R-67-042

13 DECEMBER 1967

GRARR

GODDARD RANGE AND RANGE RATE SYSTEM

DESIGN EVALUATION REPORT

Prepared for
GODDARD SPACE FLIGHT CENTER
GREENBELT, MARYLAND

Contract No. NAS 5-10555

GENERAL DYNAMICS
Electronics Division-San Diego Operations

N70-17522

DESIGN EVALUATION REPORT, GODDARD RANGE AND RANGE RATE SYSTEM

J.C. Van Caster

General Dynamics
San Diego, California

December 1967

R-67-042
13 December 1967

DESIGN EVALUATION REPORT

GODDARD RANGE AND RANGE RATE SYSTEM

Program Manager: J. C. Van Caster

Contract No. NAS 5-10555

Prepared for

Goddard Space Flight Center
Greenbelt, Maryland

Contracting Officer: Joseph M. Roberts
Technical Monitor: George C. Kronmiller, Jr.

GENERAL DYNAMICS
Electronics Division-San Diego Operations
3090 Pacific Highway, P.O. Box 127, San Diego, California 92112 • 714-298-4641

CONTENTS

CONTENTS (Continued)

CONTENTS (Continued)

CONTENTS (Continued)

CONTENTS (Continued)

TABLES

TABLES (Continued)

ILLUSTRATIONS

ILLUSTRATIONS (Continued)

ILLUSTRATIONS (Continued)

ILLUSTRATIONS (Continued)

ILLUSTRATIONS (Continued)

ILLUSTRATIONS (Continued)

SECTION 1. INTRODUCTION

1.1 OBJECTIVES

This report contains the results of a design evaluation study conducted as a part of a contract to modify the Goddard Range and Range Rate System. The study was performed for Goddard Space Flight Center by the Electronics Division of General Dynamics and is submitted in accordance with Contract NAS 5-10555, dated 25 September 1967.

The purpose of the report is to present a technical description of the total system and its operational aspects as well as to define in detail the modifications to be made. The description and design approach are supported by detailed analyses of system performance and implementation techniques.

1.2 ORGANIZATION

a. Section 1 outlines the objectives and organization of the report.

b. Section 2 summarizes the objectives and concepts underlying the modification and describes the physical and operating characteristics of the modified system.

c. Section 3 provides a physical and functional description of each subsystem and details the modifications to each equipment.

d. Section 4 consists of a design analysis for all significant parameters and functions.

e. Section 5 contains a graphical summary of system performance requirements.

f. The bibliography concluding the reports lists all documents referenced.

SECTION 2. DESIGN SUMMARY

2.1 SYSTEM OBJECTIVES

The GRARR System is designed to obtain tracking and telemetry data at VHF and S-Band frequencies from spacecraft in a wide variety of orbits. The tracking data consists of range, range rate, and angle measurements. Broad objectives of the system design include enhanced operational capability, compatibility with other systems, and growth potential. The primary features of these objectives as incorporated in this design are:

a. Enhanced Operational Flexibility.

(1) Improved system signal thresholds by the addition of parametric amplifiers and an advanced design receiver providing polarization diversity combining.

(2) Increased frequency flexibility by incorporation of fixed-step frequency shifting to provide for as many as 1000 channels within a given frequency band.

(3) Increased data capability by adding telemetry demodulators to process telemetry, range, and range-rate data simultaneously.

(4) Centralizing and automating system control functions to improve operational procedures.

(5) Increasing ranging extraction performance by using hybrid ranging codes and digital range tone extraction techniques.

(6) Operational test simulation capability for system self-exercising of the range and range rate functions to assure operational readiness on an expedient basis. This capability also provides continuous quantitative evaluation of the system capability independently of a dynamic vehicle.

(7) Capability for simultaneous reception of two signals from two different spacecraft in different frequency bands.

b. Compatibility.

(1) Inversion of the present GRARR up-link and down-link S-Band frequencies is incorporated as a step toward full compatibility with USB Systems.

(2) The system is fully compatible with the following transponders:

GRARR S-Band Crystal Transponder

GRARR S-Band Phase Locked Loop Transponder
(coherence ratio f_t/f_r = 60/48)

GRARR VHF Crystal Transponder

c. Growth Potential. Maximum possible growth potential is incorporated for expansion to a full S-Band integrated system which includes all elements of the existing STADAN, DSIF, SGLS, and USB networks. The following salient growth features have been considered:

(1) Future expansion to provide full tracking, command, and telemetry compatibility with the Apollo USB System.

(2) Future expansion to provide full tracking, command, and telemetry compatibility with DSIF and SGLS.

(3) Provisions to incorporate specific additional receiving frequency bands (400 - 410 MHz, 1435 - 1535 MHz, and 1700 - 1710 MHz) by adding the appropriate preamplifiers, mixers, and local oscillators.

(4) Provisions to extend the telemetry and command capability by adding the appropriate baseband demodulators and data processing equipment.

(5) Consideration of possible expansion, with minimum changes, to include a tracking capability with generalized ratio-type transponders which do not presently exist.

(6) Provisions to expand to computer-programmed operating sequences.

2.2 SYSTEM CONCEPTS

The GRARR System consists of ground equipment which, when operated in conjunction with suitable spacecraft transponders, will provide range, range rate, and angle data. In addition, the system is capable of transmitting commands, and of the reception and baseband demodulation of telemetry data. The system is capable of operation in the following frequency bands:

Link	VHF	S-Band
Up-link	148 - 150 MHz*	1750 - 1850 MHz
Down-link	136 - 138 MHz	2200 - 2300 MHz

*The System Signal Source is capable of providing transmitter reference frequencies from 148 to 155 MHz.

The VHF transponder in the spacecraft is a "crystal type" employing a subcarrier. In the transponder, the signal from the ground station is heterodyned to a low IF (677 to 920K Hz) and phase modulated on the RF carrier for retransmission to the ground station. For S-Band operation, either a "crystal type" or "ratio type" transponder may be used. In the "crystal type", the subcarrier frequency is either 1.4, 2.4, or 3.2 MHz. For the "ratio" or "phase-locked loop" type, the frequency transmitted by the transponder is exactly 60/48 of the frequency received.

2.2.1 Range Measurement

Range measurement is performed employing either basic sidetone ranging techniques or a hybrid ranging mode that employs sidetones and a pseudo-random binary-encoded ambiguity resolving code. The available ranging tones are:

500 KHz (S-Band operation only)
100 KHz
20 KHz
4 KHz
800 Hz
160 Hz
32 Hz
8 Hz

Any one of the three highest available tones may be selected by the operator as the highest resolution tone for a mission based upon the available transponder bandwidth or other considerations. During ranging operations, the selected highest tone is transmitted continuously and lower frequency tones are sequentially applied when required to resolve range ambiguities. For transmission, the four lowest ranging sidetones are complemented on the high side of the 4-KHz tone to produce sum frequencies of 4800 through 4008 Hz. This eliminates modulation components close to the carrier which could degrade carrier acquisition and tracking. The sequential application of all tones below the highest tone selected provides the best use of the available RF power. The lowest sidetone available, 8 Hz, establishes an unambiguous range to approximately 10,000 nautical miles. For greater ranges, within the signal threshold capability of the system, the hybrid ranging mode is employed.

In the hybrid ranging mode, an ambiguity resolving code (ARC) having a length of 32,385 bits is bi-phase modulated on the 4-KHz sidetone. The code bit rate is 4 KHz. The ARC consists of two subcodes:

Subcode	Length	Bit Length
1	2^7-1	127
2	2^8-1	255

In this mode, the unambiguous range is approximately 648,000 nautical miles.

2.2.2 Range Rate Measurement

The range rate measurement is performed using coherent doppler techniques with the doppler obtained at the effective RF carrier frequency. When "crystal type" transponders are used, the effective RF carrier is the up-link carrier. When a "ratio" type transponder is employed, the effective RF carrier is the down-link carrier. The maximum two-way doppler is ±20 KHz at VHF frequencies and ±200 KHz at S-Band frequencies. In either case, the doppler frequency is summed with a bias frequency and a measurement is made of the "time" required to count a fixed number of doppler-plus-bias frequency cycles. However both the "time base" and bias frequency are adjusted as a function of the transmitted carrier frequency so that the "time" remains constant for any given range rate. This provides "frequency-independent doppler extraction." That is, the range rate data output count is not a function of the transmitted carrier frequency.

2.2.3 Angle Measurement

Angle measurements are obtained by X-Y angle encoders on the S-Band autotracking antenna. Although the VHF antenna has no encoders, angle data can be obtained by autotracking with the VHF antenna, slaving the S-Band antenna to the VHF antenna, and recording the S-Band angle data.

2.2.4 Telemetry Demodulation

The Multifunctional Receiver includes the capability for demodulating various types of telemetry modulation. Synchronous and nonsynchronous demodulation of AM and PM is provided as well as nonsynchronous demodulation of FM. The optimal ratio-combining of the telemetry signals insures that the best possible signal-to-noise ratio is obtained in the data demodulators. The demodulator output filter bandwidths are selectable in steps from 1.5 KHz to 10 MHz for the nonsynchronous demodulator channels and from 1.5 KHz to 5 MHz for the synchronous demodulator channels.

2.3 SIMPLIFIED FUNCTIONAL DESCRIPTION

2.3.1 General

A functional block diagram of the GRARR System is shown in Figure 2-1. The system signal flow essentially common to both the range and range rate measurements is described in this subsection. The two following subsections describe the separate signal flow paths following the receiver. Sections 3 and 4 contain detailed descriptions, performance parameters, and supporting analysis for all units of the system. The description of the doppler extraction unit in Section 3 includes diagrams of frequency coherence relationships for the system.

As shown in Figure 2-1, the transmitted carrier frequency and ranging sidetones are developed in the Signal Generation Subsystem from reference signals provided by the Timing Subsystem. The ranging signal generator outputs and ambiguity resolving code (ARC) encoder signals are zero-set phase shifted and the selected tone and ARC are combined to phase-modulate the selected RF carrier. The modulated carrier is power amplified, filtered, polarized, and transmitted to the spacecraft transponder.

The system may operate with crystal or ratio-type coherent transponders. Essentially, however, with both types of spacecraft transponders, the received modulation is coherently returned to the ground station either on the RF carrier or on a subcarrier. The coherence relationships for both types of transponders are included in the system coherence diagrams provided in Section 3.6.5.

At the ground station, the S-Band autotrack antenna provides six separate signal outputs. Designating the received polarization components as A and B, the following outputs are available:

The A polarization summed signal
The B polarization summed signal
The A polarization X component
The B polarization X component
The A polarization Y component
The B polarization Y component

Six parallel channels are used for filtering, parametrically amplifying, and down-converting these signals before application to the multifunctional receiver. In four of the multifunctional receiver channels, error signals are derived for driving the antenna servo system. The two polarization components derived in the sum channels of the receiver are optimum-ratio combined to provide the best possible output signal-to-noise ratio. The composite range and range rate signal from the multifunctional receiver is applied to the subcarrier receiver. In the subcarrier receiver, the doppler information, range tones, and ARC signals are detected.

At the VHF antenna, the received signal is filtered, parametrically amplified, and supplied to the VHF receiver. The receiver derives: (1) error signals for driving the VHF antenna servos, (2) the doppler information, and (3) range tone signals.

2.3.2 Range Measurement

The received tones and ARC from either the VHF or the S-Band receiver channel are applied to the sidetone range extraction unit. In this unit, the signal-to-noise ratio of the highest frequency range tone used is enhanced by a phase-locked loop. Additional narrowbanding is made possible by the digital rate aid signal which effectively removes doppler from the range tone. In the Digital Range Tone Extractor, all lower range tones are synthesized from the highest tone and phase locked to the average phase of the received tones. Once the synthesized tones are synchronized with the lower tones, it is no longer necessary to transmit any but the highest tone.

The range extraction unit measures range by: (1) producing a start pulse that is phase coherent to the transmitted range tones, (2) producing a stop pulse that is phase coherent to the received range tones, and (3) measuring the time interval between them. This range reading is unambiguous to approximately 10,000 nmi. When the range exceeds this value the ambiguity number extraction unit which operates on the ARC is used to determine and update the number of ambiguity distances. The ambiguity number and the derived range data are multiplexed in the recording unit, formatted, encoded, and recorded by a paper punch recorder.

2.3.3 Range Rate Measurement

In the Receiver Subsystem, either of two doppler extractor units are employed; one in conjunction with the existing VHF receiver and one with the multifunctional receiver. These units perform similar functions. A frequency reference from the transmitter is combined with the doppler information on the carrier and subcarrier VCO's to derive the doppler data. The two-way doppler on a bias frequency is outputted by the receiver doppler extraction unit to the range-rate extraction unit of the Data Subsystem.

The range rate extraction unit determines doppler by measuring the time required to count a fixed number of cycles of two-way doppler-plus-bias frequency. The "time" base for counting, and the doppler data bias frequency, are adjusted as a function of transmitted frequency, so that the data outputted by the range rate extraction unit is independent of transmitted frequency.

The range rate extraction unit output is data multiplexed with other system data and recorded by the paper punch recorder.

2.4 PHYSICAL CONFIGURATION

2.4.1 Site Layouts

The relative positions of the major installations for each of the four sites is depicted in Figures 2-2 through 2-5. The configurations are based upon GSFC information updated by site surveys thus far accomplished at Rosman and Fairbanks. Straightline distances are shown between the major structures at each site although cable runs cannot, in general, be made along these routes. Exact routes and cable types have not yet been determined. In general, however, both RF and control cables will connect the instrumentation building with both antennas and the collimation tower building.

2.4.1.1 ROSMAN, TANANARIVE AND CARNARVON SITES. At these sites, the existing waveguide runs connecting the S-Band antenna and the Transmitter Trailer will be reused between the S-Band antenna and the new building, with additional sections added as required.

The 3-inch Heliax cable presently used to transmit power from the VHF transmitter to the VHF antenna will also be reused. Portions of the existing cable will be stripped back out of the gound trench, and a splice with additional lengths will be made to re-route it to the new building. Existing RF and control cables will be used where practicable.

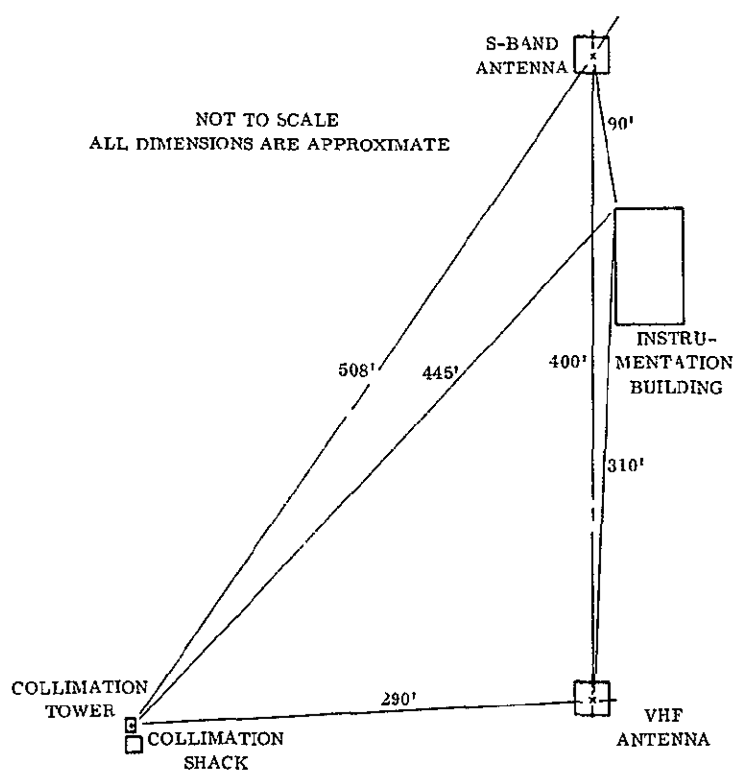

Figure 2-2. Rosman Site Layout

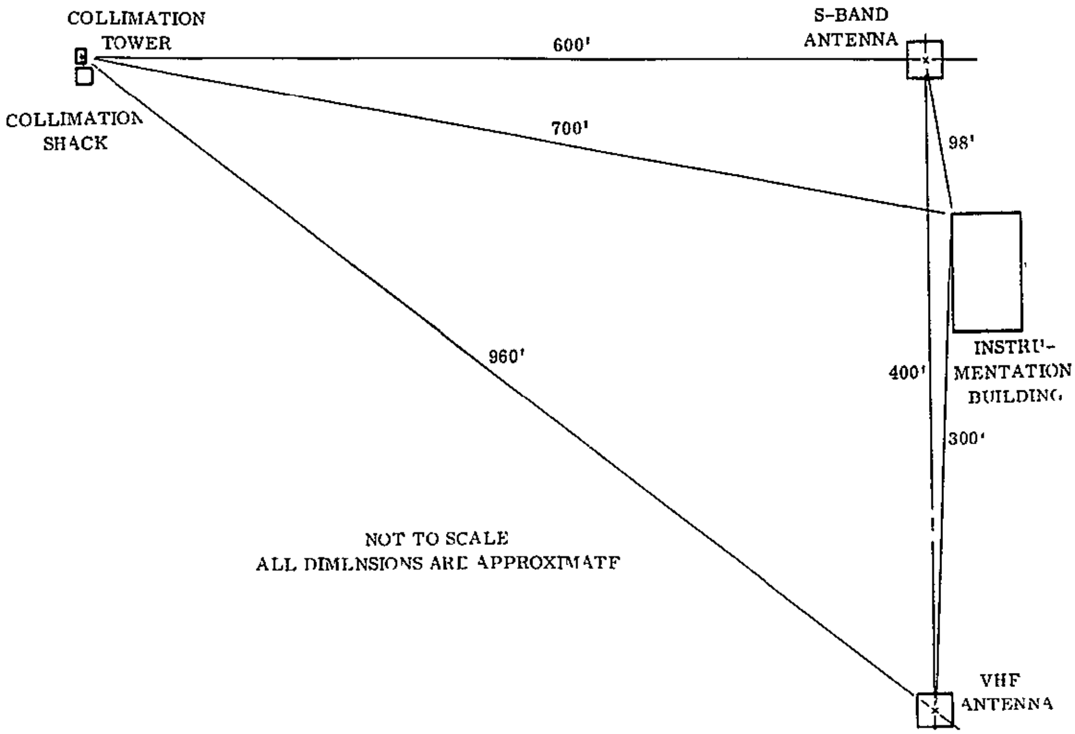

Figure 2-3. Carnarvon Site Layout

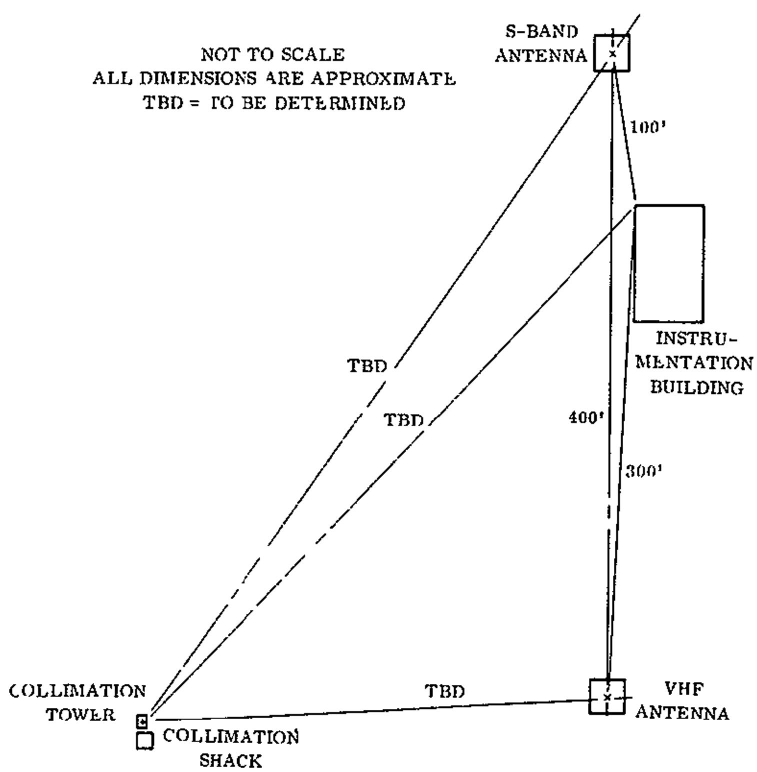

Figure 2-4. Tananarive Site Layout

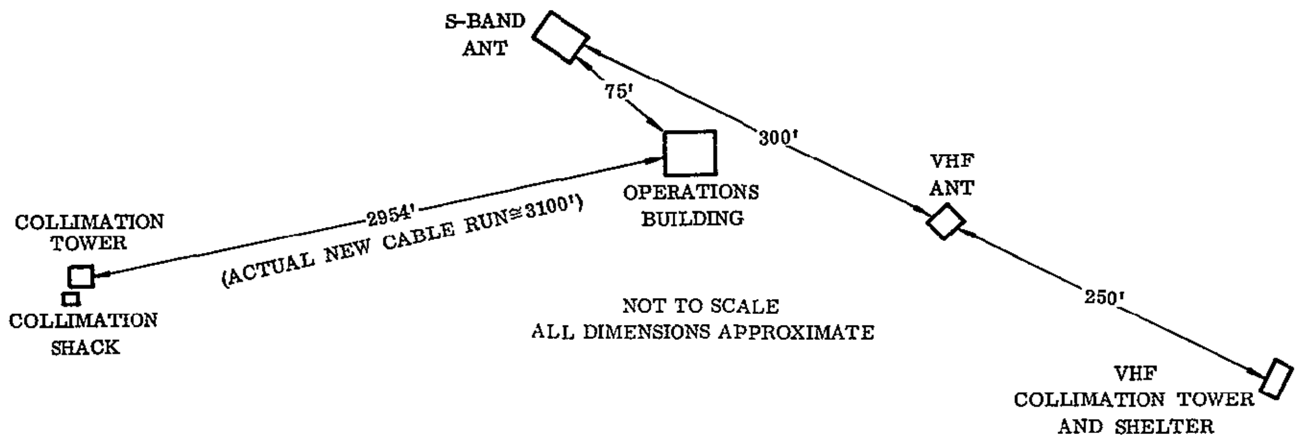

Figure 2-5. Fairbanks Site Layout

2.4.1.2 FAIRBANKS SITE. The operations building already exists at Fairbanks and no re-routing will be necessary for either the S-Band or the VHF transmitting connections. Again existing cables will be used where practicable.

2.4.2 Retained Equipment and Hardware

This paragraph lists the existing equipment to be retained and reused in whole or in part at the Rosman, Tananarive and Carnarvon sites. At the Fairbanks site, all existing equipment will be retained and reused except items specifically required to be replaced. It is expected, however, that all equipment and material at the sites will be available for reuse and that this list will serve only as a guide for evaluating design and procurement efforts.

a. General:

(1) All equipment cabinets

(2) All slides, cables, cable retractors, and associated hardware

(3) All equipment drawers and writing tables

(4) All miscellaneous brackets and mounting hardware presently used in the existing trailers

(5) All power supplies

b. Transmitter Trailer Equipment:

(1) All coaxial and waveguide components presently used in the Transmitter Trailer, and the associated bracketry

(2) All plumbing used in the present heat exchanger and the dehydrator installations, and the associated bracketry

(3) The Heat Exchanger Control Panel and its housing. (This item is to be re-installed by GSFC.)

(4) Unit 2 — VHF Final Amplifier and RF switching

(5) Unit 3 — VHF Driver Amplifier and Control

(6) Unit 4 — Power Distribution

(7) Unit 5 — S-Band Power Supply and Control

(8) Unit 6 — S-Band Klystron Amplifier

(9) Unit 7 — S-Band Calorimeter and Filter

(10) Unit 8 — Synthesizer Modulator and Test Equipment

(11) Unit 10 — Heat Exchanger

(12) Unit 11 — Dehydrator

(13) Unit 12 — Unitized Rectifier

c. Receiver Trailer Equipment

(1) Unit 1 — Recorder, Paper Analog, entire unit

(2) Unit 2 — Recorder, Punch Tape, entire unit

(3) Unit 3 — Standards:

(a) Radio Receiver, WWV (3REI)

(b) HP122AR Oscilloscope (3M1)

(c) Axis Readout Translator Register (3A2)

(d) Axis Readout Power Supply (3PS1)

(e) Power Supply, 18v, 2 amperes (3PS2)

(f) Power Supply, 18v, 1 amperes (3PS3)

(g) Power Supply, 5v, 20 amperes (3PS4)

(4) Unit 4 — Ranging and Timing

(a) Power Supply, 6v, 5 amperes (4PS1)

(b) Counter, 10 MHz (Range Rate) (4M1)

(c) Sidetone Combiner (4A1)

(d) Range Readout (4A6)

(e) Counter, 10 MHz (Range) (4M2)

(f) Prescaler, Counter (100 MHz) and Count Rate Control (4A5)

(5) Unit 5 — Receiver

(a) Power Supply, 18v, 10 amperes (5PS1)

(b) Power Supply, 28v, 10 amperes (5PS2)

(c) Power Supply, 18v, 5 amperes (5PS3)

(d) RM35A Oscilloscope (5M1)

(e) Range Tone Demodulator (5A2A9)

(6) Unit 6 — Receiver, entire unit

(7) Unit 7 — Control-Monitor Master, entire unit

(8) Unit 8 — Control-Monitor Antenna, entire unit

(9) Unit 9 — Control-Monitor, entire unit

(10) Units 11, 12, and 13 — Test Set

Most of the equipment in units 11, 12, and 13 will be retained for use as "bench type" test equipment. Three Technibilt Model DD-8T equipment carts will be provided for each site. Some of the equipment listed above will be incorporated into one or more of the subsystems, to be used as operational test equipment.

2.5 SYSTEM OPERATION

2.5.1 Carrier Frequency Selection

2.5.1.1 VHF TRANSMITTER FREQUENCY. The VHF transmitter frequency must be selected at the synthesizer or on the transmitter frequency control panel located at the control console. The VHF transmitter frequency is selectable from 148 to 150 MHz. The System Signal Source is capable of providing transmitter reference frequencies from 148 to 155 MHz. Selection is made at the console by setting four rotary switches: one nine-position switch for a 1 MHz step (marked 146 MHz to 154 MHz), and three 10-position switches for 100 KHz, 10 KHz and 1 KHz steps. There is a one-to-one correspondence between the synthesizer output frequency and transmitted frequencies; therefore, a direct indication of transmit frequency is obtained without complex switching circuits.

2.5.1.2 S-BAND TRANSMITTER FREQUENCY. The S-Band transmitter frequency may also be selected at the synthesizer or on the transmitter frequency control panel at the operators console. To set the S-Band frequency, three rotary switches are provided. To allow direct indication of the selected frequency, and since the synthesizer output frequency is multiplied by four to obtain the S-Band transmitted carrier frequency, a divide-by-four operation is provided by the switch to control the synthesizer. Three 10-position rotary switches provide increments of 10 MHz, 1 MHz, and 100 KHz to cover the transmit frequency range of 1750 MHz to 1850 MHz.

2.5.1.3 TRANSMITTER FREQUENCY SEARCH MODE. For both VHF and S-Band operation, a search mode is provided in which the frequency may be continuously varied about the selected carrier frequency. A VCO provides a variation of ±300 KHz about a selected S-Band output frequency and ±50 KHz about a selected VHF output frequency.

2.5.1.4 MULTIFUNCTIONAL RECEIVER RECEIVE FREQUENCY SELECTION. Discrete center-frequency selection and continuously variable tuning about the center frequency is provided for both VHF and S-Band operation. Center-frequency selection is made with a two-position band select switch marked 135 MHz and 2200 MHz and four rotary switches. Four 10-position rotary switches provide for steps of 10 MHz 1 MHz 100 KHz, and 10 KHz. Continuous tuning over a range of ±300 KHz is provided by a 20-turn potentiometer.

2.5.2 Modes of Operation

Major operating modes of the multifunctional receiver and the principal modes of ranging are described in the following subsections.

2.5.2.1 MULTIFUNCTIONAL RECEIVER.

2.5.2.1.1 Frequency Bands. The multifunctional receiver will operate at S-Band frequencies using the parametric amplifier-converter provided. Step and variable tuning is provided over the 2200-2300 MHz band. The capability exists for the future addition of appropriate preamplifiers and converters permitting operation in the bands between 135-139 MHz, 400-410 MHz, 1435-1535 MHz, and 1700-1710 MHz.

2.5.2.1.2 Multifunctional Receiver Modes. Eight operating modes are provided:

a. Mode A — Autotrack: The receiver will develop error voltages to position the steerable antennas in either the open-loop or closed-loop tracking modes.

b. Mode B — Autotrack and Ranging: The receiver will furnish error voltages to position steerable antennas in the closed-loop mode and supply coherent range signals at baseband.

c. Mode C — Autotrack and Telemetry (closed loop): The receiver will furnish error voltages to position steerable antennas in the closed-loop mode and supply coherently-demodulated telemetry signals at baseband. The predetection bandwidth of the telemetry channel will be variable from 10 KHz to 10 MHz.

d. Mode D — Autotrack and Telemetry (open loop): The receiver will furnish error voltages to position steerable antennas in the open-loop mode and supply non-coherently demodulated telemetry signals at baseband. Predetection bandwidth of the telemetry signal will be variable from 10 KHz to 20 MHz.

e. Mode E — Autotrack, Ranging and Telemetry: This mode will be the same as Mode B with the additional requirement of supplying coherently-demodulated telemetry signals at baseband. The predetection bandwidth of the telemetry channels will be variable from 10 KHz to 1 MHz.

f. Mode F — Ranging: The receiver will be capable of receiving and translating to baseband the coherent range signals. The predetection bandwidth required is 10 MHz.

g. Mode G — Telemetry (coherent): The receiver will be capable of receiving and translating to baseband coherent telemetry signals with a predetection channel bandwidth variable from 10 KHz to 10 MHz.

h. Mode H — Telemetry (non-coherent): The receiver will be capable of receiving and non-coherently demodulating telemetry signals with a predetection channel bandwidth variable from 10 KHz to 20 MHz.

2.5.2.2 RANGING MODES. The GRARR system can operate in: (1) a sidetone ranging mode to obtain unambiguous range to approximately 10,000 nmi, or (2) a hybrid ranging mode to obtain unambiguous range to approximately 648,000 nmi. In both modes, any one of the three highest available ranging tones, (500 KHz, 100 KHz, and 20 KHz) may be selected as the highest ranging frequency to be employed for S-Band operation. The 100 KHz or 20 KHz tone may be selected as the highest used for VHF operation. The choice may be based upon the available transponder bandwidth or other operating considerations.

2.5.3 Bandwidth Selection

In the phase-lock mode of operation the noise bandwidth of the multifunctional receiver phase-lock loops is selectable. The primary phase-lock loop corrects for the doppler frequency variation common to both signal channels. The secondary phase-lock loop corrects phase between the two sum signal input channels.

A single control provides selection of the following bandwidth combinations:

Primary Loop Bandwidth	Secondary Loop Bandwidth
3 KHz	1 KHz
1 KHz	300 Hz
300 Hz	100 Hz
100 Hz	30 Hz
30 Hz	10 Hz
10 Hz	3 Hz

2.5.4 Multifunctional Receiver Tuning Modes

A total of six tuning modes may be selected for signal acquisition by the multifunctional receiver. Three modes are provided for coherent operation and three for open loop operation.

2.5.4.1 PHASE LOCK MODE.

a. Manual Search Mode: A control is provided to tune the VCO through its entire range. The phase-lock loop is disabled in this mode so that the receiver will not lock to a signal.

b. Manual Acquire Mode: This mode is the same as the manual search mode except that the phase-lock loop is not disabled and will allow the receiver to lock on the signal and provide an indication of lock.

c. Automatic Acquire Mode: In this mode the VCO will sweep until the receiver achieves lock and provides an indication of lock. The sweep deviation and rate of deviation is proportional to the selected tracking bandwidth of the phase lock loop.

2.5.4.2 OPEN LOOP MODE.

a. Manual Tuned Mode: In this mode the receiver is continuously tunable ±300 KHz about a selectable center frequency.

b. AFC Mode: AFC is used in conjunction with manual tuning.

c. Fixed Frequency Mode: In this mode the manual tuning control is disabled and the receiver is tuned in discrete 10 KHz steps selectable at the receiver control panel.

2.5.5 Sequence of Tracking Events

The sequence of events for three primary modes of operation as described below assumes the appropriate set-up of operating controls including the selection of appropriate modes, frequencies, sampling rates, and bandwidths.

2.5.5.1 VHF ACQUIRE – S-BAND TRACK. In this operating mode, the relatively broadbeamed (≈16 degree) VHF antenna sector-scans the expected aximuth angle until the receiver acquires the 136-138 MHz carrier transmitted from the spacecraft transponder. Upon receiver acquisition of the signal, the VHF antenna is automatically switched to the autotrack mode. The relatively narrow bandwidth (≈2 degrees) S-Band antenna is slaved to the VHF antenna and also tracks the spacecraft transponder. After VHF acquisition the satellite transponder is unsquelched by S-Band transmission from the ground station and begins retransmission of the S-Band signals. The multifunctional receiver next acquires the S-Band carrier and the S-Band antenna may be switched from the slaved to autotrack mode. The S-Band system is then independent of the VHF system.

Upon acquisition of the S-Band signal by the multifunctional receiver and subcarrier acquisition by the subcarrier receiver, the transmitter carrier is sequentially modulated by ranging tones. The highest frequency range tone is acquired by a phase-locked loop and the lower frequency tones are sequentially phase matched using digital techniques. Range, range rate and angular data are derived from the transponded signal and recorded by the system. The multifunctional receiver may also receive and baseband demodulate telemetry.

2.5.5.2 VHF ACQUIRE — VHF TRACK. In this operating mode the VHF system acquires as described in the preceding paragraphs and the S-Band portions of the system and the multifunctional receiver are not activated. Range and range-rate data are similarly derived and recorded. X-Y angle signals are not available from the VHF antenna; if this data is desired, the S-Band antenna must be slaved to the VHF antenna and angle data obtained from the S-Band antenna encoders.

2.5.5.3 S-BAND ACQUIRE — S-BAND TRACK. When the expected angle data is accurately known, it is possible to initially acquire by sector scanning with the narrow beamwidth S-Band antenna. Upon receiver acquisition of the transponded S-Band signal, the S-Band antenna may be switched to autotrack. Data acquisition is then as described for the previous modes. It is also possible to slave the VHF antenna to the S-Band antenna in this mode and utilize the narrower beamwidth tracking performance of the S-Band antenna to simultaneously receive VHF data from the spacecraft.

SECTION 3. SYSTEM DESCRIPTION

3.1 PHYSICAL DESCRIPTION

3.1.1 Cabinet Arrangement

3.1.1.1 ROSMAN, TANANARIVE AND CARNARVON SITES. Since the instrumentation buildings at these sites will be new, considerable freedom is offered in equipment arrangement. Some constraints exist, however, principally in waveguide and cable entry points and window positions. Figure 3-1 depicts the operations room arrangement contemplated for the Rosman site. The console operator is positioned at a six-bay console with two additional cabinets directly behind him. These two cabinets contain controls to which the operator should have access for simulation and check-out but which are not required for actual operational control. The operator's position permits viewing both antennas through windows and surveying any operators at other cabinets. The central floor area contains two lines of five cabinets each. The lines face each other, with sufficient room between for an operator at each line if desired. Cabinet arrangement readily permits the audition of 8 more cabinets. (Information on the Rosman instrumentation building and operations room was derived from NASA architectural drawing G1-FCB-149-XXX.)

Technical panel "D", a utility power wall panel, must be relocated by GSFC to avoid interference with the dummy load cabinet (Unit 7), the location of which determines placement of the outlet for the S-Band waveguide to the antenna.

The transmitting equipment is located against the north wall of the operations room. The heat exchanger (Unit 10) will be installed on top of an outside pad provided by GSFC, near the northeast corner of the building. A shelter, complete with the primary power outlets, will be provided by GSFC to house the heat exchanger. The dehydrator (Unit 11) will be located in the mechanical equipment room.

No architectural drawing is yet available for the Carnarvon and Tananarive sites. It is anticipated, however, that the instrumentation building operations room and cabinet arrangement at Carnarvon will be similar to that at the Rosman site. At Tananarive, the existing equipment will be moved into the instrumentation building by GSFC prior to site turnover. It is anticipated that the cabinet arrangement will be significantly different at that site. It should also be noted that a new Timing Subsystem will not be provided at Tananarive since the GRARR system will share the Gemini timing system. Thus, at Tananarive, the timing cabinet and the digital phase recorder in the test signal source cabinet will be absent.

3.1.1.2 FAIRBANKS SITE. Figure 3-2 indicates the general layout of the existing operations room at Fairbanks and the proposed location of the three newly-furnished cabinets of equipment.

3.1.2 Cabinet Layouts

A tentative arrangement of equipment within cabinets is shown in the elevation views given in Figure 3-1 for the Rosman, Carnarvon, and Tananarive sites and Figure 3-2 for the Fairbanks site. As noted previously, however, the timing cabinet and the digital phase recorder in the Test Signal Source cabinet will not be present at the Tananarive site. Equipment now existing in the transmitter vans at Rosman, Carnarvon, and Tananarive is not shown since its appearance will not be modified.

The equipment is arranged in functional groups as practicable with controls and frequently-viewed displays near eye level. Growth space is provided in both the cabinets and console areas. It should be noted that the operating and viewing level for the two cabinets behind the console operator is designed for the sitting position.

Console panels and units furnished for the Fairbanks site will not be console-mounted since GSFC intends to integrate these units with the existing console.

3.1.3 Cabinet Packaging

3.1.3.1 RETAINED EQUIPMENT. All reused equipment will be relocated into their new next assembly unchanged. The new interfaces will be designed to allow reinstallation of the reused items without modification to the items. All cabinets, slides, cable retractors, handles, panel retaining screws, and other associated hardware will be retained unmodified. The retained cabinets have removable side and rear panels which are bolted in place. Existing intra-cabinet wiring harnesses and associated hardware will be used wherever practicable.

3.1.3.2 NEWLY-PROVIDED EQUIPMENT. The console, equipment cabinets, and chassis slides are categorized as newly-provided equipment herein.

a. Console: The console provided for the Rosman, Carnarvon, and Tananarive sites will be an Emcor "Low Silhouette" enclosure, consisting of six Emcor FR-72A frame sections and two 45-degree corner frames to facilitate interconsole cabling. There will be no panel between the individual frame sections.

b. Cabinets: All new cabinets provided will be Western Devices (Zero Manufacturing Co.) part number MC 1X-26-N-78 3/4-H-D-2, or equivalent. The existing cabinet presently located in each of the collimation tower buildings will be reused.

c. Slides: The slides used on new equipment will be identical to those presently installed on the existing equipment.

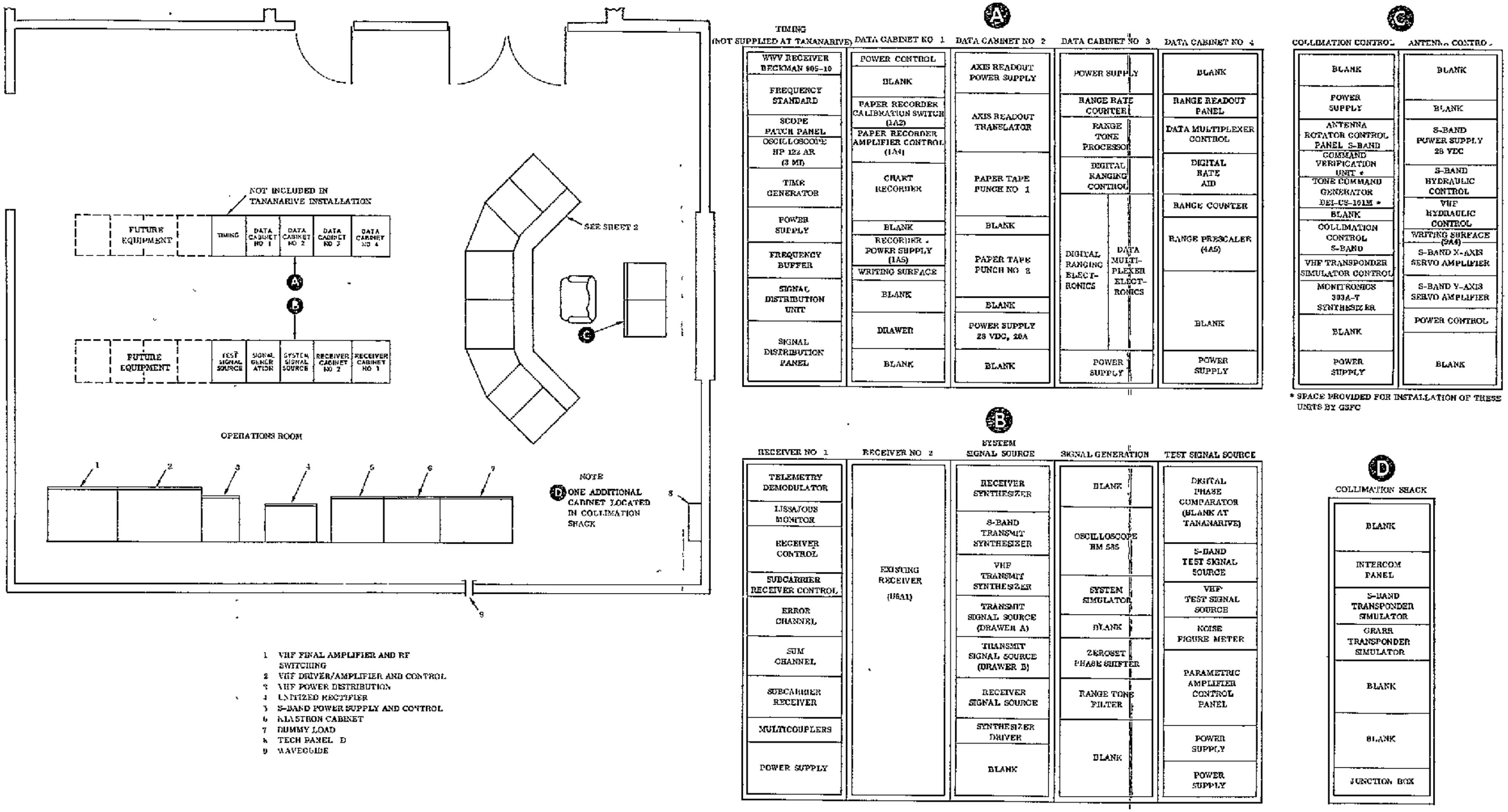

Figure 3-1. Equipment Arrangement for GRARR-1 Sites (Sheet 1 of 2)

FOLDOUT FRAME 1

FOLDOUT FRAME 2

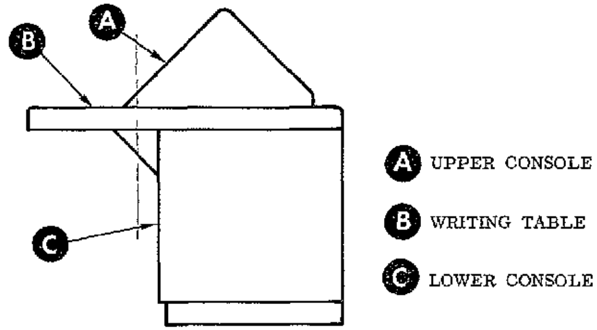

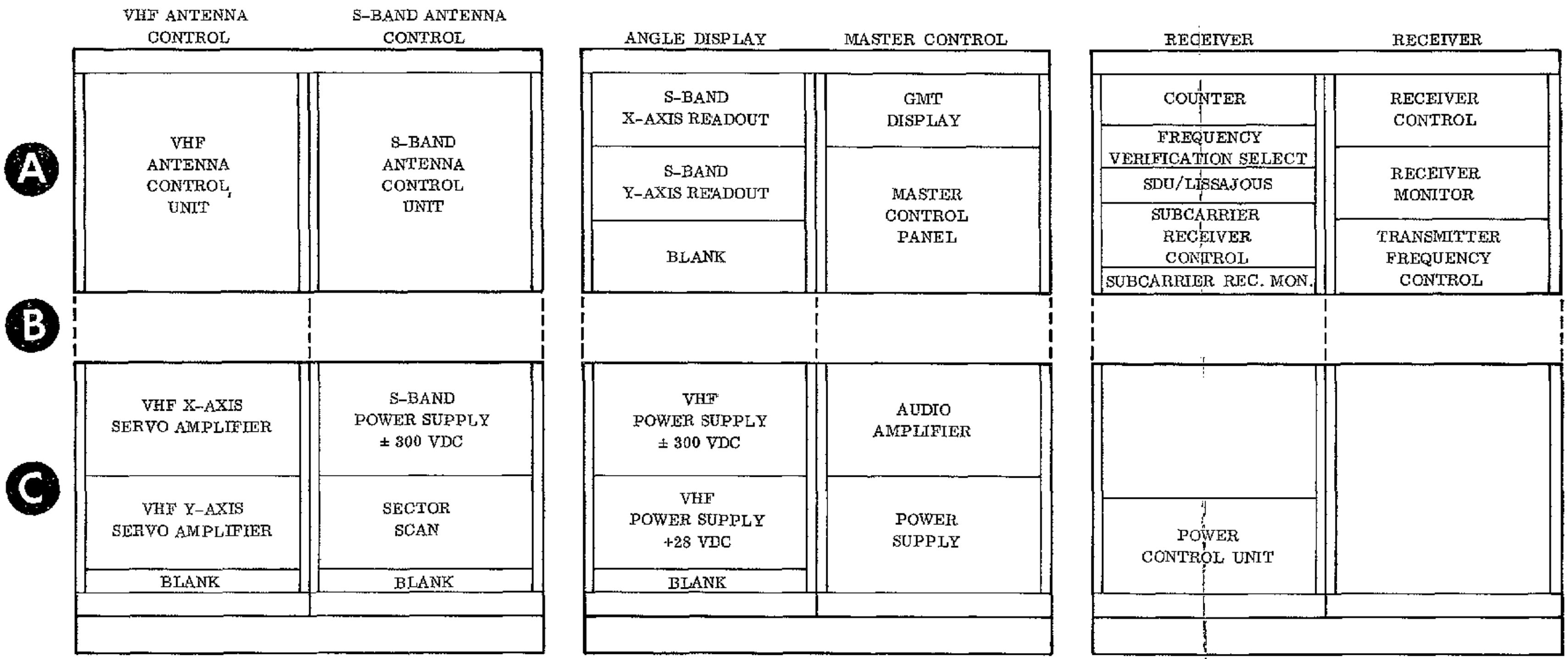

Figure 3-1. Equipment Arrangement for GRARR-1 Sites (Sheet 2 of 2)

FOLDOUT FRAME 1

FOLDOUT FRAME 2

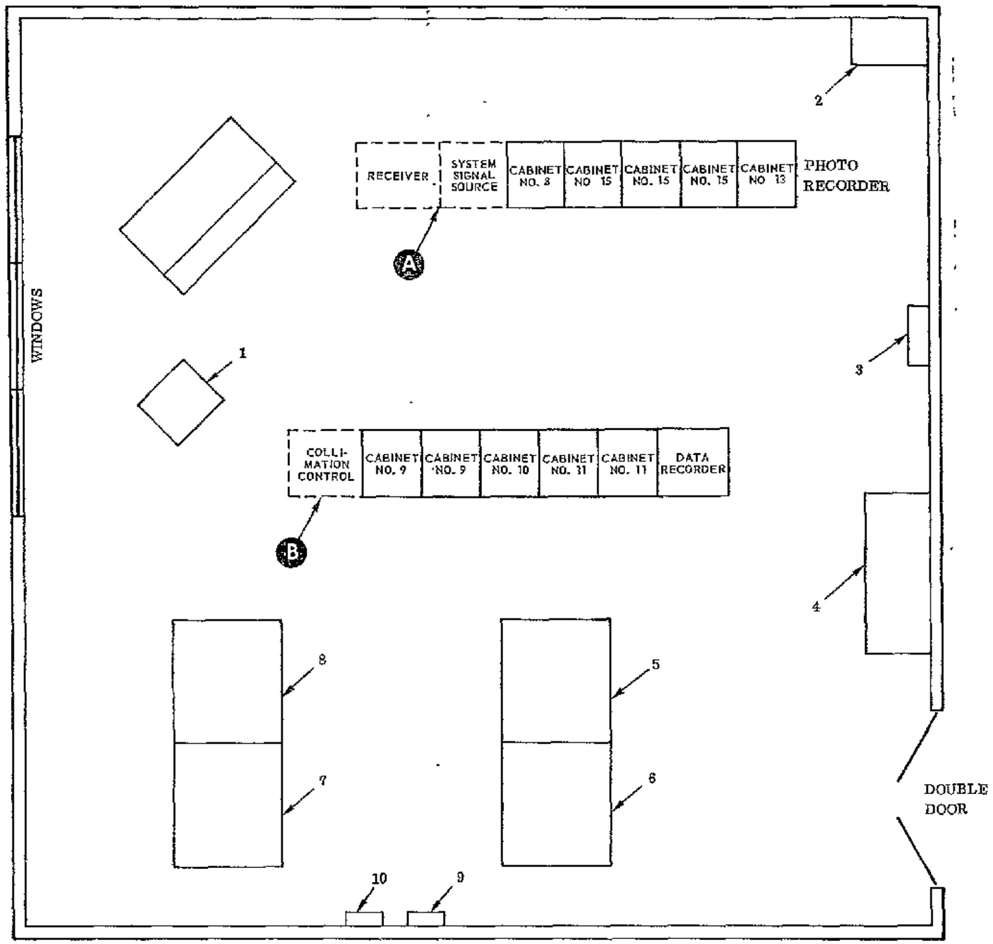

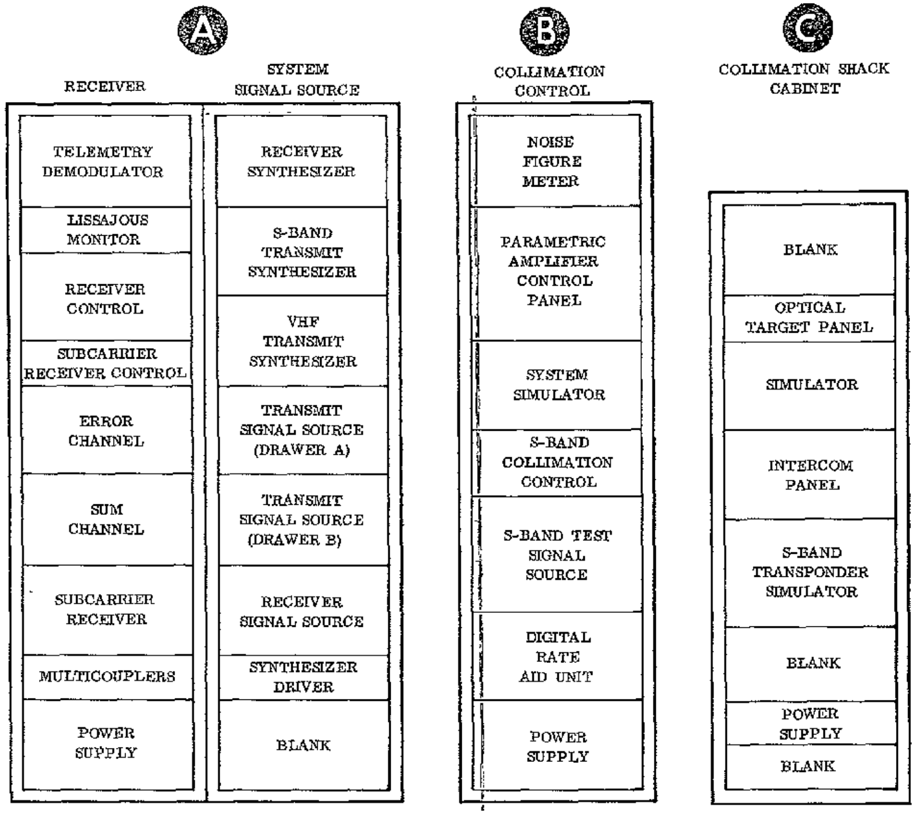

NOTE

DASHED LINES DENOTE NEW ITEMS.

C ONE ADDITIONAL CABINET LOCATED IN COLLIMATION SHACK

1. TV REMOTE DISPLAY
2. STORAGE
3. MASTER CIRCUIT BREAKERS
4. TELETYPE PRINTER
5. VHF AMPLIFIER CABINET NO. 6
6. VHF RECTIFIER AND CONTROL CABINET NO. 5
7. S-BAND AMPLIFIER CABINET NO. 3
8. S-BAND CABINET NO 4
9. VHF TRANSMITTER SWITCH
10. S-BAND TRANSMITTER SWITCH

Figure 3-2. Equipment Arrangement for Fairbanks Site

FOLDOUT FRAME 1

FOLDOUT FRAME 2

3.2 TIMING SUBSYSTEM

The Timing Subsystem provides highly accurate frequencies for subsystems within the GRARR System and generates local time signals for time-tagging data. The Timing Subsystem also provides the capability to synchronize the reference signals to WWV or other external time reference sources.

The Timing Subsystem (Figure 3-3) consists of seven functional elements:

- Standard Frequency Source
- Frequency Divider
- Digital Clock
- Time Code Generator
- Signal Distribution Unit
- Time Comparison Unit
- Emergency Power Unit

3.2.1 Standard Frequency Sources

Frequency references for the Timing Subsystem are derived from two sources. The primary source is the master oscillator which provides highly accurate and stable reference sinusoids of 5 MHz, 1 MHz and 100 KHz. The second source is a 5 MHz reference signal from other station equipment.

3.2.1.1 MASTER OSCILLATOR. The master oscillator is the basic timing and frequency reference source for the ranging system. It produces three highly stable and accurate referance frequencies; 5 MHz, 1 MHz, and 100 KHz. These signals are used in the Timing Subsystem, the Data Subsystem and the Signal Generation Subsystem as well as being provided as outputs for future use.

An internal emergency power supply is included in the master oscillator and will provide 20 hours minimum continuous operation of the oscillator in the event of ac line power failure. The batteries are rechargeable nickel-cadmium cells.

3.2.1.2 FREQUENCY BUFFER. The frequency buffer provides 5 MHz, 1 MHz, and 100 KHz reference signals derived from the master oscillator required to operate the system as well as those outputs required for the Signal Distribution Panel. This unit also provides 5 MHz, 1 MHz, and 100 KHz signals derived from an external 5 MHz source.

Each of the three inputs from the master oscillator is routed to a preamplifier. The preamplifier terminates the master oscillator signal in the proper load and then amplifies the signal for parallel distribution to output power amplifiers.

The 5 MHz input supplied from an external source is passed through a crystal filter and on to a preamplifier. The preamplifier conditions the signal for parallel distribution to an

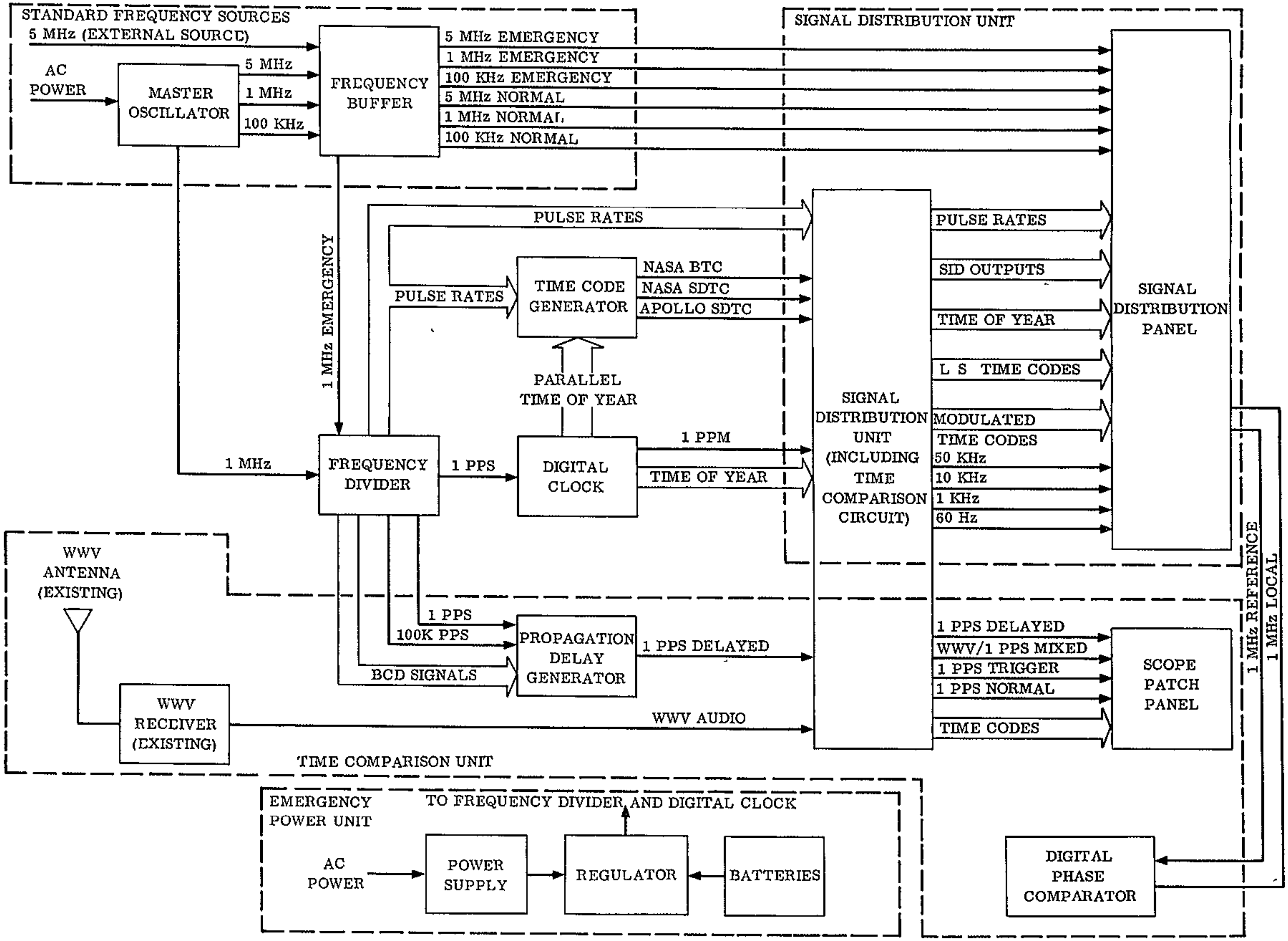

Figure 3-3. Timing Subsystem Block Diagram

output power amplifier and to a divider network for generation of the 1 MHz and 100 KHz output. The divider network consists of a divide-by-five circuit and a divide-by-ten circuit. An output of the divide-by-five circuit is filtered and amplified for parallel distribution to output power amplifier. A second output is routed to a divide-by-ten circuit. The output of the divide-by-ten circuit is filtered and amplified for distribution.

3.2.2 Frequency Divider

The Frequency Divider (Figure 3-4) processes the 1-MHZ signal from the master oscillator through a series of decade dividers to provide pulse rates which are used as reference pulses to other subsystems and to generate three time codes. The reference 1-pps signal to the Digital Clock is provided as an output of the Frequency Divider. Synchronization of the 1-pps output signal with an external time reference is accomplished by coarse and fine synchronization circuitry. If the master oscillator fails, automatic switchover to an externally-generated 1-MHz reference signal is provided.

Two 1-MHz signal inputs to the Frequency Divider are converted to square waves. A missing-pulse detector monitors the input from the master oscillator. If an interruption in the master oscillator output signal occurs, the missing-pulse detector causes the reference input to the Frequency Divider to be switched from the master oscillator 1-MHz signal to the 1-MHz external source within 1 μsec. An automatic lock-out prevents reapplication of the master oscillator until it is manually reset. A front panel display indicates which frequency source is driving the frequency dividers.

After passing through the first $\div 10$ counter (units microsecond counter, U-μsec), the resulting 100K-pps signal is converted to a sinewave by a 100-KHz filter and a high frequency resolver. A digital accumulator indicates the integral and incremental shaft rotations of the resolver for logging the oscillator frequency drift. It consists of a seven-digit counter geared to the shaft of the resolver by a 10:1 gear ratio. Thus the smallest digit is equivalent to 0.1 μsec and the most significant is equivalent to 100 msec per count. The resolver is selected to provide a continuous, linear (±1%) output as a function of the shaft rotation angle. Accumulated accuracy is maintained within ±1% of the resolver shaft position.

The output of the phase shifter is applied to a tens-of-microseconds (T-μsec) counter through a pulse shaper. The resulting 10K pps is fed to the hundreds-of-microseconds (H-μsec) counter, and the division process continues through subsequent $\div 10$ networks, down to 1-pps output from the hundreds-of-milliseconds (H-msec) counter. The 1-pps output is routed to the Digital Clock as an input and to the redundant seconds counter. In the redundant seconds counter, the 1-pps is divided by 10 and then by six with the outputs of the two counters decoded to give an indication of 1 pulse-per-minute (1 ppm). The redundant seconds counters can be reset to zero independently of the Digital Clock.

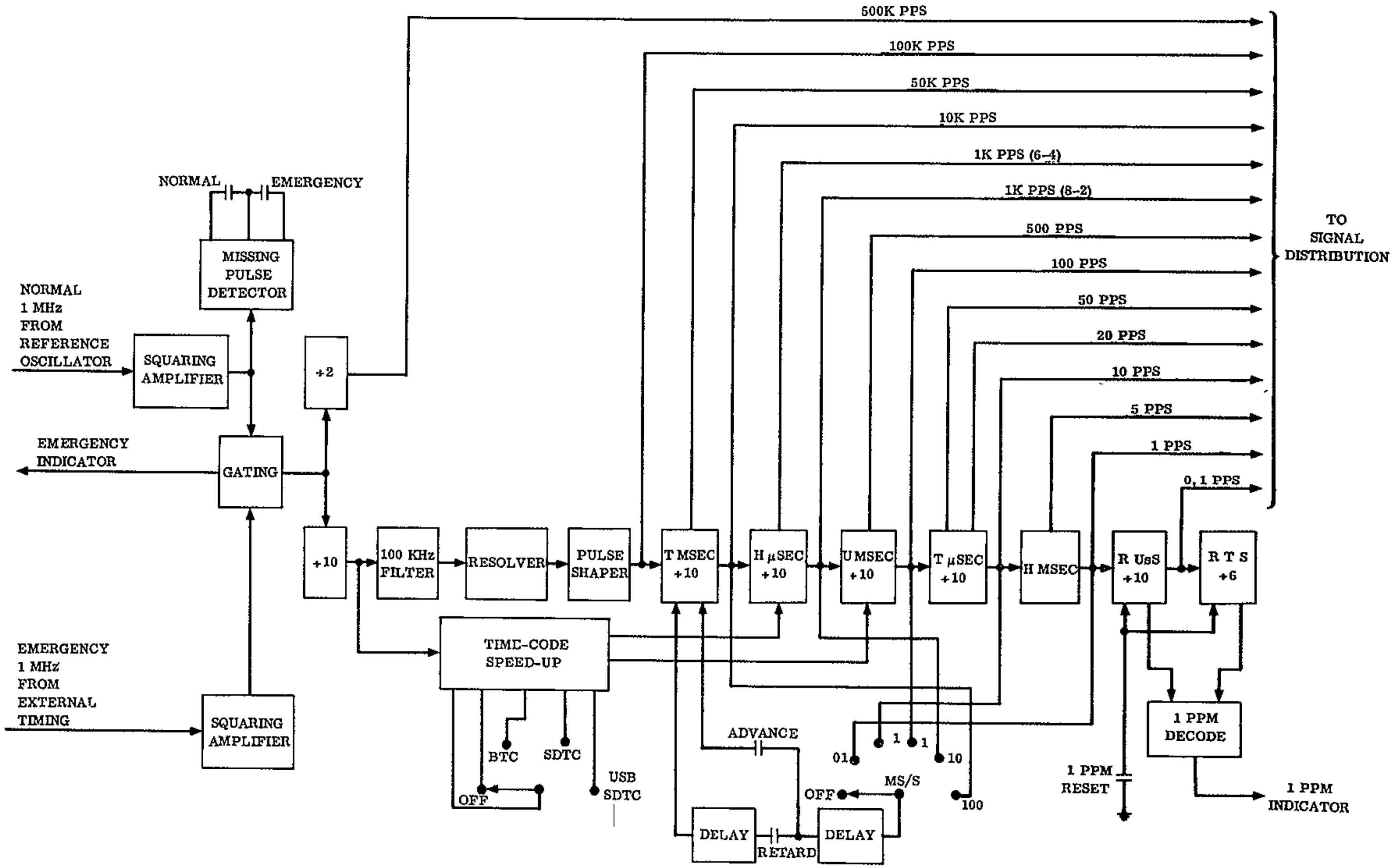

Figure 3-4. Frequency Divider

Coarse synchronization of the Timing Subsystem to WWV is accomplished by the advance-retard circuit, which adds or deletes pulses into the T-μsec counter at rates of 1, 10, 100, 1000, and 10,000 pps. These pulses are obtained from outputs in the divider chain, and through appropriate delay networks, add to or inhibit the 100K pps pulse train into the T-μsec counter. Since each pulse received by the H-μsec counter is equivalent to 0.01 msec elapsed time, the pulse rates advance or retard the accumulated time by 10 μs/sec, 100 μs/sec, 1 ms/sec, 10 ms/sec, or 100 ms/sec respectively.

The NASA and Apollo time code generating circuits can be rapidly checked by increasing the counting rate of the frequency divider and digital clock. The speed-up is accomplished by triggering the H-μsec and the U-msec counters by the 100K pps output of the T-μsec counter instead of the normal trigger inputs of 10K pps and 1K pps, respectively. This results in speeding up the time codes by factors of 10 or 100. A corresponding increase in the scope trigger frequency displays the time code on the comparison oscilloscope. A 4-position switch provides for speeding up the code rate. The position of the switch determines which code is observed and the speed-up rate required for that code. Both SDTC rates are increased by a factor of 100 and the BTC rate increased by a factor of 10. Selected pulse rates are outputs from the Frequency Divider to the Signal Distribution Unit. Each output is buffered by a separate gate circuit and is fed through an AMP Series M coaxial connector.

The frequency divider consists of 3-C μ-Pac digital modules that are primarily wired in an 8-4-2-1 BCD counting mode. The modules are housed in a 96-connector mounting bloc which, because of its open construction, does not require forced air cooling while on emergency power, thus conserving the emergency battery.

3.2.3 Digital Clock

The Digital Clock provides the required time of year display in terms of days, hours, minutes, and seconds (Figure 3-5). The unit receives a 1-pps signal from the Frequency Divider and continues the division process down to one pulse every hundred days. The display is mounted on the front panel and provision is made for manually setting the clock, which may by synchronized with standard time broadcasts or any other external reference. Output drivers also provide time-of-year (TOY) information in parallel form to the time code generator and for external signal distribution, through the AMP Series M connector.

The counters are wired in an 8-4-2-1 BCD counting mode to divide by 4, 6, 10, and 24. The following BCD outputs are thus generated:

- Units of Seconds (US)
- Tens of Seconds (TS)
- Units of Minutes (UM)
- Tens of Minutes (TM)
- Units of Hours (UH)
- Tens of Hours (TH)
- Units of Days (UD)
- Tens of Days (TD)
- Hundreds of Days (HD)

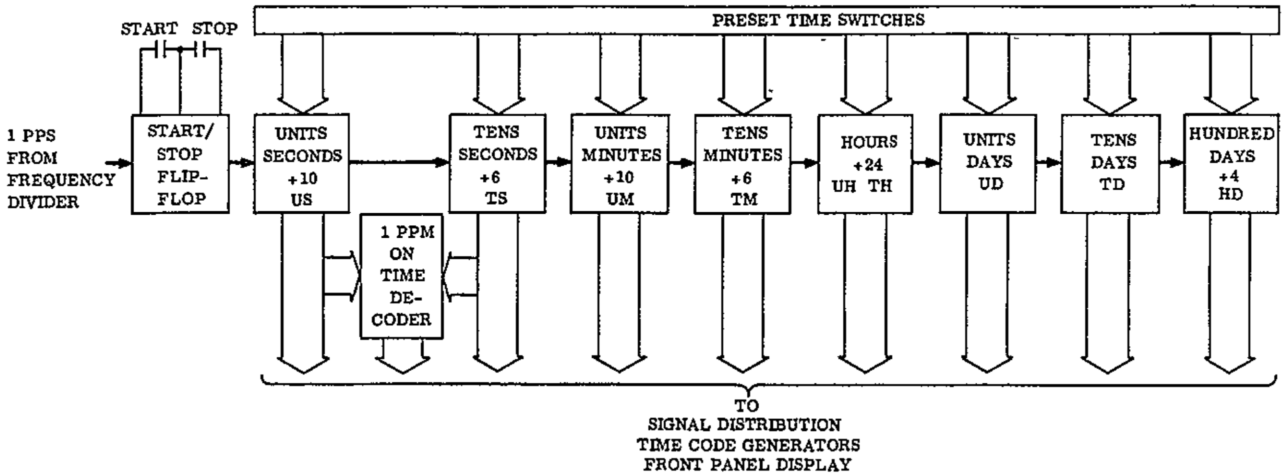

Figure 3-5. Digital Clock

The time-of-year display consists of Transistor Electronics Corporation indicators containing BCD-to-decimal converters. These indicators are not energized when operating on the emergency battery supply. Diode-isolated thumbwheel switches allow manual insertion of time-of-year into the display without first resetting the counters to zero.

The days counter is wired in a ÷24 mode such that when the units of days (UD) counter receives 24 counts, the UD and TD counters are automatically reset to zero, thereby recycling the days counter every 24 hours.

The outputs of the US and TS counters are decoded to yield a 1 ppm output one second wide and on-time. The 1 ppm signal is routed to signal distribution equipment to be provided as an output.

Manually-operated stop and start switches are provided at the input circuit for synchronizing the Digital Clock to an external 1-pps reference source. A display set switch inserts the selected TOY into the digital clock.

The Digital Clock is physically constructed from 3-C μ-Pacs. It can operate from the emergency power supply and the same cooling considerations apply as for the frequency divider.

3.2.4 Time Code Generator

The Time Code Generator accepts parallel time of year information from the Digital Clock and pulse rates from the Frequency Divider to generate the NASA Serial Decimal Time Code, the NASA 1/sec Binary Time Code, and the Apollo USB Serial Decimal Time Code.

The Time Code Generator consists of two separate subunits; the binary time code generator which generates the "1" train, "0" train, and SID strobe in addition to the binary time code, and the serial decimal time code generator which generates both the NASA and the Apollo serial decimal time codes. The three codes are generated in a dc level-shift form.

3.2.4.1 NASA 1/SECOND BINARY TIME CODE GENERATION. The 1/second binary time code generator including SID strobe, "0" train, and "1" train is shown in Figure 3-6.

The format of the NASA 1/second binary time code shown in Figure 3-7 is as follows:

Reference Marker -	Indicates the start of each one-second frame
Index Marker	Indicates the beginning of each digit in the frame
Coded Time of Year	Seconds, minutes, hours, and days; nine coded words in BCD
Control Functions	Identifies the station
Frame Time	1/second
Group Rate	10/second
Bit Rate	100/second

The SID strobe is a logic "0" signal from 908 to 948 msec after on-time and logic "1" for all other times. The "1" train is a 100-pps pulse train with 4 msec at logic "1" and 6 msec at logic "0"; the logic "1" to logic "0" transition occurs on-time. The "0" train is a 100-pps pulse train with 8 msec at logic "1" and 2 msec at logic "0" and the logic "1" to logic "0" transition on-time.

The true and complement outputs of the T-msec and H-msec counters in the frequency divider are decoded to decimal form. U-msec "8", U-msec "4", and U-msec "2" are brought in from the U-msec counter in the frequency divider and are used to generate the "1" train and the "0" train. The time-of-year information in BCD form is brought into the bit selection network from the Digital Clock.

The time-of-year information is strobed sequentially in the bit selection network by the decimal output of the H-msec decimal decoder. Time-of-year information is then assembled into proper form in the BTC assembler where the reference markers and index markers are added.

The SID strobe generator utilizes decimal "4" T-msec, "0" T-msec, "9" H-msec and binary U-msec "8" to generate the SID strobe in proper form.

3.2.4.2 SERIAL DECIMAL TIME CODE GENERATOR. The NASA serial decimal time code generator is shown in Figure 3-8.

The format for the NASA serial decimal time code shown in Figure 3-9 is as follows:

Frame Marker	Indicates the start of the 10-second time frame
Digit Marker	Indicates the start of each digit in the frame
Coded Time of Day	Five coded words in decimal indicating hours, minutes, and seconds
Frame Period	10 seconds
Group Rate	1/second
Bit Rate	10/second

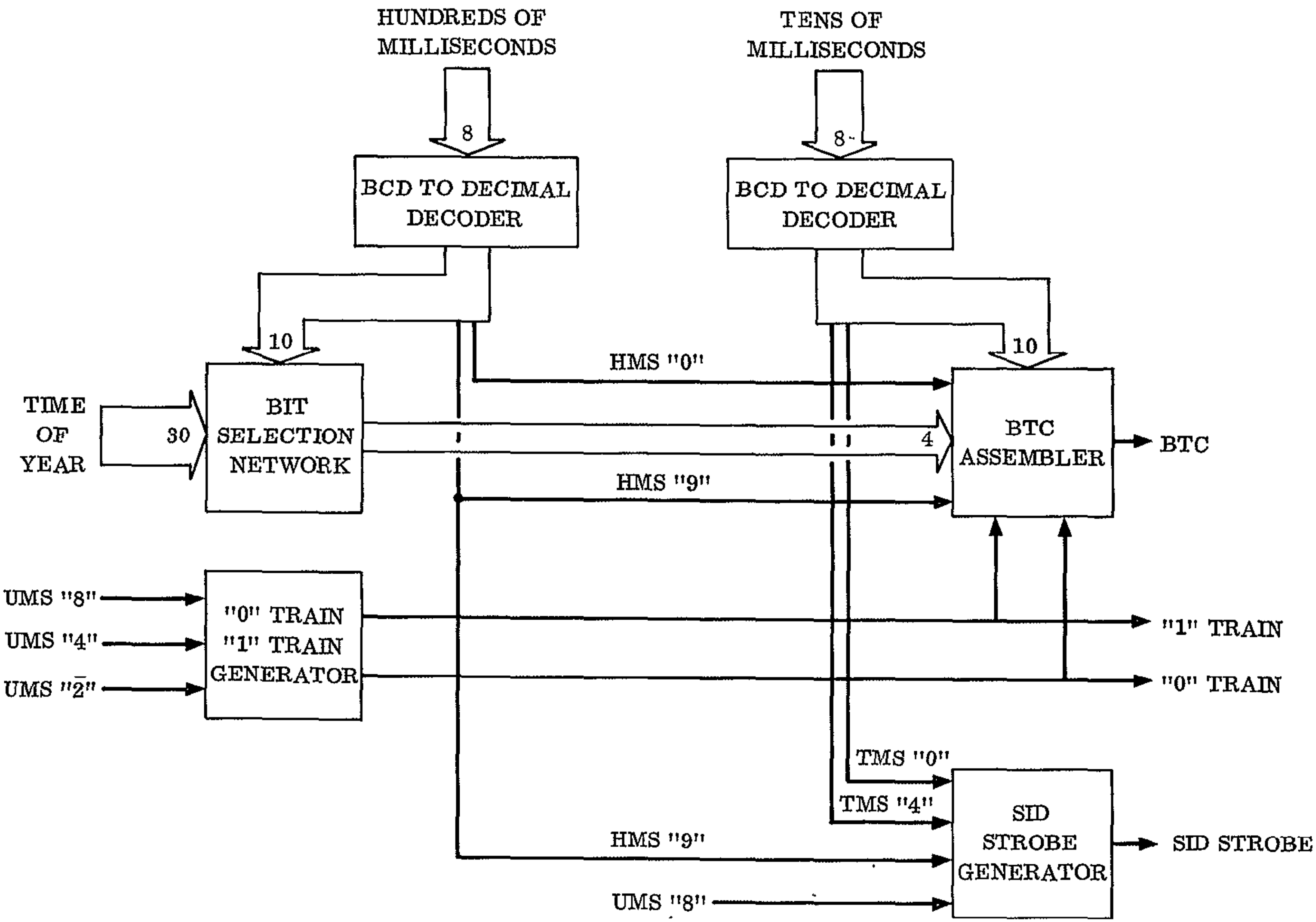

Figure 3-6. SID Strobe, "1" Train, "0" Train, and BTC Generators

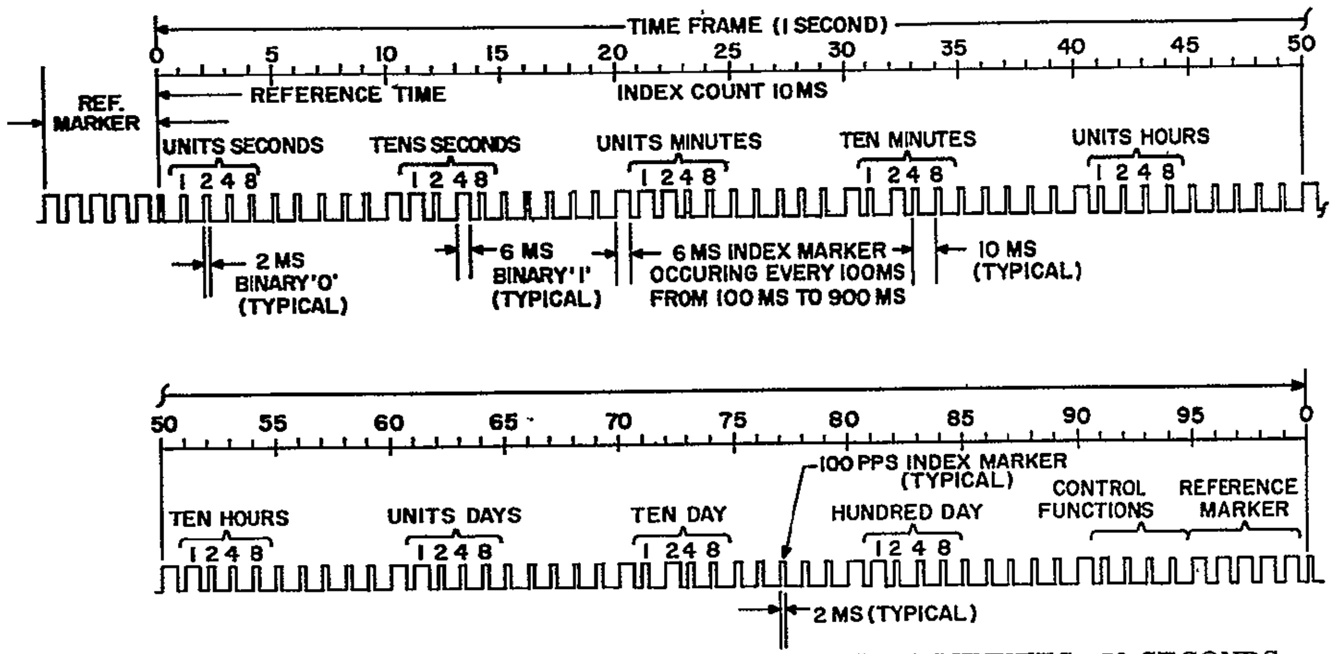

TIME AT REFERENCE MARKER IS: 121 DAYS, 10 HOURS, 23 MINUTES, 50 SECONDS.

Figure 3-7. NASA Binary Time Code Format

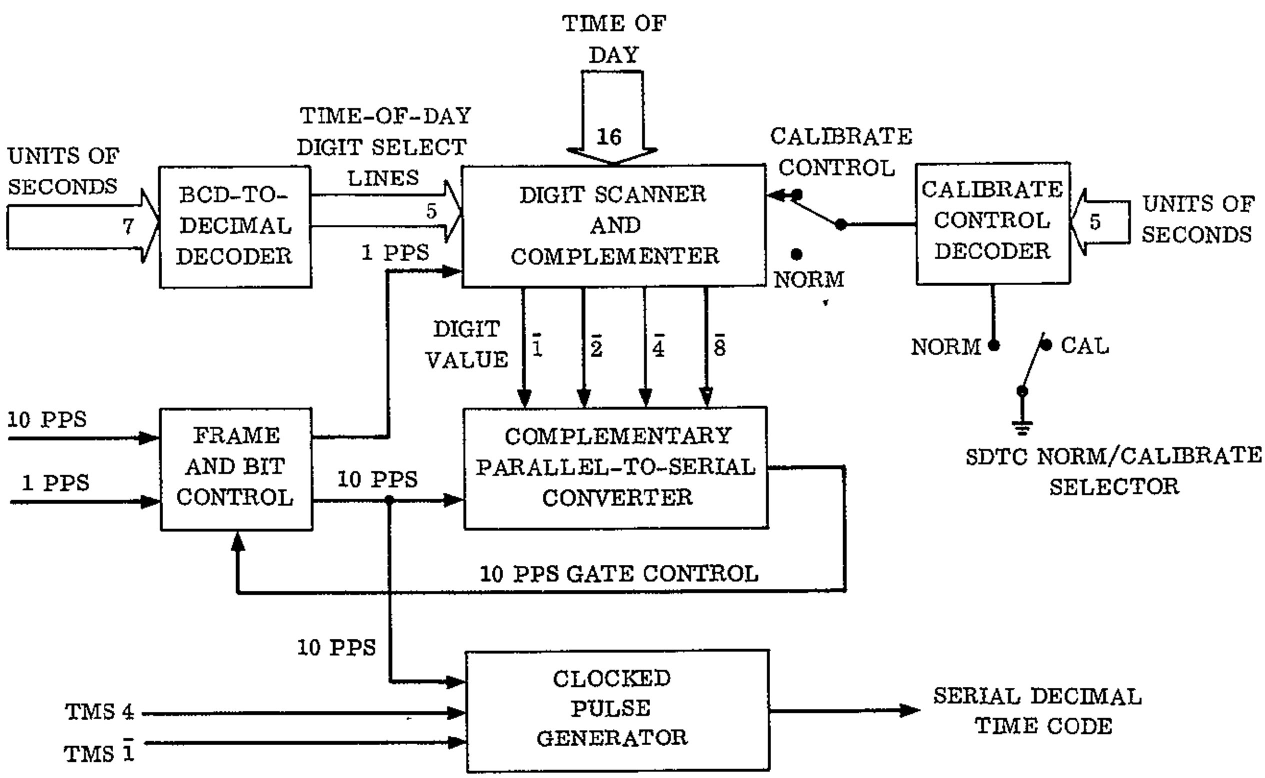

Figure 3-8. Serial Decimal Time Code Generator

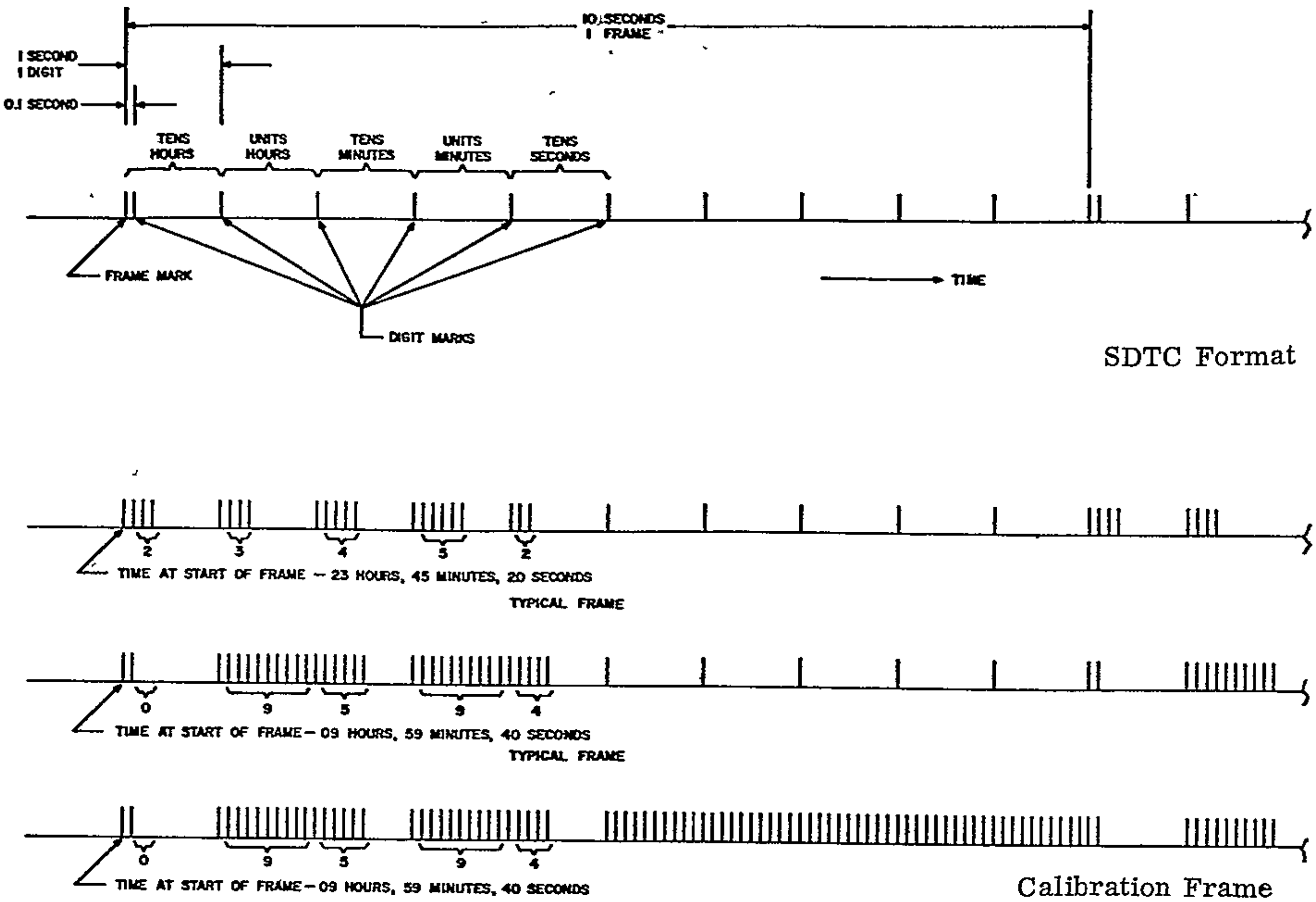

Figure 3-9. NASA Serial Decimal Time Code

Units-of-seconds from the Digital Clock are converted from 1-2-4-8 BCD to decimal 0-4. The time-of-year, from tens-of-seconds to tens-of-hours, is brought from the Digital Clock to the digit scanner and complementer. A set of gates in the digit scanner is enabled sequentially by the decimal converted units-of-seconds and pulsed at 1 pps with an output of the frame and bit control. This causes a ÷16 counter in the complementary parallel-to-serial converter to be set to the time complement once each second. For each 1 pps, the clocked pulse generator begins to output pulses at a 10-pps rate and the parallel-to-serial converter begins to output pulses at a 10-pps rate. When the ÷16 counter counts to 16, the frame and bit control 10-pps output is inhibited, thereby stopping the clocked pulse generator until the next 1-pps pulse occurs. The output of the clocked pulse generator is the NASA serial decimal time code.

3.2.4.3 APOLLO USB SERIAL DECIMAL TIME CODE GENERATOR. The Apollo USB serial decimal time code generator is shown in Figure 3-10.

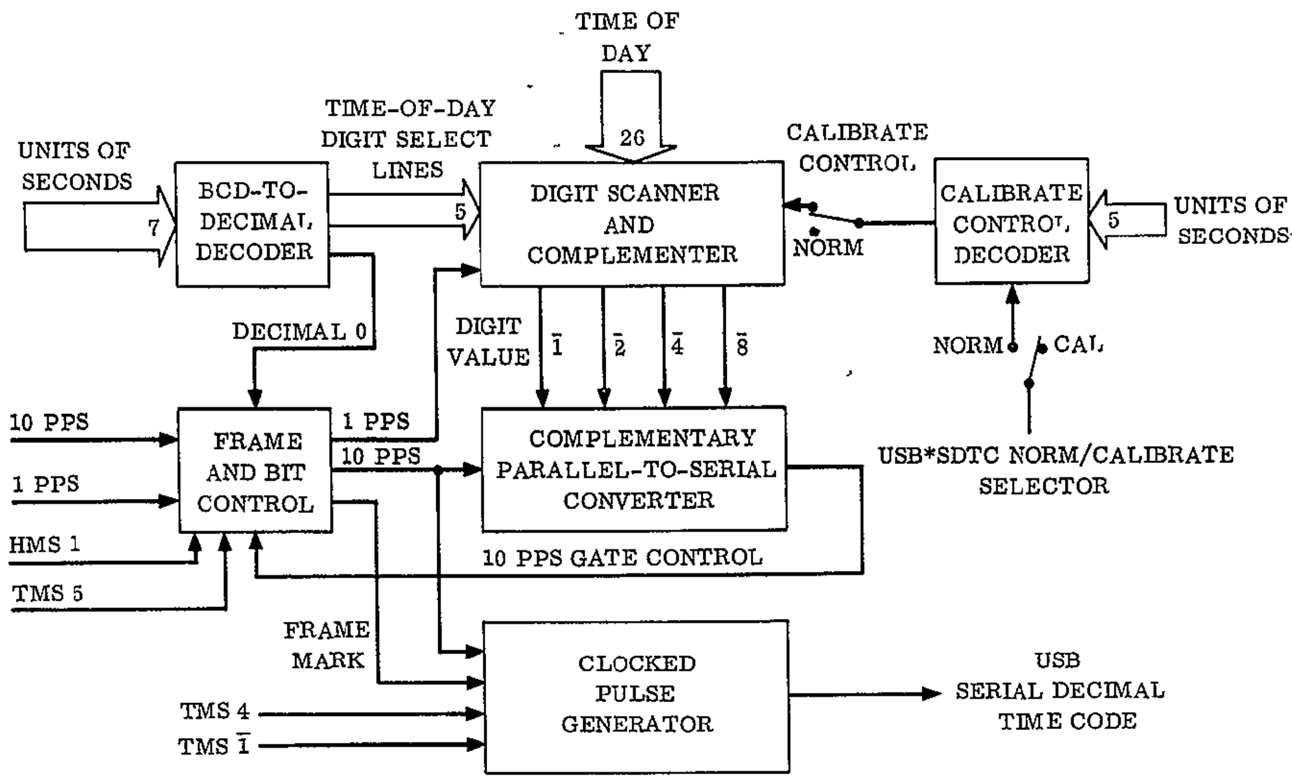

Figure 3-10. USB Serial Decimal Time Code Generator

The format for the Apollo USB serial decimal time code shown in Figure 3-11 is as follows:

Frame Marker	Indicates the start of the 10-second time frame
Digit Marker	Indicates the start of each digit in the frame
Coded Time of Day	Eight coded words in decimal indicating days, hours, minutes, seconds
Frame Period	10 seconds
Group Rate	1/second
Bit Rate	10/second

The Apollo USB serial decimal time code generator is identical to the NASA SDTC generator but with several additions. The units-of-seconds from the Digital Clock are converted to decimal 0-7 and the time-of-year from the Digital Clock includes days as well as hours, minutes and tens-of-seconds. The frame and bit control receives three additional inputs; decimal "0" from the units-of-seconds decimal decoder, hundreds of msec decimal "1" from the 1/second binary time code generator, and tens-of-msec binary 5 from the 1/second binary time code generator. The additional inputs are necessary to generate the frame mark.

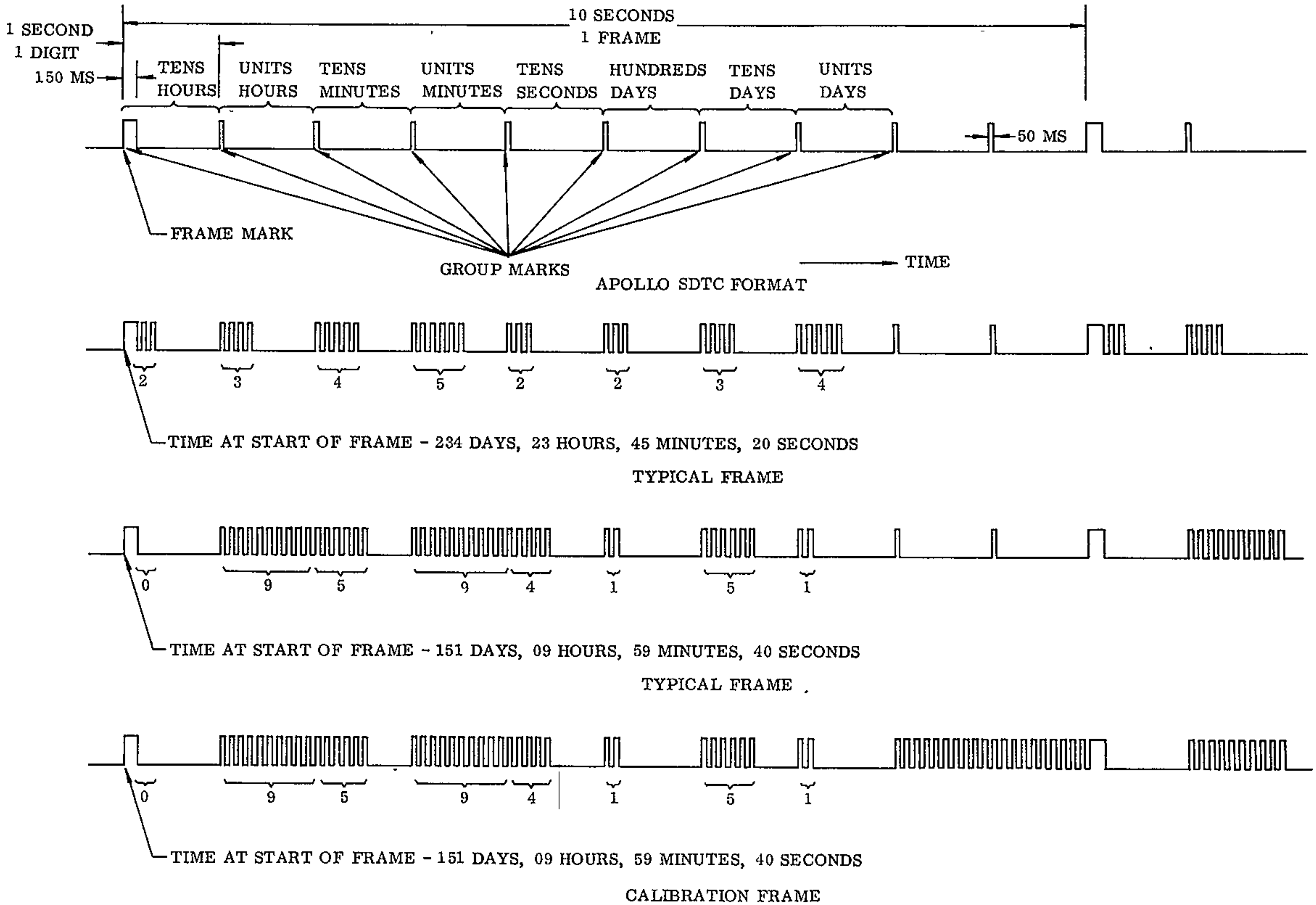

Figure 3-11. Apollo USB Serial Decimal Time Code

3.2.5 Signal Distribution Unit

The Signal Distribution Unit consists of a signal distribution chassis containing all electronics needed to provide timing signals for the system, and a signal distribution panel containing all signal output connectors.

The signal distribution chassis provides amplification for and isolation of each of the eighteen output signals listed. Each output signal is driven from an individual independent driver. Also, card space is provided for future expansion to four each of the eighteen output signals.

Two 1 MHz	Two parallel Time-of-Year
One 100 KHz	One 1/sec BTC level shift
One 50 KHz	One 1/sec BTC on a 1 KHz carrier
One 10 KHz	One 1/sec BTC on a 10 KHz carrier
One 1 KHz	One NASA Serial Decimal Time Code level shift
One 100 pps	One NASA SDTC on a 1 KHz carrier
One 1 ppm (on-time)	One NASA SDTC on a 10 KHz carrier
Two 60 Hz	One Apollo SDTC level shift
One 10 pps	One Apollo SDTC on a 1 KHz carrier
One 1 pps	One Apollo SDTC on a 10 KHz carrier
Two SID outputs	

The two SID outputs each consist of: tens-of-seconds 1, units-of-seconds 8, units-of-seconds 4, 4, units-of-seconds 2, units-of-seconds 1, "0" train, "1" train, 1/sec NASA BTC, 1K pps, and a SID strobe.

The outputs cited above have the following characteristics:

a. Pulse rates and level shift code outputs:
   Levels: 0 vdc (±0.5v) to -6 vdc (±0.5v)
   Load: 90 ohms
   Characteristic: positive-going edge "on time"

b. Sinewaves (except 60 Hz)
   Level: 1 vrms ±10%
   Load: 90 ohms
   Distortion: 1%

c. Parallel Time-of-Year
   Level: 0 vdc (20.5v) to -6 vdc (±0.5v) (negative logic)
   Load: 1K ohms

d. 60 Hz
   Level: 5 vrms ±10%
   Load: 10K ohms

e. SID Outputs:

Level: 0 vdc (±0.5v) to -6 vdc (±0.5v)

Load: 10K ohms

The sinewaves, pulse rates, and level shift codes are distributed through BNC connectors on the signal distribution panel. The parallel time-of-year outputs are provided on AMP 200277-4 connectors and the SID outputs are provided on AMP 201298-3 connectors. Mating connectors and pins are provided for the AMP connectors.

3.2.6 Time Comparison Unit

The Time Comparison Unit synchronizes the Timing Subsystem to WWV or to the existing station time. The Time Comparison Unit consists of a WWV Time Comparison Unit and a Station Time Synchronization Unit.

3.2.6.1 WWV TIME COMPARISON UNIT. The WWV Time Comparison Unit contains a WWV receiver, a WWV antenna, a propagation delay generator, a time comparison circuit, a time comparison oscilloscope, and a scope patch panel.

3.2.6.1.1 WWV Receiver and WWV Antenna. The existing WWV receiver will be retained at the Rosman and Carnarvon sites. These units, presently installed in location 3RE1, are Beckman Model 905-10 WWV receivers. At each site, the existing WWV receiver will be used with the existing antenna installations for timing signal reception.

3.2.6.1.2 Propagation Delay Generator. The propagation delay generator compensates for the propagation time of the standard time broadcasts by inserting a corresponding time compensation into the locally generated 1-pps signal from the Timing Subsystem. (See Figure 3-12.) The delay is adjustable to 1.0 sec in 10 μsec increments.

The T-μsec, H-μsec, U-msec, T-msec, and H-msec outputs of the delay divider are connected to a set of five digiswitches into which the desired delay is inserted. The outputs are brought to a coincidence comparator consisting of a 6-input AND gate. The 100K pps pulse is applied to the delay divider and strobes the comparator: the 1-pps standard pulse sets the flip-flop. When the counters in the frequency divider reach the state set into the digiswitches, the comparator generates a pulse which resets the flip-flop and the positive-going trailing edge corresponds to the preselected time delay. The pulse is routed to a delay multivibrator, which generates a pulse 1 msec wide. This pulse is the delayed 1 pps.

3.2.6.1.3 Time Comparison Circuit. The delayed 1-msec wide 1 pps from the propagation delay generator, and WWV audio from the WWV receiver are mixed in the time comparison circuit to produce a WWV signal with a 4-volt, 10-μsec wide spike superimposed. The 4-volt spike is produced from the negative-going edge of the 1-msec wide delayed 1 pps.

A delayed 1-pps scope trigger pulse is generated using the positive-going edge of the 1-msec wide delayed 1 pps. This trigger pulse will be 5 ±1 μsec in width and 18 volts in amplitude from a zero-volt base.

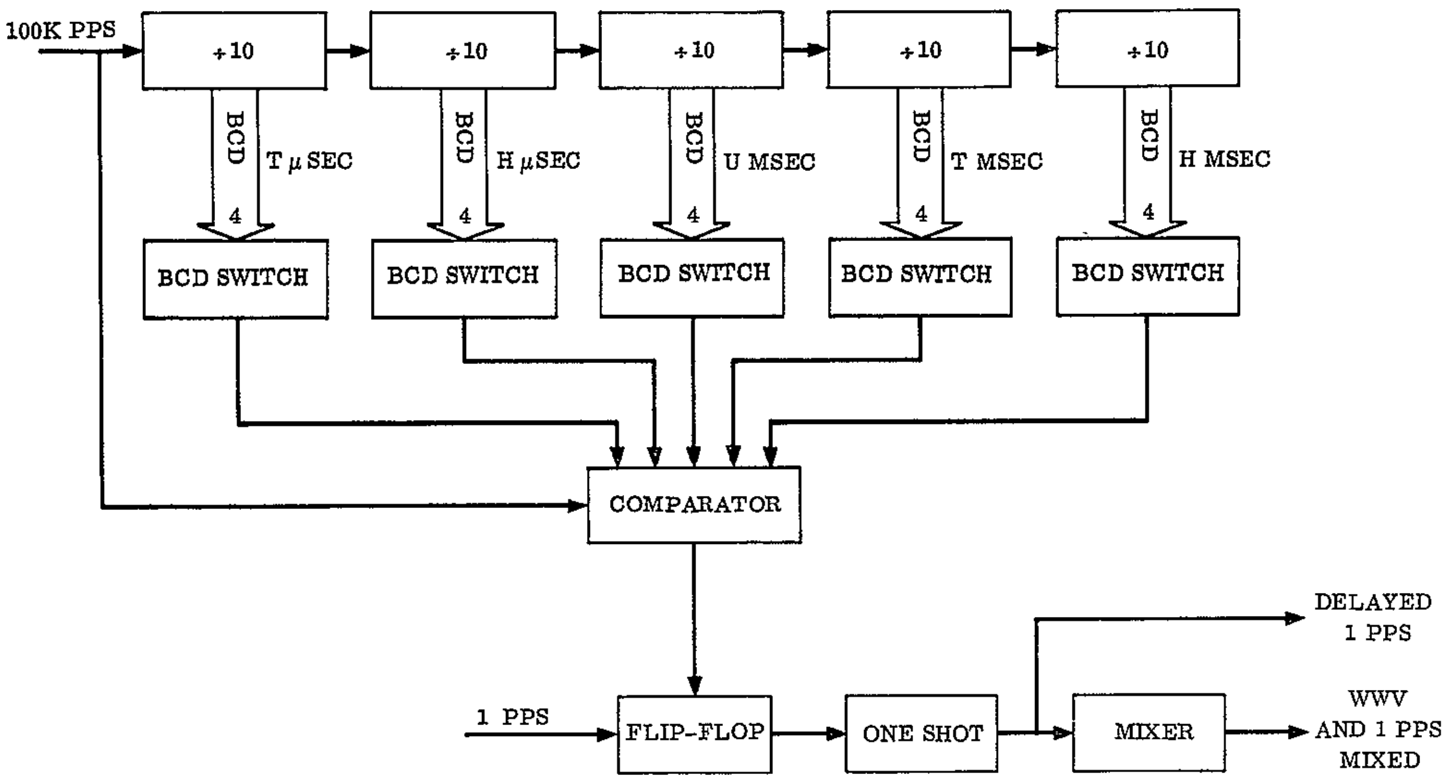

Figure 3-12. Propagation Delay Generator

3.2.6.1.4 Time Comparison Oscilloscope. The existing Time Comparison Oscilloscope will be retained at the Rosman and Carnarvon sites. HP Model 122AR oscilloscopes are presently installed in location 3A1.

3.2.6.1.5 Scope Patch Panel. The Scope Patch Panel is constructed using Trompeter type J3 panel jacks and Trompeter type PL-4 patch plugs. All scope inputs are available on this panel as well as the following signals:

- Delayed 1 pps signal
- Delayed 1 pps trigger
- WWV and time tick mixed
- NASA 1/sec BTC level shift
- NASA SDTC level shift
- Apollo SDTC level shift
- Normal 1 pps

3.2.6.2 STATION TIME SYNCHRONIZATION UNIT. The Station Time Synchronization Unit contains a Code Correlation Unit and a Digital Phase Comparator.

3.2.6.2.1 Code Correlation Unit. Code correlation circuitry is incorporated in the time code generator to check the phase and bit information from the station master code with the locally generated code. A bit-by-bit correlation is made between the two codes. If any difference is detected in corresponding bits of the code a front panel press-to-reset lamp comes on.

Phase comparison is accomplished by shaping the station code into 200-μsec pulses and shaping the local code into 0.5-μsec pulses that are delayed by 100 μsec. These signals are then fed to an inhibit gate which produces an output to set a flip-flop when the 0.5-μsec pulse falls outside the ±100 μsec limit. The flip-flop drives a front panel phase error indicator which must be manually reset.

3.2.6.2.2 Digital Phase Comparator. A digital phase comparator is used to determine the phase difference between the master oscillator and an existing station standard. Display of the phase difference versus time is provided by a chart recorder. The phase comparator tentatively chosen is a Frequency Electronics, Inc., Model FE-40A. It will utilize a 1 MHz signal derived from the external 5 MHz source as a reference, and a 1 MHz signal from the master oscillator.

The Emergency Power Supply (Figure 3-13) provides power for the Frequency Divider and Digital Clock in the event of malfunctioning of the primary power source. It consists of a series of nickel-cadmium batteries, a current limited charger with 0.1% voltage regulation, dc regulators, and monitoring meters.

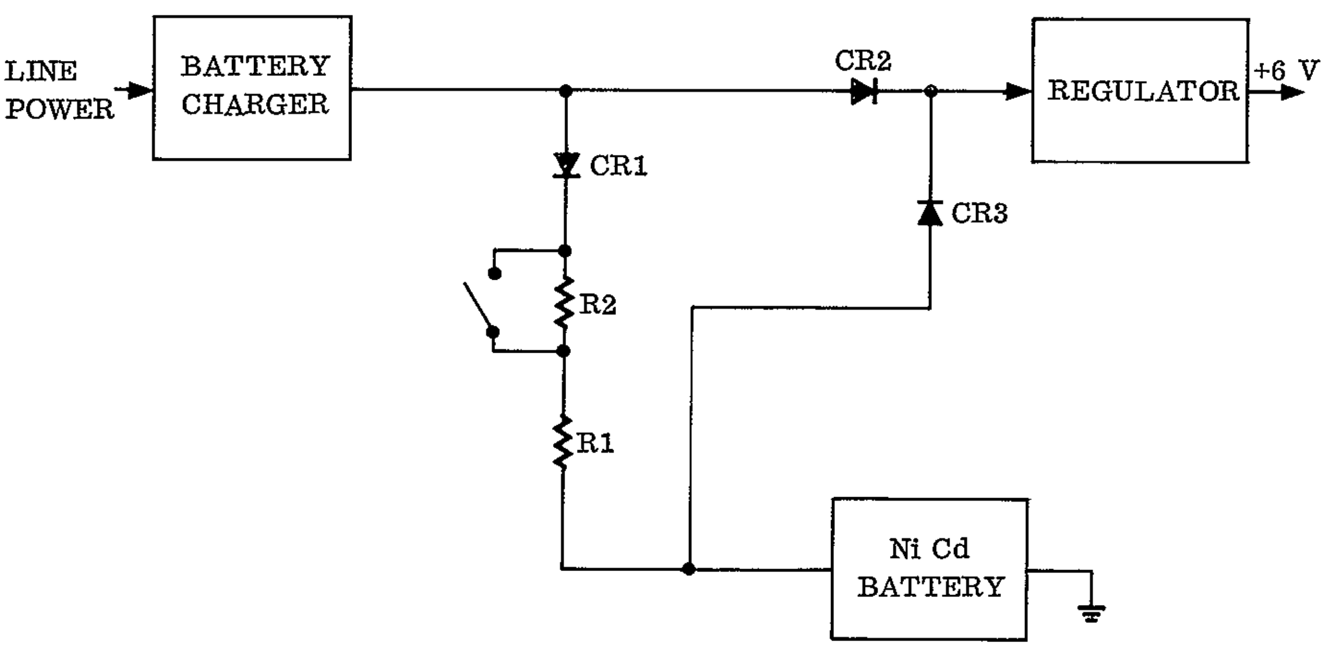

Figure 3-13. Emergency Power Supply

Primary power is converted to dc through the battery charger, which supplies power to the dc regulators for the +6 vdc outputs. The regulator is internally protected from overloads by a current-limiting circuit. During normal operation the charger furnishes a trickle charge and at the same time provides power to the regulators. In the event of an interruption of the line power, the battery (floating across the dc line) supplies the required power through diode CR3.

Diodes CR1 and CR2 prevent the charger from shorting the battery in the absence of ac power. Diodes CR2 and CR3 allow the highest voltage of either the charger or the battery to feed the power supplies.

Resistor R1 limits the battery charging rate to a safe value, and R2 is used to reduce the charge rate to extend the life of the battery.

3.2.7 Applicability

The Timing Subsystem described herein will be provided for the Rosman and Carnarvon sites. Existing Timing Subsystems will be employed at the Tananarive and Fairbanks sites.

3.3 SIGNAL GENERATION SUBSYSTEM

The Signal Generation Subsystem produces the specialized signals required for proper system operation. The subsystem consists of the following functional units:

a. Reference Pulse Generator

b. Ambiguity Resolving Code (ARC) Encoder

c. Range Tone Filter and Complementer

d. Zero-Set Phase Shifter and Sidetone Combiner

e. System Signal Source

3.3.1 Reference Pulse Generator

The Reference Pulse Generator coherently produces eight range tone frequencies and four reference pulse rates. The range tones are alternate in phase at the time of the reference pulses, and are used for ambiguity resolving in the range extraction unit. The reference pulses select the system data rate and provide system synchronization where required.

Tone and pulse frequencies are:

Range Tones	Reference Pulses
500 KHz	4 pps
100 KHz	2 pps
20 KHz	1 pps
4 KHz	6 ppm
800 Hz	
160 Hz	
32 Hz	
8 Hz	

3.3.1.1 COUNTDOWN CHAIN. Refer to Figure 3-14. A 5-MHz signal input to the Reference Pulse Generator is applied to the axis-crossing detector. The detector converts the sine wave signal to a square wave by amplification and diode-clipping. Input signal amplitude is limited by diodes to prevent overdriving the amplifier. The output waveform is shown in Figure 3-15.

The axis-crossing detector output is applied to a divide-by-five circuit providing a 1-MHz pulse of 400 nanosec duration. Figure 3-16 is a logic diagram showing the states of the three stages required to produce the output pulse.

The 1M pps output is applied to a non-inverting power amplifier. The 1M pps pulse train drives a divide-by-five circuit and a gated flip-flop, and is summed with successive divider outputs to eliminate propagation delay and minimize jitter. Jitter is maintained at less than 2 nanosec. The power amplifier drives the multiple inputs.

Referring to Figure 3-14, flip-flop A9 provides a 500 KHz square wave output. A5 divides by five to provide a 200K pps output with a 1-μsec pulse width. The 200K pps output of Q is summed with the 1M pps signal. The 200K pps, 1-μsec duration signal gates through one of five 1M-pps, 400-nanosec pulses. The output of the summing circuit is a 200K pps signal of 400-nanosec pulse duration containing the same time and jitter characteristics as the 1M-pps signal. This signal drives a flip-flop which provides a 100-KHz square wave output. A predetermined phase relationship with respect to the 500-KHz signal is maintained by the gate control inputs from the 500-KHz outputs. Figure 3-17 shows the timing relationship and logic involved in this function.

Generation of the 100-KHz through 32-Hz square wave range tones is accomplished in the same manner as the 500-KHz square wave. The 32-Hz square wave output is summed with the 64-pps and the 1M-pps signals to generate a 32-pps signal. This signal drives flip-flop (H) to produce a 16-Hz square wave. This 16-Hz square wave is summed with the 32-pps and the 1M pps signals, generating a 16-pps signal. This process of summing and dividing by two is continued for 4-Hz, 2-Hz, and 1-Hz square wave outputs. The 1-Hz square wave

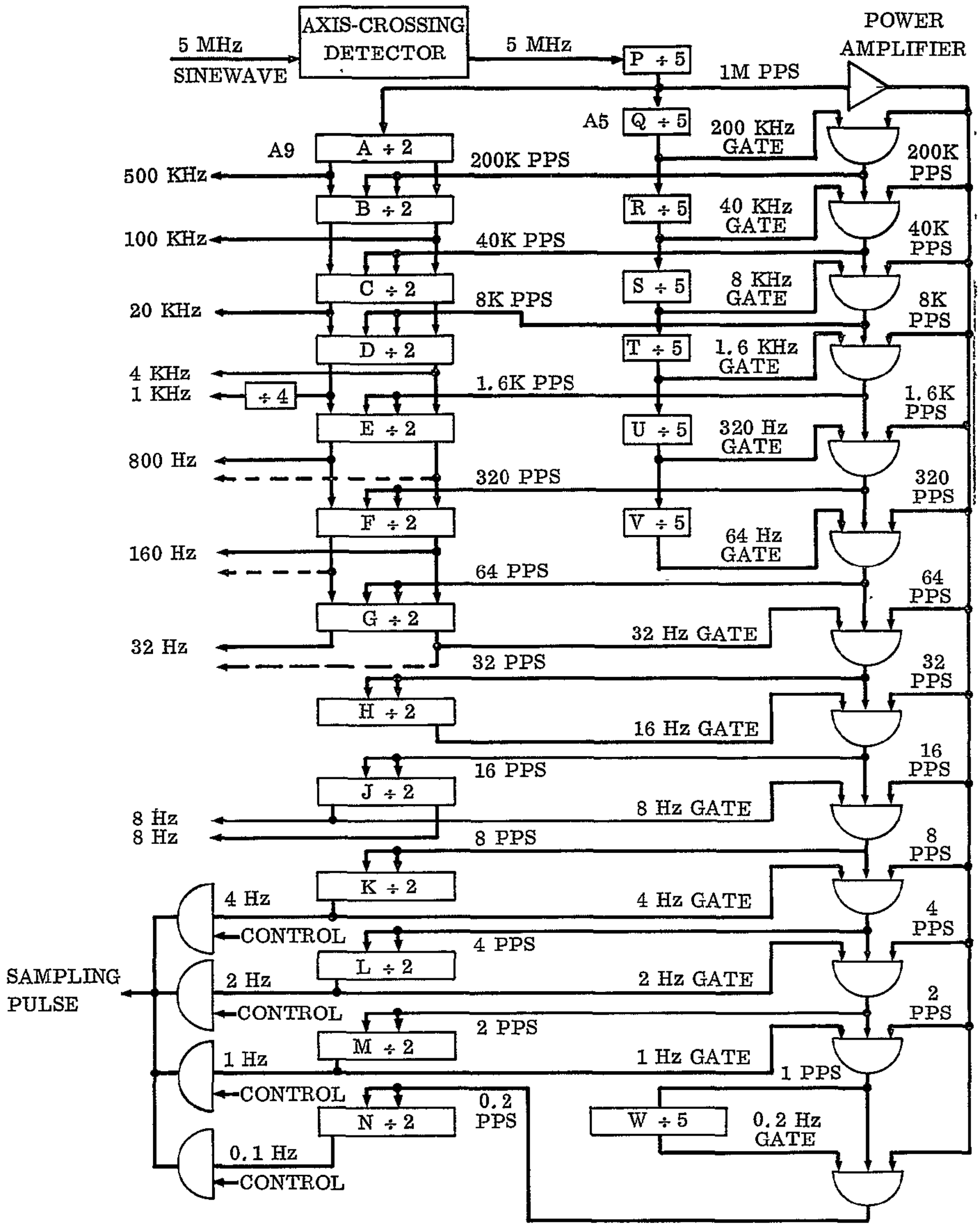

Figure 3-14. Logic Diagram of Countdown Chain

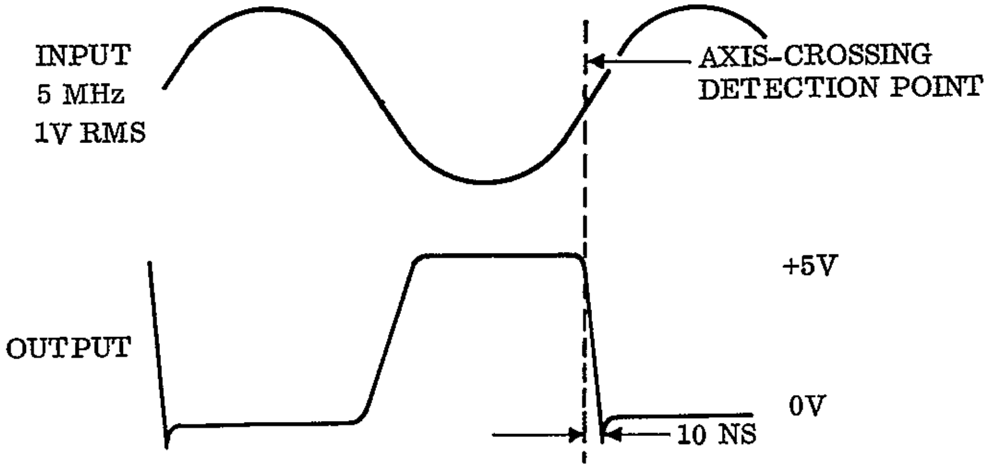

Figure 3-15. Axis-Crossing Detectors, Input and Output Signal Waveforms

output is summed to provide a 1-pps output which is then divided by five to provide a 0.2-Hz square wave. Summing provides a 0.2-pps signal which is divided by 2 to generate a 0.1-Hz square wave. All output square waves have the same jitter and time characteristics as the 1M pps signal. Therefore, all outputs occur simultaneously. Phase relationships between the output square waves and the reference sampling pulses at 4, 2, 1, and 0.1-pps are shown in Figure 3-17. The sampling pulses are square waves with the one-to-zero transition being the timing point.

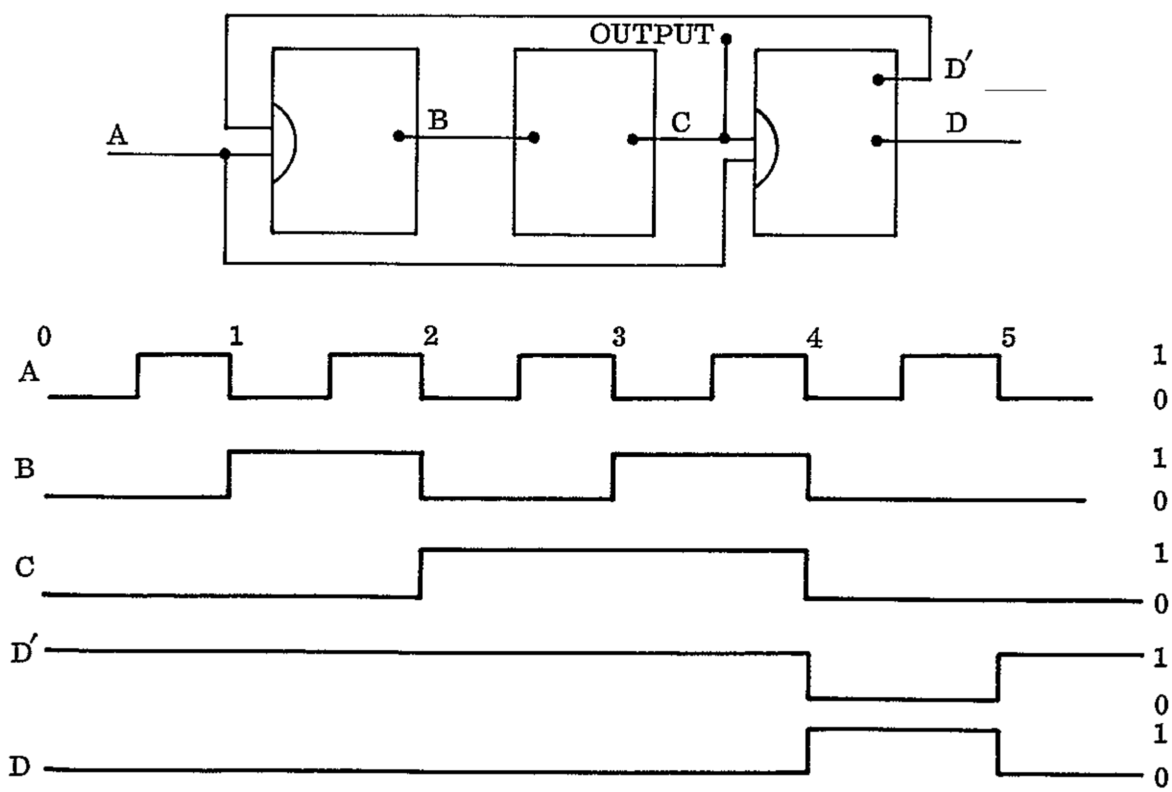

Figure 3-16. Divide-by-Five Circuit, Logic Diagram and Waveforms

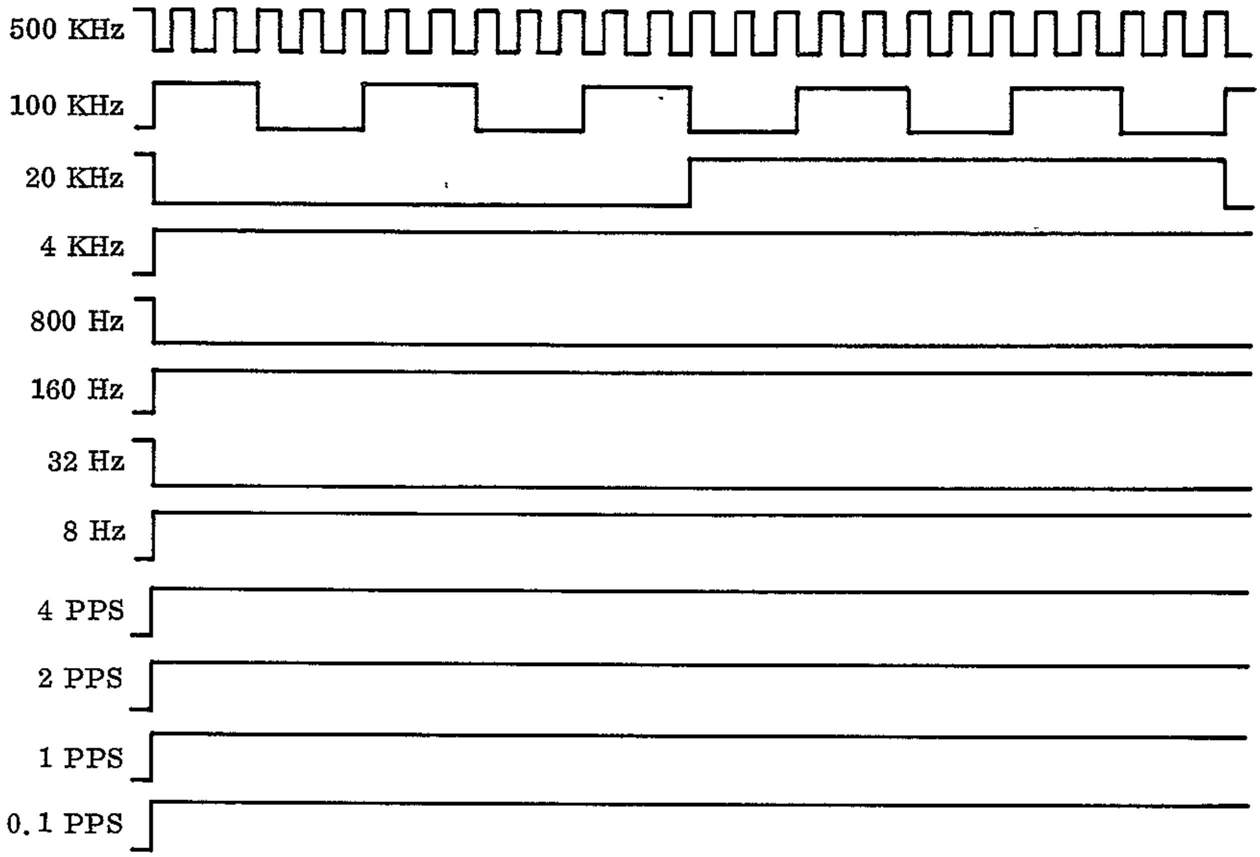

Figure 3-17. Phase Relationship of Output Signals

The 1-KHz square wave output is generated by dividing the 4-KHz square wave output by four. A definite phase relationship with respect to the sampling pulses is not maintained. The 1-KHz output is used as a clock reference in the Data Multiplexer.

Complementary outputs for the 800-Hz, 160-Hz, 32-Hz, and 8-Hz signals are generated by driving from the set and reset outputs of the gated flip-flop circuits. These complementary outputs are shown as dashed lines in Figure 3-14.

The output signals at 500-KHz through 8-Hz, are applied to transmission driver circuits. These circuits provide a 50-ohm output impedance to match the impedance of a 50-ohm coaxial cable. Additional outputs from these drivers are isolated through gate circuits. The sampling pulse signals are gated by a control NAND gate circuit. An external control signal must be applied to the control gate so that the selected sampling pulse signal is present at the output jack.

As shown in Figure 3-18, the outputs of gated flip-flop A are designated by the letters A and A′. These outputs gate the input to B and B′ of the following gated flip-flop. A one state must exist at the gate to allow the input signal C to trigger flip-flop B. Triggering is accomplished by the positive transition (trailing edge) of the signal pulse C. This point is coincident with the 1M pps positive transition and will occur prior to the gating signals A and A′ due to the circuit delay through the gated flip-flop A. Input signals at (E) at 1M pps and (C) at 200K pps are simultaneous.

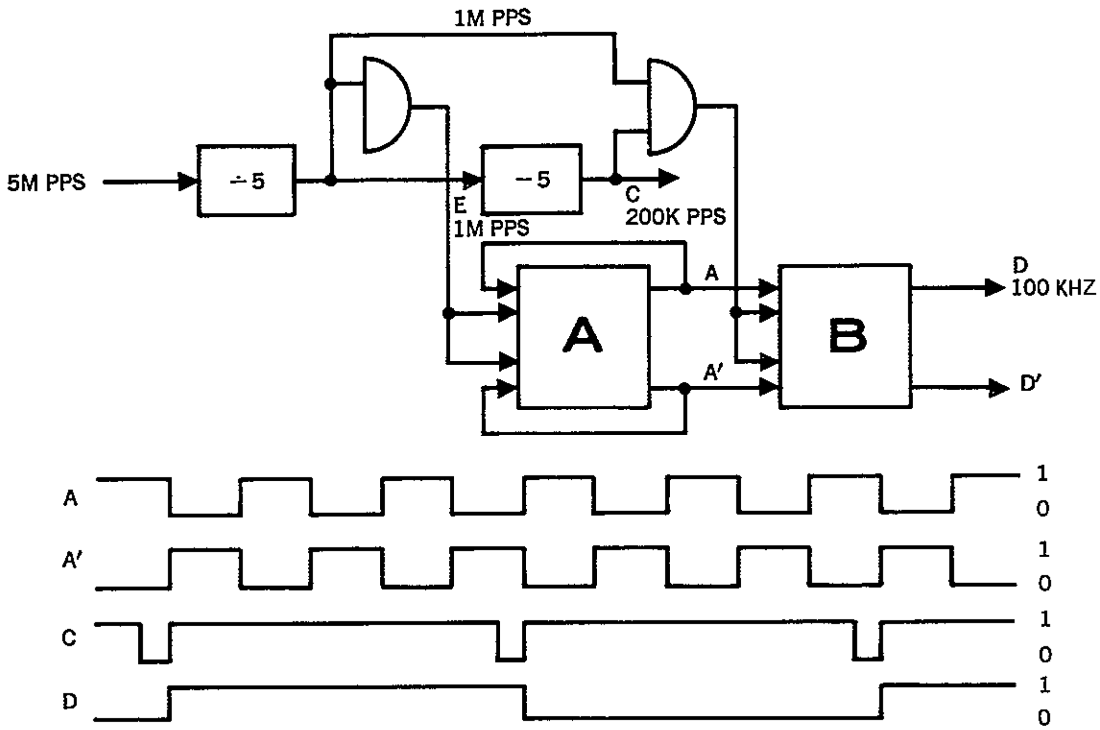

Figure 3-18. Basic Divider Components, Logic Diagram and Waveforms

Circuit delay through the gated flip-flop is 30 to 50 nanosec. Circuit delay through the AND gate is 15 to 20 nanosec. The output at point D is maintained in a definite phase relationship with respect to points A and A' by the gating function. The sidetone frequency at 500 KHz is taken from point A.

3.3.1.2 SYNCHRONIZATION CIRCUITS. The 1-pps and 0.1-pps sampling pulses are synchronized to the 1-pps and 0.1-pps outputs of the Digital Clock in the Timing Subsystem. The synchronization circuit is shown in Figure 3-19. The 1-pps point (C) of the Reference Pulse Generator drives a one-shot multivibrator which produces a 0.1-μsec positive pulse (D). The trailing edge (negative transition) triggers the gated flip-flop when gate signal (B) is in a positive state. The 1-pps input (A) from the Digital Clock is a 200-msec positive pulse. The trailing edge drives a one-shot multivibrator. This produces a 0.2-μsec negative pulse (B). These pulses are illustrated in Figure 3-20.

During a synchronous condition, the negative transition of the 0.1-μsec pulse occurs during the time the 0.2-μsec pulse exists. Therefore, flip-flop "A" is not triggered since the 0.2-μ sec pulse is at "0" volts and inhibits the negative transition triggering of the 0.1-μsec pulse as indicated in Figure 3-20; the synchronized condition exists over a maximum time of plus or minus 0.1 μsec.

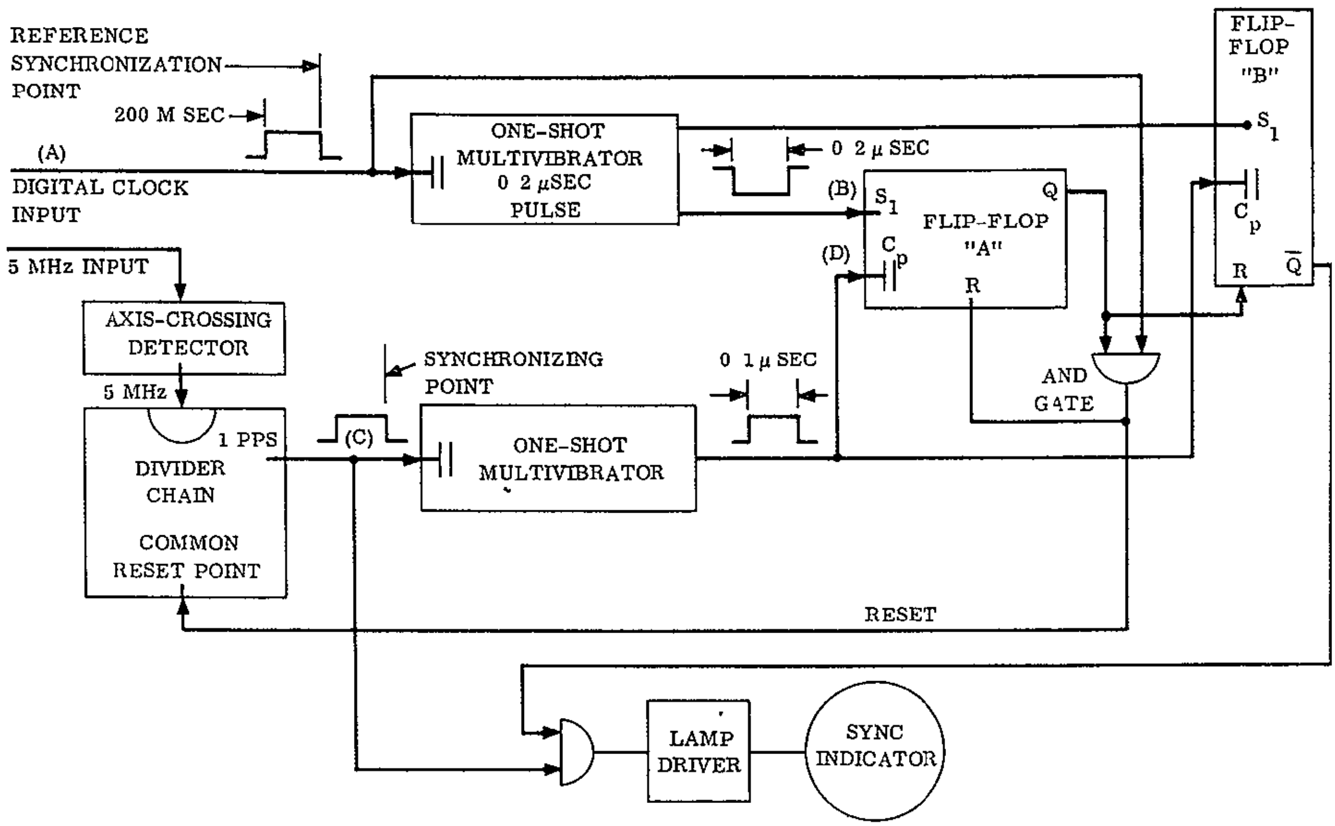

Figure 3-19. Synchronization Circuit, Logic Diagram

For a nonsynchronous condition, the trailing edge of the 0.1-μsec positive pulse will trigger flip-flops "A" and "B". The output is summed with the 1-pps input from the Digital Clock. for the 200-msec duration of the next 1-pps pulse from the Digital Clock, the Reference Pulse Generator divider is driven to a reset state by these combined signals. The trailing edge of this 200-msec pulse resets the gated flip-flop. The Reference Pulse Generator divider is allowed to count again at this time.

The trailing edge of the output of the first divide-by-five circuit occurs at 0.8 μsec after reset. This is the 1M pps signal. It should occur at 1-μsec after reset. To accomplish this, the divide-by-five circuit is reset with each stage in that state held after the fourth input signal. The third stage is reset to a set condition. The 1M pps signal now occurs at the required 1-μsec time interval. If the Reference Pulse Generator divider continues to count correctly, the 1-pps will occur one second after reset, indicating a synchronous condition.

During the synchronous condition, the 1-Hz square wave drives the front panel 1 PPS SYNC indicator. The indicator flashes at a 1-Hz rate.

When flip-flop "B" is triggered due to a nonsynchronous condition, the 1-Hz signal is inhibited by the output. The indicator lamp is then held in an on state. This condition continues until the Reference Pulse Generator divider is restarted in a synchronized state.

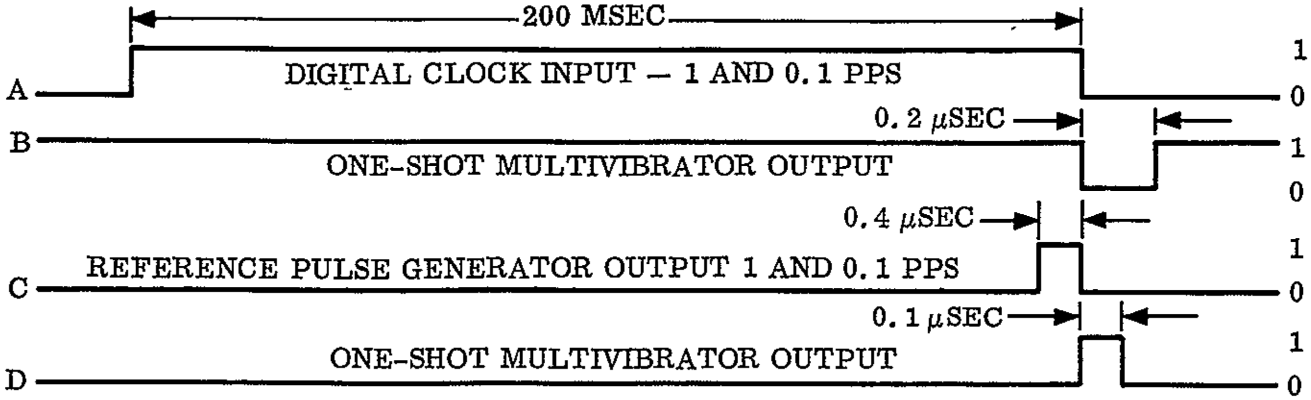

Figure 3-20. Synchronization Timing Diagram, Synchronous Condition

The 0.1-pps input pulse from the Digital Clock in the Timing Subsystem has the same characteristics as the 1-pps input. For a nonsynchronous condition, only the divide-by-five circuit, which divides the 1-pps signal to a 0.2-pps signal, is reset. The divide-by-two flip-flop, which divides the 0.2 pps to a 0.1-Hz square wave, is driven to a reset state at the signal input point. The 0.1 PPS SYNC indicator lamp on the front panel, which normally flashes at a 1-Hz rate, is held in an on state from the time the gated flip-flop is triggered until the next 0.1-pps input from the Digital Clock has occurred. The gated flip-flop is reset by the same technique used with the 1-pps synchronization circuit.

3.3.2 Ambiguity Resolving Code (ARC) Encoder

The ARC Encoder generates a pseudo-random code from a seven- and eight-bit maximal length shift register sequence for resolving ambiguities in the 8-Hz range tone. The encoder bi-phase modulates this pseudo-random code on the 4-KHz sidetone. A functional block diagram depicting these operations is given in Figure 3-21.

The 4-KHz sidetone from the Zeroset Phase Shifter and Sidetone Combiner is detected at its axis crossings and used as clock for the seven- and eight-stage shift registers and the decoder during test functions. The outputs of the shift registers are supplied to an exclusive OR circuit to produce the 32,385-bit pseudo-random code. Each of the shift registers is self-starting and fully clocked to satisfy stability and jitter requirements. They are also supplied with zero check and automatic reset circuits to remove all-zero conditions in the registers. Each stage of the registers supplies state signals to the ARC decoder.

The implementation of pseudo-random binary sequences in the form of binary waveforms which represent sequences requires specific characteristics of the binary ones and zeros in order to obtain equivalent operations between the Boolean modulo 2 addition and algebraic multiplication. The waveform used to represent a sequence is constructed by assigning a period of time, called a digit period, to each digit in the sequence and causing the waveform to be plus one (+1) when the corresponding digit is zero and minus one (-1) when the corresponding digit is one.

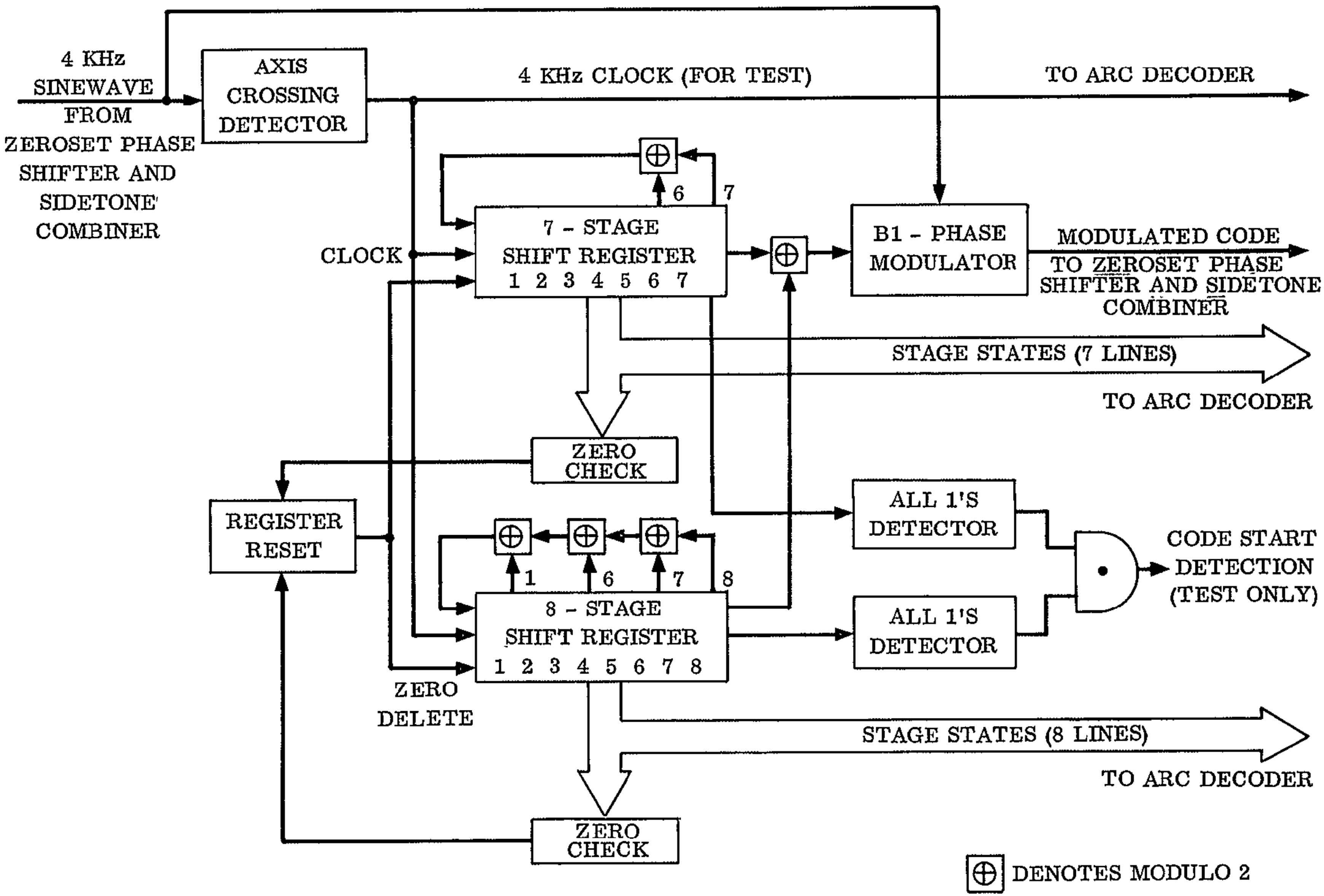

Figure 3-21. ARC Encoder Functional Block Diagram

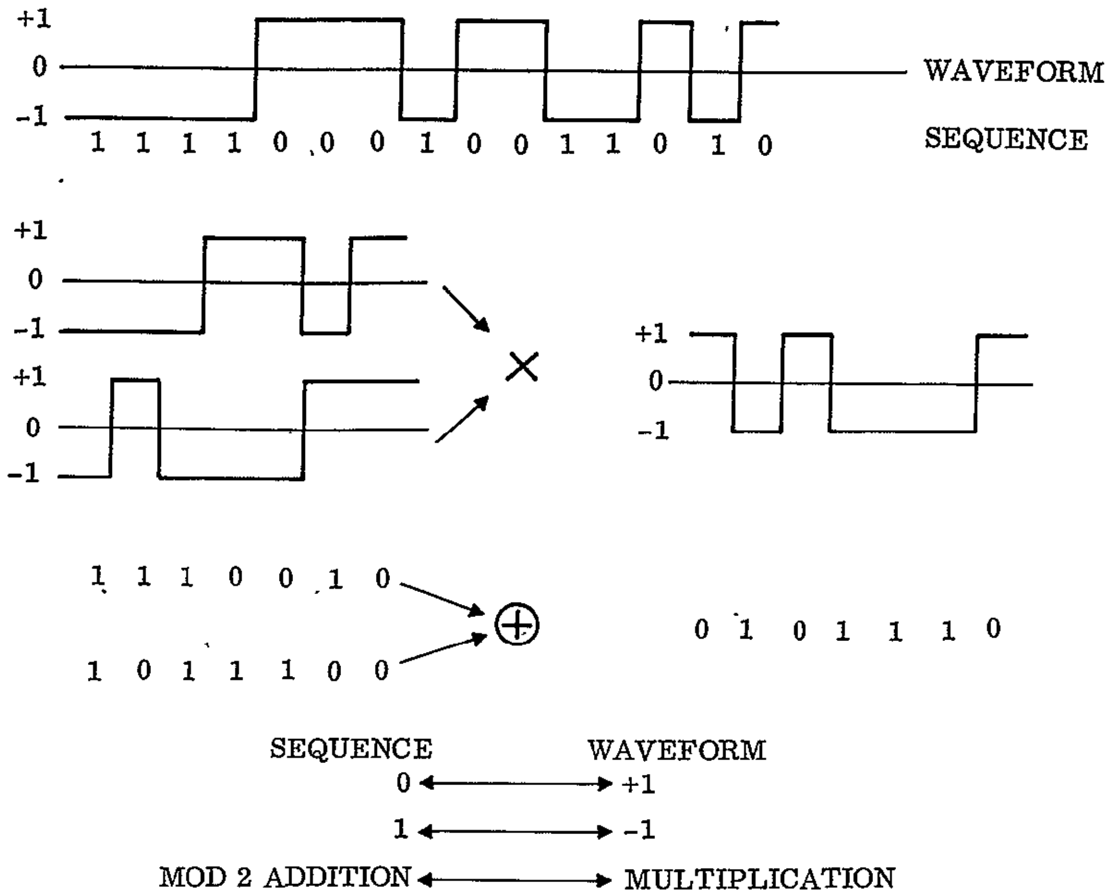

Figure 3-22. Waveforms and Sequences

Figure 3-22 illustrates the correspondence between digital sequences and digital waveforms. The code generation logic of the encoder is implemented to conserve this correspondence.

The 32,385-bit code is supplied to the bi-phase modulator for modulation of the 4-KHz sidetone. A generalized design of the bi-phase modulator and corresponding waveforms is shown in Figure 3-23. The object is to bi-phase modulate a 4-KHz sinusoidal carrier with a pseudo-random code, a code ONE representing a zero phase shift and a code ZERO representing a 180-degree phase shift. Basically, a 4-KHz sinewave is applied to a phase-splitter so that an "in-phase" or "out-of-phase" signal is available. The desired phase output is selected by a switching circuit operated by the pseudo-random code. When the code is ONE, the "in-phase" signal is switched to the load and when the code is ZERO, the "out-of-phase" signal is connected to the load. The resulting output is the desired bi-phase modulated sinewave which in turn is summed in the Zeroset Phase Shifter and Sidetone Combiner for modulation on the carrier.

The ARC encoder and decoder will be packaged in the same chassis to facilitate construction. The design will be implemented using standard integrated circuit logic cards.

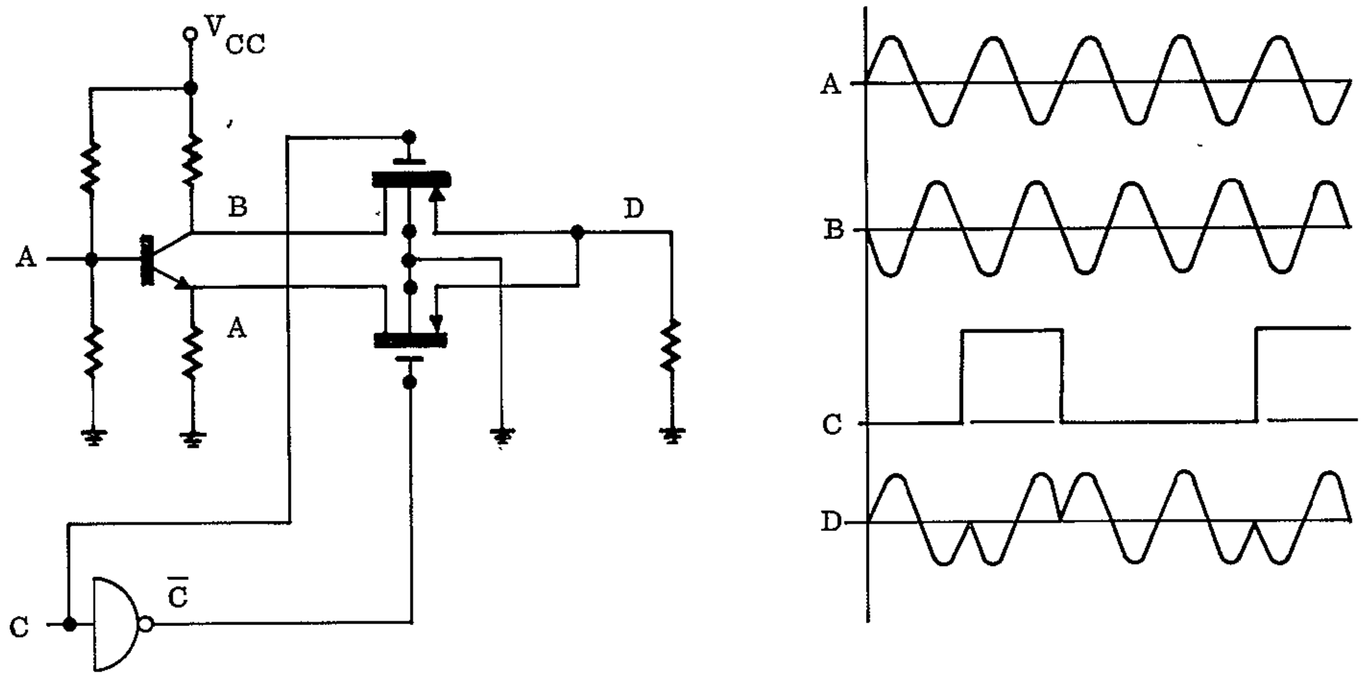

Figure 3-23. Design Concept for Bi-Phase Modulated Sinewave

3.3.3 Range Tone Filter and Complementer

This unit accepts the major range tones from the Reference Pulse Generator in the form of square waves and filters them to produce sinusoidal signals. See Figure 3-24. The major range tones are then supplied to the Data Subsystem for start pulse generation and to electromechanical phase shifters to zero-set the ranging system. The unit also provides for side tone complementing of the four minor range tones on the 4-KHz signal. These lower tones are also sent to the phase shifter for zero setting.

3.3.3.1 MAJOR RANGE TONE FILTERING. The major range tones at 500 KHz, 100 KHz and 20 KHz and the complementing range tone at 4 KHz are filtered to shape the input square waves and reduce the harmonic content to less than 1 percent for all sinewave outputs; phase stability is secondary since the reference for the start pulse generator is derived after the filter. Sufficient phase stability will be maintained, however, to prevent interference with ambiguity resolution because of misalignment of axis crossing between range tones. The most critical harmonic is the fifth. An anti-resonant circuit tuned to the fifth harmonic is used in conjunction with a single-tuned series-resonant circuit at the desired tone frequency to provide the required combination of rejection and phase stability.

As shown in Figure 3-24, the filters for the three highest range tones have outputs to the Data Subsystem in addition to their outputs to the zeroset phase shifter. These signals are used for start pulse generation.

3.3.3.2 MINOR RANGE TONE FILTERING. The minor range tones at 800 Hz, 160 Hz, 32 Hz, and 8 Hz are complemented on the high side of the 4-KHz tone using a balanced modulator arrangement. The 4-KHz signal for complementing is taken from the zeroset phase shifter so that the 4-KHz signal is zeroset prior to the modulation. In each case,

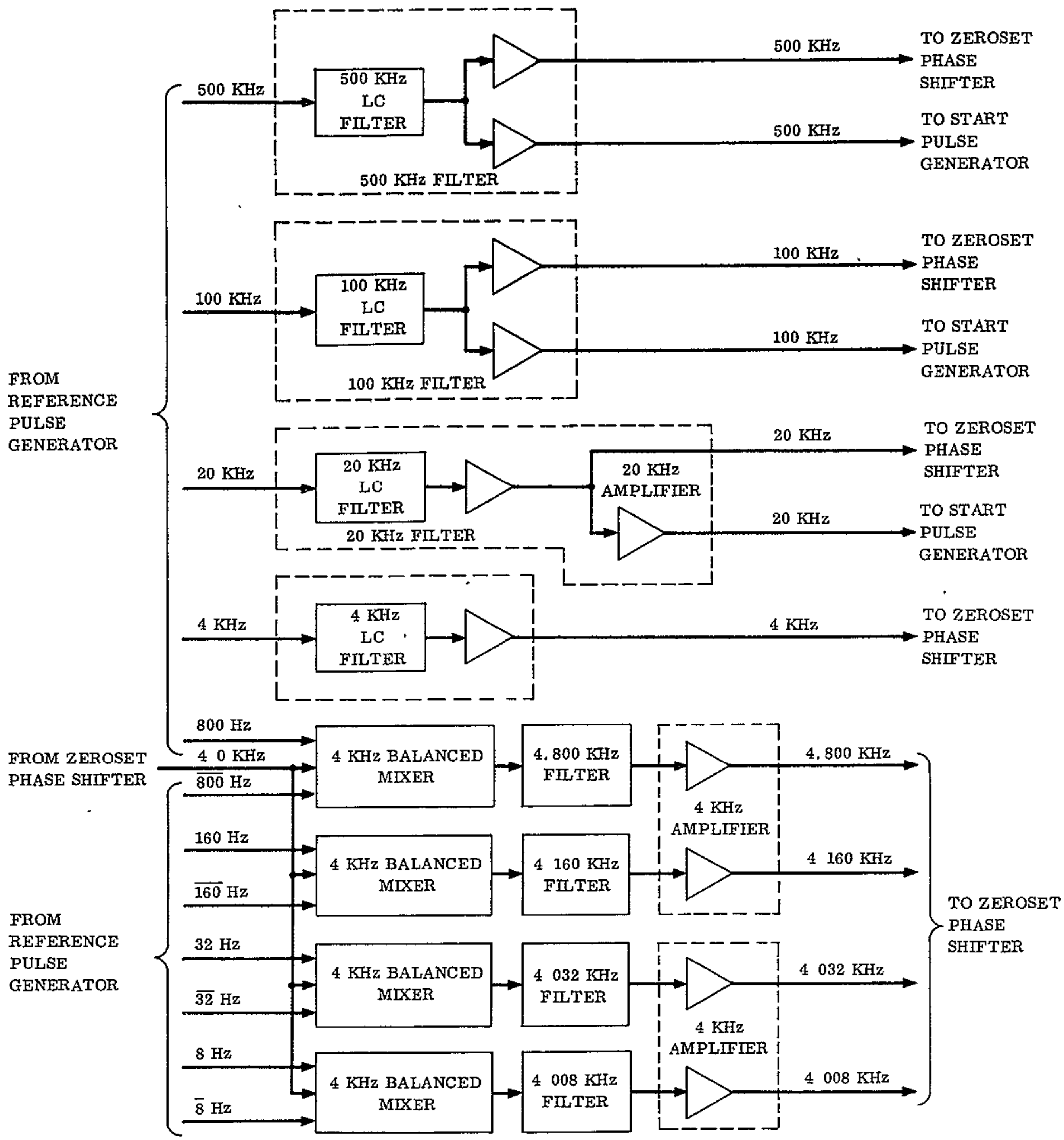

Figure 3-24. Range Tone Filter and Complementer Simplified Block Diagram

two square waves from the Reference Pulse Generator, phased 180 degrees apart, provide the proper phase relationships for the balanced modulator. The resulting complemented tone frequencies are 4.8, 4.16, 4.032 and 4.008 KHz.

Single-element crystal filters reject the undesired modulator products. The most critical filter is the 4.008 KHz filter because of the small frequency separation between the complementing input and the desired output. A single-element crystal filter with a Q of 10,000 surpresses the undesired 3.992-KHz output.

A proportional oven maintaining temperatures to within ±1° C is used for each crystal filter to maintain phase stability.

3.3.4 Zero-Set Phase Shifter and Sidetone Combiner

The Zero-Set Phase Shifter and Sidetone Combiner accepts ranging signals from the Range Tone Filter and the ARC Encoder and provides a means for adjusting the phase and amplitude of each tone. It then combines the selected tones into a composite signal suitable for driving the modulator. Figure 3-25 is a block diagram of this unit.

The major range tones and complemented minor range tones are amplified to drive zero-set electromechanical phase shifters. The phase shifters are interconnected by gearing commensurate with range tone frequency ratios to provide for overall zero-set and to compensate for the effective time delay variation between range tones.

The phase shifter in the 500-KHz channel is a carbon film sine-cosine type potentiometer with a conformity tolerance (departure from a sine wave) of less than 0.15 percent. A quadrature network between the two output arms of the potentiometer produces a continuous 360-degree phase shift. The greatest error will occur when one output is zero and the other output maximum. The conformity error (0.15 percent) is then $\tan^{-1} 0.0015$ radian or 0.085 degrees. Potentiometer accuracy is superior to that for an electrostatic type phase shifter and the attenuation is less than 10 db as compared to 30 db for the electrostatic type. Since a temperature change causes all segments of the potentiometer to change at the same rate, second-order effects are negligible. The quadrature network instability is less than 0.05 percent for a 1° C change. The wideband amplifiers incorporate negative feedback to reduce phase shift to a negligible level. A total phase error of less than 0.18 degrees is maintained for the 500-KHz channel.

The design of the lower-frequency range tone channels is similar to that for the 500-KHz channel, except that resolvers are used as the phase-shifting devices. The quadrature networks to obtain continuous phase shift on the outputs of the resolvers are the same as that for the sine-cosine potentiometer used in the 500-KHz channel.

Both manual and motor slew controls are provided for the resolver chain. Each phase shifter is mounted so that the body can be adjusted over a full 360 degrees. The manual adjustment is calibrated in 1-degree increments. Individual adjustments for the 500-KHz, 100-KHz and 20-KHz phase shifters are readable and accurate to better than 1 degree and the minor tones have readable and accurate adjustments to better than 3.6 degrees. The train braking capability prevents accidental movement of the phase shifters after final adjustment.

Each zero-set phase shifter has sufficient range of output adjustment to allow the modulation index of the tones to be varied from 0 to 1.5 radians peak. The zero-set phase shifter supplies 4-KHz to the ARC Encoder and the Range Tone Filter and Complementer.

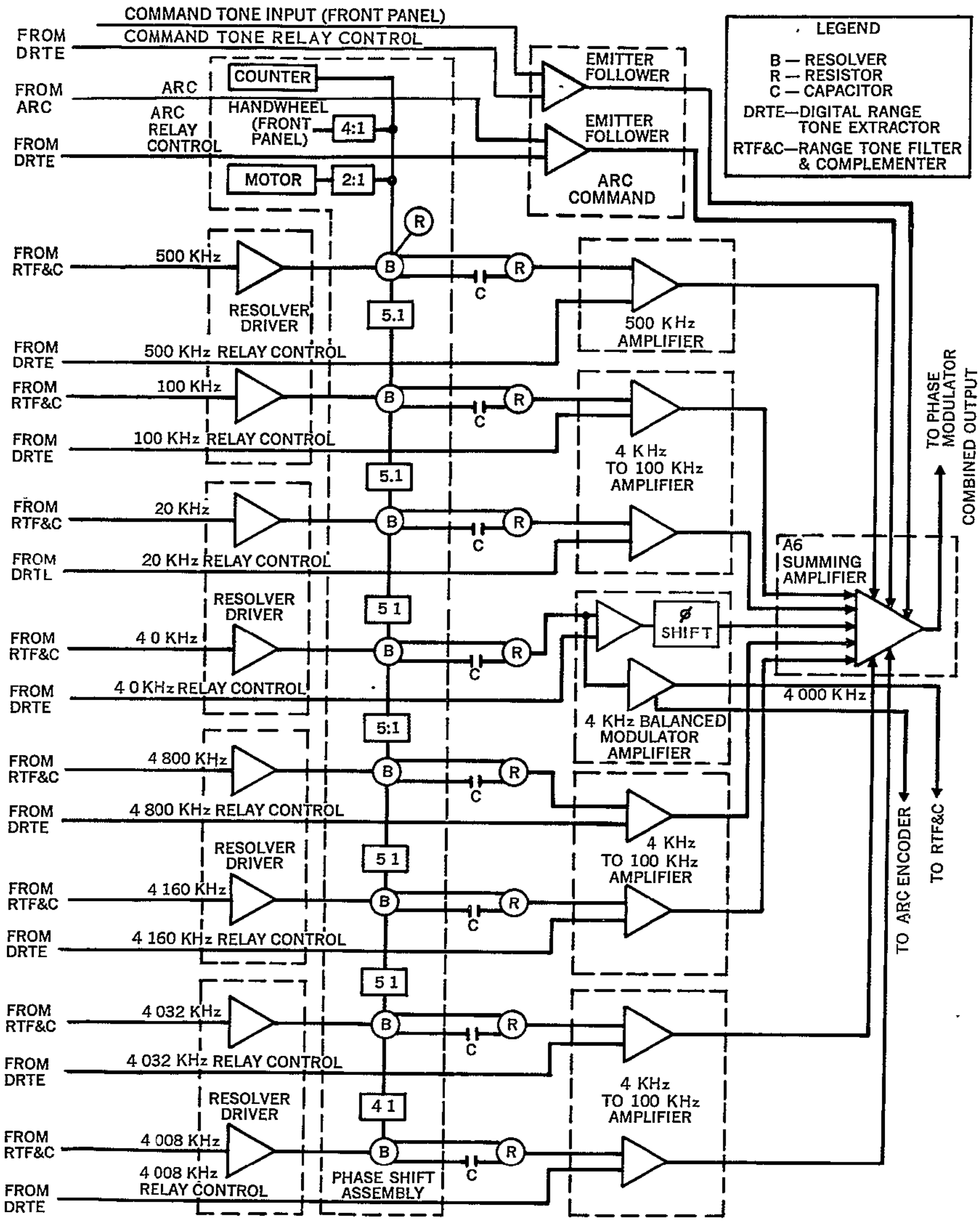

Figure 3-25. Zeroset Phase Shifter, Functional Block Diagram

The sidetone combiner linearly combines the specified transmitted tones or codes and provides a composite signal to the phase modulator of the carrier. The composite output is adjustable such that the baseband modulation index has a range of 0 to 3.0 radians peak. This output may be monitored at an isolated test point on the front panel.

Sidetone and code application is controlled by signals from the Digital Range Tone Extractor (DRTE). These signals control the input to the side tone combiner summing amplifier by means of relays in the input circuits of the individual range tone amplifiers.

The ambiguity resolving code amplifier, the command tone amplifier, and the 500 KHz, 800 Hz, 160 Hz, 32 Hz, and 8 Hz tone amplifiers have one relay in their input circuits. This relay allows these tones to be turned on and off by the DRTE. Modulation indices are adjustable from 0 to 1.5 by a potentiometer in the input circuit of each amplifier. The amplifiers for tones at 100 KHz, 20 KHz and 4 KHz have two relays, allowing each tone to be either turned off or added to the summing amplifier with one of two different modulation indices adjustable from 0 to 1.5 radians peak. Toggle switches in the relay control lines will allow the operator to manually over-ride the control signals. Manual controls will also be supplied on the composite signal and the AR code amplifier. These controls will not be on the front panel. A panel jack will allow insertion of a command tone in the uplink spectrum.

The range tone test function described in section 3.10 will be packaged within the zero-set phase shifter chassis.

3.3.5 System Signal Source

The system signal source is comprised of three functional units: (1) reference synthesizers, (2) a transmitter signal source and (3) a receiver signal source. Together these units provide all reference and local oscillator frequencies for the receiver as well as carrier frequencies for the VHF and S-Band transmitters. The system signal source also contains the phase modulators in which the composite ranging tones from the sidetone combiner are modulated upon the carrier frequencies. This unit also provides coherent frequency samples of the carrier frequencies for use by the doppler extractor. A block diagram is shown in Figure 3-26.

3.3.5.1 SYNTHESIZERS. The Hewlett Packard 5110B synthesizer driver supplies the 22 fixed reference frequencies required by each of the three HP5105A synthesizers and, in addition provides six reference frequencies to the receiver signal source. All output frequencies are coherently derived from either an internal 1 MHz reference oscillator or from an external 1 MHz or 5 MHz source. The three HP5105A synthesizers are used as indicated in the following discussion.

3.3.5.2 S-BAND TRANSMITTER SIGNAL SOURCE. The method of generating the S-Band and VHF transmitted signals and coherent reference signals is similar to that used in the Multiband Transmitter built under Contract NAS5-10508. A block diagram is shown in Figure 3-27.

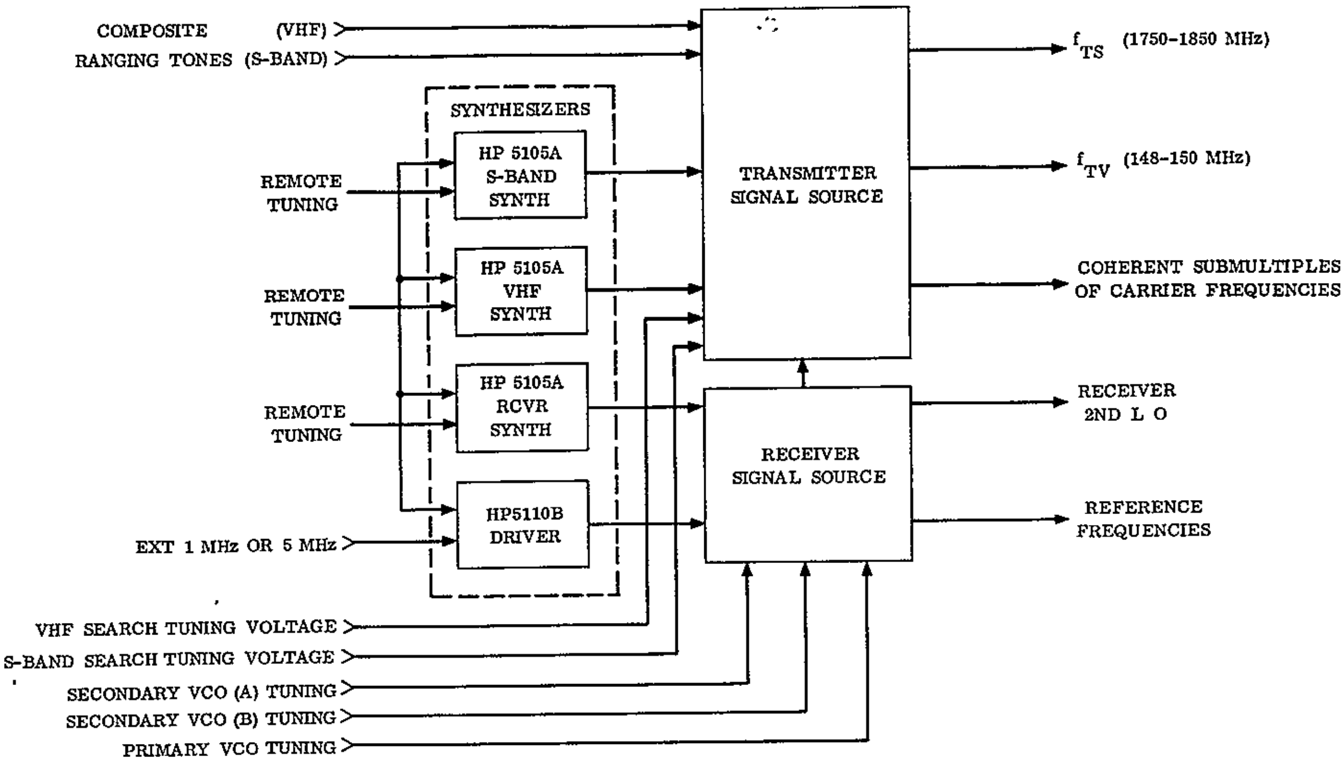

Figure 3-26. System Signal Source Block Diagram

The carrier frequency output of 1750 to 1850 MHz (in increments of 100 KHz) is derived from an HP5105A synthesizer operated at 337.5 to 362.5 MHz (stepped in increments of 25 KHz). Ranging tones linearly phase-modulate a 25 MHz carrier to 3/16 of a radian peak. The 25 MHz is derived from a high purity 1 MHz reference frequency from the HP5110B synthesizer driver. The phase-modulated 25 MHz is multiplied by eight resulting in a 200 MHz signal phase modulated to 3/2 of a radian peak.

The phase modulated signal is next translated to 875 to 925 MHz by mixing with 675 to 725 MHz signal made by doubling the input from the synthesizer. The low level output from the mixer is amplified to a 2w level to drive a ×2 varactor multiplier (similar to the Telonic TTM-4) producing the carrier frequency phase-modulated to 3 radians peak. The multiplier has a typical conversion loss of 4 db resulting in an output level of approximately 1 watt. This is attenuated to the desired transmitter input level (5 mw to 500 mw) with two front panel mounted Microlab/FXR type AX turret attenuators adjustable in steps of 1 db over a 20-db range. Non-harmonically related spurious outputs are more than 55 db below the carrier. Harmonics are more than 45 db below.

In the VCO mode, the output of a 25 MHz VCXO is substituted for the fixed 25 MHz input to the phase modulator. The VCXO frequency versus control voltage is linear to within 5 percent.

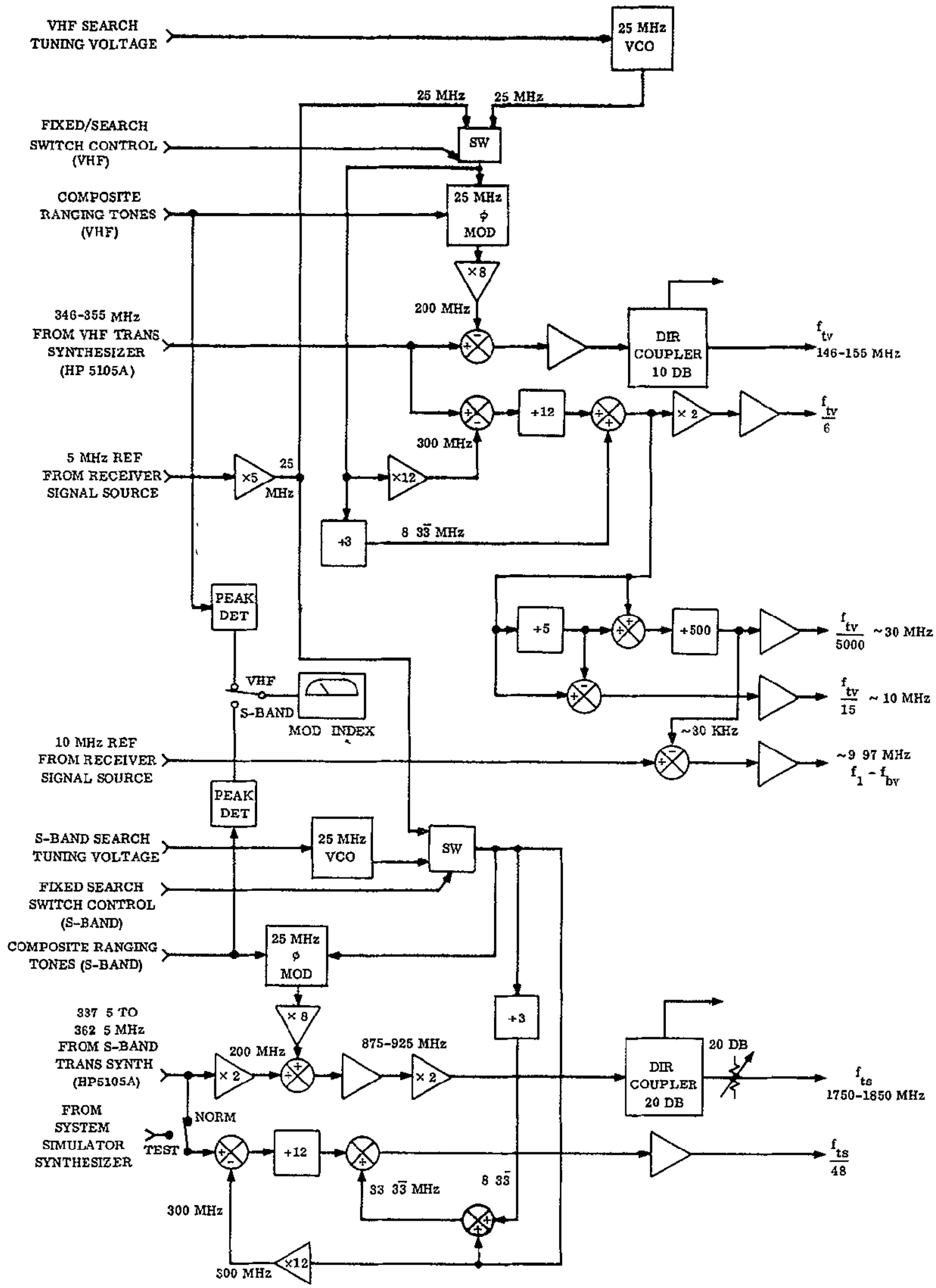

Figure 3-27. Transmitter Signal Source

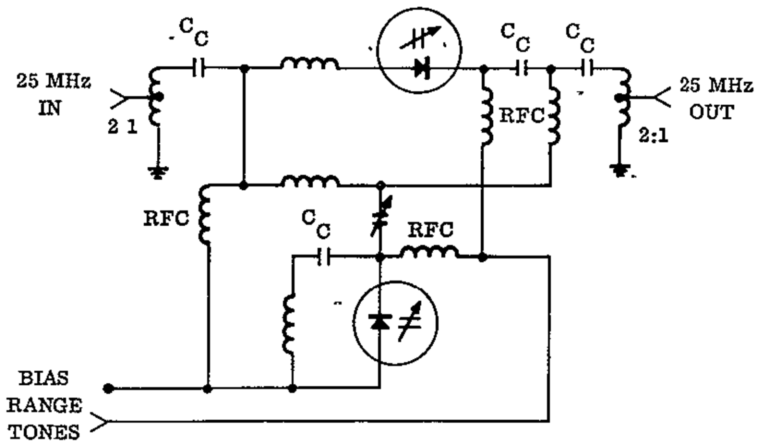

Figure 3-28. Phase Modulator

To obtain the required ±300 KHz variation at the carrier frequency, the VCXO is tuned ±18.75 KHz. The VCXO sensitivity is 3.75 KHz per volt with a tuning voltage requirement of 0 (±5) volts.

3.3.5.3 VHF TRANSMITTER SIGNAL SOURCE. The 148 to 150 MHz carrier is derived by mixing the output of an HP5105A frequency synthesizer tuned from 348 to 350 MHz (in steps of 1 KHz) with a 200 MHz phase-modulated signal. The 200 MHz signal generation is the same as discussed for the S-Band case. The maximum modulation index at 200 MHz in the VHF case, however, is 3 radians peak. A three-stage amplifier using type 2N3866 transistors provides the 1w output. Nonharmonically related spurious are more than 55 db below the VHF carrier. Harmonically related spurious will be more than 45 db down.

In the VCO mode the VHF carrier can be continuously varied over a ±50 KHz about a selected frequency. This is accomplished by substituting a 25 MHz VCXO output for the fixed 25 MHz input to the phase modulator as in the S-Band case. The VCXO control voltage requirement is 0 (±5) volts.

3.3.5.4 PHASE MODULATOR. A schematic of the phase modulator is shown in Figure 3-28. This design has been used in two recent equipment designs and provides fairly wide phase deviations while introducing negligible amplitude modulation. The modulator operates at 25 MHz with input and output impedance levels of 50 ohms. A linear change in output phase versus modulating voltage is achieved over a ±3/8 radian range. Frequency response is uniform to beyond 500 KHz with a modulating sensitivity of 4.5 degrees per volt. Measured phase distortion at maximum deviation (±3/8 radian) is the order of 1 percent and is primarily second harmonic. Fifth harmonic distortion is ~0.1 percent.

A front-panel mounted modulation index meter is provided to monitor either the VHF or S-Band index. The peak amplitude of the composite range tones at the phase modulator input is detected and the voltage developed operates the meter. The meter is calibrated in 0.1 radian increments to 3.0 peak radians full scale.

3.3.5.5 DOPPLER EXTRACTOR OUTPUTS. Coherent frequency samples of 1/6 of the VHF output ($f_{tv}/6$) and 1/48 of the S-Band output ($f_{ts}/48$) are provided for use in the doppler extractor. In addition a coherent VHF bias ($f_{tv}/5000$, approximately 30 KHz) and VHF reference frequency ($f_{tv}/15$ or approximately 10 MHz) are derived. The corresponding S-Band bias and reference frequencies ($f_{ts}/180$ and $f_{ts}/3600$, respectively) are developed in the doppler extractor using the $f_{ts}/48$ S-Band sample. This simplifies the interface between the system signal source and doppler extractor since transmitter carrier samples at different submultiples of the carrier can be introduced directly into the doppler extractor and need not be routed back to the system signal source to develop the bias and reference frequencies.

3.3.5.5.1 S-Band. The coherent $f_{ts}/48$ sample is generated in the following manner. A 300 MHz reference signal is first subtracted from the 337.5 to 362.5 MHz input from the carrier synthesizer. This 300 MHz signal is developed from the coherent 25 MHz reference signal used in the carrier frequency generation. The resultant sidestepped frequency of 37.5 to 62.5 MHz is filtered and then passed to a digital divide-by-12 circuit. The mixing process is spur-free through eight order products.

The digital divider uses Motorola type MC1013P, 70 MHz, J-K flip-flops in a fully clocked configuration. Well-filtered power supplies in conjunction with a high signal-to-noise ratio (> 60 db) at the input to the divider keep the jitter in the order of 1 to 2 nanosec.

The divided output is then mixed with a $33.3\bar{3}$ MHz reference which has also been derived from the coherent 25 MHz reference. This frequency ($33.3\bar{3}$ MHz) represents 300 MHz ÷ 12 + 400 MHz ÷ 48. The sum output is filtered through a 4-pole filter and represents the desired $f_{ts}/48$ output. All spurious are a minimum of 55 db below the desired signal.

Two outputs of 0 dbm each are provided. One goes to the doppler extractor, the second to the remote console for verifying the frequency of the S-Band carrier. Output level variation is less than ±0.5 db.

3.3.5.5.2 VHF. The $f_{tv}/6$ is derived in a similar manner. The method is the same up to the mixer following the digital divider. The second mixer input in this case is an $8.3\bar{3}$ MHz reference which represents 300 MHz ÷ 12 − 200 MHz ÷ 12. The filtered sum output is then $f_{tv}/12$.

The final $f_{tv}/6$ output is arrived at using a balanced doubler. Again, two 0 dbm (±0.5 db) outputs are provided: one to the doppler extractor, the other to the remote console for verifying the frequency of the VHF carrier. Spurious are a minimum of 55 db below the desired signal.

The VHF bias ($f_{tv}/5000$) and reference ($f_{tv}/15$) are developed from the $f_{tv}/12$ signal. The digital dividers used are the MC1013P 70 MHz flip-flops. The output levels are 0 dbm (±0.5 db) with non-harmonically related spurs down at least 55 db. Harmonics of the output are at least 30 db down.

3.3.5.6 RECEIVER SIGNAL SOURCE. The function of this drawer is to supply other units of the system with synthesized reference frequencies. In addition, the receiver second oscillator signal is generated using the input from the receiver synthesizer (HP5105A). Coherent samples of the second local oscillator are also provided ($f_{LO}/60$ and $f_{LO}/12$). The inputs required from the HP5110B are 1, 3, 3.9, 20, 30, and 36 MHz. Table 3-1 lists the various outputs.

The fixed reference frequencies are generated from the relatively spectrally pure outputs of the HP5110B Synthesizer driver (with spurious down more than 80 db). To minimize the generation of further spurs, hot carrier diode doubly-balanced mixers and balanced frequency doublers are used in conjunction with crystal and narrowband LC filters. Frequency division where required is accomplished with Motorola MC1013P digital J-K flip-flops to preclude introducing jitter. Spurious elements on reference frequencies are a minimum of 55 db down. On the 10 MHz (f_1) and 50 MHz ($f_2/2$) references, spurious elements are more than 80 db down. A block diagram of the reference frequency generation is shown in Figure 3-29

The generation of the receiver second local oscillator signal (510 to 610 MHz) requires combining the output of the receiver synthesizer with the outputs from the primary and secondary VCO's. The synthesizer output of 335-385 MHz is doubled and filtered to supply a 670 to 770 MHz signal. Subtracting 160 MHz derived from the primary and secondary VCO's results in the desired LO signal (Figure 3-30).

The primary VCO is made up of two voltage-controlled crystal oscillators which share a common control voltage input. The frequency deviation versus control voltage is opposite in each so that after subtracting, an equivalent VCO results which has twice the pulling range of a readily realizable single-stage VCXO. A block diagram is shown in Figure 3-31.

Subtracting the 6.54 MHz (±4.5 KHz) VCO signal from the 12.5 MHz (±8 KHz) VCO signal results in a 5.96 MHz (±12.5 KHz) output. Multiplying this by twelve yields 71.52 MHz (±150 KHz). To this is added the secondary VCO at 8.48 MHz to give 80 MHz (±150 KHz). Multiplying by 2 results in 160 MHz (±300 KHz).

To insure that receiver spurious responses are 70 db down, great care must be exercised in the local oscillator generation. A spurious analysis has been made to determine optimum mixing frequencies and interstage filter requirements. An additional refinement has been included following the mixer wherein the 160 MHz is subtracted from 670-770 MHz. At this point three switched filters with 30 or 40 MHz bandwidths are included. These filters divide the 100 MHz band into segments of 510 to 540, 540 to 570, and 570 to 610 MHz. The solid-state switches which select the proper filter are controlled by the setting of the 10 MHz

Table 3-1. Receiver Signal Source Outputs

Freq (MHz)	No. of Outputs	Output Level (mw)	Destination
0.010	1	1	DRA
0.390	1	1	DRA
1.5	1	1	DRA
4.5	1	1	DRA
5 ($f_1/2$)	1	1	Trans S S
9	1	1	Σ channel receiver
10 (f_1)	5	1	TLM, Σ, Δ, SC, Tr SS
$27\left(\frac{f_3 - f_2 - f_8}{60}\right)$	1	1	SC
35.416 (f_6)	1	1	SC
50 ($f_2/2$)	3	1	TLM, Σ, Δ
110	2	1	TLM, SC
56 (f_7)	1	1	SC
80 (f_8)	1	1	SC
8.5 - 10.16 ($f_{LO}/60$)	2	1	SC, Counter for Freq. Verif.
46.8$\bar{3}$ (±0.16) ($f_{LO}/12$)		1	SC
510 - 610 (f_{LO} (A))	1	50	Σ
510 - 610 (f_{LO} (B))	1	50	Σ

receiver frequency select control. The filters suppress the 110 MHz spurious caused by the third and fourth harmonic of the 160 MHz mixing with local oscillators signals in the receiver's second mixer. They also serve in removing noise components, 110 MHz from the selected frequency, from the synthesizer signal. It is imperative that noise components in this frequency band be removed from the local oscillator so that system threshold will not be degraded.

A synthesized 80 MHz signal is switched in to replace the 80 MHz VCO signal when the open-loop fixed frequency mode is selected. The 80 MHz signals from both polarizations are provided to the circuitry which derives the $f_{LO}/12$ and $f_{LO}/60$ outputs for the doppler extractor.

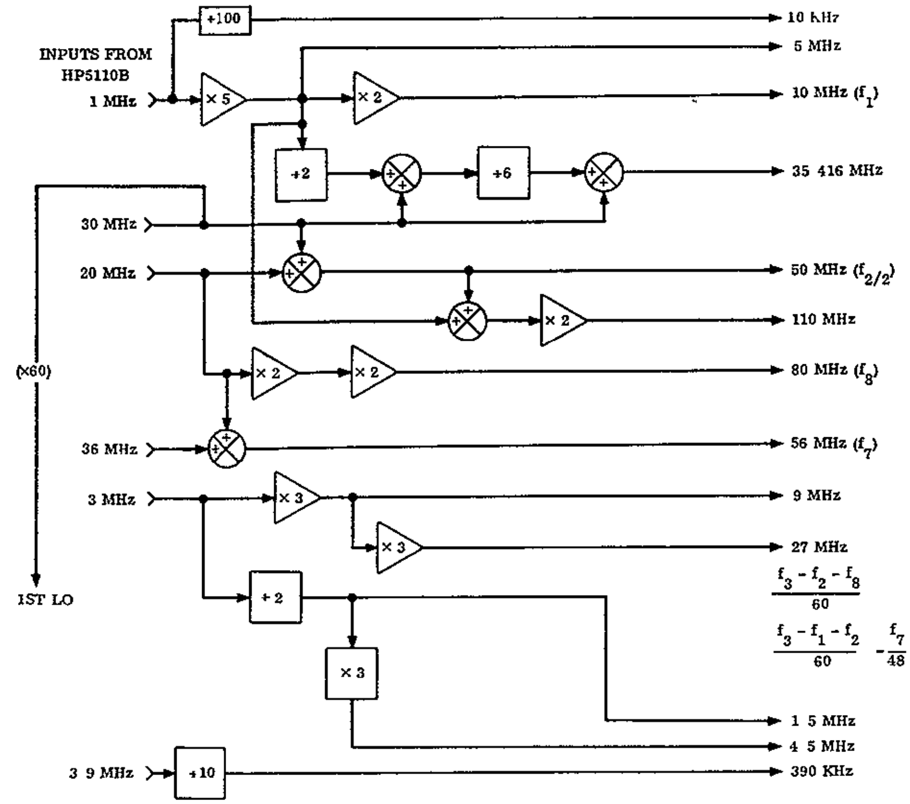

Figure 3-29. Reference Frequency Generation

The 1/12 and 1/60 submultiples of the local oscillator signal are developed by first generating $f_{LO}/2$ by subtracting 80 MHz from the 335-385 MHz input from the receiver synthesizer. A division by 3 follows using a discrete component ring divider followed by a Motorola MC1027P 120 MHz J-K flip-flop dividing by 2. The frequency developed at this point is $f_{LO}/12$. The $f_{LO}/60$ output is obtained through a divide-by-five digital divider using the MC1013P logic.

A solid state polarization selector switch controlled by a logic input from the receiver provides the correct 80 MHz signal corresponding to the polarization in use.

3.3.5.7 TRANSMITTER SYNTHESIZER CONTROLS. The VHF and S-Band transmitter frequencies may be controlled either from the transmitter frequency control panel (Figure 3-32) located at the console or locally by using the keyboard on the Hewlett-Packard 5105A synthesizers. The control mode, local or console, is determined by the setting of the remote-local switch on the synthesizer. No provision is made for programmed operation.

In addition to the controls for the synthesizers, the transmitter frequency control panel contains switches to permit selecting the search mode of operation and the associated VCO tuning controls. The tuning controls are calibrated 10-turn potentiometers.

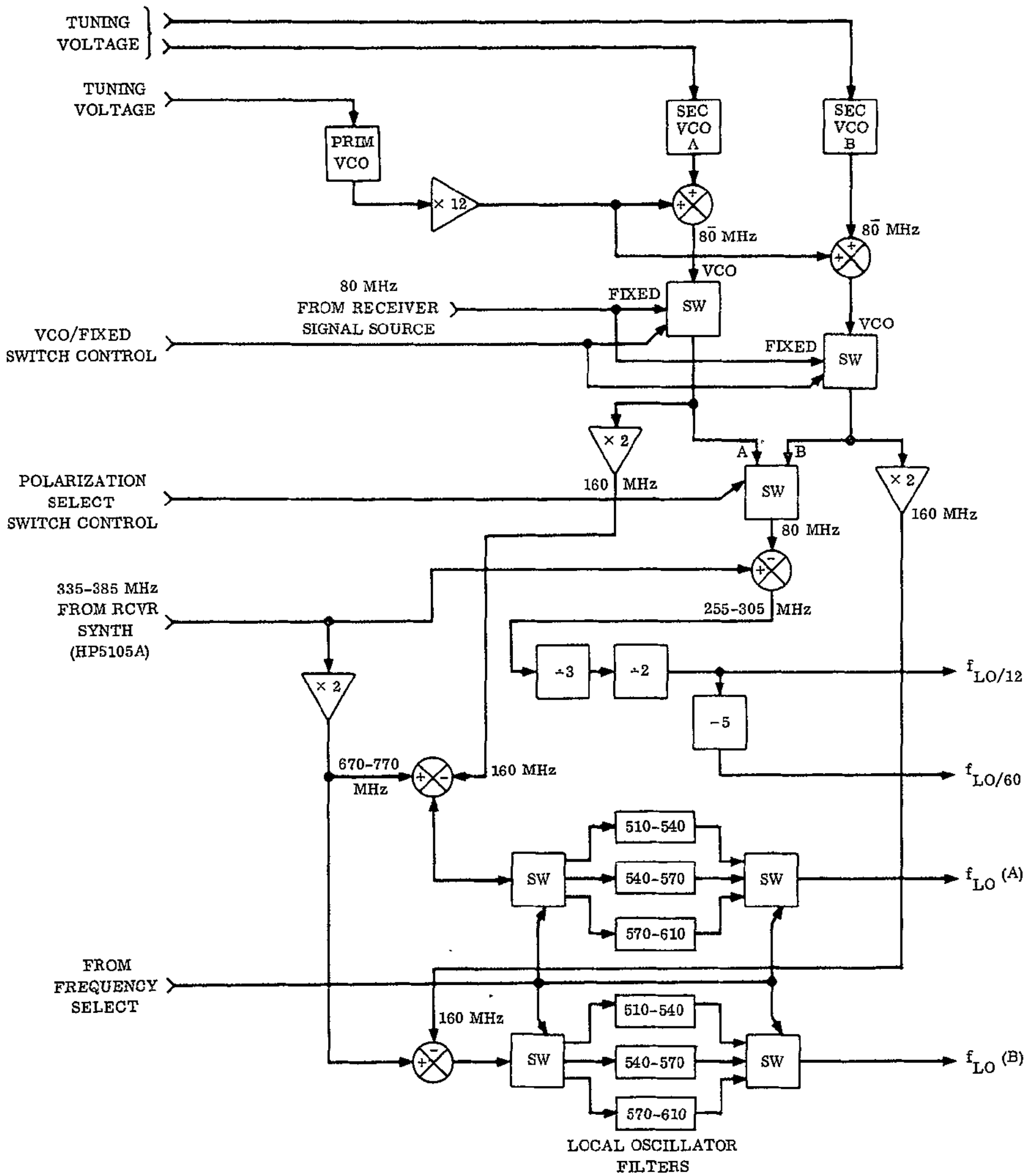

Figure 3-30. Second Local Oscillator Generation

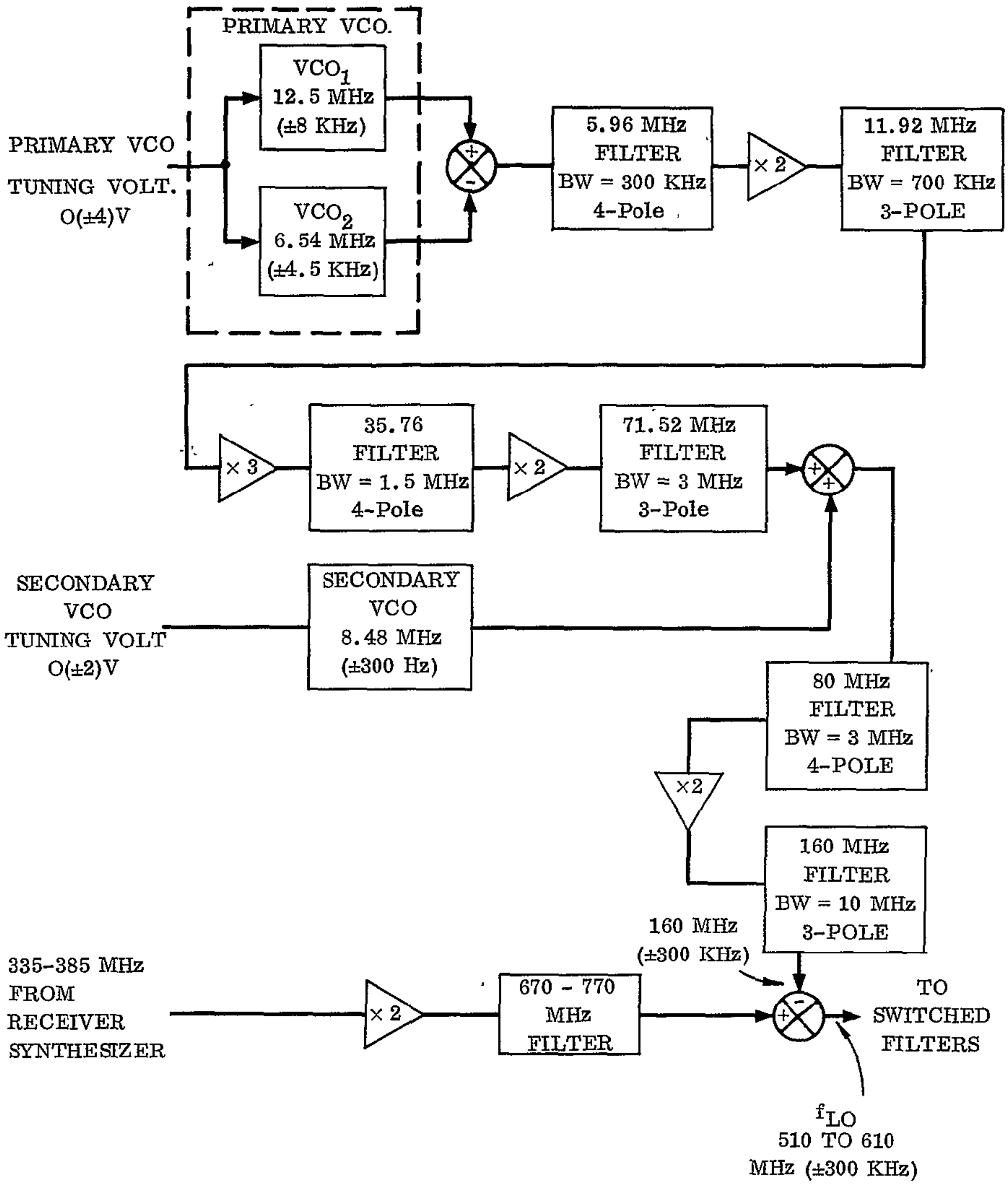

Figure 3-31. Receiver LO Generation.

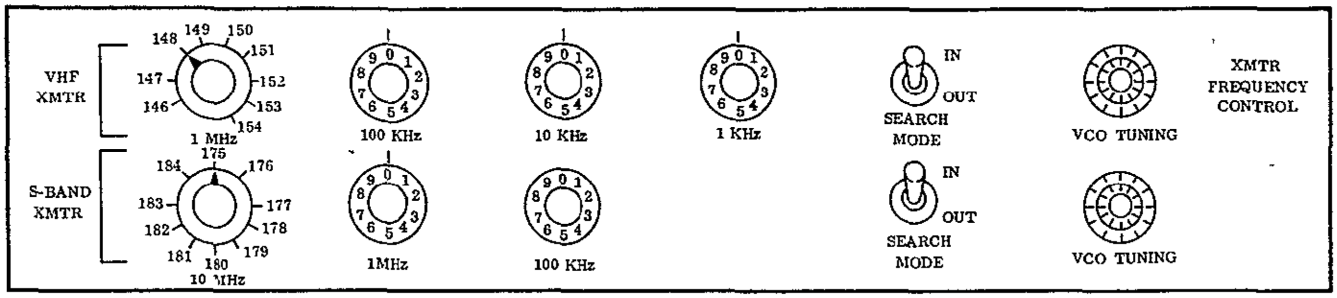

Figure 3-32. Transmitter Frequency Control Panel

3.3.5.7.1 VHF Transmitter Controls. Since there is a one-to-one correspondence between the synthesizer and transmitter frequencies, a direct indication of transmit frequency is obtained without the need for complex switching circuits. Four rotary switches are required, one nine-position to give 1 MHz steps (marked 146 through 154), and three 10-position switches for the 100 KHz, 10 KHz, and 1 KHz steps.

3.3.5.7.2 S-Band Transmitter Controls. The synthesizer frequency is multiplied by four in generating the S-Band transmitter frequency. Thus, if the transmitter frequency is to be indicated directly, the panel switches must provide an effective division by four of each indicated increment in order to properly control the synthesizer. This operation is performed directly by the switches.

3.3.5.8 RECEIVER SYNTHESIZER CONTROL. The receiver synthesizer may be controlled by a set of switches located on either receiver control panel or by external programming equipment. Synthesizer control is determined by the control mode switch on the receiver control panel located in the console. The controls are designed to provide a direct indication of receiver frequency for the 135-139 MHz and 2200-2300 MHz bands. Since the receiver synthesizer frequency is doubled in generating the second LO signal, each frequency increment indicated on the switches requires one-half that increment in the actual synthesizer frequency. In effect, the switches, in controlling the synthesizer, perform a division by two.

Transfer of control from the local to the console mode is effected by switching a -12.6 vdc line from the synthesizer to the appropriate set of switches. In the programmed control mode, a set of transistor driver circuits, one for each digit to be controlled in the synthesizer, is provided. The driver circuits convert the standardized control voltage levels from the programmer (0 and +6 volts) to the levels required by the synthesizer (0 and -12.6 volts). It should be noted that the information that the programmer must supply is the actual synthesizer frequency corresponding to the desired received signal frequency.

The receiver synthesizer controls also generate control signals used to select one of the three fixed-tuned bandpass filters in each signal path and each second LO chain. The three frequency bands in terms of the first IF frequency are 400-429.99 MHz, 430-459.99 MHz

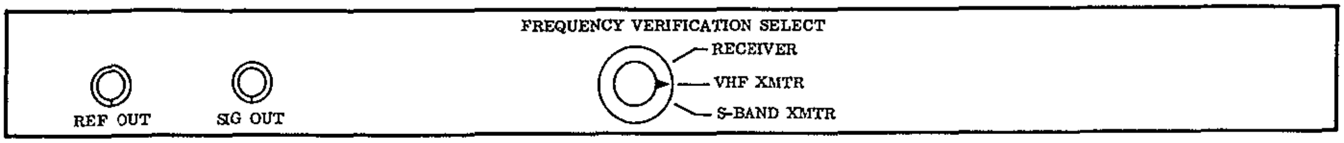

Figure 3-33. Frequency Verification Select Panel

and 460-500 MHz, corresponding to synthesizer frequency bands of 335-349.995, 350-364.995 and 365-385 MHz.

3.3.5.9 FREQUENCY VERIFICATION. The frequency verification system provides a direct reading to the nearest KHz of the VHF transmitter frequency, the S-Band transmitter frequency, or the receiver frequency. This is done by using a Hewlett-Packard 5244L electronic counter in conjunction with the Frequency Verification Select panel (Figure 3-33) to measure the ratio of a fraction of the selected transmitter frequency or the receiver second LO frequency to a similar fraction of a 17 Hz reference. Figure 3-34 is a block diagram of the system.

Three signals are supplied from the system signal source: one-sixth the VHF transmitter frequency; one-forty-eighth the S-Band transmitter frequency; and one-sixtieth the receiver second LO frequency. A 1 MHz signal from the Timing Subsystem is also supplied.

A panel switch simultaneously selects the signal to be measured and the division ratio for the 1 MHz reference signal. The ratio measurement by the counter requires the divided reference signal to be coupled to the signal input jack and the selected signal to the external time base jack of the counter.

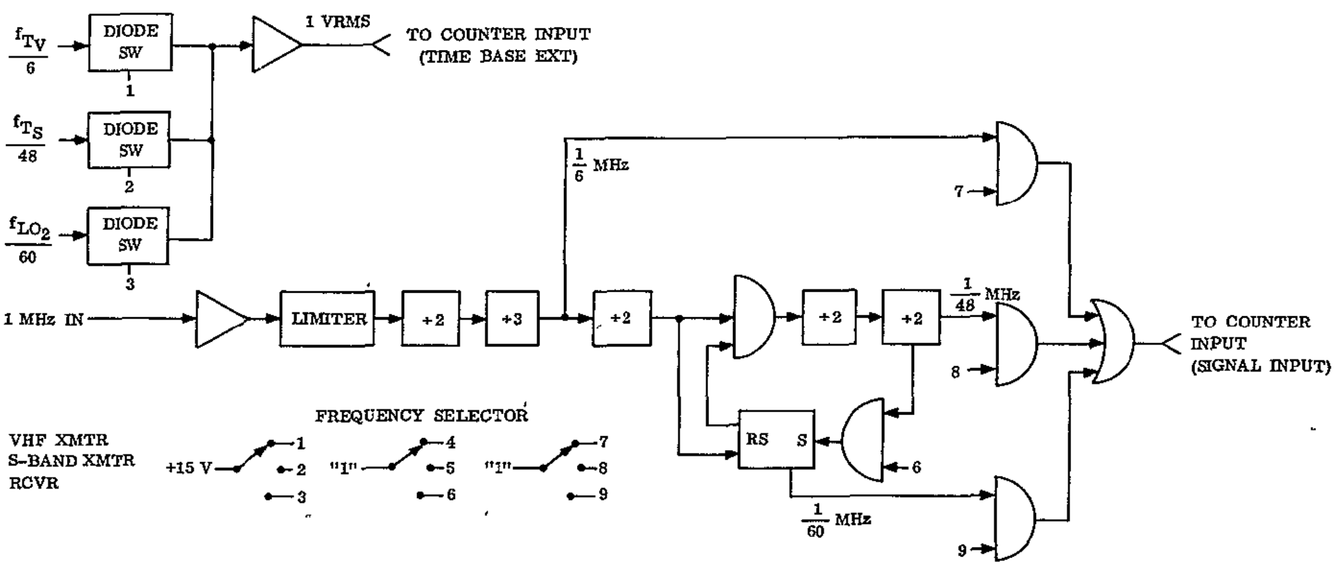

Figure 3-34. Frequency Verification Control Circuits

To provide a direct indication of the receiver frequency rather than the second LO frequency, the counter will be modified to permit resetting the four most significant digits to any desired number. The modification consists of four thumbwheel switches mounted on the front panel. These switches control the reset lines to decade counting assemblies.

In verifying the transmitter frequencies, the thumbwheel switches are all set to zero. In verifying the receiver frequency the thumbwheel switches are set to a number which depends on the receiver frequency band. Thus, if the receiver is to operate in the 2200-2300 MHz band, the thumbwheel switches would be set to 1690. In the 135-139 MHz band, the thumbwheel switches would be set to 9575.

As an example assume the receiver is set to receive at 2250 MHz. The corresponding second LO frequency is 560 MHz. With the thumbwheel switches set properly, the counter will count up from the initial setting of 1690.000 and will indicate 2250.000 MHz (1690.000 + 560.000) at the end of the count.

3.3.5.10 MECHANICAL DESIGN. The system signal source is made up of one HP5110B synthesizer driver, three HP5105A synthesizers, a transmitter signal source housed in two 10.5-inch high drawers and a receiver signal source in one 10.5-inch high drawer. All units are mounted in one equipment rack. Standard plug-in modules are used wherever possible. The transmitter and receiver signal sources operate from built-in modular power supplies manufactured by Dressen-Barnes.

3.3.6 Applicability

A full complement of equipment as described in paragraph 3.3 will be supplied at the Rosman, Carnarvon and Tananarive sites. At the Fairbanks site only a new System Signal Source as described will be supplied.

3.4 TRANSMITTER SUBSYSTEM

The Transmitter Subsystem consists of a VHF transmitter and an S-Band transmitter with associated loads and a common heat exchanger. Transmitter modifications referred to herein are applicable to the Rosman, Carnarvon and Tananarive sites.

3.4.1 VHF Transmitter

The VHF transmitter, as presently designed, will be retained in its entirety with the exception of Synthesizer-Modulator chassis 8A1. The Synthesizer-Modulator output signal will be replaced with a signal derived from the System Signal Source. The input frequency will be 148 to 150 MHz and the level will be variable from 0.1 watts to 1.0 watts. Although a variable RF input power level is not required, the 10-db control will permit adjustment of output power to facilitate testing and minimize possible arcing in coaxial and antenna elements due to overdrive conditions. A simplified block diagram of the existing VHF transmitter is shown in Figure 3-35.

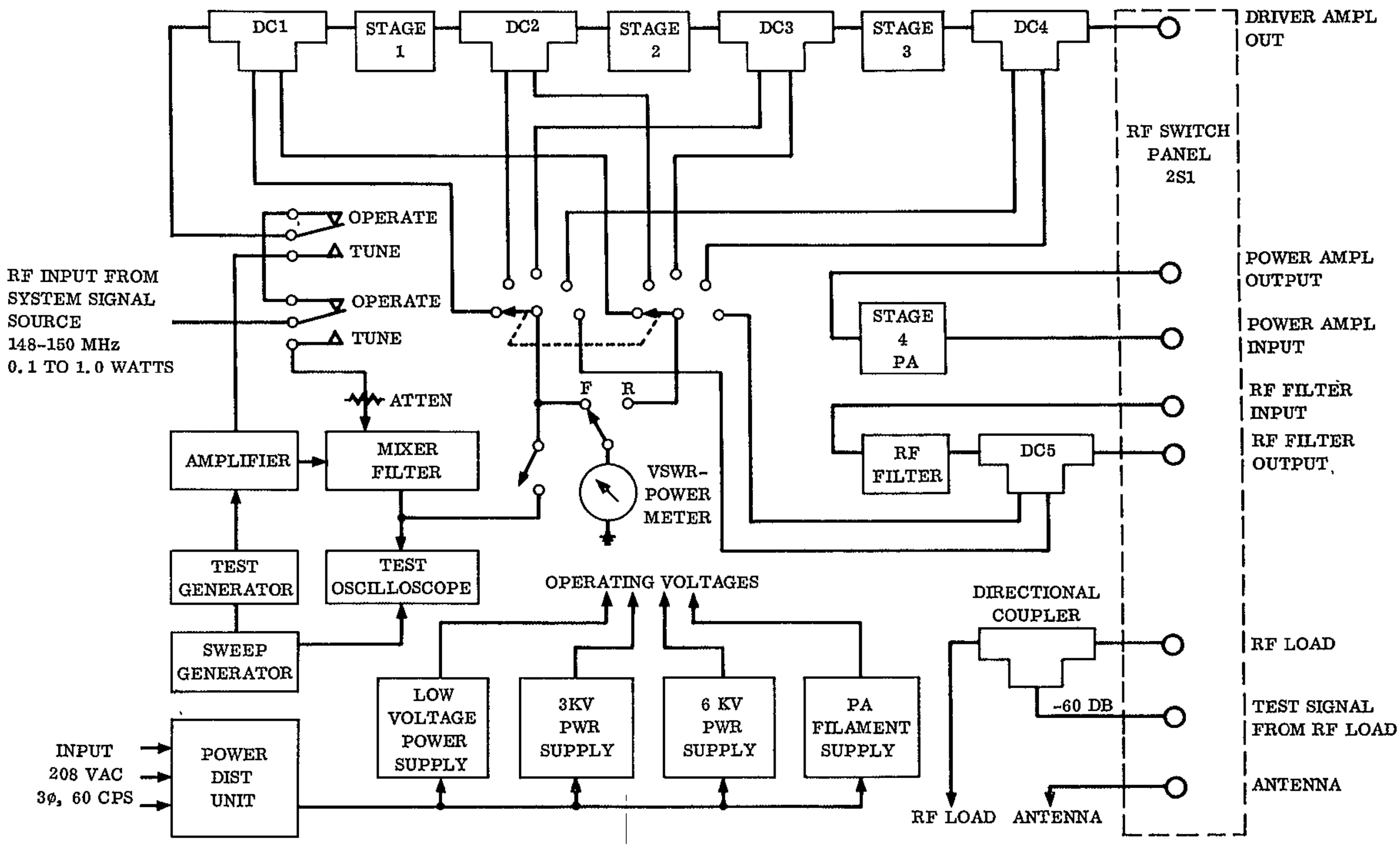

Figure 3-35. VHF Transmitter, Simplified Block Diagram

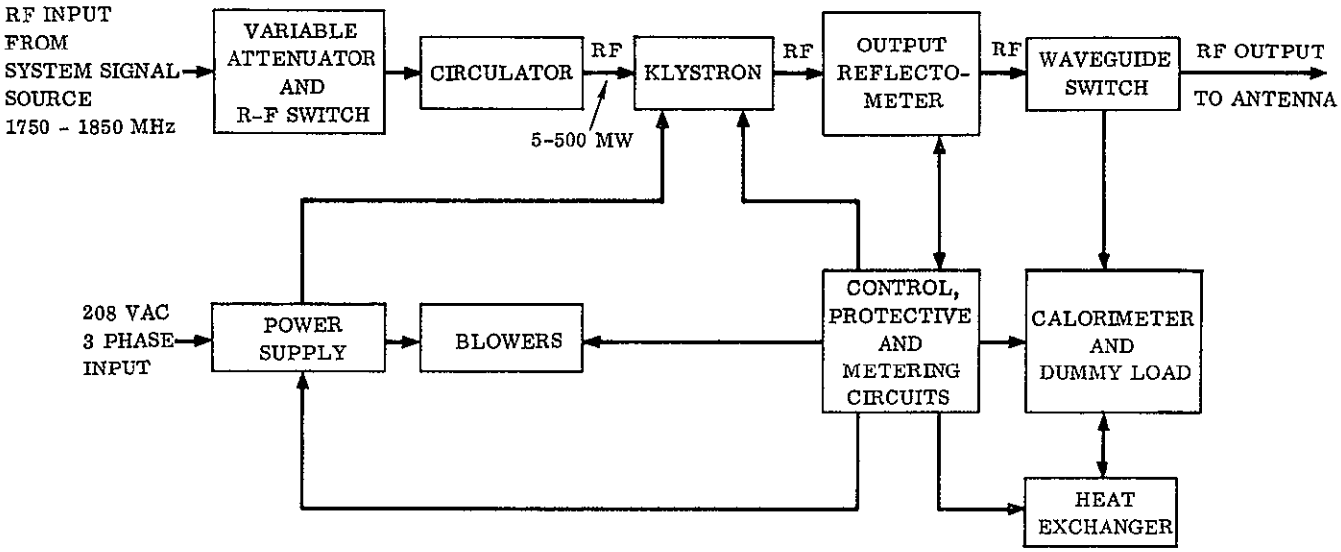

Figure 3-36. S-Band Transmitter, Simplified Block Diagram

3.4.2 S-Band Transmitter

The S-Band transmitter will be retained as presently designed except for the deletion of Synthesizer-Modulator chassis 8A1 and a Klystron amplifier change.

The variable level input signal to the transmitter klystron will be derived from the System Signal Source. An input frequency range of 1750 to 1850 MHz will be provided at power levels variable from 5 mw to 500 mw. The 20-db range of input power is controlled at the System Signal Source and will allow varying the transmitter output power from 10 kw to less than 500 watts. A simplified block diagram of the existing S-Band transmitter is shown in Figure 3-36.

In addition to the 20-db range of klystron input signal control, a 20 db ARRA Model 4414-20B variable attenuator is available and is presently installed on the existing amplifier in unit 6. The input signal from the System Signal Source will interface with the existing attenuator.

The existing klystron will be replaced with an Eimac 5KM50SJ klystron. This model is mechanically identical to the existing klystron but will require 10 db additional drive power at the new operating frequency. Gain is sacrificed to provide a broad tuning range from 1700 to 2400 MHz. A minimum input power of 890 mw will be provided at the input to the variable attenuator. This level accounts for the 2.5 db loss in the RF switch, directional coupler, circulator, and variable attenuator which precede the input port of the klystron amplifier. A 1.0 watt minimum output level from the System Signal Source will provide adequate drive for the klystron amplifier to produce a maximum power output of 10 kw.

The five RF monitor circuits are compatible with the new frequencies and input power requirements. A minor modification may be required on the RF input monitor if the existing adjustment does not provide adequate range.

3.5 ANTENNA SUBSYSTEM

The existing antenna subsystems will be used at all four sites with new S-Band feed assemblies provided to accommodate the frequency changes and polarization diversity requirements. No modifications will be made to the VHF antenna systems or to the S-Band pedestals, drive systems, reflectors, or subreflectors.

The S-Band feed assembly for the twin 14-ft antennas at the Rosman, Carnarvon, and Tananarive sites will be designed and built by the contractor. The S-Band feed assembly for the 30-ft antenna at Fairbanks will be subcontracted.

3.5.1 14-foot Antenna Feed Assembly

This subsection contains design information and outlines required modifications to the GRARR-1 S-Band antennas at Rosman, Carnarvon, and Tananarive. Figures 3-37 and 3-38 are simplified diagrams depicting the relative positions of the elements in the feed assembly. The modification will consist of the following:

a. Replace the transmitter feed horn with a feed horn designed to properly illuminate the subreflector and the secondary reflector in the new frequency band, and to mate with the new polarizer assembly.

b. Replace the transmitter-polarizer assembly with a remotely-controlled polarizer assembly.

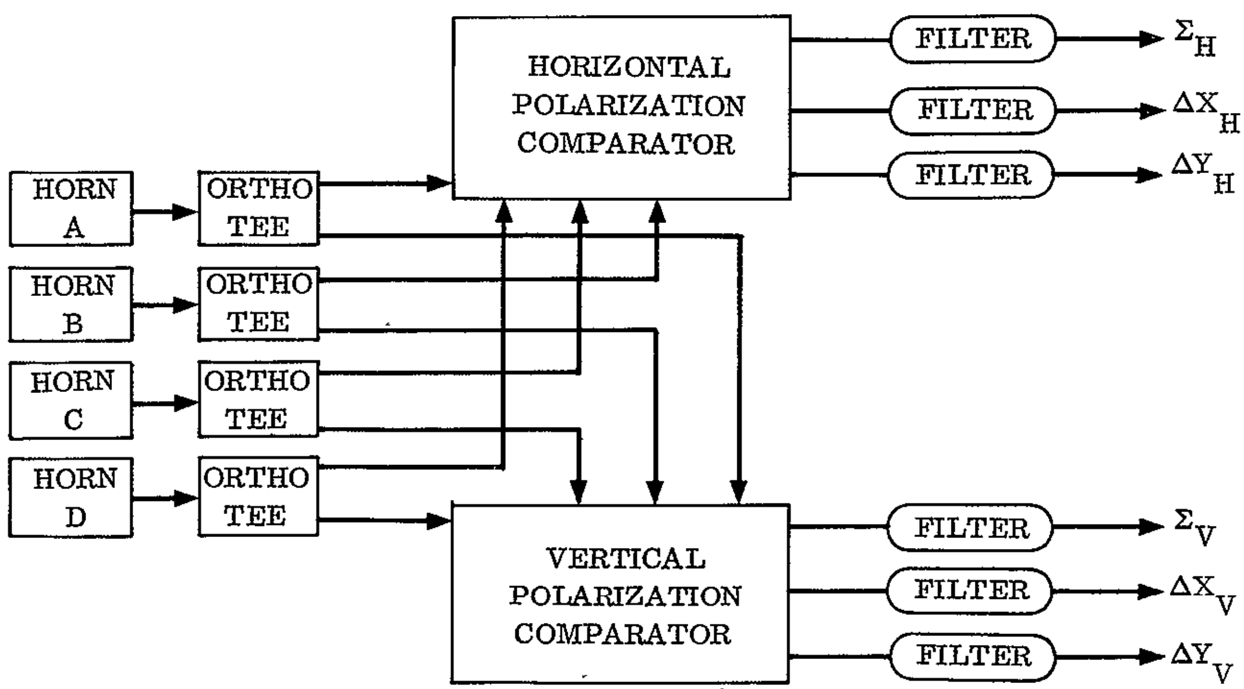

Figure 3-37. S-Band Antenna Receive Assembly

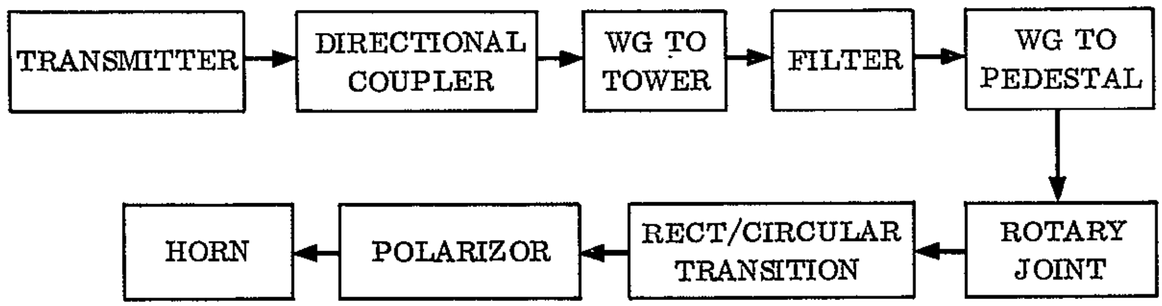

Figure 3-38. S-Band Antenna Transmit Assembly

c. Replace the square-to-rectangular waveguide transition in the existing transmitter assembly with a circular-to-rectangular transition in order to mate to the new polarizer assembly.

d. Replace the rotary joint assemblies in both the azimuth and elevation transmitter channels with new rotary joints tuned to the new frequency band.

e. Install the waveguide transmit filter and incorporate the additional sections of waveguide needed between the Y-axis rotary joint and the transmitting antenna assembly to accommodate changes in the physical dimensions of the new feed assembly and filter.

f. Replace the receiver four-horn monopulse assembly with a new four-horn monopulse assembly to properly illuminate the existing subreflector and secondary reflector in the new receive frequency band.

g. Replace the receive feed horn output polarizers with a set of orthomode couplers which will couple out both horizontally and vertically-polarized signals from the four-horn monopulse system.

h. Replace the existing waveguide monopulse comparator with a set of two monopulse comparators; one for horizontal polarization and one for vertical polarization, both optimized to operate in the new receiver frequency band.

i. Replace the existing filter assemblies with new filter assemblies tuned to pass the new receiver frequency band.

3.5.1.1 FEED HORN. The transmit antenna feed horn must be redesigned to operate over the new transmit frequency range from 1750 MHz to 1850 MHz. The square aperture pyramidal horn presently installed on the antenna will be scaled to the new band. Since the new frequency range is lower than the present frequency range, the feed horn aperture size and length must be increased to obtain equivalent performance. This will maintain the present subreflector illumination and, therefore, maintain the present antenna efficiency and side-lobe level performance.

Physical measurements on an installed feed assembly at Rosman, N. C., agree with available drawings. The present feed horn has the following design parameters:

Aperture Side - 20 inches
Flare Length - 32.6 inches
Flare Angle - 18 degrees

Scaling this feed horn design to a center frequency of 1800 MHz from 2250 MHz gives the following values:

Aperture Side - 25.0 inches
Flare Length - 40.8 inches
Flare Angle - 18 degrees

The above aperture size and flare length cause the horn length to increase from 30.8 inches to 38.5 inches. Measurements made at the Rosman site indicate the increase in horn length will not create any mechanical problems.

3.5.1.2 POLARIZER ASSEMBLY. The transmit polarizer being considered is a section of circular waveguide with four sets of three pins each. The four sets of pins are located symmetrically around the circular waveguide at 90-degree intervals. Opposing sets of pins will work together to generate the necessary 90-degree phase shift for circular polarization. The circular waveguide will be approximately 4.5 inches in diameter. The pins will be spaced about 1.65 inches apart with the two end-elements extending into the waveguide 0.91 inches and the center element extending into the waveguide 1.08 inches. The axial ratio of the polarization ellipses will not exceed 2.5 db for either circular polarization mode. A rectangular-to-circular waveguide transition will be needed with this polarizer. The transition will be a gradual taper from WR430 waveguide to circular waveguide. Taper length will be sufficient to maintain a low VSWR over the 2200-2300 MHz band.

The opposing-pin polarizer assemblies will be inserted upon command to provide the desired sense of circular polarization. When one set of six opposing pins is inserted into the waveguide, the alternate set of pins will be withdrawn. Pin actuation will be solenoid controlled. Cover pressure panels over the solenoids will maintain waveguide pressurization.

3.5.1.3 TRANSMIT FILTER. The transmit filter will be a low-pass filter to 1900 MHz in WR430 waveguide. It is to have an insertion loss of less than 0.2 db from 1750 MHz to 1850 MHz and 55 db at 2200 MHz. Filter ripple is expected to be 0.1 db or less over the bandwidth of 1750 to 1850 MHz with a VSWR of 1.3:1 or less. The power-handling capability will be 15 kw of CW power. No extra equipment will be used to cool the filter. The physical size of the filter will be approximately 4.5 × 2.25 × 20 inches. It will be located and mechanically supported at the base of the antenna tower. It will be purchased from a qualified vendor. A heat analysis of a typical filter is contained in section 4.5.

3.5.1.4. TRANSMIT ROTARY JOINT. The transmit rotary joint for the new bandwidth will be designed by direct scaling of the present rotary joint. The waveguide dimensions, other than length, are not expected to change. The length of the new rotary joint will be approximately 16 inches. No interference with any existing structure is anticipated.

3.5.1.5 RECEIVE ANTENNA MODIFICATIONS. Analysis of the present receive feed at 2250 MHz dictates its replacement. The total capture angle of the subreflector is 34 degrees and 4 minutes. At 2250 MHz the first null of the present feed will occur at 14 degrees and 48 minutes off axis due to the array factor for 1.94 wavelength spacing between elements.

The present aperture dimensions of the feed will be scaled by a factor of 0.757. Thus, the new receive aperture will be 15.2 inches square. The aperture will consist of four horns spaced at 1.47 λ at 2250 MHz. The aperture phase variation across each individual horn element will not exceed 1/8 λ. Each horn will have a square aperture of 7.57 inches. By utilizing the design principle of directly scaling each dimension the performance currently being achieved on the GRARR-1 sites could be expected again at the new frequency of 2250 MHz.

The contractor has taken antenna dimensions from the ASI drawings and analyzed the configuration to determine the expected antenna performance at 2250 MHZ with a scaled feed. This analysis is presented in Section 4.5.

3.5.1.6 ORTHOMODE TEE. To obtain two orthogonal polarizations simultaneously, an orthomode tee will be used consisting of two sections of aluminum WR430 waveguide connected at right angles similar to a folded magic tee in the E-plane. The inputs to the tee are cross-polarized. The output from the orthomode tee will be through square waveguide propagating only the $TE_{1,0}$ and the $TE_{0,1}$ waveguide modes. The waveguide will be 3.38 inches square in its internal dimensions; optimum for low insertion loss and the rejection of higher order modes.

3.5.1.7 MONOPULSE COMPARATOR. The monopulse comparator will be an arrangement of 3/2 λ "rat-race" hybrid rings of the coaxial or stripline type with type-N connectors. The hybrids will be packaged to eliminate any phase or amplitude variation between hybrids and to ensure each hybrid will be designed to exhibit greater than 35 db isolation over the pass band of 2200 to 2300 MHz. The VSWR over the band will not exceed 1.3:1. Particular emphasis will be taken to insure optimum results from the comparator at the presently specified operating frequency of 2250 MHz. The comparator will be purchased from a qualified vendor.

The comparator network and the horn array will be linked by coaxial cable. The cable will be 0.5-inch diameter Spir-O-line, Prodelin Part Number 61-500 (RG252/U). Cable attenuation at 2000 MHz is 4.0 db per 100 feet; the estimated loss over the 3-foot length preceding the comparator is 0.12 db. Prodelin Part Number 76-500 Type N connectors will be used.

Precomparator phase balance will be insured by time domain reflector and slotted section techniques. The overall monopulse feed performance will be verified by radiation pattern and short circuit technique measurements taken at General Dynamics.

The following characteristics are expected from the feed-monopulse comparator assembly for both vertical and horizontal polarization. Precomparator amplitude unbalance is expected to be less than 0.2 db. Precomparator phase unbalance is expected to be less than 3 degrees. The isolation between comparator sum and difference ports should exceed 35 db. Post-comparator phase unbalance should not exceed 10 degrees. The resultant radiation characteristic of the boresight axis is expected to exhibit a null in excess of 35 db relative to the sum channel pattern at 2250 MHz.

The boresight shift about the mechanical axis should not exceed 2 percent of the half-power beamwidth of the sum patterns. Reflections from the surrounding area will probably cause this value to be exceeded due to the poor sidelobe characteristic of the difference pattern

3.5.1.8 FILTER. The required 190 db rejection between the transmitter and the preamplifier is extremely difficult to achieve and to measure with standard techniques. Allowing for 70 db between the two antennas requires that the filters have 120 db isolation. The proposed filter will be installed in each of the feed monopulse outputs to the preamplifier. Six filters will be required per system. The filter design will be a bandpass filter with the following characteristics. The bandpass insertion loss will be less than 0.5 db. The VSWR will be less than 1.3:1. This VSWR is consistent with the 0.1 db ripple specification rather than the specified VSWR of 1.1:1. The bandpass will be a minimum of 100 MHz at the 0.2 db point. The ripple over the pass band shall be less than 0.1 db. The rejection of signals 100 MHz away from the center frequency will exceed 28 db. Filters will be purchased from a qualified vendor.

3.5.1.9 ESTIMATED ANTENNA PERFORMANCE. The following antenna performance is anticipated for all 14-foot antenna assemblies based on the analysis outline in Section 4.5

(a) Transmit Function

Frequency	1750-1850 MHz band
Power	15KW average
Polarization	left and right circular
Axial Ratio	2.5 DB
Gain	34.5 DB (45% efficiency)
Sidelobes	13 DB first sidelobe
	21 DB Spillover sidelobe at 20° off axis

VSWR	1.2:1
Beamwidth	2.5 - 3.0 degrees

(b) Receive Function

Frequency	2200-2300 MHz band
Polarization	Sum perpendicular to Y linear X error perpendicular to Y linear Y error perpendicular to Y linear Sum parallel to Y linear X error parallel to Y linear Y error parallel to Y linear
Gain	35 DB minimum (33% efficiency)
Sidelobes	13 DB first sidelobe 22 DB Spillover at 34° off axis
Beamwidth	2.0 - 2.5 degrees
VSWR	1.5:1 over bandwidth except 1.2:1 for 2249 to 2257 MHz

(c) Tracking Function

Sidelobes	13 db first sidelobes 20 db spillover sidelobes at 20 degrees off axis
Null depth	35 db
VSWR	1.5:1

3.5.2 30-FOOT ANTENNA FEED ASSEMBLY. The modifications at the Fairbanks site include replacing the existing S-Band antenna feed to accommodate the new frequencies. It is anticipated that this feed-diplexer subsystem will be subcontracted to Rantec Corporation, Calabasas, California. It is considered to be a major subcontract item. Rantec has supplied similar feeds for the GRARR System as well as for the Unified S-Band Tracking System.

Figure 3-39 shows in broad form the single aperture feed system planned. The feed/diplexer system, composite receive, transmit, and tracking type, will have the following required characteristics:

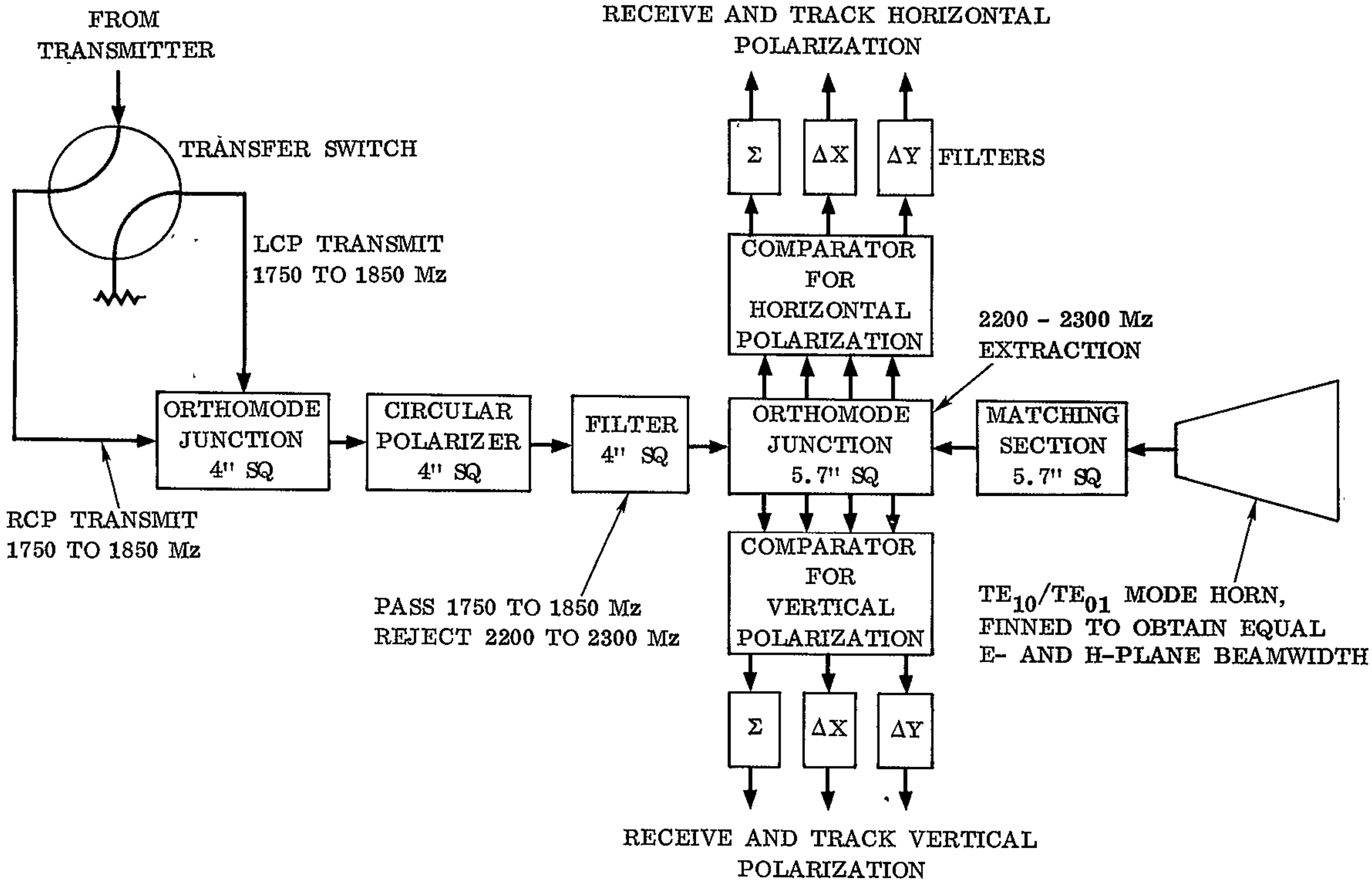

Figure 3-39. S-Band Antenna Feed Assembly for Fairbanks

a. Transmit Function

Frequency	-	1750-1850 MHz band
Power	-	15 kw average
Polarization	-	left and right circular
Axial Ratio	-	2.5 db
Gain	-	41.5 db minimum
Sidelobes	-	15 db minimum down
VSWR	-	Either 1.2:1 maximum over any 20 MHz portion of the transmit band, or 1.3:1 maximum over the entire band

b. Receive Function

Frequencies	-	2200-2300 MHz band
Polarization	-	Sum perpendicular to Y linear
	-	X error perpendicular to Y linear
	-	Y error perpendicular to Y linear
	-	Sum parallel to Y linear
	-	X error parallel to Y linear
	-	Y error parallel to Y linear
Gain	-	42 db minimum
Sidelobes	-	15 db minimum
Beamwidth	-	Sum channel, between 0.8 and 1.2 degrees
VSWR	-	1.2:1 with random spikes up to 1.5:1

c. Tracking Function

Sidelobes	-	15 db down minimum
Null depth	-	35 db
VSWR	-	1.5:1

The feed will be installed in the existing structure without extensive structural modifications. The mounting ring presently in the Fairbanks antenna will be used to attach the feed system.

This feed system is very similar to that used for Unified S-Band 30-foot antenna systems on the Apollo program. Approximately twelve of these types have been installed throughout the world.

The filter in the transmit line is crucial to the success of this feed design. It is now expected (since the 2130 MHz transmit band is eliminated) that a highly reliable, high performance feed can now be built. Rantec, Inc., has had prior success with filters of this design.

3.5.2.1 TRANSFER SWITCH. The transfer switch used to change the polarization (right or left circular) is a waveguide transfer switch manufactured by Ramcor, Inc. It operates from 115 vac single phase and is integral to the feed system.

3.5.2.2 TRANSMIT ORTHOMODE JUNCTION. This junction is designed for the best bandwidth characteristics. One input is injected straight into the square waveguide through a transition and forms an in-line end port, giving one of the linear modes. The other linear mode is injected into the side of the waveguide and is prevented from reflecting back to the in-line input by fins (septas) which function as the matching element (back cavity short) for the side input.

3.5.2.3 CIRCULAR POLARIZER. The circular polarizer is a square waveguide in which a series of obstacles are introduced to, in effect, retard the linear polarized phase of the two orthogonal components. The waveguide then appears inductive 45 degrees to one component and capacitive 45 degrees to the other, thereby producing the 90-degree phase shift required for circular polarization.

3.5.2.4 TRANSMIT FILTER. This filter is a band-reject type in square waveguide rejecting 2200-2300 MHz. Rejection is accomplished by resonant sections which present high series impedances at the reject band of frequencies. It can be compared to a transmission line where several parallel resonant circuits at the reject frequencies are in series with the line. The elements are one-quarter wave cavities which interrupt the series currents where the coupling apertures present low impedances to the transmit frequencies. This design presents no resonant buildups at the transmit frequencies. A Chebychev model is used as the basis for the original design; the final design is usually a combination of Chebychev and maximally flat.

3.5.2.5 RECEIVE ORTHOMODE JUNCTION. This junction couples the receive outputs representing the errors and sums of vertical and horizontal polarizations. It consists of square waveguide wherein the transmit frequency signals are propagated relatively untouched. There are two sets of hybrids for each horizontal and vertical polarization. Each hybrid is connected to a combination of magic tees in the comparator. Inputs to the hybrids couple through four ports associated with the generated horizontal and vertical voltages.

3.5.2.6 VERTICAL AND HORIZONTAL COMPARATORS. The vertical and horizontal comparators are similar. They produce the sum, ΔX, and ΔY voltages for the receiver and tracking information. For the vertical polarization section, there are four coupling apertures into each waveguide. For the sum signal, the four ports produce a $TE_{1,0}$ mode in square waveguide. The same four apertures are phased to excite the $TE_{2,0}$ mode and can phase the $TE_{1,1}$ and $TM_{1,1}$ simultaneously. The three phases are required by the comparator to produce the voltages representing sum, ΔX, and ΔY. The horizontal comparator phases in the $TE_{0,1}$, $TE_{0,2}$, $TM_{1,1}$ and $TE_{1,1}$ modes

3.5.2.7 HORN. The horn is a square pyramidal type without separation. Fins are provided to produce equal E- and H-plane beamwidths.

3.5.2.8 MATCHING SECTION. This is a typical matching iris arrangement. Matching is accomplished after the other structures are built up and their empirical impedance determined by measurement. The matching coupling is then adjusted for optimum.

3.5.2.9 RECEIVE FILTERS. The receive filters are bandpass types intended to reject the transmit frequencies. They are of standard design, utilizing in-line tuned cavities with adjacent coupling. The field between the receive filters and the comparator coupling input apertures is such that it does not favor the transmit frequencies. The field is comparable to a waveguide below cutoff, a situation further increasing transmit frequency rejection.

3.5.2.10 MECHANICAL DESIGN. The mechanical structure depends upon making the feed cone strong enough to resist the shear forces. The sag of the cone will be kept within the cone limits. The feed is an all-waveguide structure. A simple bracket attachment will be developed to mount the assembly (in addition to the feed-mounting ring). The weight of the total structure is expected to be approximately 500 pounds.

3.5.2.11 VSWR. It is expected that because of the rather stringent filter, orthomode junction, and coupler designs, the VSWR in the receive feed may, at random narrow points (approximately 5 MHz apart), rise to a maximum of 1.5:1; however, the design will meet the 1.2:1 VSWR requirement over most of the specified receive band. It is possible to provide tuning adjustments to move a random point away from a much-used frequency.

3.5.2.12 SIDE LOBE LEVELS. It is predicted that side lobe levels will be 15 db minimum rather than the 18 db design goal.

3.5.2.13 SUBREFLECTOR. The presently-installed subreflector subassembly associated with this cassegrain feed system is assumed satisfactory and only minor readjustments are anticipated.

3.6 RECEIVING SUBSYSTEM

The description of the Receiving Subsystem which follows is subdivided according to major functional assemblies of the subsystem: (1) Parametric Amplifier-Converter, (2) Multicouplers, (3) Multifunctional Receiver, (4) Subcarrier Receiver, (5) Doppler Extractor, and (6) the Digital Rate Aid Unit.

3.6.1 Parametric Amplifier - Converter

The Parametric Amplifier - Converter assembly will be a major subcontract item. It is anticipated that the subcontractor will be Airborne Instruments Laboratory (AIL), New York. Subcontractor evaluation has shown AIL to have the necessary capability to produce the required assembly and a history of satisfactory production of similar units.

The assembly will consist of two units: (1) a parametric amplifier-converter unit mounted on the antenna, and (2) a control panel in the Instrumentation Building. For the Rosman, Carnarvon and Tananarive sites, the antenna-mounted unit will be installed externally at the rear of the reflector. For the Fairbanks site, the antenna-mounted unit will be installed in the enclosure directly behind the feed assembly. The Parametric Amplifier-Converter assembly will have the following required characteristics:

Input Frequency	2200 to 2300 MHz
Channels	6
Pumps	2
Stages Per Channel	2
Bandwidth (3 db)	100 MHz
Noise Figure	2 db maximum
Gain (Adjustable)	25 to 35 db
Gain Stability	±1 db
Impedance	50 ohms
Dynamic Range	Threshold to -50 dbm
Phase Stability	10 degrees differential between channels
VSWR (Input)	1.5 to 1
VSWR (Output)	1.75 to 1
Weight	175 lb maximum

With the first IF selected as 400 to 500 MHz, the required first local oscillator frequency is 1800 MHz. A 30-MHz fixed reference will be supplied to the parametric amplifier-converter unit by the receiver synthesizer of the System Signal Source. The 30 MHz will be multiplied by 60 within the parametric amplifier-converter unit to obtain the 1800 MHz local oscillator frequency.

3.6.1.1 ENVIRONMENT. Combining the general environmental requirements with the specific environmental requirements for antenna-mounted equipment has led to the following temperature requirements being placed on all four of the parametric amplifier-converter units.

a. Operate to specifications at temperatures between +120°F and 0°F.

b. Survive and operate with degraded performance at temperatures from +120°F to +130°F and from 0°F to -20°F.

Although lower outside temperatures are experienced at the Fairbanks site, the unit at that site will be in the wheelhouse enclosure where the temperature should not fall below -20°F.

3.6.1.2 TWO-STAGE CHANNELS. Analysis has shown that the two-stage per channel approach has several inherent characteristics that increase the performance:

a. Noise Figure: Greater assurance of meeting the 2 db specification.

b. Bandwidth: The wide bandwidth of 100 MHz (and greater) makes remote tuning and varactor selection much less critical.

c. Gain: A large reserve of stable gain is available in the event of gain deterioration in other parts of the system.

d. Reliability: Should one stage fail, the gain reduction will be only 2 db; the noise figure will increase to 4.9 db for first-stage failure and 2.0 db for second-stage failure.

3.6.1.3 CONTROL PANEL. This unit will contain klystron and bias voltage power supplies. Provisions will be incorporated to allow operation of the pump attenuator (parametric amplifier gain control) and adjustment of the parametric amplifier bias voltage from the control panel.

Also incorporated into the control panel will be circuits for monitoring the pump klystron output power and mixer diode bias current. The controls and monitor circuit on the control panel will consist of the above items and those required in the equipment specification.

Two klystron power supplies will be mounted in the instrumentation building, one for each pump klystron in the antenna enclosure. All operating parameters of the klystron will be monitored on the control panel.

3.6.1.4 ANTENNA ENCLOSURE. The enclosure will contain all the RF hardware and solid-state power supplies required for operation and will be thermally insulated. A redundant thermostatically-controlled heater circuit will maintain the interior temperature close to that of the highest ambient temperature (+120°F). The units within the enclosure can be divided into two main groups: (1) the parametric amplifier, and (2) the down converter.

Major components of the parametric amplifier include the circulator, parametric amplifier mount, directional coupler, pump filter, pump attenuator, power divider, isolator, and klystron. When combined, these components form the six-channel parametric amplifier providing the low-noise gain needed to mask the converter noise figure. Basically, the amplifier is a one-port negative-resistance amplifier with a circulator separating the input port from the output port. Amplification takes place in a diode mount comprised of a varactor diode, signal circuit, idler circuit, and pump feed network. All six amplifiers of each stage are pumped from a common klystron. Pump power is directed to the individual channels by hybrids. Pump level is controlled by a motor-driven attenuator that provides amplifier gain control. A band-pass filter in the pump circuit of each amplifier reduces interchannel coupling, thus ensuring the required 50 db of channel-to-channel isolation.

Each converter channel consists of a fixed tuned preselector, a balanced mixer, and a transistor IF amplifier. The IF amplifier will be centered at 450 MHz with a 1-db bandwidth in excess of 100 MHz. Each converter channel will be separate to ensure the decoupling required for 50 db overall isolation. Coupling through the local oscillator divider will be kept at the required level by using high-isolation balanced mixers and by dividing the local oscillator power with hybrids. The local oscillator signal will be derived from a solid-state frequency multiplier. The frequency multiplier will be driven by a 30 MHz signal at +7 dbm from the System Signal Source. Frequency multiplier output will be fixed at 1800 MHz at sufficient power to drive the six balanced mixers.

3.6.1.5 PARAMETRIC AMPLIFIER CONVERTER COMPONENTS. Significant elements of the parametric amplifier-converter are discussed below.

3.6.1.5.1 Circulator. The input circulator separates the input and output ports of the parametric amplifier and reduces the effects of any external impedance variations. The circulator will have a minimum isolation of 28 db at the signal frequency, a maximum loss of 0.2 db, and a maximum SWR of 1.10.

With the parametric amplifier operating at a gain of 13 db, the high isolation of the circulator will limit the SWR (looking into the amplifier) to less than 1.50.

An additional input circulator will not be needed since sufficient isolation can be obtained in one circulator to meet all stability specifications.

3.6.1.5.2 Parametric Amplifier. The parametric amplifier mount is a balanced diode configuration identical to a unit being supplied to NASA. The amplifier, which was developed at AIL, offers four unique features:

a. Separation of signal and idler frequencies without the use of filtering

b. A broadband pump circuit

c. A voltage-tunable idler circuit

d. Replacement of varactor diodes without disassembly of the mount.

The signal-idler isolation is accomplished by cancelling the idler currents in the signal current connection by proper phasing of the two idler currents generated by mixing the signal and pump frequencies in the diodes. The elimination of external filtering ensures maximum bandwidth. The broadband pump circuit consists of a two-step waveguide transformer. The waveguide dimensions are chosen such that the pump circuit is "cut-off" to the idler frequency, thus precluding idler loading.

The diode mount to be used for this equipment is designed for varactor diode replacement. The varactor diodes are removed and replaced simply by removing the large knobs protruding from the mount body. The method is similar to that employed for diode replacement in a balanced mixer.

3.6.1.5.3 Pump Attenuator. The pump attenuator is a motor-driven unit controlled from the control panel. A DC motor operating through a gear reducer provides accurate control of pump level to the amplifier mounts. Provisions are included to prevent damage to the attenuator from attempting to run the attenuator element beyond mechanical design limits.

3.6.1.5.4 Klystron and Power Divider Network. The VA266A klystron used in this equipment was chosen because of a long warranteed life of 5000 hours. The klystron will be operated below its rated output power capacity, thus ensuring maximum life.

The pump power divider network consists of a series of waveguide hybrids and couplers. The design is such that isolation is maintained between the channels of the parametric amplifier-converter at the sum and idler frequencies of the parametric amplifiers. A single element filter at the pump input to each parametric amplifier will ensure the required isolation between channels.

3.6.1.5.5 Directional Coupler. A 17-db directional coupler preceding each of the six channels will permit monitoring the parametric amplifier noise figure or injecting a test signal.

3.6.2 Multicouplers

3.6.2.1 ELECTRICAL DESIGN. The multicouplers used in the GRARR System will consist of low noise-figure broadband amplifiers followed by passive hybrid power dividers. Each of the two sum channels has a 25 db gain amplifier followed by five cascaded hybrids and two 3 db attenuators. Six outputs are provided at a level 15 db above the amplifier input. Each error channel has a 25 db gain amplifier followed by a hybrid divider and two 7 db attenuators. The gain of the error channel multicouplers is therefore the same as the sum channels. The multicoupler gain of 15 db is sufficient to meet the specified 6 db noise while not compromising the high signal level performance.

In Figure 3-40, signal levels are shown for the threshold case, -161 dbm, and the maximum input case, -50 dbm, at the antenna preamplifier input. Note that a gain of 25 db (+35 db in the preamplifier converter and -10 db cable loss) is assumed ahead of the multicouplers. Should the antenna cable loss be less than 10 db, the preamplifier converter gain can be reduced, so that the gain preceding the multicoupler remains 25 db. As indicated in Figure 3.6.2, the use of a 400-500 MHz amplifier with a 3.5 db noise figure permits a 6 db noise figure at the multicoupler input, assuming a second converter design as pictured. Such an amplifier is commercially available from several sources. The hybrids at the output of the multicouplers will provide a minimum of 30 db isolation between outputs.

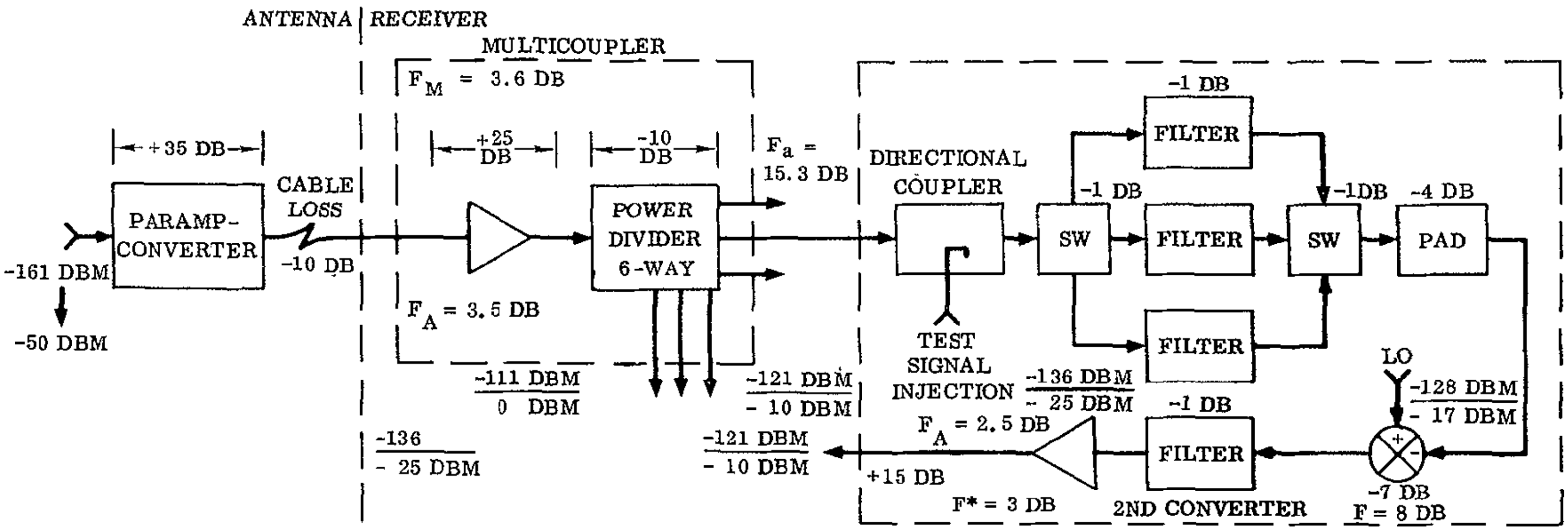

$$F_R = F_M + \frac{F_C - 1}{G_M} = 2.27 + \frac{34.1-1}{31.6} = 5.2 \text{ DB}$$

(IF CABLE LOSSES BETWEEN MULTIPLIER AND CONVERTER = 2 DB, $F_R = 2.27 + \frac{50.1 + 2.5}{31.6} = 2.27 + 1.67 = 3.94$ OR 5.95 DB

Figure 3-40. Multicoupler and Second Converter Gain Distribution

3.6.2.2 MECHANICAL DESIGN. Both the amplifiers and the hybrids are integrally-packaged sealed units, which require no maintenance. They will be mounted on a flat vertical panel at the lower rear of the receiver rack. The power supply for the amplifiers will also be mounted on the panel. In this manner the multicouplers are self-contained and may be relocated should future additions to the Receiver Subsystem require it.

3.6.3 Multifunctional Receiver

This description of the Multifunctional Receiver (MFR) is subdivided into detailed discussions according to the following breakdown:

a. Sum and Error Channel

b. Telemetry Demodulator

c. Spectrum Display Unit and Lissajous/Monitor

d. Receiver Control and Monitor Panels

e. Mechanical Design

3.6.3.1 SUM AND ERROR CHANNEL DESIGN. Throughout the design development discussed here and dealing with the gain distribution in the sum and error channel IF amplifiers, two important requirements were carefully weighed. One requirement, that the amplifier stages remain linear in the presence of large noise power at phase lock threshold, imposed signal maintenance at a relatively low level in the wideband stages. However, this imposed the second requirement; avoiding degradation in the signal-to-noise ratio of high-level wideband signals, since residual circuit noise power becomes significant with respect to the signal power. The gain distribution has therefore been assigned with these two conflicting requirements as boundaries. That is, the signal level has been set as high as possible, consistent with the high noise power requirement, at the critical locations in the receiver.

In this receiver, all gain control is performed in the second IF amplifier. Therefore, it is at the output of the amplifier that the signal level determines the signal-to-noise ratio for a high level wideband signal. (This ratio is sometimes called the "ultimate signal-to-noise ratio", since the output signal-to-noise ratio ceases to become a function of the input signal-to-noise ratio.)

The signal and noise calculations shown on the diagrams that follow indicate that a poor signal-to-noise ratio (about 15 db) will exist in the 20 MHz IF/BW under strong signal conditions.

The specification requires that means be provided for improving this signal-to-noise ratio to at least 30 db. To accomplish this, a 20 db attenuator, controlled by the telemetry S/N switch, is inserted into the third IF amplifier signal path of each sum and error channel.

This causes the signal level at the output of the second IF amplifier to assume a new level 20 db above the normal operation level. Calculations indicate that the 30 db signal-to-noise ratio may then be met. The compromise for this action is that as phase-lock threshold is approached, limiting action will occur due to the high noise power. The overall effect will be to degrade phase-lock threshold by 10 to 20 db in the narrower tracking bandwidths. The telemetry output from the wideband combiner, where the second IF amplifier outputs are diversity combined, are attenuated by 20 db when the telemetry S/N switch is thrown, in order that all signal levels remain consistent at the demodulators.

An overall block diagram of the 6-channel Multifunctional Receiver including the S-Band preamplifier-converter is shown in Figure 3-41. The operating frequencies selected in the frequency analysis are indicated on the diagram, as well as the significant functional blocks. Directional couplers are indicated in each IF path for the insertion of fault isolation signals. Outputs from each sum channel IF amplifier are provided to drive the ranging demodulator with uncombined signals in a test mode. In this mode a manual patch at the rear of the sum channel drawer permits the ranging system to be tested with any effects of polarization diversity combining removed. A manually operated switch is also provided at this point to select the VCO input to the doppler extractor corresponding to the patched-in sum channel.

3.6.3.1.1 Second Converter. Gain distribution for the second converter is shown in Figure 3-40. The three switched filters which precede the converter divide the 100 MHz receive band according to the center frequencies and bandwidths discussed in the frequency analysis, Paragraph 4.3. Control signals for the switches are obtained from the receiver frequency select controls, located on the receiver control panel.

The switches are 3-position PIN diode types having isolations greater than 55 db. A 4 db pad is inserted between the filters and the double-balanced mixer in order to provide a good impedance match for the filters. The filter characteristics in the two sum channels must be carefully controlled in order that the differential group delay remain small. The 4 db pad will sufficiently isolate small differences in the mixer impedance to insure stable operation. The filter following the mixer is a simple two-pole design which removes the local oscillator and input signal from the second IF and determines the noise bandwidth of the second IF. The filter exhibits a flat response over a 20 MHz bandwidth and a noise bandwidth of approximately 32 MHz. A low-noise amplifier follows the filter. The noise figure and gain of this stage permit the overall noise figure of 6 db at the multicoupler input to be attained.

3.6.3.1.2 Second IF Amplifier Gain Distribution. A detailed diagram for the second IF amplifier is given in Figure 3-42. The tabulated numbers on this diagram and the others that follow are:

S = Signal power (dbm)

N_i = Input noise power (dbm)

N_s = Internally-generated noise referred to the input (dbm)

N_t = Total noise, $N_s + N_i$ (dbm)

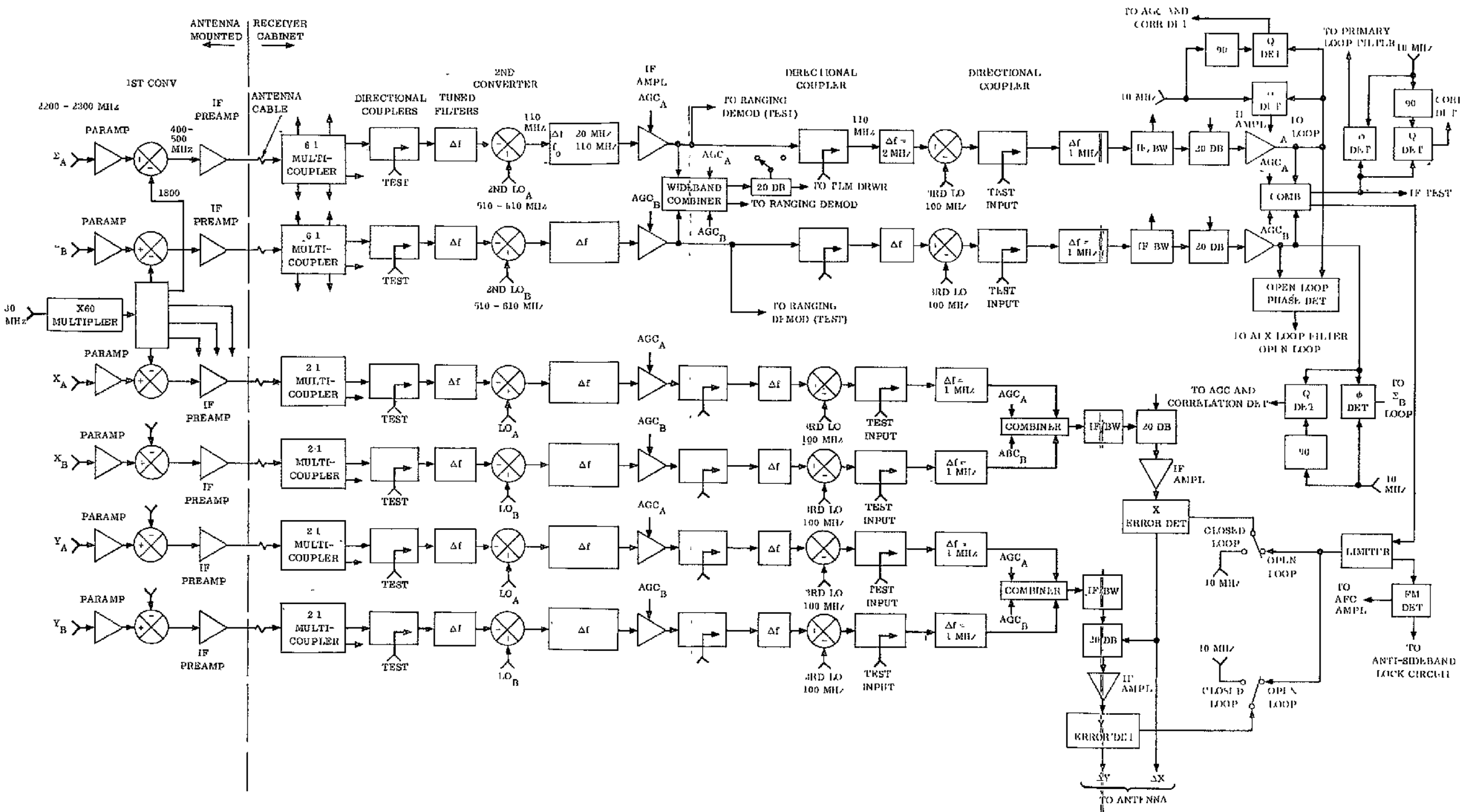

Figure 3-41. Multifunctional Receiver Block Diagram

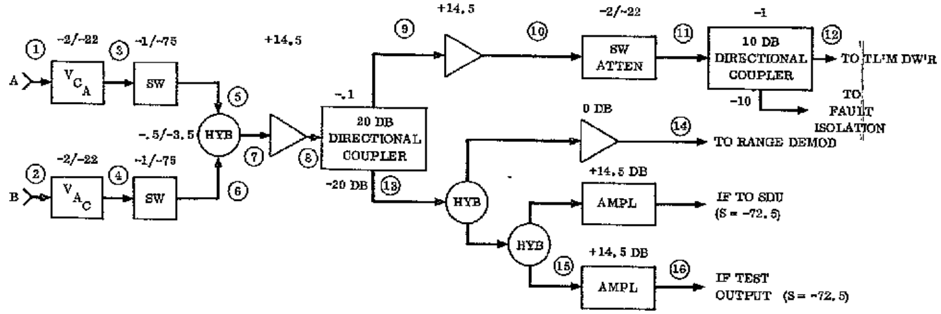

	1	2	3	4	5	6	7	8
S = -159 BOTH CHANNELS	S = -68 N_i = - 6 N_s = -91 N_t = - 6	S = -68 N_i = - 6 N_s = -91 N_t = - 6	S = -76 N_i = -14 N_s = -98 N_t = -14	S = -76 N_i = -14 N_s = -98 N_t = -14	S = -77 N_i = -15 N_s = -99 N_t = -15	S = -77 N_i = -15 N_s = -99 N_t = -15	S = -74.5 N_i = -15.5 N_s = -92.5 N_t = -15.5	S = -60 N_i = - 1 N_s = -99 N_t = - 1
S = -50 (BOTH CHANNELS)	S = -68 N_i = -94.5 N_s = -91 N_t = -89.4	S = -68 N_i = -94.5 N_s = -91 N_t = -89.4	S = -76 N_i = -97.4 N_s = -98 N_t = -94.9	S = -76 N_i = -97.4 N_s = -98 N_t = -94.9	S = -77 N_i = -95.9 N_s = -99 N_t = -94.2	S = -77 N_i = -95.9 N_s = -99 N_t = -94.2	S = -74.5 N_i = -94.7 N_s = -92.5 N_t = -90.5	S = -60 N_i = -76.0 N_s = -99 N_t = -76.0
S_A = -50 S_B = -161	S = -68 N_i = -95.5 N_s = -97 N_t = -93.2	S = -68 N_i = - 4 N_s = -77 N_t = - 4	S = -70 N_i = -95.2 N_s = -98 N_t = -93.4	S = -90 N_i = -25 N_s = -24 N_t = -21.9	S = -71 N_i = -94.4 N_s = -99 N_t = -93.1	S = -165 N_i = - 96.9 N_s = - 99 N_t = - 94.9	S = -74.5 N_i = -94.8 N_s = -92.5 N_t = -90.5	S = -60 N_i = -76 N_s = -99 N_t = -76
S = -50 (BOTH CHANNELS) 20 DB S/N RATIO SWITCH IN	S = -48 N_i = -90.9 N_s = -91 N_t = -88	S = -48 N_i = -90.9 N_s = -91 N_t = -88	S = -56 N_i = -96 N_s = -98 N_t = -93.9	S = -56 N_i = -96 N_s = -98 N_t = -93.9	S = -57 N_i = -94.9 N_s = -99 N_t = -93.5	S = -57 N_i = -94.9 N_s = -99 N_t = -93.5	S = -54.5 N_i = -94 N_s = -92.5 N_t = -90.2	S = -40 N_i = -75.7 N_s = -99 N_t = -75.7

	9	10	11	12	13	14	15
S = -159 BOTH CHANNELS	S = -59.1 N_i = - 1.1 N_s = -92.5 N_t = - 1.1	S = -45.6* N_i = +13.4 N_s = -97 N_t = +13.4	S = -47.6 N_i = +11.4	S = -48.6 N_i = +10.4	S = -80 N_i = -21 N_s = -99 N_t = -21	S = -83.5 N_i = -24.5	S = -87 N_i = -28
S = -50 (BOTH CHANNELS)	S = -60.1 N_i = -76.1 N_s = -92.5 N_t = -76.0	S = -45.6 N_i = -61.5 N_s = -97 N_t = -61.5	S = -47.6 N_i = -63.5 N_s = -98 N_t = -63.5	S = -48.6 N_i = -63.5	S = -80 N_i = -96 N_s = -99 N_t = -94.2	S = -83.5 N_i = -97.6	
S_A = -50 S_B = -161	S = -60.1 N_i = -76.1 N_s = -92.5 N_t = -76	S = -45.6 N_i = -61.5 N_s = -97 N_t = -61.5	S = -47.6 N_i = -63.5 N_s = -98 N_t = -63.5	S = -48.6 N_i = -63.5	S = -80 N_i = -96 N_s = -99 N_t = -94.2	S = -83.5 N_i = -97.6	
S = -50 (BOTH CHANNELS) 20 DB S/N RATIO SWITCH IN	S = -40.1 N_i = -75.8 N_s = -92.5 N_t = -75.7	S = -25.6 N_i = -61.2 N_s = -77 N_t = -61.1	S = -49.6 N_i = -81.6 N_s = -99 N_t = -81.5	S = -48.6 N_i = -82.5	S = -60 N_i = -95.7 N_s = -99 N_t = -94.1	S = -63.5 N_i = -98.2	

*AMPLIFIER SATURATED AT ϕ THRESHOLD

Figure 3-44. Wideband Combiner Gain Distribution

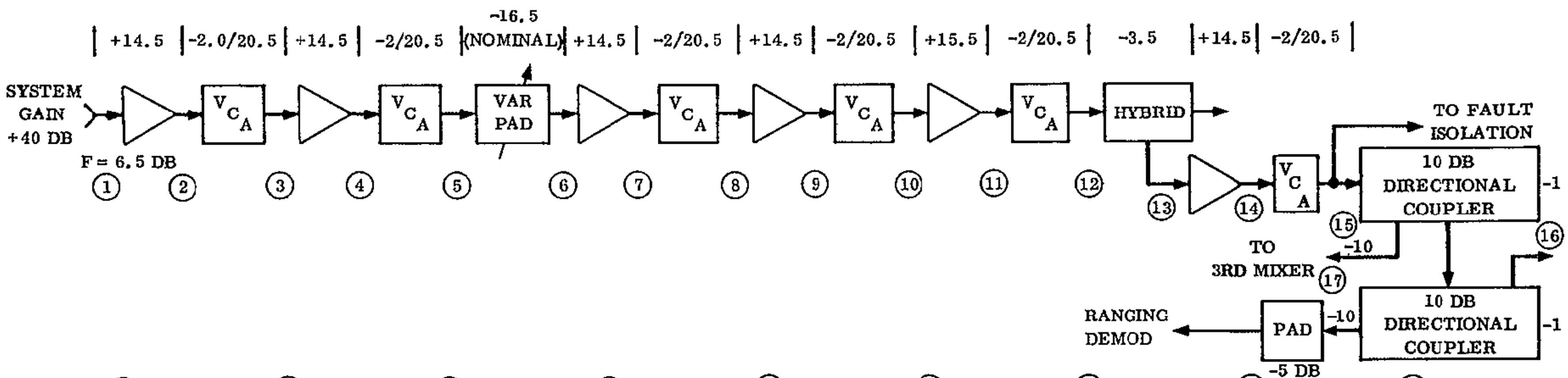

S = -161 INPUT

Point	S	N_i	N_s	N_t
1	-121	- 57	- 92.5	- 57
2	-106.5	- 42.5	- 97	- 42.5
3	-108.5	- 44.5	- 92.5	- 44.5
4	-94	-30	-97	-30
5	-96	-32	-82.5	-32
6	-112.5	- 48.5	- 92.5	- 48.5
7	-98	-34	-97	-34
8	-100	- 36	- 92.5	- 36
9	-85.5	-21.5	-97	-21.5
10	-87.5	-23.5	-92.5	-23.5
11	-73	- 9	-97	- 9
12	-75	-11	-99	-11
13	-78.5	-14.5	-92.5	-14.5
14	-64	0	-92.5	-14.5
15	-66	- 2	-99	- 2
16	-68	- 4		
17	-76	-12		

S = -59 ANTENNA INPUT

Point	S	N_i	N_s	N_t
1	-10	-57	-92.5	-57
2	+ 4.5	-42.5	-78.5	-42.5
3	-16	-64	-92.5	-64
4	- 1.5	-49.5	-78.5	-49.5
5	-22	-70	-88.5	-70
6	-38.5	-86 5	-92.5	-85.5
7	-24	-71	-78.5	-70.3
8	-44.5	-91.0	-92.5	-88.7
9	-30	-74.2	-78.5	-72.8
10	-50.5	-92.3	-92.5	-89.4
11	-36	-74.9	-78 5	73 3
12	-56.5	-93.5	-99	-92.4
13	-60	-95.9	-92.5	-90.9
14	-45.5	-76.4	-78.5	-74.4
15	-66	-94.9	-99	-93.5
16	-68	-95.5		
17	- 76	-103.5		

Figure 3-42. Second IF Amplifier Gain Distribution

The signal and noise powers at each interstage point in the IF amplifier are shown for input signal levels at the antenna preamplifier of -161 dbm and -50 dbm. The level of -161 dbm is the threshold value in the 3 Hz secondary loop bandwidth, assuming a noise density of -174 dbm/Hz at the preamplifier. Since the noise figure at this point will actually be 2 db, or an equivalent noise density of -172 dbm/Hz, the actual threshold in the secondary loop will be -159 dbm. However, the gain distribution has been calculated using the -161 dbm figure, to give some additional margin at threshold.

Referring to Figure 3-42, six building-block amplifiers and six VCA's provide the required gain and gain control. The output at point (16) is maintained at -68 dbm by the AGC system. This is the maximum allowable signal level at which the final VCA can operate and remain a linear device at the threshold noise power levels. This signal is sent to the wideband combiner and eventually to the wideband telemetry demodulators. Therefore, it is this signal level which determines the "ultimate signal-to-noise ratio".

Figure 3-43 shows the gain distribution when the telemetry S/N switch is thrown. Note that the signal level at point (16) is now -48 dbm.

Subsequent level analysis in the telemetry demodulator section (Paragraph 3.6.3.2) shows that this level is sufficient to obtain a 30 db signal-to-noise ratio in the 20 MHz IF/BW. The output at point (17) is sent to the third converter. Since this signal is translated to the third IF for phase lock and autotrack purposes, the ultimate signal-to-noise ratio is unimportant. Therefore this output is provided at a level 8 db below the output telemetry output, in order to minimize the telemetry signal-to-noise ratio degradation.

An additional signal is provided at a level corresponding to point (13) on the diagram. This output permits a future addition of a separate IF amplifier signal which would be gain-controlled to a higher output level. The additional output would be combined in a second wideband diversity combiner used for telemetry signals only. This addition would remove the necessity for operating the telemetry S/N switch.

3.6.3.1.3 Wideband Diversity Combiner. Figure 3-44 presents the gain distribution for the wideband diversity combiner. The signal and noise conditions for several different input signal conditions are shown. Levels are also shown for the strong signal condition (-50 dbm) with the telemetry S/N switch thrown.

For the condition where a strong signal exists in one sum channel and a weak signal in the other, it is necessary to switch the weaker signal completely off. Otherwise, the noise from the weaker channel would degrade the signal-to-noise ratio of the strong channel. Logic circuits will be used to sense a differential signal level between polarizations of 12 db, and operate the switches.

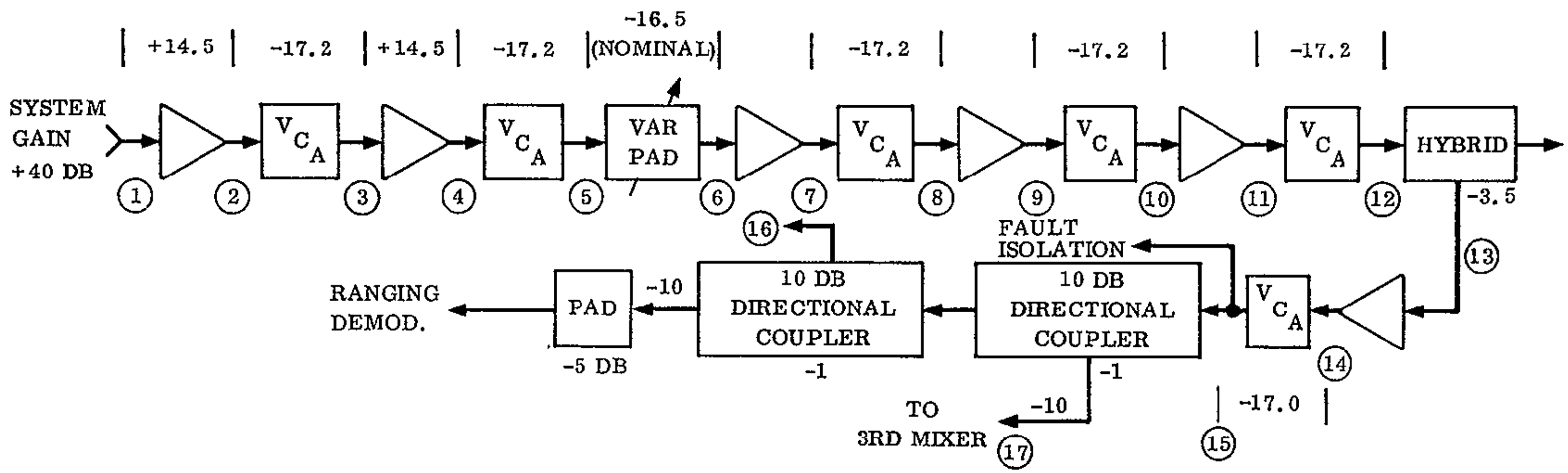

S = -50

Point	S	N_i	N_s	N_t
1	-10	-57	-92.5	-57
2	+ 4.5	-42.5	-81.8	-42.5
3	-12.7	-59.7	-92.5	-59.7
4	+ 1.8	-45.2	-81.8	-45.2
5	-15.4	-62.4	-82.5	-62.4
6	-31.9	-78.9	-92.5	-78.7
7	-17.4	-64.2	-81.8	-64.1
8	-34.6	-81.3	-92.5	-81.0
9	-20.1	-66.5	-81.8	-66.4
10	-37.3	-83.6	-92.5	-83.1
11	-22.8	-68.6	-81.8	-68.4
12	-40	-85.6	-99	-85.4
13	-43.5	-88.9	-92.5	-87.3
14	-29.0	-72.8	-82.0	-72.3
15	-46.0	-89.3	-99	-88.9
16	-48	-90.9		
17	- 58	-100.9		

Figure 3-43. Second IF Amplifier Gain Distribution (20 db S/N Switch In)

The VCA's which control the combiner in a close approximation of the ideal maximal ratio (as analyzed in Paragraph 4.3) are the standard building-block units. However, the control characteristic for the VCA will be shaped to provide the required linear transfer function. The phase shift in these VCA's over the first 10 db of gain variation is less than 3 degrees. This is a negligible amount for detection at the coherent ranging and telemetry demodulators.

Separate combined outputs are provided for telemetry and ranging. The ranging output is provided at a lower level (-83.5 dbm) in order to avoid noise saturation at phase lock threshold. The telemetry output is provided at a high level (-48.6 dbm) in order to preserve the signal-to-noise ratio of wideband signals. Other outputs are supplied for test purposes and for the spectrum display unit.

3.6.3.1.4 Sum Channel Third Converter and IF Amplifier. Gain distribution is shown in Figure 3-45. The most important criterion used in assigning gain distribution in this signal path is discrimination against strong interfering signals which could overload the receiver. Therefore, filters are placed as early as possible in the signal-path to provide maximum protection.

The wideband second IF amplifiers which precede the third converter are capable of handling signal strengths 70 db greater than the desired signal at phase-lock threshold. An interfering signal falling within the 2 MHz filter which precedes the third mixer will overload the mixer at a level approximately 60 db above the desired signal. Immediately following the mixer, the IF bandwidth is narrowed to 1 MHz. A 60-db overload capability is maintained to the filter bank, where the narrower band IF filters are selected. When the 10 KHz IF filter is selected, an interfering signal up to 60 db above the desired signal must fall within 5 KHz of the received signal before overload takes place.

Each of the four narrower IF filters (10, 30, 100 and 300 KHz bandwidths) is followed by a pad and phase-shift circuit adjusted to match the center frequency phase shift and insertion loss of each filter.

A 20 db attenuator is switched into the signal path at point (11), when the telemetry S/N switch is thrown, to redistribute the gain as discussed previously. Outputs from the sum channel third IF amplifier are distributed to the secondary phase detectors, the narrowband combiner, the open loop phase detector, and a third IF test output.

3.6.3.1.5 Sum Channel Narrowband Combiner and Reference Limiter. The signal and noise levels for the narrowband combiner are shown in Figure 3-46. The narrowband combiner circuits are essentially the same as the wideband combiner circuits. The same VCA building block will be used here, and therefore common control circuits may be used.

The combined output signal sent to the primary phase detector is also provided as a test signal output. The combined signal is also hard-limited in cascaded sideband-cancelling limiters and amplified for use in the open loop error product detectors and AFC discriminators.

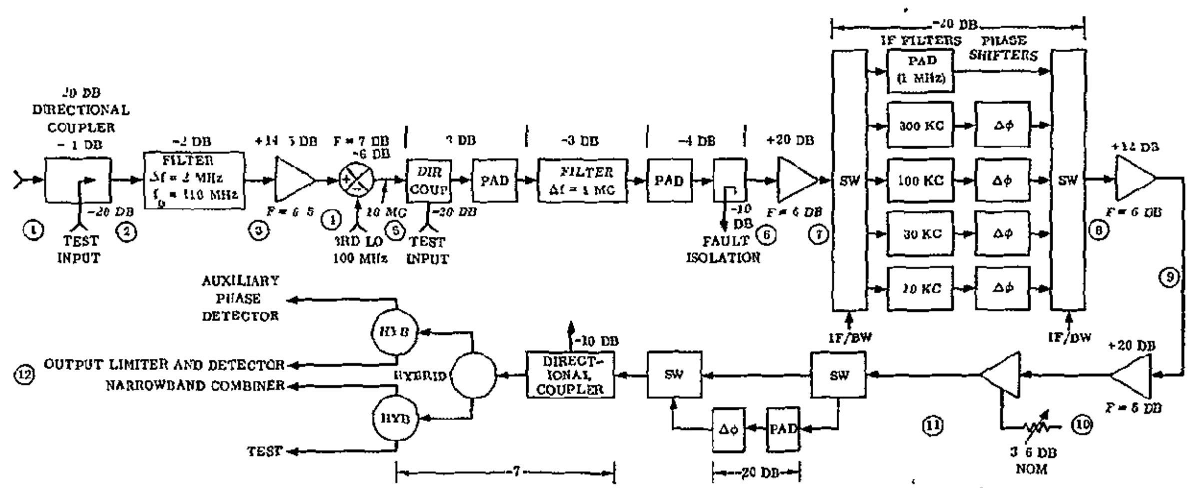

S = -161 INPUT

	1	2	3	4	5	6	7	8	9	10	11	12
S	-76	-76.1	-78.1	-63.6	-69.6	-79.6	-59.6	-79.6	-67.6	-47.6	-34	-41
N_i	-12	-12.1	-26.1	-11.6	-17.6	-30.6	-10.6	-50.6	-38.6	-18.6	-5	-12
N_s	-98.9	-97	-104.5	-104	-101	-108	-94	-128	-128	-128	-134	
N_t	-12	-12.1	-26.1	-11.6	-17.6	-30.6	-10.6	-50.6	-38.6	-18.6	-5	
BW	32 MHz	32 MHz	2 MHz	2 MHz	2 MHz	1 MHz	1 MHz	10 KHz	10 KHz	10 KHz	10 KHz	

S = -50 INPUT (OPEN LOOP 1 MHz)

	1	2	3	4	5	6	7	8	9	10	11	12
S	-76	-76.1	-79.1	-63.6	-69.6	-79.6	-59.6	-79.6	-67.6	-47.6	-34	-41
N_i	-103.5	-97.6	-105.5	-88.5	-94.4	-106.5	-84.2	-103.8	-90.4	-70.3	-56.7	-63.7
N_s	-99.9	-97	-101.5	-104	-101	-108	-94	-108	-108	-108	-134	
N_t	-97.6	-94.5	-100.0	-88.4	-93.5	-104.2	-83.8	-102.4	-90.3	-70.3	-56.7	
BW	32 MHz	32 MHz	2 MHz	2 MHz	2 MHz	1 MHz	1 MHz	1 MHz	1 MHz	1 MHz	1 MHz	

S = -134 INPUT (OPEN LOOP (10 KHz)

	1	2	3	4	5	6	7	8	9	10	11	12
S	-79	-79.1	-81.1	-66.6	-72.6	-82.6	-62.6	-82.6	-70.6	-50.6	-37	-44
N_i	-44	-44.1	-58.1	-43.6	-49.6	-62.6	-42.6	-82.6	-70.6	-50.6	-37	-44
N_s	-98.9	-97	-104.5	-104	-101	-108	-94	-128	-128	-128	-134	
N_t	-44	-44.1	-58.1	-43.6	-49.6	-62.6	-42.6	-82.6	-70.6	-50.6	-37	
BW	32 MHz	32 MHz	2 MHz	2 MHz	2 MHz	1 MHz	1 MHz	10 KHz	10 KHz	10 KHz	10 KHz	

S = -114 (BOTH INPUTS) (OPEN LOOP 1 MHz)

	1	2	3	4	5	6	7	8	9	10	11	12
S	-79	-79.1	-81.1	-66.6	-72.6	-82.6	-62.6	-82.6	-70.6	-50.6	-37	-44
N_i	-64	-64.1	-78.1	-63.6	-69.6	-82.6	-62.6	-82.6	-70.6	-50.6	-37	-44
N_s	-98.9	-97	-104.5	-104	-101	-108	-94	-108	-108	-108	-114	
N_t	-64	-64.1	-78.1	-63.6	-69.6	-82.6	-62.6	-82.6	-70.6	-50.6	-37	
BW	32 MHz	32 MHz	2 MHz	2 MHz	2 MHz	1 MHz						

BW = 1 MHz (points 7–12)

Figure 3-45. Sum Channel 3rd Mixer and 3rd IF Amplifier Gain Distribution

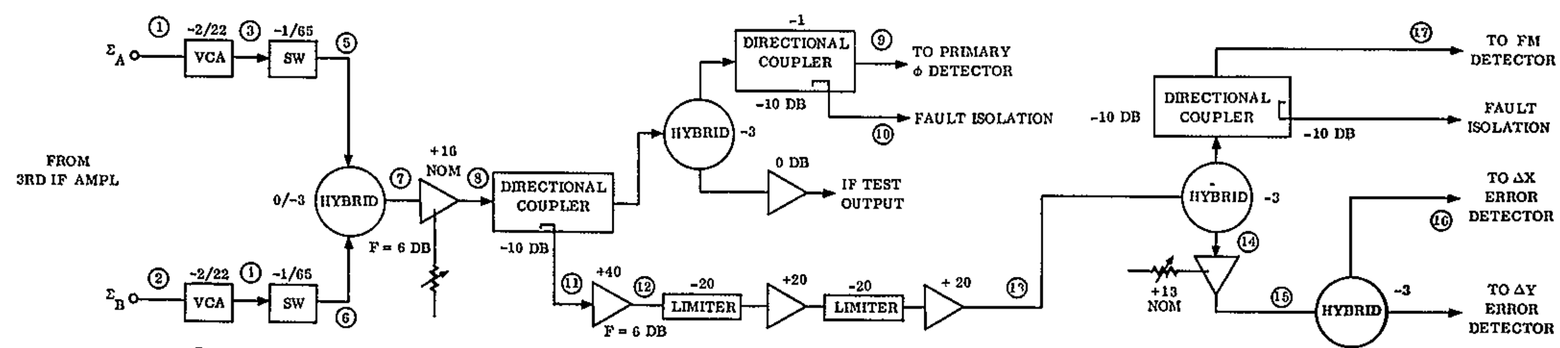

S = -159 (BOTH CHANNELS)

Point	S	N_i	N_s	N_t	BW
1	-41	-14	-126	-14	10 KHz
2	-41	-14	-126	-14	
3	-49	-22	-133	-22	
4	-49	-22	-133	-22	
5	-50	-23	-134	-23	
6	-50	-23	-134	-23	
7	-47	-23	-128	-23	
8	-31	-7	-134	7	
9	-36	-12			
10	-35	-11			
11	-41	-21	-128	-21	

S = -134 (BOTH CHANNELS) OPEN LOOP BW = 10 KHz

Point	S	N_i	N_s	N_t
1	-44	-44	-126	-44
2	-44	-44	-126	-44
3	-52	-52	-133	-52
4	-52	-52	-133	-52
5	-53	-53	-134	-53
6	-59	-53	-134	-53
7	-50	-53	-128	-53
8	-34	-37	-134	-37
9	-39	-42		
10	-38	-41		
11	-44	-47	-128	-47
12	-4	-7	-128	-7
13	-4	-7		
14	-7	-10		
15	+6	+3		
16	+3	0		
17	-8	-11		

S = -50 (BOTH CHANNELS) OPEN LOOP BW = 1 MHz

Point	S	N_i	N_s	N_t	BW
1	-41	-63 7	-106	-63 7	1 MHz
2	-41	-63 7	-106	-63 7	
3	-19	-71 7	-113	-71 7	
4	-49	-71 7	-113	-71 7	
5	-50	-72.7	-114	-72 7	
6	-50	-72 7	-114	-72 7	
7	-47	-72 7	-108	-72 7	
8	-31	-56 7	-114	-56 7	
9	-36	-61.7			
10	-35	-60 7			
11	-41	-66 7	-108	-66 7	
12	-1	-26 7	-91	-26 7	
13	-1	-26 7			
14	-1	-29 7			
15	+9	-16 7			
16	+6	-19 7			
17	-5	-307			

S_A = -50
S_B = -161

Point	S	N_i	N_s	N_t	BW
1	-41	-63 7	-13 2	-63 7	10 KHz
2	-11	-12	-132	-12	10 KHz
3	-43	-65 7	-133	-65 7	10 kHz
4	-63	-24	-69	-24	10 KHz
5	-44	-66 7	-134	-66 7	10 KHz
6	-128	-89	-134	-89	10 KHz
7	-47	-69 7	-128	69.7	

Figure 3-46. Narrowband Combiner and Reference Limiter Signal and Noise

3.6.3.1.6 Primary and Secondary Phase Detectors. The signal and noise levels for threshold levels in the secondary loop bandwidths are shown in Figure 3-47. In the closed loop mode, the IF/BW is selected as a function of tracking bandwidth as either 10 KHz or 100 KHz. This is necessary to maintain a reasonable signal-to-noise ratio in the narrower bandwidths and to minimize delay in the widest bandwidth. For the same reasons, two crystal filters are included in the phase detector module. Using the bandwidths indicated in Figure 3-47 the threshold signal-to-noise ratio at the phase detector is -17 db. Allowing a peak-to-rms noise ratio of 10 db, the phase detectors must be capable of detecting without limiting for noise peaks 27 db greater than the signal. Prior experience in the design of similar detectors, together with preliminary design work in this circuit indicate that the residual dc offset from the phase detectors, due to temperature, aging, and noise unbalance effects will be approximately 38 to 40 db below the signal output. When the loops are locked, this residual error is less than 0.8 degrees, which can be neglected in determining threshold and dynamic performance of the loop.

3.6.3.1.7 Error Channel Third Converter and IF Amplifier. Signal and noise levels for the error channel third converter and IF amplifier are shown in Figure 3-48. The design of the circuits shown on this diagram is identical to that for the sum channel circuits. The same degree of overload protection from strong interfering signals is provided here.

The four error channels are separately converted and filtered to a 1 MHz IF/BW as detailed in Figure 3-47. However, before further filtering is performed, the separate polarizations are combined in the narrowband error channel combiner. Figure 3-49 details the signal and noise levels in the error channel combiner and third IF amplifiers. By combining at this point in the signal path, the number of IF filters is reduced. That is, the 10 KHz, 30 KHz, 100 KHz and 300 KHz error channel IF bandwidths are selected after the A and B channels are combined.

A 20 db attenuator selected by the telemetry S/N switch is included in the error channels, as it was in the sum channels, in order that error detector calibration remains unchanged when the switch is thrown.

3.6.3.1.8 Error Product Detector. In Figure 3-50, signal and noise levels are shown for the threshold cases in both open and closed loop modes. An error signal level is indicated 15 db below the sum channel level, consistent with Paragraph 4.5.4.4.1.1.1 of the specification.

The dual quad detector itself, and the amplifier stages which drive it, are sufficiently broadband to operate over a 1 MHz bandwidth. Therefore, to select open or closed-loop mode it is necessary only to switch a narrowband noise filter into the signal path in the closed-loop mode, and switch the 10 MHz reference signal into the reference driver stage. A post-detection filter and amplifier amplify the error signal to the required 10 volt output level.

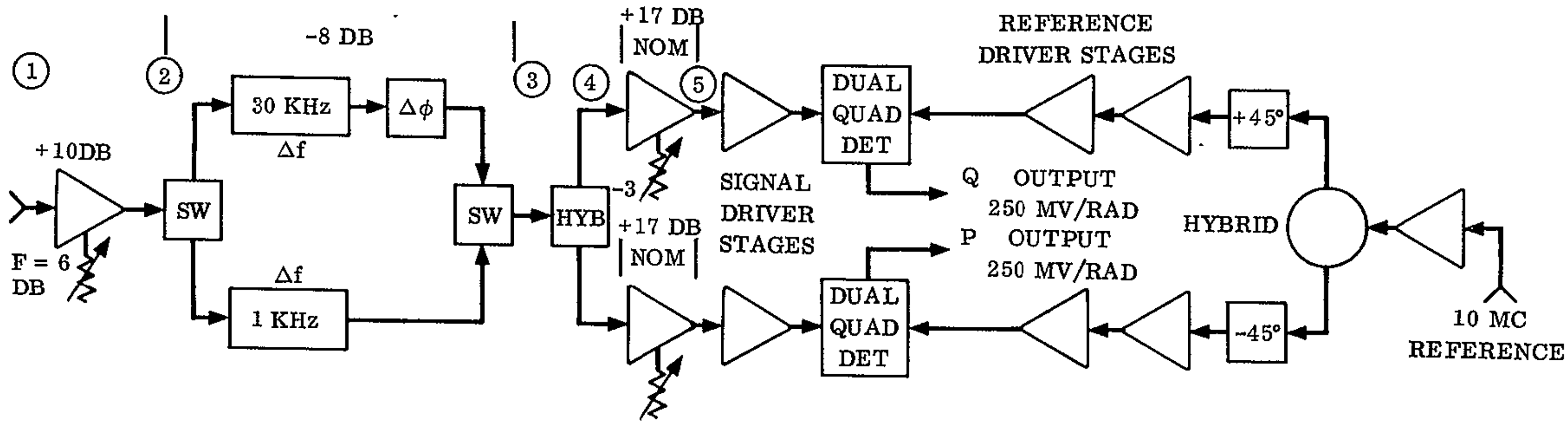

	PRIMARY TRACKING BW	IF/BW	1 LEVELS	2 LEVELS	3 LEVELS	Δf	4	5
S = -161	10 Hz	10 KHz	S = -41	S = -31	S = -39	1 KHz	S = -42	S = -25
			N = -12	N = -2	N = -20		N = -23	N = -6
	30 Hz	10 KHz	S = -41	S = -31	S = -39	1 KHz	S = -42	S = -25
			N = -17	N = -7	N = -25		N = -28	N = -11
	100 Hz	100 KHz	S = -41	S = -31	S = -39	30 KHz	S = -42	S = -25
			N = -12	N = -2	N = -20		N = -23	N = -6
	300 Hz	100 KHz	S = -41	S = -31	S = -39	30 KHz	S = -42	S = -25
			N = -17	N = -7	N = -25		N = -28	N = -11
	1000 Hz	100 KHz	S = -41	S = -31	S = -39	30 KHz	S = -42	S = -25
			N = -22	N ≐ -12	N = -30		N = -33	N = -16
	3000 Hz	100 KHz	S = -41	S = -31	S = -39	30 KHz	S = -42	S = -25
			N = -27	N = -17	N = -35		N = -38	N = -21

Figure 3-47. Phase Detectors Gain Distribution

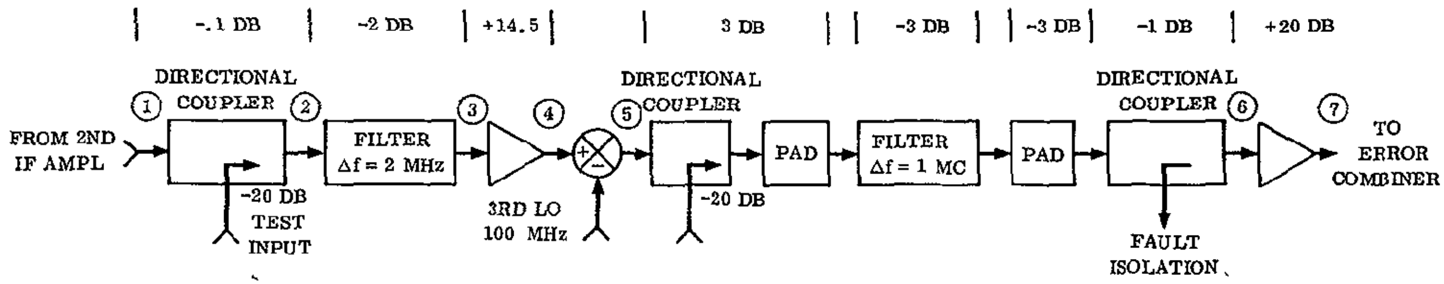

		①	②	③	④	⑤	⑥	⑦
S = -161	S	-76	-76.1	-78.1	-63.6	-69.6	-79.6	-59.6
	N_i	-12	-12.1	-26.1	-11.6	-17 6	-30.6	-10.6
	N_s	-98.9	-97	-104.5	-104	-101	-108	-94
	N_t	-12	-12.1	-26.1	-11.6	-17.6	-30.6	-10.6
	BW	32 MHz	32 MHz	2 MHz	2 MHz	2 MHz	1 MHz	1 MHz
S = -50 BOTH INPUTS OPEN LOOP (1 MHz)	S	-76						-59.6
	N_i	-103.5						-84.2
	N_s	-98.9						
	N_t	-97.6						
	BW	32 MHz						1 MHz
S = -134 BOTH INPUTS OPEN LOOP (10 KHz)	S	-79						-62.6
	N_i	-44						-42 6
	N_s	-98.9						
	N_t	-44						
	BW	32 MHz						1 MHz
S = -114 BOTH INPUTS OPEN LOOP (1 MHz)	S	-79						-62.6
	N_i	-64						-62.6
	N_s	-98.9						
	N_t	-64						
	BW	32 MHz						1 MHz

Figure 3-48. Error Channel Third Converter and IF Amplifier Gain Distribution

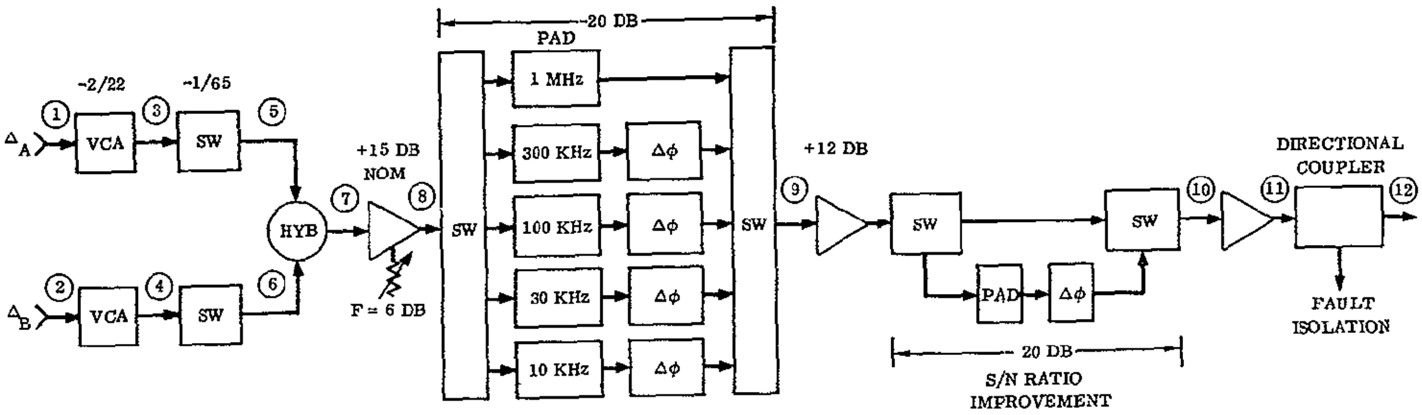

S = -159
BOTH
CHANNELS

	1	2	3	4	5	6
S	-59.6	-59.6	-67.6	-67 6	-68 6	-68 6
N_i	-12.6	-12.6	-20 6	-20 6	-21.6	-21.6
N_s	-106	-126	-113	-113	-114	-114
N_t	-12.6	-12 6	-20 6	-20.6	-21 6	-21 6
BW	1 MHz	1 MHz	→ 1 MHz			

	7	8	9	10	11	12
S	-65.6	-50.6	-70.6	-58 6	-38.6	-39.6
N_i	-21.6	-6 6	-46.6	-34.6	-14 6	-15 6
N_s	-114	-94	-128	-128	-128	
N_t	-21.6	-6 6	-46.6	-34.6	-14.6	
BW	→	1 MHz	10 KHz	→ 10 KHz		

S = -50
BOTH CHANNELS
OPEN LOOP
BW = 1 MHz

	1	2	3	4	5	6
S	-59.6	-59.6	-67.6	-67 6	-68.6	-68 6
N_i	-84.2	-84 2	-92.2	-92.2	-93 2	-93 2
N_s	-106	-106	-113	-113	-114	-114
N_t	-84.2	-84.2	-92.2	-92.2	-92.2	-92.2
BW	1 MHz → 1 MHz					

	7	8	9	10	11	12
S	-65.6	-50.6	-70 6	-58 6	-38 6	-39.6
N_i	-92 2	-77.1	-97	-84 7	-64.7	-65 7
N_s	-108	-94	-108	-108	-108	
N_t	-92.1	-77	-96.7	-84 7	-64.7	
BW	1 MHz → 1 MHz					

Figure 3-49. Error Channel Combiner and Third IF Amplifier Gain Distribution

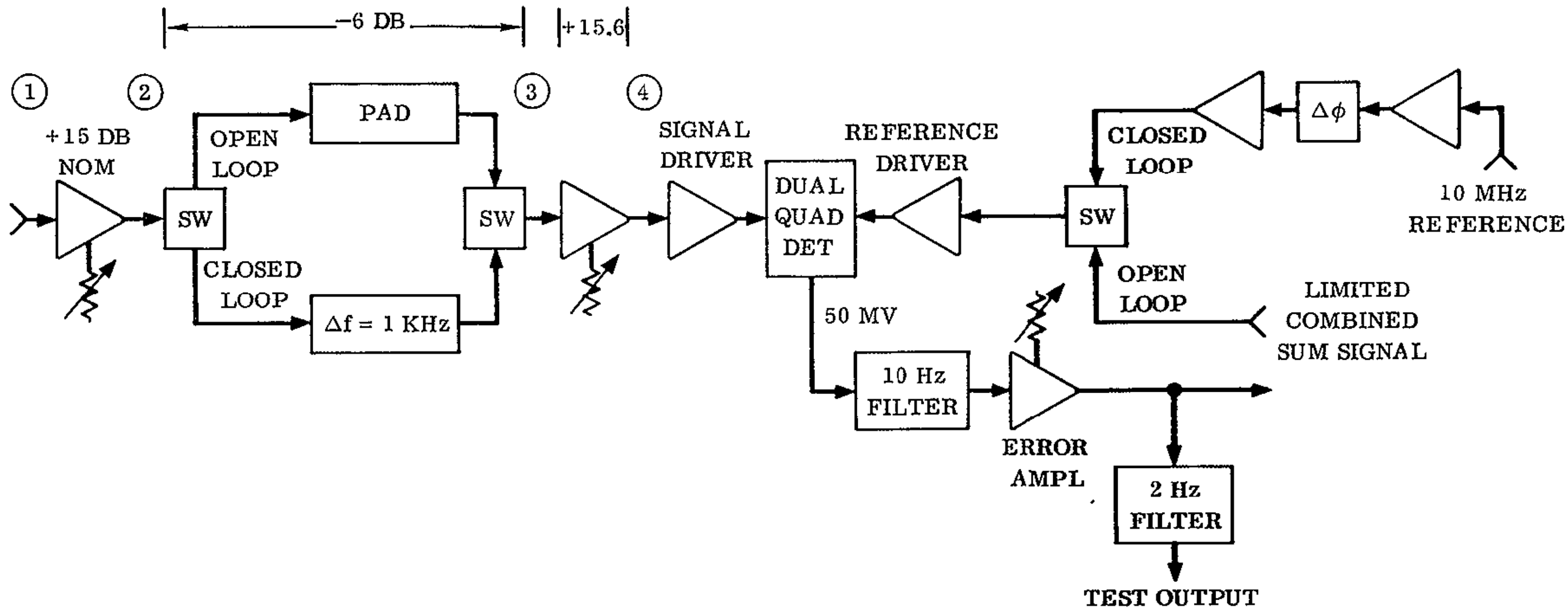

	MODE	IF/BW	1	2	3	4
S_3 = -159 AT BOTH SUM CHANNELS S_Δ = -174 BOTH ERROR CHANNELS	CLOSED LOOP	10 KHz	S = -54.6 N = -15.6	S = -39.6 N = -.6 BW = 1 KHz	S = -45.6 N = -16.6	S = -30 N = -1
S_Σ = -134 BOTH SUM CHANNELS S_Δ = -149 BOTH ERROR CHANNELS	OPEN LOOP	10 KHz	S = -57.6 N = -42.6	S = -42.6 N = -27.6	S = -48.6 N = -33.6	S = -33.6 N = -18.6

Figure 3-50. Error Product Detector Gain Distribution

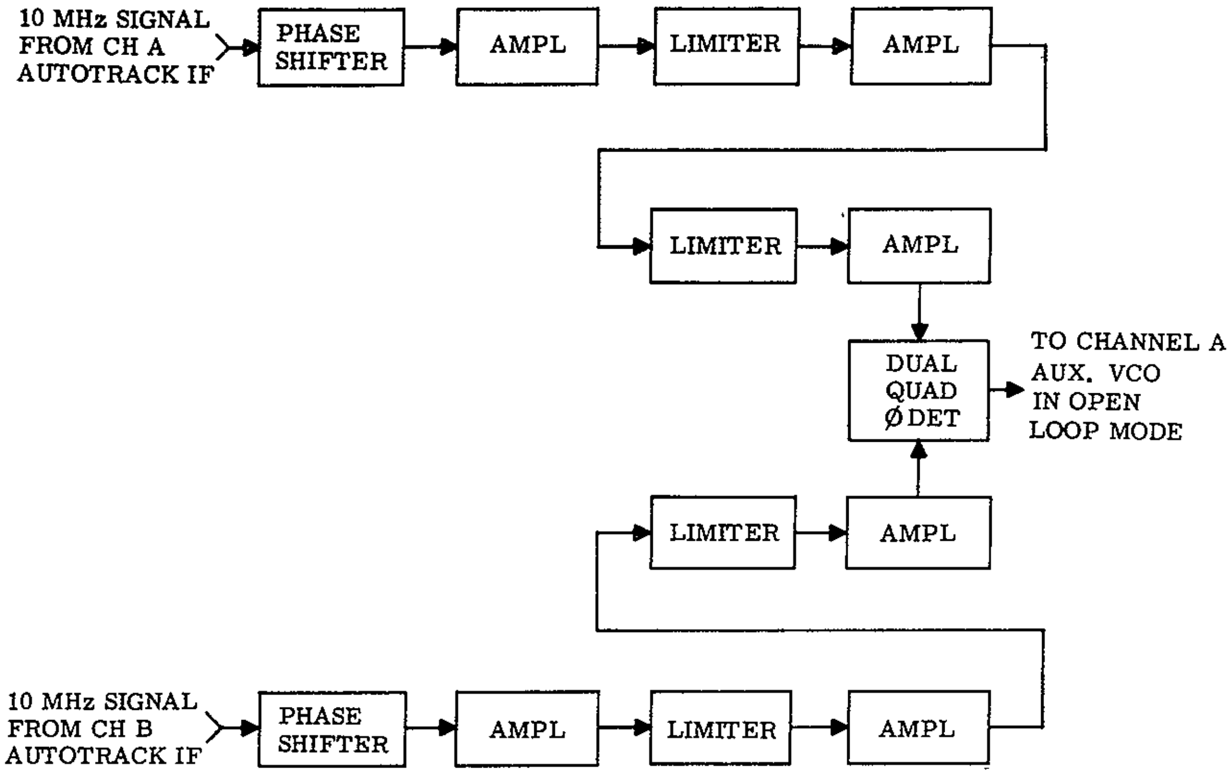

Figure 3-51. Open Loop Phase Detector

3.6.3.1.9 <u>Open Loop Phase Detector</u>. The open loop phase detector multiplies the two sum channel signals together to provide an error signal to the channel A secondary phase-lock loop in the open loop mode. Figure 3-51 is a functional block diagram of the open-loop phase detector. The phase shifters at each sum channel input provide a total phase difference between channels of 90 degrees at the dual quad phase detector. Therefore, a zero error signal will result at the detector output when the two input signals are in phase.

3.6.3.1.10 <u>Local Oscillator and Reference Signal Distribution</u>. Figures 3-52 and 3-53 detail the methods which distribute the system signal source signals to the receiver third converter and phase detectors. Each phase shifter has a phase adjustment range in excess of 180 degrees. The phase shifters are a constant-amplitude circuit, developed by General Dynamics for the Advanced Polarization Diversity Autotrack Receiver (APDAR) system. The third local oscillator signals are phase shifted 180 degrees at 50 MHz and then doubled to 100 MHz. In this manner, a full 360 degrees of phase adjustment is available to align the autotrack error channels. The four error channel phase shifters will be located on the front panel of the error channel drawer, as will the local (receiver cabinet) X and Y channel error meters. Rapid alignment of the autotrack system is thereby provided whenever a new operating frequency is selected.

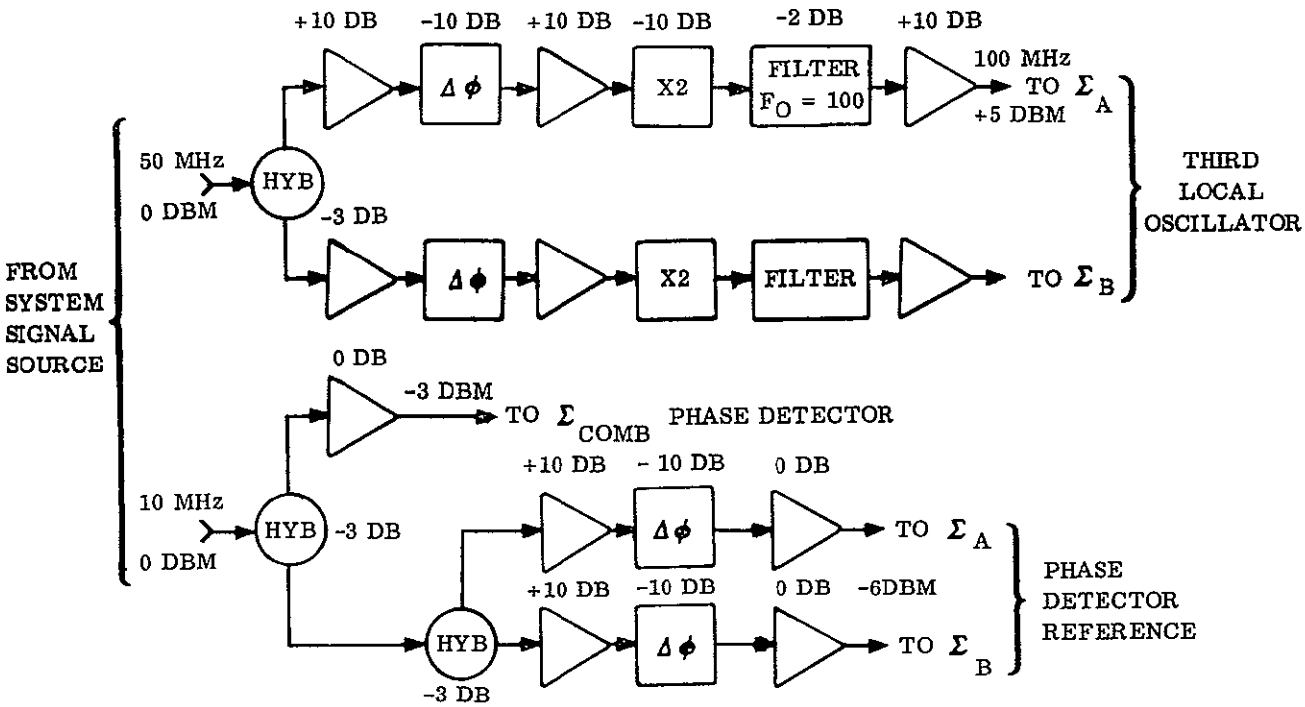

Figure 3-52. Local Oscillator and Reference Signal Distribution, Sum Channel Drawer

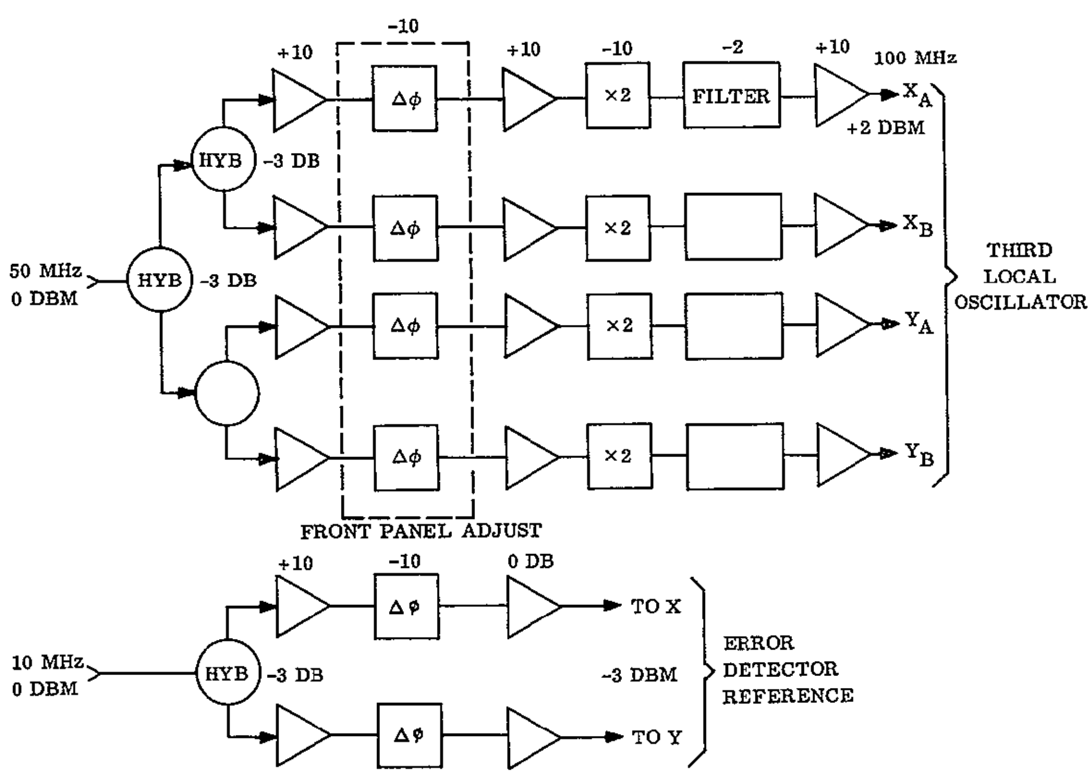

Figure 3-53. Local Oscillator and Reference Signal Distribution, Error Channel Drawer

A receiver phasing diagram is shown in Figure 3-54. Eleven phase shifters are indicated. These are sufficient to properly align the six receiver channels in the open-loop and closed-loop modes for autotrack and diversity combining. The phasing sequence is as follows:

a. Set $\Delta\phi$ No. 1 and No. 2 for proper phase at the narrowband combiner and primary phase detector.

b. Set $\Delta\phi$ No. 3 and No. 4 for proper phase at the wideband combiner.

c. Set $\Delta\phi$ No. 5 for proper phase at the open loop phase detector, while locked in the closed loop mode.

d. Set $\Delta\phi$ No. 6, 7, 8, and 9 for proper phase at error combiners and error product detectors while in the open loop mode.

e. Set $\Delta\phi$ No. 10 and 11 for proper phase at the error product detectors while in the closed loop mode.

3.6.3.1.11 AFC Discriminators and Sideband Lock Detectors. Figure 3-55 is a block diagram of the discriminator circuits used for AFC and sideband lock detection. The limited sum signal is split in hybrids and applied to 10 MHz FM discriminator-driven circuits. Two discriminators are used for the AFC function, a 30 KHz crystal discriminator and a 100 KHz "frequency domain" discriminator. The discriminator outputs are coupled to a single pole, 4-position FET switch which is controlled by the IF bandwidth switch.

The 30 KHz discriminator output is used for the 10 and 30 KHz IF bandwidths, a scale factor reduction of 3-to-1 being made for the 30 KHz IF bandwidth. The 300 KHz discriminator output is selected for all other IF bandwidths, a scale factor reduction of 3-to-1 being made for IF bandwidth switch positions of 300 KHz to 20 MHz.

The selected discriminator output is filtered, amplified and coupled to the dead-zone circuit. A dead-zone adjustment is provided which permits the width of the dead zone to be varied from essentially zero to more than ±5 percent of the discriminator bandwidth. In the AFC tuning mode, the dead-zone circuit output is switched into the primary VCO control circuit.

The anti-sideband lock circuits derive their information from FM discriminators. A non-zero signal from the discriminators indicates the receiver is detuned from the center of the received signal spectrum. In addition to the two discriminators mentioned above, a third narrowband (3 KHz) discriminator is required in order to detect lock to sideband frequencies as close as 100 Hz from the carrier. An additional frequency conversion from the

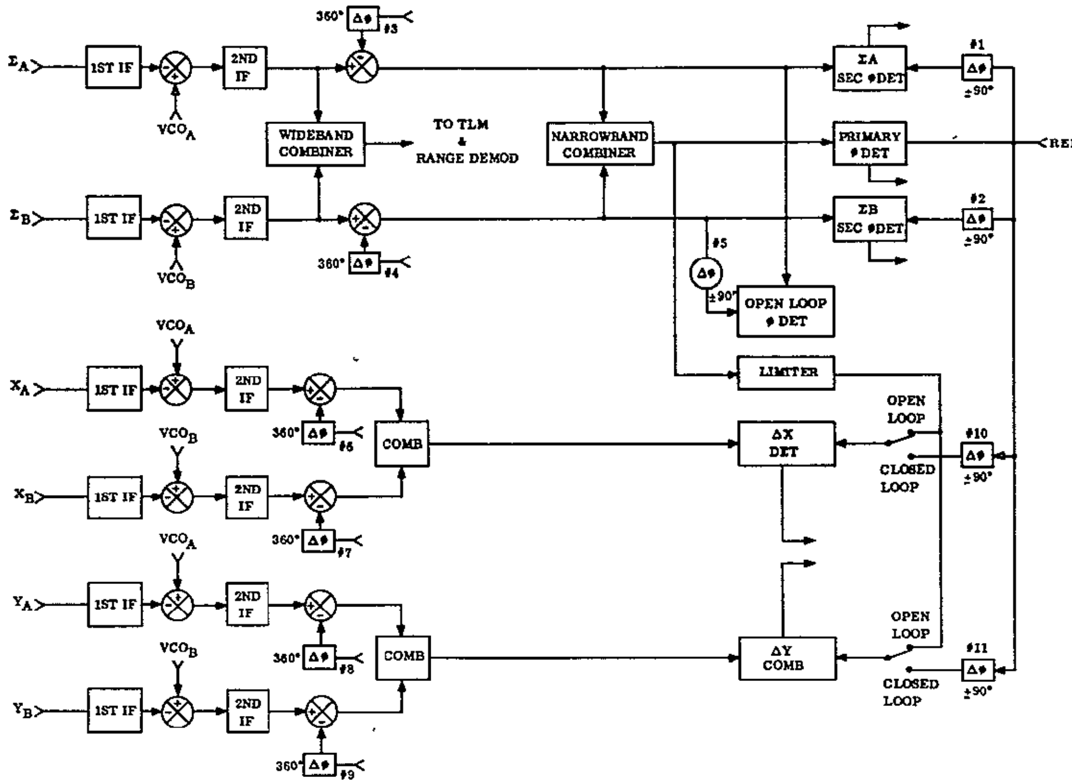

Figure 3-54. Receiver Phasing Diagram

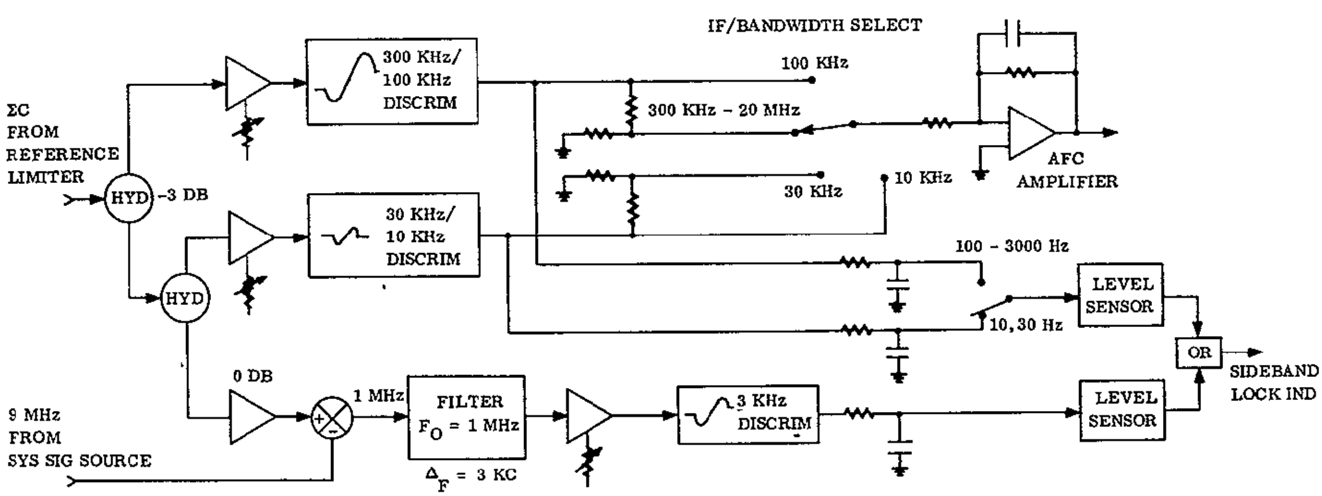

Figure 3-55. AFC Discriminators and ASL Detectors

third IF of 10 MHz down to 1 MHz is necessary since a stable 3 KHz bandwidth discriminator is not practical at 10 MHz.

The outputs of the discriminators selected as a function of tracking bandwidth in accordance with Table 3-2 below are coupled to level-sensing circuits.

Table 3-2. Tracking Bandwidths and Discriminator Outputs

TR/BW	IF/BW (KHz)	Discriminators		
		3 KHz	10 KHz	100 KHz
10	10	X	X	
30	10	X	X	
100	100	X		X
300	100	X		X
1000	100			X
3000	100			X

The level sensor generates an output when the magnitude of its input exceeds a preset threshold. The level sensor outputs are coupled via an OR gate to the sideband lock indicator driver and to the phase lock loop control circuits through the ASL disable switch.

The thresholds of the sideband lock detectors occur at signal-to-noise ratios of about +10 db in the predetection bandwidths of the FM discriminators. Thus, the 3 KHz discriminator will be capable of providing useful information for input signal levels greater than -129 dbm (assuming an input-noise spectral density of -174 dbm/Hz and a signal spectrum width less than 3 KHz). The corresponding thresholds for the 10 KHz and 100 KHz discriminators are -124 and -114 dbm, respectively.

3.6.3.1.12 Closed Loop Controls. The method of implementing the primary phase-lock loop filter is shown in Figure 3-56.

In the Manual Tuning position of the Tuning Mode control, the primary loop filter is configured as shown in Figure 3-56A. The input from the phase detector is not connected, however, so that phase-lock acquisition will not occur. The tuning control potentiometer in conjunction with the voltage divider network causes the VCO tuning control output to vary symmetrically about ground potential. Ten turns of the 20-turn potentiometer tune the VCO over its full range. Five turns at each end of the range are available for additional control rotation in the memory mode.

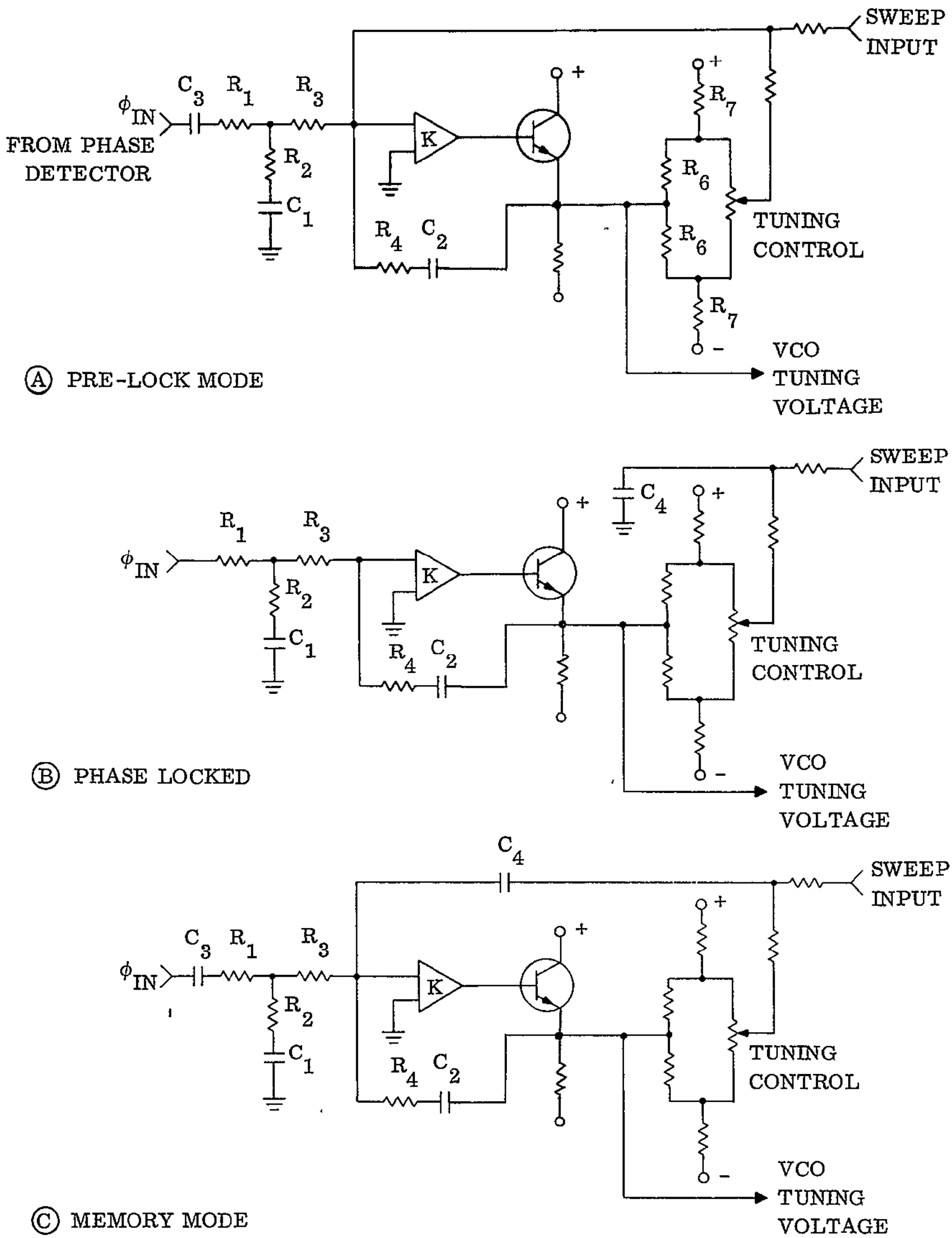

Figure 3-56. Primary Loop Modes of Operation

In the Manual APC mode, the phase detector output is connected to the loop filter through C_3. In this configuration the loop is "closed", although ac is coupled through C_3, and is a second-order type due to the dc shunting of the active filter capacitor, C_2. This acquisition circuit has been used in a number of phase-lock equipments designed by the General Dynamics. It has been found successful in avoiding the false lock problem which other types of acquisition circuits sometimes evince on noisy signals, near threshold.

Phase-lock is sensed when a dc voltage is developed by the quadrature detector, at which time the correlation circuits cause the loop to switch to the configuration shown in Figure 3-56B. In this mode the phase detector output is dc-coupled and the loop is in the required third-order configuration. The memory capacitor, C_4, is connected and will charge to a voltage proportional to the VCO tuning voltage.

In the sweep APC mode, a sweep voltage is added as a forcing function to the tuning control feedback voltage. After phase lock has occurred, the correlation circuits disable the sweep generator.

If the loop should unlock, the filter switches to the memory mode shown in Figure 3-56C. Here the charge stored on C_4 holds the VCO tuning voltage at the level where lock was lost. Then, both the tuning control and sweep can vary the VCO tuning voltage about the "remembered" tuning level.

When the Memory Erase button is depressed, C_4 is discharged, and the loop is returned to original configuration.

The provisions for prevention of sideband lock are not shown on the block diagram.

The circuit features described below are tentative and are subject to revision depending on the results of planned laboratory tests on a phase-lock receiver. In the MAN APC tuning mode, sideband lock is indicated on the receiver control panel. The operator may then depress the primary loop lock pushbutton which places the primary loop in the memory mode and disables the correlation amplifier. At the same time the operator may tune the VCO sufficiently far away from the undesired signal to avoid reacquisition and may then release the pushbutton.

In the SWP APC mode, when phase lock occurs the output of the sideband lock detector is examined. If a sideband lock is indicated, the inputs to the correlation detectors are interrupted and the VCO sweep is restarted. After a period of time (which is a function of the tracking bandwidth) sufficient to move the undesired signal beyond the acquisition bandwidth of the primary loop, the inputs to the correlation detectors are reconnected and the loop is again capable of acquiring a signal.

The secondary loop filters are second-order as discussed in the diversity phase-locked loop analysis.

The secondary loops acquire phase lock unaided in a diversity lock loop. The normal locking sequence of the primary and two secondary loops is as follows.

a. The primary and one of the secondary loops will lock up essentially simultaneously.

b. The remaining secondary loop will pull into lock provided that the difference in frequency between the two auxiliary VCO's is less than its pull in range. This requirement dictates that the auxiliary VCO's have excellent long-term stability to keep the frequency difference to 15 Hz or less. The pull-in range for the narrowest bandwidth of 3 Hz is approximately 15 Hz.

3.6.3.1.13 Fault Isolation. Throughout the gain distribution diagrams in the foregoing sections, output signals are indicated for fault isolation purposes. It is planned that a standard building-block submodule will be used throughout the receiver for this purpose. The submodule will consist of a broadband step-up transformer followed by a diode peak detector. The fault determination consists of injecting test signals into the receiver at the different intermediate frequencies and measuring the detected dc levels.

Sufficient detectors will be included to fault isolate to the module level. The detected levels will be available at test points on the top of each module, and will be wired to a pin on the module connector.

3.6.3.2 TELEMETRY DEMODULATORS. A simplified block diagram of the telemetry system is given in Figure 3-57. The telemetry system has been divided into two subsystems; a narrowband system which handle signals having a predetection bandwidth of 10 KHz to 1 MHz and a wideband system which handles signals having predetector bandwidths from 3 MHz to 20 MHz. Each system contains a set of six demodulators: three coherent demodulators for AM, PM (sinusoidal transfer characteristic), and PM (linear transfer characteristic) and three non-coherent demodulators for AM, FM and PM.

A signal at the second RF of 110 MHz is supplied to the telemetry system from the wideband combiner in the sum channel drawer. This signal is split in a 10 db directional coupler, the larger fraction being supplied to the wideband system. This is done to avoid excessive degradation of the output signal-to-noise ratio at the wider predetection bandwidths.

The wideband telemetry signal is amplified in a 110 MHz RF amplifier and applied to a bank of demodulators. The wideband RF amplifier is provided with automatic gain control. The AGC is required because the input signal level to the telemetry system is controlled by the autotrack system AGC and the RF bandwidth of the autotrack RF is narrower than that of the wideband telemetry system. Thus, in the open loop mode the signal power supplied from the wideband combiner may be higher for a wideband signal than for a narrowband signal. The outputs of the wideband demodulators are applied to a solid state switch controlled by the demodulator selector on the receiver control panel.

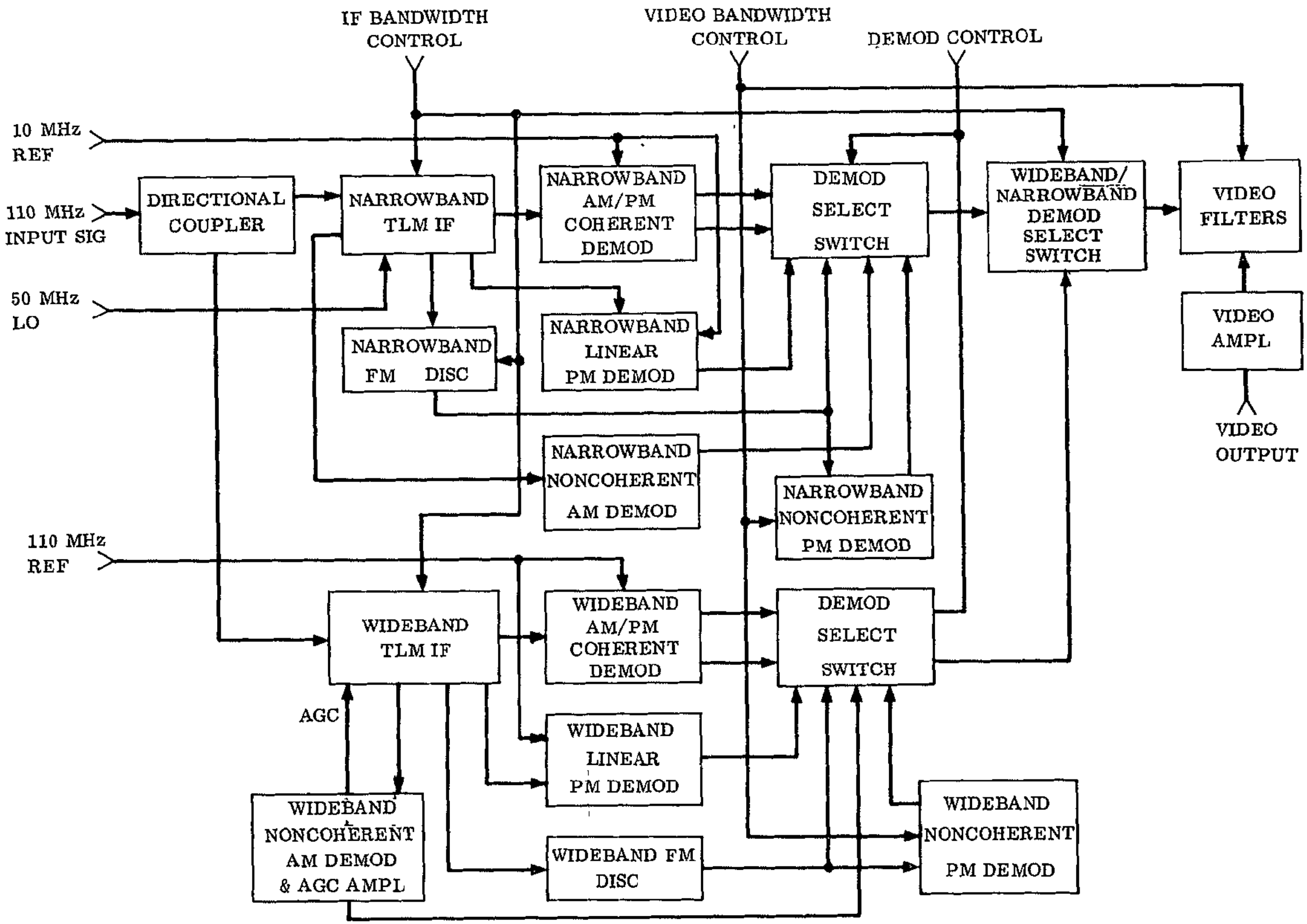

Figure 3-57. Telemetry System Simplified Block Diagram

Narrowband telemetry signals are down-converted to the third IF of 10 MHz, demodulated and applied to the demodulator switching circuit. The outputs from the wideband and narrowband demodulator switching circuits are applied to another switch used to select either the wideband or narrowband signal. This switch is controlled by the IF bandwidth switch on the receiver control panel. For the three highest bandwidths, a signal from the wideband demodulators is selected.

The selected signal is switched through one of a set of nine linear-phase lowpass filters with 1 db bandwidths ranging from 1.5 KHz to 10 MHz and amplified. A video gain control located on the local receiver control panel adjusts the level of the input signal to the final video amplifier. This gain control will be useable regardless of which of the three control modes, local, console, or programmed, is in effect.

3.6.3.2.1 Narrowband Mixer and IF Amplifier. A block diagram and gain map of the narrowband telemetry mixer and IF amplifier is given in Figure 3-58. Signal and noise levels through the chain are given for strong signal (-50 dbm input) cases with the signal-to-noise improvement switch on and off. With the receiver set for a maximum signal-to-noise ratio, the input signal-to-noise ratio to the telemetry system is 33.9 db in a 32 MHz bandwidth (corresponding to 48.9 db in a 1 MHz bandwidth) and the output signal-to-noise ratio (1 MHz bandwidth) to the narrowband demodulators is 37.9 db. Thus, the signal-to-noise ratio is degraded by 11 db. It is possible to avoid a large part of this degradation by placing more gain ahead of the mixer and filter bank. However, this would increase the vulnerability of the system to extraneous signals outside the IF amplifier passband. A tradeoff was made, therefore, between strong signal-to-noise ratio and overload susceptibility. The narrowband telemetry system will be capable of handling without overload extraneous signals, in the passband of the 2.5 MHz filter preceding the mixer, which are up to 60 db greater than the desired signal.

With the signal-to-noise improvement switch off, the input signal-to-noise ratio to the telemetry system is 14.9 db in a 32 MHz bandwidth (corresponding to 29.9 db in a 1 MHz bandwidth). The output signal-to-noise ratio for the 1 MHz bandwidth is 29.2 db which is 8.7 db worse than the ratio when the improvement switch is on. This ratio is adequate for most purposes and so, in general, the signal-to-noise improvement switch may be left off when a narrowband telemetry signal is being received.

The 110 MHz input signal to the telemetry system comes from the wideband combiner. The system bandwidth at this point is 32 MHz. The signal is split in a 10 db directional coupler. The larger fraction is sent to the wideband telemetry system. The remaining signal is passed through a 2.5 MHz bandwidth filter to a double balanced mixer. Local oscillator drive for the mixer is derived by doubling a 50 MHz signal supplied from the receiver signal source. The doubler output is passed through a 2-pole filter which, together with the doubler, provides more than 80 db suppression of the fundamental and third harmonic. The 100 MHz output is amplified to a level of +7 dbm. The amplifier following the mixer is capable of delivering +10 dbm without compression. Thus, it can handle extraneous signals 62 db greater than the desired signal.

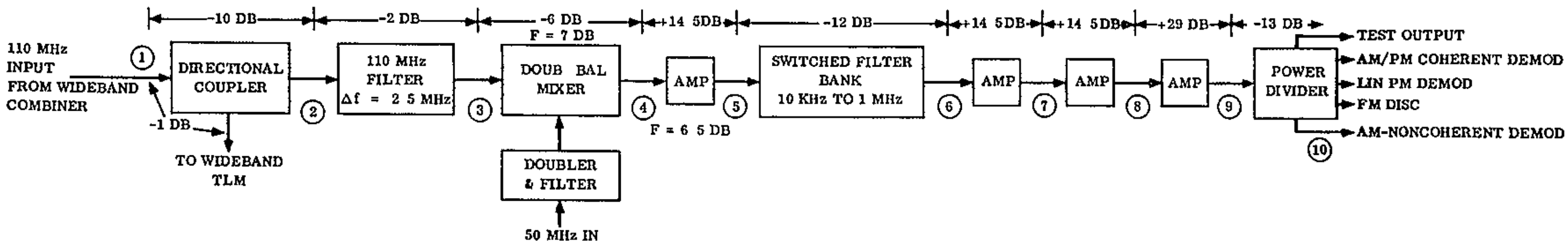

SIG CONDITION*	CODE	1	2	3	4	5	6	7	8	9	10
I	A	-48.6	-58.6	- 60.6	- 66 6	- 52.1	- 64 1	- 49.6	- 35 1	- 6 1	-19.1
	B	-82.5	-92.4	-103.5	-105 6	- 86.3	-103.3	- 87 5	- 73	- 44	-57
	C	-99	-99	-102	-102 5	-109	-107.5	-107.5	-107 5	-114	
	D	-82.4	-91.5	- 99 6	-100 8	- 86.3	-101 9	- 87.5	- 73	- 44	
II	A	-48 6	-58.6	- 60 6	- 66.6	- 51 1	- 64 1	- 49.6	- 35 1	- 6.1	-19 1
	B	-63.5	-73 5	- 85.5	- 91.4	- 76 5	- 93 6	- 78.8	- 64 3	- 35.3	-48 3
	C	-99	-99	-102	-102.5	-109	-107 5	-107.5	-107.5	-114	
	D	-63.5	-73 5	- 85 4	- 91 1	- 76 5	- 93 3	- 78 8	- 64.3	- 35.3	
BW		32	32	3	3	3	1	1	1	1	1

* I - STRONG SIGNAL CASE - TLM S/N INCREASE SWITCH IN
II - STRONG SIGNAL CASE - TLM S/N INCREASE SWITCH OUT

NOTES ALL LEVELS IN DBM
A = INPUT SIGNAL LEVEL
B = INPUT NOISE LEVEL
C = INTERNALLY GENERATED NOISE LEVEL REFERRED TO INPUT OF STAGE
D = TOTAL NOISE LEVEL (B + C)

Figure 3-58. Narrowband TLM Mixer and IF Amplifier

The filter bank consists of five filters with 1 db bandwidths of 10, 30, 100, 300, and 1000 KHz and their associated diode switches, gain- and phase-matching networks. The phase-matching circuits are provided so that the phase shift of the signal through the filter bank will be the same regardless of which filter is selected. The gain-matching networks are required to compensate for differences in filter insertion loss. The signal out of the filter bank is amplified and applied to a 5-way resistive power divider which supplies a test signal as well as the signals for the various narrowband demodulators.

3.6.3.2.2 Narrowband Coherent AM and PM Sinusoidal Demodulators. Figure 3-59 is a block diagram of the narrowband telemetry coherent AM and PM sinusoidal demodulators. The input signal from the power divider in the narrowband IF amplifier is split in a hybrid and applied to double balanced mixers. Feedthrough of reference signal from one mixer to the signal input of the other mixer is kept small by virtue of the port-to-port isolation of the hybrid and the inherent suppression of the double-balanced configuration. The hybrid provides about 30 db suppression and the mixer 40 db suppression for a total of 70 db with a reference level of +7 dbm into the mixers. The amount of reference signal from one mixer feeding through to the signal input of the other is about -63 dbm, or 41 db below the signal.

The 10 MHz reference signal from the system signal source is split in a hybrid, amplified, and applied to a phase shifter (of the type used in the phase matching networks in the narrowband IF filter bank) with an adjustment range of ±120 degrees. The phase shifter output is split, one-half being applied to a fixed 45-degree phase lead network and the other half to an adjustable 45-degree phase lag network. The adjustment range is approximately 20 degrees and permits the required reference quadrature phase relationship with the signal to the PM demodulator to be set with a relatively high degree of resolution.

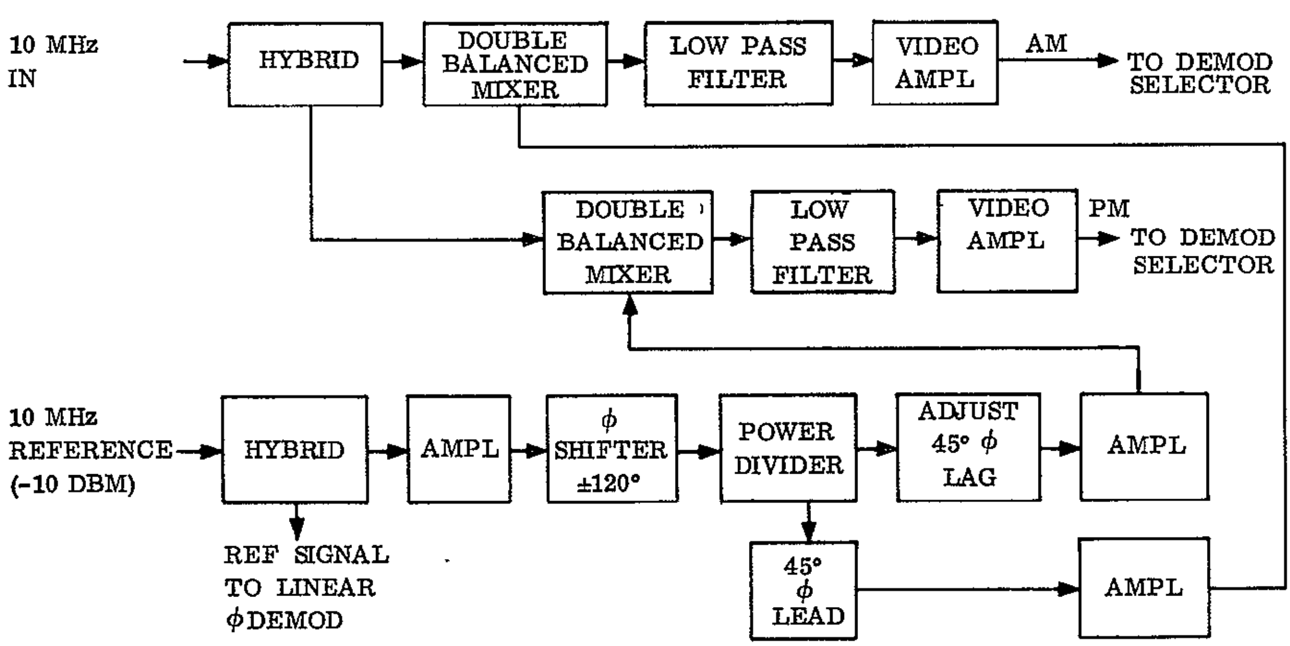

Figure 3-59. Narrowband Coherent AM and PM Demodulators

The outputs of the balanced mixers are passed through low-pass filters, amplified, and sent to the demodulator selector. The low-pass filters are 3-pole with a 2.5 MHz cut-off frequency and are used primarily to reduce the level of the 20 MHz products from the mixer as well as the 10 MHz reference fed through.

A level adjustment with a range of 10 db is provided at the input to each video amplifier. These adjustments are used to set each amplifier output for a level of 110 mv rms for standard modulation (50 percent AM and 1 radian peak phase modulation).

The video amplifiers, Fairchild ua 702C integrated circuits, have a differential input and so lend themselves readily to a dc balance adjustment. The dc adjustment is necessary to balance out the dc voltage developed by the AM demodulator.

3.6.3.2.3 Narrowband Coherent Linear Phase Demodulator. Figure 3-60 is a block diagram of the coherent linear phase demodulator. The circuit consists essentially of a flip-flop whose duty cycle is a linear function of the phase difference between the reference and input signal. Integrating the output of the flip-flop then results in a voltage which is a measure of this phase difference. Although it is theoretically possible to have a range of ±180 degrees, practical considerations limit the range. A range of ±120 degrees has been chosen as a reasonable design goal. This requires that the flip-flop be capable of resolving pulses which may be separated by only 16.7 nanosec (corresponding to a phase difference between signal and reference of 60 degrees at 10 MHz).

The input signal from the narrowband IF amplifier is amplified, limited and differentiated, and used to set the flip-flop. The reference which is also limited and differentiated resets the flip-flop. With no phase modulation, the phase of the reference is adjusted to produce a 50 percent duty cycle in the flip-flop. The flip-flop is a current-mode design capable of

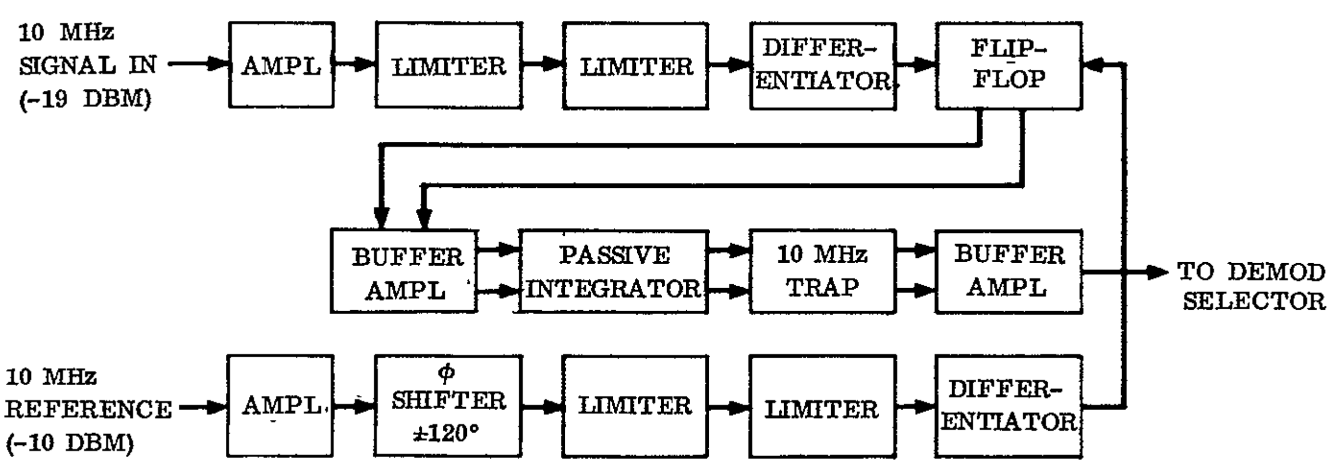

Figure 3-60. Narrowband Linear Phase Demodulator

operation at rates of 100 MHz or of resolving pulses spaced 10 nanosec apart. In order to obtain zero dc output with no modulation applied and to avoid dc shifts as a result of temperature changes and power supply variations, both flip-flop outputs are used. This approach also helps to reduce even-order distortion terms.

The flip-flop outputs are coupled via a dual current-mode inverter stage to passive integrators. The integrators are designed to cut-off at 2 MHz which gives about 14 db rejection of the 10 MHz fundamental and 14 degrees of phase shift for a modulation frequency of 500 KHz. Additional rejection of the fundamental is obtained from 10 MHz traps preceding the final buffer amplifier. The final amplifier is a Fairchild ua 702C connected for unity gain. A level control with a 10 db range is provided at the amplifier output.

3.6.3.2.4 Narrowband FM Demodulator. Figure 3-61 is a block diagram of the narrowband FM demodulator. The 10 MHz signal is amplified, limited, and split in a 3-way resistive power divider. The power divider outputs are applied to discriminator driver circuits. The discriminator driver circuits contain adjustments which control the signal level supplied to the discriminators. These adjustments are normally set to obtain 2.8 volts peak-to-peak at the telemetry system output for a peak-to-peak frequency deviation equal to 80 percent of the IF bandwidth.

The three discriminator circuits are designed to have peak-to-peak separations of 30 KHz, 300 KHz and 1 MHz. The discriminator outputs are coupled to a single pole 5-position solid state switch which is controlled by the IF bandwidth switch on the receiver control panel. The output of the 30 KHz discriminator is selected for IF bandwidths of 10 and 30 KHz, and the 300 KHz discriminator for IF bandwidths of 100 and 300 KHz. The switch, in addition to selecting the appropriate discriminator output, also reduces the selected discriminator output by a factor of three for the 30 KHz and 300 KHz IF bandwidths by switching in a resistive divider.

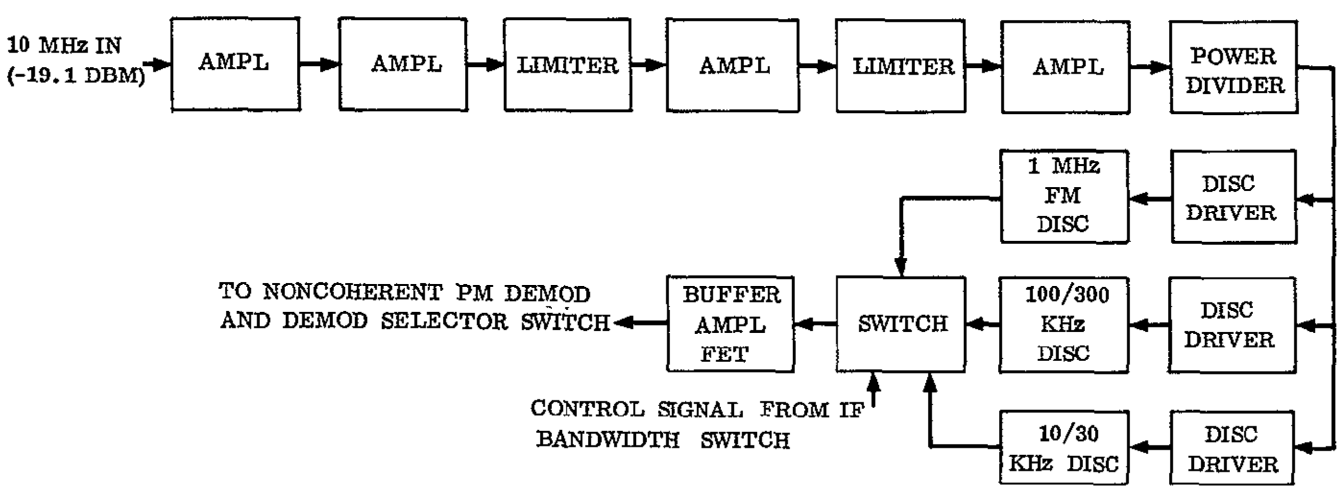

Figure 3-61. Narrowband FM Demodulator

A crystal discriminator is used in the 30 KHz circuit. The 300 KHz and 1 MHz circuits use frequency domain, or staggered-circuit, discriminators. The selected discriminator output is coupled via a high input impedance, unity-gain buffer amplifier to the demodulator selector switch and the narrowband non-coherent PM demodulator.

3.6.3.2.5 Narrowband Non-Coherent AM and PM Demodulators. Figure 3-62 is a block diagram of the narrowband non-coherent AM and PM demodulators. These circuits will be packaged in a single module.

a. Non-Coherent AM Demodulator. The 10 MHz input signal from the narrow IF amplifier is amplified to a level of +3 dbm and stepped up by a 3:1 transformer. The resulting signal at a level of nearly 1 volt rms is applied to a half-wave diode detector. The detector transfer characteristic is linearized by forward biasing the diode. The detector output is coupled through a 3-pole low-pass filter to one input of a unity-gain Fairchild ua702C video amplifier. A dc offset adjustment is applied to the other input of the amplifier. A level control (10 db range) is placed at the output rather than the input of the amplifier so that the offset and level adjustments may be completely independent of each other.

b. Non-Coherent PM Demodulator. Phase modulation is recovered by integrating the output of the FM discriminator. A signal from the narrowband FM discriminator is applied via a unity-gain buffer amplifier to a solid state (FET) single pole, 6-position switch. The switch is controlled by the video bandwidth switch on the receiver control panel. The switch couples the signal into one of six single-stage RC integrators. A common capacitor is used for all six integrators, the appropriate resistor being selected by the switch.

The integrators are designed to have a breakpoint at a frequency equal to one percent of the video bandwidth. The breakpoints, therefore, will range from 15 Hz to 5 KHz for video bandwidths of 1.5 KHz to 500 KHz. The one percent value was chosen as a reasonable compromise between the range over which the conversion from FM to PM is effective and the amount of attenuation produced at the maximum modulation frequency.

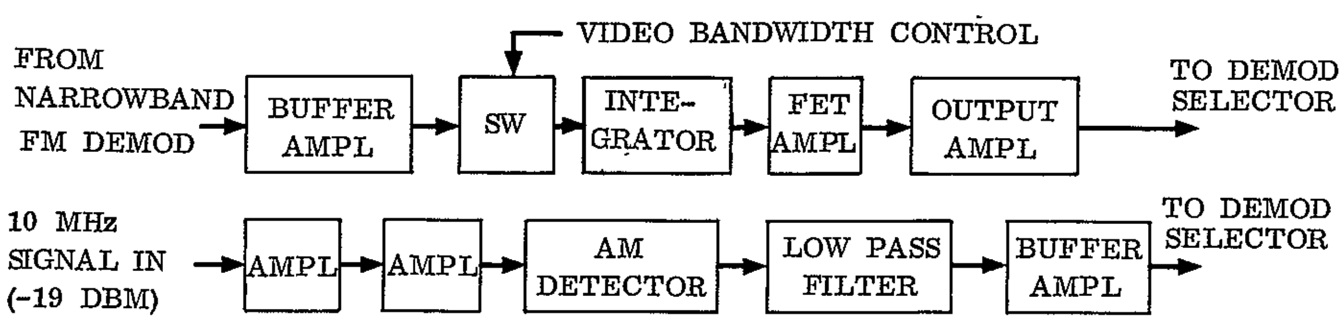

Figure 3-62. Narrowband Non-Coherent AM and PM Demodulator

The integrator output is ac-coupled via a source follower to the output amplifier. The ac coupling is employed since the dc offset resulting from errors in the AFC loop in the main receiver is comparable in magnitude to the desired signal level at the output of the integrator. The gain of the output amplifier, a Fairchild ua702C, is 40 db. A dc offset adjustment is provided at one input to the amplifier to balance out the dc voltage at the other input due to the source follower.

3.6.3.2.6 Wideband IF Amplifier. Figure 3-63 is a block diagram of the wideband telemetry IF amplifier. The 110 MHz input signal derived from the directional coupler in the narrowband telemetry IF amplifier is amplified and applied to a voltage-controlled attenuator. The input amplifier is capable of delivering up to 10 dbm without compression and so will not overload on extraneous signals up to 45 db greater than the desired signal. In the worst case where the telemetry threshold is about -110 dbm (corresponding to unity signal-to-noise ratio in a 3 MHz bandwidth) extraneous signals at input levels of -65 dbm can be handled without overload.

Automatic gain control of the wideband IF amplifier is required to maintain the correct signal levels to the non-coherent demodulators. With the main receiver in the open-loop mode and wideband telemetry signals being received, the autotrack predetection bandwidth will be 1 MHz. The main receiver AGC will act to maintain the signal power in a 1 MHz bandwidth constant. The signal power seen by the telemetry system will, therefore, be a function of the spectral distribution of the input signal. Assuming a 20 MHz uniformly-distributed spectrum, the signal input power to the telemetry system will be 13 db greater (-36.6 dbm) than the power level indicated on the block diagram.

The VCA attenuation is variable from 2 to 22 db. In the closed loop mode, the VCA is set for 2 db. In the open loop mode, the VCA is controlled by a signal derived from the wideband non-coherent AM detector. The output of the VCA is coupled to the wideband filter bank which consists of 3 MHz, 10 MHz, and 20 MHz band-pass filters and their associated diode switches and gain and phase matching networks. Only one phase-matching network is employed to match the phase shift of the 3 MHz filter to that of the 10 MHz filter. No phase compensation of the 20 MHz filter is required since this filter is not used for coherent detection. The gain-matching networks are required to compensate for the different insertion losses of the filters.

3.6.3.2.7 Wideband Coherent AM and PM Demodulators. Figure 3-64 is a block diagram of the coherent AM and PM demodulators. The 110 MHz input signal from the wideband IF amplifier is amplified, split in a hybrid, and applied through adjustable voltage controlled attenuators to Relcom M6E double-balanced mixers. The variable attenuators are controllable over a 6 db to 16 db range and are used to set the demodulated signal level to the demodulator selector switch at 110 mv rms (at 50 percent AM or 1 radian peak deviation). Phase shift in the attenuator at 110 MHz over the 10 db range used is less than 5 degrees.

The outputs of the mixers are coupled via low-pass filters (3-pole, 10 MHz cut-off

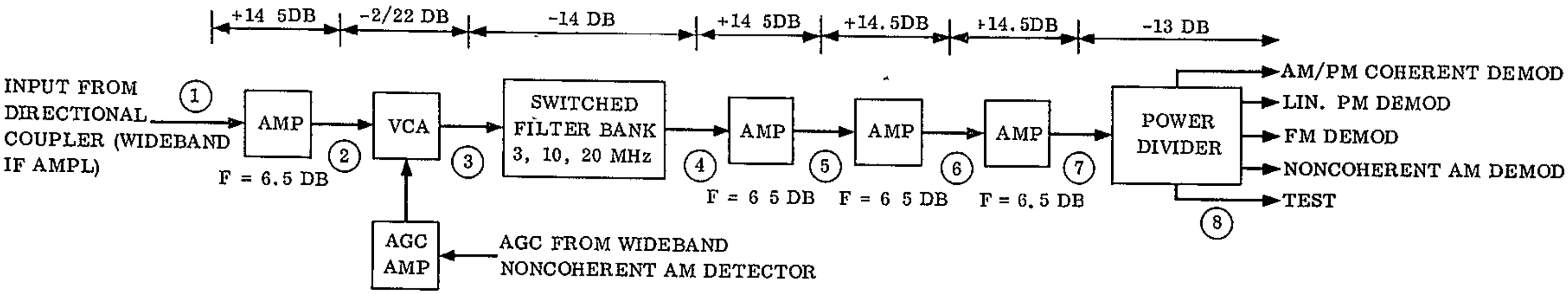

SIG CONDITION*	CODE	①	②	③	④	⑤	⑥	⑦	⑧
I	A	-49.6	-35.4	-37.1	-51.1	-36.6	-22.1	- 7.6	-20.6
	B	-83.5	-68.5	-70.5	-86.5	-71.3	-56.8	-42.3	-55.3
	C	-92.5	-99	-99	-94.5	-94.5	-94.5	-94.5	
	D	-83.0	-68.5	-70.5	-85.8	-71.3	-50.8	-42.3	
II	A	-49.6	-35.1	-37.1	-51.1	-36.6	-22.1	- 7.6	-20.6
	B	-63.5	-49	-51	-67	-52.5	-38	-23.5	-36.5
	C	-92.5	-99	-99	-94.5	-94.5	-94.5	-101	
	D	-63.5	-49	-51	-67	-52.5	-38	-23.5	
BW (MHz)		32	32	32	20	20	20	20	20

* I - STRONG SIGNAL CASE - TLM S/N INCREASE SWITCH IN
II - STRONG SIGNAL CASE - TLM S/N INCREASE SWITCH OUT

NOTES ALL LEVELS IN DBM
A = INPUT SIGNAL LEVEL
B = INPUT NOISE LEVEL
C = INTERNALLY GENERATED NOISE LEVEL REFERRED TO INPUT OF STAGE
D = TOTAL NOISE LEVEL (B + C)

Figure 3-63. Wideband Telemetry IF Amplifier

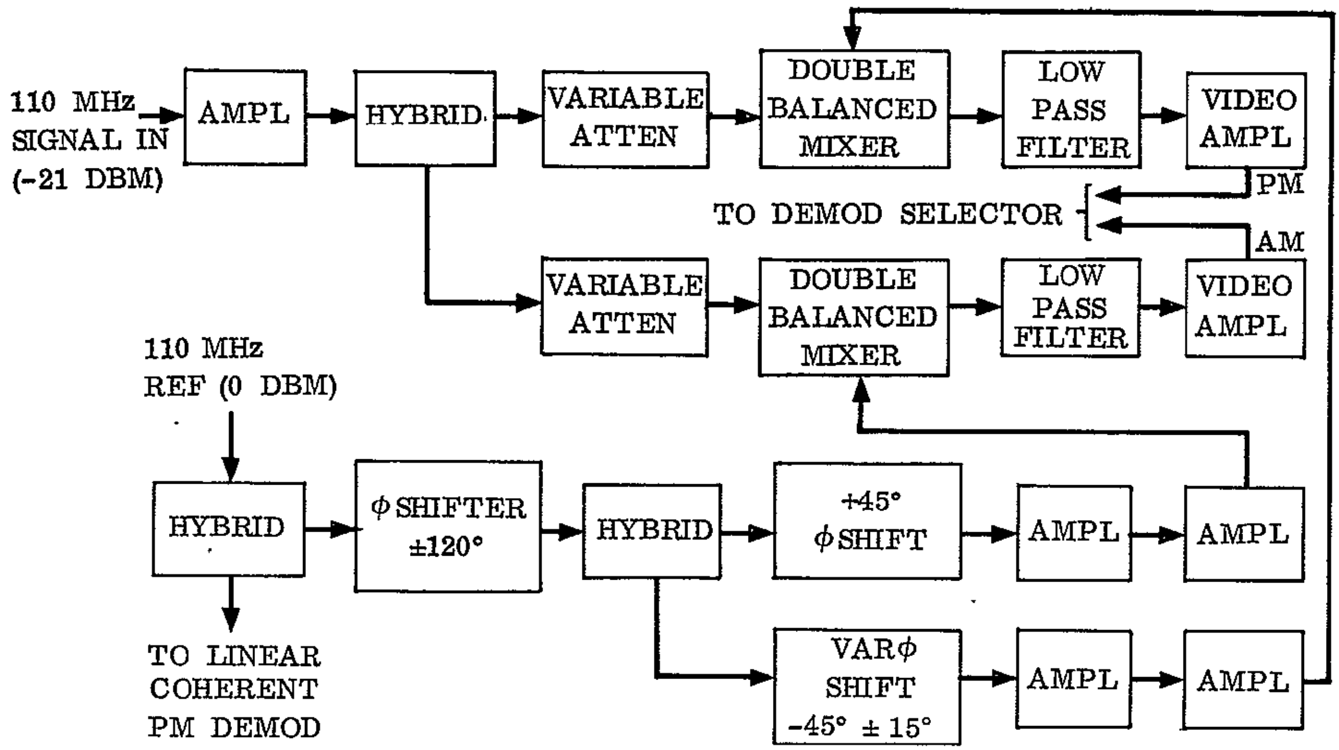

Figure 3-64. Wideband Coherent AM/PM Demodulators

frequency) to Fairchild ua 702C video amplifiers. Each amplifier has a gain of 20 db. A dc offset adjustment is provided at one input of the AM video amplifier to balance out the dc normally developed in the AM demodulator.

The 110 MHz reference signal from the system signal source is split in a hybrid with half the power being supplied to the coherent linear phase demodulator. The remaining signal is passed through a phase shifter with a range of ±120 degrees, split in a hybrid, and applied to a fixed 45-degree phase lead network and an adjustable 45-degree (±15 degrees) phase lag network.

The two reference signals are amplified to +7 dbm and supplied to the mixers.

3.6.3.2.8 Wideband Linear Coherent PM Demodulator. Figure 3-65 is a block diagram of the linear coherent PM demodulator. The design approach is different from that taken for the narrowband linear phase demodulator since wide-range crossover type demodulators are impractical at 110 MHz. The linear transfer characteristic is obtained in this case by clipping the input signal applied to a double balanced mixer. The maximum possible demodulation range for this circuit is 180 degrees.

The 110 MHz input signal at a level of about -21 dbm is amplified to about +5 dbm and applied to a series current-mode clipper which utilizes well-matched hot carrier diodes.

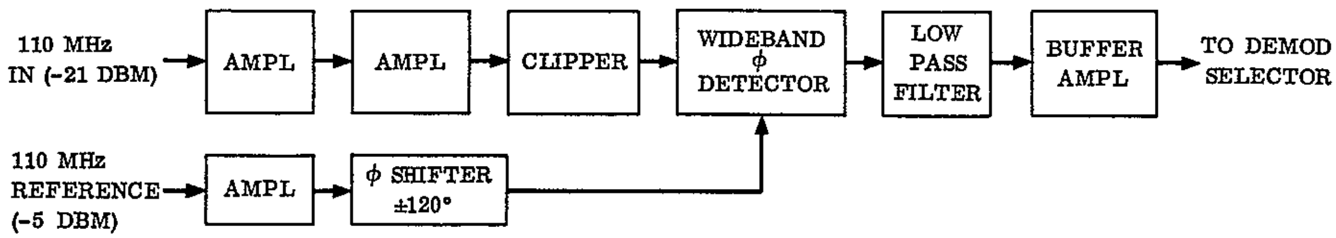

Figure 3-65. Wideband Linear Coherent Phase Demodulator

The clipper is designed not only to produce a flat-topped output but to minimize phase variations of the output with input amplitude changes. The clipper output circuit must be extremely broadband in order to preserve the wave shape of the clipped signal.

The clipped output is fed directly to a broadband double balanced mixer, an Anzac Model SMX-10, or equivalent. The mixer is capable of working over a frequency range of 0.2 to 1000 MHz.

The output of the mixer is linearly proportional, over a range of more than ±60 degrees, to phase deviations of the input signal with respect to the reference. The output is passed through a 3-pole low pass filter (10 MHz cut-off) to the output buffer amplifier. The amplifier, a Fairchild ua 702C, has a gain of 20 db.

3.6.3.2.9 Wideband FM Demodulator. Figure 3-66 is a block diagram of the FM demodulator. The 110 MHz input signal is amplified and limited in sideband-cancelling limiters utilizing hot-carrier diodes. The limited signal is split in a hybrid and applied through driver circuits to the two discriminators.

One discriminator designed for a peak separation of 10 MHz is used at IF bandwidths of 3 and 10 MHz. The other discriminator is designed for a peak separation of 20 MHz. The FM demodulator output level is set by controlling the drive level to the discriminators.

The discriminator outputs are coupled to a solid state single-pole, 3-position switch controlled by the IF bandwidth switch on the receiver control panel. In addition to selecting the discriminator output, the switch provides a scale factor change for the 10 MHz discriminator by switching in a resistive divider in the 10 MHz IF position.

In order to obtain good high frequency response beyond 10 MHz, the switching circuit is implemented by a diode quad rather than field-effect transistors as in the case of the narrow-band FM discriminator. A dc adjustment is provided in each switch to balance out dc offsets in the discriminator circuit itself as well as dc offset due to unbalance of the diodes in the quad.

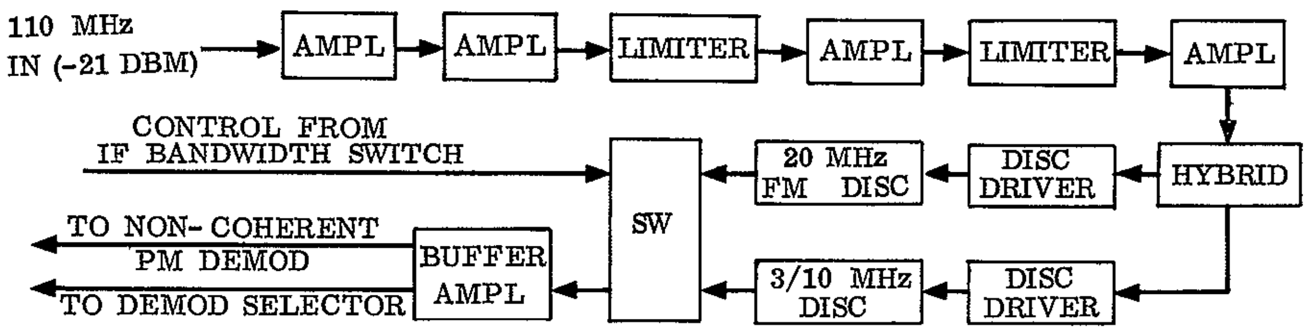

Figure 3-66. Wideband FM Demodulator

The output buffer amplifier, a Fairchild ua 702C, provides a signal to the wideband non-coherent phase demodulator as well as the demodulator selector switch.

3.6.3.2.10 Wideband Non-Coherent AM and PM Demodulator. The non-coherent AM and PM demodulators are contained in the same module. A block diagram is given in Figure 3-67.

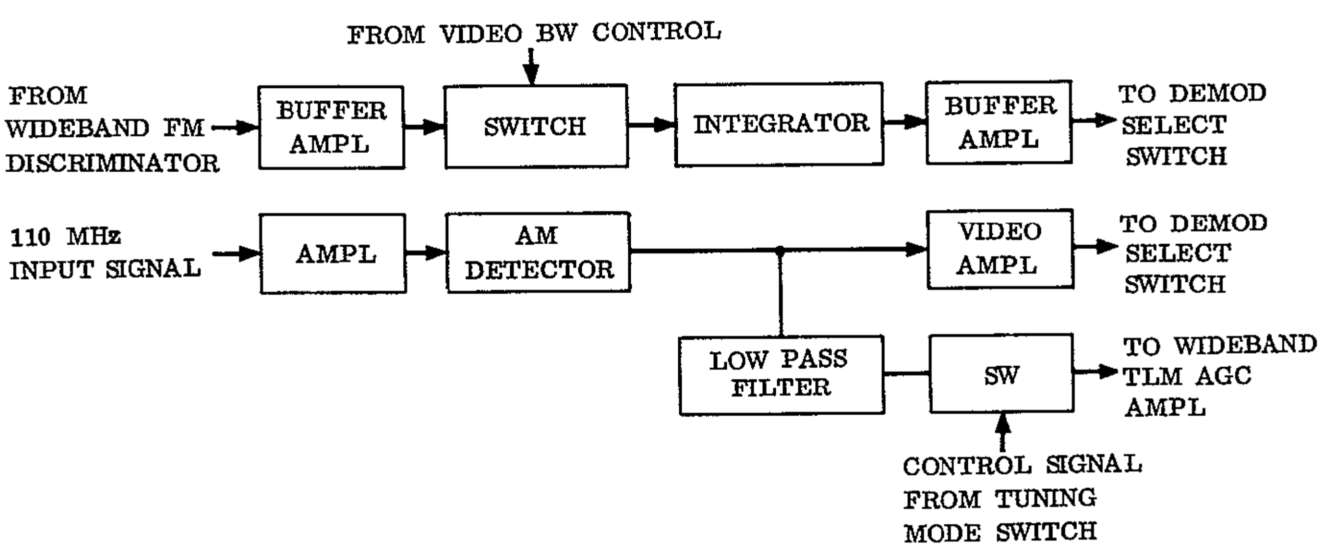

Figure 3-67. Wideband Non-Coherent AM and PM Demodulators

a. Non-coherent AM Demodulator. The amplified 110 MHz input signal is applied to a linearized, half-wave hot-carrier diode detector. The output of the detector is coupled via a unity-gain video amplifier to the demodulator selector switch.

The detector output is also coupled via a long time constant (about 1 second) low-pass RC filter to an FET switch. The switch is controlled by the tuning mode switch on the receiver control panel. When any of the three open-loop tuning modes is selected, the smoothed AM detector output is coupled to the AGC amplifier in the wideband IF amplifier.

b. Non-coherent PM Demodulator. The principle of operation for the wideband PM demodulator is the same as that for the narrowband demodulator. The integrators are designed here, also, to have a breakpoint at 1 percent of the video filter bandwidth. The integrator breakpoints then are at 15 KHz, 50 KHz, and 100 KHz.

The switch is a single pole, 3-position switch controlled by the video bandwidth switch in the 1.5 MHz, 5 MHz, and 10 MHz positions. Diode quads are also used here to achieve the required bandwidth.

3.6.3.2.11 Demodulator Selector. Figure 3-68 is a block diagram of the demodulator selector circuits. The sets of signals from the wideband and narrowband demodulators are applied to solid state single-pole, 6-position switches controlled by the demodulator selector on the receiver control panel. Switching of the narrowband demodulator signals is done with field-effect transistors. The wideband signals are switched with diode quads. Selection of either a wideband or narrowband telemetry signal is made by a switch controlled by the IF bandwidth switch. The wideband signal is selected for IF bandwidths of 3, 10, and 20 MHz.

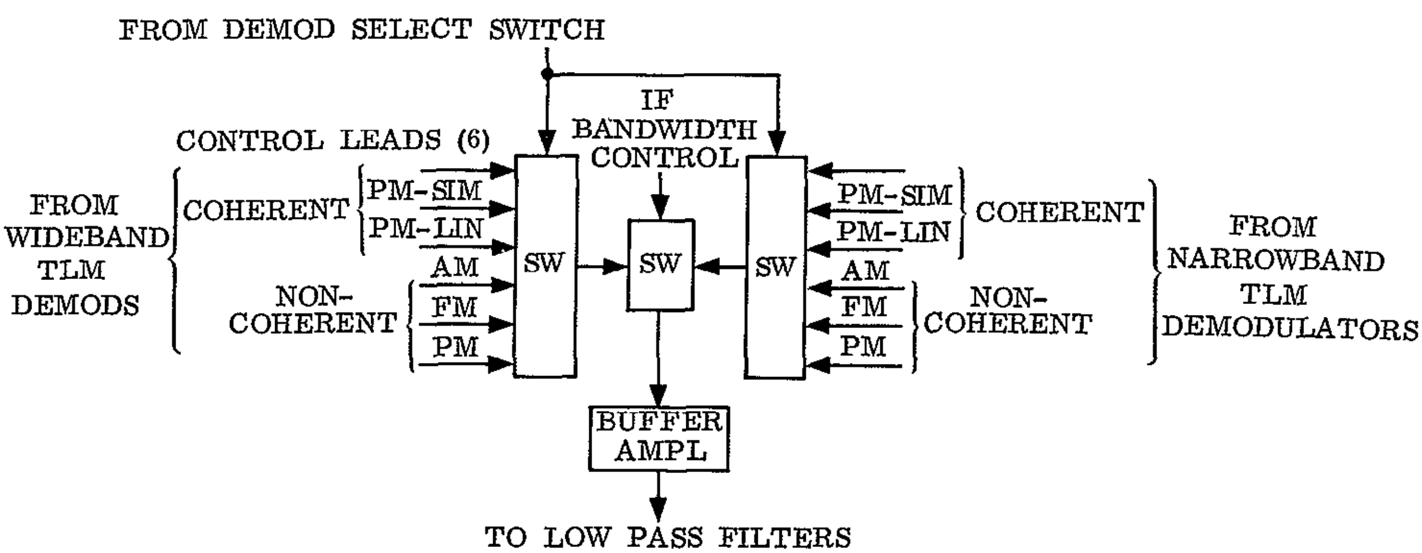

Figure 3-68. TLM Demodulator Selector

3.6.3.2.12 Low Pass Filter and Video Amplifier. Figure 3-69 is a block diagram of the low pass filter and video amplifier module. The selected demodulator is switched through a low-pass filter to the buffer amplifier. The low-pass filters are 6-pole, linear phase with 1 db bandwidths ranging from 1.5 KHz to 10 MHz. Switches for the 1.5 KHz to 500 KHz filters are n-channel JFET types. Diode quad switches are used for the 1.5, 5, and 10 MHz filters.

The output of the buffer amplifier is coupled to a variable attenuator having an adjustment range of 2 to 12 db. The attenuator is controlled from the local receiver control panel. This control is effective in all three receiver control modes; local, console, and programmed.

The output amplifier is designed to have a gain of 20 db and a 1 db bandwidth of 15 MHz. It is capable of delivering more than 6 volts peak-to-peak into a 90 ohm load. Normally, the attenuator is set so that the amplifier output is 2.8 volts peak-to-peak for 50 percent AM, ±1 radian PM, or FM with peak-to-peak frequency deviation equal to 80 percent of the IF bandwidth.

3.6.3.2.13 Mechanical Design. The telemetry system is packaged in a slide-mounted drawer having a panel height of 10.5 inches. The circuits are contained in the standard plug-in modules described earlier. It is estimated that 16 to 18 modules will be required.

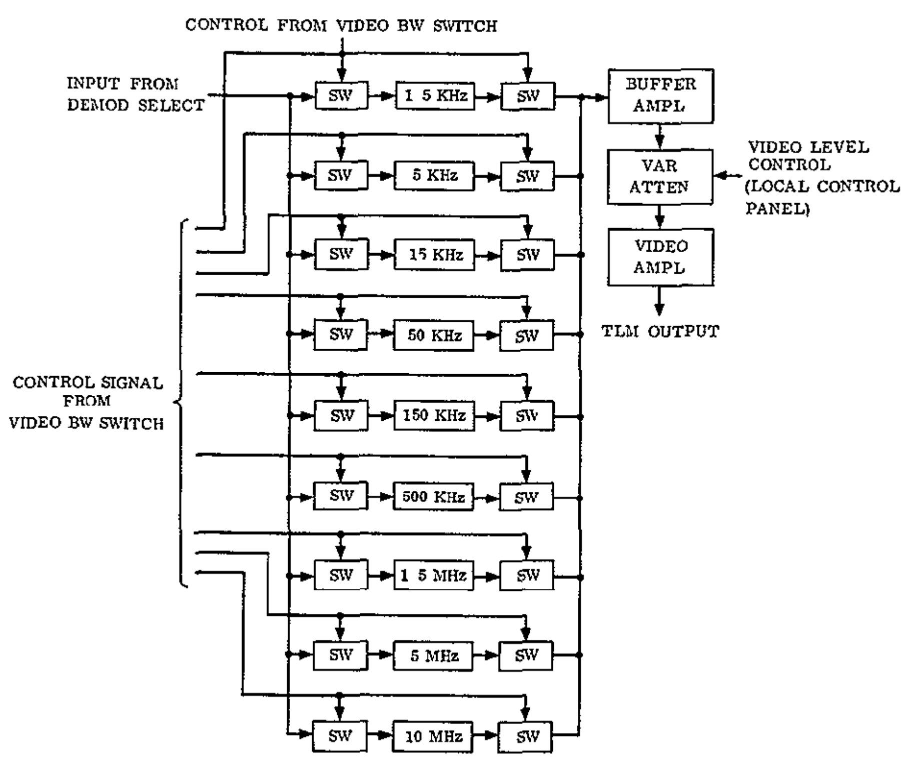

Figure 3-69. Low-Pass Filters and Video Amplifiers

3.6.3.3 SPECTRUM DISPLAY AND LISSAJOUS MONITOR UNIT.

3.6.3.3.1 Lissajous Monitor Unit. A local Lissajous monitor will be provided at the receiver as a visual aid to acquisition. The remote Lissajous monitor will be incorporated in the Spectrum Display Unit. Each monitor will provide Lissajous representations of the secondary VCO's, secondary phase detectors, main phase detectors for the Multifunction Receiver (MFR) and the narrowband phase detector for the subcarrier receiver.

The local monitor will consist of a Benrus type RA840C solid state X-Y indicator with horizontal and vertical amplifier plug-in units (Figure 3-70). The unit has a 1-1/2 × 3 in. rectangular cathode ray tube with external graticule 4 × 8 cm square. The horizontal and vertical sensitivity is 0.1 volt per centimeter.

A functional block diagram of the local Lissajous monitor unit is provided in Figure 3-71. The "Q" and "P" outputs from each phase detector are applied to the horizontal and vertical amplifiers respectively and the resultant circle is viewed on the scope. The input may be selected as either linear or limiting. The linear mode is used for checking phase detector gain and balance while the limiting mode is used prior to phase lock to keep the display within the bounds of the scope face to aid in acquisition. Low pass filters for the vertical and horizontal inputs are selected at the front panel in steps of 1, 10, 100, 1000, 10,000 Hz. An unfiltered input is also provided and must be used when the secondary VCO's are viewed.

3.6.3.3.2 Spectrum Display Unit. The spectrum display unit is located at the remote control console. The unit includes circuits for remote monitoring the Lissajous patterns discussed above. A functional block diagram of the spectrum display unit is shown in Figure 3-72. The display is made up of the Benrus type RA840C X-Y indicator and appropriate vertical and horizontal amplifiers. The Lissajous monitor will be implemented the same way as the local Lissajous monitor.

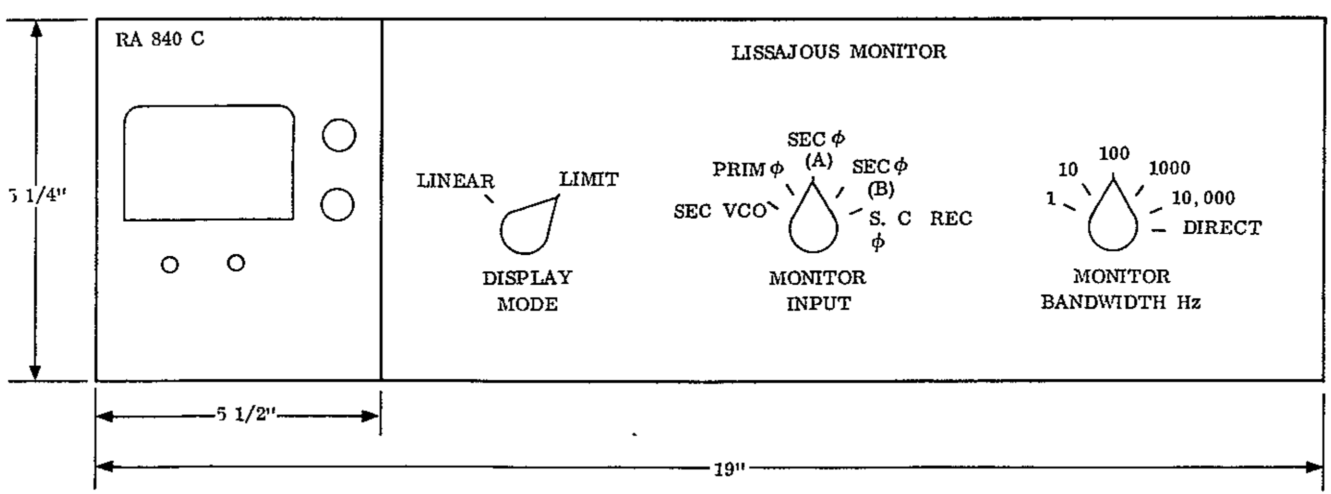

Figure 3-70. Local Lissajous Monitor Unit Panel

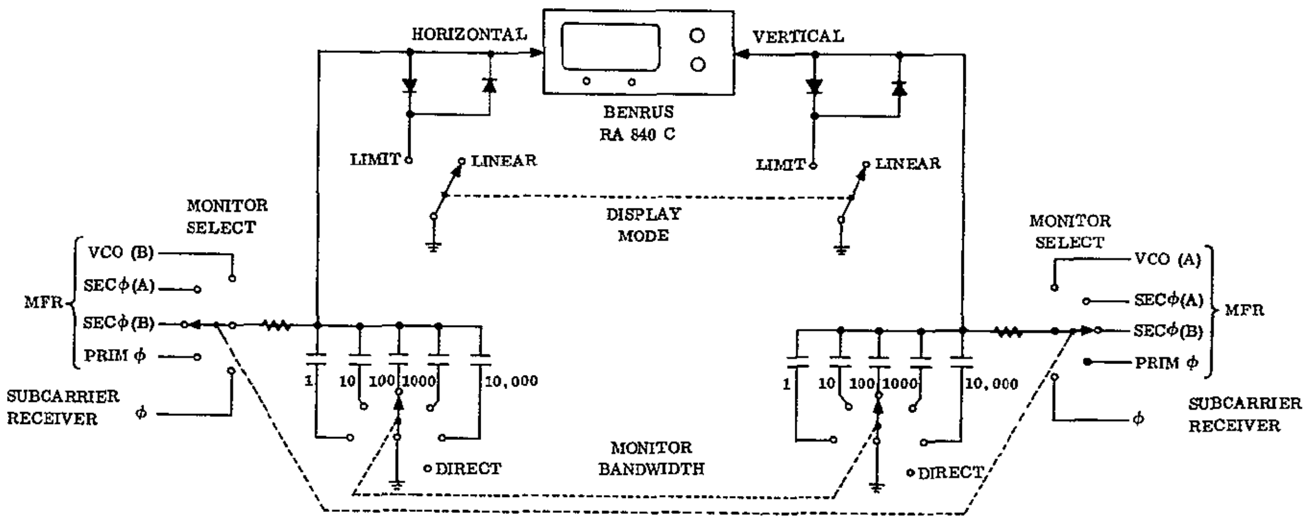

Figure 3-71. Local Lissajous Monitor Unit

The spectrum display unit is capable of operating with the combined MFR sum channel IF (110 MHz) or the subcarrier receiver IF (10 MHz). Linear or logarithmic display will show the appropriate IF spectrum.

a. Mixers and IF Amplifiers. The wideband 110 MHz IF signal from the multifunction receiver is converted to 25 MHz by mixing with a 135 MHz VCO in a double-balanced mixer. The subcarrier receiver 10 MHz input is first up-converted to 110 MHz by mixing with a 100 MHz crystal controlled oscillator in a double-balanced mixer. The input to the 110/25 MHz mixer is selected by solid state switches controlled from the front panel.

The 25 MHz out of the mixer is filtered and amplified in a wideband amplifier consisting of standard amplifiers and VCA's providing 50 db of manual gain control range. This range is adequate since the inputs are gain controlled. The 25 MHz is down-converted to 10.7 MHz by mixing with a 35.7 MHz crystal-controlled oscillator in a double-balanced mixer. The 10.7 MHz signal is filtered, amplified, and sent to one of three narrowband filters. The filters are selected by diode switches controlled from the front panel. The filter used depends on the VCO sweep rate.

The 10.7 MHz signal is fed to a Linear-Logarithmic (LIN-LOG) amplifier. The amplifier consists of several cascaded common-emitter amplifiers followed by a video detector. A simplified schematic is shown in Figure 3-73. The final transistor is used only as a

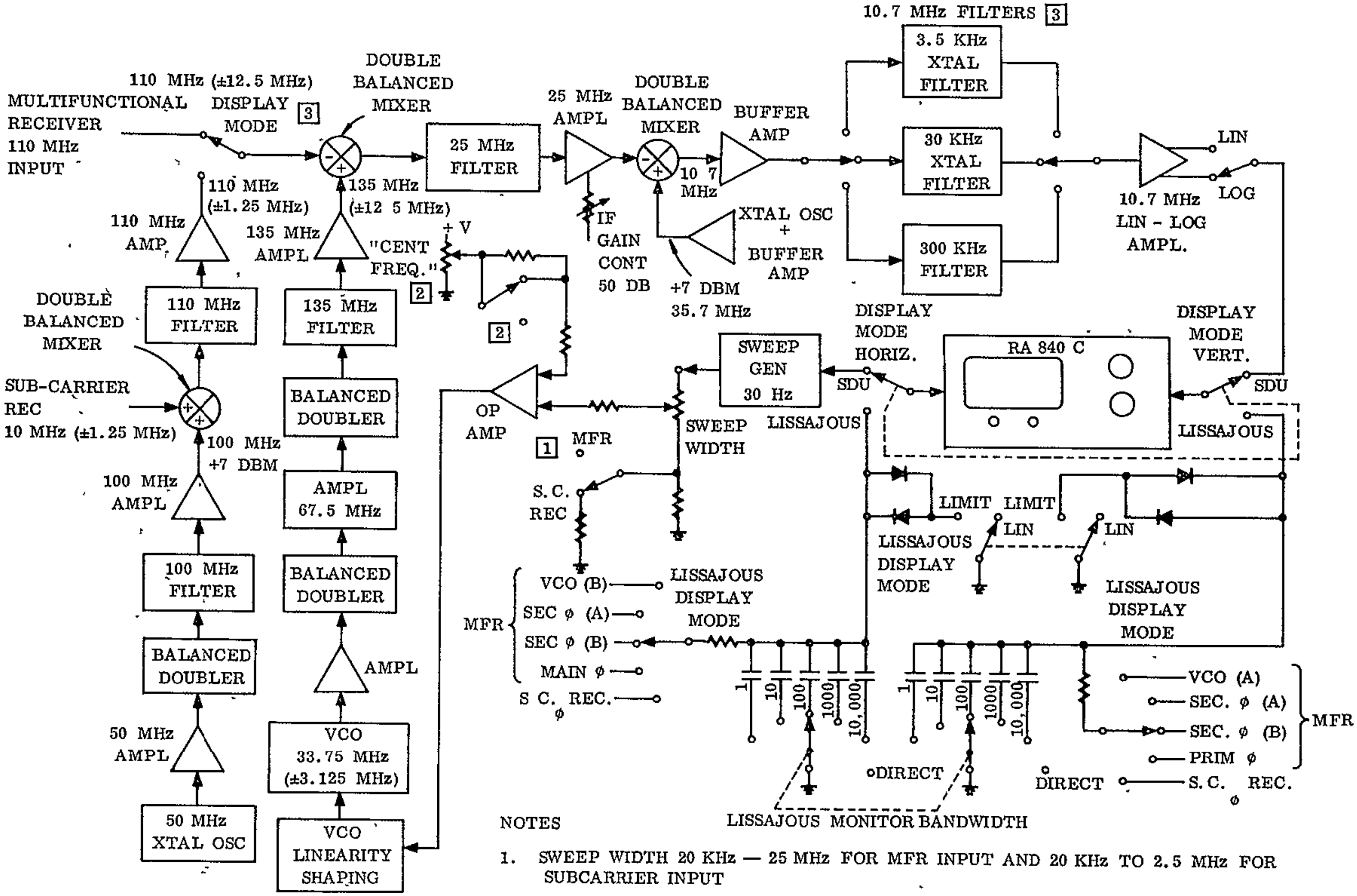

NOTES

1. SWEEP WIDTH 20 KHz — 25 MHz FOR MFR INPUT AND 20 KHz TO 2.5 MHz FOR SUBCARRIER INPUT
2. "CENT FREQ." CONSISTS OF 10-TURN POTENTIOMETER WITH MICRODIAL CALIBRATED FOR 0 - 1,000. SMALLEST INCREMENT EQUALS 20 KHz FOR MFR AND 2 KHz FOR SUBCARRIER RECEIVER.
3. 110 MHz AND 10.7 MHz SWITCHING IS SOLID STATE.

Figure 3-72. Spectrum Display/Lissajous Monitor Block Diagram

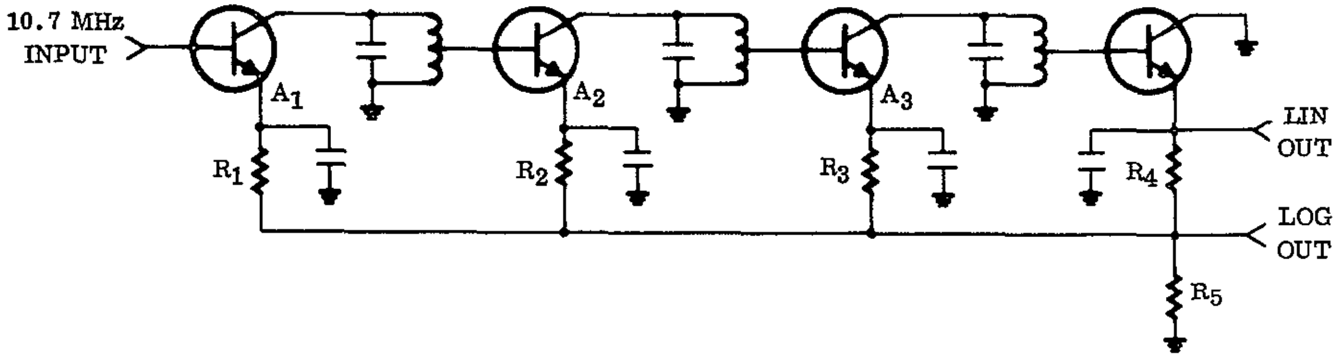

Figure 3-73. LIN-LOG Amplifier

detector. For low-level signals the first three stages amplify the signal linearly and the detected output is a linear function of the input voltage. The LOG-OUT receptacle is grounded for the linear mode. As the signal level increases, stages A_1, A_2 and A_3 begin to detect the signal and apply video signals into summing resistor R_5. The progressive saturation of the amplifier stage continues as the input signal level increases causing the voltage across R_5 to follow a logarithmic curve. The linear or logarithmic output is then applied to the vertical amplifier of the CRT.

b. VCO and LO Generation. A 30-Hz sweep generator sweeps the horizontal deflection plates and is also used to sweep the VCO providing the first LO of 135 MHz. The output of the sweep generator is fed to an operational amplifier. The sweep width is controlled by the magnitude of the voltage at this point. The Sweep Width control varies this from 20 KHz to 25 MHz for the Multifunction Receiver and 20 KHz to 2.5 MHz for the subcarrier receiver mode.

The output of the operational amplifier is shaped and applied to a varicap in the oscillator circuit to provide a linear frequency versus voltage output. The center frequency of the oscillator is adjusted by changing the fixed bias on the varicap.

The VCO nominal center frequency is 33.75 MHz and is pulled ±3.125 MHz. The output of the VCO is multiplied by four in two balanced doubler circuits to obtain the required local oscillator of 135 MHz (±12.5 MHz). The multiplied output is amplified to +7 dbm in standard broadband amplifiers.

c. Mechanical Description. The Spectrum Display/Lissajous Monitor Unit is a completely self-contained unit including power supplies. The unit is completely solid state except for the display tube in the X-Y indicator. All amplifiers and mixers will be standardized as much as possible with the building blocks used in the receiver portions of the equipment. Standard sub-modules will be used to package the circuits.

This unit is mounted with chassis slides to facilitate maintenance and alignment. All controls essential to operation are front panel mounted (Figure 3-74). Alignment adjustments will be accessible from the top of the modules.

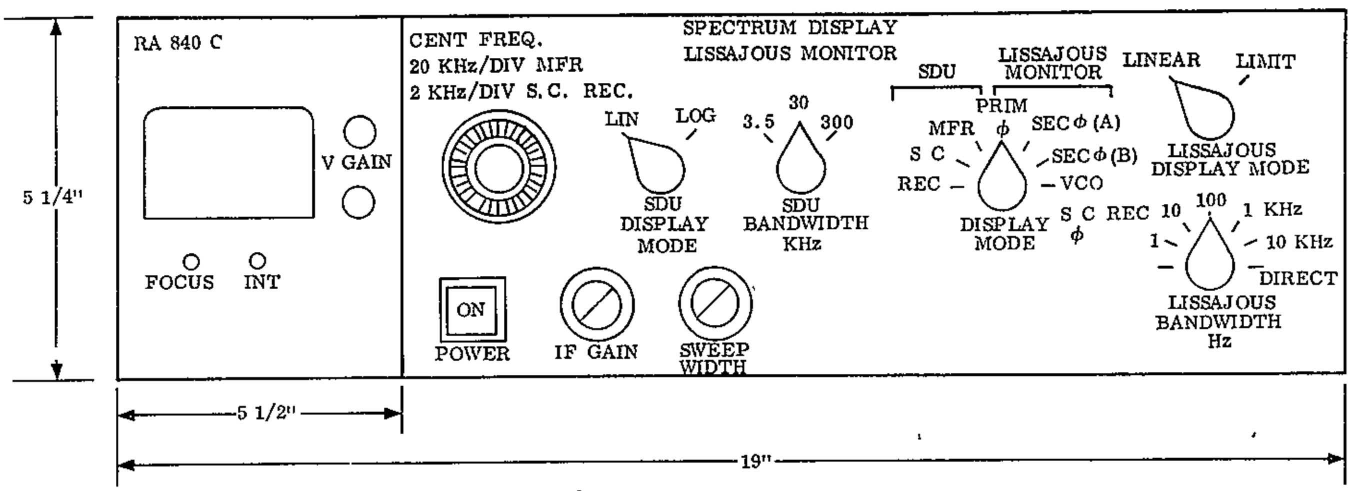

Figure 3-74. Spectrum Display/Lissajous Monitor Unit Panel

3.6.3.4 RECEIVER CONTROL AND MONITOR PANELS. Two control panels and one monitor panel will be provided.

3.6.3.4.1 Receiver Control Panel. Two receiver control panels are supplied, one located at the control console (See Figure 3-75) and the other locally in the receiver rack. The panels are identical except that the local panel has a video level control rather than the control mode switch. In addition, three lamps are provided on the local level to indicate the position of the control mode switch at the console. Panel height is 10.5-inches.

The control mode switch provides a +6-volt line to the switches on either the local receiver control or console receiver control panels (except for the synthesizer control switches which require -12.6 volts). In addition, the control mode switch selects analog control voltages from the channel A and channel B gain controls and the VCO tuning control. When program control is selected, a set of diode AND gates is enabled permitting control from external programming equipment. In addition, a fixed control voltage is applied to the primary VCO to center the frequency. It has been assumed in the design that control signals from the programmer will not be coded.

The only circuitry required behind the console control panel is an integrated 1-watt audio amplifier driven by a signal from the primary loop phase detector. A chassis located behind the local control panel contains the logic circuits for generating control functions other than those indicated directly by the various panel controls. In addition, the chassis contains the driver circuits which power the lamps on the receiver monitor panel.

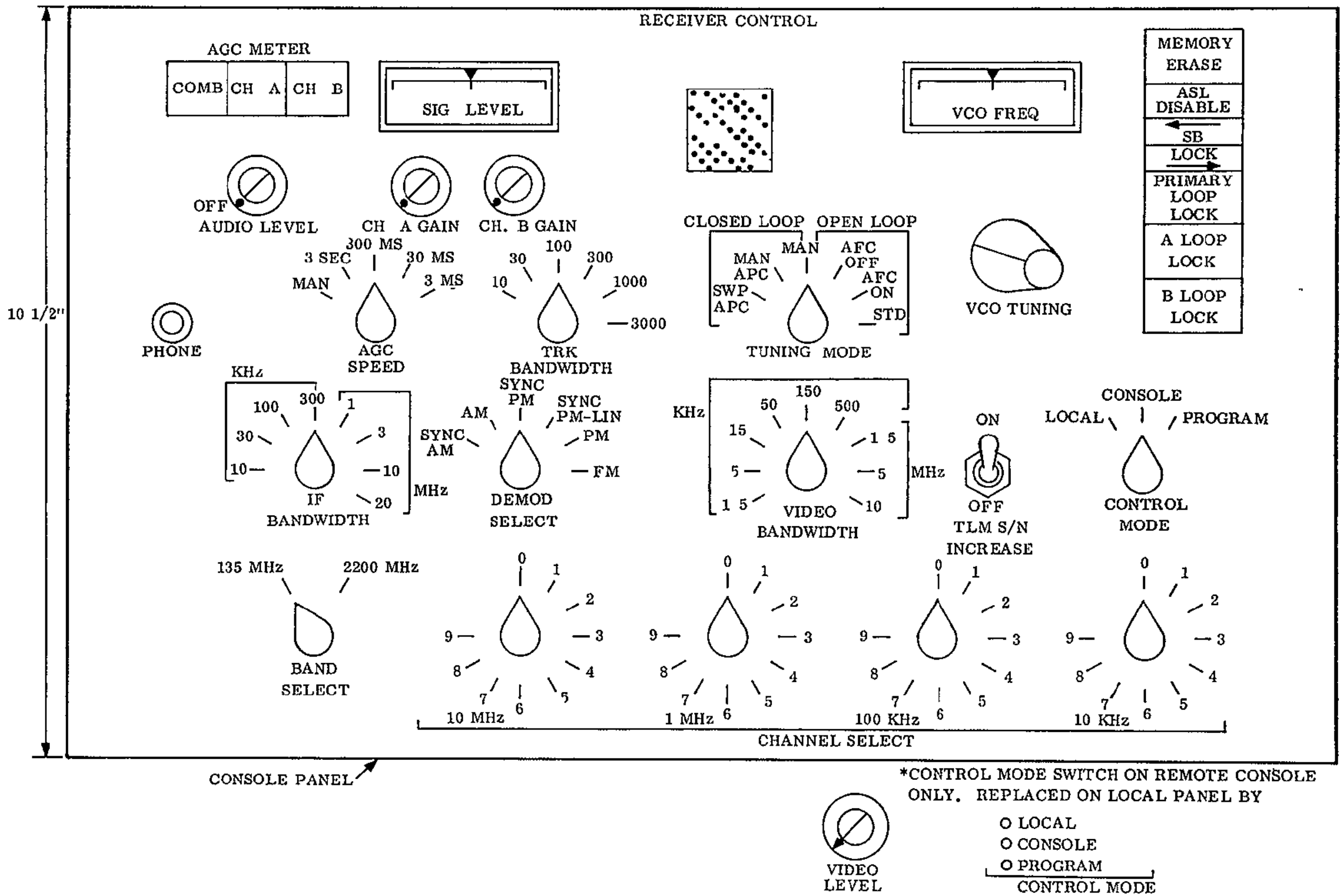

Figure 3-75. Receiver Control Panel

The switches used for frequency selection have been described previously in the section on receiver synthesizer controls. The other switches and their control functions are as follows:

a. TRK BW: a 6-position switch which selects primary loop bandwidths of 10, 30, 100, 300, 1000 and 3000 Hz. The switch simultaneously selects the corresponding secondary loop bandwidths, the predetection autotrack IF bandwidth, the primary and secondary loop phase detector predetection bandwidths, prelock gain, primary loop correlation time constant, sweep speed and range, and anti-sideband lock circuit bandwidth.

b. TUNING MODE: a 6-position switch which provides three closed loop modes of operation; manual, manual acquisition, and sweep acquisition; and three open loop modes; manual, AFC, and fixed frequency. The actual controlled functions include:

(1) AGC selection — either coherent AGC voltages developed in the secondary loop phase detector or non-coherent diode detector voltages.

(2) Phase error — In closed loop operation switches the phase error outputs of the loop phase detectors into the loop filters or in open loop operation the output of the open loop phase detector into the channel A loop filter.

(3) Autotrack IF bandwidth — In closed loop operation transfers control of the autotrack IF bandwidth from the IF BW switch to the TRK BW switch.

(4) Error Product Detector Reference — switches the reference to the product detector from a fixed 10 MHz signal in the closed loop mode to the limited combined sum signal in the open loop mode. In addition, for closed loop operation narrowband crystal filters are switched into the error signal paths.

(5) VCO Control — Allows the primary VCO to be controlled by the output of the primary loop filter or the AFC circuit. In the STD position, the VCO signal is removed from the second LO subsystem and a fixed frequency substituted.

(6) Correlation Enable — Provides enabling signals to the primary and auxiliary correlation amplifiers in the MAN APC and SWP APC positions.

(7) Sweep Enable — Provides an enabling signal to the sweep generator in the SWP APC position.

c. IF BW: An 8-position switch which controls the telemetry IF bandwidth and the open loop autotrack IF bandwidth. In the 1, 3, 10, and 20 MHz positions the autotrack IF bandwidth is 1 MHz. This switch also selects either the wideband or narrowband telemetry demodulator output, the wideband output being selected in the 3, 10, and 20 MHz positions. In addition, the switch selects the appropriate telemetering FM demodulator output and the discriminator output for AFC.

d. Video BW: A 9-position switch which, in addition to selecting the telemetry post detection bandwidth, switches the time constants of the integrators in the non-coherent PM demodulators.

e. TLM S/N Increase: This switch in the ON position changes the gain distribution in the sum channel receiver so as to produce a strong signal-to-noise ratio of at least 30 db in a 20 MHz IF bandwidth.

The functions of the remaining selector switches, AGC SPEED, DEMOD SELECT and AGC METER are self-explanatory. Five indicators which show the status of the phase lock loops are provided. Three of the indicators, memory erase, sideband lock, and primary loop lock are pushbutton switch lights. If the receiver should drop lock, the memory light will go on. The memory circuit may be deactivated by depressing the pushbutton.

Depressing the primary loop lock pushbutton disables the primary loop correlation detector and switches the receiver to the memory mode. The sideband lock indicator has a split lens, one half indicating ASL disable, and the other half sideband lock. Depressing the push-button disables the anti-sideband lock circuits in the receiver and illuminates the ASL disable light. When the ASL circuits are used and phase lock to a sideband occurs, the SB lock light is turned on.

Signal level and VCO frequency meters are provided. The signal level meter is calibrated in dbm from -50 to -160. The VCO frequency meter is calibrated from -300 KHz to +300 KHz.

3.6.3.4.2 Receiver Monitor Panel. The receiver monitor is contained on a 5.25-inch panel as shown in Figure 3-76. The indicator lights provide verification of the actual receiver operational setup for any of the three control modes. Expected life of the indicator lamps is 16,000 hours.

X and Y error signals supplied to the antenna system are indicated on the two panel meters. X and Y error signals are also displayed on another pair of panel meters located on the error channel drawer. Two-position switches associated with each meter permit a 10:1 change in meter sensitivity.

3.6.3.5 MECHANICAL DESCRIPTION. The multifunctional receiver, excluding the control and monitor panels, is contained in four rack-mounted drawers.

3.6.3.5.1 Sum Channel Drawer. This drawer accepts the two sum channel inputs from the multicoupler and performs all the signal processing to accomplish phase lock control, AGC, AFC, diversity combining and all other operations performed on the received sum signals. Input local oscillator signals and control signals from the system signal source and local/remote receiver control are used to accomplish these operations.

Output signals include gain-controlled IF signals for the telemetry drawer and the ranging demodulator in the subcarrier receiver drawer, AGC and diversity combiner control signals,

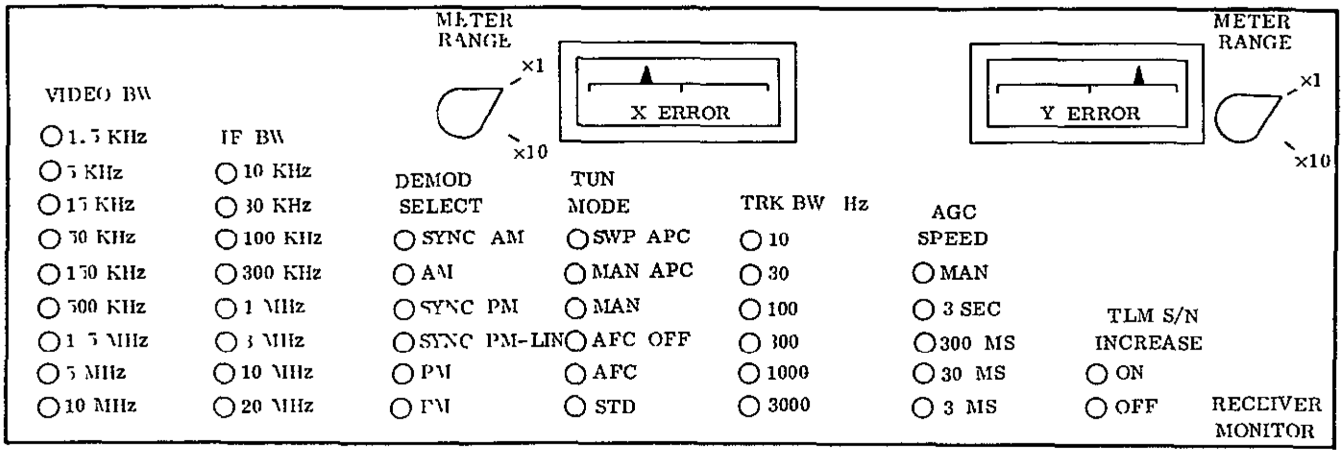

Figure 3-76. Receiver Monitor Panel

and local oscillator and reference signals for the error channel drawer.

3.6.3.5.2 Error Channel Drawer. This drawer accepts the four-error channel inputs from the multicoupler and performs the signal processing to develop antenna steering information in both open and closed-loop modes. Input local oscillator signals and control signals from the system signal source, sum channel drawer, and local/remote receiver controls are used in these operations.

3.6.3.5.3 Telemetry Drawer. This drawer accepts the wideband combined second IF from the sum channel drawer and performs all signal processing to accomplish demodulation of AM, FM, and PM signals for all the specified bandwidths.

3.6.3.5.4 Power Supply Drawer. This drawer provides regulated dc voltages for the three major drawers described above.

3.6.3.5.5 Drawer Assembly. Each of the drawers is a slide-mounted 10.5-inch high chassis. A standard plug-in module is used through the receiver. The module is vertically mounted and approximately $2 \times 4 \times 6$ inches in size. It is held in place by two screws accessible from the top of the module. The module cover is secured with two quarter-turn fasteners. With the cover removed, both the front and back sides of the circuit board are accessible.

3.6.3.5.6 Building Block Design. The multifunctional receiver and subcarrier receiver design will make maximum use of standard building block sub-modules. Over the past year the Electronics Division of General Dynamics has developed a family of broad-band amplifiers, mixers, and voltage-controlled attenuators packaged in small crystal-can enclosures. The broad-band characteristics of these circuits allow them to be used at frequencies from 1 MHz to over 300 MHz. The use of such circuits is beneficial to GSFC, since logistic and maintenance costs are reduced by such standardization, as well as to General Dynamics, since duplication of design effort is avoided.

Some of the building block modules already developed include:

a. Type I Amplifier

Frequency	1 MHz to 300 MHz
Gain	+14.5 db
Noise Figure	6.5 db at 110 MHz
Impedance	50 ohm nominal input and output; VSWR 1.4:1
Time Delay	1.7 nanosec
Application	Second IF amplifier

b. Type II Amplifier

Frequency	1 MHz to 100 MHz
Gain	20 db
Noise Figure	6 db at 10 MHz
Impedance	50 ohm nominal input and output; VSWR 1.4:1
Application	Third IF amplifier General purpose amplifier

c. Variable Gain Amplifier

Frequency	1 MHz to 100 MHz
Gain	10 db to 20 db (potentiometer adjust)
Application	Third IF amplifier General purpose amplifier

d. Type III Amplifier

Frequency	1 MHz to 250 MHz
Gain	0 db
Impedance	50 ohm nominal input and output; VSWR 1.2:1
Application	Isolation amplifier

e. Voltage-Controlled Attenuator

Frequency	10 MHz to 150 MHz
Attenuation	-2 db to -22 db (log-linear control)
Impedance	50 ohms nominal; VSWR 1.2:1

f. Double Balanced Mixer

Frequency	500 KHz to 500 MHz
Conversion Loss	6-7 db
LO Isolation	30 db

g. Balanced Doubler

Frequency	500 KHz to 500 MHz
Conversion Loss	10 db
Harmonic Rejection	Fundamental - 30 db; 3rd Harmonic - 30 db
Impedance	50 ohms nominal

h. Directional Coupler

Frequency	500 KHz - 400 MHz	
	10-db type	20-db type
Insertion Loss	1 db	0.1 db
Directivity	40 db at 100 MHz	25 db at 100 MHz

Other types of building blocks are required in the design of the multifunctional receiver. Preliminary design work has been initiated on several types, which include: (1) a phase shifter (±90 degrees) operating at 10 MHz, 50 MHz, and 110 MHz, (2) a phase detector for 10 MHz operation with a 65 db dynamic range (dc offset to saturation level), and (3) an RF switch with 75 db isolation.

3.6.4 Subcarrier Receiver

A functional block diagram of the subcarrier receiver and range demodulator is illustrated in Figure 3-77.

The function of the subcarrier receiver is to accept the 110 MHz IF from the wideband combiner, demodulate the subcarrier (crystal transponder) or range tones (phase-locked loop transponder) phase-modulated on the primary carrier, track the subcarrier, and demodulate the range tones phase-modulated on the subcarrier. The subcarrier receiver is capable of operating with either the S-Band or VHF carrier and corresponding subcarriers.

Besides the demodulated range tones, this receiver also supplies a VCO output to the doppler extractor for range rate determination and a 10 MHz IF to the spectrum display unit for viewing the subcarrier and its ranging sidetones.

Since the subcarrier undergoes the same signal dynamics as the primary carrier, a third-order phase-locked loop identical to the composite diversity locked loop in the multifunctional receiver will be used.

The 110 MHz IF from the wideband combiner is gain-controlled and arrives at the input to the range demodulator at a constant level of -83.5 dbm. This signal is amplified and coherently detected in a wideband double-balanced phase detector. The output of the phase detector is fed to a video amplifier to provide range tones for use with a phase-locked loop transponder.

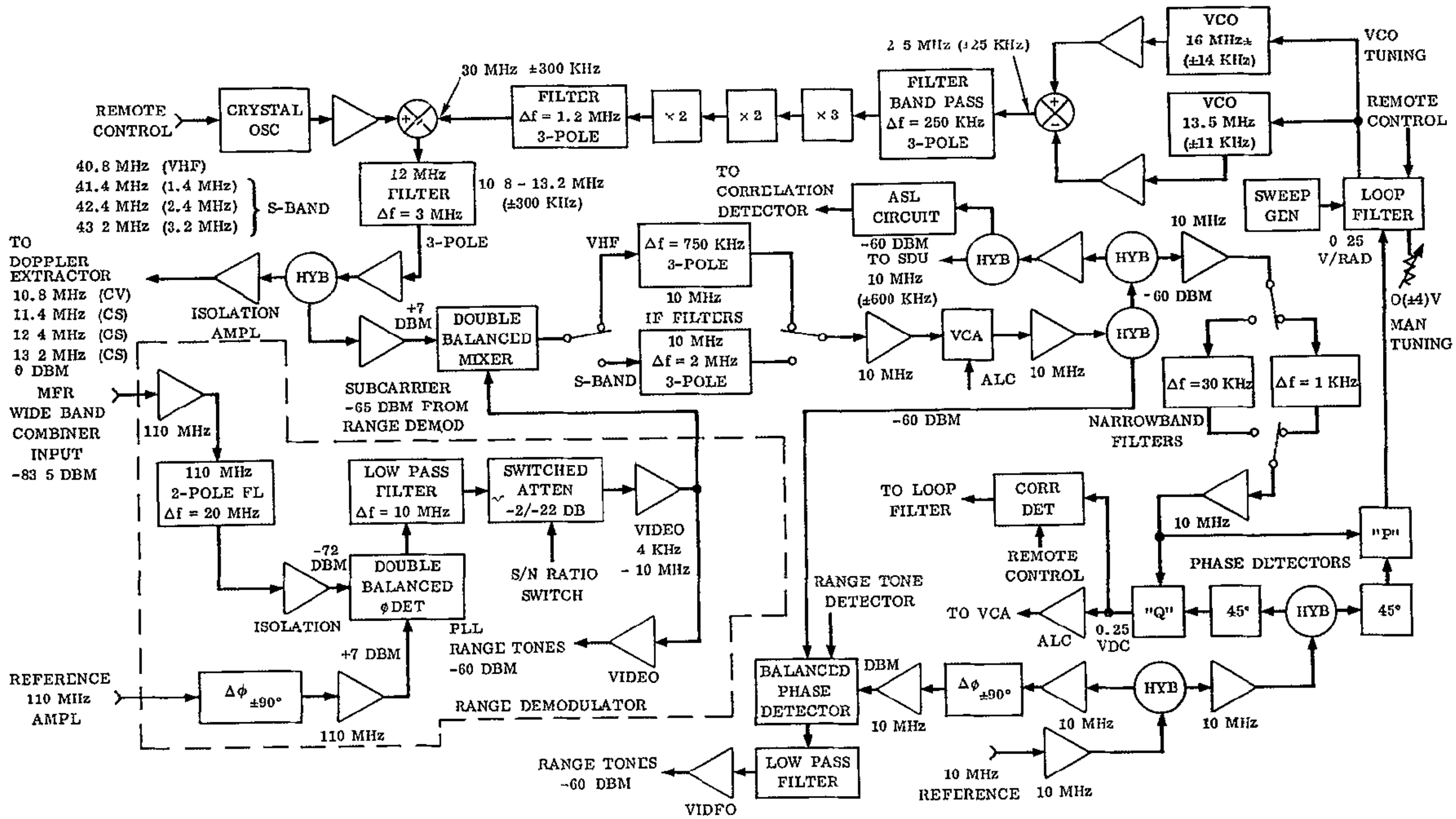

Figure 3-77. Subcarrier Receiver/Range Demodulator Functional Block Diagram

The range tones are demodulated in a wideband coherent phase detector. The 10 MHz reference signal is derived from the system signal source and is coherent with the 10 MHz used in the multifunctional receiver. The detected range tones are amplified in a wideband video amplifier to a level of -60 dbm (nominal).

The 10 MHz input to the narrowband phase detector is filtered in 1 KHz or 30 KHz single-pole crystal filter. The filters are selected as a function of the tracking bandwidth to improve the signal-to-noise ratio at the input to the phase detector. The signal and reference are power split to drive two phase detectors 90 degrees apart. The output of the amplitude detector is used to control the automatic leveling circuit necessary to maintain constant range tone amplitude for different subcarrier modulation indices. The output of the "P" detector or phase detector is used to control the VCO frequency and thereby close the loop.

3.6.4.1 RANGE DEMODULATOR. Figure 4-22 illustrates the gain distribution for the range demodulator and subcarrier receiver from the 110 MHz input to the demodulated subcarrier output. Also included in the diagram is a noise analysis indicating signal and noise levels at various points. The noise analysis is carried out for threshold in the 10 Hz tracking bandwidth, strong signal, and strong signal with the signal-to-noise ratio improvement switched in. Equal carrier and subcarrier power is also assumed.

The signal level into the first amplifier is held fixed by the main receiver AGC to -83.5 dbm. However, the noise varies from -97.6 dbm for strong signals to -24.5 dbm for threshold signals. Therefore, care must be taken to prevent the amplifiers and phase detector from limiting on noise peaks. Considering noise peaks 13 db above rms noise, the maximum power handled by the amplifiers is +3 dbm peak at the output. The amplifiers used are standard broadband stages which can supply up to +10 dbm rms or +13 dbm peak power without compression. Two amplifiers are used to adequately isolate the 110 MHz reference signal from the main receiver. The amplifiers plus the balanced phase detector provide about 120 db of isolation. Additional isolation is provided in the MFR.

The 110 MHz predetection filter shapes the response to have a 3 db bandwidth of 20 MHz and a 1 db bandwidth of 14 MHz. The filter is a 2-pole maximally flat design to minimize the group delay. The filter is sufficiently wide to approximate a linear phase characteristic over the band of interest. Analysis of group delay stability indicates that the predetection filtering contributes little to the overall delay.

The 110 MHz reference signal from the system signal source is passed through a variable phase shifter having a range of greater than 180 degrees and amplified to a level of +7 dbm at the phase detector input. This level is 22 db above the rms noise at threshold and is more than adequate to prevent the phase detector from limiting on noise.

The double-balanced phase detector to be used is the Relcom Model M6E double-balanced mixer. With a reference level of +7 dbm the single sideband conversion loss is 6 db; phase detector sensitivity is 143 mv per radian into a 50-ohm load when driven with 0 dbm of signal power. This mixer will handle inputs of +1 dbm without appreciable compression.

The output of the phase detector is filtered in a 2-pole low pass filter with a 3 db bandwidth of 10 MHz and a 1 db bandwidth of 7 MHz. The video amplifier following the filter has a frequency response flat from essentially dc, to allow passage of the 4 KHz range tones for the phase-locked loop transponder, to over 10 MHz to minimize the delay to the subcarrier and higher frequency-modulating signals. Another wideband video amplifier delivers the range tones to the range tone extractor. Both video amplifiers are integrated circuits.

A 20 db attenuator is switched in when the signal-to-noise ratio improvement is switched in. This attenuator reduces the subcarrier and range tones to compensate for the 20 db increase in IF at the phase detector input. Therefore, the range tone and subcarrier are maintained at a constant level for either mode of operation. However, the threshold is degraded when the signal-to-noise improvement switch is used due to limiting ahead of the 20 db attenuator.

3.6.4.2 MIXER AND IF AMPLIFIER. The subcarrier output from the range demodulator for equal carrier and subcarrier power is -65 dbm. The noise at threshold is -11 dbm. This noise level is sufficiently low so that limiting in the mixer does not occur. The mixer used is identical to the phase detector already discussed. The high degree of balance obtained in this mixer virtually eliminates spurs in the 10 MHz passband.

Since the VCO is chosen higher than the IF, spurs occur at $3F_{sig}$, and $2F_{LO} - 5F_{sig}$. Data on the mixer when driven with +7 dbm of LO power and -10 dbm signal power shows these spurs down 61 and 86 db, respectively. For signal levels lower than -10 dbm the spurious response improves. For frequencies less than 50 MHz the isolation between the LO port and the IF port is 40 db.

For the S-Band subcarriers of 1.4, 2.4, and 3.2 MHz, a three-section filter further attenuates the LO and spurious frequencies. In this case the filter is flat for a band ±600 KHz from center frequency to allow the 500-KHz range tones to pass through undistorted.

In the VHF case, the LO and image rejection requirements imply a much narrower filter since the subcarrier is only 677 - 920 KHz. The major range tones for VHF operation are only 20 KHz, therefore, a narrower filter will be switched in for VHF operation.

The IF signal after filtering passes through a voltage-controlled attenuator and is amplified before being power split to drive the wideband range tone detector, the spectrum display unit, and the narrowband phase lock loop. The VCA has a range of 20 db. From Figure 4.3.15 it can be seen that this range is more than adequate to maintain constant range tone outputs for the expected variations of modulation indices.

The amplifiers used throughout for the 10 MHz IF are standard broadband amplifiers having a gain of approximately 20 db. External provisions are made to reduce this gain for certain requirements. A variable gain version of this amplifier will also be used in the 10 MHz IF signal path.

3.6.4.3 WIDEBAND RANGE TONE DETECTOR AND VIDEO AMPLIFIER. The circuits used to implement demodulation of the range tones from the subcarrier are essentially the same as those used for demodulating the subcarrier from the carrier. The double-balanced phase detector and video amplifier will be identical. The signal at the input to the phase detector will be held at -60 dbm by the ALC circuit. Noise at this point is a maximum of -13 dbm at threshold for the 10 Hz tracking bandwidth.

The 10 MHz reference signal is amplified to a level of +7 dbm at the phase detector. The amplifiers used are identical to those used in the 10 Hz IF signal path. The variable phase shifter required to properly phase the reference to the signal is the same type as that of the 110 MHz phase shifter.

The gain control circuit maintains the subcarrier level constant independent of its modulation index with respect to the primary carrier. Also, since the gain control works off the subcarrier level, the input to the range tone demodulator will be constant and independent of the modulation on the subcarrier. However, the range tone output will vary as a function of its modulation index with respect to the subcarrier. The gain of the video amplifier will be less than 10 db.

3.6.4.4 NARROWBAND PHASE DETECTORS. Figure 4-23 illustrates the gain distribution for the signal path to the narrowband phase detectors. The 10 MHz IF signal is filtered in narrowband single-pole crystal filters prior to the phase detector inputs. The function of the filter is to limit the noise power into the detector and hence, ease the dynamic range over which the detector must operate. The filter is single pole to introduce minimum phase lag into the loop.

The filter to be used in the 10, 30, and 100 Hz tracking bandwidth is the 1 KHz 3 db bandwidth filter (noise bandwidth is 1.57 KHz). In this case the worst signal-to-noise ratio is -16 db at threshold in the 10 Hz bandwidth. The 30 KHz (47 KHz noise bandwidth) filter is used for the 300, 1000, and 3000 Hz tracking bandwidths. In this case the worst case signal-to-noise ratio is -17 dbm in the 300 Hz bandwidth at threshold. The phase detector designed allows operation at much lower signal-to-noise ratios.

The phase detector, reference drive, and signal drivers are identical for both the "P" and "Q" phase detectors. The same design is also used throughout the multifunctional receiver. The phase detector is a dual-quad which has extremely good balance, not only as a function of temperature and time, but also as a function of input noise level. The reference and signal drivers are complementary emitter followers providing a low impedance drive to the phase detector. The output of the "P" phase detector is fed to the loop filter. The output of the "Q" detector, which is 90 degrees out of phase with the "P" detector and thus becomes an amplitude detector, drives the ALC amplifier to maintain the phase detector constant at 0.25 volt/radian.

3.6.4.5 AUTOMATIC LEVEL CONTROL. A simplified schematic diagram of the automatic level control (ALC) circuit is shown in Figure 3-78. A gain control is necessary in the subcarrier receiver to maintain constant range tone outputs independent of subcarrier

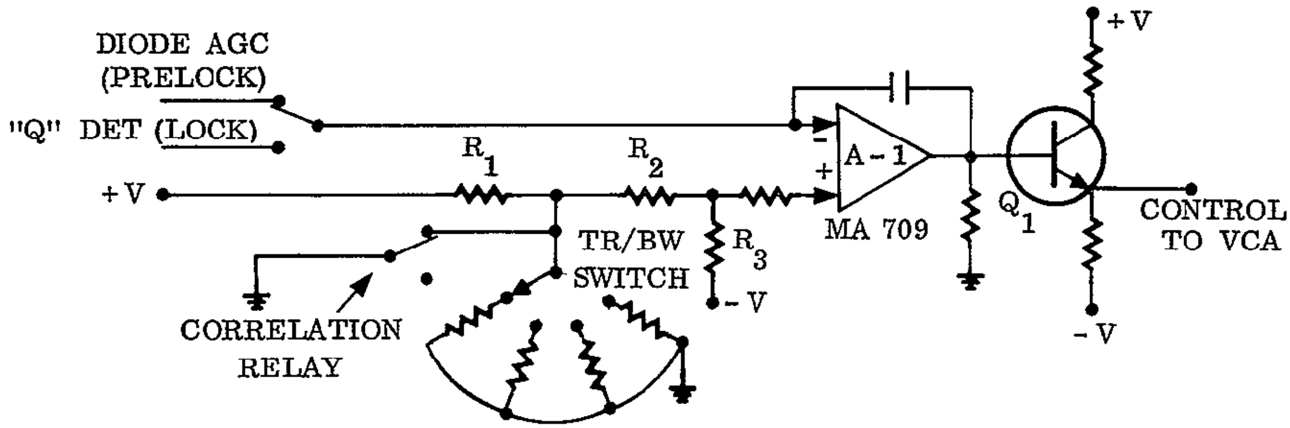

Figure 3-78. ALC Amplifier

modulation indices. The gain control circuit must also work prior to subcarrier phase lock to prevent saturation on noise.

Consider the phase lock condition first. When the subcarrier is phase locked, a -0.25 vdc signal is applied to the inverting input of operational amplifier A-1 from the "Q" or synchronous amplitude detector. In this condition the junction of R_1 and R_2 is grounded and the divider network of R_3 and R_2 establishes -0.25 vdc bias at the noninverting input to the amplifier. Since amplifier A-1 is a very high gain device, a slight change in the "Q" detector voltage produces a proportional change in control voltage at Q_1. The control voltage changes the attenuation of the VCA in the IF signal path in a direction to reduce the change at the "Q" detector output and thus maintain a constant signal level.

Prior to phase lock, since the output of the "Q" detector is zero, the VCA will have minimum attenuation and amplifiers prior to the phase detector could saturate on noise, hindering acquisition of weak signals. There is no danger of saturating on strong signals since the main receiver AGC keeps the level at the range demodulator constant. To eliminate this problem a diode detector is provided, just ahead of the narrowband filter in the IF path, which has a dc output proportional to the rms noise at this point. In this case the junction of R_1 and R_2 is not grounded, but is held to a voltage dependent on the tracking bandwidth. This allows the prelock gain to be a function of tracking bandwidth, which is desirable for acquisition purposes. The ALC loop recirculates in the same manner as for the phase lock case.

3.6.4.6 PHASE LOCK LOOP FILTER AND SWEEP GENERATOR. Figure 3-79 illustrates the implementation of the loop filter required in the third-order phase-lock loop. The circuit takes on three different configurations as shown.

In the prelock manual acquisition position of the tuning mode control, the loop filter is configured as shown in Figure 3-79A. Prior to phase lock, the phase detector input is ac-coupled to prevent phase detector offsets from saturating the operational amplifier. In this

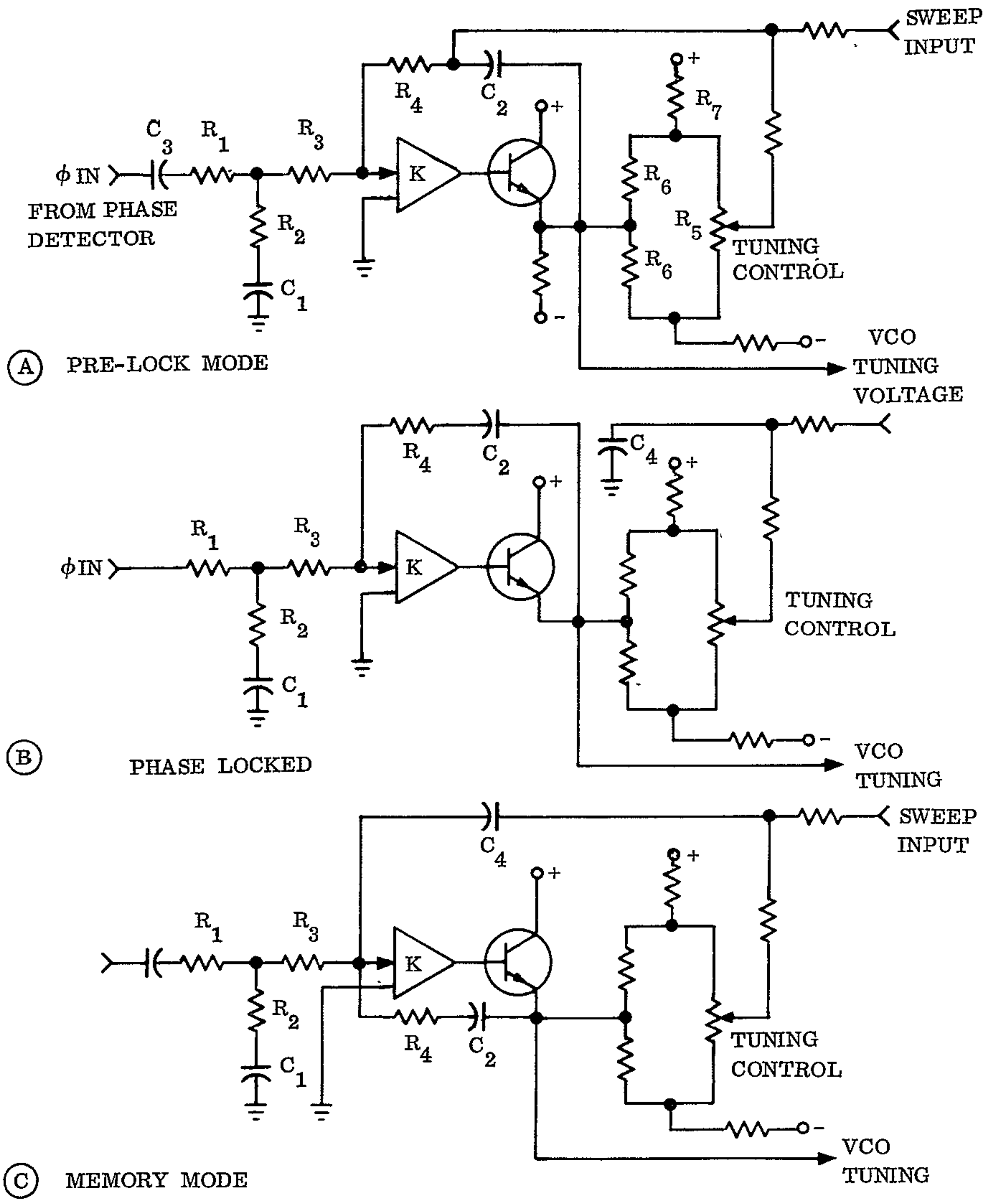

Figure 3-79. Loop Filter Modes of Operation

mode, capacitor C_2 is effectively shorted out by the tuning control. The loop is now a second-order loop with only the passive integrator (R_1, R_2, and C_I) in the circuit.

Tuning of the VCO in the acquisition (prelock) mode is as follows. Because of the very high gain of the amplifier ($K \approx 1 \times 10^6$), the resistive feedback maintains the voltage at the wiper of the tuning potentiometer at essentially zero. Therefore the VCO tuning voltage and, hence, the VCO frequency is directly proportional to the value of R_5.

Tuning control R_5 is a 20-turn potentiometer. The center ten turns are used to control the VCO over its entire range. Five turns at each end of the range are available for additional rotation in the memory mode. In the sweep acquisition mode a triangular voltage waveform is added to the manual tuning voltage.

When acquisition has occurred, the manual tuning control (or sweep control) is disabled and the phase detector is dc-coupled to the loop filter as shown in Figure 3-79B. The resistive bypass is removed from C_2 and the loop is now third order. Memory capacitor C_4 is connected and will charge to a voltage proportional to the VCO tuning voltage.

If the loop should unlock, the filter switches to the memory mode as shown in Figure 3-79C. The charge stored on C_4 holds the VCO tuning voltage at the level where lock was lost. However, both the tuning control and sweep can vary the VCO tuning voltage about the "remembered" tuning level.

In the manual search mode the phase detector is not connected to the loop filter and phase lock cannot occur. The correlation detector is also disabled in this mode.

The sweep generator used in the automatic acquisition mode is an integrator type utilizing an operational amplifier as an active element. A bistable multivibrator generates a gate which is integrated to generate a symmetrical sweep waveform. The sweep generator is disabled when phase lock occurs or when the tuning control is not in the automatic acquisition mode. The sweep rates are selected as a function of tracking bandwidth. A functional block diagram is shown in Figure 3-80.

3.6.4.7 CORRELATION DETECTOR AND ANTI-SIDEBAND LOCK CIRCUIT. The function of the correlation detector is to sense phase lock and perform the necessary switching functions to configure the loop filter, as shown in Figure 3.6.14, necessary to track the doppler on the subcarrier. A simplified schematic is shown in Figure 3.6.15. When phase lock is achieved the correlation detector energizes a series of relays which switch a number of functions including phase lock indication, manual and sweep tuning disable, and frequency memory storage. Also the AGC error is switched from the diode detector to the "Q" phase detector.

The input to the correlation detector is the output of the "Q" phase detector. Prior to phase lock, this signal consists of "beat note" and noise. This signal is filtered as a function of tracking bandwidth prior to the correlation switch. When the subcarrier frequency is co-

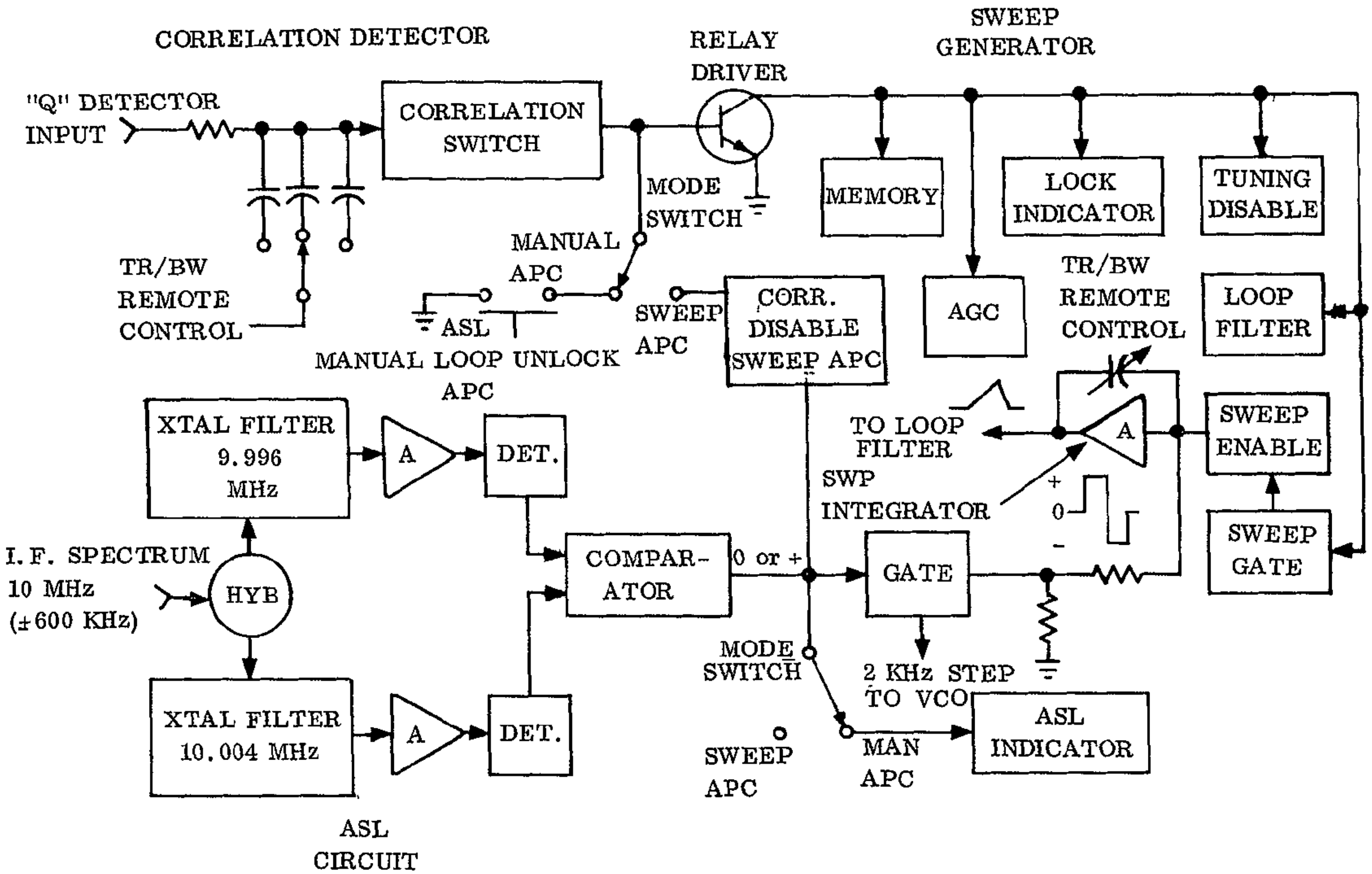

Figure 3-80. ASL Circuits, Correlation Detector Sweep Generator

herent with the reference frequency a negative dc voltage appears on the "Q" detector output and causes the correlation switch to trigger "on" energizing the relay driver which, in turn, energizes the other required switching functions. When lock is lost, the correlation switch returns to its prelock condition and the loop assumes the "memory" condition previously described.

Also included in Figure 3-80 is circuitry necessary to prevent the subcarrier receiver from locking up to 4 KHz sidetones. The method used takes advantage of the knowledge of the specific frequency to guard against. Thus, threshold of the anti-sideband lock (ASL) is improved because it is a narrowband scheme.

The 10 MHz IF signal supplied to the SDU is split and drives two filters. The filters are 2-pole crystal filters centered at 4 KHz above and below 10 MHz. The filters are approximately 1 KHz wide to accommodate the possibility of an 800 Hz sideband of the 4 KHz signal. Thus, the bandwidth of the ASL circuit is approximately 1 KHz. A discriminator technique would require a 9.6 KHz bandwidth resulting in a lower threshold.

The outputs of the filters are amplified, detected, and sent to a comparator circuit. If the receiver is locked to the subcarrier the 4 KHz sidebands would be equal in amplitude and the dc signals applied to the comparator would be equal. In the event of sideband lock there will be an output from only one of the filters and unequal dc signals are applied to the comparator.

The comparator is set up to provide an output only when unequal signals are applied at the input. The comparator will be adjusted to tolerate a preset difference without switching.

When sideband lock occurs in the manual acquisition mode the output of the comparator is sent to an indicator on the control panel. A pushbutton switch on the control panel unlocks the loop by disabling the relay driver.

In the automatic acquisition mode the receiver unlocks automatically as soon as sideband lock is sensed by the comparator. The loop is then in the memory mode and the sweep continues in the direction it was going before it was interrupted. However, to prevent the receiver from locking up immediately to the same sideband, a small offset voltage must be applied to the VCO to step it toward the carrier frequency. To do this, a fixed amount of the output voltage of a multivibrator, which drives the integrator in the sweep circuit, is coupled to the tuning voltage. The sense of this voltage agrees with the tuning direction and the VCO is stepped toward the carrier frequency. Since we are only concerned with the 4 KHz sidebands the VCO can be stepped about 2 KHz, independent of tracking bandwidth.

3.6.4.8 VCXO AND LOCAL OSCILLATOR DESIGN. The local oscillator necessary for converting the subcarrier to a constant 10 MHz is made up of a voltage-controlled oscillator, controlled by the narrowband phase lock loop, and a fixed-frequency crystal oscillator whose frequency is selected with the subcarrier switch on the subcarrier receiver control panel.

The VCXO will be made up of two VCXO's. This method, together with careful component selection and circuit design, should enable the VCO to meet the 3° rms phase jitter specification.

As illustrated in Figure 3-77 the two VCO's used will be at center frequencies of 16 MHz and 13.5 MHz with pulling ranges of ±14 KHz and ±11 KHz, respectively. These frequencies and pulling ranges were chosen to provide a spurious-free area for the difference frequency and also to make the two VCXO's agree with the assumptions developed during analysis. As can be seen, the pulling ranges of the two VCXO's are nearly the same and therefore nearly maximum stability improvement of $\sqrt{2}$ can be expected. The frequency vs voltage slopes of the two VCXO's are opposite in sign and their difference equals ± 25 KHz.

The two VCXO's are mixed in a double-balanced mixer and filtered in a 3-pole bandpass filter to remove undesired products. The difference frequency of 2.5 MHz (±25 KHz) is amplified and multiplied by 12 to give an output of 30 MHz (±300 KHz). The times-12 circuit consists of a transistor tripler followed by two balanced-doubler circuits with amplifiers and filters between multiplying operations. The final VCXO output is filtered and applied to a double-balanced mixer.

The other input to the mixer is a crystal-controlled oscillator. The crystal oscillator supplies one of four possible frequencies, dependent on the mode of operation and the frequency of the subcarrier. Diodes are used to switch crystals into the circuit which determines the oscillator frequency. Three crystals are used for the S-Band subcarriers of 1.4, 2.4 and 3.2 MHz. A fourth crystal is used for the center frequency, 800 KHz, of the VHF subcarrier. Since the VHF subcarrier varies from 677 KHz to 920 KHz with a maximum doppler of ±20 KHz or a total of 283 KHz plus variations in the crystal transponder frequency. The 600 KHz tuning range of the VCXO is more than adequate to cover the VHF frequency variation.

The mixed output frequencies of 10.8 MHz (VHF), 11.4, 12.4, and 13.2 MHz (S-Band) are filtered to remove unwanted products and provide a clean LO to the input mixer. The filter has a flat bandwidth of 10.5 to 13.5 MHz to accommodate doppler shifts and frequency changes. The filtered signal is amplified and sent to the mixer at +7 dbm.

A local oscillator output is also provided for the doppler extractor for use in obtaining range rate information. This output is of the form:

$$f_1 + K' 48 f_c - KK' f_t \text{ (S-Band)}$$

$$f_1 + KK' f_{TV} - 13K' f_{cv} \text{ (VHF)}$$

and is mixed with the multifunctional receiver input to remove the f_c terms.

3.6.4.9 MECHANICAL DESIGN. The Subcarrier Receiver will be rack mounted with chassis slides to facilitate maintenance and alignment. The receiver circuits will be packaged in standard plug-in modules. The drawer housing the Subcarrier Receiver and Doppler Extractor will use 10.5-inches of panel space.

The Subcarrier Receiver is capable of being completely controlled from the control panel in the rack or the remote control panel at the control console. All control voltages from the remote control panel are 0 or 6 vdc.

3.6.4.10 SUBCARRIER RECEIVER CONTROL PANEL. The control panel for the subcarrier receiver also includes the controls necessary to operate the doppler extractor since the doppler extractor and subcarrier receiver are housed in the same drawer. Two control panels will be provided. One will be located locally in the receiver rack and one is located in the remote control console. This panel is a standard 5.25-inch rack panel.

The equipment is operated entirely by the controls on the control panel. Digital control voltages (0 and +6v) are sent to the receiver to perform the required switching.

Figure 3-81 shows a view of the subcarrier receiver control panel. A panel-mounted meter indicates the VCO frequency. An integrated-circuit audio amplifier drives a front panel speaker. The phase detector is connected from the receiver to the audio amplifier, providing an audio indication of phase lock. Most switches on the front panel are self-explanatory.

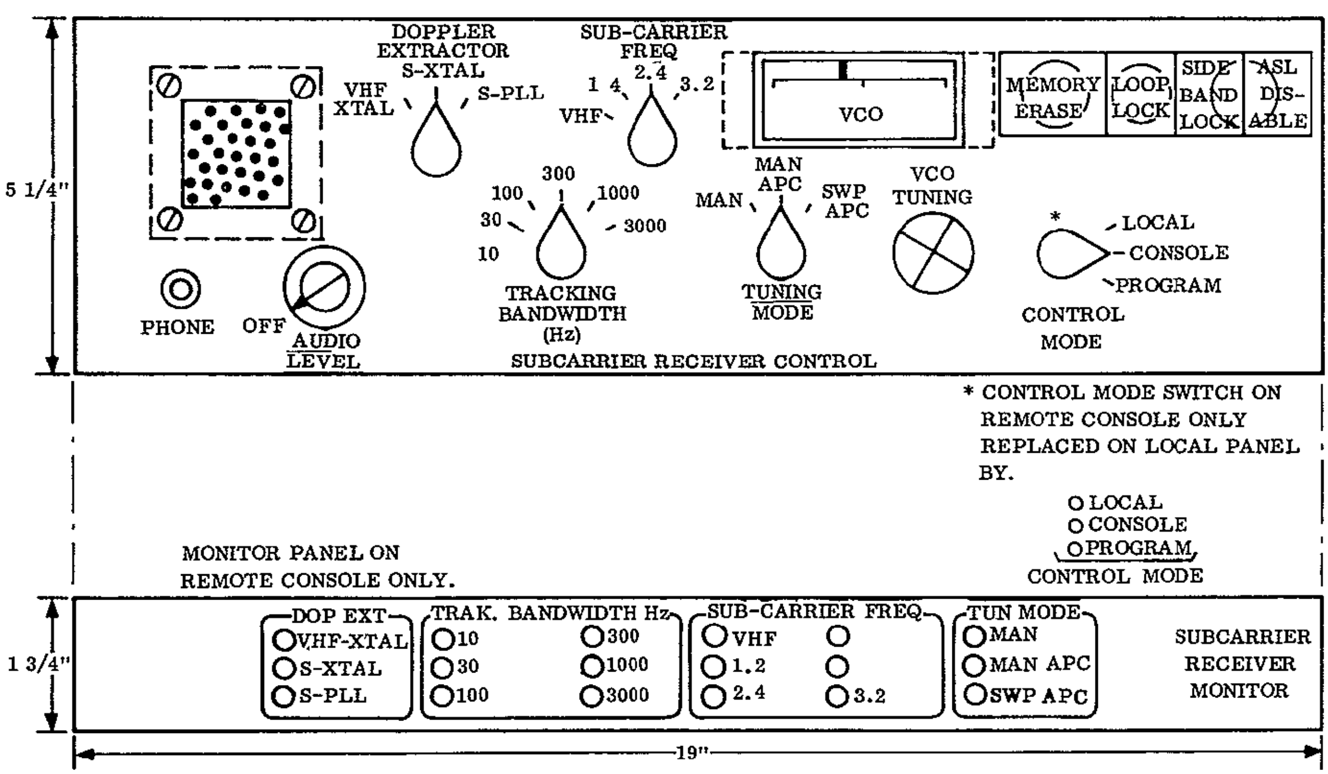

Figure 3-81. Subcarrier Receiver Monitor and Control Panels

The "Memory Erase", "Loop Lock", and "Sideband Lock" indicators are pushbutton switches with illuminated lenses. When the receiver goes into the memory mode the "Memory Erase" button illuminates. To remove the memory function, the "Memory Erase" light is simply pressed.

The "Loop Lock" indicator is illuminated when phase lock is achieved. Pressing the indicator disables the correlation detector, placing the receiver in the memory mode. The receiver can then be returned to its pre-lock condition by pressing the "Memory Erase" indicator.

The "Sideband Lock" indicator has a split lens. One-half the lens indicates "ASL DISABLE" and the other half indicates "SIDEBAND LOCK". Pressing the "sideband lock" indicator completely disables the anti-sideband lock circuits (ASL) in the receiver and this is indicated by the ASL DISABLE light. When the ASL circuits are used and sideband lock occurs in the manual acquisition mode, the SIDEBAND LOCK is illuminated. The receiver is then unlocked by pressing the "Lock" indicator.

The remote and local control panels are the same except for the "Control Mode" switch. The remote control panel at the console is the master and selects the method by which the receiver is operated. The local panel then indicates this selection.

3.6.4.11 SUBCARRIER RECEIVER MONITOR PANEL. The subcarrier receiver monitor panel is located in the remote control console. The panel indicates the switching functions performed by the control panel by illumination of the appropriate indicators. This panel is a standard 1.75-inch rack panel.

3.6.5 Doppler Extractor

The function of the doppler extractor is to extract doppler information from the RF carrier and subcarrier for the purpose of determining range rate data. The doppler extractor receives inputs containing doppler information from the multifunction receiver VCO and the subcarrier receiver VCO. Appropriate bias frequencies are supplied by the system signal source. The output of the doppler extractor goes to the range rate extractor and the digital rate aid unit. The doppler extractor unit will be located in the same drawer as the subcarrier receiver.

3.6.5.1 FREQUENCY INDEPENDENT DOPPLER EXTRACTION. The velocity of a satellite is determined by measuring the two-way doppler frequency shift on the transmitted frequency. The actual measurement performed involves the determination of the time interval required for a fixed number of doppler cycles, offset from zero by a fixed bias frequency, to pass through a gate. This gate then admits a reference frequency into a counter which counts the reference frequency for the time interval determined by the gate. The number of counts of the reference frequency f_r is:

$$T_c = \frac{Nf_r}{f_b + f_d} \tag{1}$$

where

T_c = Number of counts of frequency, f_r

N = Preset number of doppler plus bias cycles

f_r = Reference frequency

f_b = Bias frequency

f_d = Two-way doppler frequency = $f_t \frac{(2V)}{C}$

f_t = Transmit frequency

c = Speed of electromagnetic propagation

V = Satellite velocity with respect to station

then

$$T_c = \frac{Nf_r}{f_b + f_t\left(\frac{2V}{C}\right)} \tag{2}$$

As indicated by the above expression the velocity measurement is a function of f_t. Therefore, for precise velocity measurements, the transmitted frequency must be very accurately known and a precise measurement is required every time f_t is changed.

A method removing the dependency of the velocity measurement on the transmit frequency derives the reference and bias frequencies from the same source as the transmitted frequency.

From equation (2) it is seen that if the transmitted frequency changes, T_c remains constant for a given velocity if f_b and f_r change by the same factor. Therefore, if all frequencies involved are coherently related to the transmit frequency and the transmitted frequency changes, the bias and reference change by the same amount. This results in a constant T_c. In the GRARR system the nominal bias and reference frequencies are:

f_b (VHF) = 30 KHz

f_b (S-Band) = 500 KHz

f_r = 10 MHz

3.6.5.2 SYSTEM COHERENCE RELATIONSHIPS. The following symbols will be used throughout the discussion.

S-Band:

f_t = ground transmitter frequency (uplink)

f_c = transponder, crystal oscillator frequency

ρ = phase-locked transponder multiplication constant

$60f_c$ or ρf_t = transponder, carrier frequency (downlink)

$48f_c - f_t$ = subcarrier frequency (crystal transponder 1.4, 2.4, 3.2 MHz)

f_B = doppler extractor bias frequency (500 KHz nom)

f_r = doppler reference frequency (10 MHz nom)

VHF:

f_{TV} = ground transmitter frequency (uplink)

f_{cv} = transponder, crystal oscillator frequency

$12f_{cv}$ = transponder, carrier frequency (downlink)

$f_{TV}-13f_{CV}$ = subcarrier frequency (677-920 KHz)

f_{BV} = doppler extractor bias frequency (30 KHz nom)

f_r = doppler reference frequency (10 MHz nom)

Also:

K = one-way frequency multiplier due to doppler, for a fixed transmitter and moving receiver = $1 + V/C$

K′ = one-way frequency multiplier due to doppler, for a fixed receiver and moving transmitter = $\dfrac{1}{1 - V/C}$

$\rho(KK'-1)f_t$ = two-way doppler frequency shift corresponding to transmitted frequency ρf_t.

Figures 3-82, 3-83, and 3-84 show how a frequency independent doppler scheme is implemented for the GRARR system. The expressions used on the diagrams are completely general and the same scheme would work with any operating frequencies. The only limitation on the system is that the crystal transponder multiplier constants are $\frac{12f_{TV}}{13}$ (VHF) and $\frac{60}{48} f_T$ (S-Band). Also the phase-locked loop transponder transmitted frequency must be generated by a times 60 multiplier and $\rho f_t/60$ is available to the doppler extractor. The diagrams show only one polarization channel. The appropriate switching of VCO's takes place in the system signal source.

3.6.5.2.1 <u>S-Band Phase-Lock Transponder System Frequency Coherence Relationships</u>. Figure 3-82 is a flow diagram showing the frequency relationships of the GRARR system utilizing a ratio type phase-locked (PLL) transponder showing frequency-independent doppler extraction. The generalized factor, ρ, is the coherence ratio. The dotted lines in the diagram separate the functions performed in the multifunction receiver, doppler extractor and system signal source.

The transmitted frequency f_T is shifted to Kf_T on the uplink, multiplied by ρ in the transponder, and re-transmitted to the receiver. The downlink frequency is shifted by K' and becomes $K'K\rho f_t$. The signal frequency processing is defined by equations at various points in the system.

The downlink frequency is converted and phase-locked, in the multifunctional receiver, to a 10 MHz reference coherent with the transmitted frequency f_t. The VCO frequency then contains the doppler information of the downlink signal. The VCO is then processed in the doppler extractor to produce a bias plus doppler signal $[f_B + \rho(KK'-1)f_t]$ where $\rho(KK'-1)f_t$ is in effect the two-way doppler on the downlink signal ρf_t. As shown in the diagram, $f_B = \frac{\rho f_t}{60 \times 75}$. The reference f_r for the time counter is $\frac{\rho f_t}{225}$.

From equation (2):

$$T_c = \frac{N\left[\frac{\rho f_t}{225}\right]}{\frac{\rho f_t}{60 \times 75} + \rho f_t\, KK'-1} = \frac{N/225}{\frac{1}{60 \times 75} + (KK'-1)}$$

Therefore the counts, T_c, are independent of the transmitted frequency and the airborne transponder since ρ and f_t cancel out of the equation. The resulting range rate data is, therefore, independent of ρ and f_t as well as changes in transmitted frequency. This approach provides a capability for operation with any phase-locked loop transponder within the frequency range of the multifunction receiver.

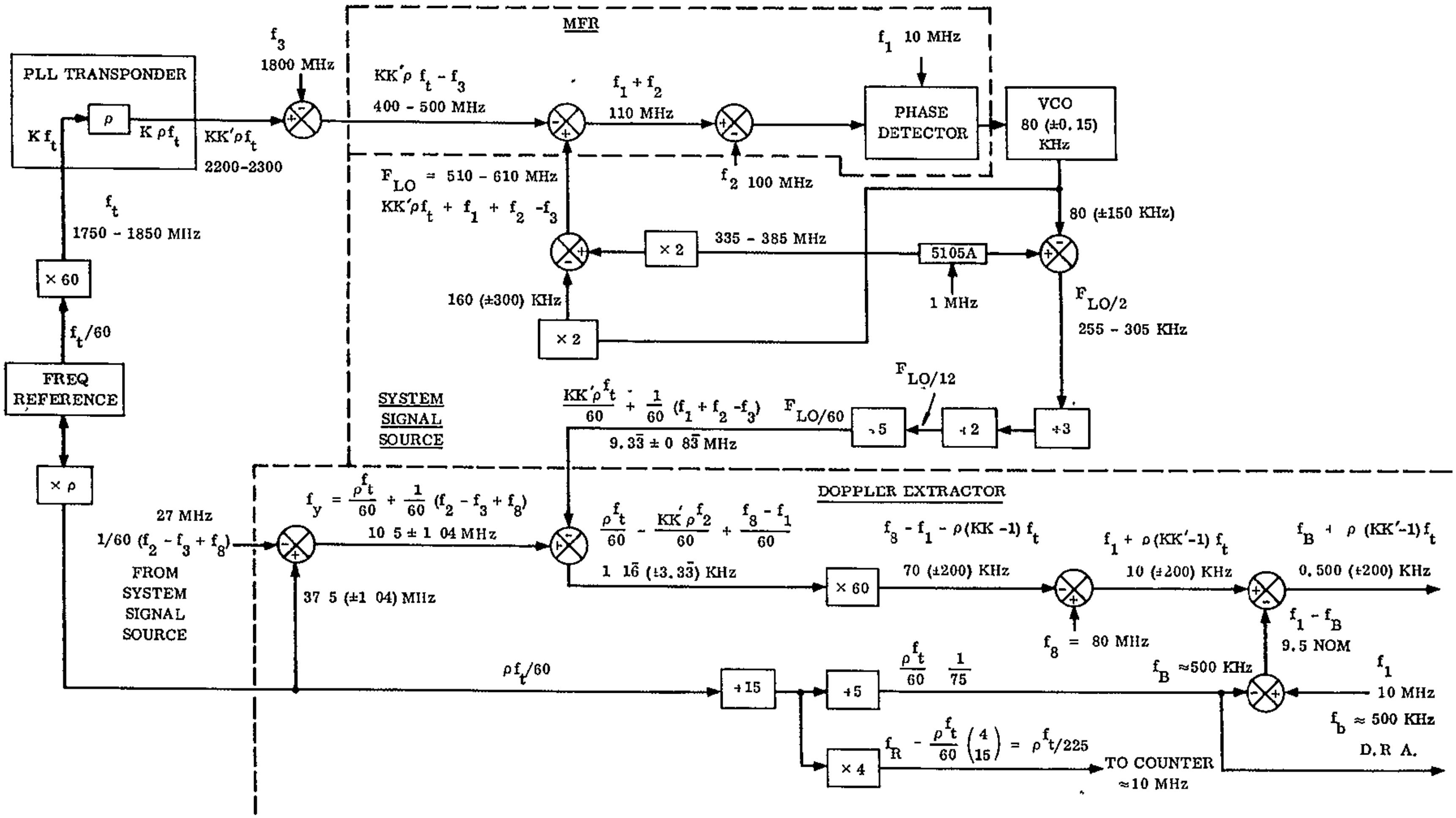

Figure 3-82. System Frequency Coherence Relationship (PLL Transponder)

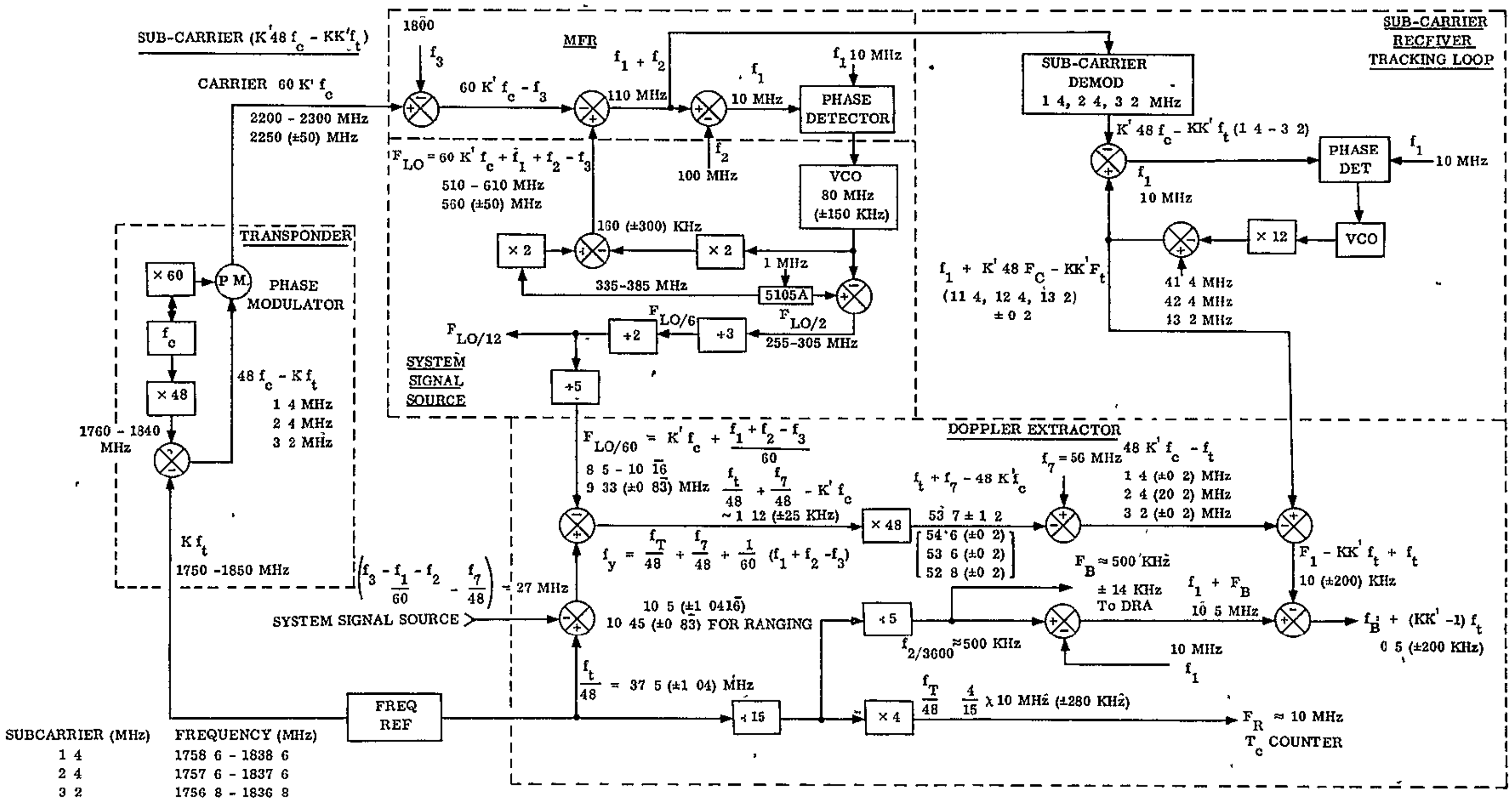

Figure 3-83. System Frequency Coherence for S-Band Crystal Mode

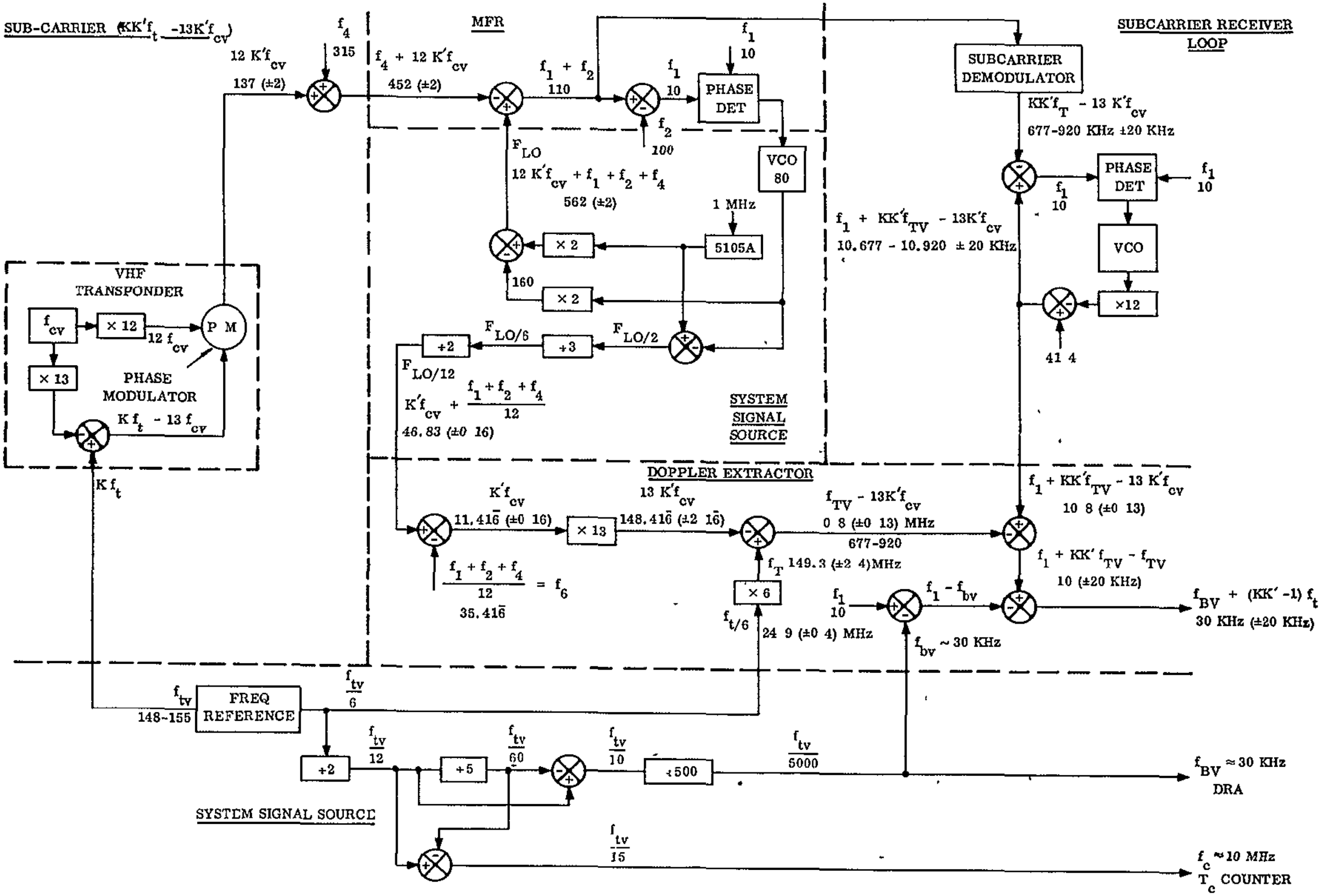

Figure 3-84. System Frequency Coherence (VHF Crystal Transponder)

3.6.5.2.2 S-Band Crystal Transponder, System Frequency Coherence Relationships. Figure 3-83 is a flow diagram showing the frequency coherence relationships for the GRARR System utilizing an S-Band crystal transponder. In this case the uncertainty in the transponder crystal oscillator frequency as well as variations in the transmitted frequency must be removed. The diagram is shown only for the case where downlink frequency is equal to (60/48) f_t. If transponders with different multiplying constants are used, appropriate changes indicated by the equations in the flow diagram, must be made to the system.

In the crystal transponder case, the downlink signal consists of a carrier, $60f_c$, and one of three possible subcarriers, $48f_c - f_t$, (1.4, 2.4, or 3.2 MHz). The carrier frequency is shifted by K′and becomes $K'f_c$. The subcarrier frequency undergoes the same doppler shift as if it were transmitted directly. Since f_t is shifted to Kf_t at the transponder, the received subcarrier looks like, $K'(48f_c - Kf_t)$.

The carrier frequency is phase locked in the multifunctional receiver exactly as in the PLL mode. However, in this case the VCO contains no information about the transmitted frequency doppler. The subcarrier signal has this information. Therefore, the subcarrier is removed from the carrier in the ranging demodulator and phase-locked to the 10 MHz reference in the subcarrier receiver.

The doppler extractor inputs now come from the multifunction receiver VCO, which contains the doppler information on the carrier frequency ($K'60f_c$), and from the subcarrier VCO which contains doppler information on the carrier and the transmitted frequency. As shown in Figure 3-83 the two signals are properly mixed and multiplied to remove the crystal oscillator frequency f_c. The resultant output of the doppler extractor is the bias frequency f_B, plus the two-way doppler shift on the transmitted frequency, f_T $(KK'-1)$.

Also from the diagram, $f_B = \frac{f_t}{3600}$, and f_r, the reference frequency to the counter, equals $\frac{f_t}{180}$. Therefore, the expression for T_c becomes

$$T_c = \frac{Nf_t/180}{\frac{f_t}{3600} + f_t\,(KK'-1)} = \frac{N/180}{\frac{1}{3600} + (KK'-1)}$$

and the range rate data is independent of the transponder crystal frequency or the ground transmitted frequency.

3.6.5.2.3 VHF Crystal Transponder, System Frequency Coherence Relationships. The operation of the VHF crystal mode is very similar to that of the S-Band crystal mode. The flow diagram containing the important relationships for this case is shown in Figure 3-84. In this case the transponder output frequency is $\frac{12}{13}$ f_{tv} and therefore a lower frequency than the transmitted frequency.

The inputs to the doppler extractor, consisting of MFR VCO and subcarrier VCO signals, are multiplied and mixed to provide an output frequency consisting of the bias frequency, f_{Bv}, plus the two-way doppler shift on the transmitted frequency, f_{Tv} (KK′-1). The bias frequency is $\frac{f_{Tv}}{5000}$ and the reference frequency, f_r is $\frac{f_t}{15}$. The number of counts, T_c, becomes:

$$T_c = \frac{N/15}{\frac{1}{5000} + (KK'-1)}$$

Again the range rate data is independent of transmitted frequency or transponder crystal frequency.

3.6.5.3 DOPPLER EXTRACTOR DESIGN. Figure 3-85 shows a functional block diagram of the doppler extractor unit. This unit is designed as a single integrated unit of mixers, multiplier, filters, and solid state switches capable of operating with crystal or phase-locked loop transponders at VHF or S-Band frequencies. Appropriate switching circuitry and controls have been incorporated so that the same basic hardware can be used for all modes of operation.

The unit will operate with any PLL transponder ratio, ρ, as long as $\frac{\rho f_t}{60}$ is supplied to the doppler extractor unit. A second, and obvious, requirement is that ρf_t must lie within the frequency band of the multifunctional receiver. Although the unit will operate with any PLL ratio, ρ, the crystal S-Band and VHF modes are limited to transponder multiplier constants of 60/48 and 12/13, respectively. The expressions in Figures 3-82 and 3-84 enable one to readily calculate new frequencies resulting from a system parameter change.

Figure 3-85 indicates the operating frequencies at various points. Comparison of these frequencies with corresponding points on the flow diagrams of Figures 3-82, 3-83, and 3-84 will illustrate which circuitry is used with a particular mode of operation. Operation is best understood by referring to the frequency expressions at each point in the diagrams and tracing the operations through to the output.

The frequencies at each point in Figure 3-85 and their deviation assume a 100 MHz receiver bandwidth (2200-2300 MHz) and a maximum doppler shift of ±200 KHz for the S-Band cases. The VHF frequencies allow a received band of 137 MHz (±2 MHz) and maximum doppler of ±20 KHz. Allowance is also made for oscillator variations in the crystal modes. A summary of the basic doppler extractor frequencies is given in Table 3-3 and the frequencies required by the synthesizer are given below.

Fixed Frequencies:

f_1 = Third IF, 10 MHz

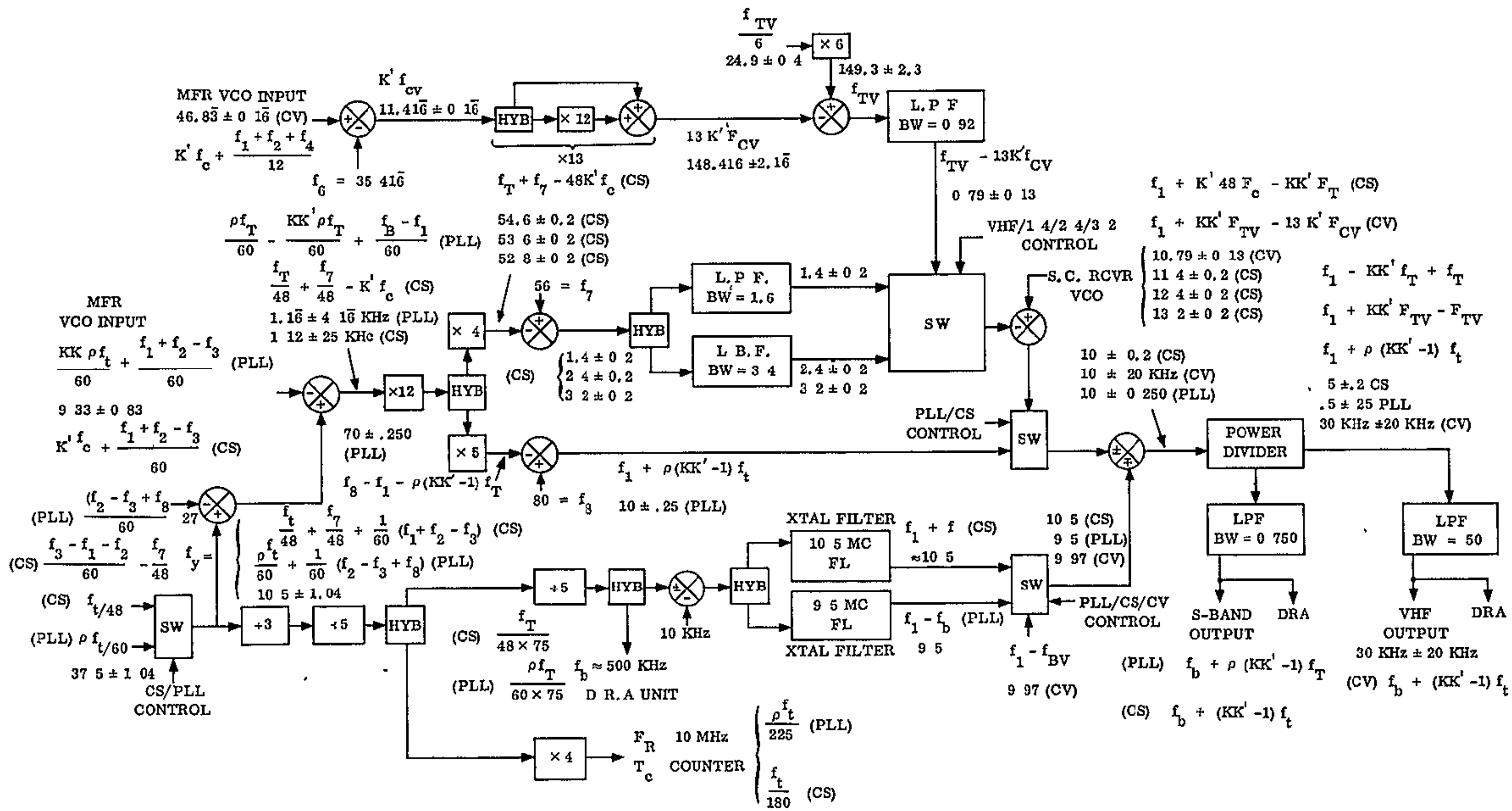

Figure 3-85. Doppler Extractor Functional Block Diagram

Table 3-3. Doppler Extractor Input/Output Summary

Transponder Mode	Receiver* Input	Output
Crystal S-Band (cs)	$K'f_c + \frac{1}{60}(f_1 + f_2 + f_3)$ (9.33 MHz ± 0.83 MHz)	$f_B + (KK' - 1) f_T$ (≈500 KHz ±200 KHz)
Crystal VHF (cv)	$F'f_c + \frac{f_1 + f_2 + f_4}{12}$ (46.83 MHz ± 0.16 MHz)	$f_{BV} + (KK' - 1) f_{TV}$ (≈30 KHz ± 2. KHz)
Phase-Locked Loop (PLL)	$\frac{\rho KK'f_T}{60} + \frac{1}{60}(f_1 + f_2 - f_3)$	$f_B + \rho(KK' - 1) f_T$ (≈500 KHz ± 200 KHz)

*This input actually comes from the system signal source, but it is the receiver VCO frequency. Appropriate polarization switching takes place in the VCO chain to provide one output to the doppler extractor.

f_2 = Second LO 100 MHz (synthesizer supplies $\frac{f_2}{2}$ = 50 MHz)

f_3 = S-Band first LO 1800 MHz

f_4 = VHF first LO 315 MHz

$f_6 = \frac{1}{12}(f_1 + f_2 + f_4)$ = 35.416 (VHF crystal)

f_7 = 56 MHz (used for crystal S-Band)

f_8 = 80 MHz (PLL transponder)

$$\left.\begin{array}{l} \text{(cs)}\ \dfrac{f_3 - f_1 - f_2}{60} - \dfrac{f_7}{48} \\[2ex] \text{(PLL)}\ \dfrac{f_2 - f_3 + f_8}{60} \end{array}\right\} = 27\ \text{MHz}$$

b. Variable Frequencies:

$$(cs)\ f_t/48 = 37.5 \pm 1.04 \text{ MHz}$$

$$(PLL)\ \rho F_t/60 \approx 37.5 \pm 0.83 \text{ MHz}$$

$$(cv)\ \frac{f_{TV}}{6} = 24.9 \pm 0.4 \text{ MHz}$$

$$(cv)\ f_1 - f_{BV} = 10 \text{ MHz} - \frac{f_{TV}}{5000} = 10.97 \text{ MHz (nom)}$$

To facilitate easy patching for applications with PLL transponders, the S-Band bias frequency and reference frequency are generated in the doppler extractor unit. Patching in $\rho f_t/60$ at the doppler extractor unit allows frequency-independent doppler extraction for any factor ρ. The VHF bias and reference frequencies are generated in the system signal source.

All mixers used in the doppler extractor unit will be Relcom model M6E double-balanced mixers because of their excellent spurious response. The doppler extractor frequencies f_7 (56 MHz) and f_8 (80 MHz) were selected to provide a good spurious response throughout. They also establish a convenient frequency of about 1 MHz to the S-Band multiplier chains.

The filtering shown in Figure 3-85 is the origin of the most critical problems. The 9.5 MHz and 10.5 MHz filters necessary in generating $f_1 + f_B$ and $f_1 - f_B$ are narrowband crystal filters since the variation on the 500 KHz is only ±14 KHz. These narrowband filters safely reject the 10 MHz signal as well as the image frequencies. The 9.97 MHz signal for VHF is filtered in a crystal filter in the system signal source, where it is generated.

The switched low-pass filters in the crystal S-Band mode and the low-pass filter in the VHF mode are designed to eliminate 2-2 spurs caused by mixing two frequencies very close together.

All circuits in the doppler extractor unit will be standarized as much as possible with circuits in other portions of the equipment. Broadband amplifiers will be used with filters to provide desired bandwidths. Standard balanced doublers will be used as much as possible in the multiplying chains. Integrated circuit digital dividers are used to generate F_R and F_B.

The circuits necessary to implement the doppler extractor unit will be packaged in standard submodules and mounted in the drawer with the subcarrier receiver. Control of the doppler extractor unit will be effected from the subcarrier receiver control panels.

3.6.6 Digital Rate Aid Unit

The function of the Digital Rate Aid Unit is to develop signals with frequencies equal to a bias plus range tone dopplers. This information is developed by dividing the carrier doppler information from the Doppler Extractor by a number approximately equal to the frequency ratio of the transmitted carrier to the range tone frequency. This signal is used to cancel the frequency dynamics on the received major tones, thereby allowing the use of range tone tracking filters with very narrow bands for improvement of the signal-to-noise ratio of the major tones.

The Digital Rate Aid Unit receives the bias-plus-doppler for either S-Band or VHF from the Doppler Extractor. Through a series of mixers, filters, and dividers, three signals containing doppler data are developed and are provided to the Range Tone Processor which contains the range tone loops. Figure 3-86 is a functional block diagram of the Digital Rate Aid Unit.

Two separate paths are used to develop the doppler information for the range tone loops. The bias frequency and the bias frequency plus doppler inputs to the separate paths are used to develop the 500 KHz range tone loop doppler information independently of variation in the bias frequency. This is accomplished by subtraction of the bias frequency from the bias frequency plus doppler rate-aid signal.

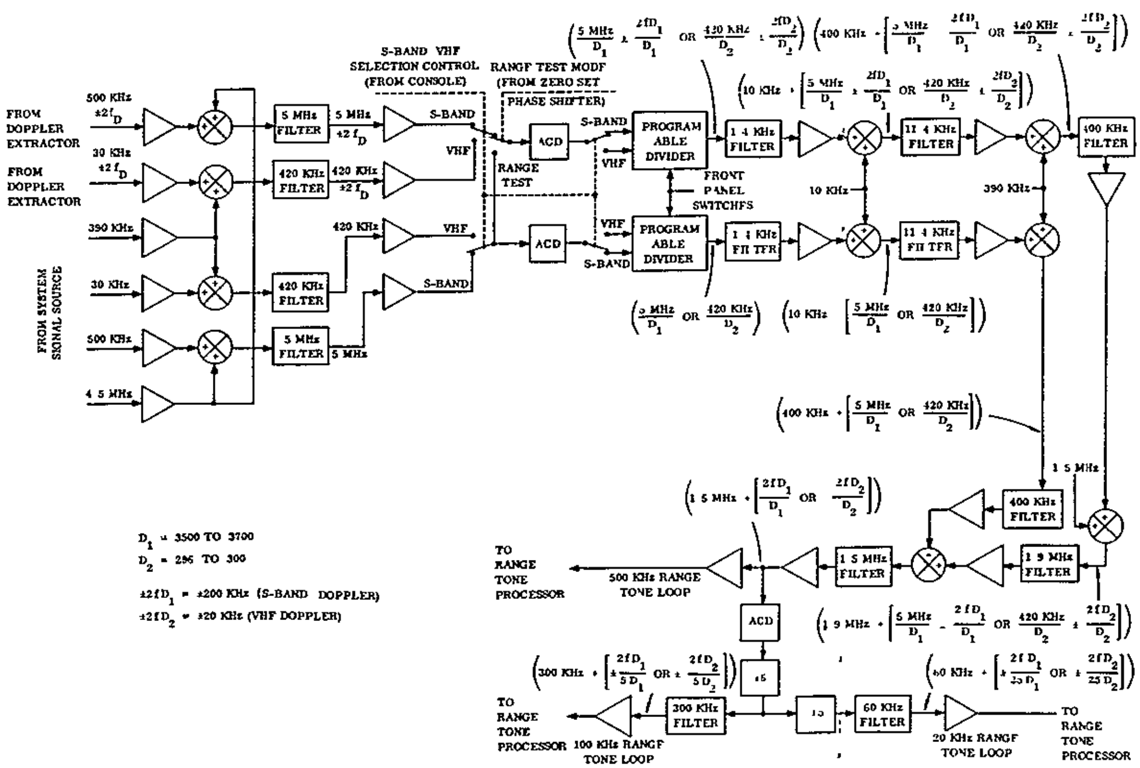

Figure 3-86. Digital Rate Aid Unit Block Diagram

3.6.6.1 5 MHZ MIXERS AND FILTERS. The 5 MHz mixer in the bias-plus-doppler path must be capable of mixing bias-plus-doppler, from 300 KHz to 700 KHz, with a 4.5 MHz signal. With maximum negative doppler, the mixer output will be 4.8 MHz and with maximum positive doppler, 5.2 MHz. The filter following the mixer must be capable of passing the two frequencies and all frequencies between. At the maximum negative doppler condition, the mixer will also have an undesired mixer product output, at 5.1 MHz; within the passband of the filter. A double balanced mixer is used to provide 30 db attenuation of this spurious output and thereby limit its contribution to phase jitter to less than 0.72 nanosec rms at 5 MHz, or less than 1.4 degrees rms.

The 5 MHz filter in the bias-plus-doppler path is a four-pole Butterworth filter centered at 5 MHz with a bandwidth of 400 KHz. A four-pole filter was chosen to provide additional attenuation of the spurious products near the passband of the filter.

The mixer in the bias-only path mixes the 4.5 MHz from the system signal source and the 500 KHz bias frequency. This mixer is identical to the mixer in the bias-plus-doppler path. Variations in the bias frequency amount to ±3 percent of the bias nominal frequency of 500 KHz. This small variation does not cause additional undesirable mixer products to place restrictions on the following 5 MHz filter. Therefore, the closest undesirable mixer products are ±500 KHz away from 5 MHz. Since the mixer provides 30 db of attenuation to the undesirable products, a single-section 100 KHz Butterworth filter is adequate to provide the desired selectivity and attenuation of the unwanted signals. The phase jitter contributions of the undesired mixer products are negligible.

3.6.6.2 420 KHZ MIXERS AND FILTERS. The first mixers in the VHF bias-plus-doppler path and the bias-only path are double balanced mixers. The mixer in the bias-only path mixes 390 KHz and the 30 KHz VHF bias to obtain 420 KHz. By using a double balanced mixer the 390 KHz fundamental and the 450 KHz product are attenuated by, typically, 35 db. The filter following is a two-section Butterworth filter with a bandwidth of 10 KHz and center frequency of 420 KHz. This filter provides an additional attenuation of 30 db at 390 KHz and 450 KHz and renders the phase jitter contribution of these two signals to a negligible value. The mixer in the bias-plus-doppler path mixes 390 KHz and 30 KHz ± 20 KHz. A characteristic of a double balanced mixer is high rejection of the two fundamentals and of the even harmonics of these signals. Typically the fundamental is rejected by 30 db, the even harmonics by 55 db or more, and the odd harmonics by 50 db or more.

The bandpass filter in the bias-plus-doppler path has a center frequency of 420 KHz and a bandwidth of 40 KHz. The four-section filter will further attenuate the 390 KHz fundamental by 15 db. Total contribution to phase jitter as a result of the mixer and filter is less than 6.67 nanosec or 1.02 degrees at 420 KHz.

3.6.6.3 AXIS-CROSSING DETECTORS. The axis-crossing detectors in the bias-plus-doppler and bias-only paths are high gain amplifiers. The output stages of the amplifiers are driven from cutoff to saturation with an input signal of ±0.05 volts. The phase jitter contribution of the axis-crossing detectors at 5 MHz is less than 1 nanosec rms or 1.8 degrees rms, and at 420 KHz the contribution is 3.5 nanosec or 0.5 degrees rms.

3.6.6.4 PROGRAMMABLE DIVIDERS. The programmable dividers in both the bias-only and bias-plus-doppler paths are synchronous decade counters. The maximum count of the dividers is controlled by three thumbwheel switches on the front panel of the Digital Rate Aid Unit. To set the divider, the switches are set to the transmit frequency minus 1750 rounded off to the nearest 1 MHz for S-Band, or to the transmit frequency rounded off to the nearest 1 MHz for VHF.

For S-Band, the incoming signal in both paths can be divided by any number between 3500 and 3700 in increments of two. The VHF signals can be divided by any number between 296 and 300 in increments of two. For both VHF and S-Band, this amounts to dividing the signals by a number equal to twice the transmit frequency rounded to the nearest 1 MHz.

The output frequency of the divider in the bias-plus-doppler path is nominally 1.4K pps and will vary approximately ±100 pps depending on the transmit frequency and the doppler frequency. The output frequency of the divider in the bias-only path is nominally 1.4K pps and will vary approximately ±50 pps depending on the transmit frequency. Both path outputs are filtered by identical wideband two-section filters.

3.6.6.5 11.4 KHZ MIXERS AND FILTERS. The 11.4 KHz mixers in both paths are double balanced mixers and both receive, as one input, 10 KHz from the system signal source. In the bias-plus-doppler path the second input is nominally 1.4 KHz varying ±100 Hz, and in the bias-only path the second mixer input is nominally 1.4 KHz varying ±50 Hz. The outputs of the mixers to the filters are nominally 11.4 KHz. Both filters are two-section Butterworth bandpass filters with bandwidths of 300 Hz centered at 11.4 KHz. Mixer and filter contributions to phase jitter are insignificant.

3.6.6.6 400 KHZ MIXERS AND FILTERS. The nominal 11.4 KHz signals in the bias-plus-doppler path and the bias-only path are each mixed with 390 KHz, derived from the system signal source, in double balanced mixers. The mixer outputs are nominally 401.4 KHz. The output of each mixer is fed to a three-section Butterworth filter centered at 400 KHz with a 5 KHz bandwidth. Sufficient rejection of fundamental and spurious signals is provided by the mixer-filter combination to render their contributions to phase jitter negligible.

3.6.6.7 1.9 MHZ MIXER AND FILTER. The nominal 401.4 KHz in the bias-plus-doppler path and 1.5 MHz from the system signal source are mixed in a double balanced mixer to obtain 1.9 MHz nominal. The mixer output is routed to a two-section Butterworth filter centered at 1.9 MHz and having a bandwidth of 100 KHz. The phase jitter contribution of the mixer-filter combination is negligible.

3.6.6.8 1.5 MHZ MIXER AND FILTER. The signal generated in the bias-only path and the signal generated in the bias-plus-doppler path are mixed down to 1.5 MHz (±60 Hz). The effect of this mixing action removes from the doppler information those frequency deviations caused by variations in the bias frequency.

The 1.5 MHz filter is a two-section bandpass filter with a bandwidth of 100 KHz centered at 1.5 MHz. The filter-mixer combination contributes negligible phase jitter to the output signal. The buffered output of the 1.5 MHz filter in the Digital Rate Aid unit is fed to the 500 KHz range tone loop in the Range Tone Processor. The filter output is further processed within the Digital Rate Aid Unit to derive 100 KHz and 20 KHz range tone rate aid signals.

3.6.6.9 100 KHZ AND 20 KHZ RANGE TONE GENERATION. The 1.5 MHz (±60 Hz) signal from the 1.5 MHz filter is sent to an axis-crossing detector where the signal is squared for digital division. The axis-crossing detector is a high gain amplifier whose output stage is driven from cutoff to saturation upon application of an input signal of ±0.05 volts. The contribution to phase jitter is 1.5 nanosec or 0.81 degrees at 1.5 MHz. The output of the axis-crossing detector is divided by five in a synchronous divider yielding 300K pps (±12 pps). The 300K pps is further divided by five synchronously to yield 60K (±2.4) pps.

The 300K pps output of the first divider is filtered by a two-section bandpass filter centered at 300 KHz with a bandwidth of 15 KHz. The output of this filter, after buffering, is sent to the 100 KHz tone loop in the Range Tone Processor. The 60K pps output of the second divider is filtered by a two-section filter with a bandwidth of 3 KHz centered at 60 KHz. This output is sent to the 20 KHz tone loop in the Range Tone Processor.

3.6.7 Applicability

The receiver subsystems to be provided are applicable for the Rosman, Carnarvon, Tananarive, and Fairbanks sites, the elements of which are listed as follows:

a. S-Band Parametric Amplifier - Converter

b. Multicouplers.

c. Multifunctional Receiver.

d. Subcarrier Receiver.

e. Doppler Extractor.

f. Digital Rate Aid

3.7 DATA SUBSYSTEM

The Data Subsystem consists of the following units:

Range Extraction Unit
Range Rate Extraction Unit
Recording Unit

The subsystem processes the demodulated range and range rate data from the Receiver Subsystem, compares these data signals with reference signals, and records the resultant range and range rate information along with suitable identification information. A block diagram of the Data Subsystem is presented in Figure 3-87.

3.7.1 Range Extraction Unit

The Range Extraction Unit (Figure 3-88) consists functionally of the sidetone extraction unit and the ambiguity number extraction unit. The sidetone extraction unit measures range by producing a start pulse phase coherent to the transmitted range tones and a stop pulse phase coherent to the received range tones, and then measuring the time interval between them. This range reading is unambiguous to a distance determined by the lowest sidetone used (8 Hz). When the range exceeds this distance, the ambiguity number extraction unit determines and updates the number of ambiguity distances by the use of an ambiguity resolving code (ARC). The system can operate in a sidetone ranging mode which utilizes only the sidetone range extraction unit or in a hybrid ranging mode which utilizes both the sidetone range extraction unit and the ambiguity number extraction unit.

3.7.1.1 RANGE TONE PROCESSOR. The range tone processor drawer contains the major range tone tracking loops, the 4 KHz tone decomplementer, and minor tone phase detectors. The processor provides signal-to-noise improvement on the major ranging tone and compares the phase of the synthesized minor tones to the phase of the received minor tones. A simplified block diagram is shown in Figure 3-89. As shown by the diagram, only the highest frequency range tone is actually tracked and filtered by a phase-locked loop. By selection, however, the loop will operate at either 500 KHz, 100 KHz, or 20 KHz.

3.7.1.1.1 Major Range Tone Tracking Loop. A simplified block diagram of the major range tone tracking loop configured for 500 KHz is shown in Figure 3-90. The loop utilizes digital rate aiding which reduces the respective range tone doppler and doppler rate to 0.03 percent when working with the S-Band receiver and to 0.30 percent when working with the VHF receiver. The rate aiding is implemented by mixing the rate aid signal with the range tone signal ahead of the phase lock loop and mixing the VCXO output with the same rate aid signal after the phase lock loop. The rate aiding signal frequencies are listed in Table 3-4.

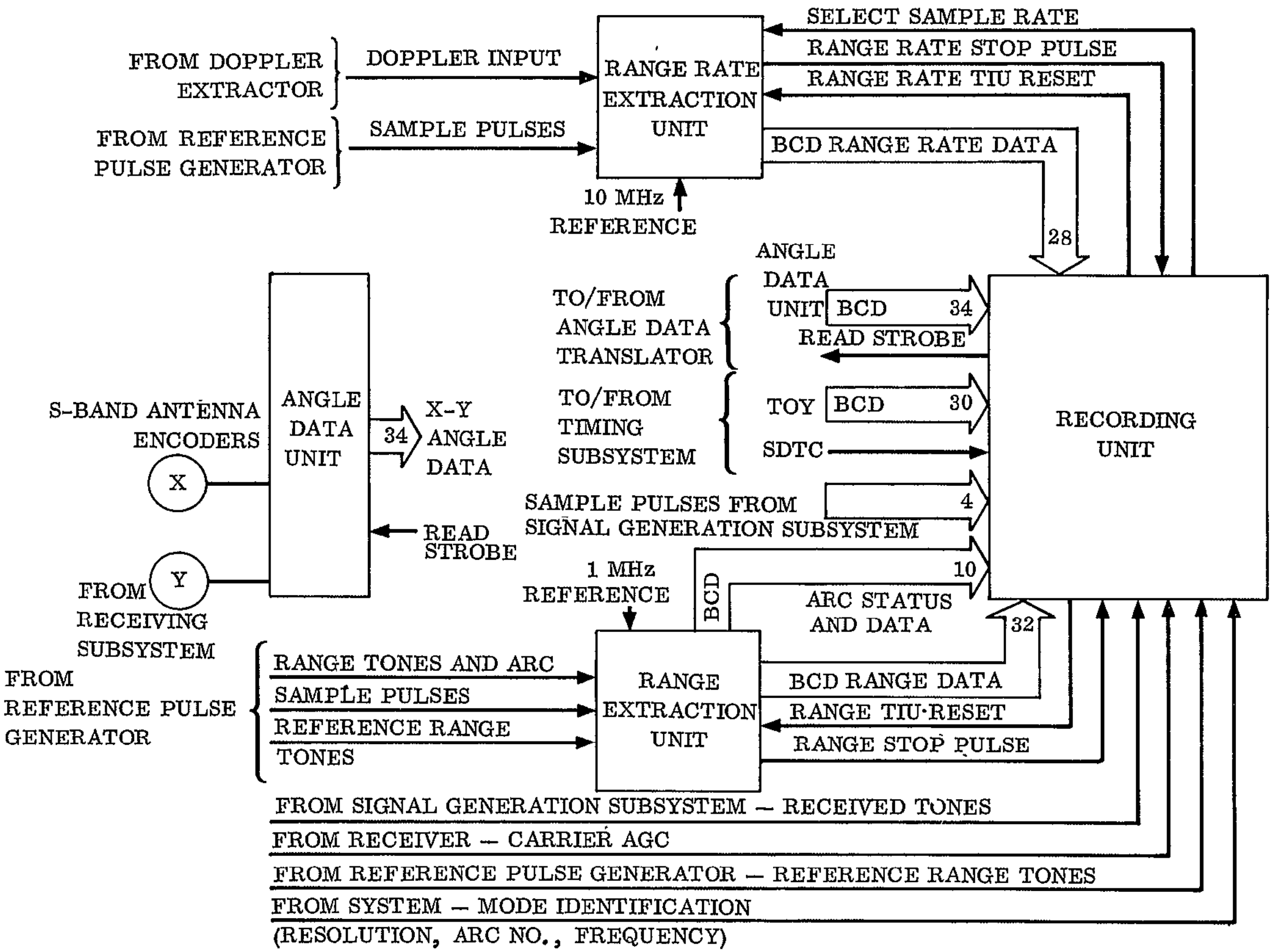

Figure 3-87. Data Subsystem Functional Block Diagram

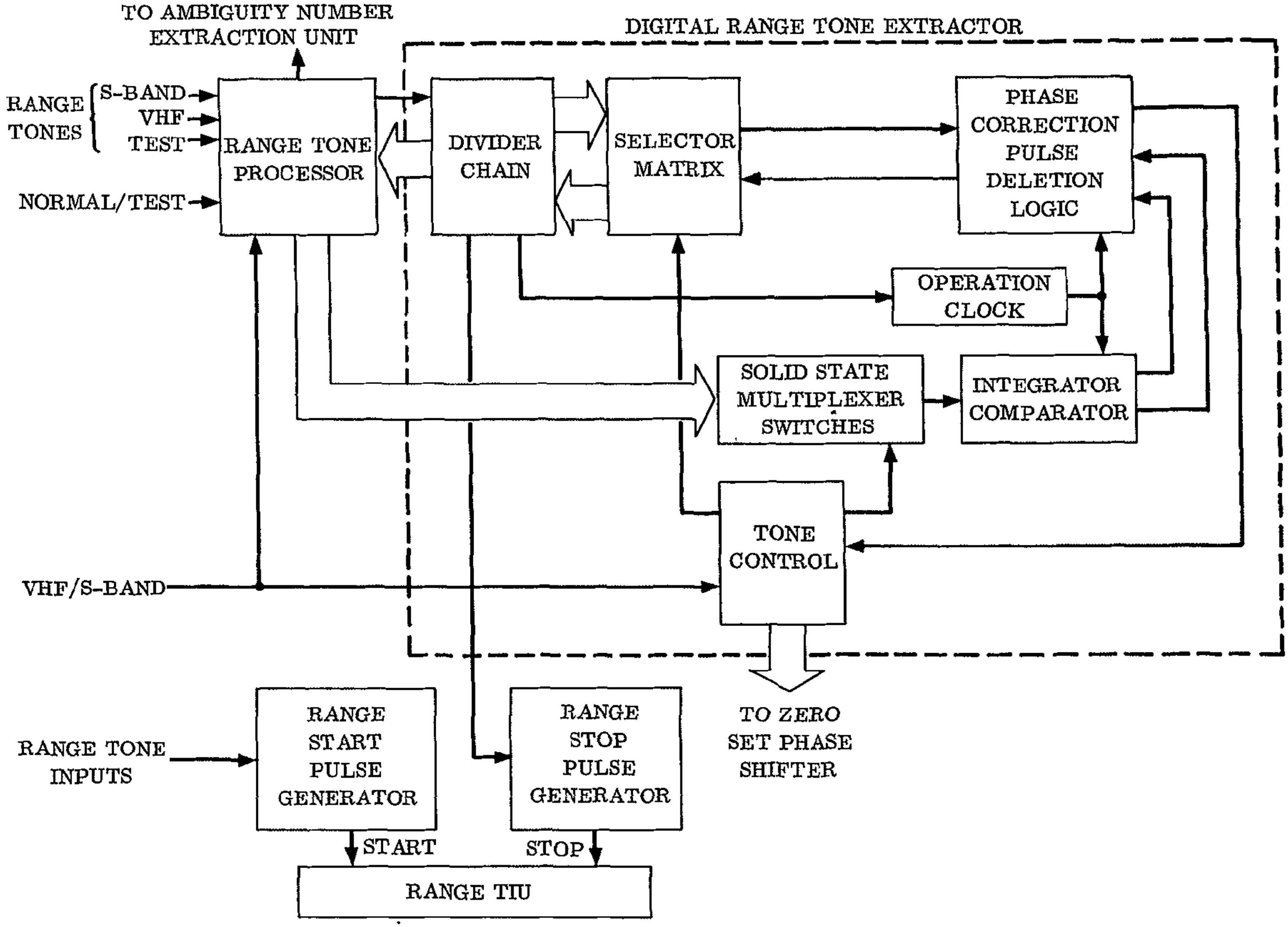

Figure 3-88. Range Extraction Unit

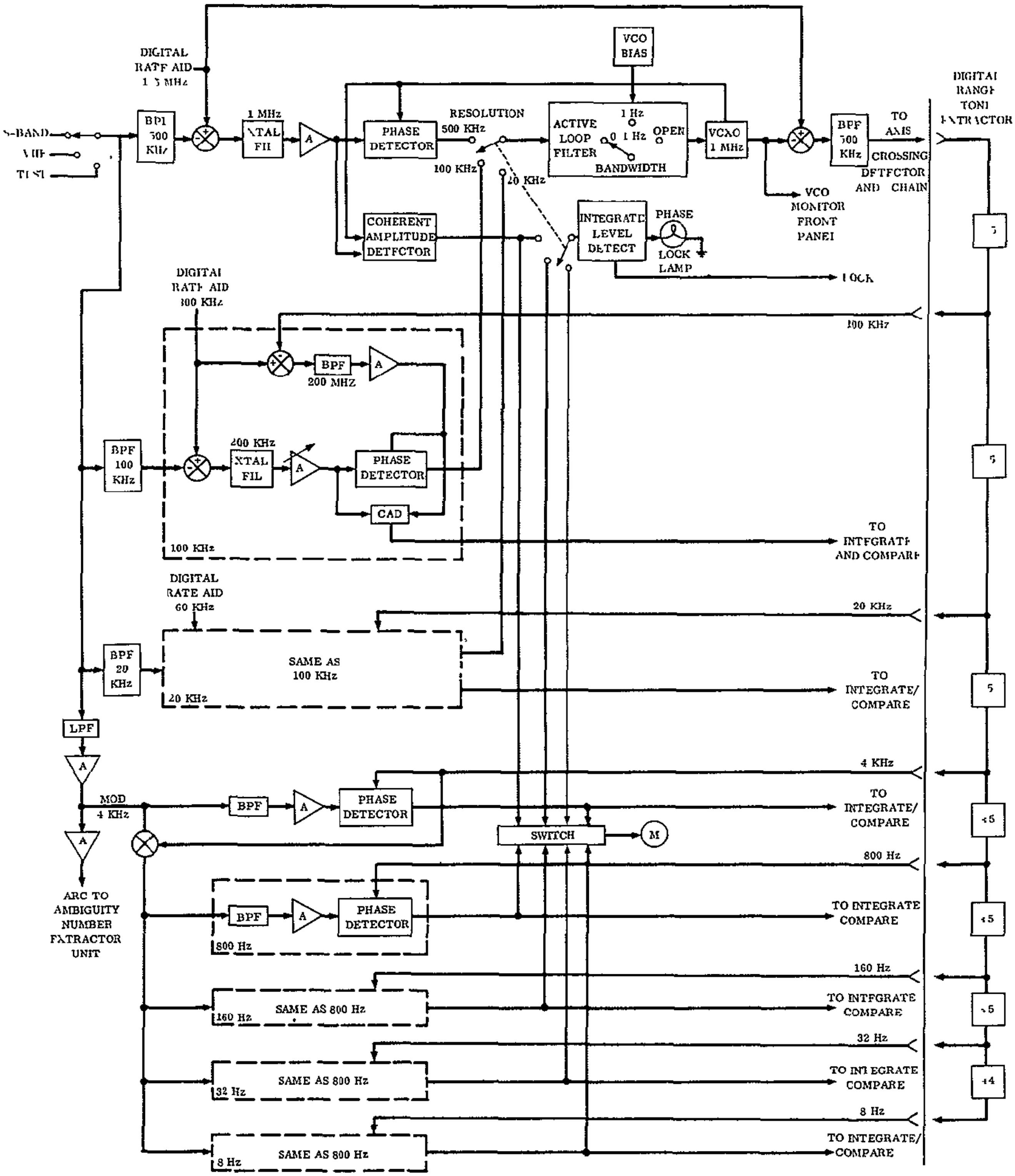

Figure 3-89. Range Tone Processor

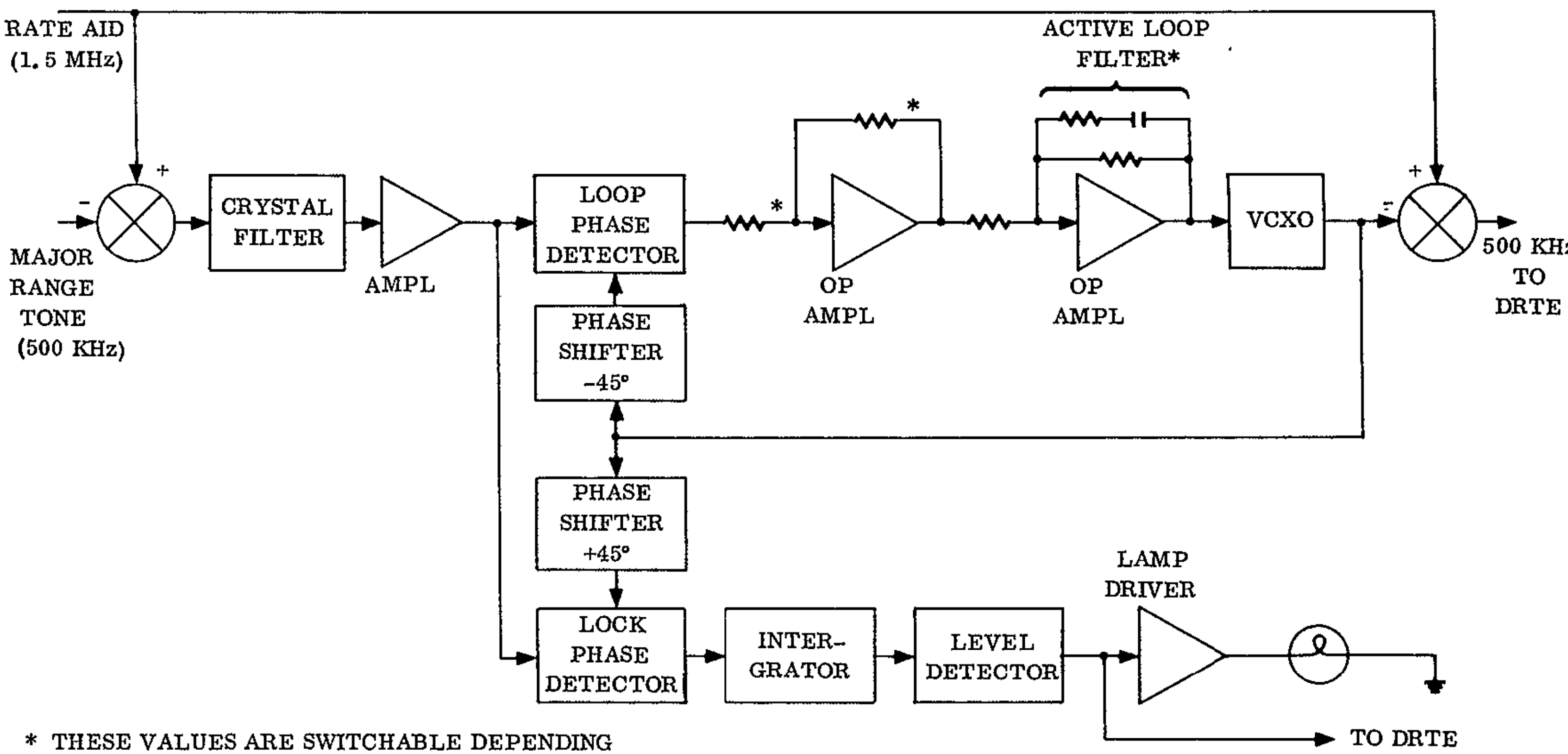

* THESE VALUES ARE SWITCHABLE DEPENDING ON THE MAJOR RANGE TONE AND THE BAND-WIDTH SELECTION

Figure 3-90. Major Range Tone Tracking Loop Configured for 500 KHz Tone

Table 3-4. Rate and Signal Frequencies

Range Tone Loop	S-Band	VHF
500 KHz	1.5 MHz $\pm 2D_{500\ KHz}$ (±0.03%)	--
100 KHz	0.3 MHz $\pm 2D_{100\ KHz}$ (±0.03%)	0.3 MHz $\pm 2D_{100\ KHz}$ (±0.30%)
20 KHz	60 KHz $\pm 2D_{20\ KHz}$ (±0.03%)	60 KHz $\pm 2D_{20\ KHz}$ (±0.3%)

The mixing process ahead of the phase lock loop may be critical because of the choice of the rate aid bias frequencies. The choice is necessary, however, for compatibility with the Fairbanks site. In each range tone loop the second harmonic of the range tone is also the IF. This will require a well-balanced mixer so that the range tone does not contain improper phase information. A four-diode bridge with well-balanced transformer feeds should suffice if matched diodes are also used.

The rate aiding process allows a narrowband filter to be used ahead of the phase detector. This filter is advantageous because it allows the phase detector to work down to a lower signal level before it "thresholds" due to the noise power. The worst-case signal-to-noise condition occurs using 100 KHz in VHF. In this case, S/ϕ is +4.5 db-Hz and the signal-to-noise at the input to the phase detector will be -8 db (which is above the detector threshold signal-to-noise) if the noise bandwidth of the filter is 17.5 Hz. This bandwidth results in a Q of 9000 which can only be achieved with a crystal filter. A single-pole crystal filter will be used to minimize the effects of phase shift versus frequency on loop acquisition. The bandwidth of the crystal filters will be wide enough such that the phase shift due to expected doppler results in neglectable phase error. An RF amplifier (with approximately 66-db of gain) following the crystal filter drives the phase detector. Its gain will be switchable, in the 100 KHz loop, by 4.6 db to compensate for the difference in the level of the 100 KHz tone when it is used as the high tone or second tone.

The rate aided and filtered range tone is phase-compared with the VCXO signal in a loop phase detector with a sensitivity of 1 volt/radian. The detector will be identical to the rate-aid mixers in circuit configuration except that it will have resistors in series with the bridge diodes. The output impedance of the detector must be such that no adverse loading effects occur when the range tone select switch is in any of the three resolution positions (different loading occurs on the detector because a different dc amplifier configuration is used for each tone).

The output of the phase detector is amplified and filtered by an active filter before driving the VCXO. The dc amplifier compensates for the decrease in loop phase gain when operating with the 100-KHz or 20-KHz range tone. The same VCXO is used for all range tones;

however, the output to the VCXO is divided by 5 when operating with the 100-KHz range tone and divided by 25 when operating with the 20-KHz range tone; thus the respective decrease in loop gain.

The active filter parameters must be changed when a new noise bandwidth is selected. Only feedback and input resistors will be changed. If the capacitor is changed, capacitor voltage will vary and unlock the loop when switching to a new noise bandwidth. The operational amplifier will be a commercially-available linear integrated operational amplifier approved for military applications. These amplifiers exhibit input offset voltages and currents which must be balanced out. The loop filter will be shared by the major range tones and will be appropriately configured by a relay and/or a mechanical switch. The voltage-controlled oscillator will be a crystal oscillator with oven temperature control. The expected requirements are for a center frequency of 1 MHz, a frequency stability of 0.042 ppm for 30 days, a sensitivity of 0.5 Hz/volt, a tuning range of ±2 Hz, and a phase jitter of less than 0.1 degree rms.

A lock-indicating circuit is necessary mainly to initiate the DRTE digital phase matching process. The circuit consists of a quadrature phase detector driving an integrator. The integrator output is detected by a zener-controlled switch illuminating a lamp and delivering an output to the DRTE. The total lock-up time and indication time will not exceed 2.5 sec. The lock-indication circuit will be shared by the major range tones and will be configured by a relay and/or a mechanical switch.

3.7.1.1.2 Minor Tone Phase Detectors and 4 KHz Decomplementer. The block diagram in Figure 3-91 shows the phase detector arrangement used for the 100 KHz and 20 KHz tone when they are used as the second tone. The phase-lock loop circuitry is utilized by switching the phase detector reference signal from the VCXO output to the output from a mixer. The mixer produces the difference frequency between the rate aid signal and the synthesized tone. The rate aided range tone and the synthesized rate aided range tone are then phase-compared by a quadrature phase detector whose output is used in the digital phase matching process.

Figure 3-92 is a simplified block diagram of the 4 KHz decomplementer and minor tone phase detectors. The expected bandwidths and filter types are shown. The minor tone phase detector will be a simple transistor type with the signal on the base, the reference introduced at the emitter, and the output at the collector. The decomplementer (the 4 KHz mixer) will probably be a four-diode bridge fed by transistors. Balance is not critical for this mixer.

3.7.1.1.3 Front Panel and Packaging. The front panel is depicted in Figure 3-93. The VCO section incorporates a small dc meter to monitor the VCO control voltage. The VCO FREQ CONTROL is a 5-turn variable resistor which applies a dc voltage to the VCO control input. The FREQ MONITOR will be a BNC jack.

The RANGE TONE PHASE meter and RESOLUTION SELECT switch are used in conjunction with the DRTE during manual digital phase matching.

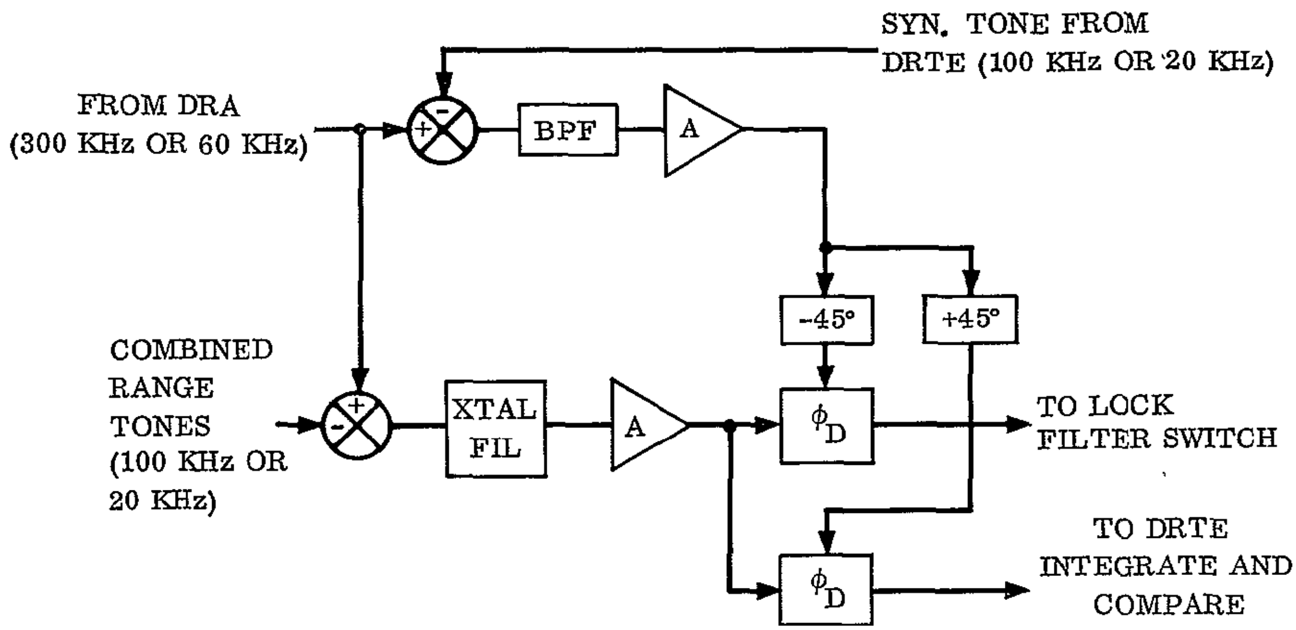

Figure 3-91. Phase Detecting 100 KHz and 20 KHz Tones Used as Second Tones

The Resolution Select function, Bandwidth Select function, and the Range Tone Phase lock indicator will be paralleled to the control console. Note that when acquiring lock, the loop bandwidth will be 1 Hz although the bandwidth selector may be in the 0.1 Hz position. If the 0.1 Hz position is selected, the bandwidth will be automatically decreased to 0.1 Hz after acquisition.

The circuits will be mounted on printed circuit cards housed in card cages. The card cages will be fabricated of metal with insertable shields for EMI isolation between cards.

3.7.1.2 DIGITAL RANGE TONE EXTRACTOR. The Digital Range Tone Extractor (DRTE) will consist of a frequency-divider chain synthesizing the range sidetones, a manual and automatic circuit for digitally phase-matching the synthesized tones to the received range tones, and a control function which selects the range tones for transmission. The control function also directs the sequencing of the range sidetones and the modulation index for each according to the transmitted frequency, either S-Band or VHF Band; the major range tone selected at 500 KHz, 100 KHz, or 20 KHz; and the ambiguity selected at 160 Hz, 32 Hz, 8 Hz or hybrid, which includes the ARC code transmission and decoding.

The Divider Chain is depicted in Figure 3-94. The input frequency is 500 KHz received from the Range Tone Processor. An axis-crossing detector converts the input sinewave to a square wave which is applied to a 3-stage divider to produce a 200K pps signal. The 500 KHz signal controls the dc inputs to a flip-flop. The output is a 100 KHz squarewave with a phase relationship relative to the 500 KHz as depicted in Figure 3-95.

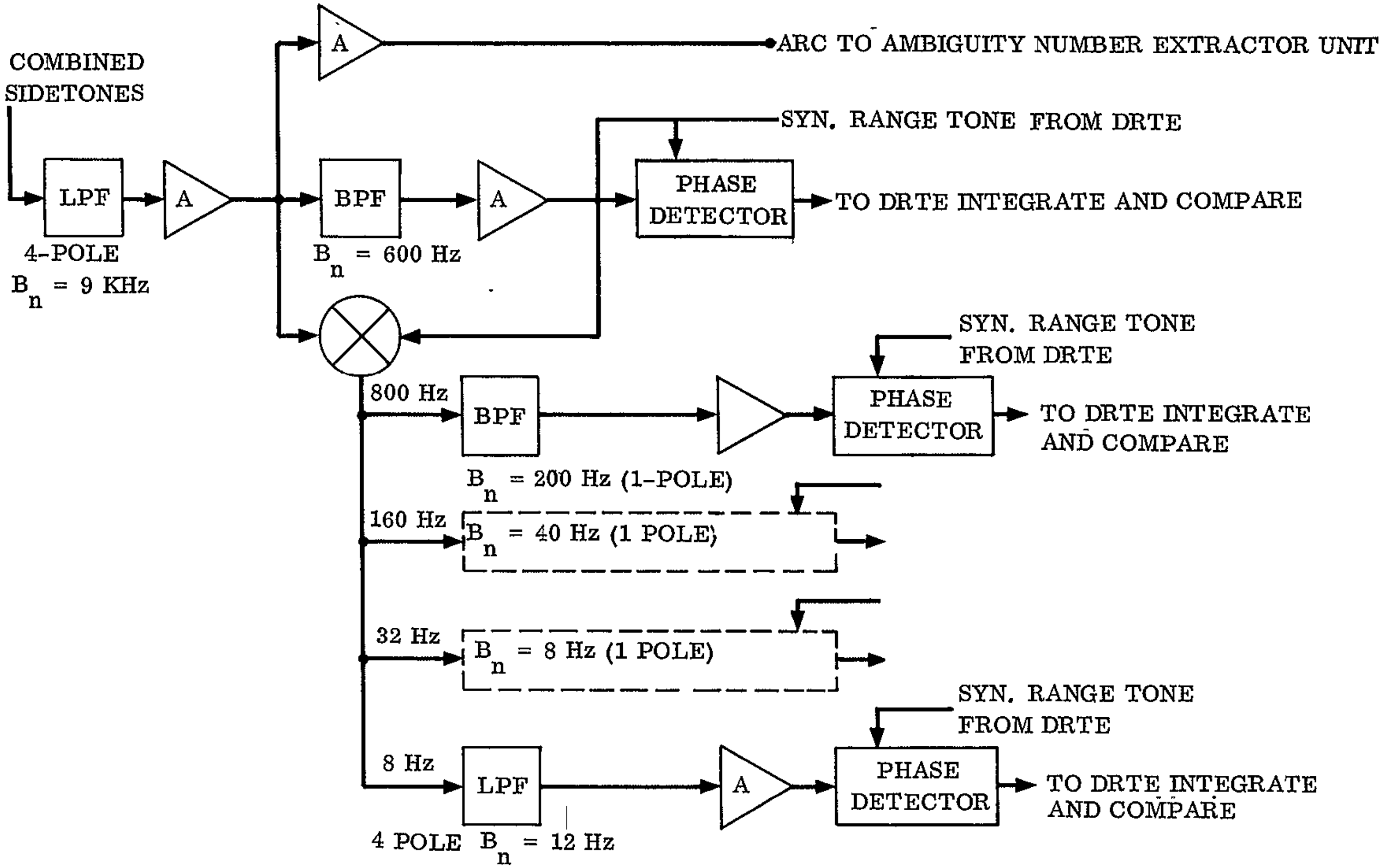

Figure 3-92. Decomplementer and Minor Tone Loops

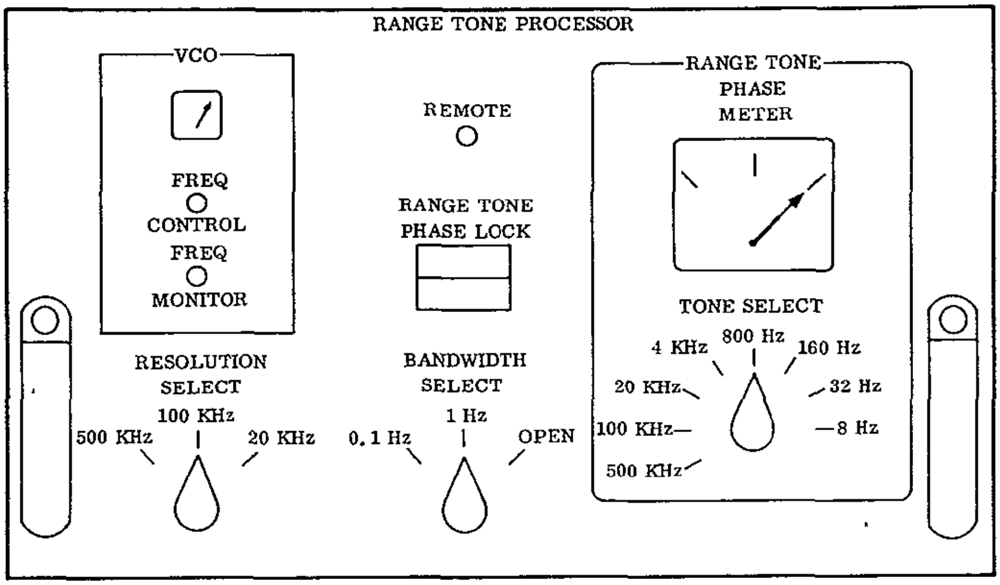

Figure 3-93. Range Tone Processor Front Panel

The 200K pps signal is further divided down to 40K pps. The 40K pps signal drives a flip-flop with the 100 KHz squarewave as input to the dc controls. The output of this flip-flop is a 20 KHz squarewave maintaining a phase relationship with the 100 KHz signal. The same sequence of dividing and gating is continued to produce 4 KHz, 800 Hz, 160 Hz, and 32 Hz. The 32 Hz signal is divided by four to provide an 8 Hz squarewave signal.

The tone control section of the Digital Range Tone Extractor is shown in Figure 3-96. The primary function of this circuitry is to control the range tone modulation. The circuit design incorporates manual, semi-automatic, or automatic operation; 500 KHz, 100 KHz or 20 KHz resolution; S-Band or VHF transmission; and phase lock signals from the major range tone phase-lock loop circuitry and the digital phase-matching circuitry. Table 3-5 indicates in sequential order the modulation index applicable for each tone for selected resolution and transmission frequencies. The table indicates the sidetone applied when sequencing from the major range tone through to the lowest frequency ambiguity tone required.

The range sidetones at 100 KHz, 20 KHz, 4 KHz, 800 Hz, 160 Hz, 32 Hz, and 8 Hz, are received and phase-detected in the range tone processor. Outputs of these phase detectors are routed to the Digital Range Tone Extractor for integration. The planned integration circuitry is shown in Figure 3-97. This design will provide low noise error for long integration times since one side of the integrating capacitor is connected to ground. The transfer function of this design is

$$E_o/E_i = \frac{A}{s\,CR_1 + \frac{1}{R_L} + 1 - \frac{R_1}{R_2}A + \frac{R_1}{R_2}}$$

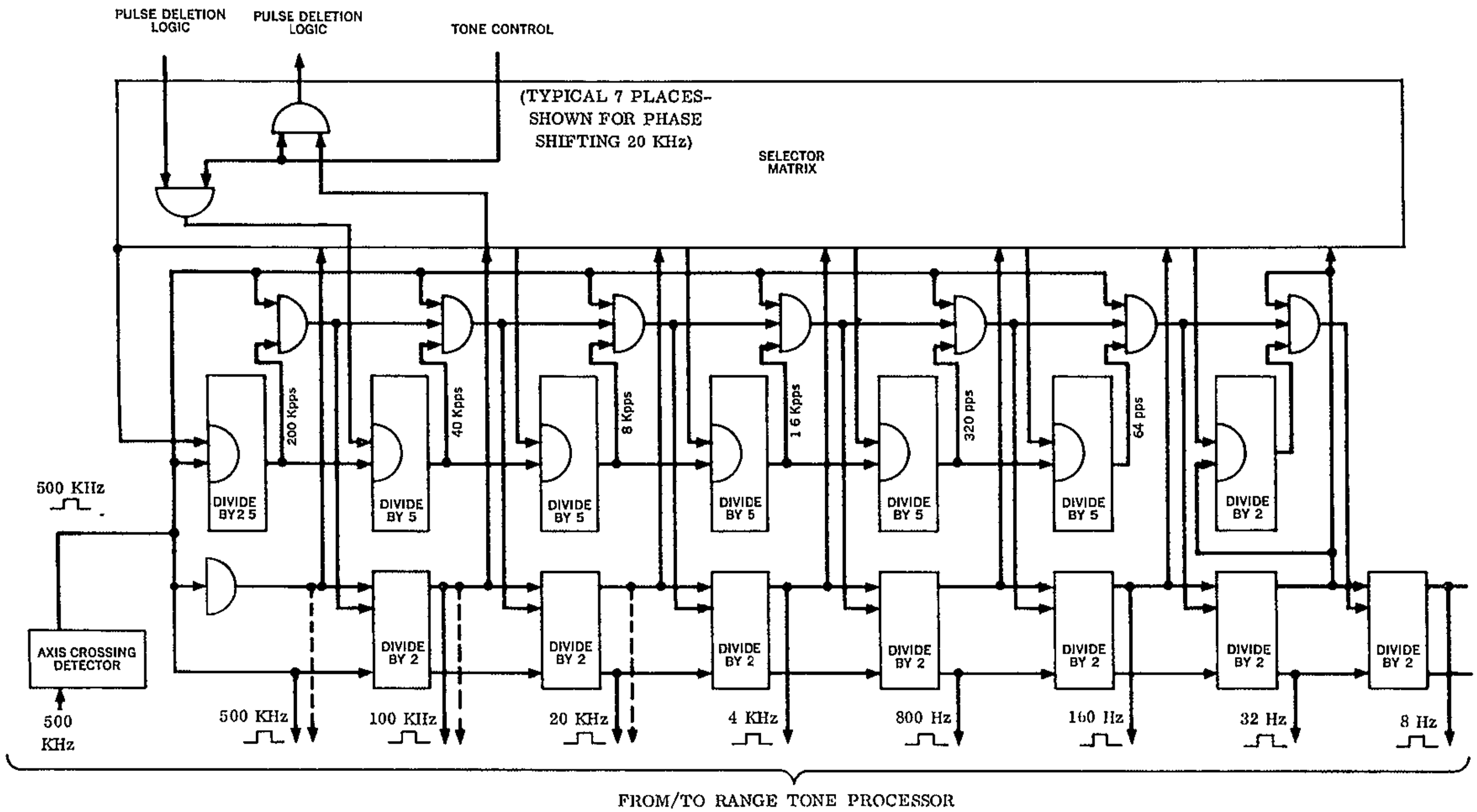

Figure 3-94. DRTE Divider Chain and Selector Matrix Block Diagram

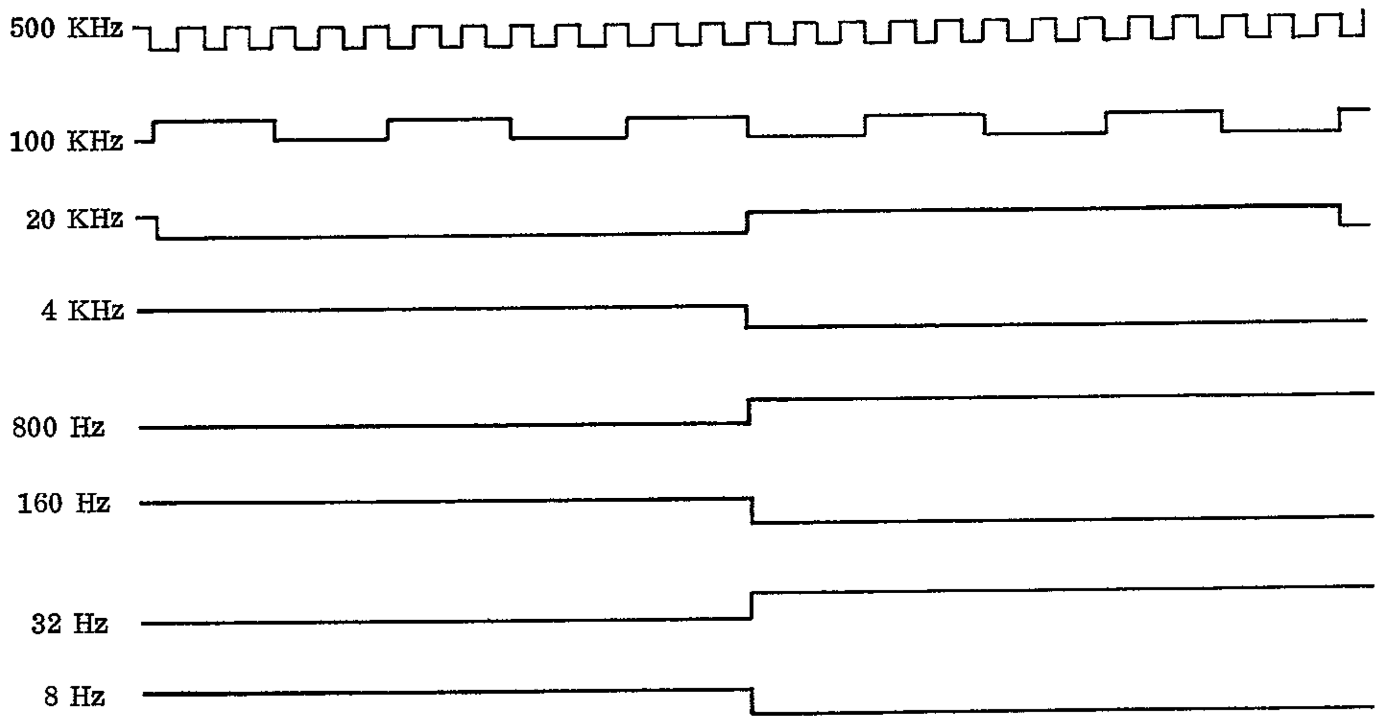

Figure 3-95. DRTE Divider Chain Outputs

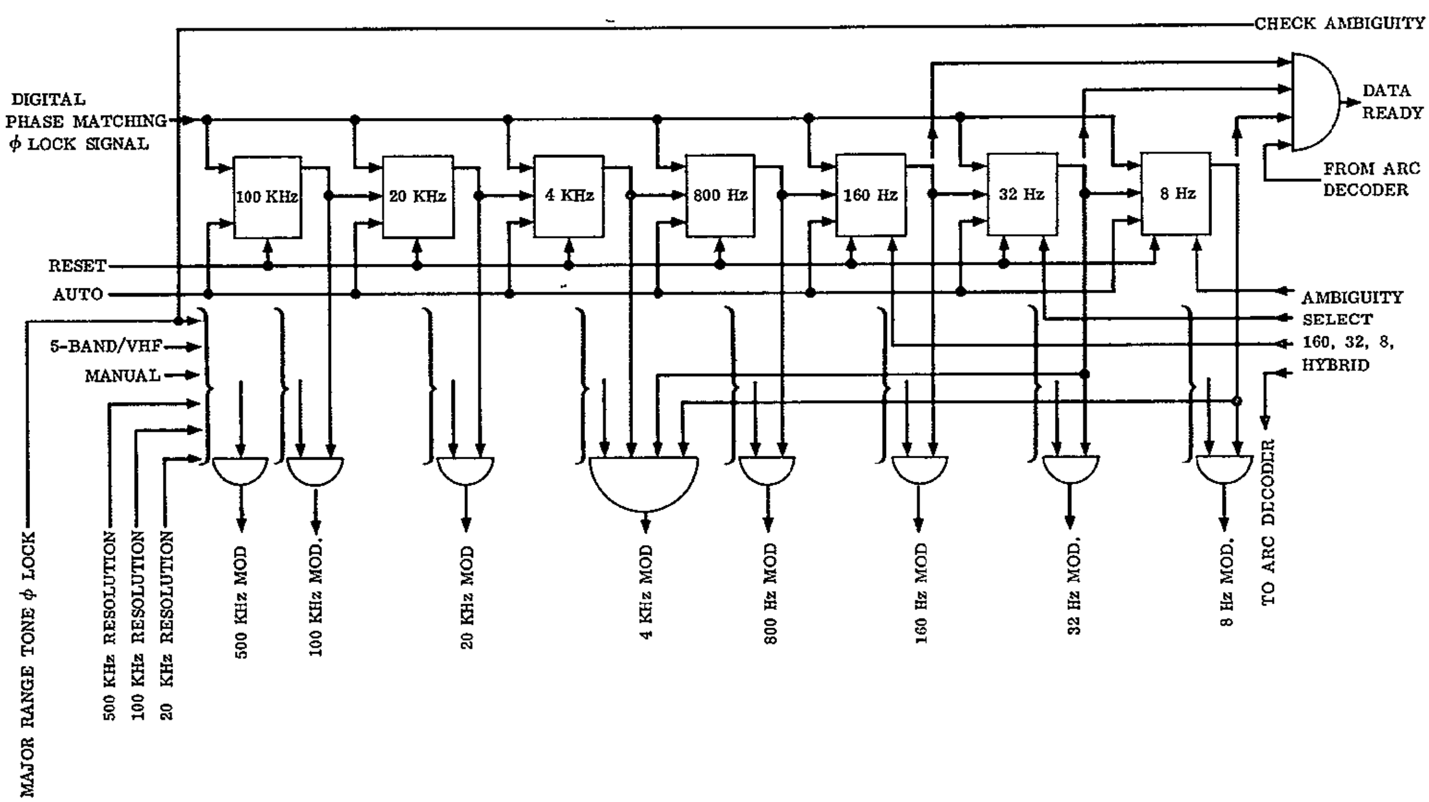

Figure 3-96. DRTE Tone Control

Table 3-5. Modulation Sequencing

500 KHz β=1.06	100 KHz β=1.06	100 KHz β=0.7	20 KHz β=1.06	20 KHz β=0.7	4 KHz β=0.7	4 KHz β=0.3	4.8 KHz β=0.7	4.16 KHz β=0.7	4.032 KHz β=0.7	4.008 KHz β=0.7	ARC β=0.7	
X												
X		X										
X				X								
X					X							
X							X					S-Band, 500 KHz Resolution
X								X				
X									X			
X										X		
X											X	
X												
	X											
	X			X								
	X				X							
	X						X					
	X							X				S-Band, 100 KHz Resolution
	X								X			
	X									X		
	X										X	
	X											
			X									
			X		X							
			X				X					
			X					X				S-Band, 20 KHz Resolution
			X						X			
			X							X		
			X								X	
			X									
		X				X						
		X		X		X						
		X			X							
		X				X	X					
		X				X		X				VHF, 100 KHz Resolution
		X							X			
		X								X		
		X				X					X	
		X				X						
				X		X						
				X	X							
				X		X	X					
				X		X		X				VHF, 20 KHz Resolution
				X					X			
				X						X		
				X		X					X	
				X		X						

NOTE β=Modulation Index

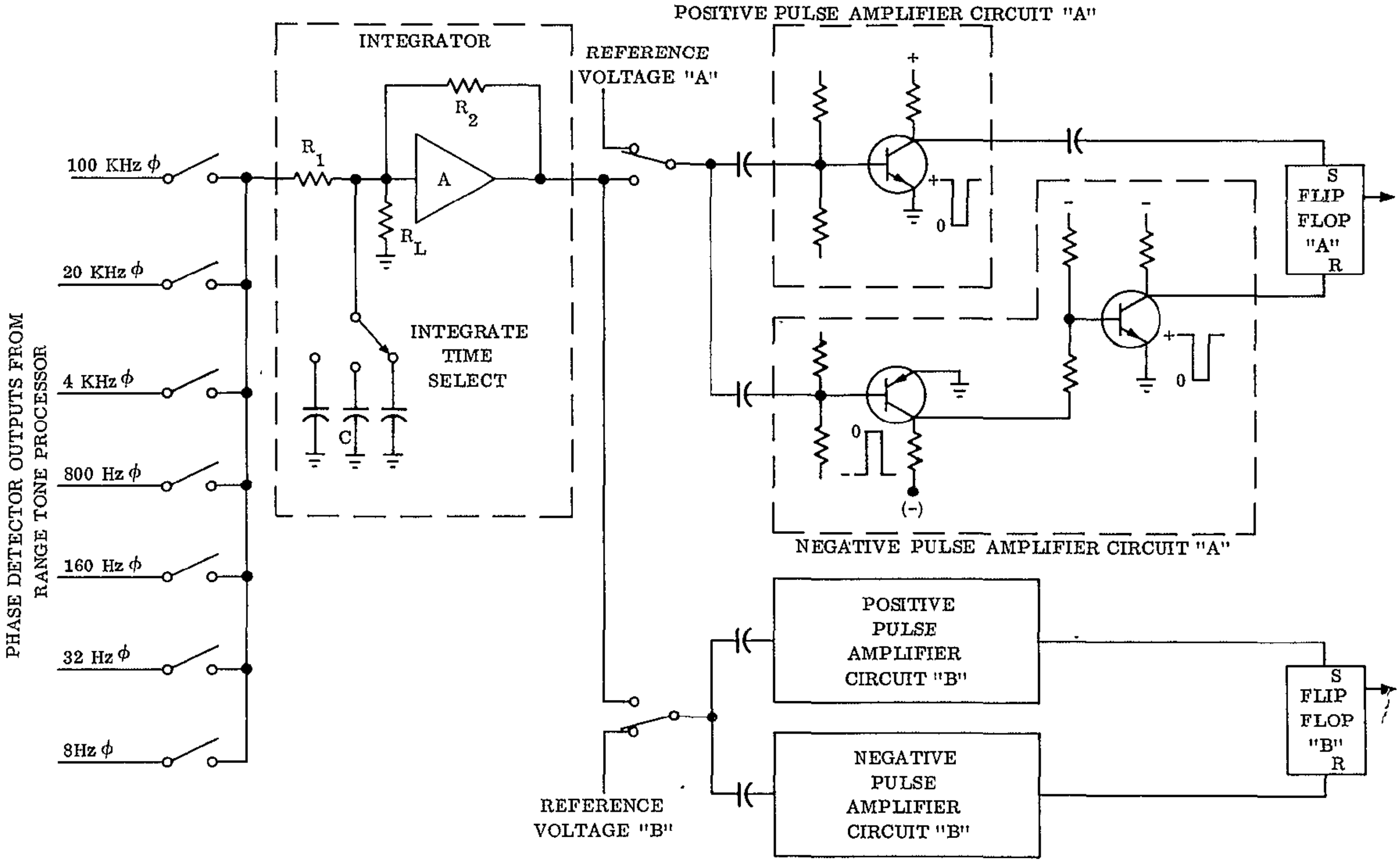

Figure 3-97. Integrator/Comparator

True integration is realized if

$$\frac{1}{R_L} + 1 - \frac{R_1}{R_2} A + \frac{R_1}{R_2} = 0$$

This can be very closely approximated in practice. The integrator will contain capacitors appropriate to the three integration time periods of 0.063, 1, and 10 seconds. The output of the integrator is connected to two comparator circuits which compare the integrator output to reference voltages. The outputs of the comparator circuits are then connected to pulse amplifier circuits which drive flip-flop direct inputs. The pulse amplifier circuits are complementary and each is biased in the ON state. Therefore a signal pulse of either polarity with respect to the reference voltage will generate a trigger pulse at the flip-flop direct inputs. The flip-flop will be placed in a state determined by the polarity of the signal pulse.

This circuitry performs the same function as a Schmitt trigger but offers greater stability since the pulse circuit is capacitively-coupled and temperature-compensated. No field adjustments are required.

Outputs of the integrator/comparator are routed to the pulse deletion logic circuitry shown in Figure 3-98. The phase detector outputs for a 360-degree phase shift and the digital representation at the output of the integration and comparison circuitry in truth table form are shown in Figure 3-99.

The pulse deletion logic circuitry deletes pulses in the divider chain to produce a 72 degree phase shift of a specified sidetone frequency. The pulse train at 10 times the frequency of the sidetone frequency to be phase shifted is inhibited. One pair of pulses of this pulse train equals 72 degrees of the sidetone frequency being phase matched. Therefore, deleting a pair of pulses at 10 times the sidetone frequency will phase shift the sidetone frequency by 72 degrees. Selecting the pair of pulses is accomplished by gating at 5 times the sidetone frequency. The pair of pulses to be deleted occurs during one cycle of the frequency at 5 times the sidetone frequency being phase matched. Phase shifts of 72 degrees, 144 degrees, and 216 degrees are provided by deleting 1, 2, or 3 pairs of pulses of the signal at 10 times the pulse train frequency. Phase shifting in these 3 discrete steps is required by the digital phase-shifting circuitry.

In phase-shifting the 100 KHz sidetone frequency, cycles of the 500 KHz frequency are deleted. In phase-shifting the 8 Hz sidetone frequency, pairs of pulses of the pulse train at 8 times the sidetone frequency, 64 pps, are deleted. Ninety-degree phase shifts are produced for each pair of pulses deleted. The pulse deletion logic receives the two flip-flop outputs and performs the necessary logic to delete pairs of pulses in the divider chain. As indicated in Figure 3-99, five possible phase positions result in three combinations of flip-flop outputs. The ambiguity of positions 1 and 3, and 4 and 5 is resolved by the pulse deletion logic sequence of operations. The case for 8 Hz is shown in Figure 3-100.

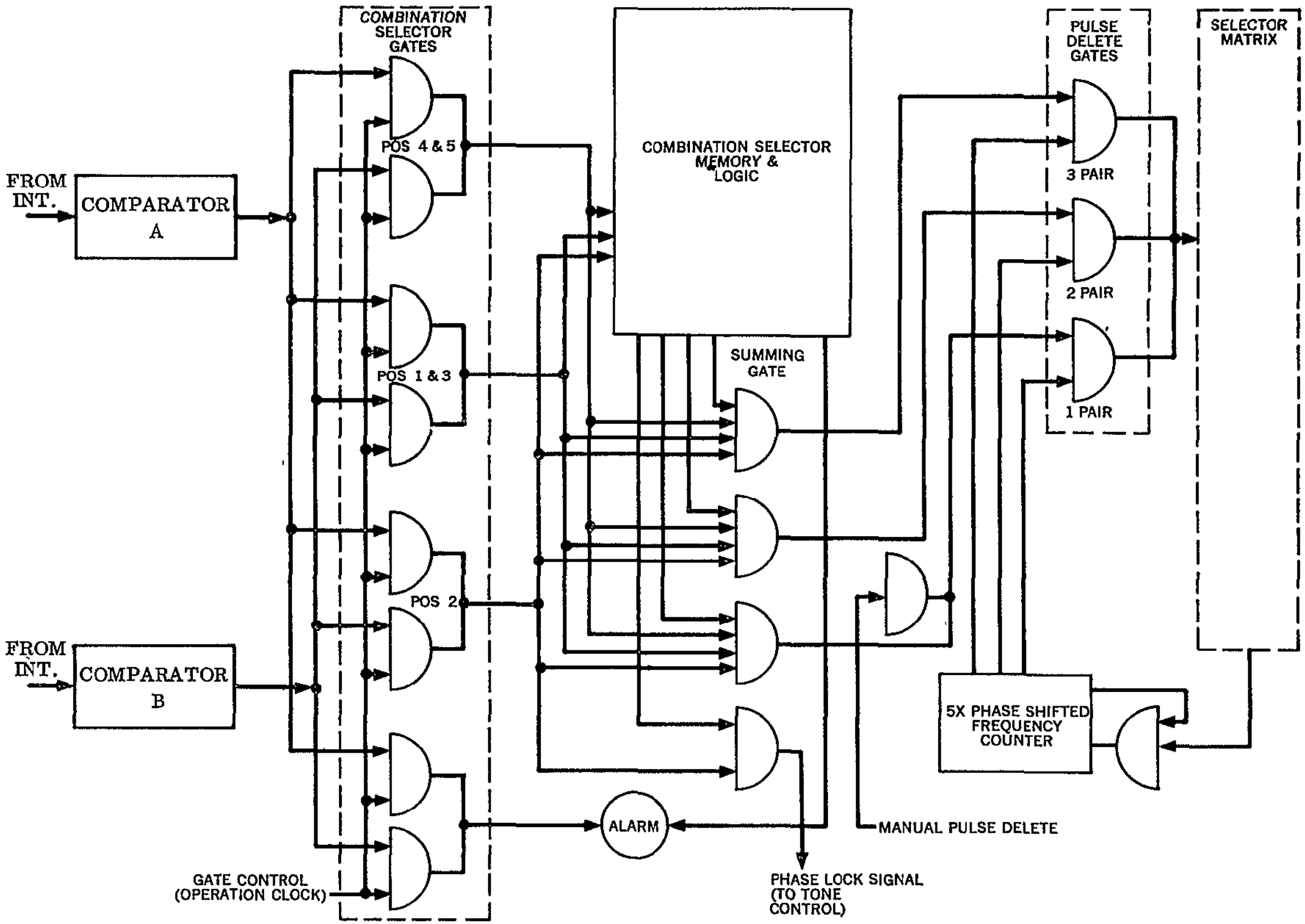

Figure 3-98. DRTE Pulse Deletion Simplified Logic

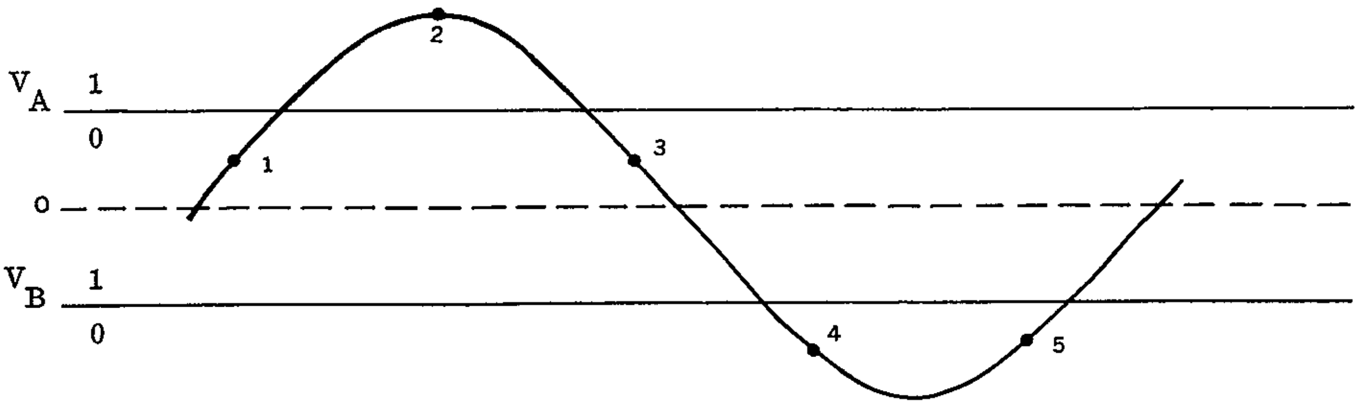

TRUTH TABLE

	SIGNAL RESPECTIVE TO V_A	SIGNAL RESPECTIVE TO V_B
1	0	1
2	1	1
3	0	1
4	0	0
5	0	0

Figure 3-99. 100 KHz to 32 Hz Phase Sensing Logic

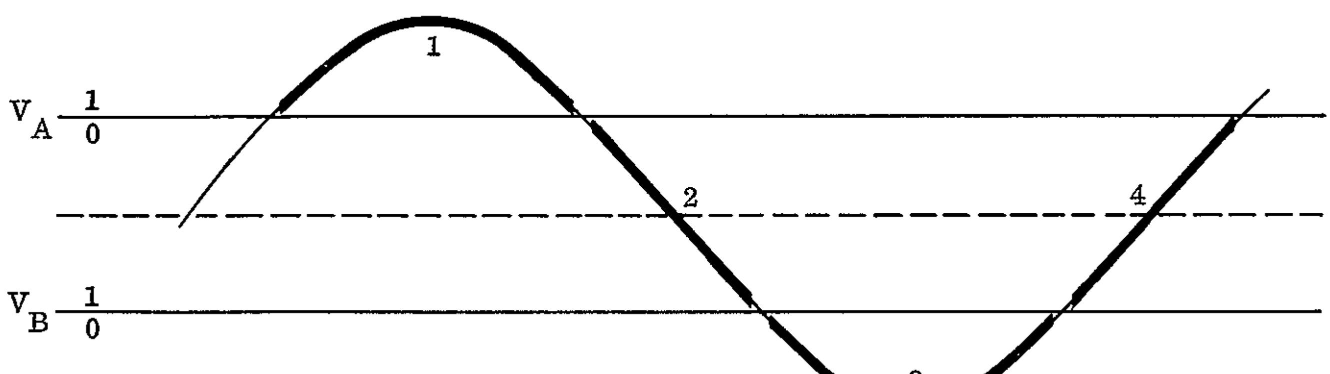

TRUTH TABLE

	SIGNAL RESPECTIVE TO V_A	SIGNAL RESPECTIVE TO V_B
1	1	1
2	0	1
3	0	0
4	0	1

Figure 3-100. Phase Sensing Logic for 8 Hz

A simplified logic diagram of the pulse deletion logic is shown in Figure 3-98. Flip-flop outputs are summed in the combination selector gates to produce an output from one gate only. A fourth combination gate detects an impossible combination and triggers an alarm signal located on the DRTE front panel. The three possible combination gates drive the combination selector memory logic and summing gates. In general, a memory flip-flop is triggered for each combination input signal. It is summed with the following combination signals according to the logic of Tables 3-6 and 3-7. The memory outputs control the summing gates. The summing gate outputs are routed to the pulse delete gates. For a signal input combination or series of combinations a summing gate will be operated by the memory and logic. Summation with a combination gate output will result in applying a signal at one input of the pulse delete gates. The second input to the pulse deletion gates is provided by the "5 × phase-shifted frequency" counter. Referring to Figure 3-101, the counter input is the waveform at 5 × the sidetone frequency being phase shifted. The shaded areas of Figure 3-101 denote the time interval for each output with respect to the divider chain pulses to be deleted.

The counter output signals occur during 1, 2, or 3 pairs of pulses in the divider chain. When these signals are applied at the pulse delete gate in conjunction with the signal from the memory and logic circuitry, the pulse delete gate selected by the memory and logic circuitry will pass the counter output signal to the selector matrix. As shown in Figure 3-98, the counter circuitry is also tied to a gate at the counter input. This gate inhibits the input signal after one output sequence from the counter. The counter is reset by the 8 Hz signal controlling the operation clock. The pulse delete gate signals inhibit the respective divider chain counter stage from receiving input pulses.

In normal operation the pulse deletion logic will apply a signal to the summing gate controlling the phase-lock signal to the tone control function after the predetermined sequence of flip-flop input signal combinations has occurred. At this time the memory circuits are reset to receive the next combination selector gate inputs. If a wrong sequence of combination signals occurs, the memories are reset and the alarm light is displayed on the front panel until a phase-lock condition occurs.

Manual control of the pulse deletion logic is accomplished by manually applying the memory and logic output at the 1-pair pulse delete gate. The 8-Hz control signal to the operation clock sequences the actual pulse-inhibiting operation in the divider chain. The selector matrix interfaces the pulse deletion logic function with the divider chain function. It controls (1) the source of the signal from the divider chain to the pulse deletion logic, and (2) the inhibit gate in the divider chain for the signal from the pulse deletion logic. Sidetone selection in the tone control controls the selector matrix gates.

3.7.1.3 RANGE START PULSE GENERATOR. The range start pulse generator is shown in Figure 3-102. As shown by this block diagram, the three highest frequency range tones at 20 KHz, 100 KHz, or 500 KHz are received and squared by axis-crossing detectors. The outputs of these axis-crossing detectors are gated by the mode selected to the clock input of flip-flop A. The phase relationship maintained by the three major range tones is shown in Figure 3-103. The 500 KHz tone is the major range tone selected for 500 KHz resolution,

Table 3-6. Digital Range Tone Extractor Gate Control Logic for 32 Hz to 100 KHz Range Tones

First Comparison Result*		Action Required	Second Comparison Result		Action Required	Third Comparison Result		Action Required
A	B		A	B		A	B	
1	1	None (wait for next comparison)	1	1	Give in-lock indication			
			Any other		Give alarm and start over			
0	1	Delete 1 pair of pulses (72°)	1	1	None (wait for next comparison	1	1	Give in-lock indication
						Any other		Give alarm and start over
			0	0	Delete 3 pairs of pulses (216°)	1	1	Give in-lock indication
			Any other		Give alarm and start over	Any other		Give alarm and start over
0	0	Delete 2 pairs of pulses (144°)	1	1	Give in-lock indication			
			0	1	Delete 1 pair of pulses (72°)	1	1	Give in-lock indication
						Any other		Give alarm and start over
			Any other		Give alarm and start over			
1	0	Give alarm and start over						

*Logical states of analog comparator outputs

Table 3-7. Digital Range Tone Extractor Gate Control Logic for 8 Hz Range Tone

First Comparison Result		Action Required	Second Comparison Result		Action Required	Third Comparison Result		Action Required
A	B		A	B		A	B	
1	1	None (wait for next comparison)	1	1	Give in-lock indication			
			Any other		Give alarm and start over			
0	1	Delete 1 pulse (90°)	1	1	None (wait for next comparison)	1	1	Give in-lock indication
						Any other		Give alarm and start over
			0	0	Delete 2 pulses (180°)	1	1	Give in-lock indication
			Any other		Give alarm and start over	Any other		Give alarm and start over
0	0	Delete 2 pulses (180°)	1	1	Give in-lock indication			
			Any other		Give alarm and start over			
1	0	Give alarm and start over						

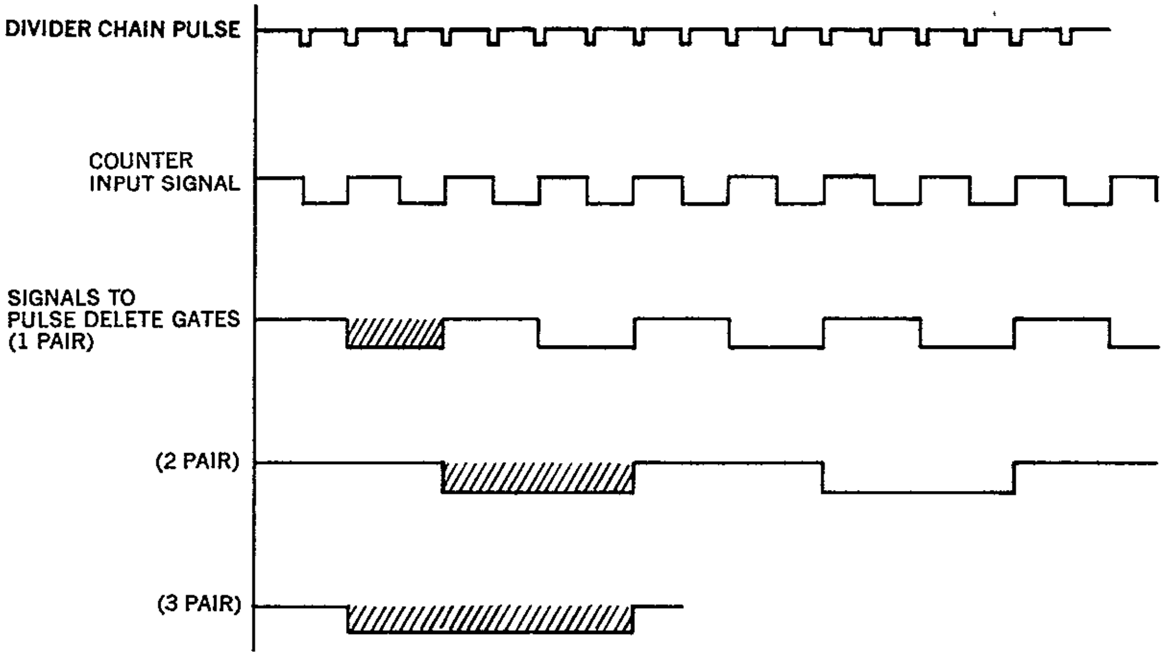

Figure 3-101. DRTE Time Interval Outputs Respective to the Divider Chain Pulses

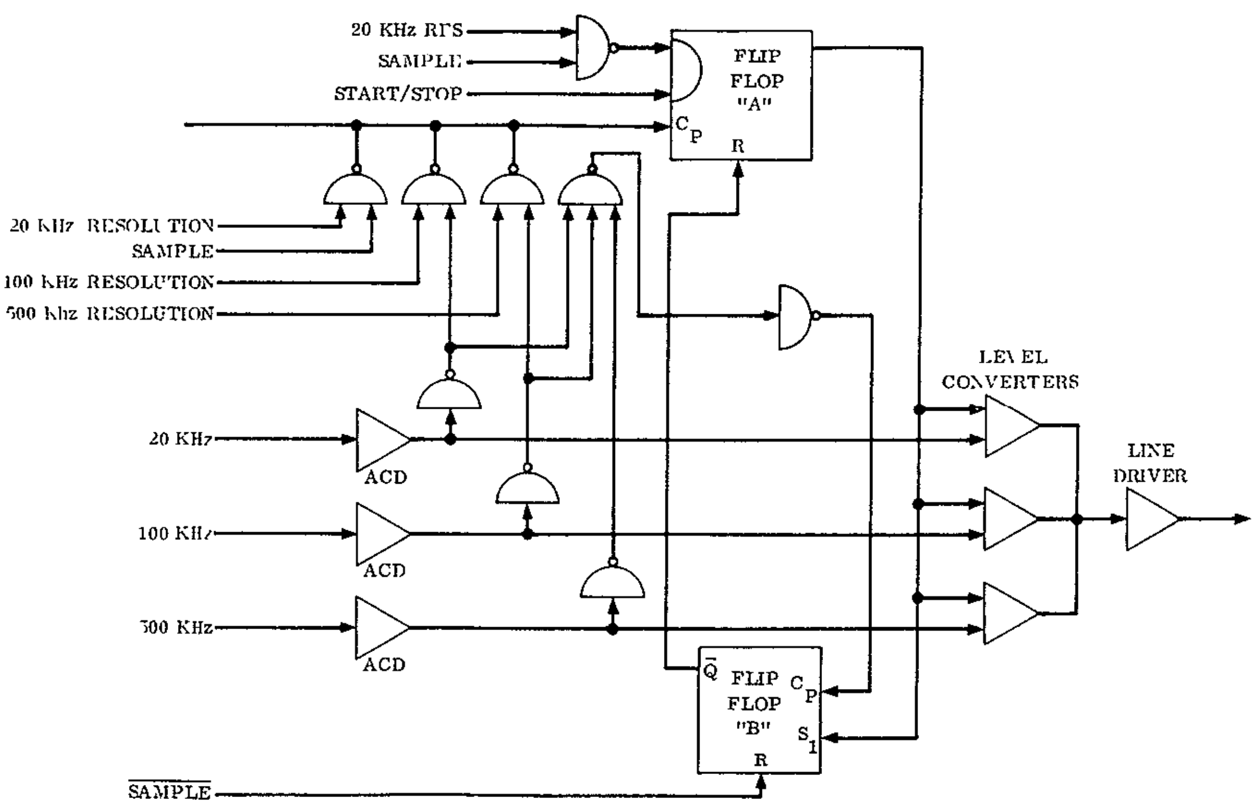

Figure 3-102. Range Start Pulse Generator

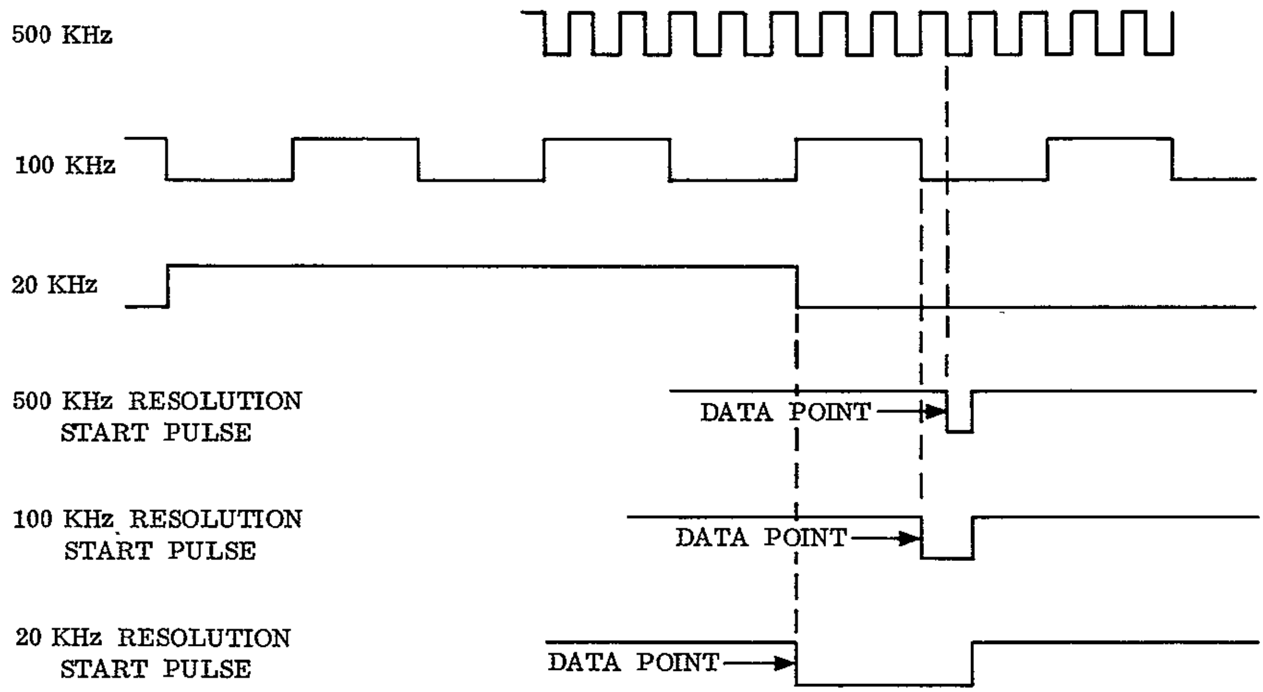

Figure 3-103. Major Range Tone Phase Relationships

100-KHz is the major range tone selected for 100 KHz resolution, and 20 KHz is the major range tone selected for 20 KHz resolution. In all cases the first negative transition of the major range tone after the sample period has started is the data point for the range start pulse. This is indicated in Figure 3-103.

For 20 KHz resolution only the 20 KHz tone is used. In this mode, flip-flop A, which controls the level converter inputs, is triggered by the sample pulse signal. The first negative transition of the 20 KHz signal after the sample pulse is the range start signal data point. Flip-flop A is reset by flip-flop B. Flip-flop B is triggered by a 500 KHz pulse gated to the flip-flop clock input by the 20 KHz and 100 KHz signals.

For 100 KHz resolution, the 20 KHz and 100 KHz tones are used to generate the range start pulse. Flip-flop A is triggered by the 20 KHz signal. The next negative transition of the 100 KHz is the range start signal. Flip-flop B is triggered in the same manner as for 20 KHz resolution.

For 500 KHz resolution, the 500 KHz, 100 KHz, and 20 KHz tones are used to generate the range start pulse. Flip-flop A is triggered by the 20 KHz and 100 KHz signals summed together. The 500 KHz signal is gated through to the level converter as the range start pulse. Flip-flop B is triggered in the same manner as for 20 KHz and 100 KHz resolution and resets flip-flop A.

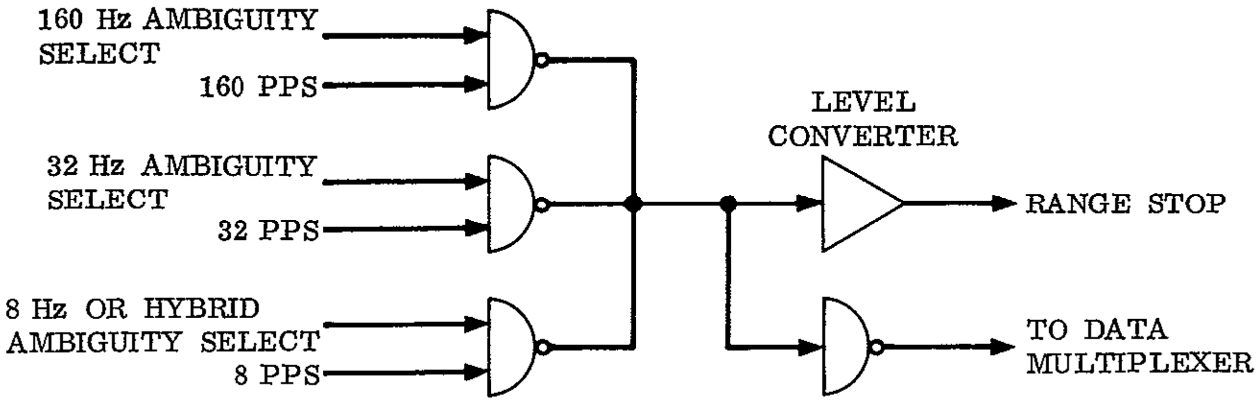

Figure 3-104. Range Stop Pulse Generator

In all cases the range start pulse is a single negative pulse at the level converter outputs. The start pulse generator circuitry will add no jitter to the pulse characteristics above that contributed by the axis-crossing detectors. This will be no more than 3.5 nanosec rms for 500 KHz and 100 KHz and 20 nanosec for 20 KHz. The output impedance of the pulse circuitry is 50 ohms, the output is adequate to drive the counter input directly.

3.7.1.4 RANGE STOP PULSE GENERATOR. Figure 3-104 is a block diagram of this unit. As indicated, inputs to the circuit are the ambiguity select functions and associated frequencies at 160 pps, 32 pps, or 8 pps. These frequencies are generated by the frequency divider chain of the Digital Range Tone Extractor. The pairs determine the rate at which the stop pulses are generated: 160, 32, or 8 pps. These pulses drive a level converter, thus providing the negative range stop pulses. The leading edge, negative transition, of the range stop pulses is the data point.

3.7.1.5 RANGE TIME INTERVAL UNIT. The Range Time Interval Unit consists of three assemblies comprising a 100 MHz time interval counter and an associated 8-digit decimal readout. Figure 3-105 shows the functional relationship of the assemblies. The three assemblies are part of the present installation; the Eldorado Model 1045M 100 MHz Prescaler in 4A5; the CMC Time Interval Unit Model 757BN in 4A2; the Range Readout in 4A6. These assemblies will be relocated.

The time interval measurement is obtained by counting 100 MHz pulses in two decade counters of the prescaler. The divided 1 MHz output from the two decades is fed to six decade counters of the CMC 757BN counter. The resultant eight decades of BCD decimal information are fed to the data system for use. A pulse from the data system resets the prescaler and counter for the next pair of start/stop pulses. Measurement resolution is 10 nanosec.

3.7.1.6 AMBIGUITY NUMBER EXTRACTION UNIT. The Ambiguity Number Extraction Unit (Figure 3-106) utilizes the transmitted and received pseudo-random binary codes to determine a range ambiguity number which represents the number of 8 Hz ambiguities which must be added to the basic range number to determine the true unambiguous range.

NOTE

In modulo two, two binary numbers are added digit by digit such that an even number of ones produces a zero result and an odd number of ones produces a one result.

The code utilized is generated by combining, in modulo two, the outputs of two maximal length binary shift counters. The counters, 7 and 8 stages in length, respectively, produce 127 and 255 unit sub-codes which, when combined in modulo two, produce a 32, 385 unit code. This 32, 385 unit code, when transmitted at 4 KHz, is unambiguous to a range of approximately 1.2 million km.

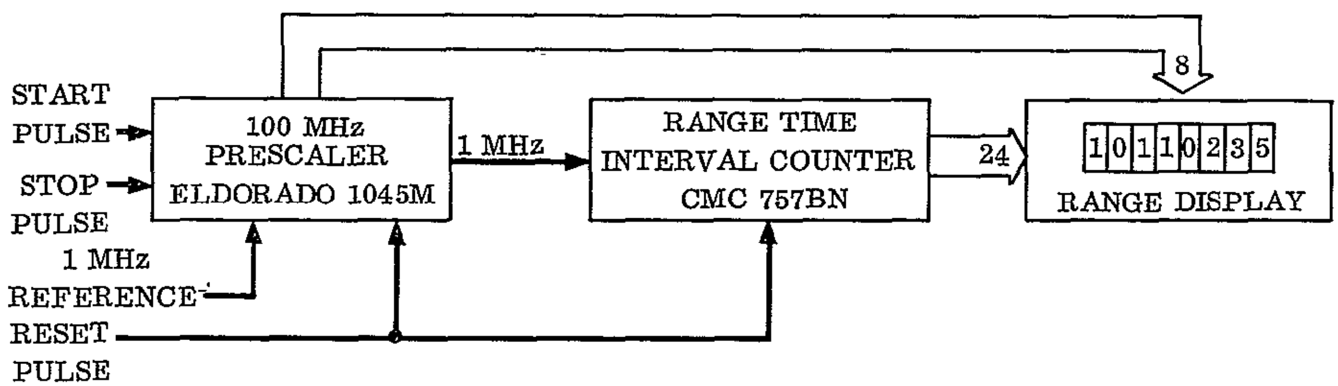

Figure 3-105. Range Time Interval Unit

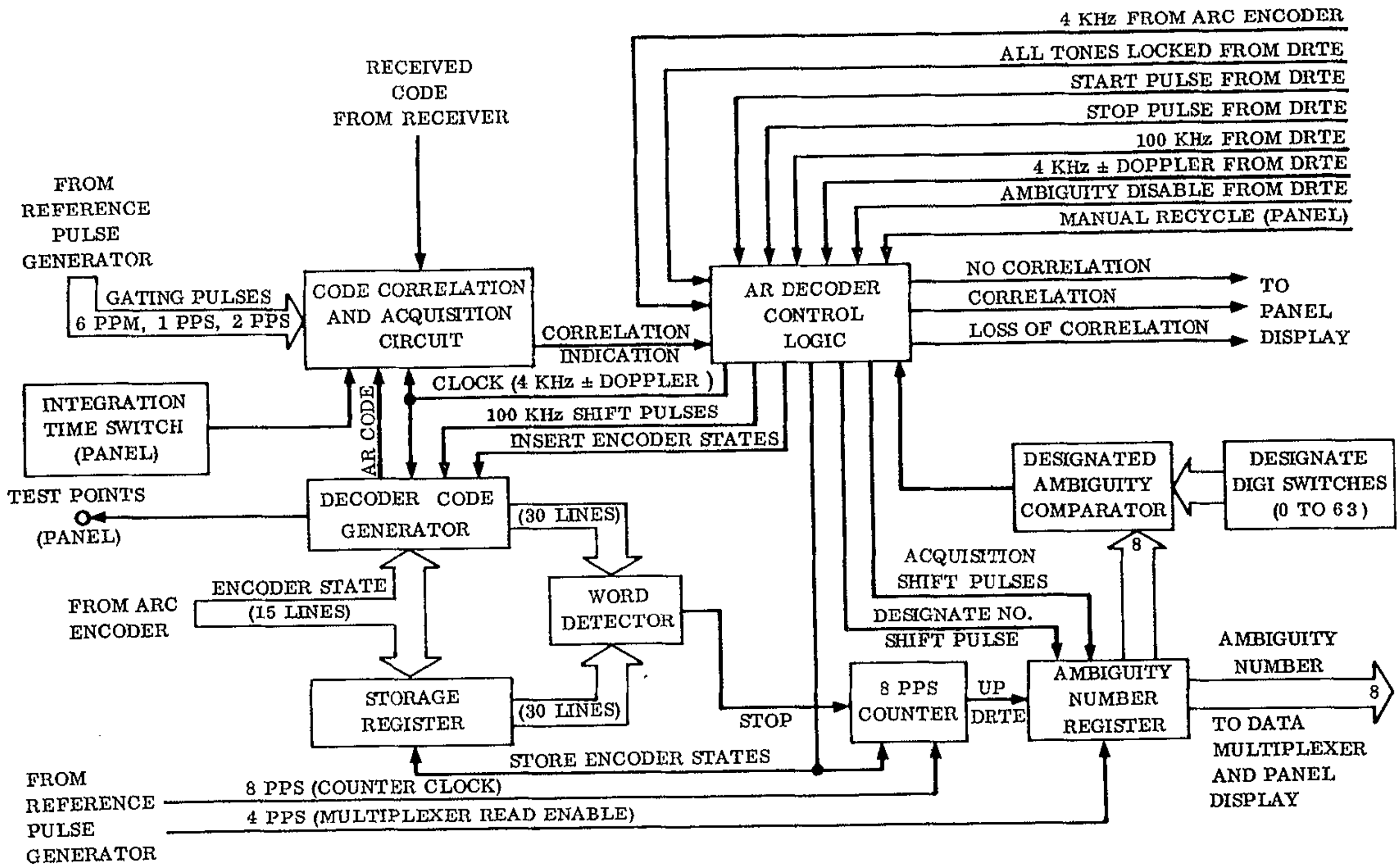

Figure 3-106. Ambiguity Number Extraction Unit Functional Block Diagram

Two operations are involved in producing and maintaining the range information derived from these codes. The first operation results in synchronization of the local receive or decoder code generator with the received code, which is actually the transmitted code delayed by transit time and corrupted with noise. This is called the acquisition operation. The second operation takes place after the acquisition phase and consists of utilizing the synchronized decoder code generator in conjunction with the transmitter or encoder code generator and the sidetone ranging system to obtain the appropriate range ambiguity number. Note that once the acquisition phase is complete it is no longer necessary to transmit the code. It is only necessary to transmit the 4 KHz clock which runs the decoder code generator.

3.7.1.6.1 Code Acquisition. Code acquisition or synchronization consists of synchronizing the received code with the decoder code generator. Figure 3-107 is a flow chart of the process. The transmitted code is stored in the code generator (Figure 3-106) upon occurrence of the range start pulse. When the range stop pulse occurs, the code generator is allowed to count from the received 4 KHz reference. The sidetone ranging system has thus accounted for ranges which are fractions of the basic 8 Hz range tone in the start and stop pulse time delay.

Although the code generator is counting in synchronism with the received code, it differs in phase or time by the number of whole 8 Hz ambiguities which were included in the start and stop pulse delay. The decoder generator is therefore stepped out to a trial designate ambiguity number selected by the operator on the front panel. This stepping is accomplished by adding 10 pulses to the 8-stage decoder register and 7 pulses to the 7-stage encoder register for each 8 Hz ambiguity. The effect is to advance the decoder generator 31,885 bits, which is the same as retarding the generator by 500 bits or 1/8 sec in range. Stepping is accomplished at a 100 KHz rate between adjacent 4 KHz clock pulses so as not to disturb the basic synchronism of the received code and the decoder code generator. After the trial number is reached, the two codes are compared by the correlation detector.

The correlation detector, Figure 3-108 determines whether correlation exists between the decoder code generator and the received code. Correlation is a measure of the certainty with which we may predict that two signals are alike in the presence of random noise disturbances. Pseudo-random codes are characterized by auto-correlation functions which exhibit a sharp positive peak at the point of correlation or match and a slightly negative value at all other displacements. For all values of displacement of the received code, with respect to the transmitted code, the input to the integrator (shown in Figure 3-108) will approximate a balanced waveform of negative and positive excursions. However, at the point of correlation, a positive full-wave rectified signal will appear at the input to the integrator to produce an integrator output.

Figure 3-109 shows the waveforms for the correlated case. Note that the sum signal input to the integrator (signal 6) is as predicted and results in a positive integrator output. If integration is over a suitable period of time, the threshold of the detector circuit is exceeded and correlation indication is generated. Integration times of 1 sec and 10 sec are switch-selectable at the front panel. An analysis of integration time is given in Section 4.10.

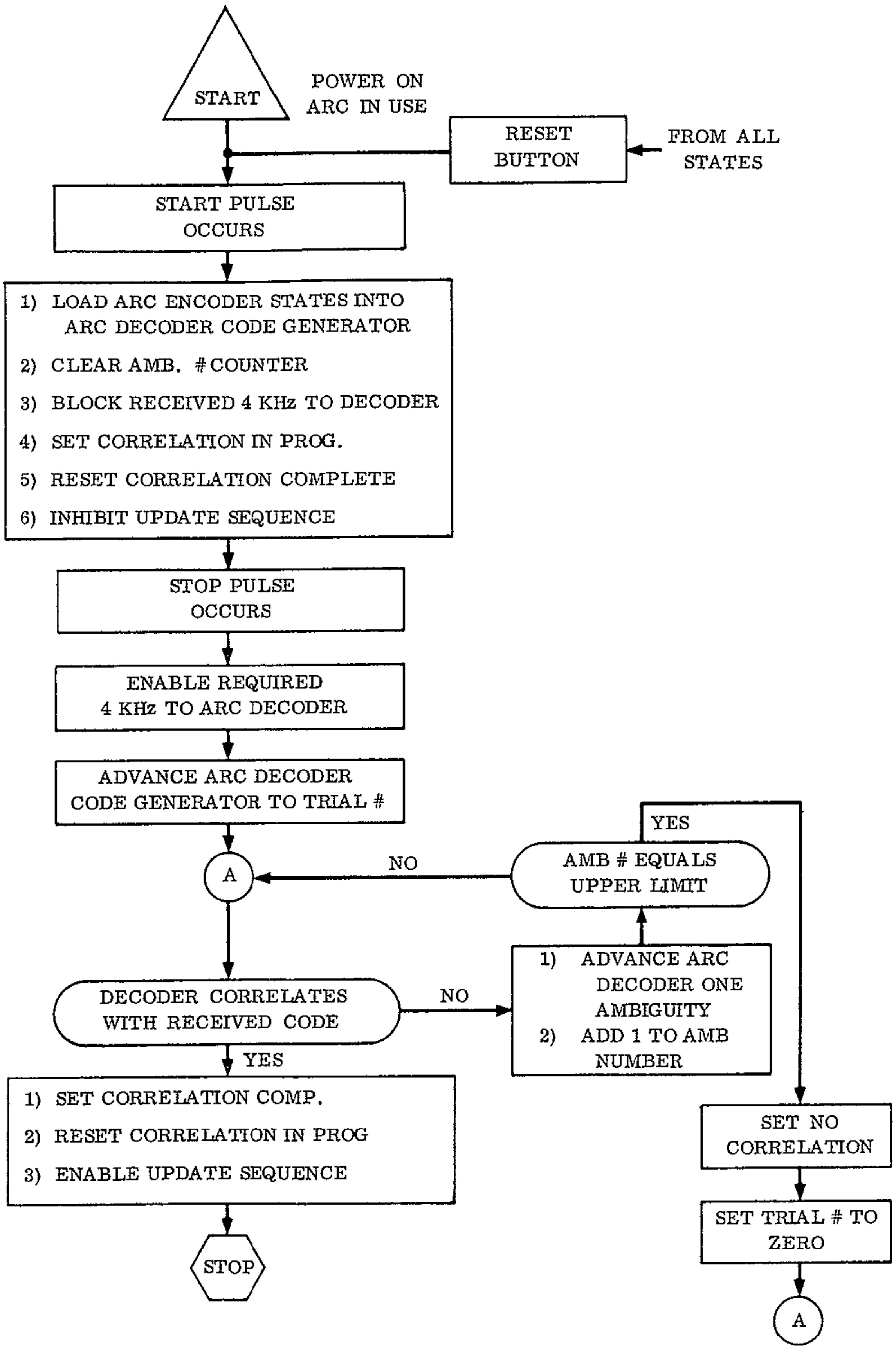

Figure 3-107. Synchronization Flow Chart

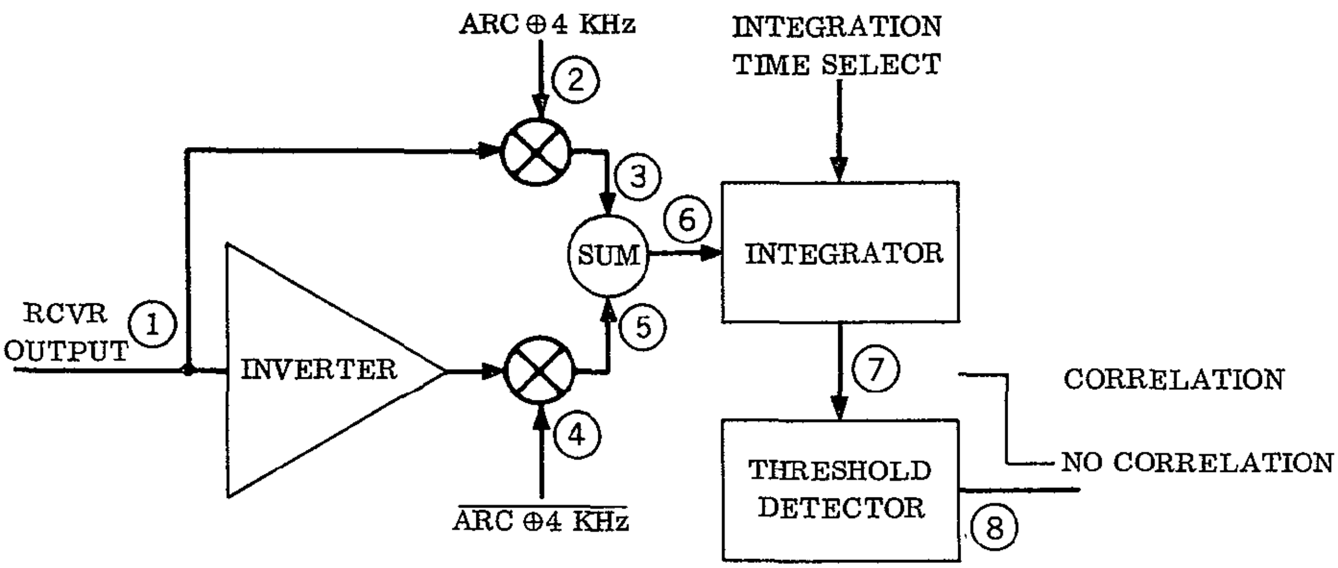

Figure 3-108. Correlation Detector

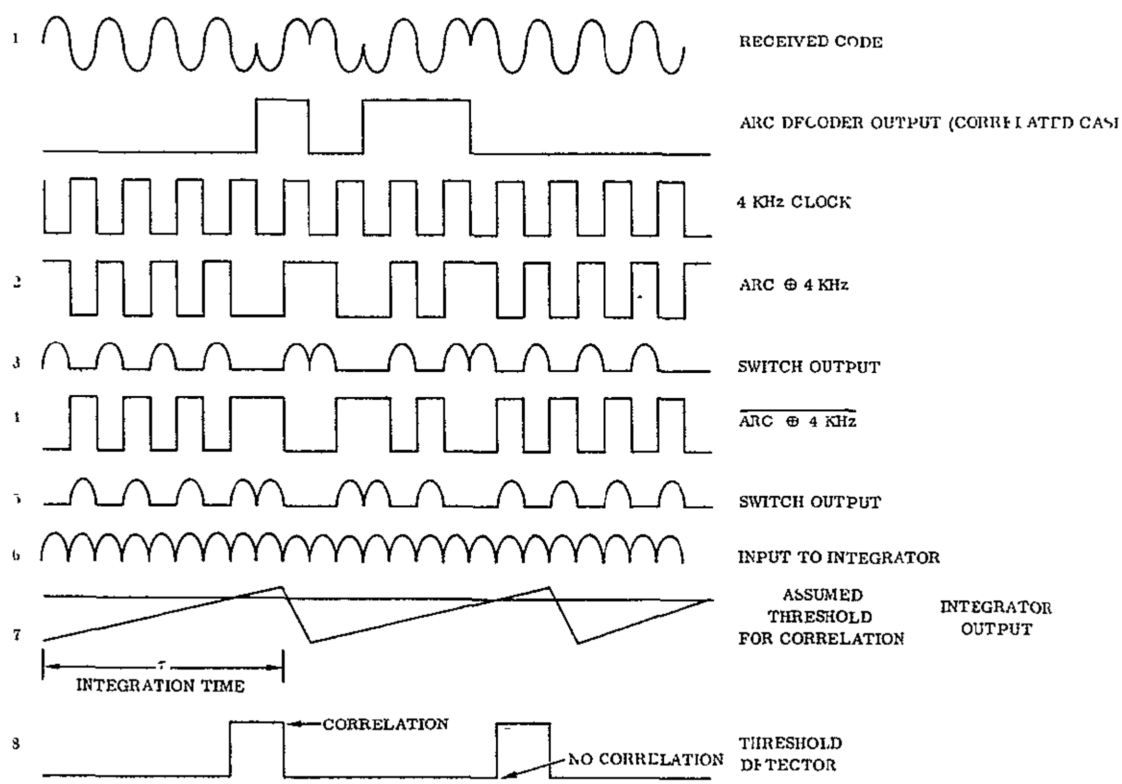

Figure 3-109. Waveforms in Correlation Detector

3.7.1.6.2 Ambiguity Number Updating. Once acquisition or synchronization is complete, it is only necessary to continue to apply the received 4 KHz clock to the decoder code generator and range information will be generated by the observed time displacement between the decoder code and the encoder code. Occurrence of the start pulse marks the beginning or synchronization point of the encoder code. This start pulse may then be used to cause transfer of the encoder generator states which marks the code start point. The encoder code generator states are stored in the storage register upon occurrence of the start pulse. A continuous comparison is made between this code word and the contents of the decoder code generator, driven from the received 4 KHz clock. When a match is obtained we have determined the time interval between the two codes which is our measure of range. It is only necessary to start and stop a counter in synchronism with the start pulse and stop it when this comparison is achieved to complete the measurement. The counter counts from the 8 pps reference since we wish only to know the number of 8 cps ambiguities involved. This process is detailed in the flow chart of Figure 3-110.

3.7.1.7 ANALOG PHASE DETECTORS. Two types of inputs are applied to the analog phase detector (Figure 3-111). The inputs from the Receiver Subsystem consist of eight

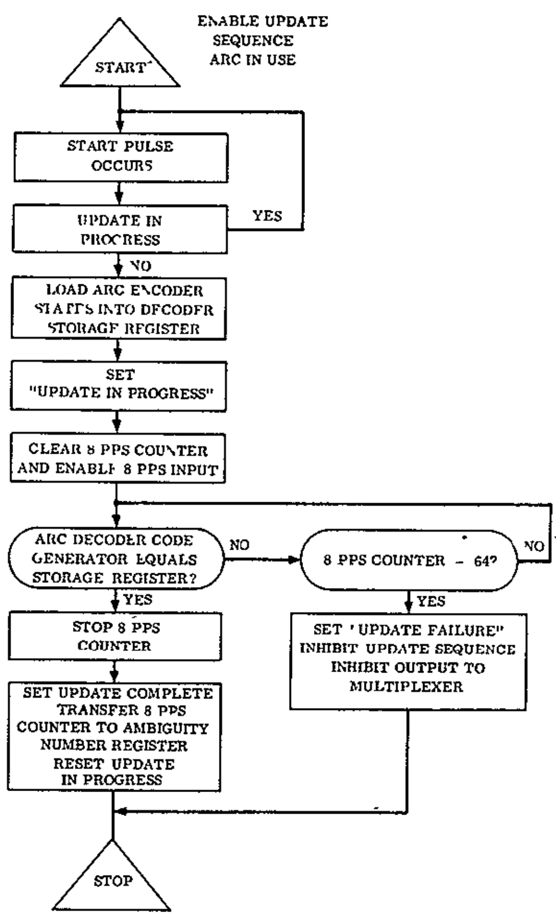

Figure 3-110. Update Flow Chart

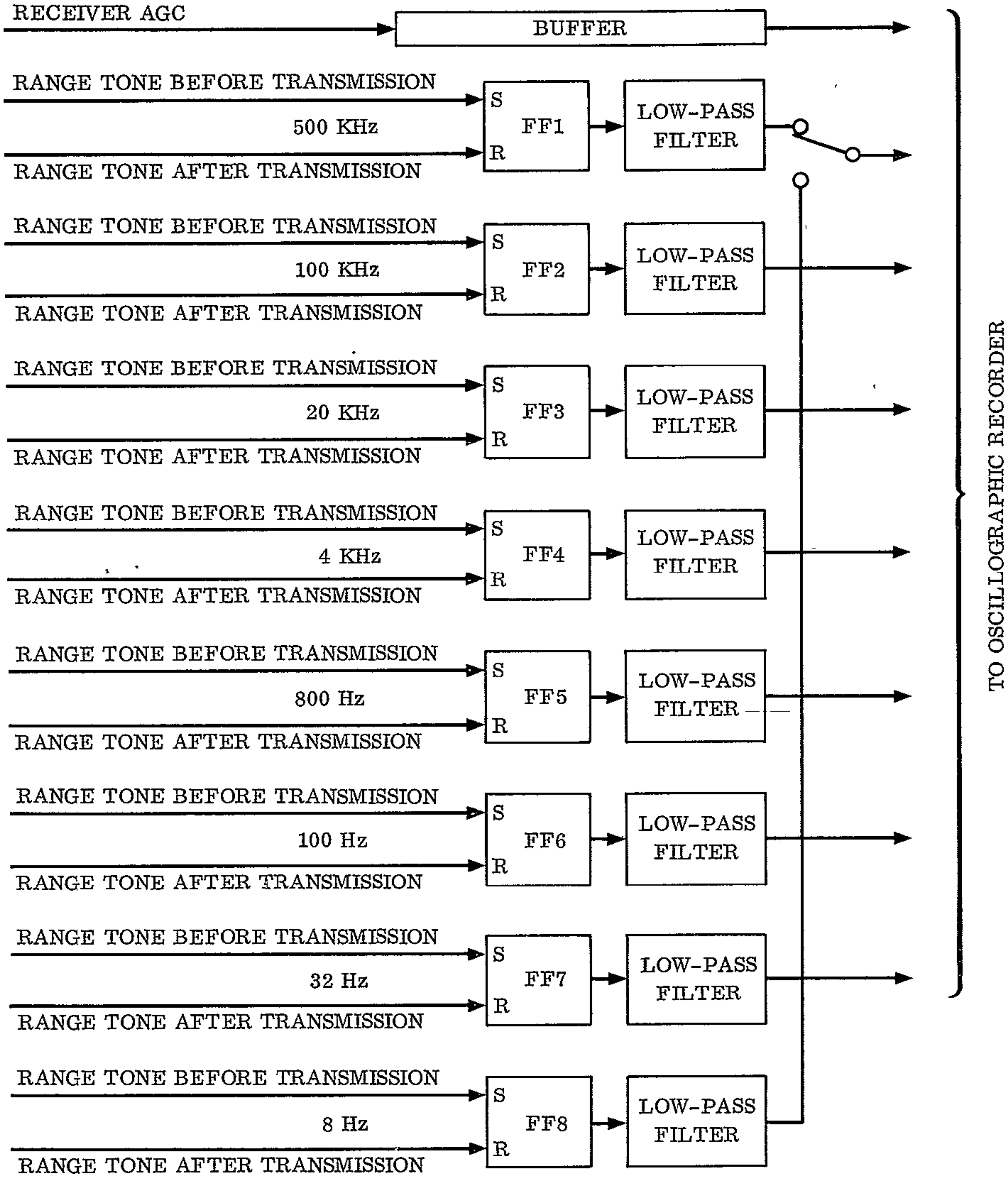

Figure 3-111. Analog Phase Detectors

sidetone signals which have been synthesized to square waves by the Digital Range Tone Extractor. These sidetone signals are delayed in phase commensurate with the range of the vehicle being tracked. The second group of inputs is received from the Reference Pulse Generator in the Signal Generation Subsystem and consists of reference square waves. Each of the received analog signals is applied to the set input of a separate flip-flop circuit. Each of the eight reference inputs drives the reset input of its respective flip-flop. The set signal will cause the flip-flop to change state if the circuit is in a reset state when it is applied.

The outputs of the eight analog phase detectors are passed through low-pass filters. Outputs of the low pass filters for the 100 KHz, 20 KHz, 4 KHz, 800 Hz, 160 Hz, and 32 Hz phase data are supplied directly to the Analog Recorder. Outputs for the 500 KHz and 8 Hz phase data are supplied to the Digital Range Tone Extractor where one or the other is selected by a front panel switch and then routed to the Analog Recorder via the Reference Pulse Generator.

3.7.2 Range Rate Extraction Unit

The Range Rate Extraction Unit determines doppler by measuring the time required to count a fixed number of cycles of two-way doppler plus bias frequency.

The two-way doppler on the S-Band carrier has a maximum frequency of approximately ±200 KHz with a 500 KHz bias frequency. For the VHF carrier, the maximum two-way doppler

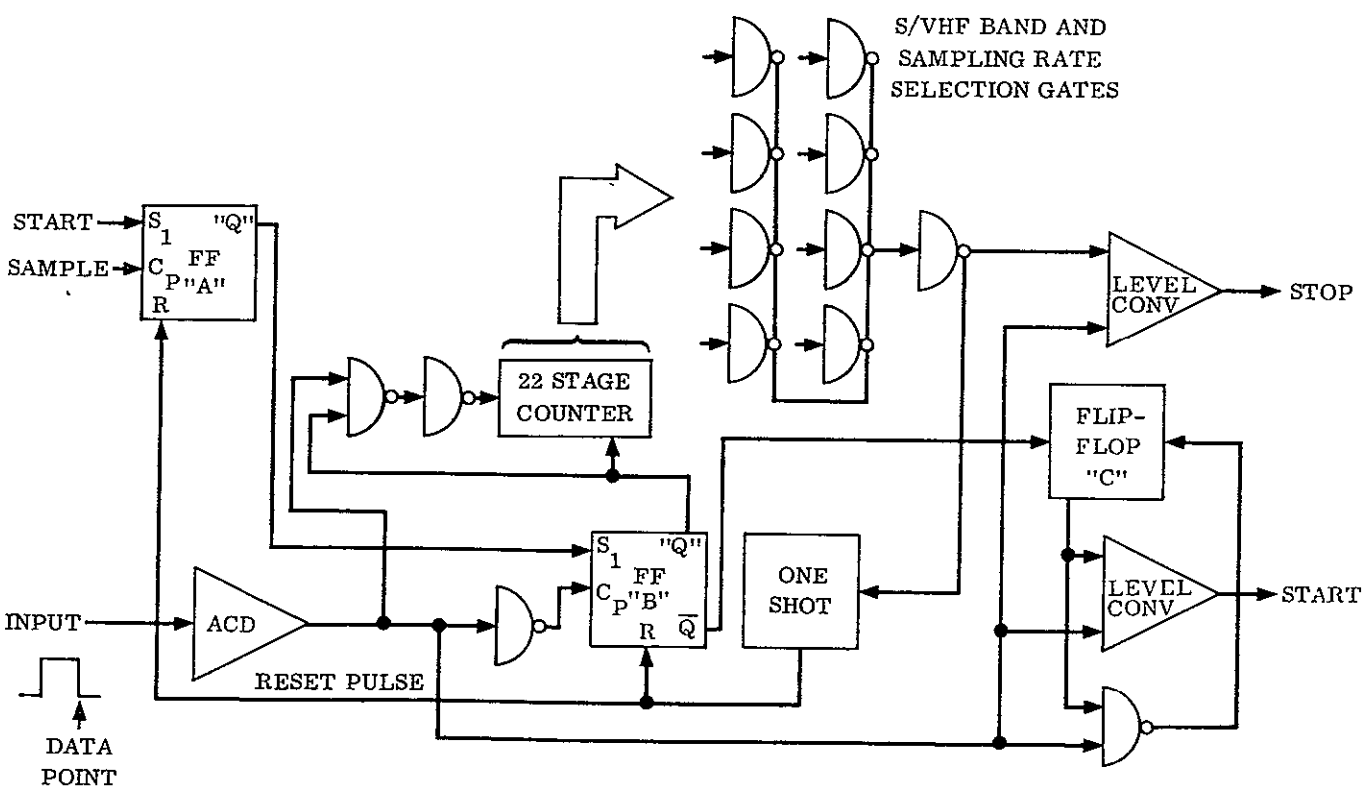

Figure 3-112. Range Rate N-Cycle Counter

frequency is ±20 KHz with a 30 KHz bias frequency. The range rate extraction unit consists of an N-cycle counter and the range rate time interval unit.

3.7.2.1 N-CYCLE COUNTER. Figure 3-112 is a block diagram of the N-cycle counter. The number of cycles to be counted and the sampling rates for the VHF and S-Band modes are given in Table 3-8.

Table 3-8. Counting and Sampling Rates

Recording Rate	S-Band (N Counter)	VHF (N Counter)
4/sec	65,503	4,093
2/sec	131,007	8,187
1/sec	229,263	14,328
6/min	3,133,956	182,182

In the S-Band mode the bias frequency is 500 KHz with a ±200 KHz doppler. In the VHF-Band mode the bias is 30 KHz with a ±20 KHz doppler frequency. These frequencies are received at the axis-crossing detector. Flip-flop A is triggered by the first sampling pulse following the operation of the start control. Flip-flop A sets the dc control on flip-flop B such that the first positive transition of the input data signal will trigger flip-flop B and remove the reset control on the twenty-two stage counter. The input data negative transition is the proposed data point. The pulse will be transferred through as the start pulse with the trailing edge as the data point.

The counter will count this pulse as the first of the group in the sampling period. Eight selection gates select one of the counts shown in Table 3-8. The input data signal pulse is thus gated out as a stop pulse when the counter reaches the selected count. Here also, the data point is the trailing edge of the pulse. Figure 3-113 depicts the time relationships for the start and stop pulses. Flip-flop C controls the start pulse such that only one pulse is transferred out to the TIU for a sample period. Flip-flop C is triggered on by flip-flop B. This occurs at the first positive transition of the input data signal. Flip-flop C is turned off on the next positive transition at the data point. Since flip-flop C controls the start pulse level converter only one start pulse is generated.

It should be noted in Table 3-8 that the slowest sampling rate provides a 300 KHz bias plus doppler signal. The time interval per cycle for this frequency is 1/300 Ksec. The required count at the 6/min sampling rate is 3,133,956 which will require $10^{-6}/0.3 \times 3.133956 \times 10^{6} = 10.44$ sec. Thus the 10 sec time interval is exceeded for this extreme condition.

3.7.2.2 RANGE RATE TIME INTERVAL UNIT. The Range Rate Time Interval Unit, a CMC Model 757BN Time Interval Unit located presently in 4M1, will be retained. This unit

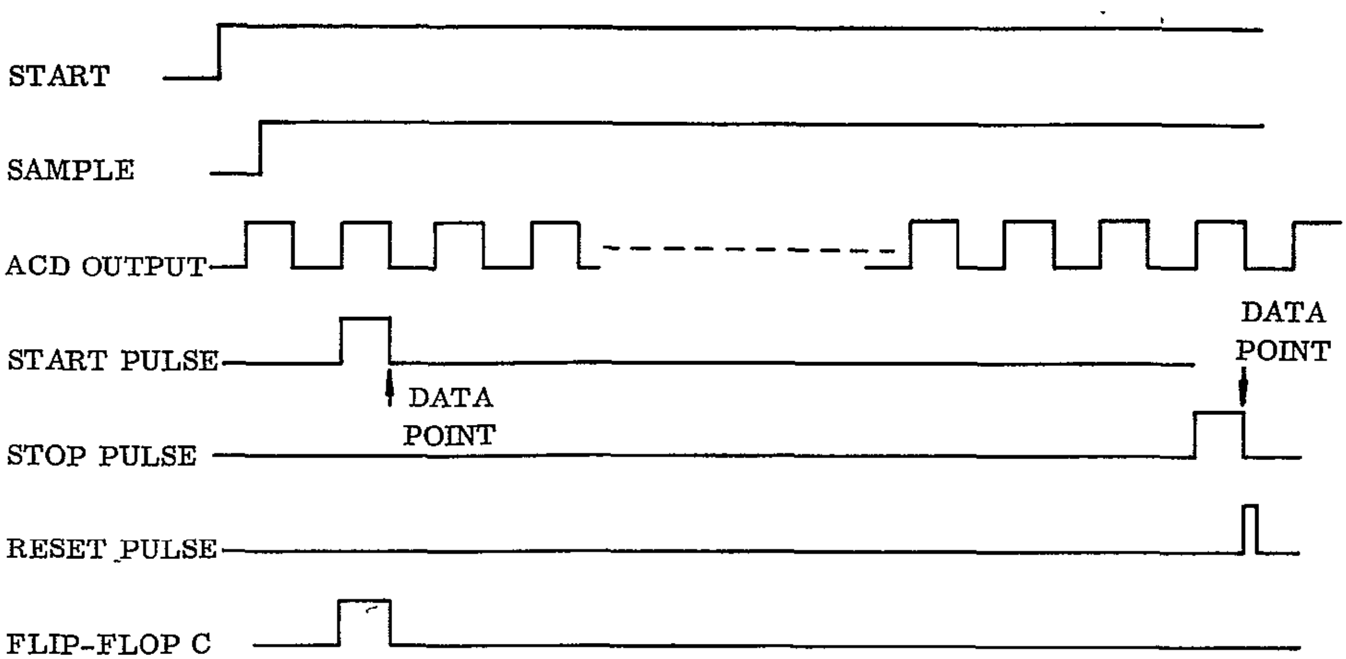

Figure 3-113. Timing Relationships

counts a 10 MHz reference from the Frequency Synthesizer. The count is controlled by a start and stop pulse from the range rate N-cycle counter. The time interval between the start and stop pulses is measured by counting the 10 MHz pulses, giving a resolution of 0.1 μsec. The accumulated time interval measurement is read out when required by the data system and then reset for the next count.

3.7.3 Recording Unit

The function of the recording unit (Figure 3-114) is to receive data inputs from the system and process, format, and record them on a suitable medium for later use. Both oscillographic paper records and punched paper tape are utilized. Range system phase detector outputs are recorded along with receiver AGC on the oscillographic recorder to provide a coarse range measurement. A standard Goddard data message is recorded on the paper tape in Baudot five-level teletype format which contains all pertinent system data.

3.7.3.1 DATA MULTIPLEXER. The Data Multiplexer (Figures 3-115 and 3-116) receives the system data and performs the tasks of formatting, time-tagging, and buffering prior to data entry into the paper tape recorder. Input data will consist of the following items:

	Item	Source	Size	Characteristic
a.	X, Y Angle Data	Angle Data Translator	34 bits	BCD
b.	Time-of-Year	Time Code Generator	30 bits	BCD
c.	Q/D Identification	Receiver Subsystem Signal Generation Subsystem	4 bits	Binary
d.	ARC Number	ARC Decoder	8 bits	BCD

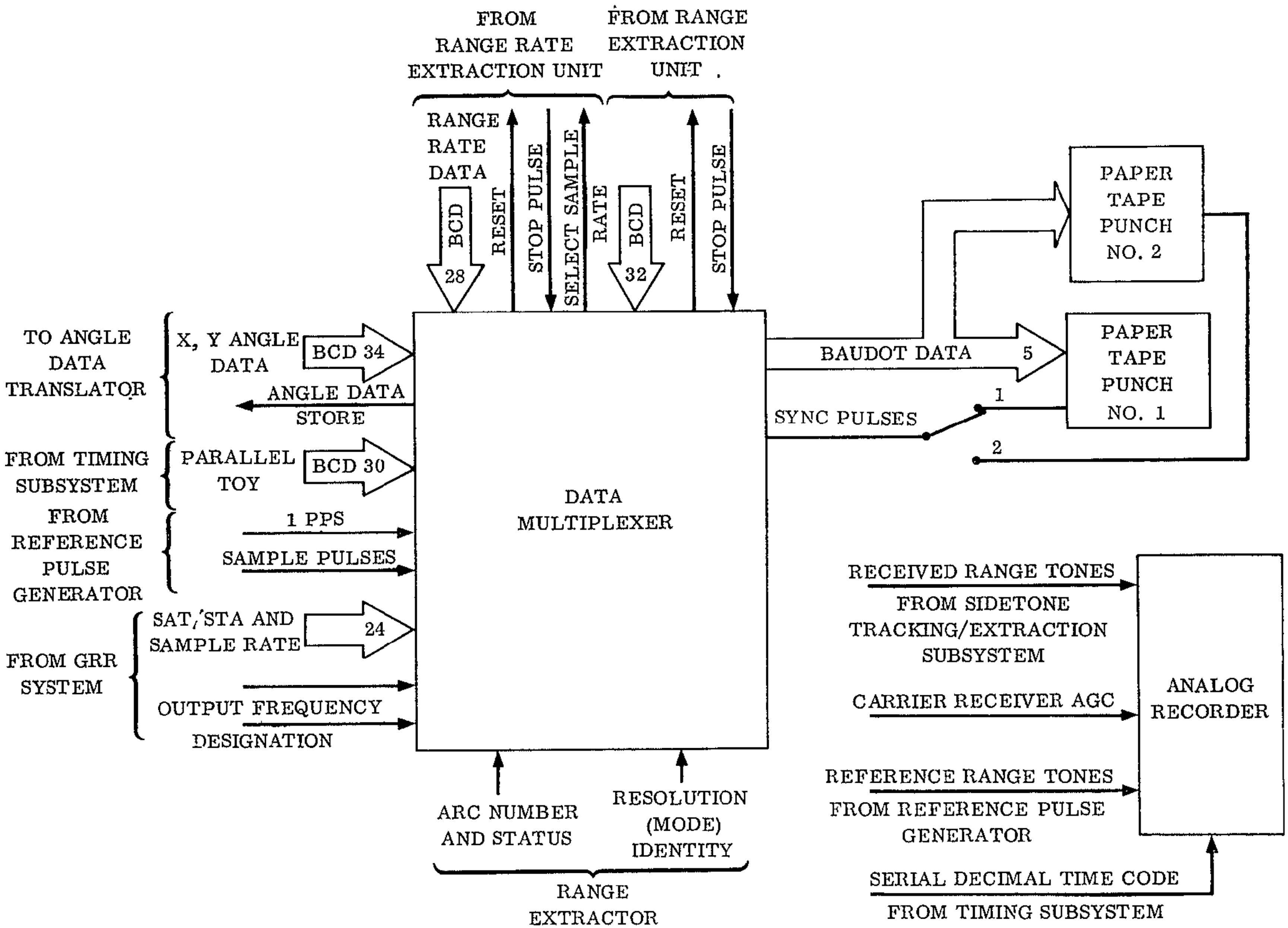

Figure 3-114. Recording Unit Signal Flow

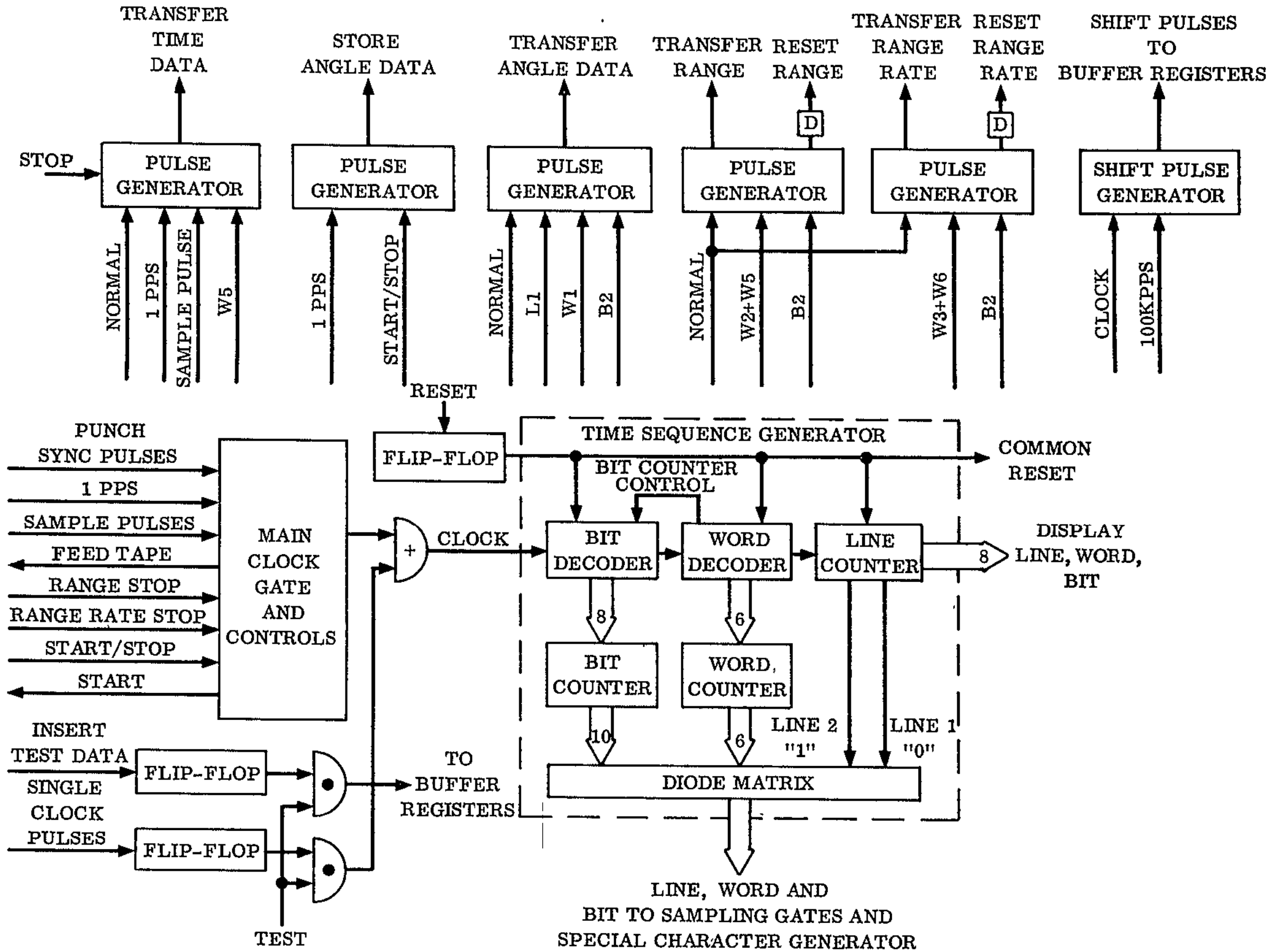

Figure 3-115. Data Multiplexer Time Sequence and Pulse Generators Functional Block Diagram

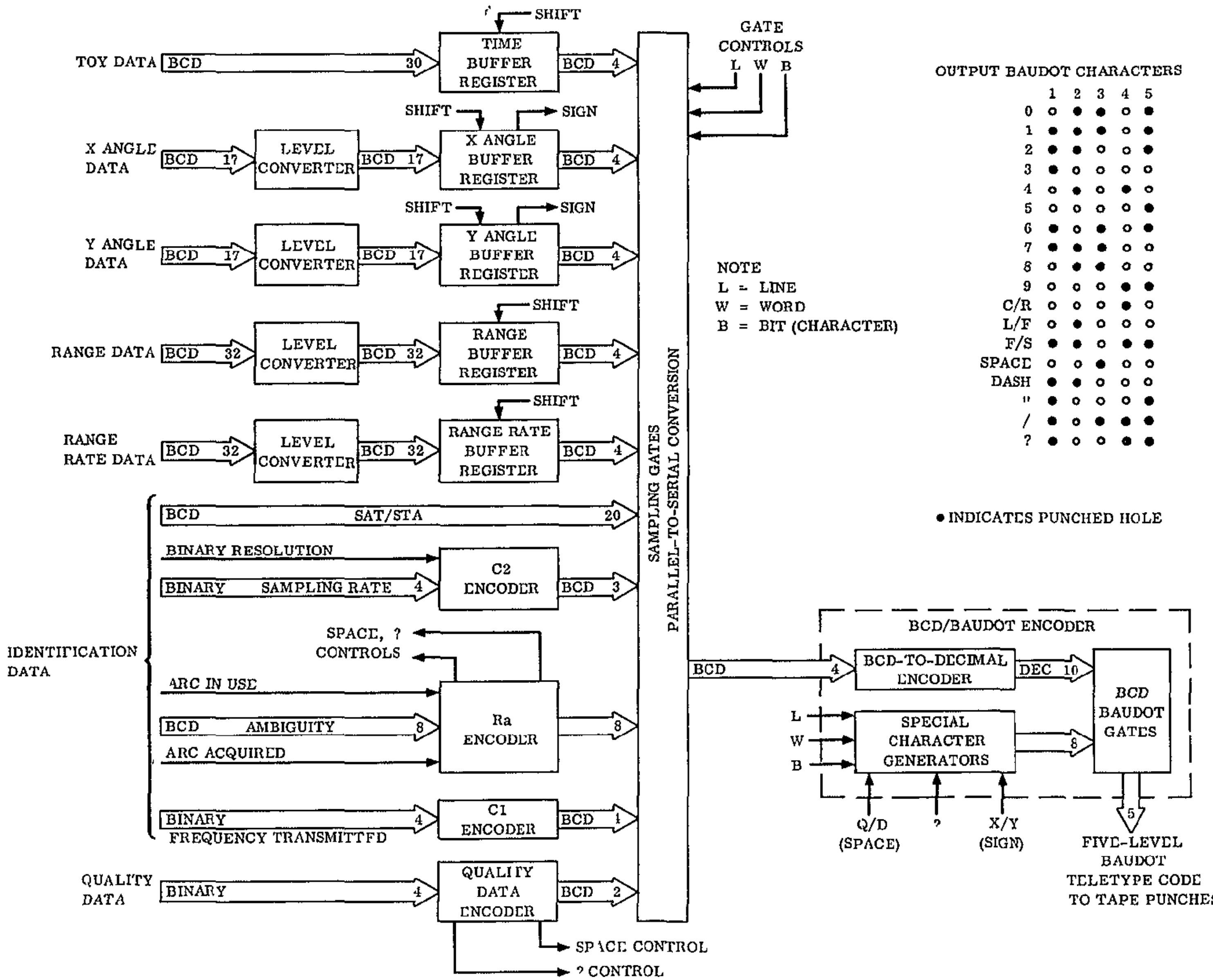

OUTPUT BAUDOT CHARACTERS

	1	2	3	4	5
0	o	●	●	o	●
1	●	●	●	o	●
2	●	●	o	o	●
3	●	o	o	o	o
4	o	●	o	●	o
5	o	o	o	o	●
6	●	o	●	o	●
7	●	●	●	o	o
8	o	●	●	o	o
9	o	o	o	●	●
C/R	o	o	o	●	o
L/F	o	●	o	o	o
F/S	●	●	o	●	●
SPACE	o	o	●	o	o
DASH	●	●	o	o	o
"	●	o	o	o	●
/	●	o	●	●	●
?	●	o	o	●	●

● INDICATES PUNCHED HOLE

Figure 3-116. Data Multiplexer Simplified Block Diagram

	Item	Source	Size	Characteristic
e.	ARC Status	ARC Decoder	2 bits	Binary
f.	Range Data	Range Time Interval	32 bits	BCD
g.	Range Rate Data	Range Rate Time Interval	28 bits	BCD
h.	Resolution ID	Range Extractor	1 bit	Binary
i.	Sat/Sta ID	Control Panel	20 bits	BCD
j.	Sample Rate ID	Control Panel	4 bits	Binary

This input data will be stored as required and converted from binary or BCD to the required Baudot teletype code. The output data will be recorded by the existing BRPE-9 Teletype Tape Perforators in a format as shown in Figure 3-117. This format consists of two lines of 52 characters each containing four samples of range and range rate information time-tagged by a days, hours, minutes and seconds time word contained in the first line. The time word displayed is the time of the first range and range rate word contained in the first line; subsequent samples are spaced from this time by the sample intervals of the selected sample rate. Thus, at four samples per second, a complete data format will be recorded once per second. At six samples per minute, 40 seconds are required to record a complete format.

Certain system data will be encoded to provide maximum information transfer while utilizing minimum recording time. The encoding charts for these characters, the C1, C2 and Q/D (Quality Data) are shown in Tables 3-9, 3-10, and 3-11.

Table 3-9. C1 Character Encoding

S-Band			VHF	BCD				Decimal
A	B	C		8	4	2	1	
1				0	0	0	0	0
	1			0	0	0	1	1
		1		0	0	1	0	2
			1	0	0	1	1	3

Note:: S-Band Frequency (A) = that which gives the 3.2 MHz subcarrier
S-Band Frequency (B) = that which gives the 2.4 MHz subcarrier
S-Band Frequency (C) = that which gives the 1.4 MHz subcarrier

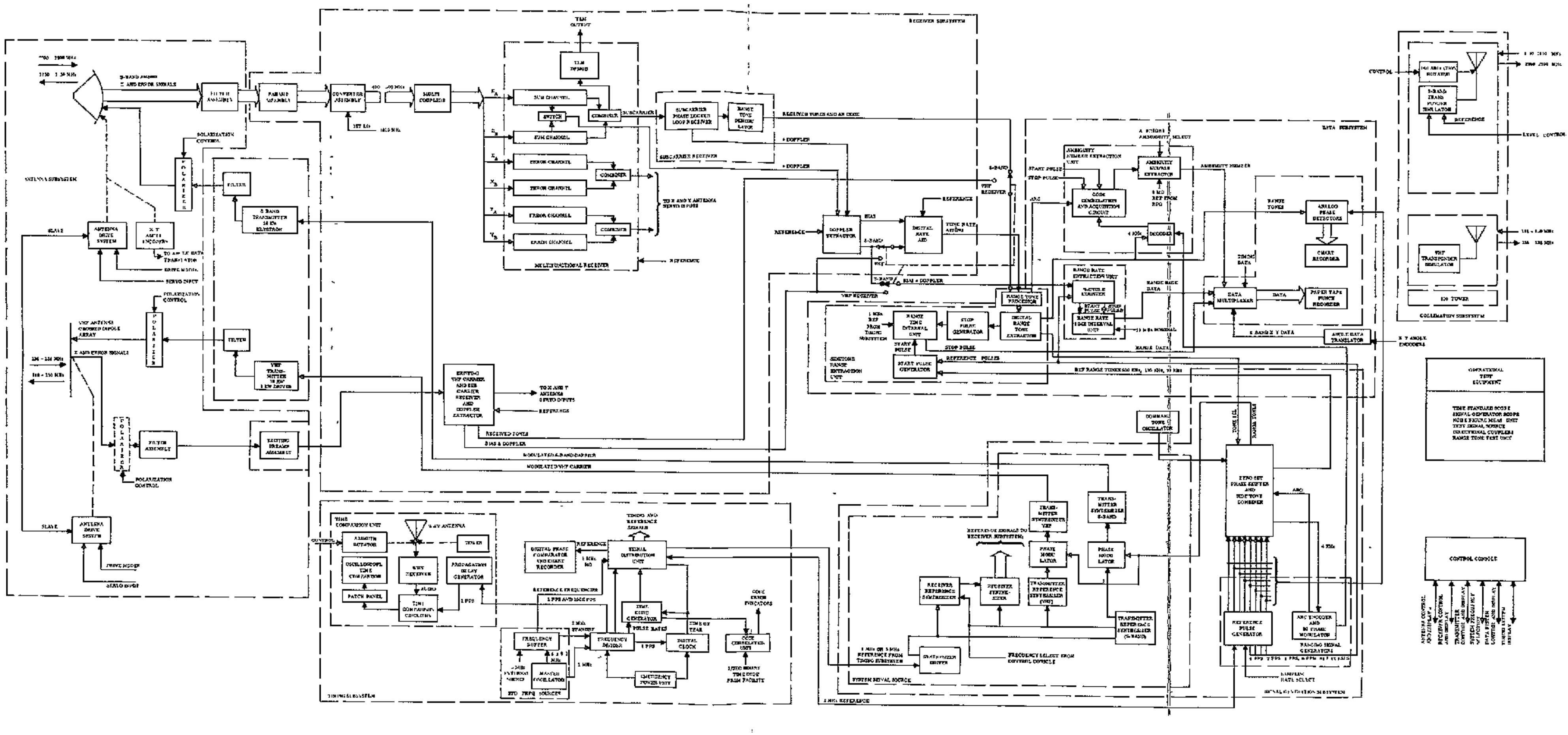

Figure 2-1. Functional System Block Diagram

FOLDOUT FRAME 1

FOLDOUT FRAME 2

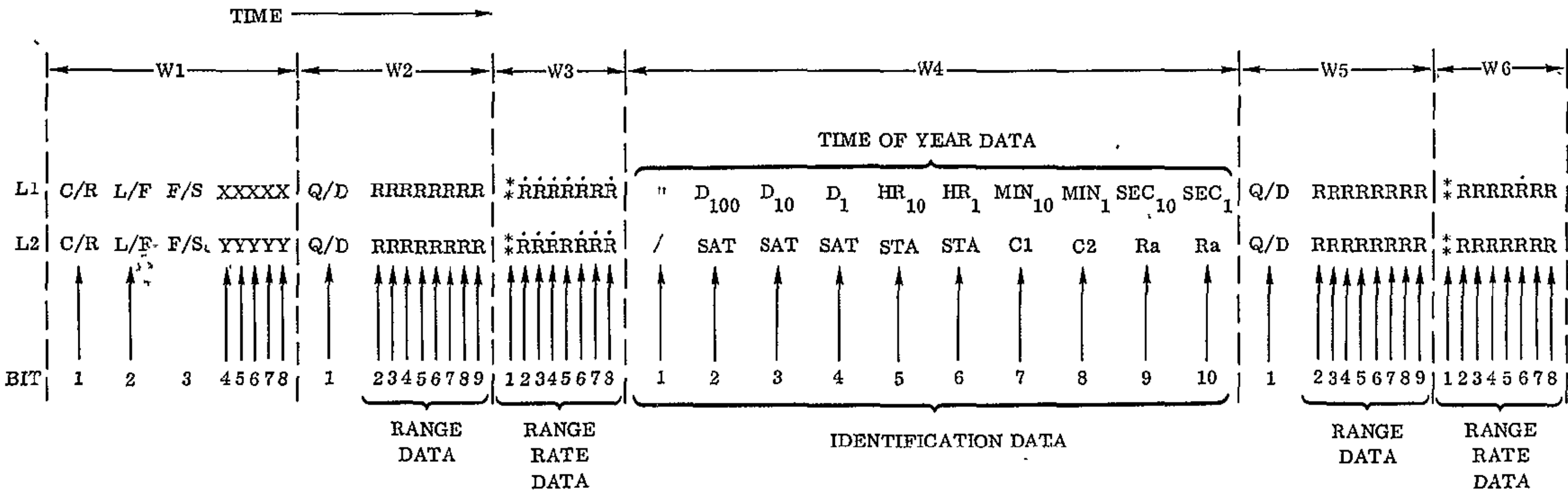

C/R	CARRIAGE RETURN
L/F	LINE FEED
F/S	FIGURE SHIFT
X	ANTENNA POSITION (SIGN AND FOUR DECIMAL
Q/D	QUALITY DATA (SPACE INDICATES ALL LOOPS LOCKED AND RANGE TONES ON)
$\dot{R}$	RANGE RATE (00000000-99999999)
SEC	SECONDS (00-59)
MIN	MINUTES (00-59)
R	RANGE (00000000 - 99999999)
HR	HOURS (00-23)
D	DAYS (000-365)
Y	ANTENNA POSITION (SIGN AND FOUR DECIMAL DIGITS)
SAT	SATELLITE IDENTIFICATION (000-999)
STA	STATION IDENTIFICATION (00-99)
C1	SPACE CRAFT FREQUENCY
C2	SAMPLE RATE (0-4) AND RESOLUTION
Ra	RANGE AMBIGUITY * (00-63)

NOTE: DATA IS TO BE PUNCHED IN STANDARD BAUDOT 5-LEVEL CODE

THERE ARE 52 CHARACTERS IN EACH LINE, MAKING A TOTAL OF 104 CHARACTERS TO BE TRANSMITTED SERIALLY

*SPACE = ARC NOT IN USE, ? = ARC NOT ACQUIRED,
** 0 = SAMPLE RATE AT 6/MIN, SPACE = SAMPLE RATE AT 4 2 OR 1/SEC

Figure 3-117. Output Data Format

Table 3-10. C2 Character Encoding

Resolution		Data Rate				BCD				Decimal
20 KHz	100 KHz or 500 KHz	1/sec	2/sec	4/sec	6/min	8	4	2	1	
1		1				0	0	0	0	0
1			1			0	0	0	1	1
1				1		0	0	1	0	2
1					1	0	0	1	1	3
	1	1				0	1	0	0	4
	1		1			0	1	0	1	5
	1			1		0	1	1	0	6
	1				1	0	1	1	1	7

Table 3-11. Q/D Character Encoding

Failure	BCD				Decimal
	8	4	2	1	
Receiver Carrier Loop	0	0	0	0	0
Receiver Subcarrier Loop	0	0	0	1	1
Antenna Not Auto Track	0	0	1	0	2
Digital Range Tone Extractor	0	0	1	1	3

The Data Multiplexer will be physically located in a vertical pull-out drawer adjacent to the Digital Range Tone Extractor and other digital units. The unit will be constructed principally of integrated circuit logic cards.

A control panel located adjacent to the digital unit will contain the principal controls and indicators required. Figure 3-118 shows the proposed layout. The control panel will permit the operator to select the system sample rate and the mode of operation of the multiplexer. In the test mode a selectable pattern of numbers will be inserted in the buffer registers so that proper operation of the unit may be checked. Thumbwheel switches are provided for selection of the Station and Satellite Identification number. Visual displays will be provided for the status of Quality Data and Spacecraft Frequency.

3.7.3.2 PAPER TAPE PUNCH. The paper tape punch receives Baudot-coded teletype characters on five parallel lines from the Data Multiplexer and records these at the required rate on standard five-level paper tape. Two paper tape punches will be retained. One punch will be operated at a time. Punch No. 1 or Punch No. 2 can be selected on the Master Control Panel.

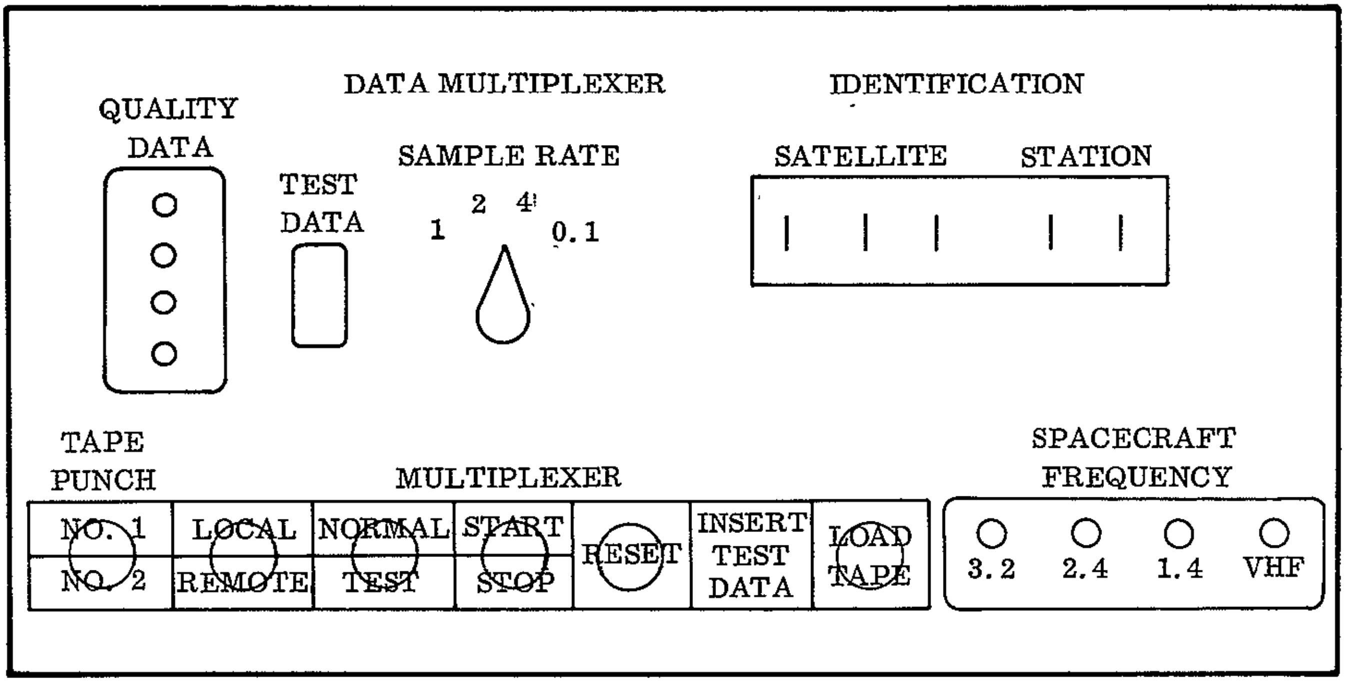

Figure 3-118. Data Multiplexer Control Panel

3.7.3.3 ANALOG CHART RECORDER. The existing Sanborn Recorder contained in Cabinet 1 will be retained as the Analog Chart Recorder. New analog phase detectors will be fabricated and installed to output the required analog phase information to seven channels of the recorder. The eighth channel will record receiver AGC. The marker channel will record the NASA serial decimal time code for time identification of data.

3.7.3.4 ANGLE DATA UNIT. The Angle Data Unit (Figure 3-119) provides a measurement of antenna angle position which is recorded by the data subsystem. The angle data unit consists of two S-Band antenna angle encoders and an S-Band translator unit. Two remote indicators on the console provide a visual indication of antenna position.

All necessary equipment exists in the present installation and will be retained and relocated as required. The angle translator is a Datex TR-111 with associated power supply. Data output from this unit is in the form of X-position and Y-position words, each 17 bits in length. Each word is comprised of four 4-bit BCD digits and one sign bit. These data are routed to the Data Multiplexer and recorded on the paper tape punch.

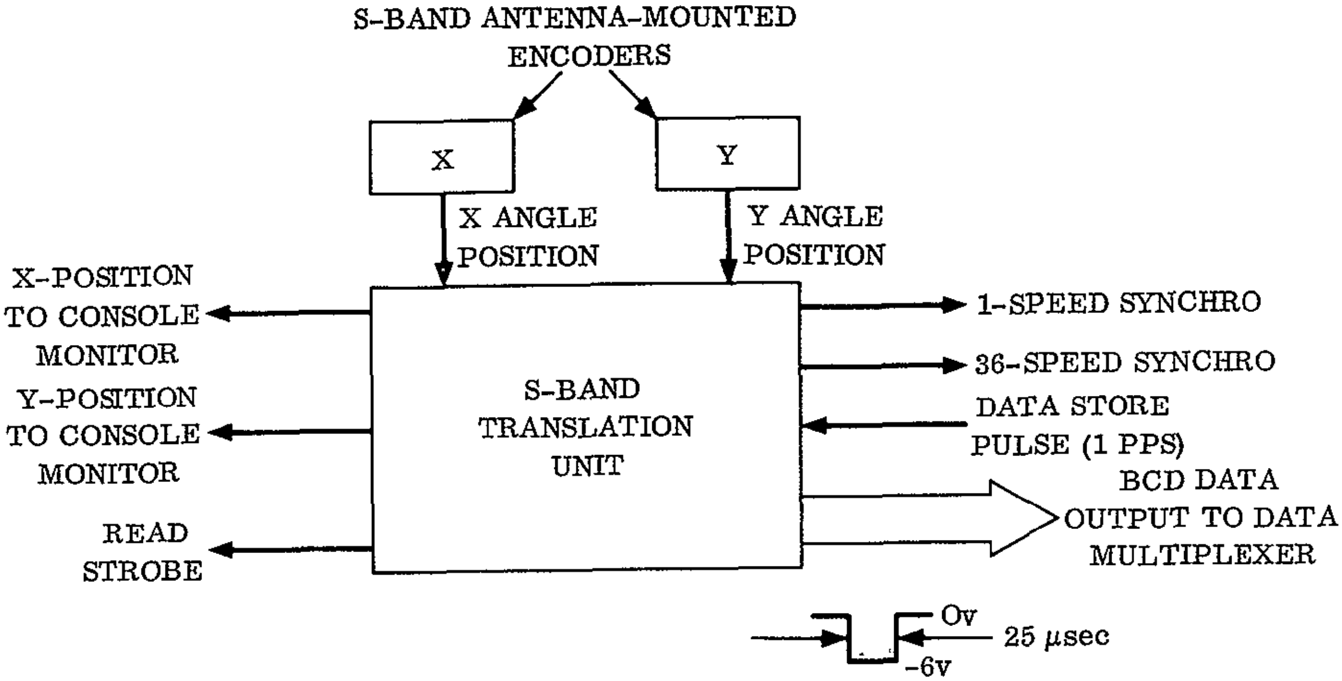

Figure 3-119. Angle Data Unit Functional Block Diagram

3.7.4 Applicability

The Data Subsystem as described in the preceding paragraphs will be supplied at the Rosman, Carnarvon, and Tananarive sites.

3.8 COLLIMATION SUBSYSTEM

The Collimation Subsystem is used for boresighting and checking both the S-Band and the VHF antennas, for zero-setting the Ranging System, and for performing system tests including threshold measurements. It consists of tower-mounted VHF and S-Band antennas, VHF and S-Band transponder simulators housed in a cabinet at the base of the tower, remote controls and indicators located in the instrumentation building, and all necessary interconnection cabling. The tower, and present VHF collimation system equipment, will be retained in its entirety. The original VHF Pole Beacon is not considered part of the collimation tower installation and will not be retained. New cabling will connect the tower elements of the subsystem with the collimation remote control panel in the instrumentation building. The S-Band portions of the tower will be completely modified to incorporate a new antenna with polarization control and a new transponder simulator. The new S-Band transponder simulator will receive on frequencies between 1750 and 1850 MHz and transmit on frequencies between 2200 and 2300 MHz.

3.8.1 Boresight Antenna

The new S-Band antenna provided will be a 3-foot diameter parabolic reflector with a suitable feed selected to provide optimum linear polarization with a minimum of cross-polarization component. Gain of the assembly will be a nominal 20 db. The first side lobe suppression will be typically 17 db. Cross-polarization of this antenna configuration is typically -20 db. The entire assembly is fabricated as an integral structure and is bolted to the face of the polarization positioner. The antenna feed output line is located at the center behind the vertex and is fed through the center tube of the positioner where it is attached to a flexible RG 9/U cable, allowing the antenna to rotate between its plus and minus 90-degree positions. The output of the RG 9/U cable is connected to the existing semi-rigid RG-232/U transmission line which carries signals to the collimation enclosure at the base of the tower.

3.8.2 Antenna Rotator

The selected polarization positioner will be remotely controlled. Its controls and indicators will be installed in the collimation control cabinet located in the instrumentation building. The polarization positioner is capable of rotating the parabolic antenna at better than 1 rpm in a 30-mph wind. Positioner rotation is continuous and reversible. Polarization position is limited to ±90 degrees by precision limit switches. The drive shaft is hollow to permit passage of RF plumbing.

3.8.3 Transponder Simulators

Two transponder simulators are required: A GRARR S-Band simulator and a VHF simulator. S-Band simulators will be supplied to the Fairbanks, Tananarive, Rosman, and Canarvon sites. Parts from the existing S-Band Pole Beacons will be used to fabricate these simulators. It is assumed that the existing VHF simulator is adequate and will be retained without modification.

The S-Band simulator will furnish the necessary capability for boresighting the S-Band antenna, for zero-setting the S-Band equipment, and for performing threshold measurements and system tests. Selection of fixed attenuators may be required at each site due to the different distances between the collimation tower, the antennas, and the instrumentation building.

A functional block diagram of the proposed S-Band Simulator is shown in Figure 3-120. The S-Band simulator will use solid state circuitry and will be capable of operation by remote control from the instrumentation building. The simulator will be rack-mounted in the collimation tower enclosure. At sites where a rack-mounted version of the VHF simulator is available, it will be integrated into the equipment rack.

3.8.3.1 GRARR S-BAND SIMULATOR. The GRARR S-Band Simulator will receive S-Band carrier frequencies within the band between 1750 and 1850 MHz which are modu-

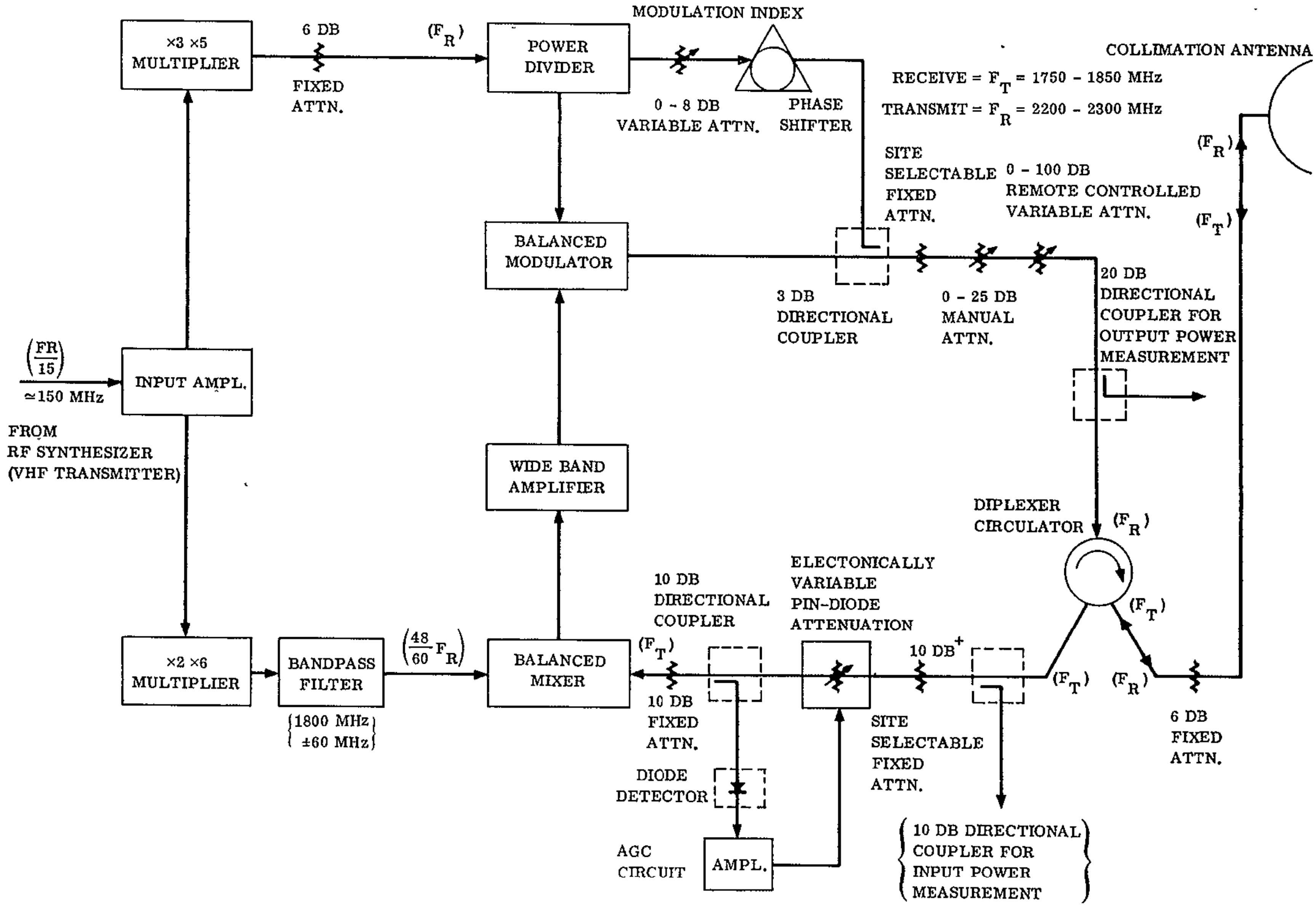

Figure 3-120. S-Band Transponder Simulator, Functional Diagram

lated with range sidetones. Through mixing of the transponder input signal with a local oscillator signal, an IF (subcarrier) of 1.4, 2.4, or 3.2 MHz is derived. These IF contain all range tones originally impressed on the received carrier. The IF signals are amplified and subsequently mixed with a local oscillator in a balanced modulator. The resultant output is a suppressed carrier flanked by subcarriers equally spaced spectrally above and below the desired carrier. Additionally, the range tones are present and complemented on the subcarriers. As the output signal passes through a directional coupler, a carrier of the same frequency as the suppressed carrier is injected. The phase amplitude of the injected carrier reinforces the suppressed carrier to produce an output carrier with a relative level dependent upon the desired modulation index. The output transmitter frequency will be between 2200 and 2300 MHz.

To achieve design simplicity, the S-Band transponder simulator will not use a local oscillator to develop mixer and carrier frequencies. The required frequency will be supplied to the transponder via coaxial cable from a frequency synthesizer located in the instrumentation building. The VHF transmitter reference synthesizer will be used to produce this signal of $f_R/15$ (f_R ranges from 2200 to 2300 MHz). This is possible because the VHF equipment will not be operated while the S-Band collimation system is in use. This will permit the operator in the instrumentation building to exercise complete control of both the received and transmitted frequencies of the S-Band transponder simulator in the collimation enclosure.

Transponder output level is calibrated in 1-db increments, over a 100-db range, by a continuously variable attenuator remotely controlled from the collimation control rack in the instrumentation building.

Typically, the S-Band transponder will have a maximum carrier output power level of -8 dbm at the output of the 3-db coupler shown in Figure 3-120. This will ensure sufficient dynamic range in the remote-controlled output attenuator to test the system.

A signal level analysis summary for the S-Band collimation system is given in Table 3-12.

The power level of the received signal at the input of the balanced mixer will be typically maintained at 0 dbm. This will be accomplished by a series of fixed attenuators and an electronically controlled pin-diode attenuator as shown in Figure 3-120. The pin-diode attenuator will be controlled by an automatic gain control circuit using a diode detector. The bias of this circuit will be adjustable so that the AGC circuit can be adjusted to each site. The dynamic phase delay contributed by the variable attenuator will be typically less than 1 nanosec. A typical thermal noise figure for this type attenuator is 0.5 db at the received frequencies between 1750 and 1850 MHz. The harmonic distortion products caused by the pin-diode attenuator will be at least 40 db below the fundamental output.

The main function of the pin-diode and the AGC circuit is to maintain a given power level at the input to the mixer so that the power ratio of the received signal to the local mixer frequency will remain constant even though the S-Band transmitter power is varied between 200 w and 10 kw.

3.8.3.2 COMPONENTS. Basically, the transponder will be packaged in four modules installed in a rack-mounted drawer with slides. Each module will be electrically shielded by a metal enclosure. Circuit modules will be as follows:

Table 3-12. S-Band Collimation Signal Level

S-Band Transponder Simulator to Receiver				
	Rosman	Tananarive	Carnarvon	Fairbanks
Transponder Carrier Power Level at 3 db Directional Coupler Output	-8 dbm	-8 dbm	-8 dbm	-8 dbm
Site Selectable Attenuator	15 db	15 db	15 db	15 db
Manual Attenuator	25 db	25 db	25 db	25 db
Remote Controlled Attenuator	100 db	100 db	100 db	100 db
Coaxial Losses	2 db	2 db	2 db	2 db
Input/Output Pad	6 db	6 db	6 db	6 db
Miscellaneous Losses	2.5 db	2.5 db	2.5 db	2.5 db
Collimation Antenna Gain	24 db*	24 db*	24 db*	26.5 db**
Space Attenuation (1)	83.6 db	83.4 db	85.2 db	97.7 db
Receiver Antenna Gain	36.5 db	36.5 db	36.5 db	42 db
Minimum Power at Receiver	-181.6 dbm	-181.4 dbm	-183.2 dbm	-187.7 dbm
Receiver Sensitivity	-159 dbm	-159 dbm	-159 dbm	-159 dbm
Threshold Test Margin	22.6 db	22.4 db	24.2 db	28.7 db
*3-ft parabolic **4-ft parabolic	(1) Taken at 2250 MHz			

Table 3-12. S-Band Collimation Signal Level (Continued)

Transmitter to S-Band Transponder Simulator				
	Rosman	Tananarive	Carnarvon	Fairbanks
Maximum Transmitter Power	+70 dbm	+70 dbm	+70 dbm	+70 dbm
Minimum Transmitter Power	+53 dbm	+53 dbm	+53 dbm	+53 dbm
Transmitter Antenna Gain	35.5 db	35.5 db	35.5 db	41.5 db
Space Attenuation (2)	81.8 db	81.6 db	83.4 db	95.4 db
Collimation Antenna Gain	22 db*	22 db*	22 db*	24.8 db**
Miscellaneous Losses	1.5 db	1.5 db	1.5 db	1.5 db
Input/Output Pad	6 db	6 db	6 db	6 db
Coaxial Losses	2 db	2 db	2 db	2 db
Site Selectable Attenuation	10 db	10 db	10 db	10 db
Maximum Input to Transponder (3)	26.2 dbm	26.4 dbm	24.6 dbm	21.4 dbm
Minimum Input to Transponder (3)	9.2 dbm	9.4 dbm	7.6 dbm	4.4 dbm

* 3-ft parabolic
** 4-ft parabolic
(2) Taken at 1800 MHz
(3) At input to pin-diode attenuator

a. Amplifier Module: This assembly will consist, essentially, of three amplifiers. The input amplifier will be tuned to a reference frequency of 150 MHz (±4 MHz) and provide adjustable gain with a typical maximum gain of 15 db. The input amplifier will drive two isolated output amplifiers, each providing 15-db gain. One output amplifier will drive the ×12 multiplier; the other will drive the ×15 multiplier.

b. ×12 Multiplier: The ×12 multiplier will consist of an input amplifier, a transistor doubler, a power amplifier, and a ×6 step recovery diode multiplier and cavity filter. The output of the ×12 multiplier will function as the local oscillator signal to the balanced mixer.

c. ×15 Multiplier: The ×15 multiplier will consist of an input amplifier, a solid state tripler, a power amplifier, and a ×5 step recovery diode multiplier and cavity filter. The output of the ×15 multiplier will function as the S-Band input to the balanced modulator as well as the transmitted carrier. The multiplying stages of the ×12 and ×15 multipliers are staggered such that neither unit generates identical frequencies thereby assuring isolation between the two multipliers. By using an input tripler in the ×15 module and an input doubler in the ×12 module, it is possible to keep the multiplier frequencies at least 150 MHz apart.

d. Wideband Amplifier: The wideband amplifier will amplify the subcarrier frequencies (1.4, 2.4 or 3.2 MHz) from the mixer. Minimum amplifier bandwidth will be 10 KHz to 100 MHz. The large bandwidth is required to ensure that the signal differential phase delay through the transponder will be less than ±10 nanosec and the total phase delay will be less than 50 nanosec.

The required gain and bandwidth will be achieved by cascading parallel amplifiers. Bandwidths throughout the transponder multiplier will be sufficient to permit operation over the transmitted frequency range of 2200 to 2300 MHz.

The transmitter will be capable of simulating a modulation index of between 0.5 and 1.5 radians peak by adjustment of a variable attenuator between the power divider and the 3-db directional coupler.

3.8.4 Auxiliary and Control Equipment

Remote control of the S-Band transponder simulator will be accomplished via cables from the collimation control cabinet in the instrumentation building. Relays and variable attenuator controls will be mounted within the S-Band transponder simulator located in the equipment cabinet in the collimation enclosure (Figure 3-121). The VHF transponder simulator and S-Band boresight antenna controls will be mounted in the collimation control cabinet located in the instrumentation building.

3.8.4.1 POWER CONTROL. Remote power control on, off, and standby functions will be provided for the S-Band transponder simulator. The remote power control will be located at the collimation control cabinet in the instrumentation building. The standby function will be provided only if required for the operation of equipment heater blankets or other similar accessories.

3.8.4.2 VARIABLE ATTENUATOR CONTROL. Two variable attenuators with ranges from 0 - 100 db and 0 - 25 db will be provided for adjusting the output power level of the S-Band transponder simulator. These attenuators will be located within the transponder simulator. The 0 - 25 db attenuator will be manually controlled and provided with a position lock. The 0 - 100 db variable attenuator will be driven by a servo repeater (Figure 3.8.2) remotely controlled from the collimation control cabinet in the instrument building. The remote control system will have a vernier of 1-db increments over the full range.

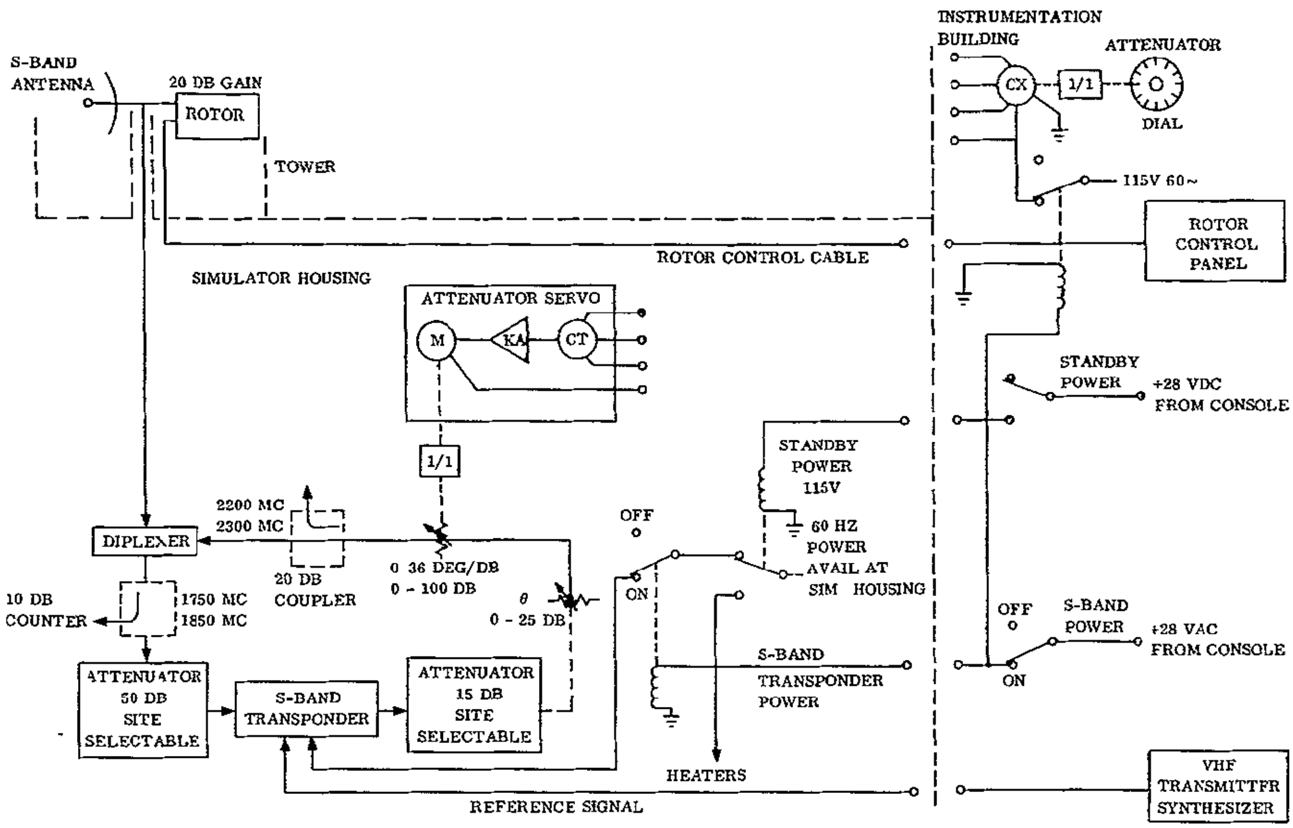

Figure 3-121. S-Band Transponder Simulator System Diagram

3.8.4.3 DIRECTIONAL COUPLERS. A 10-db directional coupler will be provided so that power measurements can be made of the ranging signal received at the collimation tower enclosures.

A 20-db directional coupler will be provided in the output circuit of the collimation transponder to allow power measurement.

3.8.5 Applicability

The Collimation Subsystem as described in this section applies to the sites at Rosman, N.C. Carnarvon, Australia, and Tananarive, Republic of Malagasy. The site at Fairbanks, Alaska will not receive a new boresite antenna or new antenna rotator.

3.9 CONTROL CONSOLE

The Control Console provided will serve as the central control and monitor station for the system during a tracking mission. To provide the operator with adequate controls and displays, the Control Console will require six cabinet sections in the main console and two additional standard racks located directly behind the operator as shown in Figure 3-1.

The Control Console is functionally divided into four sections: VHF antenna control, S-Band antenna control, receiver and system signal source control, and system monitor and control. The VHF antenna control panel from the existing installation will be installed in one of the console sections. The existing S-Band antenna controls will occupy two console sections.

The receiver and system signal source controls require two sections. The remaining section will be used for system monitor and control functions.

The console selected for the Rosman, Carnarvon, and Tananarive sites is a six-bay low silhouette model manufactured by the Emcor Division of Borg-Warner. Simultaneous control access and indicator surveillance by two operators is facilitated by a console arrangement of the two main bays flanked on both sides by two-bay wings joined to the main bays at 45 degrees. Each bay consists of an upper control panel section sloped 45 degrees for convenience of operation, a writing shelf, and a lower vertical panel section.

Two standard cabinets, identical in appearance to the existing cabinets, will be installed behind the Control Console. The operator will normally sit between these cabinets and the console. The two cabinets will contain the collimation control equipment and the servo amplifiers and hydraulic controls for both the VHF and S-Band antennas.

New controls will be provided for the console in three categories: system control and monitor, system signal source controls, and receiver controls.

3.9.1 System Control and Monitor

The system control and monitor portion of the console will contain remote controls and indicators for the Transmitter Subsystem, the Timing Subsystem, the Signal Generation Subsystem, and the Data Subsystem. A summary follows.

3.9.1.1 TRANSMITTER SUBSYSTEM. Controls and indicators provided will be as follows:

a. S-Band Transmitter:

TRANSMITTER ON/OFF switch
CONSOLE CONTROL/LOCAL CONTROL indicator
S-BAND TRANSMITTER READY indicator
S-BAND TRANSMITTER ALARM indicator

b. VHF Transmitter:

TRANSMITTER OFF/ON switch
TRANSMITTER ALARM indicator
CONSOLE CONTROL/LOCAL CONTROL indicator
1 KW READY indicator
10 KW READY indicator

3.9.1.2 TIMING SUBSYSTEM. One GMT display will be provided.

3.9.1.3 SIGNAL GENERATION SUBSYSTEM. Controls and indicators for the ARC Encoder will be provided as follows:

AMBIGUITY NUMBER switch	Variable from 0 to 63: A local/remote interlock provides for either local or console control of the ambiguity number.
INTEGRATE TIME-SELECT switch	Settings for 1 sec or 10 sec.
CORRELATION/NO CORRELATION/ CORRELATION IN PROCESS indicators	Indications of correlation status.
CONSOLE CONTROL/LOCAL CONTROL indicator	

3.9.1.4 DATA SUBSYSTEM. Controls and indicators will be provided for four assemblies:

a. Range Tone Processor

RESOLUTION SELECT switch	For 500 KHz, 100 KHz, or 20 KHz.
BANDWIDTH switch	For 0.1 Hz, 1 Hz, or open bandwidths.
PHASE LOCK indicator	Denoting major range tone in or out of lock.

b. Digital Range Tone Extractor (DRTE):

AMBIGUITY SELECT switch	For selection of 160 Hz, 32 Hz, 8 Hz, or the hybrid system.
OPERATING MODE SELECT switch	For auto, semi-auto, or manual.
AMBIGUITY CHECK switch	Initiate ambiguity check.
INTEGRATE TIME SELECT switch	For 0.0625, 1, or 10 sec.
DRTE RESET switch	For operator-initiated reset.
DIGITAL PHASE MATCH ALARM indicator	
DATA READY indicator	

c. Data Multiplexer:

SAMPLE RATE SELECT switch	For 4, 2, 1, or 0.1 sec.
MULTIPLEX ON/OFF switch	For operator control from console.
MULTIPLEXER RESET switch	For operator reset from console.

d. Paper Tape Punch:

TAPE #1 ON/TAPE #2 ON	TAPE punch status indication.
TAPE #1 LOW/TAPE #2 LOW	Low TAPE indication.

3.9.1.5 ADDITIONAL CONTROLS AND INDICATORS. In addition to the foregoing, the system control and monitor functions will include:

a. A polarization select switch for the S-Band antenna.

b. An indicator which illuminates when the system noise test is in process.

c. Switches and indicators denoting local or remote control status for the various subsystem of the station.

d. A headset jack for intercom functions.

3.9.2 System Signal Source Functions

A discussion of the remote controls and indicators for the System Signal Source accompanies the unit descriptions provided in paragraph 3.3.5.

3.9.3 Receiver Control Functions

A discussion of the remote controls and indicators for the Receiver Subsystem accompanies the unit descriptions provided in paragraphs 3.6.3 and 3.6.4.

3.10 OPERATIONAL TEST EQUIPMENT

The operational test equipment will consist of test instrumentation required to perform normal routine day-to-day checks on system operation and calibration. Subsequent paragraphs describe the test equipment units and their integration within the overall ground tracking system.

3.10.1 Timing Subsystem Oscilloscope

The existing oscilloscope for time standard determination will be utilized at the Rosman, Carnarvon, and Tananarive sites. The oscilloscope provides the means for checking the internal Timing Subsystem against WWV broadcasts and making the appropriate corrections. It is assumed that the existing oscilloscopes are Tektronix RM561 or Hewlett-Packard 122A types and can be used without modification. These units are adequate for the intended purpose.

3.10.2 Signal Generation Subsystem Oscilloscope

The Signal Generation Subsystem oscilloscope provides the means for measuring and setting the phase and modulation indices of the range tones and serves as a general-purpose test and calibration unit. A Tektronix Model 585A oscilloscope with a Type 82 Dual-Trace Plug-in will be provided to perform the aforementioned functions. The oscilloscopes and associated plug-ins provided will be installed in permanent racks at Rosman, Carnarvon, and Tananarive. The Fairbanks site will utilize the existing oscilloscope and plug-in for the intended function. Paint matching of panels to cabinets will be provided for the new equipments.

The RM 585A oscilloscope is a rack-mounted model which will fit a standard 19-inch rack. The principle electrical characteristics include a dc to 85 MHz bandwidth, delayed time base, 10 mv/cm verticle sensitivity with a Type 82 plug-in, and dc coupling. Bandwidth is limited to 80 MHz at maximum sensitivity.

The Type 82 plug-in has a dual-trace capability, each trace channel having a bandwidth of 80 MHz with a maximum sensitivity of 10 mv/cm and a maximum risetime of 4.5 nanosec. This plug-in is designed for operation with the Model 585A oscilloscope without an external adapter assembly.

3.10.3 Noise Figure Measurement Unit

An automatic noise figure measurement unit will be provided. This unit will consist of a test signal power-divider, a noise source, coaxial switches, parametric amplifier couplers, a power supply, and an associated instrumentation panel for monitoring the system noise figure. The noise source (including modulator and power supply), the power divider, the parametric amplifier couplers, and the coaxial switches will be located at the antenna assembly. The remote instrumentation and IF signal switching will be located in the instrumentation building.

Figure 3-122 is a functional block diagram of the S-Band Test Signal System showing the method for injecting noise into the parametric amplifiers. System noise figure measurement will be accomplished independently on each channel by switching the noise source at the amplifier input and by switching each IF input to the noise figure meter. A 6 db isolator will couple the IF signal to the noise figure meter. No coaxial switches are used in the RF input lines to the parametric amplifiers.

The purpose of injecting a noise testing signal is to measure the relative sensitivity of each of the six channels of the Receiving Subsystem so that changes in sensitivity with time may be detected. Additionally, while measuring receiver sensitivity, the effects of antenna position, atmospherics, etc., can be determined.

The overall sensitivity of the Receiving Subsystem is proportional to T_{op}, where, for a single response receiver

$$T_{op} = T_a + T_e$$

with

T_a = antenna temperature

T_e = effective input noise temperature of the receiver

The automatic noise figure monitor to be provided measures total receiving system performance consisting of antenna losses, sky noise temperature, and receiver noise temperature contributions. For T_a, the assumed value is 0.5 db (35° K); sky noise temperature is assumed to be 15°K. Therefore, T_{op} was selected for measurement since the system can be calibrated with this technique. T_{op} lumps the antenna contribution with the RF component and receiver characteristics. This method measures the ability to detect input signals, but does not isolate troubles if they occur.

The sensitivity measurement is made by injecting a known noise level into the front end of the parametric amplifier through a directional coupler and observing the voltage change at the second detector, after sufficient video amplification. The relationships for a linear detector are:

$$T_{op} = \frac{\Delta T V}{2 \Delta V}$$

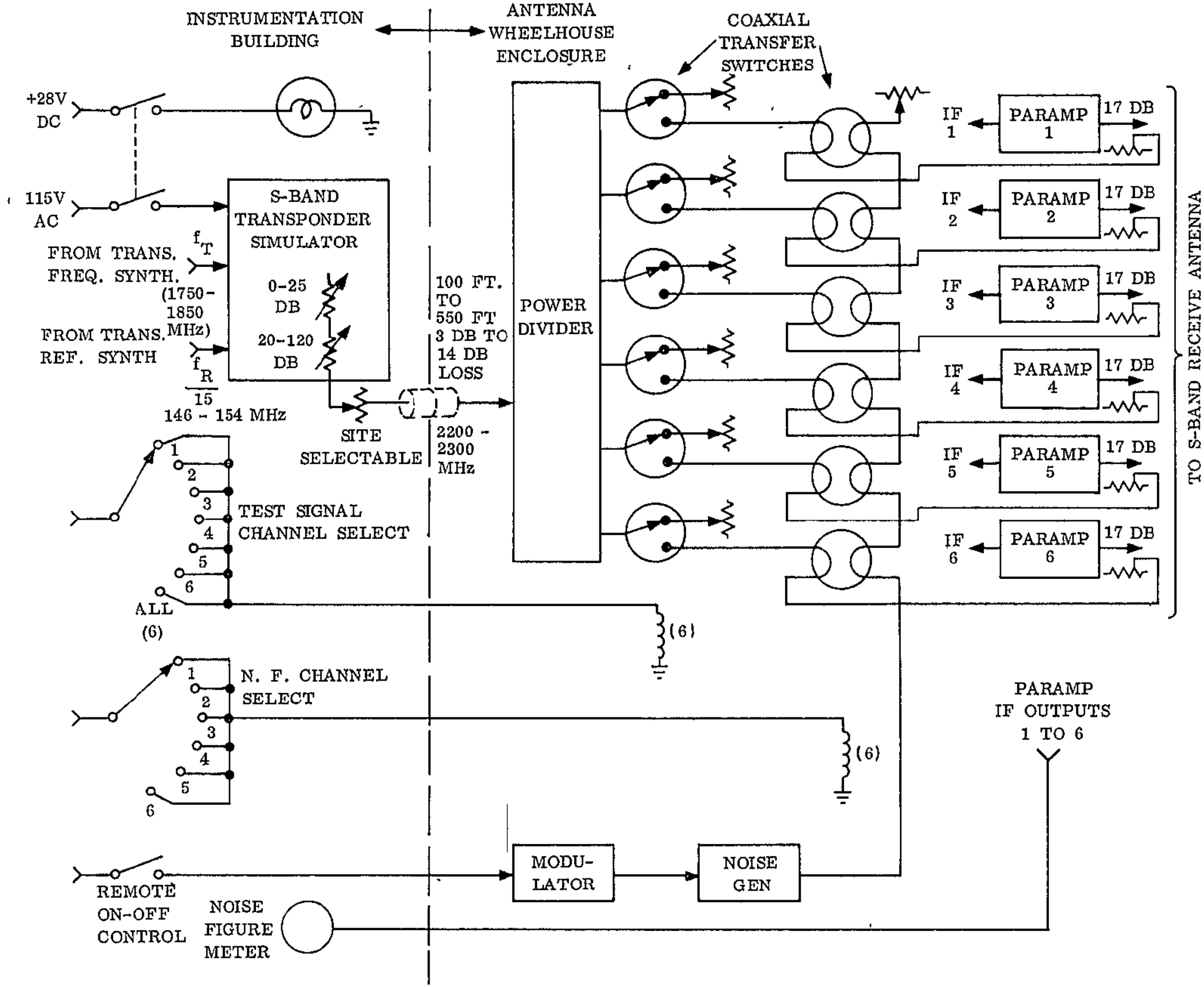

Figure 3-122. S-Band Test Signal System Functional Block Diagram

where

ΔT = injected noise level in °K

V = Voltage level at the linear detector with no injected noise level

ΔV = change in voltage level at the detector for a given ΔT

It can be seen that if ΔT and V are set to precisely known quantities, then a measurement of ΔV will yield T_{op}.

The accuracy of T_{op} will be ±0.2 db (20°K) at 2.45 db. Reduced accuracies at high noise figures are anticipated. If the previously assumed value of T_a is 50° K, the overall system noise figure, including a 170° K parametric amplifier will be 2.45 db (220° K).

If the noise figure equipment is operated during normal operation of the system, an average value of approximately 100° K is added to the system, degrading system sensitivity of one channel only by approximately 0.6 db.

3.10.4 Test Signal System

The test signal system provides a means of measuring system threshold and provides the necessary signal to set up the autotrack receiver AGC circuitry for the S-Band Subsystem. An S-Band transponder simulator will be provided to perform this function. Control of the test signal will be accomplished from a panel located in the instrumentation building. Test signal injection to each parametric amplifier channel separately, or to all channels simultaneously, will be accomplished remotely on the antenna assembly by means of coaxial switches and a power divider. A block diagram of the S-Band test signal system is shown in Figure 3-122.

The S-Band test signal is generated by an S-Band transponder which is essentially identical in design to the S-Band transponder simulator used in the Collimation Subsystem. (Refer to Paragraph 3.11 for a discussion of the transponder simulator and Figure 3-123 which shows a block diagram of the transponder simulator test signal.) Differences in design include a manual attenuator control and separate input and output connections to eliminate a diplexer. The S-Band input signal is derived from the transmitter frequency synthesizer which provides a signal with the required range tones. The output signal of the transponder simulator passes through two calibrated variable attenuators providing 125 db of signal control to the parametric amplifier input. A maximum input signal level of -70 dbm is anticipated due to losses in the power divider, directional coupler, 550 feet of coaxial cable, and variable attenuators.

Signal injection to the parametric amplifiers is accomplished through 17 db couplers which are also used for noise signal injection, as discussed in the foregoing paragraphs. The subcarrier power level will be at -8 dbm corresponding to a modulation index of 1.5.

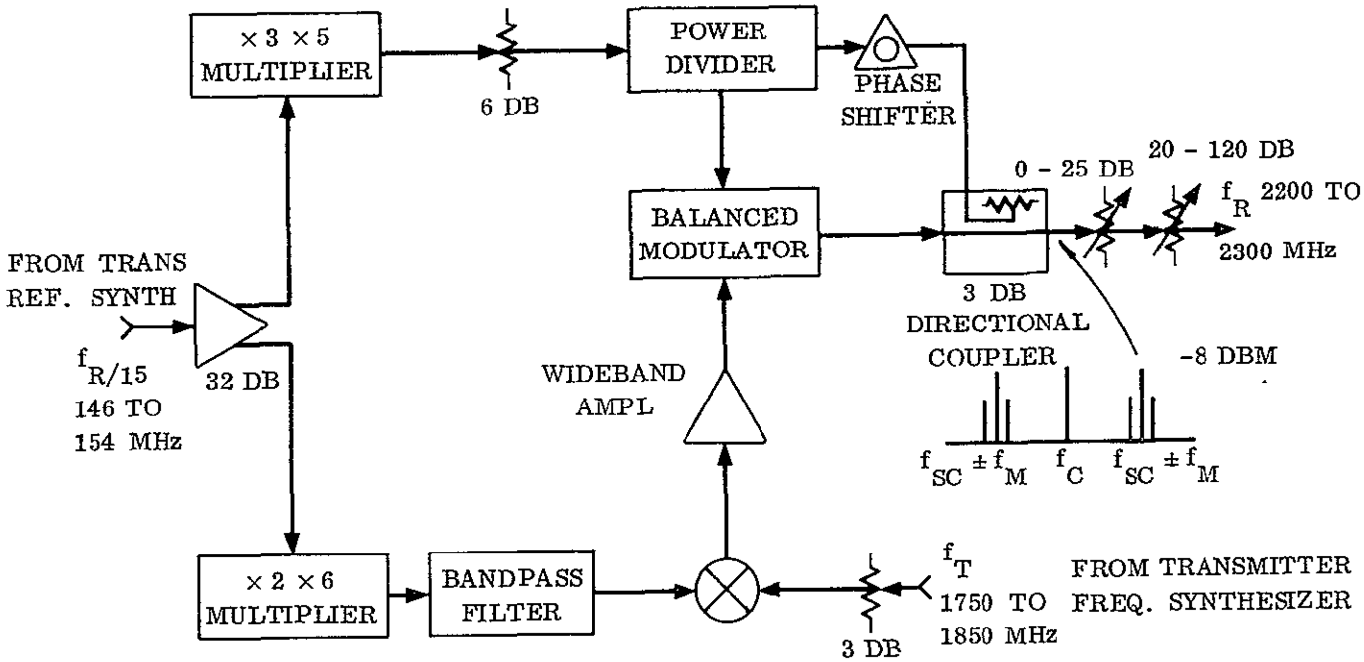

Figure 3-123. S-Band Transponder Simulator Test Signal Block Diagram

3.10.5 Range Tone Test Function

The range tone test function, Figure 3-124, allows testing of the range tone loops independently of the transmitter and receiver. Implementing of this test function will:

a. Provide constant 1.5 MHz, 300 KHz and 60 KHz bias frequency outputs from the digital rate aid unit to allow lockup of the range tone loops (described in Paragraph 3.6.6).

b. Provide an input to the range tone loops (range tone extractor) consisting of the range tone combiner output linearly added to an internal variable noise source.

The range tone test function switch will be located in the zero-set phase shifter (providing adequate space is available in the chassis for the noise test module). Actuation of the switch disables the VHF and S-Band receiver output and energizes the noise source and associated summing amplifier. The range tone level set is pre-set internally to provide an input to the range tone loops identical to that previously supplied by the receivers (≈350 μV per range tone).

The noise source of −157 dbm per Hz is adjustable over a 40 db range through use of a 7-stage, 100 db gain amplifier. The resultant amplifier output will be a series of range tones

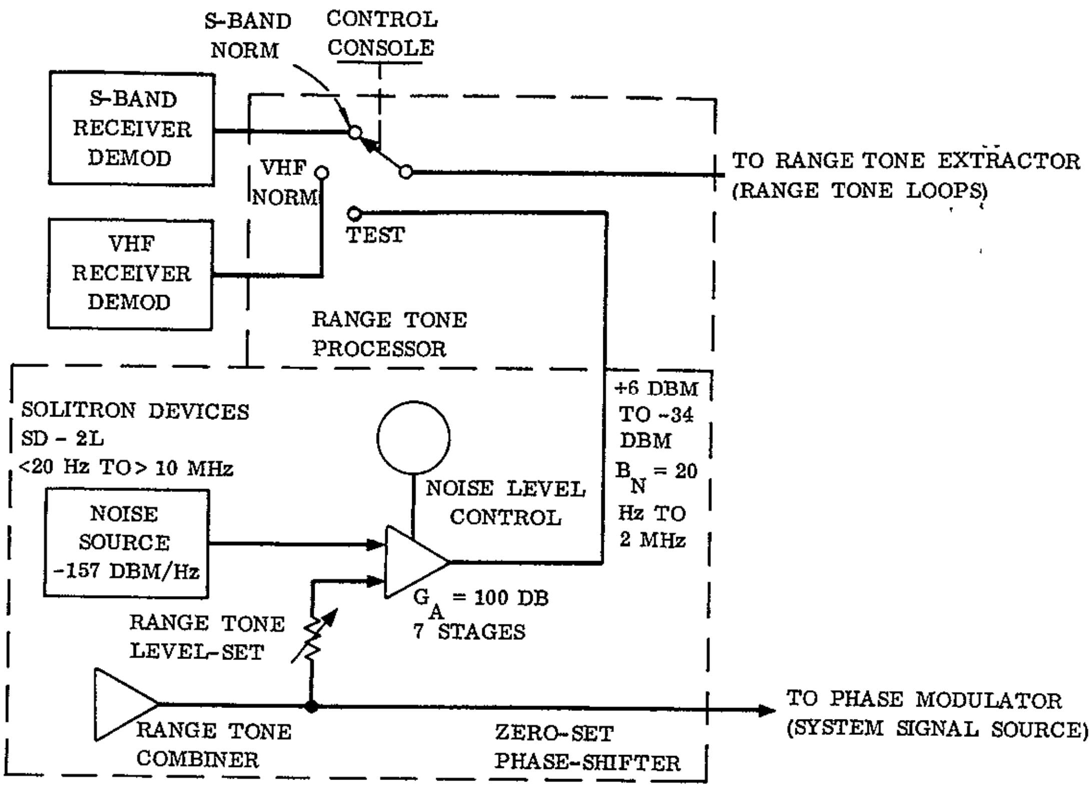

Figure 3-124. Range Tone Test Function Functional Block Diagram

complemented with white noise in a band of approximately 20 Hz to 2 MHz. The white noise level will be adjustable to simulate signal-to-noise ratios occurring at 10 db below carrier (or subcarrier threshold) to approximately 30 db above threshold. This range of control provides a wide range of signal degradation for determining data quality extracted under various noise conditions. Since the highest tone to be used will be 500 KHz, a 2 MHz noise bandwidth appears adequate.

A Solitron SD-2L noise diode (solid state) is intended as the noise generator. This device produces 17 db of excess noise above room ambient (293°K) over a 20 Hz to 10 MHz band. The spectrum is considered to be "white noise" over the entire bandwidth. The amplifier and associated roll-off network will narrow-band the noise to approximately a 2 MHz bandwidth.

A brief analysis of signal levels yields the following:

Range tone loop input (range tone)	=	-57 dbm
Noise source	=	-157 dbm/Hz
Amplifier gain	=	100 db
Available noise power (Bw = 1 Hz)	=	-57 dbm/Hz

Range tone signal-to-noise power density	=	0 db
Amplifier bandwidth (2 MHz)	=	63 db
Total noise power available (max)	=	+6 dbm (-57 dbm/Hz + 63 db)

In combining the range tones with the noise source at the input to the 100 db gain amplifier, a large isolation is achieved between the noise amplifier and the signal path terminating at the phase modulator in the system signal source. Due to reduced loading on the modulation signal, the amplifier may remain in the circuit during normal system operation. The B+ supply voltage will be removed from the noise source and the amplifier during normal operation.

3.10.6 Applicability

The operational test equipment discussed above for the test signal system and automatic noise figure measurement will be provided for the Fairbanks, Rosman, Carnarvon, and Tananarive sites. The Signal Generation Subsystem oscilloscope (Tektronix 585A/Type 82) and the range tone test function are provided only for the Rosman, Carnarvon and Tananarive installations.

3.11 TRANSPONDER TEST SET

The following discussion is confined to equipment to be modified. Equipment and parts retained without modification are not discussed.

3.11.1 Transmitter

The transmitter will have six major module changes (three voltage-controlled RF oscillators and three ×16 multipliers) but will be retained in its present housing.

3.11.1.1 VOLTAGE-CONTROLLED RF OSCILLATOR MODIFICATION. These modules will be electrically redesigned and repackaged. Figure 3-125 is a block diagram of the new voltage-controlled RF oscillator. One module will contain the three channel 14 oscillators, another the three channel 24 oscillators, and the third the three channel 32 oscillators. The oscillator switching arrangement is shown in Figure 3-126; note that the power supply dc voltage ($+V_b$) is switched to the proper oscillator stage. This switching arrangement is offered to meet the intent of the specification although there is not an on-off power switch for each oscillator as may be implied by the specification. The circuits will be mounted on both sides of a T-frame module identical in size to the present modules and suitable for mounting into the existing bathtubs.

The oscillator stage is shown schematically in Figure 3-127. For the required frequency range (±120 KHz), the stability of this oscillator is expected to produce a maximum of 6 degrees rms phase jitter at the subcarrier phase detector output when in the 50 Hz noise

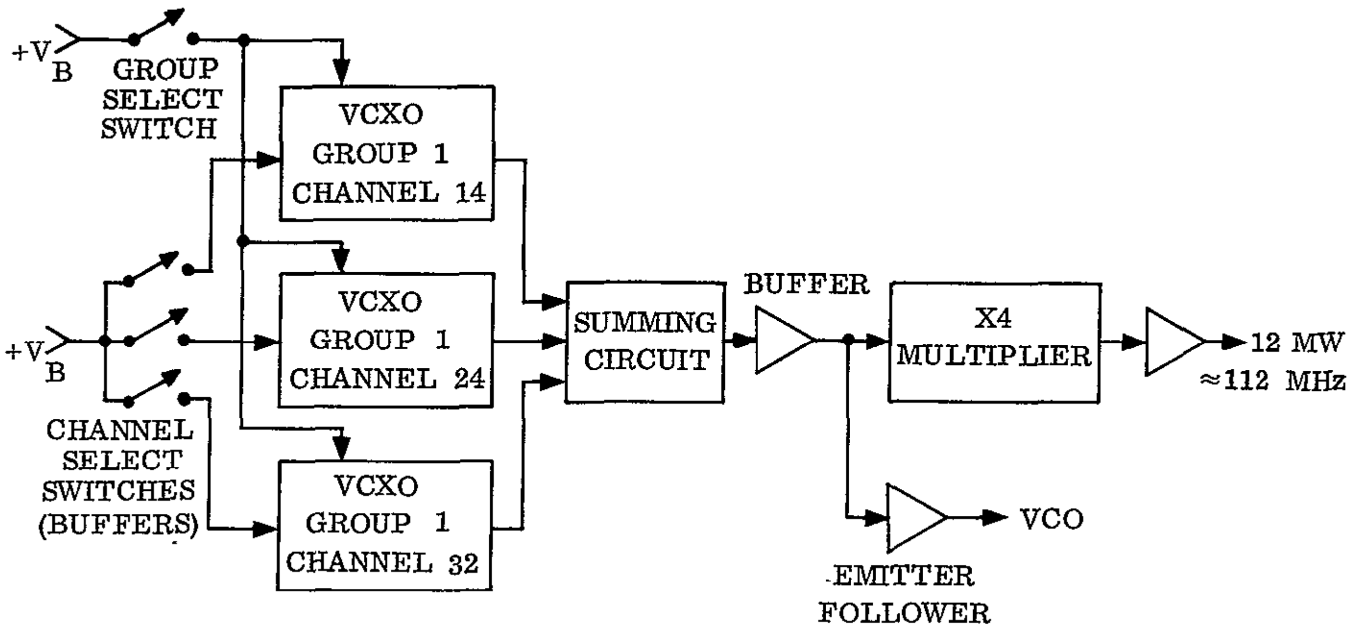

Figure 3-125. Voltage-Controlled RF Oscillator Block Diagram

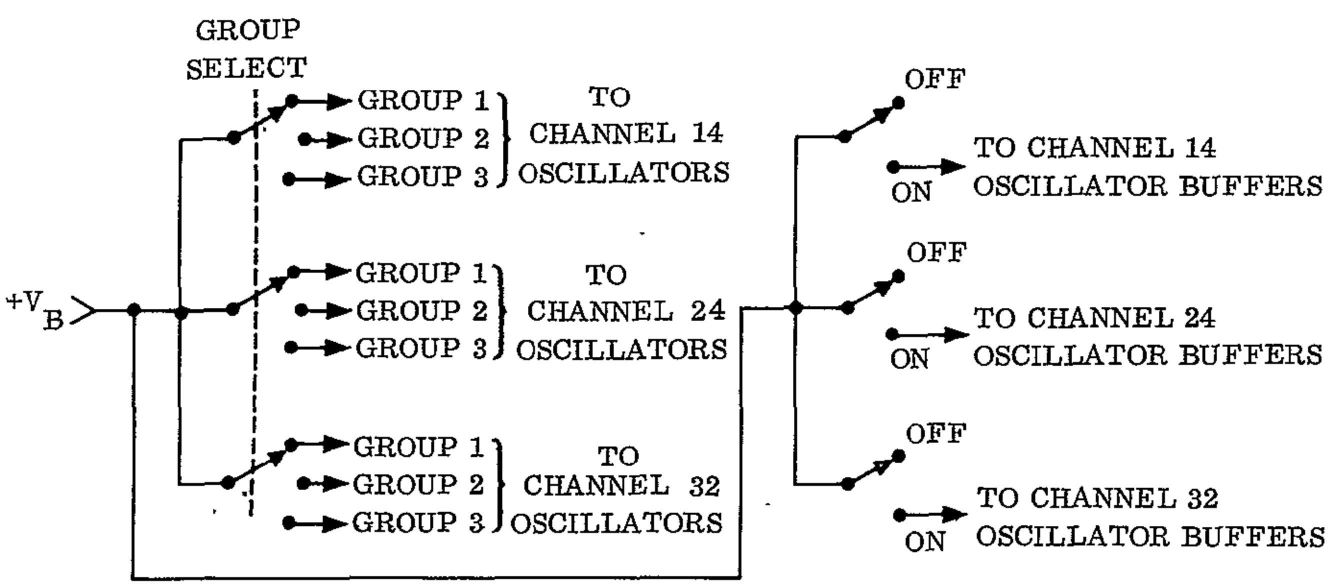

Figure 3-126. Oscillator Switching Diagram

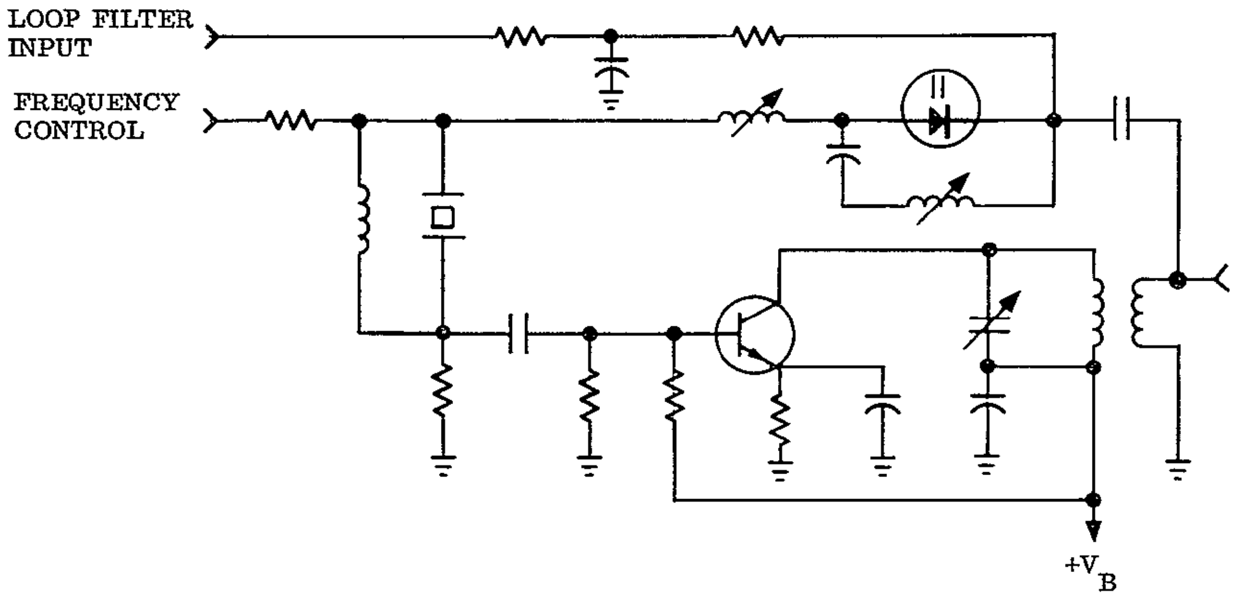

Figure 3-127. Schematic Diagram of VCXO Stage

bandwidth mode. This measurement is strongly dependent on the jitter contributed by the present subcarrier oscillators. Based on an expected maximum jitter of 5.5 degrees rms due to the redesigned wider-range subcarrier VCO, crystal selection for the transmitter VCXO is mandatory. The expected crystal yield is 30 to 40 percent.

3.11.1.2 ×16 FREQUENCY MULTIPLIER PHASE MODULATOR MODIFICATIONS. These three modules will be electrically redesigned and repackaged. Figure 3-128 is a block gram of one module. The phase modulator will be a series single-tuned circuit where the phase through the network is changed by varying the junction capacitance of a varicap. This circuit will produce 5.4 degrees peak of phase variation. Sensitivity will be controlled with a screwdriver adjustment on the front panel. The limiting amplifier will provide 3 to 4 db

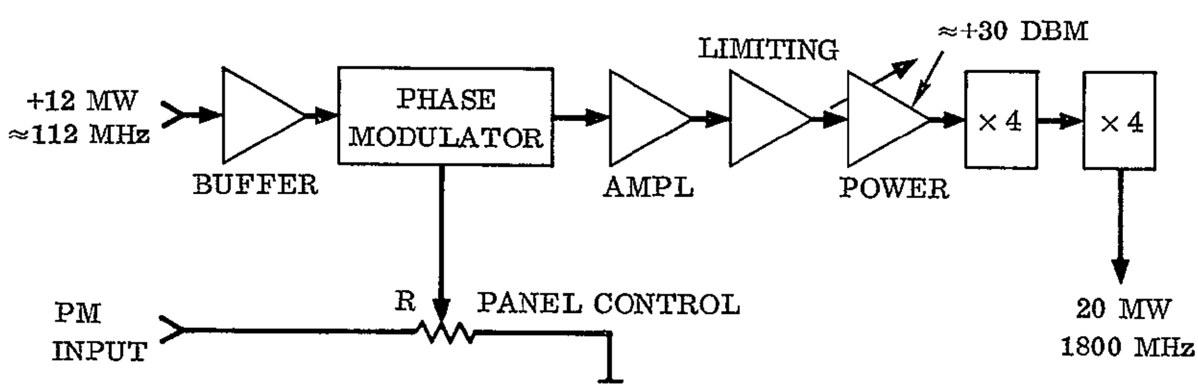

Figure 3-128. ×16 Frequency Multipliers — Phase Modulator Block Diagram

of limiting. The power amplifier will be a single 2N3866 stage with the gain controlled by adjusting the emitter current. This variable adjustment is used to set the output power of each channel to 1 mw as read at the DIRECT jack on the front panel. The ×16 multiplier may remain in the same network configuration with the element values scaled in accordance with the frequency decrease using existing varactor diode types. The use of step-recovery diode multiplication for the final stage will also be considered for this design.

3.11.1.3 CHANNEL ISOLATION. The channel power combining method is shown in Figure 3-129. It differs from the present method in that one power divider is replaced with a power divider with more isolation (19 db per manufacturer's specification), and the other power divider is replaced with a 3-db directional coupler whose directivity is 25 db. The manufacturer of the power divider indicated that, at 1800 MHz, the isolation would increase from the specified 19 db to 20 db or more. This method is offered to meet the intent of the specification by providing 20 db isolation between channels even though load isolators are not used as separate entities.

3.11.1.4 FRONT PANEL. The front panel will have a new control to select any one of three frequency groups. Photographs in the existing manual for this drawer indicate that the control can be mounted to the right and slightly above the variable attenuator dial. If possible, the control will be mounted above the channel controls; this cannot be verified until inspection of the drawer after delivery.

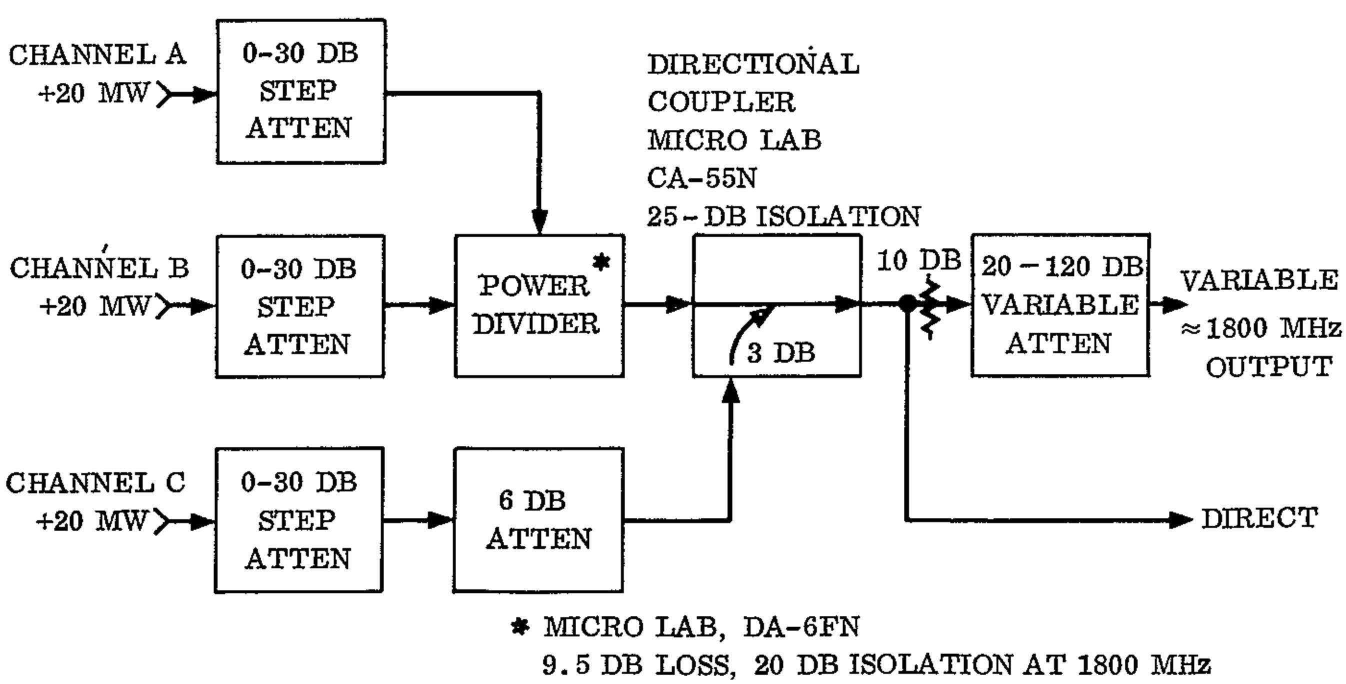

Figure 3-129. Channel Power Combining

The MOD ADJ knob for each channel will be removed and the shaft of the variable resistor will be recessed beneath the front panel surface. The end of the shaft will have a screwdriver blade receptacle, thus making it a front panel screwdriver adjustment.

3.11.2 Receiver

The receiver will require one major module change to the carrier VCXO and minor circuit modifications to the subcarrier VCO. The present receiver housing will be retained. The RF converter hardware will remain with the transponder simulator and is discussed with the simulator in Paragraph 3.11.3.

3.11.2.1 CARRIER VCXO MODIFICATIONS. This module will be electrically redesigned and repackaged. Figure 3-130 is a block diagram of the new VCXO module. The three oscillators will be identical in electrical design except for the resonant frequency of the crystal. To select the proper channel, the dc voltage from the power supply is switched to the proper oscillator. The circuits will be mounted on both sides of a T-frame module identical in size to the present VCXO module and suitable for mounting into the existing bathtubs.

The oscillator is shown schematically in Figure 3-127. For the required frequency range, the stability of this oscillator is such that it is expected to produce a maximum of 6 degrees phase jitter as measured at the carrier receiver phase detector output in the 20 Hz noise bandwidth mode, when the receiver is locked to the transponder simulator, and there is no input to the simulator from the test transmitter. This stability will be achieved by selecting crystals. The crystal yield will probably be 50 percent.

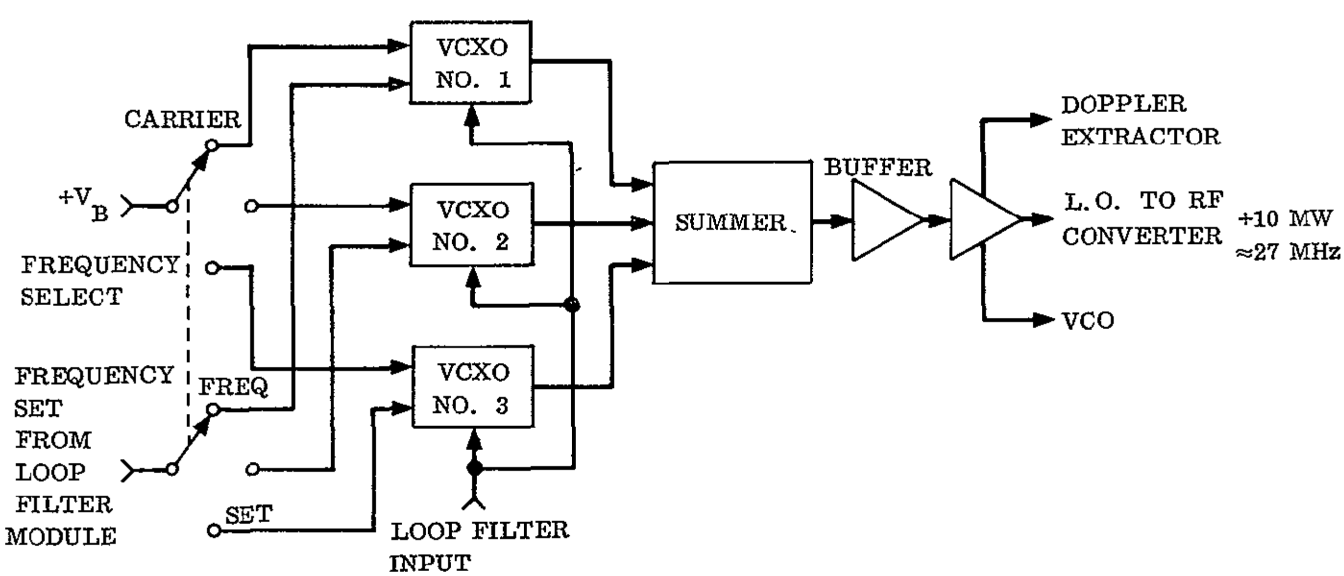

Figure 3-130. VCXO Chassis Block Diagram

3.11.2.2 SUBCARRIER VCO MODIFICATIONS. The subcarrier VCO's must be modified to operate over a control range of ±120 KHz instead of their present range of ±100 KHz. This can be done by increasing the L-to-C ratio of the collector tank circuit. The increase in percentage change of tank capacitance will enable the greater frequency change. The new frequency range may increase the mean-square-phase error of the oscillators. Under any conditions these oscillators cannot have more than 5.5 degrees rms phase jitter as measured at the subcarrier phase detector output. This requirement stems from the specification on the transmitter phase jitter which requires that the total system phase jitter be not more than 6 degrees rms measured at the subcarrier phase detector output.

3.11.2.3 FRONT PANEL. The front panel will incorporate a new control for switching receiver input frequencies. The knob for this control (Carrier Frequency Select) will be mounted between the carrier test jacks and the present nameplate; the nameplate may be moved to ease installation. The knob and control mechanism will be identical to the Subcarrier Freq. Select function.

3.11.3 Test Equipment Unit

The only new pieces of test equipment to be supplied are a new 3-channel transponder simulator/RF converter drawer replacing the existing drawer, an HP 6266A power supply to drive the transponder in place of the Trygon-M36-5, and an HP-5245L counter (supplied only for one system to replace the HP-524C). The transponder mount drawer will require modifications.

3.11.3.1 TRANSPONDER SIMULATOR/RF CONVERTER. The Transponder Simulator/RF Converter drawer contains the receiver RF converter modules and the transponder simulator modules.

3.11.3.1.1 Receiver RF Converter. A block diagram of the receiver RF converter is given in Figure 3-131. The switching function for low-level and high-level received inputs will be incorporated using coaxial switches and a front panel control.

The ×5 multiplier in the ×80 module will be a varactor type using a PC-116 varicap. The power amplifier will be a single 2N3866 stage. The ×16 multiplier will be of the same design as that used in the test transmitter; the element values will be scaled in accordance with the frequency difference. The same varactor types now in the present ×60 module will be used.

The new cavity filter, operating at approximately 2200 MHz, will be similar in design to the present 1645 MHz cavity filter. If at all possible, the present MIXER/PREAMPL module will be used. Tests must be conducted, after delivery to the contractor, to determine gain, bandwidth, and noise figures. If the module is unacceptable, a new commercial low noise mixer and a contractor-designed preamplifier will be used.

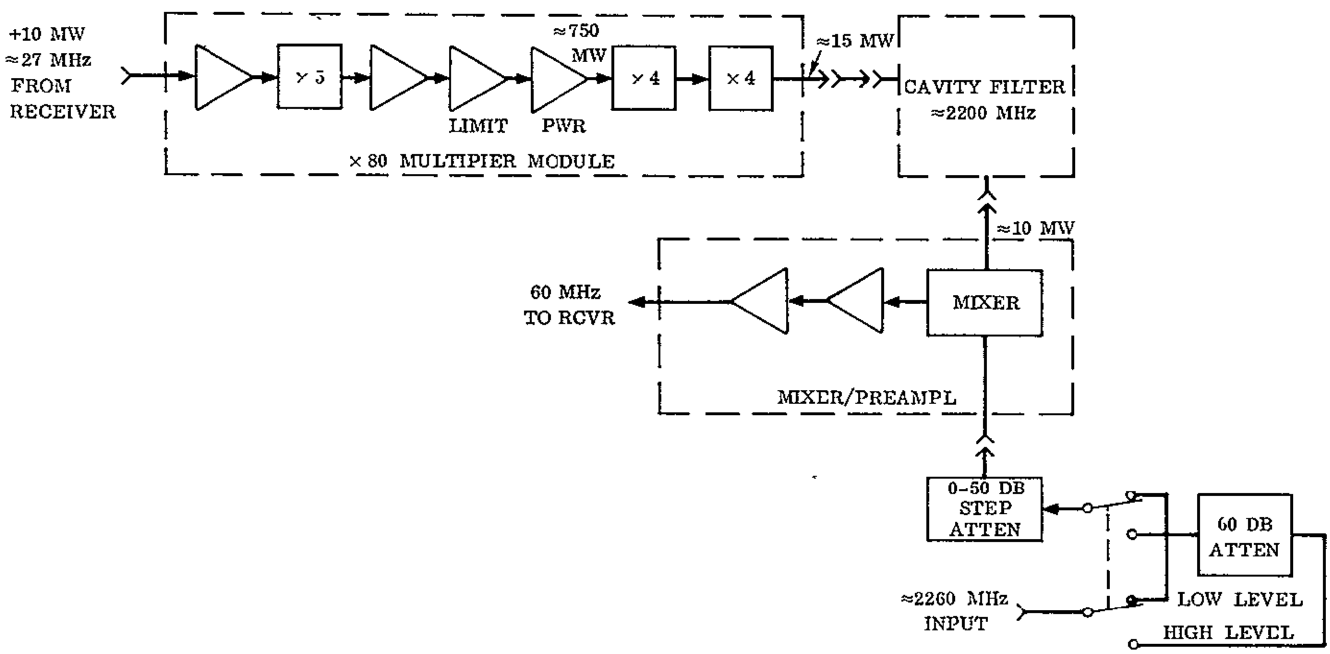

Figure 3-131. Receiver RF Converter Block Diagram

3.11.3.1.2 Transponder Simulator. Figure 3-132 shows a block diagram for the transponder simulator. The simulator will have a time delay of approximately 12.5 nanosec with 8.5 nanosec contributed by the wideband amplifier and 4.0 nanosec due to the RF path length. The simulator is designed such that, when driven with 0 dbm from the test transmitter, the modulation index shall be 1.5 radians.

The RF oscillator module contains three oscillators which are selected one at a time by a front panel control routing the dc power to the proper stage. The ×5 multiplier in this module will be a varactor type using a PC-116 varicap. The amplifiers following the ×5 multiplier will be switched off whenever the TRANSPONDER/SIMULATOR mode control on the Transponder Mount Drawer is in the TRANSPONDER position. This is done to prevent EMI problems when testing a transponder.

The ×15 multiplier will consist of an input amplifier, a power amplifier, a ×3 varactor multiplier, a ×5 step recovery diode multiplier, and a cavity filter. The output of the ×15 multiplier will function as the S-Band input to the balanced modulator as well as the transmitted carrier.

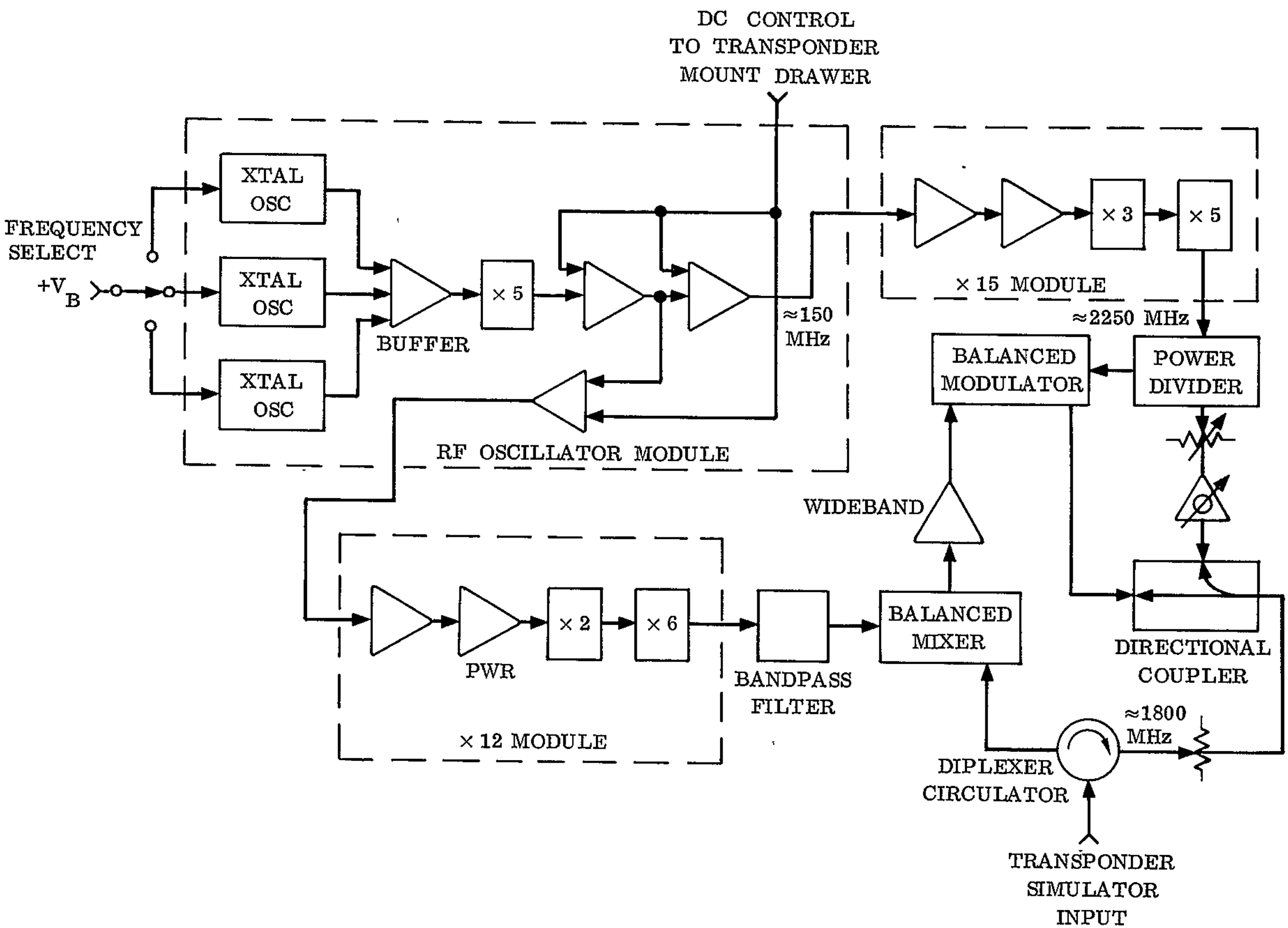

Figure 3-132. Transponder Simulator Block Diagram

The ×12 multiplier will consist of an input amplifier, a power amplifier, a varactor doubler, a ×6 step recovery diode multiplier, and a cavity filter. The ×12 multiplier output will provide the local oscillator signal to the balanced mixer.

The wideband amplifier will be an RC-coupled, 3-stage amplifier with 36 db of gain and a minimum bandwidth of 100 MHz per stage. High f_t transistors like the 2N3866 will be used.

The module circuitry will be mounted on extruded aluminum T-frames and enclosed in EMI tight metal containers. Figure 3-133 depicts the RF CONVERTER/TRANSPONDER drawer front panel.

3.11.3.2 TRANSPONDER MOUNT DRAWER MODIFICATIONS. The requirement to monitor the transponder power supply voltage will require using the spare jacks mounted on the front panel.

A new diplexer must be supplied because of the new frequency groups. The diplexer will have sufficient isolation to permit proper operation of both the transmitters at high signal and the receivers at low signal conditions. A new control will be mounted to the right of the power lamp and above the input current monitoring jacks. The control will switch the diplexer output port from the transponder to the transponder simulator as shown in Figure 3-134. When this control is in the transponder simulator mode the transponder will be terminated in a 5-watt 50-ohm load. The $+V_b$ interrupt output line goes to the simulator to disable its output when in the transponder mode.

Front panel jack labeling must be changed in accordance with the preceding modifications.

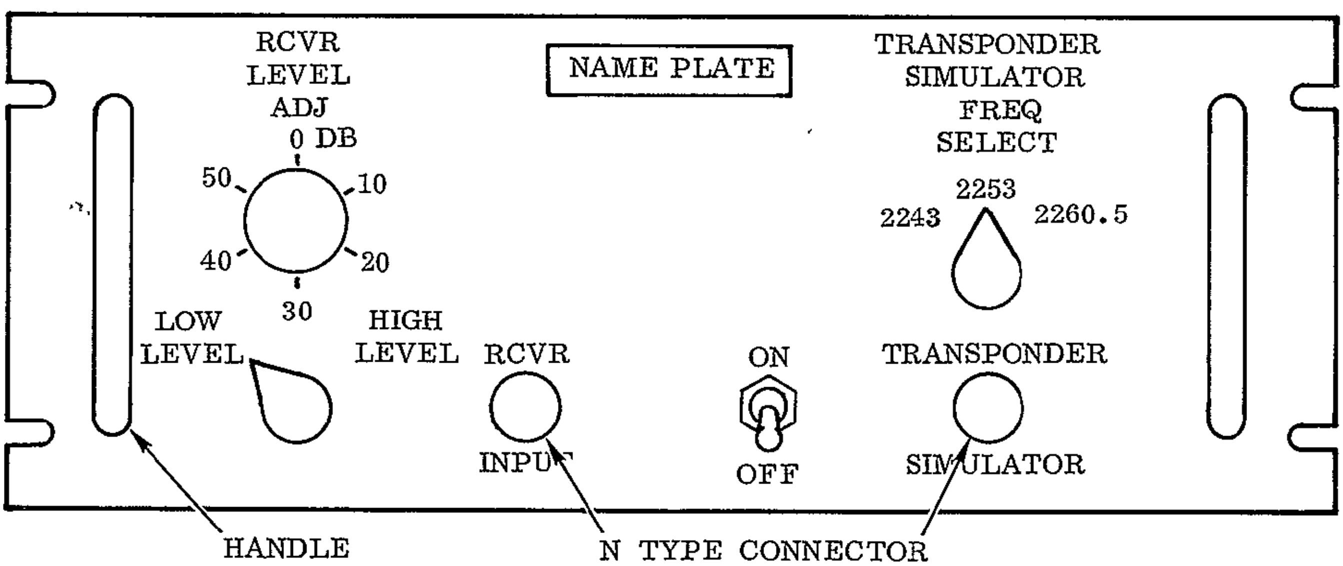

Figure 3-133. RF Converter/Transponder Drawer Panel

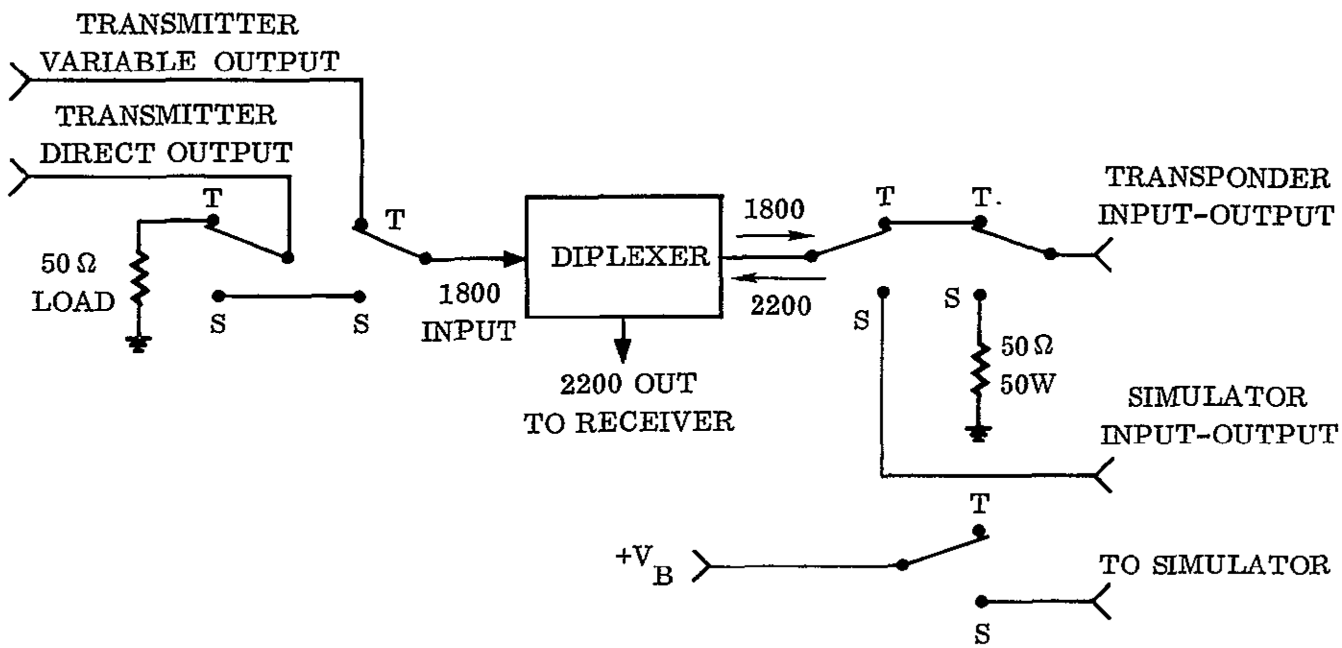

Figure 3-134. Diplexer Switching Arrangement

3.12 SYSTEM SIMULATOR

3.12.1 Functional Description

The function of the System Simulator is to provide S-Band carrier and subcarrier doppler simulation. Simulation of other dynamic system parameters such as signal and noise levels and range variation are provided by the collimation subsystem, the test signal source, the range tone test function, and the zero-set phase shifter. The doppler simulation provided by the System Simulator exercises the carrier and subcarrier receivers as well as the doppler extractor and range rate extraction unit. Thus the system may be exercised all the way through data print-out.

Doppler simulation is achieved by combining the inherent capability of the system signal source with one additional coherent but tunable reference frequency source (an additional HP5105 synthesizer). Although the one additional synthesizer is termed the "system simulator", it is, in fact, only a portion of the equipment used for simulation.

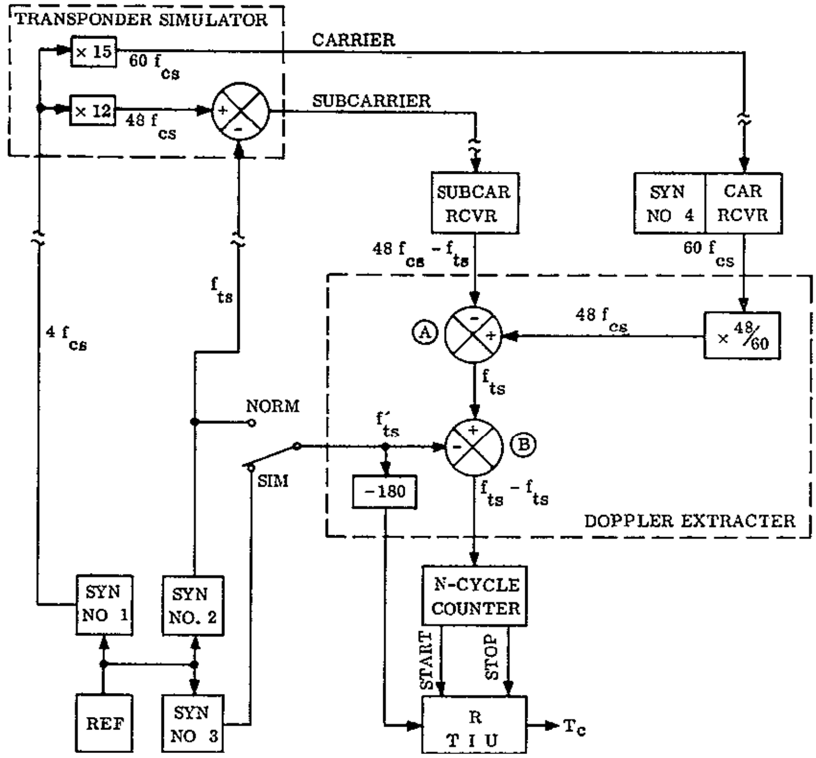

Figure 3-135. Doppler Simulation Simplified Functional Block Diagram

Figure 3-135 is a functional block diagram showing signal flow for doppler simulation. The diagram is simplified and does not show bias frequency offsets or actual hardware implementation. It is intended to show only the basic signal flow and control points.

To provide the controlled S-Band doppler simulation necessary to obtain quantitative doppler data, there are three basic reference frequencies which must be independently variable and exactly known. These are:

f_{ts} — the S-Band carrier frequency transmitted by the ground station

f'_{ts} — the "apparent" transmitted frequency as supplied to the doppler extractor.

f_{cs} — the reference frequency for the transponder simulator

For normal system operation, the transmitted frequency, f_{ts}, and the apparent transmitted frequency, f'_{ts}, supplied to the doppler extractor are the same. The two signals are both controlled by the S-Band transmitter synthesizer (Syn. No. 2). This is necessary to implement "frequency independent doppler extraction". For doppler simulation, these two reference frequencies must be independently controllable but both known. Synthesizer No. 3

provides the additional controlled source. The third reference frequency, f_{cs}, is generated by synthesizer No. 1 which is normally used to provide the VHF transmitter reference. (This is actually done for any operation using the S-Band transponder simulator.)

The frequency of synthesizer No. 1 can be varied to simulate down-link carrier doppler. This will exercise the carrier receiver and other elements in the carrier receiver path. Varying synthesizer No. 4 (receiver reference synthesizer) will also exercise the carrier receiver phase-lock loop. Note that the long-term phase excursions of synthesizer No. 1 are cancelled at mixer A and do not affect the range rate data.

The frequency of synthesizer No. 2 can be varied to simulate subcarrier doppler. This will exercise the subcarrier receiver and other elements of the subcarrier processing circuitry. By proper control of synthesizers No. 2 and 3 together, the doppler extractor and all elements of the range rate extractor will be exercised. Note that if the frequencies of synthesizers No. 2 and 3 are set equal, the effective doppler is zero due to subcarrier cancellation at mixer B.

Thus by proper control of synthesizers No. 1, 2 and 3, any combination of carrier and subcarrier doppler may be simulated. The transponder simulator shown in the figure may be either the transponder simulator in the collimation subsystem or the S-Band test signal source which is part of the operational test equipment.

The system simulator will be implemented using an HP 5105 synthesizer located in the signal generation cabinet. The synthesizer output will be injected into the system in the system signal source as shown in Figure 3-27.

3.12.2 Applicability

The system simulator will be provided for all four sites.

SECTION 4. SYSTEM DESIGN ANALYSIS

4.1 SIGNAL DYNAMICS

The GRARR system is designed to track space vehicles in a wide variety of orbits. In order to determine maximum possible system dynamics, Reference 1 analyzed the case shown in Figure 4-1. It was assumed that the tracking station was located on the equator and that the satellite traversed an elliptical orbit with apogee of 60,000 nautical miles and perigee of 150 nautical miles. The orbit was also assumed to be traversed in a direction opposite to the direction of the earth's rotation. For the analysis, the orbital system synchronization was varied so that the tracking site was directly under the satellite at perigee (Case I) and at geocentric angles of $\pi/2$ (Case II), $3/4\pi$ (Case IV), and π radians (Case III) from the perigee or zero geocentric angle direction.

Table 4-1 lists approximate numerical maxima for R, $\dot{R}$, $\ddot{R}$, $\dot{\phi}$, and $\dot{\phi}$. Note that maxima do not occur simultaneously except for the acceleration ($\ddot{R}$) and zenith angle rate ($\dot{\phi}$).

The two-way doppler frequency shift, D (Hz) in a frequency, f (Hz), due to a radial velocity, $\dot{R}$ (m/sec), is given on page 72 of Reference 2 as:

$$D = \frac{2\dot{R}f}{C} \tag{1}$$

where C = velocity of light (3×10^8 meters/sec).

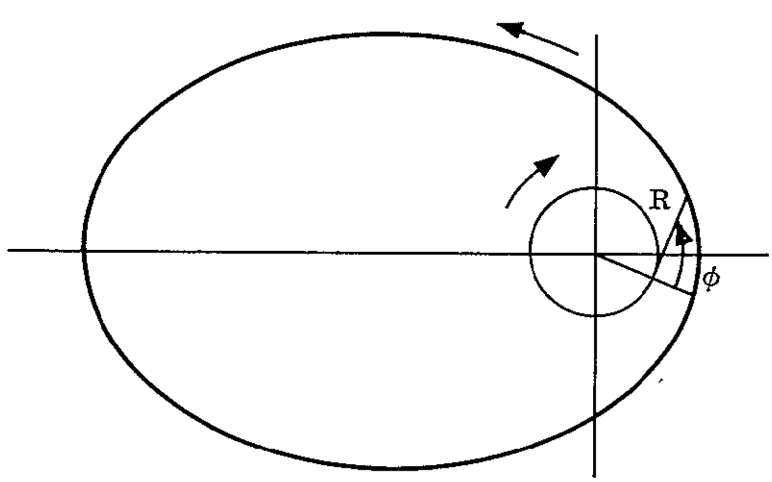

Figure 4-1. Worst Case System Dynamics

Table 4-1. Approximate "Worst Case" Orbital Parameters

Case	Range R (meters)	Rate $\dot{R}$ (m/sec)	Acceleration $\ddot{R}$ (m/sec^2)	Zenith Angle ϕ (rad)	Angle Rate $\dot{\phi}$ (rad/sec)	Angle Acceleration $\ddot{\phi}$ (rad/sec^2)
3	$\boxed{1.12 \times 10^{8}}$	-5.02×10^{1}	-1.85×10^{-2}	-1.35	7.94×10^{-5}	2.84×10^{-10}
1	1.83×10^{6}	$\boxed{1.08 \times 10^{4}}$	1.19×10^{-1}	1.50	1.37×10^{-3}	-1.08×10^{-5}
1	2.78×10^{5}	0.0	$\boxed{4.35 \times 10^{2}}$	0.0	$\boxed{4.00 \times 10^{-2}}$	0.0
1	3.03×10^{5}	4.36×10^{3}	3.37×10^{2}	4.13×10^{-1}	3.38×10^{-2}	$\boxed{-9.6 \times 10^{-4}}$
*Numerical maxima are boxed.						

The two-way doppler rate, $\dot{D}$ (Hz/sec), can be found from the time derivative of Equation 1.

$$\dot{D} = \frac{2\ddot{R}f}{C} \tag{2}$$

Table 4-2 lists the two-way maximum doppler frequency shift, D_{max}, in the GRARR system frequencies computed by substituting $\dot{R}_{max}$ and the frequency into Equation 1. The two-way doppler frequency rates, $\dot{D}$, occurring at the same time as D_{max} are listed in the next column. Table 4-2 also lists the maximum two-way doppler frequency rates, D_{max}, occurring at $\ddot{R}_{max}$.

The values of D concurrent with $\dot{D}_{max}$ are listed in the adjointing column.

4.2 MODULATION AND SIGNAL STRENGTH ANALYSIS

During ranging operations, the GRARR system is capable of transmitting range tones and a range ambiguity resolving code to a spacecraft on either VHF or S-Band frequencies. The available range tones are 500 KHz, 100 KHz, 20 KHz, 4 KHz, 800 Hz, 160 Hz, 32 Hz, and 8 Hz. All tones below 4 KHz are transmitted as upper sidebands of the 4 KHz tone. The operator may choose which of the three highest tones will be used for range resolution; the 500 KHz tone is available for S-Band only. The lower tones are used sequentially for range resolution. VHF transponders require the presence of a 4 KHz, 4.008 KHz, or 4.016 KHz holding tone to gate the transponder. The ambiguity resolving code is a pseudo-random sequence of 32,385 bits having a 4 KHz bit rate and bi-phase modulated on the 4 KHz range tone.

Table 4-2. Two-Way Doppler Frequency Shift and Doppler Frequency Shift Rates for $\dot{R}_{max}$ and $\ddot{R}_{max}$

System Frequency (Hz)	When $\dot{R}$ is Maximum		When $\ddot{R}$ is Maximum	
	D_{max} (Hz)	$\dot{D}$ (Hz/sec)	D (Hz)	$\dot{D}_{max}$ (Hz/sec)
2.30×10^{9}	1.66×10^{5}	1.83×10^{1}	0.0	6.68×10^{3}
1.85×10^{9}	1.33×10^{5}	1.47×10^{1}	0.0	3.86×10^{3}
1.48×10^{8}	1.07×10^{4}	1.18×10^{1}	0.0	4.30×10^{2}
1.36×10^{8}	9.78×10^{3}	1.08×10^{1}	0.0	3.95×10^{2}
5.00×10^{5}	3.6×10^{1}	3.97×10^{-3}	0.0	1.45×10^{0}
1.00×10^{5}	7.20	7.93×10^{-4}	0.0	2.90×10^{-1}
2.00×10^{4}	1.44	1.59×10^{-4}	0.0	5.80×10^{-2}
4.00×10^{3}	2.88×10^{-1}	3.17×10^{-5}	0.0	1.16×10^{-2}
800.	5.76×10^{-2}	6.35×10^{-6}	0.0	2.32×10^{-3}
160.	1.15×10^{-2}	1.27×10^{-6}	0.0	4.65×10^{-4}
32.	2.3×10^{-3}	2.54×10^{-7}	0.0	9.3×10^{-5}
8.	5.6×10^{-4}	6.35×10^{-8}	0.0	2.3×10^{-5}

At the spacecraft transponder, the signal from the ground is heterodyned to a low IF (677 to 920 KHz for VHF and 1.4, 2.4, or 3.2 MHz for S-Band) and phase modulated on the RF carrier for retransmission to earth.

The VHF transponder is a single channel unit while the S-Band unit may receive and retransmit up to two channels simultaneously.

This section provides an analysis of the spectral power distribution and signal strengths in the GRARR system.

4.2.1 Modulation Analysis

The theory of phase modulation, which is employed in the GRARR system, is treated in Reference 3 and in standard texts on modulation theory. The formulas required to analyze the spectrum of a carrier modulated by n tones are listed below.

The power in the modulated carrier relative to the total power is:

$$\frac{P_c}{P_{tot}} = \prod_{j=1}^{n} J_o^2 (A_j) \tag{3}$$

where

P_{tot} = total power (power in unmodulated carrier)

P_c = power in modulated carrier

A_j = carrier deviation in radians produced by the j^{th} modulating tone

$\prod_{j=1}^{n}$ = product of n terms

$J_m(A_j)$ = Bessel function of the first kind and of order "m"

Since the total power, P_{tot}, remains constant, the power in the modulated carrier, P_c, is seen to be a function of the number and amplitudes of the modulating tones.

The power in the two sidebands of the i^{th} tone relative to the total power is approximately:

$$\frac{P_{ti}}{P_{tot}} = 2 \frac{J_1^2 (A_i)}{J_o^2 (A_i)} \prod_{J=1}^{n} J_o^2 (A_j) \tag{4}$$

Dividing Equation 4 by Equation 3 gives the ratio of the power in the two sidebands of the i^{th} tone to the power of the modulated carrier.

$$\frac{P_{ti}}{P_c} = 2 \frac{J_1^2 (A_i)}{J_o^2 (A_i)} \tag{5}$$

This shows that the ratio of a tone sideband power, $P_{ti}/2$, to the modulated carrier power, P_c, is fixed by the phase deviation, A_i, produced by that tone and is independent of the presence of other modulating tones.

These expressions are used to determine the spectral power distributions in the uplink and downlink signals for a variety of modulation conditions.

Table 4-3 lists the modulation indices for the modulating tones and the sideband level in db relative to the modulated and the unmodulated carrier for the VHF earth-to-space signal. Three possible modulation cases are shown. Figure 4-2 is a graphical presentation of the spectral levels for Case 1 of Table 4-3.

Table 4-3. VHF Earth-to-Space Relative Spectral Levels

Spectral Component	Modulation Index (radians)	Referenced to Unmodulated Carrier (db)	Referenced to Modulated Carrier (db)
Case 1			
Modulated Carrier		- 2.4	0.0
Highest Tone Sideband	0.7	-11.0	- 8.6
Second Tone or Code Sideband	0.7	-11.0	- 8.6
Holding Tone Sideband	0.3	-18.8	-16.4
Case 2			
Modulated Carrier		- 2.2	0.0
Highest Tone Sideband	0.7	-10.8	- 8.6
Second Tone Sideband (4.000 or 4.008 of 4.016)	0.7	-10.8	- 8.6
Case 3			
Modulated Carrier		- 1.3	0.0
Highest Tone Sideband	0.7	- 9.9	- 8.6
Holding Tone Sideband	0.3	-17.7	-16.4

Similarly, Table 4-4 lists the earth-to-space spectral levels for two modulation cases on an S-Band signal and Figure 4-3 depicts Case 1 graphically.

Three modulation cases for the VHF space-to-earth signal are tabulated in Table 4-5 and Case 1 is shown graphically in Figure 4-4.

Tables 4-6 and 4-7 list spectral levels for one-channel and two-channel S-Band space-to-earth signals, respectively, and Figures 4-5 and 4-6 display the spectra.

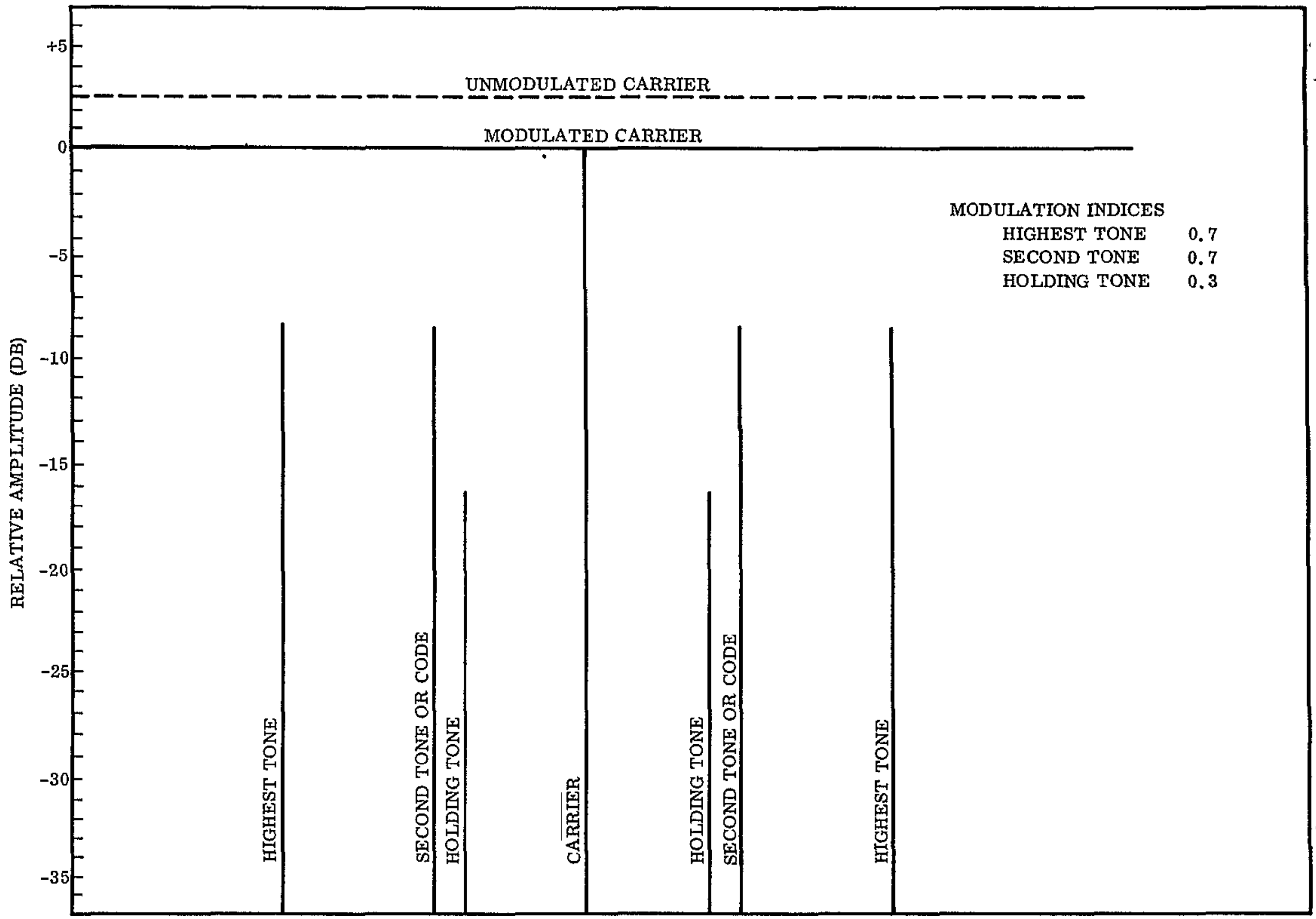

Figure 4-2. VHF Uplink Spectrum (Case 1, Table 4-3)

Table 4-4. S-Band Earth-to-Space Relative Spectral Levels

Spectral Component	Modulation Index (radians)	Referenced to Unmodulated Carrier (db)	Referenced to Modulated Carrier (db)
Case 1			
Modulated Carrier		- 3.7	0.0
Highest Tone Sideband	1.06	- 7.9	- 4.1
Second Tone or Code Sideband	0.7	-12.3	- 8.6
Case 2			
Modulated Carrier		- 2.6	0.0
Highest Tone Sideband	1.06	- 6.8	- 4.1

Table 4-5. VHF Space-to-Earth Relative Spectral Levels

Spectral Component	Modulation Index (radians)	Referenced to Unmodulated Carrier (db)	Referenced to Modulated Carrier (db)
Case 1			
Modulated Carrier		- 1.1	0.0
(Unmodulated Subcarrier Sideband)	(0.7)	(- 9.6)	(- 8.6)
Modulated Subcarrier Sideband	0.7	-12.1	-11.0
Highest Tone Sideband	0.7	-20.6	-19.5
Second Tone or Code Sideband	0.7	-20.6	-19.5
Holding Tone Sideband	0.3	-28.4	-27.3
Case 2			
Modulated Carrier		- 1.1	0.0
(Unmodulated Subcarrier Sideband)	(0.7)	(- 9.7)	(- 8.6)
Modulated Subcarrier Sideband	0.7	-11.9	-10.8
Highest Tone Sideband	0.7	-20.4	-19.3
Second Tone or Code Sideband	0.7	-20.4	-19.3

Table 4-5. VHF Space-to-Earth Relative Spectral Levels (Continued)

Spectral Component	Modulation Index (radians)	Referenced to Unmodulated Carrier (db)	Referenced to Modulated Carrier (db)
Case 3			
Modulated Carrier		- 1.1	0.0
(Unmodulated Subcarrier Sideband)	(0.7)	(- 9.7)	(- 8.6)
Modulated Subcarrier Sideband	0.7	-11.0	- 9.9
Highest Tone Sideband	0.7	-19.5	-18.4
Holding Tone Sideband	0.3	-27.3	-26.2

Table 4-6. S-Band Space-to-Earth Relative Spectral Levels (One Channel Operation)

Spectral Component	Modulation Index (radians)	Referenced to Unmodulated Carrier (db)	Referenced to Modulated Carrier (db)
Case 1			
Modulated Carrier		- 5.8	0.0
(Unmodulated Subcarrier Sideband)		(- 5.1)	(+ 0.7)
Modulated Subcarrier Sideband	1.5	- 8.8	- 3.0
Highest Tone Sideband	1.06	-12.9	- 7.1
Second Tone or Code Sideband	0.7	-17.4	-11.5
Case 2			
Modulated Carrier		- 5.8	0.0
(Unmodulated Subcarrier Sideband)		(- 5.1)	(+ 0.7)
Modulated Subcarrier Sideband	1.5	- 7.7	- 1.9
Highest Tone Sideband	1.06	-11.8	- 6.0

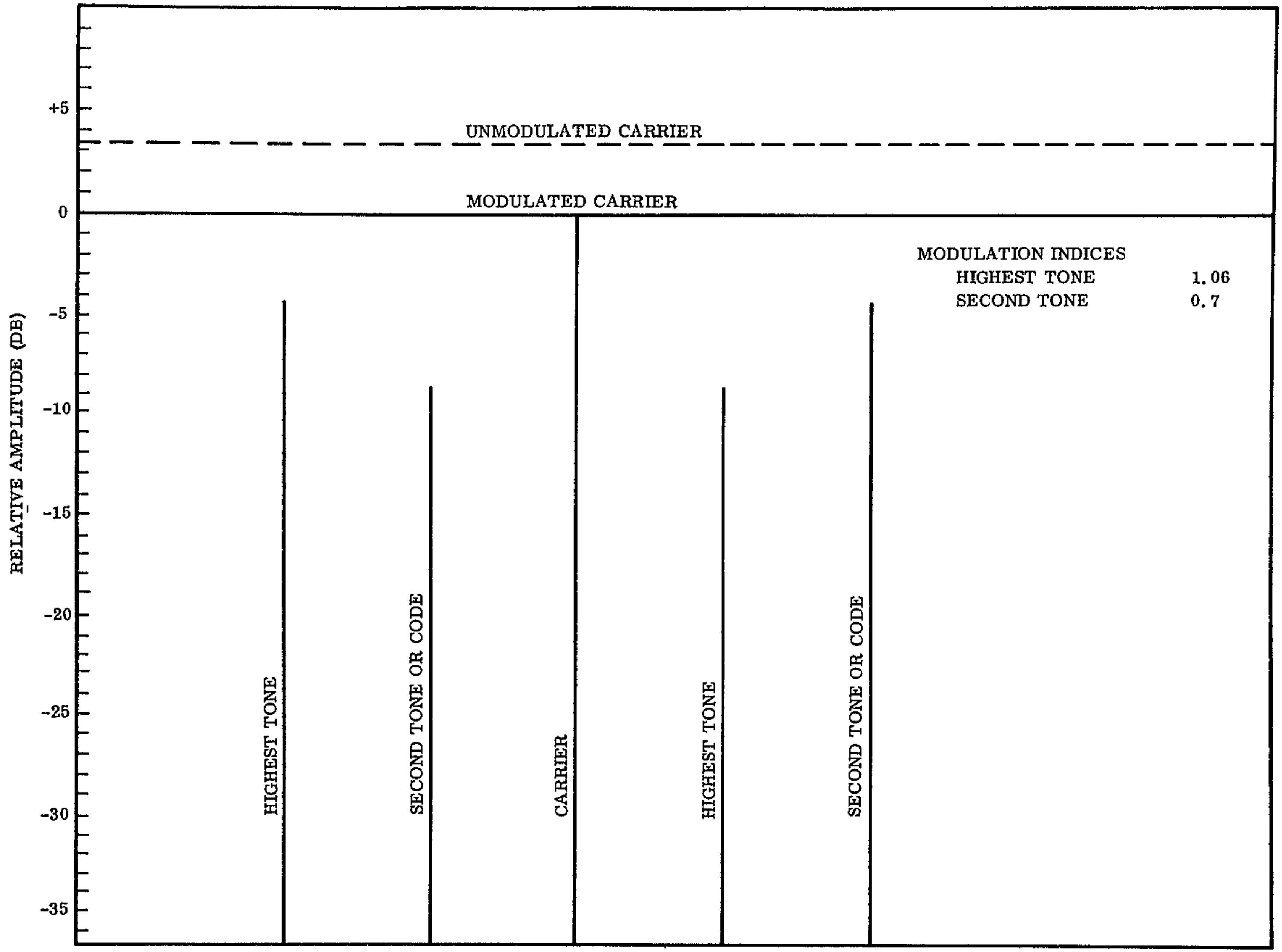

Figure 4-3. S-Band Uplink Spectrum (Case 1, Table 4-4)

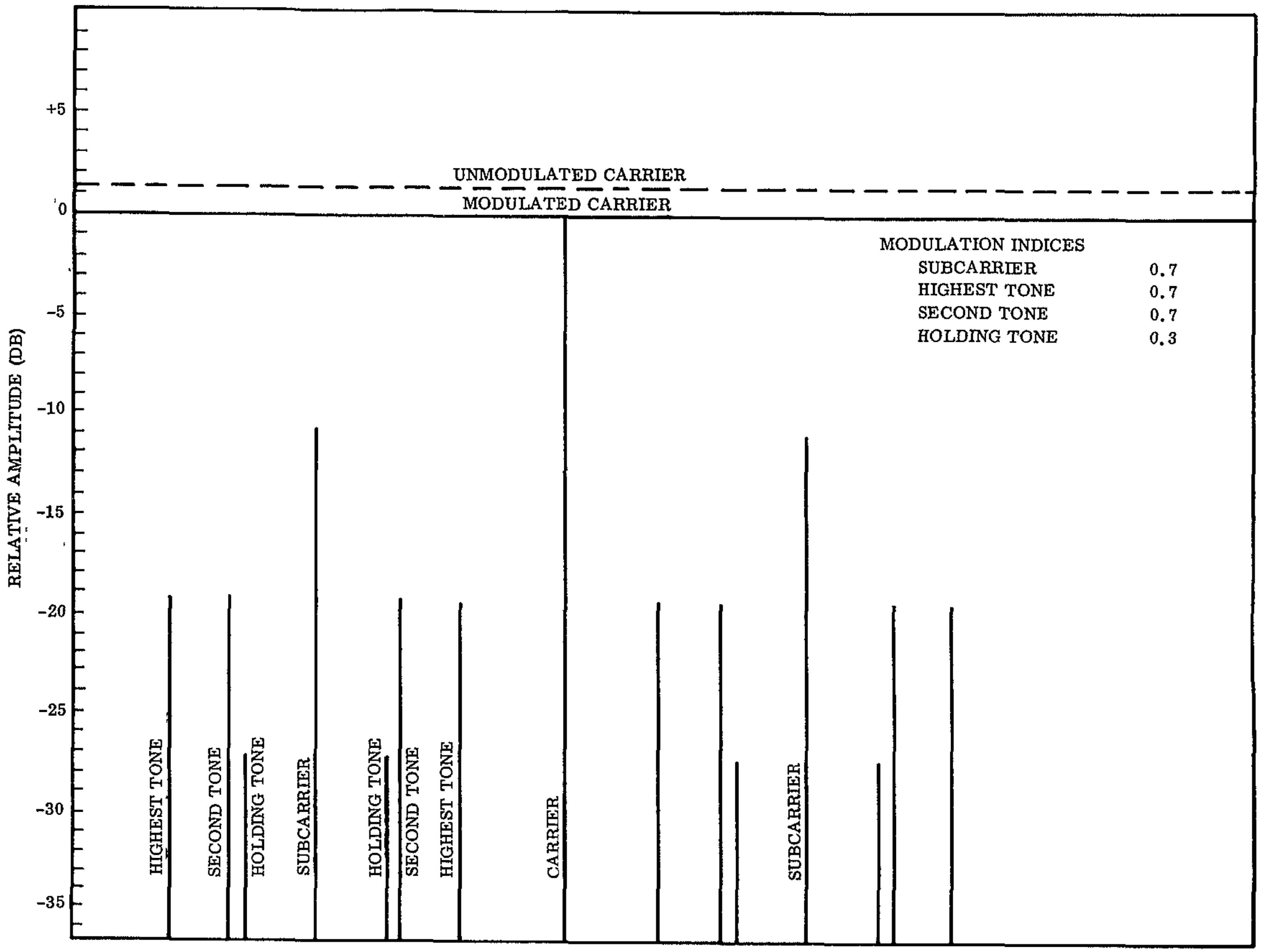

Figure 4-4. VHF Downlink Spectrum (Case 1, Table 4-5)

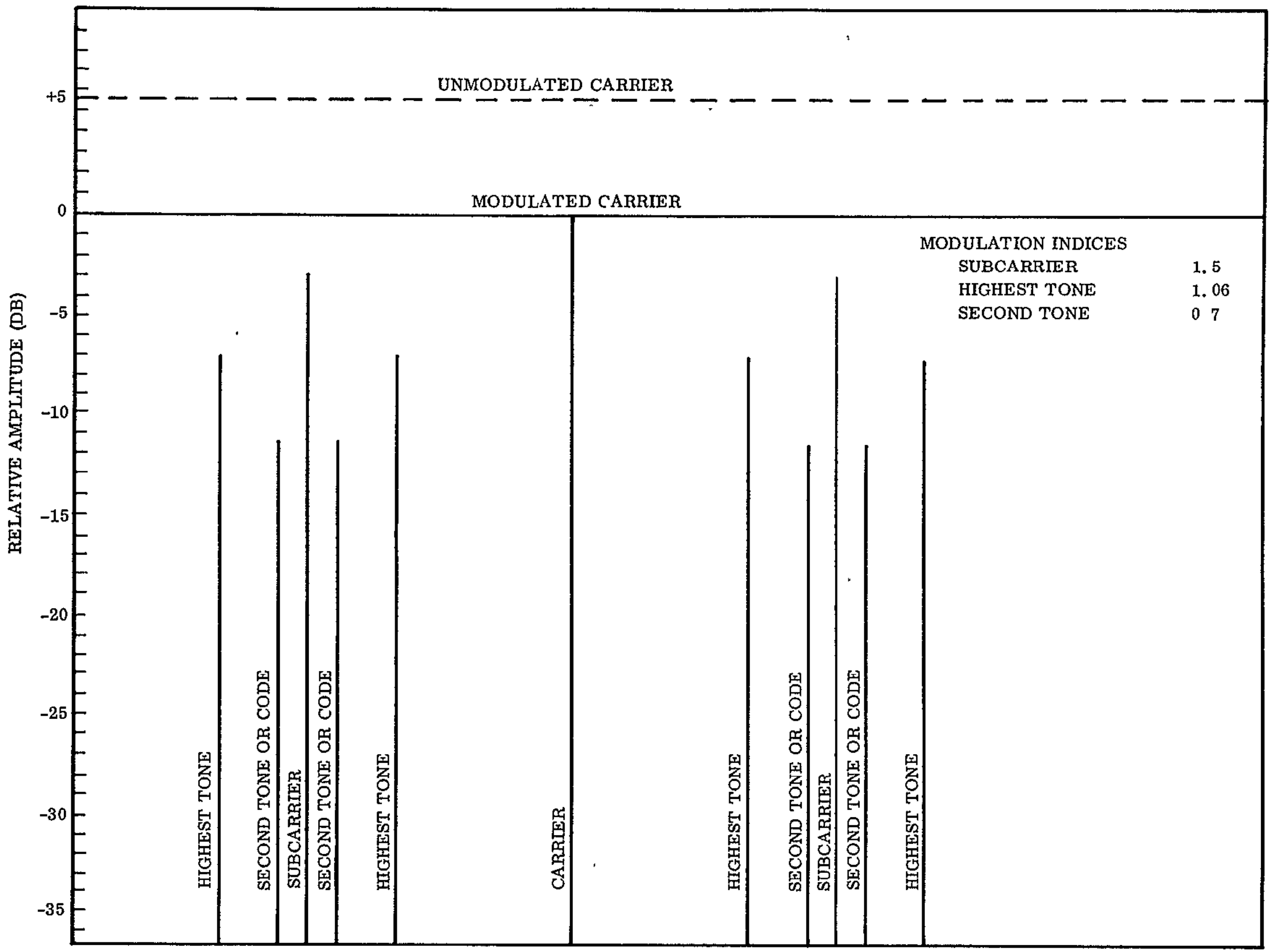

Figure 4-5. S-Band Downlink, One-Channel Spectrum (Case 1, Table 4-6)

Table 4-7. S-Band Space-to-Earth Relative Spectral Levels (Two-Channel Operation)

Spectral Component	Modulation Index (radians)	Referenced to Unmodulated Carrier (db)	Referenced to Modulated Carrier (db)
Case 1			
Modulated Carrier		- 2.5	0.0
First and Second (Unmodulated Subcarrier Sideband)	(0.75)	(-10.4)	(- 7.9)
Modulated Subcarried Sideband	0.75	-14.1	-11.6
Highest Tone Sideband	1.06	-18.3	-15.7
Second Tone or Code Sideband	0.70	-22.7	-20.2
Case 2			
Modulated Carrier		- 2.5	0.0
First (Unmodulated Subcarrier Sideband)	(0.75)	(-10.4)	(- 7.9)
Modulated Subcarrier Sideband	0.75	-14.1	-11.6
Highest Tone Sideband	1.06	-18.3	-15.7
Second Tone or Code Sideband	0.70	-22.7	-20.2
Second (Unmodulated Subcarrier Sideband)	(0.75)	(-10.4)	(- 7.9)
Modulated Subcarrier Sideband	0.75	-13.0	-10.5
Highest Tone	1.06	-17.2	-14.6
Case 3			
Modulated Carrier		- 2.5	0.0
First and Second (Unmodulated Subcarrier Sideband)	(0.75)	(-10.4)	(- 7.9)
Modulated Subcarried Sideband	0.75	-13.0	-10.5
Highest Tone Sideband	1.06	-17.2	-14.6

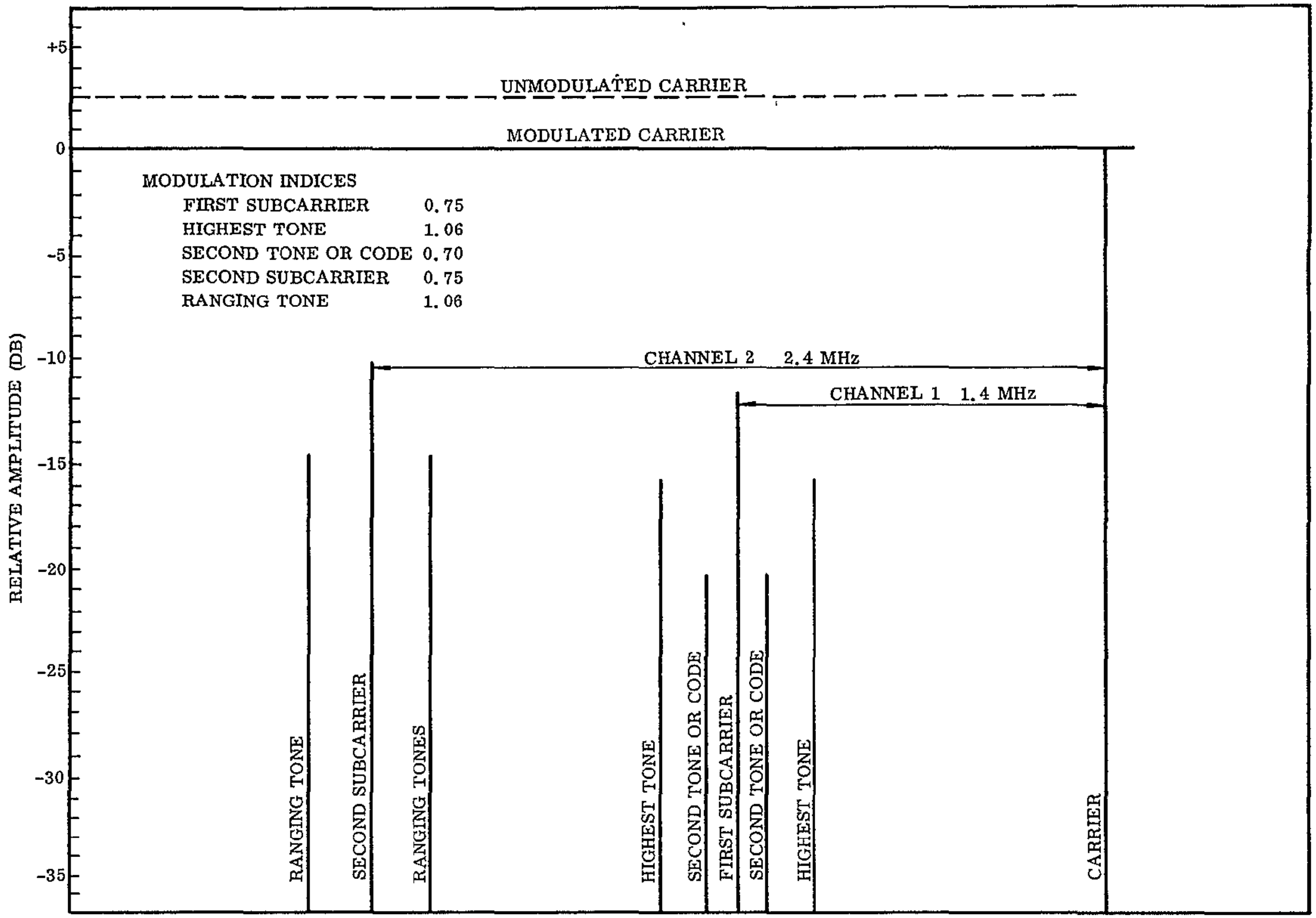

Figure 4-6. S-Band Downlink, Two-Channel Spectrum (Case 2, Table 4-7)

4.2.2 Downlink Relative Power Summary

Table 4-8 summarizes the relative downlink power levels of the VHF carrier and modulating tones with respect to the power in the unmodulated VHF downlink carrier for each of the possible modulation cases.

Similarly, Table 4-9 summarizes the relative power levels for the S-Band downlink.

Table 4-8. VHF Space-to-Earth Power Summary Relative to Total Received Power

Case	Modulated Carrier	Modulated Subcarrier	Highest Tone	Second Tone or Code	Holding Tone
1. Modulation Index (rad) Relative Power (db)	 -1.1	0.7 -9.1	0.7 -14.6	0.7 -14.6	0.3 -22.4
2. Modulation Index (rad) Relative Power (db)	 -1.1	-0.7 -8.9	- 0.7 -14.4	- 0.7 -14.4	
3. Modulation Index (rad) Relative Power (db)	 -1.1	0.7 -8.0	0.7 -13.5		0.3 -21.3

4.2.3 Downlink Signal-to-Noise Power Density

This section presents a derivation of the total received signal-to-noise power density ratio. Since certain system parameters (e.g., transponder output power and antenna gain) vary from mission to mission and station to station, only a normalized case is presented. Any particular case can be readily derived by making adjustments to the assumed parameters.

The total received signal-to-noise power density can be expressed as

$$(S/\phi)_T = \frac{P_T G_T G_R L A_s}{K T_s} \tag{6}$$

where

$(S/\phi)_T$ = received signal-to-noise power density ratio

P_T = transponder power output

G_T = transponder antenna gain

G_R = ground antenna gain

Table 4-9. S-Band Space-to-Earth Power Summary Relative to Total Received Power

Case	Modulated Carrier	Modulated Subcarrier	Highest Tone	Second Tone or Code	Modulated Second Subcarrier	Highest Tone	Second Tone Tone
One-Channel Operation							
1. Modulation Index (rad) Relative Power (db)	 -5.8	1.5 - 5.8	1.06 - 6.9	0.7 -11.4			
2. Modulation Index (rad) Relative Power (db)	 -5.8	1.5 - 4.7	1.06 - 5.8				
Two-Channel Operation							
1. Modulation Index (rad) Relative Power (db)	 -2.5	0.75 -11.1	1.06 -12.3	0.70 -16.7	0.75 -11.1	1.06 -12.3	0.70 -16.7
2. Modulation Index (rad) Relative Power (db)	-2.5 -2.5	0.75 -11.1	1.06 -12.3	0.70 -16.7	0.75 -10.0	1.06 -11.2	
3. Modulation Index (rad) Relative Power (db)	 -2.5	0.75 -10.0	1.06 -11.2		0.75 -10.0	1.06 -11.2	

L = system loss factor

K = Boltzmann's constant = 1.37×10^{-23} Joules/°K

T_s = total system noise temperature

A_s = free space attenuation = $\left(\frac{C}{4\pi RF}\right)^2$

where

C = velocity of propagation = 3×10^5 Km/sec

R = range in Km

F = downlink carrier frequency in Hz

Using the parameters listed below, the total received VHF signal-to-noise power density ratio is plotted in Figure 4-7 as a function of range. Note that the system loss factor (including polarization mismatch, atmospheric absorption, and miscellaneous losses) has been set at 0 db, thus giving the maximum density. Note also, that a 1-watt transponder power level is used.

P_T	transmitted power 1 watt	+30.0 dbm
G_T	spacecraft antenna gain	0.0
G_R	ground antenna gain	19.0 db
L	system loss	0.0
$1/KT_s$	(T_s assumed to be 584°K)	+171.0 dbm
A_s	space loss for F = 136 MHz and R = 10^3 KM	-135.1 db
	Total	84.9 db

The assumed S-Band downlink parameters are given below. Figure 4-8 shows the corresponding received signal-to-noise power density ratio. Again, the system loss factor has been set to 0 db.

P_T	transmitted power 1 watt	+30.0 dbm
G_T	spacecraft antenna gain	0.0 db
G_R	ground antenna gain	36.5 db
L	system loss factor	0.0 db
$1/KT_s$	(T_s assumed to be 463°K)	+172.0 dbm
A_s	space loss for F = 2.3 GHz and R = 10^3 Km	-159.6 db
	Total	78.9 db

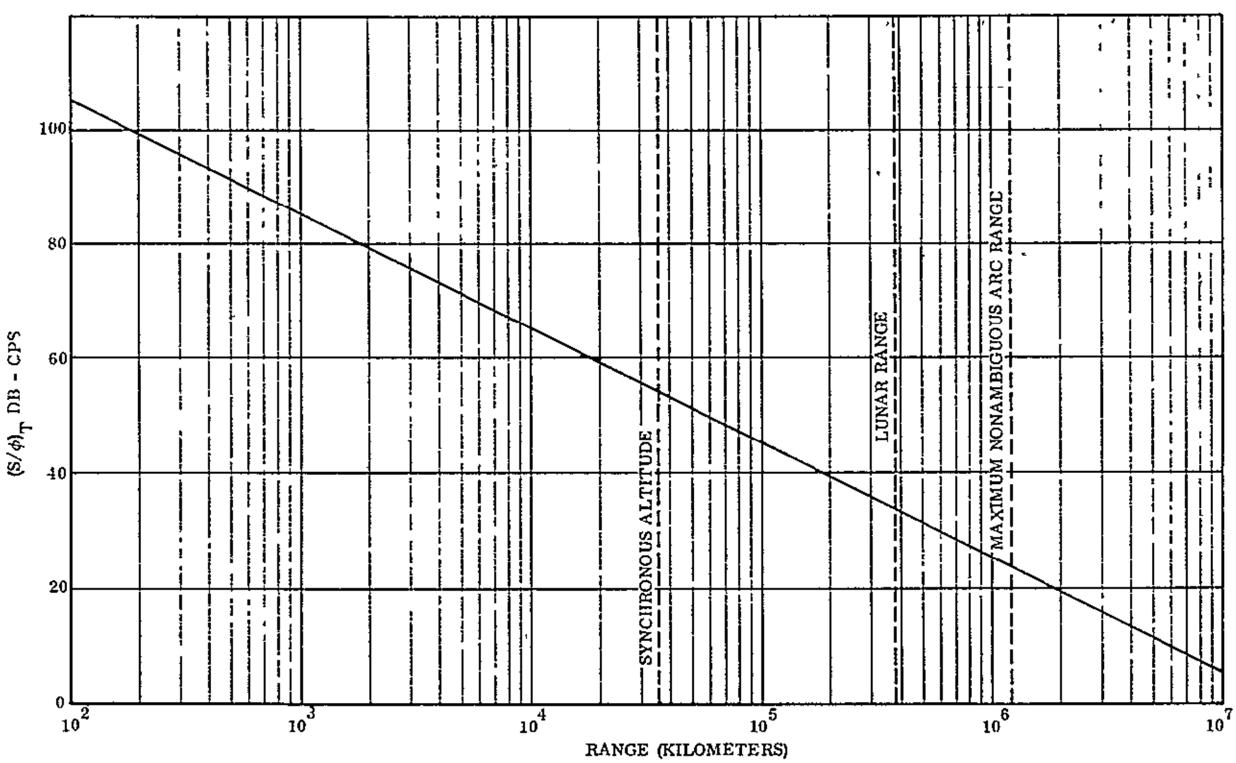

Figure 4-7. VHF Downlink Signal-to-Noise Power Density Ratio vs. Range ("Normalized" Case)

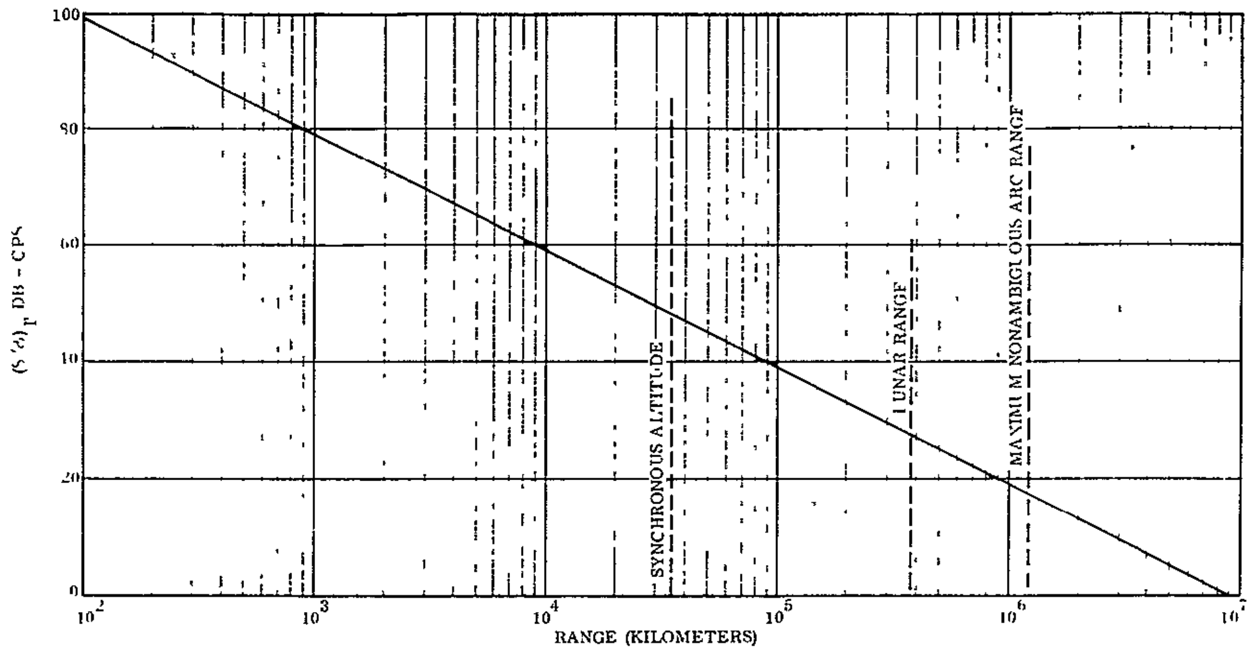

Figure 4-8. S-Band Downlink Signal-to-Noise Power Density Ratio vs. Range ("Normalized" Case)

4.3 RECEIVER ANALYSIS

4.3.1 Receiver Frequency Selection

Operating frequencies for the multifunctional receiver (MFR) have been further analyzed since the submission of the original proposal. A new computer program has been developed which adds a level analysis to the computation. The new program functions in the same manner as did the first in that a frequency mixer, accompanied by an input and output filter, is assumed. The input signal and local oscillator are then searched through a predetermined range and the output is examined for undesired combinations of the input and local oscillator signal. In addition, the new program examines each spurious response calculated and compares its level at the output of the mixer to the specified spurious response. The level calculation makes use of preprogrammed rejection levels for various order spurs, as well as peculiar rejection levels for special combinations of signal and local oscillator harmonics. For example: a $5F_S - F_L$ spur and $4F_S - 2F_L$ spur are both 6th-order terms, but the $4F_S - 2F_L$ spur will be rejected in a balanced mixer by a greater degree than will the $5F_S - F_L$ spur. Also entered in the level calculation is the shape factor of the input and output filters. That is, the attenuation of the filter skirts is subtracted from the spurious level for any input signal or output spur which falls outside of the flat band of the filters.

Therefore, the printout from this computer program will indicate spurious-free regions including those where the level calculation indicates that in-band spurs are below the specified spurious rejection level. For GRARR applications, this level is 70 db.

4.3.1.1 SELECTION OF THE FIRST IF. The level analysis program has been used to examine the five frequency bands required to operate with the MFR. Figure 4-9 presents the spurious-free regions selected by the computer. Figure 4-10 is a sample print-out for the 2200-2300 MHz mixer. Mixer design data shown in Figure 4-11 was entered in the computer to permit a level analysis. The entered data consists of two data sets. The first set lists a general relationship between spurious level and order through the 9th order. The second data set lists data for particular spurs obtained from published data and from measurements performed at the Contractor's facility. In the computer calculation for a given spur, the information from data set 2 always has priority over that from data set 1.

The results shown in Figure 4-9 indicate a relatively wide selection of first intermediate frequencies are available, based on consideration of the first mixer only. If a choice is made so that a portion of the 100 MHz first IF overlaps the 400-410 MHz band (which permits this band to be received without conversion) then the region from 310 MHz to 451 MHz is essentially available. Note that several small gaps occur in this region due to the 135-139 MHz band.

However, to make a final selection for the first IF, it is necessary to weigh considerations other than just this computer output. That is, while this program has reduced considerably the number of trial and error calculations required to choose the first IF, there are several trade-offs to be resolved. These include:

a. Choice of a first IF which permits the local oscillator signals to be synthesized easily from available signals.

b. Frequency limitations of mixers and preamplifiers.

c. Choice of a first IF which permits a 20 MHz band to be translated to the second IF.

Of the three considerations listed above, the third has the most significance. That is, the requirement to handle a 100 MHz bandwidth at the first IF dictates that the center frequency be as high as possible to minimize the percentage bandwidth, $\Delta f/f_o$, since the spurious problems in the second mixer increase rapidly as this percentage increases. Based on this consideration, 450(±50) MHz was tentatively selected as the first choice. A thorough study was then made to examine the following: (1) generation of first local oscillator signals for the four receive bands, (2) generation of the adjustable second local oscillator signal and the required doppler extractor sub-multiple outputs, and (3) the conversion to the second IF of a 20 MHz wide data bandwidth, with various filter configurations preceding the second mixer. Each of these areas of investigation indicated that the choice of 400 - 500 MHz was optimum. Figure 4-12 depicts each of the first converters and suggests the method for deriving the first local oscillator signals. All local oscillator drive signals are available from a Hewlett-Packard 5110B frequency synthesizer.

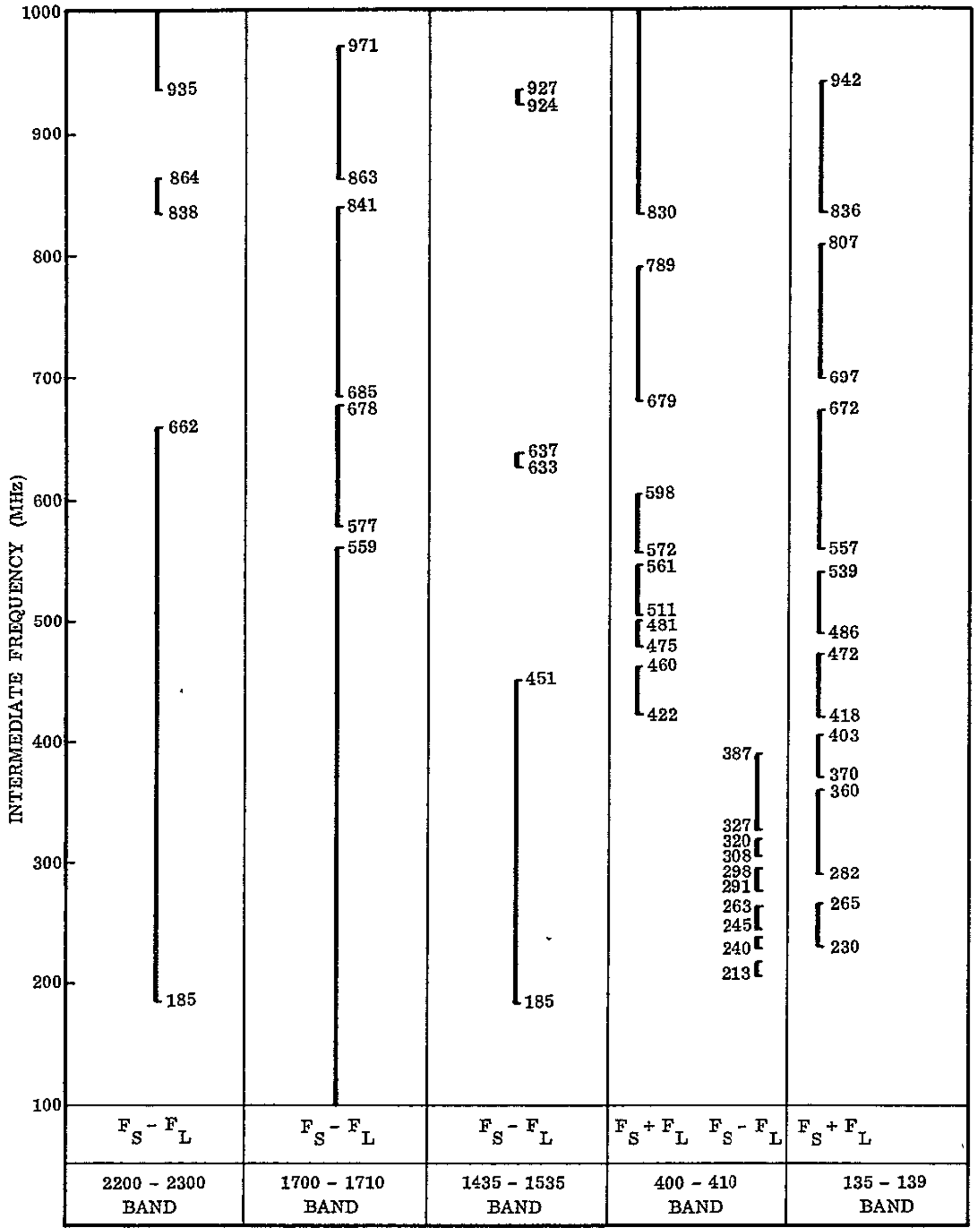

Figure 4-9. Possible Spurious-Response Free Regions

SPUR FREE IF SYNTHESIS

ALL SPURS THROUGH THE 9TH ORDER

CONVERTER M1-----------------------------------LOW SIDE DIFFERENCE MIXING (IF=FS-FL)

ALL FREQUENCIES IN MHZ ALL SPURS DOWN 70DB

INPUT DATA	INPUT	OUTPUT	
FREQ CONSIDERED	2250.0000	100 0000-10000 0000	
FLAT BANDWIDTH	100 0000	100.0000	
FILTER SHAPE FACTOR	3.0000	1.0000	FOR A CUTOFF FREQ. DOWN 70DB

SPUR FREE IF FREQUENCIES		SPURS LIMITING FREQUENCY		SIZE OF
MINIMUM	MAXIMUM	LOWER LIMIT	UPPER LIMIT	BAND
185.715	661.905	3FS -3FL	3FS -4FL	476.190
838.096	864 286	3FS -4FL	-2FS 4FL	26.190
935.715	1014 287	-2FS 4FL	2FS -3FL	78.572

Figure 4-10. Printout of 2200-2300 MHz Converter Spur-Free Regions

MIXER DESIGN DATA

SPUR ORDER	DB DOWN
1	10
2	0
3	30
4	40
5	45
6	50
7	55
8	65
9	70

MIXER DESIGN DATA CONTINUED

INPUTED SPURS---DB DOWN

0FS	1FL	25	0FS	2FL	35	0FS	3FL	40	0FS	4FL	45	0FS	5FL	55	0FS	6FL	55
0FS	7FL	70	1FS	0FL	20	2FS	0FL	50	3FS	0FL	70	4FS	0FL	70	5FS	0FL	70
6FS	0FL	70	7FS	0FL	70	2FS	-1FL	70	2FS	-2FL	70	3FS	-1FL	55	3FS	-2FL	70
3FS	-3FL	30	4FS	-1FL	70	4FS	-2FL	70	4FS	-3FL	70	4FS	-4FL	65	5FS	-1FL	70
5FS	-2FL	70	5FS	-5FL	70	6FS	-1FL	70	-1FS	2FL	40	-1FS	3FL	10	-1FS	4FL	45
-1FS	5FL	35	-1FS	6FL	50	-2FS	2FL	70	-2FS	3FL	70	-2FS	4FL	60	-2FS	5FL	70
-3FS	3FL	30	-3FS	4FL	70												

Figure 4-11. Input Data

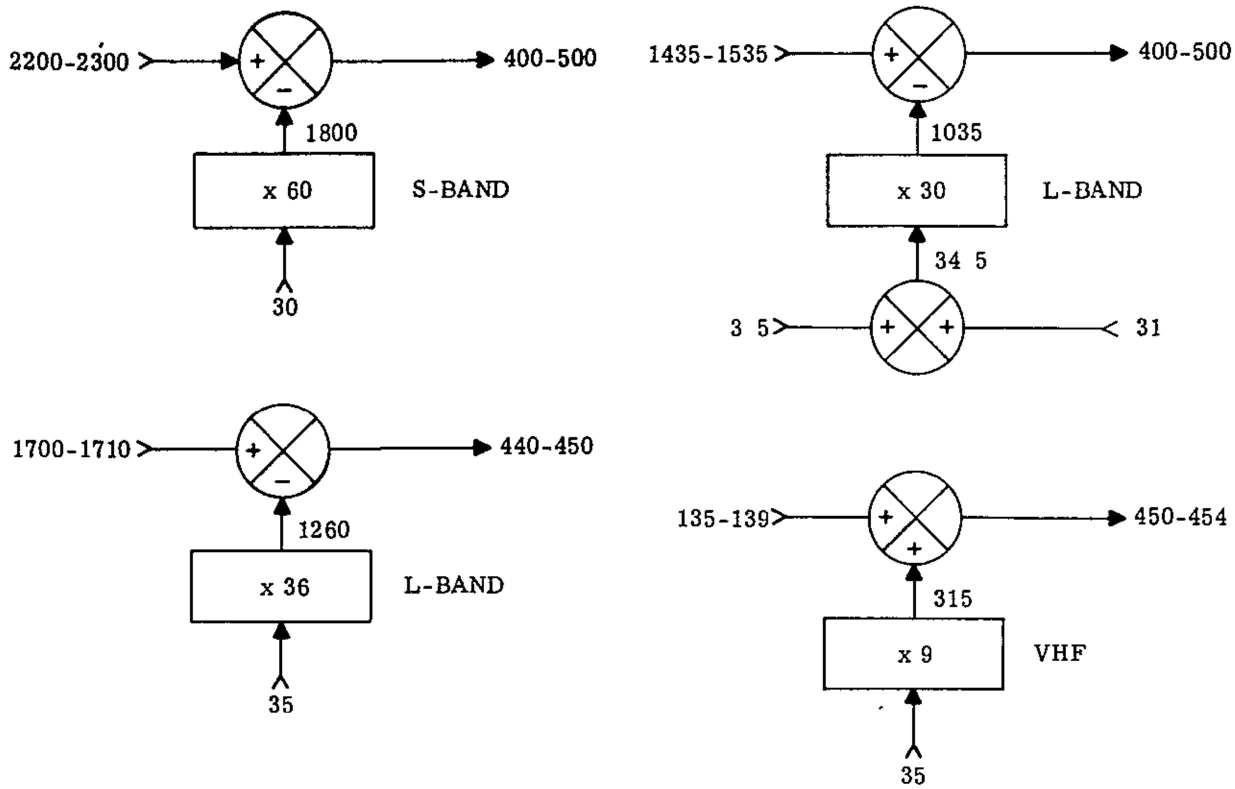

Figure 4-12. First Converters Used with MFR

4.3.1.2 SELECTION OF THE SECOND IF. Computational analysis for the second conversion rapidly established that a wide selection for a second IF was available, using "high-side" mixing (F_L - F_S = IF), if a 20 MHz wide tunable filter preceded the mixer. Such filters, however, are questionable in a diversity ranging system such as GRARR where the group delay stability must be carefully maintained. In a polarization diversity ranging system, either sum channel or a combination of both may supply the range tone data. Therefore, the group delays of each sum channel must be closely matched. Paragraph 4.5.4.5.4.1 of the specification states that the variation shall be less than 3.5 nanosec between channels over the signal dynamic range. While the delay variation through the tunable filters could be corrected for any given setting to less than 3.5 nanosec, this degree of matching could not be maintained over the 80 MHz tuning range of the filters. Any readjustment of the filters would require a new calibration and adjustment of sum channel delay.

To avoid this situation, the Contractor has investigated an alternate filtering scheme preceding the second mixer. An arrangement with switched-selected filters has been analyzed which avoids the problems inherent with the tunable filter. One constraint on the switched filter design is that a 20 MHz overlap must exist between adjacent filters in order to permit any 20 MHz portion of the 100 MHz band to be converted to the second IF. At the same time, a 70 db spurious response must be maintained.

Several other factors affecting the choice of the second IF are apparent. If an IF less than 100 MHz is chosen, then a severe interference problem can exist due to second LO cross-talk, when more receivers are added to the system. That is, the second LO from one MFR could appear within the receive band of another MFR. This problem is removed if the second IF is greater than 100 MHz.

On the other hand, as the second IF is increased, the requirements for minimum phase and group delay variations versus AGC become more difficult to solve. Therefore, it is desirable to select a second IF greater than 100 MHz, but no greater than is necessary to avoid the interference problem.

A frequency of 110 MHz was selected and computer analyses were made with several different switched-filter combinations. The results indicated that the spurious response specification of 70 db could be met using three switched filters. The lowest order spur that could be troublesome was $2F_L - 2F_S$. The three filters shown in Figure 4-13 were chosen to minimize this spur equally on all of the three positions. In each case the interfering signal which would cause the $2F_L - 2F_S$ spur is 30 MHz removed from the flat bandwidth of the filters. This is adequate to meet the 70 db specification. Fifth and seventh order spurious responses caused by $3F_S - 2F_S$ and $4F_S - 3F_L$ occur in band in the selected combination. However, these responses have been measured by the Contractor for a double-balanced hot carrier diode mixer similar to the one which will be used in the MFR. Both of these spurs were down greater than 75 db from the desired response using the operating levels that will exist in the receiver.

4.3.1.3 SELECTION OF THE THIRD IF. A wide selection of spurious-free frequencies, ranging from 7.5 to 25 MHz, is available according to a computer analysis. The choice then may be made with simplicity of the system signal source as a criterion, as well as compatibility with the existing VHF GRARR ranging equipment. 10 MHz is a logical selection since the system signal source design can then function with either the new or old VHF doppler extractor. Also, the third LO is 100 MHz, and the reference signals for the various phase detectors are directly synthesized from outputs available from the HP 5110B driver.

The operating frequencies selected for the MFR and the associated first converters are summarized in Table 4-10.

Table 4-10. MFR Operating Frequencies

Receive Band (MHz)	1st LO (MHz)	1st IF (MHz)	2nd LO (MHz)	2nd IF (MHz)	3rd LO (MHz)	3rd IF (MHz)
135 - 139	315	450 - 454	560 - 564	110	100	10
400 - 410	-	400 - 410	510 - 520	↑	↑	↑
1435 - 1535	1035	400 - 500	510 - 610			
1700 - 1710	1260	440 - 450	550 - 560	↓	↓	↓
2200 - 2300	1800	400 - 500	510 - 610	110	100	10

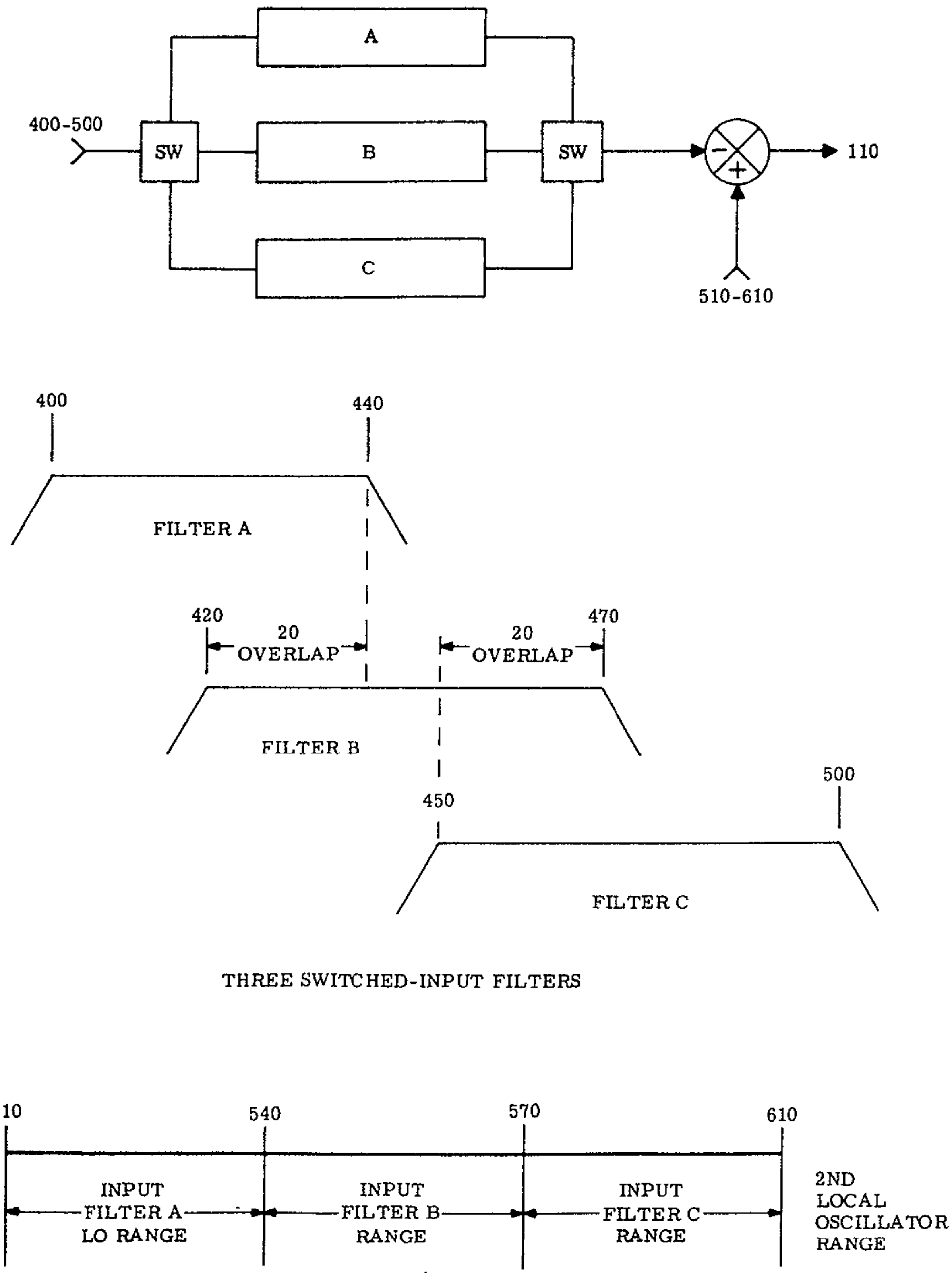

Figure 4-13. Second Converter with Three Input Filters

4.3.2 Diversity Phase Lock Loop Analysis

A linearized model of the diversity phase lock loop which will be used in the multifunctional receiver is shown in Figure 4-14. The assumptions made in this model are that the primary and both secondary loops are locked, with small error signals, and that the receiver AGC circuits hold the input signals constant, as well as provide the proper weighting signals, A_A and A_B, to the diversity combiner.

The subscript notations "A" and "B" used on the diagram refer to the two received polarizations. The following definitions can be made:

$\theta_{INA}(s)$ = Laplace transform of Channel A input phase

$\theta_{INB}(s)$ = Laplace transform of Channel B input phase

$\theta_{OA}(s)$ = Laplace transform of Channel A output phase

$\theta_{OB}(s)$ = Laplace transform of Channel B output phase

$\theta_{VA}(s)$ = Laplace transform of Channel A secondary loop output phase

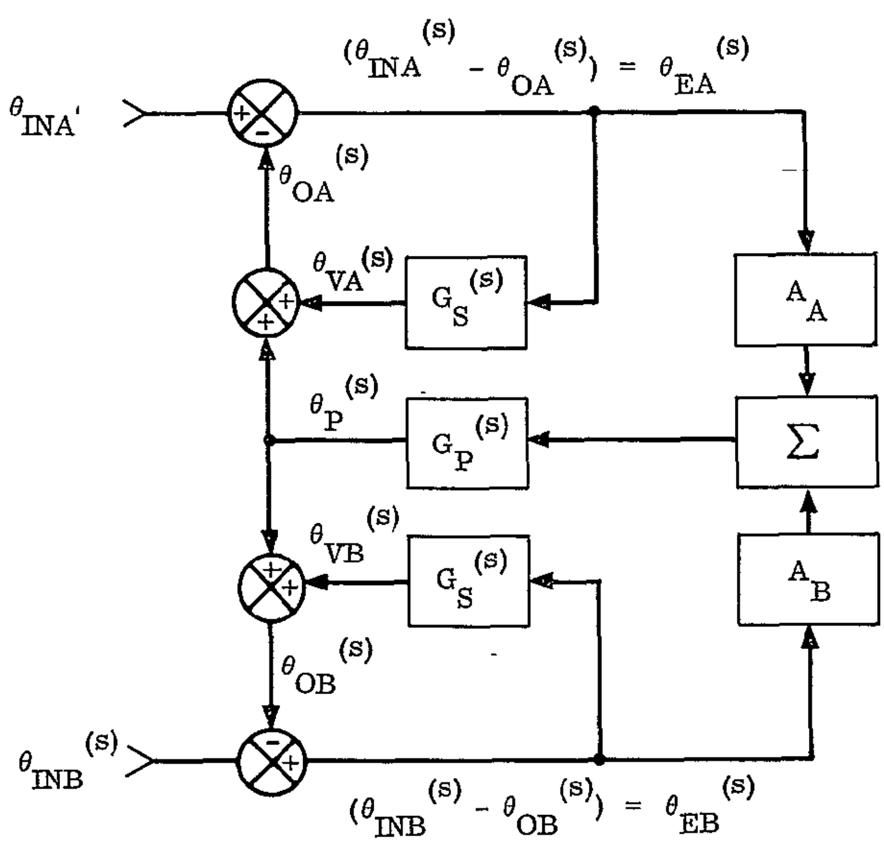

Figure 4-14. Linear Model, Diversity Phase Lock Loop

$\theta_{VB}(s)$ = Laplace transform of Channel B secondary loop output phase

$\theta_P(s)$ = Laplace transform of primary loop output phase

$G_S(s)$ = Open Loop transfer function of secondary loop

$G_P(s)$ = Open Loop transfer function of primary loop

$A_A = \dfrac{a_A}{a_A + a_B}$, $A_B = \dfrac{a_B}{a_A + a_B}$ are the weighting functions for the diversity combiner.

The open loop equation for each channel can be written. (The Laplace operator notation is dropped for simplicity.)

$$\theta_{OA} = \theta_{VA} + \theta_P = \theta_{EA} G_S + (A_A \theta_{EA} + A_B \theta_{EB}) G_P \quad (1)$$

$$\theta_{OB} = \theta_{VB} + \theta_P = \theta_{EB} G_S + (A_A \theta_{EA} + A_B \theta_{EB}) G_P \quad (2)$$

Also, the weighted average output phase,

$$\theta_O = A_A \theta_{OA} + A_B \theta_{OB}$$

can be defined and obtained from equations (1) and (2).

$$\theta_O = A_A \theta_{OA} + A_B \theta_{OB} = \left[A_A \theta_{EA} + A_B \theta_{EB}\right] G_S + \left[A_A \theta_{EA} + A_B \theta_{EB}\right] G_P \quad (3)$$

The weighted average input phase is also defined,

$$\theta_{IN} = A_A \theta_{INA} + A_B \theta_{INB}$$

and note that

$$\theta_O = \theta_P + A_A \theta_{VA} + A_B \theta_{VB}$$

Therefore, equation (3) can be rearranged.

$$\theta_O = (\theta_{IN} - \theta_O)\, G_S + (\theta_{IN} - \theta_O)\, G_P \quad \text{or} \tag{4}$$

$$\frac{\theta_O}{\theta_{IN} - \theta_O} = G_S + G_P = G_O$$

We now define, $G_O = G_S + G_P$, as the sum of the primary and secondary open loop functions and

$$\frac{\theta_O}{\theta_{IN}} = \frac{G_O}{1 + G_O} = C_O \tag{5}$$

That is, the primary and secondary open loop transfer functions add together to form a resultant open loop function, G_O, and a closed loop function, C_O, which determine how the average input phase is tracked.

Similarly, the weighted average input phase difference θ_{IND}, and output phase difference, θ_{OD}, can be defined:

$$\theta_{IND} = A_A \theta_{INA} - A_B \theta_{INB}$$

$$\theta_{OD} = A_A \theta_{VA} - A_B \theta_{VB}$$

Then from equations (1) and (2)

$$\theta_{OD} = \left[A_A \theta_{EA} - A_B \theta_{EB}\right] G_S \tag{6}$$

Since $A_A \theta_{EA} - A_B \theta_{EB} = (A_A \theta_{INA} - A_A \theta_{VA}) - (A_B \theta_{INB} - A_B \theta_{VB})$

$$\theta_{OD} = (\theta_{IND} - \theta_{OD})\, G_S \quad \text{or} \tag{7}$$

$$\frac{\theta_{OD}}{\theta_{IND} - \theta_{OD}} = G_S$$

$$C_S = \frac{G_S}{1 + G_S} = \frac{\theta_{OD}}{\theta_{IND}} \tag{8}$$

That is, the secondary loop filter is required to track only the input phase differences between received polarizations. This result is important in determining the design of the primary and secondary loop filters. The primary loop filter can be designed so as to track essentially all input signal dynamics which are common to both polarizations, while the secondary loops respond only to the differences between polarizations. This design yields the maximum advantage of the diversity loop which is that the secondary loops acquire phase lock automatically without aiding controls. If the secondary loops were permitted to track carrier doppler shift, for example, then a secondary channel which lost lock during a deep polarization fade might be unable to reacquire unaided at the end of the fade. This would occur since a frequency difference would exist between the locked and unlocked secondary VCO's.

Therefore, the design approach described in the following paragraph was chosen to minimize the dynamic response of the secondary loops to input signal dynamics common to both polarizations.

4.3.2.1 PRIMARY AND SECONDARY LOOP SELECTION. Based on the results from equations (5) and (8) above, the loop design involves determining G_O and G_S, since G_P must then result from $G_P = G_O - G_S$.

A model of the composite phase lock loop, C_O, is shown in Figure 4-15. This model is convenient for determining the dynamic response of the diversity loop to inputs common to both polarizations. The assumption is made that the secondary loops correct for differences between polarizations. The model is valid without this assumption when the received signal levels differ by more than 12 db, since the diversity combiner essentially removes the weaker signal from the loop.

The closed loop transfer function C_O, must track the specified frequency ramps (Specification Paragraph 4.5.4.2.3) without exceeding a steady state phase error of 0.1 radians.

The specification implies a third order loop filter, since a second order type is incapable of following the specified rates while remaining locked.

The composite third order loop filter design to be used in the MFR has the following idealized open and closed loop functions.

$$G_O = \frac{9/4\ \omega_o \left(s + \frac{\omega_o}{3}\right)^2}{s^3} \tag{9}$$

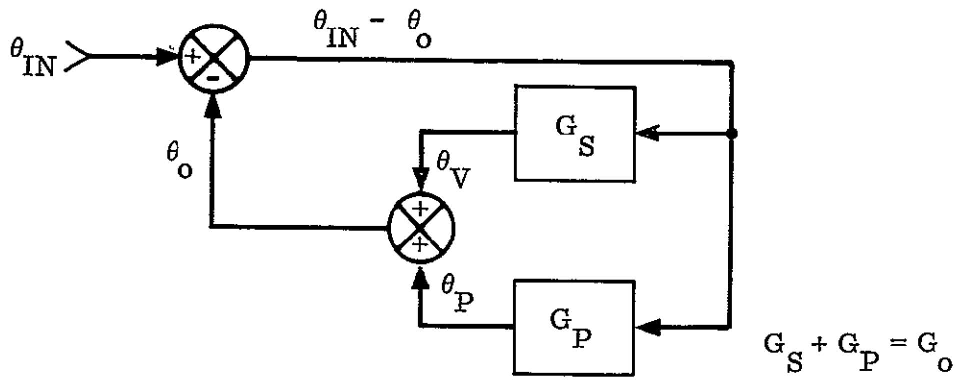

Figure 4-15. Simplified Composite Phase Lock Loop

$$C_O = \frac{G_O}{1 + G_O} = \frac{9/4\ \omega_o \left(s + \frac{\omega_o}{3}\right)^2}{\left(s + \omega_o\right)^2 \left(s + \frac{\omega_o}{4}\right)} \tag{10}$$

This transfer function has been used by the Electronics Division in other phase lock receivers (SC-755, APDAR, ATSR Carrier Receiver-Demodulator).

The two-sided noise bandwidth of the loop is obtained from

$$2B_{nO} = \frac{1}{2\pi} \int_{-\infty}^{\infty} \left|C_O(j\omega)\right|^2 d\omega \tag{11}$$

which can be evaluated from a tabulation given in Reference 9.

Then, the one-sided noise bandwidth is

$$\underset{(Hz)}{B_{nO}} = 0.743\ \omega_o \text{ rad/sec} \tag{12}$$

The secondary loop filter design to be used is a second order type with the idealized open and closed loop functions.

$$G_S = \frac{\sqrt{2}\,\omega_S\left(s + \frac{\omega_S}{\sqrt{2}}\right)}{s^2} \tag{13}$$

$$C_S = \frac{G_S}{1 + G_S} = \frac{\sqrt{2}\,\omega_S\left(s + \frac{\omega_S}{\sqrt{2}}\right)}{s^2 + \sqrt{2}\,\omega_S\,S + \omega_S^2} \tag{14}$$

The selection of this loop design for the secondary loop filter is based on several practical considerations regarding the operation of the receiver. Since the secondary loops must acquire without operator aid, that is, unassisted by VCO tuning, a second order loop has definite advantage over a first order loop (Reference 10). A third order type filter is undesirable in the secondary loop since the secondary VCOs would then tend to track the input frequency ramp in conjunction with the primary VCO. As equation (8) indicates, the secondary loops are required to track only the input differences between polarizations. Since these differences are essentially phase shifts due to multipath effects and satellite motion, the dynamic pulling range of the secondary VCOs need not be large. This factor is in agreement with the requirement that a channel which has faded and unlocked, reacquire automatically. The locked and unlocked secondary VCOs will be close in frequency, if the primary VCO has been tracking the input doppler shift during the fade, and reacquisition can occur.

The noise bandwidth of the secondary loops is found:

$$2B_{nS} = \frac{1}{2\pi}\int_{-\infty}^{\infty} \left|C_S(j\omega)\right|^2 d\omega \tag{15}$$

$$\underset{(\mathrm{Hz})}{B_{nS}} = 0.530\ \omega_S\ (\mathrm{rad/sec}) \tag{16}$$

The specification requires the approximate ratio

$$\frac{B_{nO}}{B_{nS}} \cong 3 \cong \frac{0.743\omega_o}{0.53\ \omega_S}$$

Therefore, $\omega_S = 0.468\ \omega_o$.

For some tracking bandwidth positions, the ratio of primary and secondary bandwidths is 3.33 which modifies the expression only slightly.

We can now find the expression for G_P, the idealized open loop transfer function of the primary loop. From equation (4)

$$G_P = G_O - G_S = \frac{9/4\ \omega_o \left(s + \frac{\omega_o}{3}\right)^2}{s^3} - \frac{\sqrt{2}\ (0.468\ \omega_o \left(s + \frac{0.468\ \omega_o}{\sqrt{2}}\right)}{s^2}$$

$$G_P = \frac{1.59\ \omega_o\ (s + 0.477\ \omega_o)\ (s + 0.329\ \omega_o)}{s^3} \tag{17}$$

The idealized primary and second loop filters can therefore be defined as

$$F_P = \frac{1.59\ \omega_o\ (s + 0.477\ \omega_o)\ (s + 0.329\ \omega_o)}{K_{vP} K_\phi s^2} \tag{18}$$

$$F_S = \frac{2\ (0.468\ \omega_o)\ s + \frac{0.468\ \omega_o}{2}}{K_{vS} K_\phi s} \tag{19}$$

where the K's are the constants for the primary and secondary VCOs and phase detectors. Figure 4-16 is a linear model of the diversity tracking loop.

The filters will be implemented as shown in Figure 4-17. The filters are designed such that the passive filters, R_1, R_2, C_2 and R_5, R_6, C_3, are not loaded by R_3 and R_8. The ratio of R_1/R_2 is made 200 in order to minimize the static error due to a frequency ramp. The gain of the operational amplifier, K_A, is not less than 10^6. Therefore the primary filter transfer function is

$$F_{(p)} = \left[\frac{R_2}{R_1 + R_2}\right]\left[\frac{R_4}{R_3}\right]\left[\frac{S + \frac{1}{C_1 R_2}}{S + \frac{1}{C_1 (R_1 + R_2)}}\right]\left[\frac{S + \frac{1}{C_2 R_4}}{S + \frac{1}{(R_4 + [K + 1]\ R_3)\ C_2}}\right] \tag{20}$$

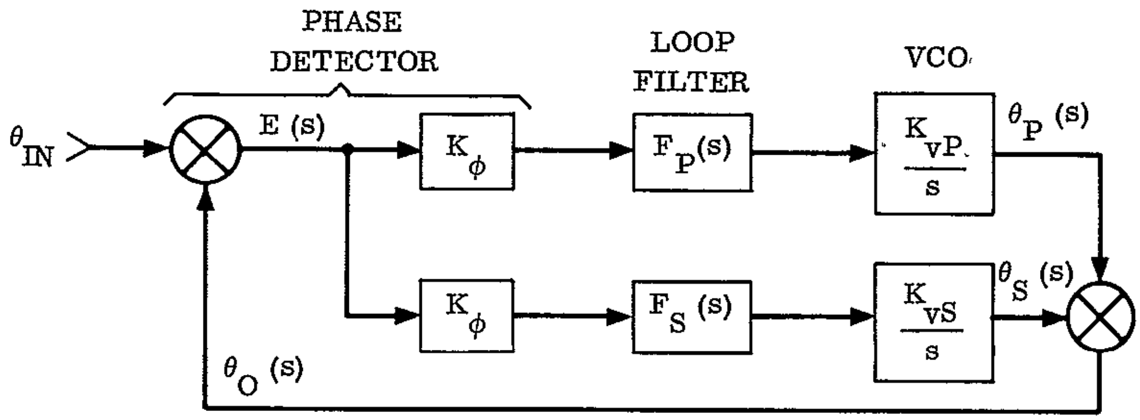

Figure 4-16. Composite Phase Lock Loop

We set

$$\frac{1}{C_1R_2} = 0.477\ \omega_o \quad \text{and} \quad \frac{1}{C_2R_4} = 0.329\ \omega_o$$

Then

$$\frac{1}{C_1(R_1 + R_2)} = 0.00238\ \omega_o \quad \text{and} \quad \frac{1}{C_2(R_4 + [K+1]\,R_3)} \approx \frac{1}{KC_2R_3}$$

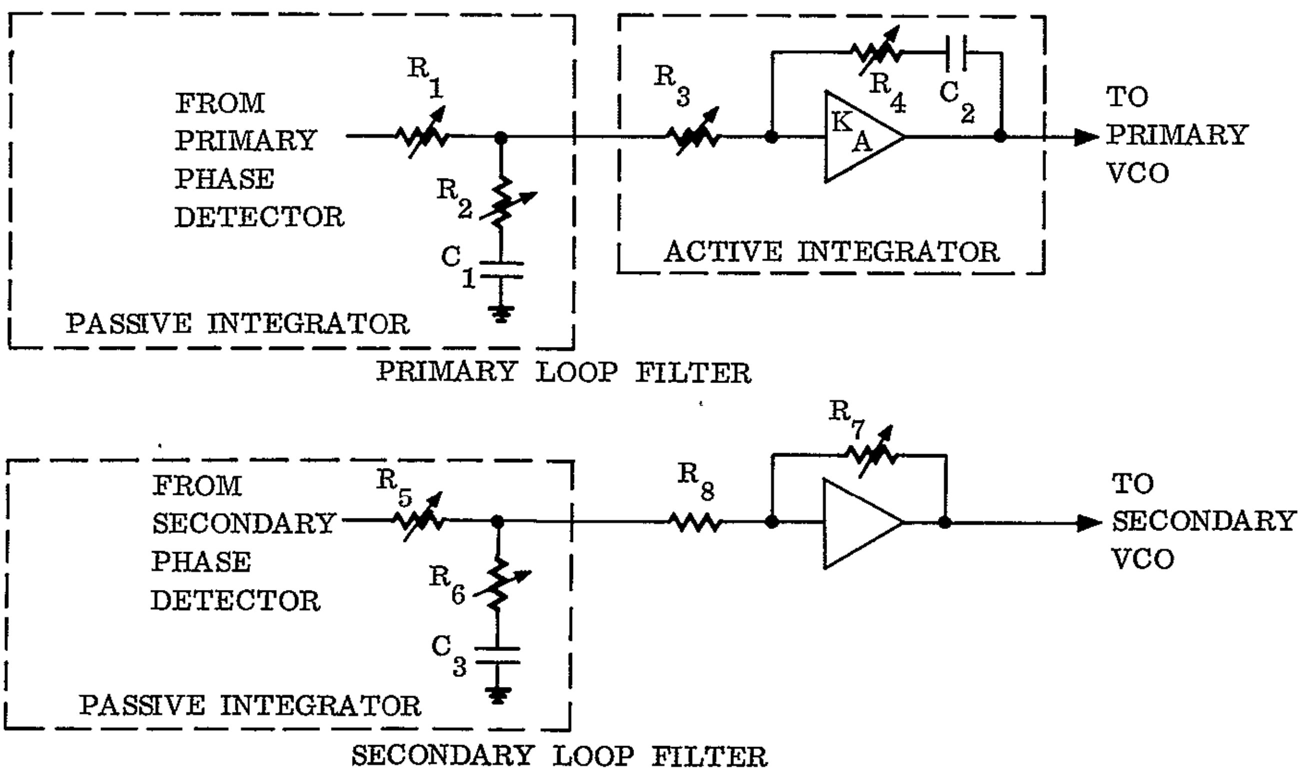

Figure 4-17. Loop Filters

The phase detector and VCO constants for the primary loop are:

$$K_{vP} = 75 \text{ KHz/v} = 4.71 \times 10^5 \text{ rad/sec-v}$$

$$K_\phi = 0.25 \text{ v/rad}$$

For purposes of determining the values of resistors R_1 through R_4 for the different tracking bandwidths, the poles $\frac{1}{C_1(R_1+R_2)}$ and $\frac{1}{K C_2 R_3}$ can be neglected. Therefore, from equations 18 and 20, the required expression is

$$\left(\frac{R_4}{R_3}\right)\left(\frac{R_2}{R_1+R_2}\right)(K_{vP})(K_\phi) = 1.59\ \omega_o$$

$$\left(\frac{R_4}{R_3}\right)\left(\frac{4.71)\ (0.25)\ (10^5)}{200}\right) = 1.59\ \omega_o \text{ and } R_4/R_3 = 27.0 \times 10^4\ \omega_o$$

The pole of the active integrator can now be determined

$$\frac{1}{KC_2R_3} = \frac{27.0\ (10^{-4})\ \omega_o}{KC_2R_4} = 8.89\ \omega_o^{\ 2}\ (10^{-10}) \text{ rad/sec}$$

This pole can be neglected for most dynamic calculations since the pole of the passive filter is more significant. For example, in the 3000 Hz bandwidth, where $\omega_o = 4.04 \times 10^3$ rad/sec

$$\frac{1}{C_1(R_1+R_2)} = 0.00237(4.04)\ 10^3 = 9.56 \text{ rad/sec}$$

while

$$\frac{1}{KC_2R_3} = 8.89(4.04)^2\ (10^6)(10^{-10}) = 0.0145 \text{ rad/sec}$$

The primary open loop function is then

$$G_P = \frac{1.59\,\omega_o\,(s + 0.477\,\omega_o)(s + 0.329\,\omega_o)}{s^2\,(s + 0.00237\,\omega_o)} \tag{21}$$

The secondary filter transfer function as implemented is

$$F_S = \left[\frac{R_7}{R_8}\right]\left[\frac{R_6}{R_5 + R_6}\right]\left[\frac{s + \dfrac{1}{C_3 R_6}}{s + \dfrac{1}{C_3 (R_5 + R_6)}}\right] \tag{22}$$

In this filter, $(R_5 + R_6) \approx 15R_6$. The ratio is not made larger in order that the zero frequency gain of the filter, R_7/R_8, be minimized. This is desirable in order to minimize the required pulling range of the secondary VCOs due to such static input errors as phase tracking errors, phase alignment errors and drift in operational amplifiers. The imperfection in this integrator does not compromise the operation of the diversity loop since long term frequency differences between polarizations are not experienced.

The secondary open loop transfer function is then:

$$G_S = \frac{\sqrt{2}\,(0.468\,\omega_o)\left(s + \dfrac{0.468}{\sqrt{2}}\,\omega_o\right)}{s\left(s + \dfrac{0.0335}{\sqrt{2}}\,\omega_o\right)} = \frac{0.662\,\omega_o\,(s + 0.331\,\omega_o)}{s\,(s + 0.024\,\omega_o)} \tag{23}$$

The composite open loop filter can now be found

$$G_O = G_P + G_S = \frac{1.59\,\omega_o (s+0.477\,\omega_o)(s+0.329\,\omega_o)(s+0.024\,\omega_o) + 0.662\,\omega_o s\,(s+0.331\,\omega_o)(s+0.00237\,\omega_o)}{s^2 (s+0.00237\,\omega_o)(s+0.024\,\omega_o)}$$

and the composite error function is

$$\frac{\epsilon}{\theta_{in}} = \frac{1}{1+G_O} = \frac{s^2\,(s+0.00237\,\omega_o)\,(s+0.024\,\omega_o)}{s^2 (s+0.00237\,\omega_o)(s+0.024\,\omega_o) + 1.59\,\omega_o (s+0.477\,\omega_o)(s+0.329\,\omega_o)(s+0.024\,\omega_o) + 0.662\,\omega_o s\,(s+0.331\,\omega_o)(s+0.00237\,\omega_o)} \tag{24}$$

The steady state error due to a frequency ramp can be determined by applying the final value theorem to the error equations.

$$\lim_{t \to \infty} \epsilon(t) = \lim_{s \to 0} \left[\frac{\epsilon(s)}{\theta_{in}}\right] \cdot \theta_{in} \cdot s = \left[\frac{\epsilon(s)}{\theta_{in}}\right] \cdot \frac{\ddot{\theta}}{s^3} \cdot s$$

The result is

$$\epsilon = \frac{0.0095\ (\ddot{\theta})}{\omega_o^2}$$

Taking the 3000 HZ bandwidth, the error due to frequency ramp of $20 \times 10^6 (\mathrm{Hz})^2$ is found to be 0.073 radians which is within the specified 0.1 radian error for such an input. It is of interest to note that the pole, $\frac{1}{KC_2R_3}$, is negligible for the frequency ramps and VCO range specified for the MFR. In the 10 Hz bandwidth, the time for the specified $200(\mathrm{Hz})^2$ ramp to traverse the 600 KHz VCO range is 3000 seconds.

The time constant for the active filter pole is $\frac{10^9}{1.26\omega_o^2} = 2.74(10^6)$ seconds, or about 1000 times greater than the maximum traverse time. Therefore the assumption of a perfect integrator in the active filter is valid for the specified conditions.

The contribution of the secondary VCO to the output of the composite filter due to an input ramp is of interest since the result will determine the required pulling range of the secondary VCO. Recall from preceeding discussions that it is desirable to minimize the response of the secondary loops to input signals common to both channels. Using the model of Figure 4-15

$$\theta_v = \frac{\theta_{in} G_S}{1+G_O}$$

For a step input phase acceleration, $\ddot{\theta}/s^3$, (frequency ramp)

$$\theta_v = \frac{\theta}{s^3}\left[\frac{0.662\ \omega_O (s+0.331\ \omega_O)(s+0.00237\ \omega_O)}{s^2(s+0.00237\ \omega_o)(s+0.024\ \omega_o)+1.59\ \omega_o (s+0.477\ \omega_o)(s+0.329\ \omega_o)(s+0.024\ \omega_o)+0.662\ \omega_o\ s(s+0.331\ \omega_o)(s+0.00237\ \omega_o)}\right]$$

The solution for the above expression is found to contain a frequency term $\frac{K_1}{s^2}$ and a phase term $\frac{K_2}{s}$. The remaining terms are transients which damp to zero. Note that no $\frac{K}{s^3}$ (frequency ramp) term appears in the error expression, which indicates that the secondary loop does not track the doppler shift on the input signal. However, of interest is the frequency step term which is found to be

$$\frac{K_1}{s^2} = \frac{0.084}{\omega_o} \frac{\ddot{\theta}}{s^2} \tag{26}$$

The maximum step phase acceleration input permitted can be defined as that which produces a peak transient error of $\pi/2$ radians. It can be shown (Reference 11) that for the composite filter this value is

$$\ddot{\theta} = \frac{\omega_o^2 \, \pi/2}{0.56} \tag{27}$$

This is the peak error which would occur at each of the three phase detectors for a step phase acceleration common to both channels. Substituting into equation (26)

$$K_1 = \frac{0.084 \, \omega_o \, \pi/2}{0.56} = 0.236 \, \omega_o \text{ (rad/sec)}$$

For the 3000 Hz bandwidth

$$K_1 = 0.236(4.04)(10^3) = 953 \text{ rad/sec} = 152 \text{ Hz}$$

Therefore, the secondary VCO need have a dynamic pulling range of at least several hundred Hz to accommodate this dynamic input.

4.3.3 Subcarrier Receiver Phase-Locked Loop Analysis

Since the specifications for phase-locked operation of the subcarrier receiver are the same as those for the composite diversity-locked loop of the multifunction receiver, a third order

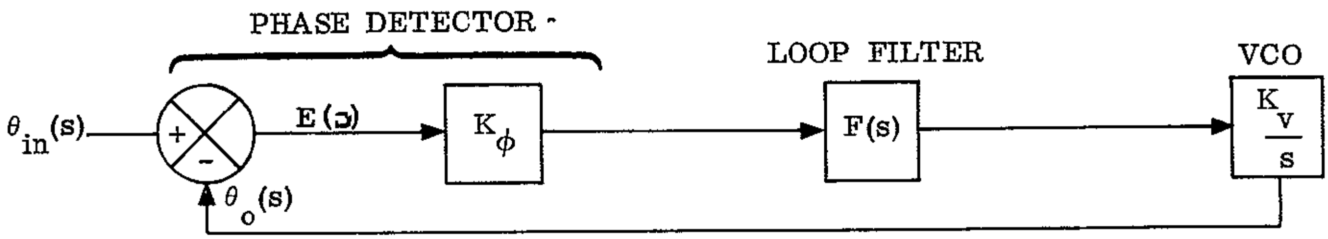

Figure 4-18. Simplified Subcarrier Tracking Loop Model

carrier tracking loop will be designed. An automatic leveling control maintains the subcarrier signal level constant at the phase detector input and, therefore, the loop bandwidth is independent of modulation index. A simplified linear model of the subcarrier tracking loop is given in Figure 4-18.

The important transfer functions for the loop are:

$$\text{Open Loop, } G(s) = \frac{\theta_o(s)}{E(s)} = \frac{K_\phi K_v F(s)}{s} \tag{1}$$

$$\text{Closed Loop, } C(s) = \frac{\theta_o(s)}{\theta_{in}(s)} = \frac{G(s)}{1 + G(s)} = \frac{K_\phi K_v F(s)}{s + K_\phi K_v F(s)} \tag{2}$$

$$\text{Error Function} = \frac{E(s)}{\phi_{in}(s)} = \frac{1}{1 + G(s)} = \frac{S}{s + K_\phi K_v F(s)} \tag{3}$$

where

$\theta_{in}(s)$ = Laplace transform of the input phase function

$\theta_o(s)$ = Laplace transform of the output phase function (VCO)

$E(s)$ = Laplace transform of the VCO tracking error

K_ϕ = phase detector gain constant in volts/radian

K_v = VCO gain constant in radians/sec/volt

$F(s)$ = Laplace transform of loop filter transfer-function

The closed loop transfer function to be used is taken from the work of Mallinckrodt (Reference 11).

$$C(s) = \frac{9\,\omega_o \left(s + \frac{\omega_o}{3}\right)^2}{4\left(s + \frac{\omega_o}{4}\right)\left(s + \omega_o\right)^2} \qquad (4)$$

where ω_o is a parameter that adjusts the loop bandwidth.

Solving equation (2) for G(s)

$$G(s) = \frac{C(s)}{1 - C(s)}$$

Substituting the closed loop transfer function from equation (4) gives the required open loop transfer function.

$$G(s) = \frac{9\,\omega_o \left(s + \frac{\omega_o}{3}\right)^2}{4\,s^3} \qquad (5)$$

From equations (3) and (5) the error function associated with the Mallinckrodt filter is:

$$\frac{E(s)}{\theta_{in}(s)} = \frac{s^3}{\left(s + \frac{\omega_o}{4}\right)\left(s + \omega_o\right)^2} \qquad (6)$$

Plots of the open loop, closed loop, and error functions for the third order loop are given in Figures 4-19 and 4-20.

The two-sided noise bandwidth of the loop is defined as

$$2B_n = \frac{1}{2\pi}\int_{-\infty}^{\infty} \left|C(j\omega)\right|^2 d\omega \qquad (7)$$

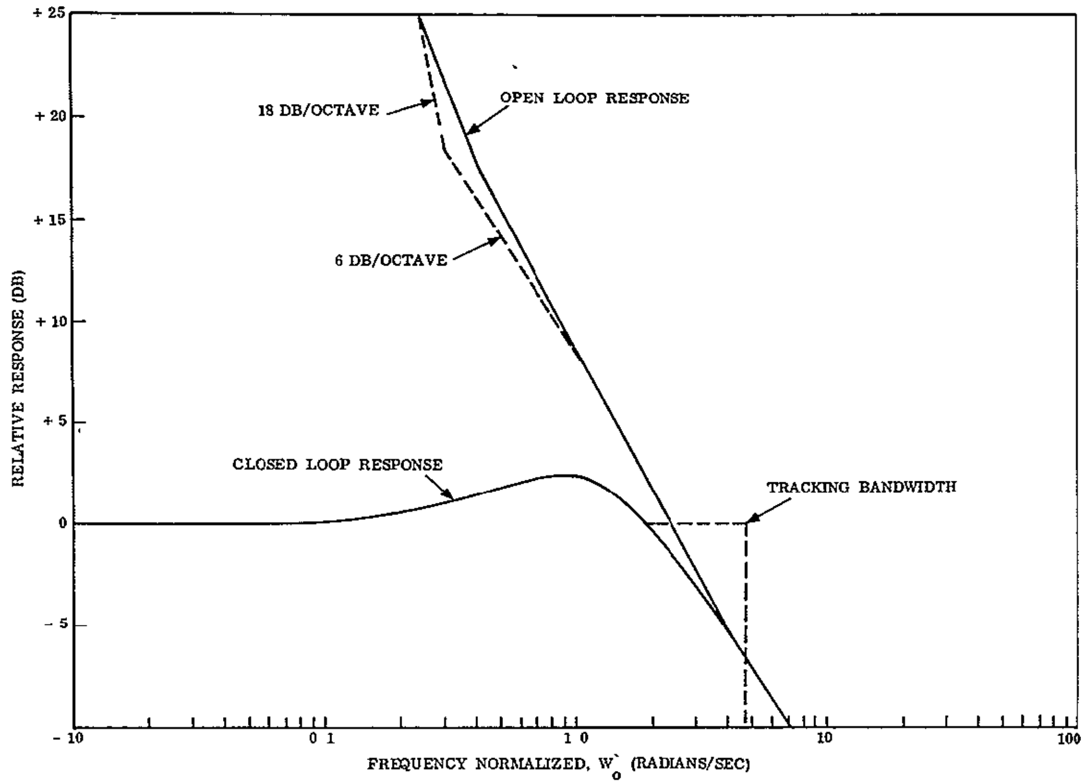

Figure 4-19. Open and Closed Loop Response

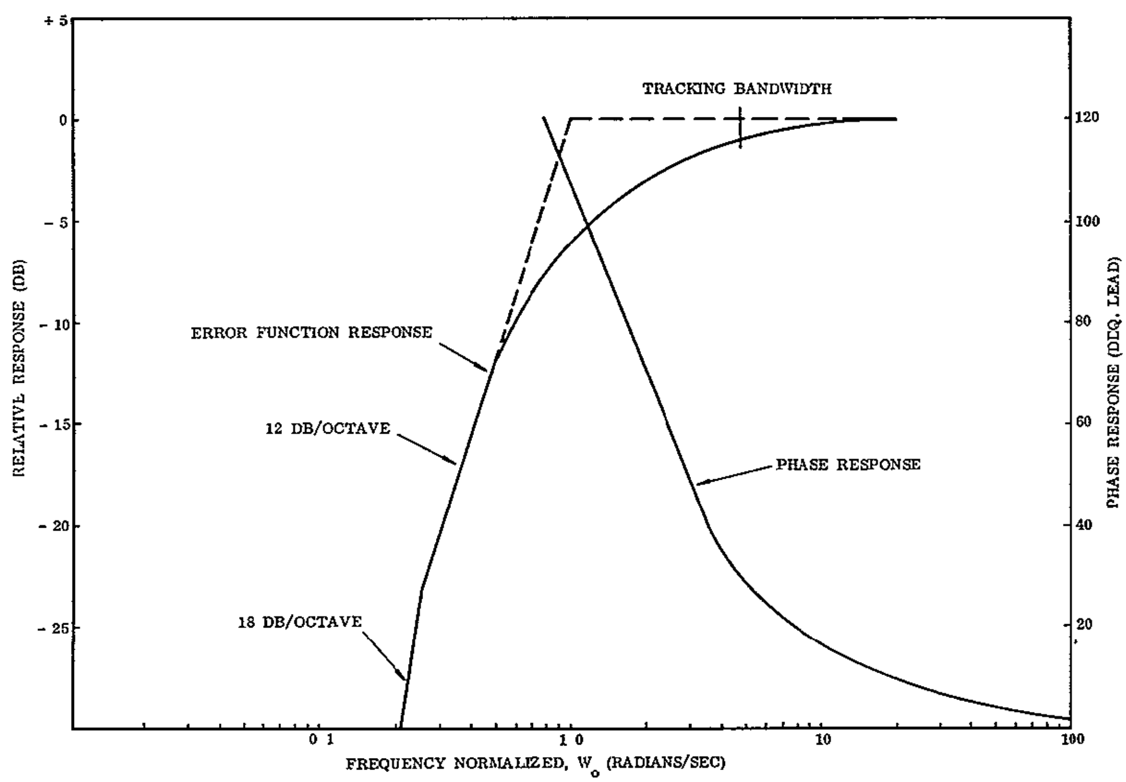

Figure 4-20. Error Function Response

This is evaluated by use of the tables in Reference 9.

$$2B_n = \frac{297}{200}\omega_o = 1.485\,\omega_o$$

or the one-sided loop bandwidth in Hz (loop tracking bandwidth)

$$B_n = 0.743\,\omega_o \tag{8}$$

where ω_o is given in radians per second.

Expressing B_n in radians per second equation (8) becomes

$$B_n = 4.67\,\omega_o \text{ (rad/sec)}$$

Solving equations (1) and (5) for F(s) gives the required loop filter transfer function.

$$F(s) = \frac{9\,\omega_o\left(s + \frac{\omega_o}{3}\right)^2}{4K_\phi K_v s^2} \tag{9}$$

This filter is implemented by the network shown in Figure 4-21. If it is assumed that R_3 does not load the passive integrator network (R_1, R_2, and C_1) and that the amplifier gain is very large ($R_3 > 100R_2$ and $K \approx 1 \times 10^6$), the filter transfer function is given by:

$$F(s) = \left(\frac{R_2}{R_1 + R_2}\right)\left(\frac{R_4}{R_3}\right)\left(\frac{s + \frac{1}{R_2C_1}}{s + \frac{1}{(R_1 + R_2)\,C_1}}\right)\left(\frac{s + \frac{1}{R_4C_2}}{s + \frac{1}{KR_3C_2}}\right) \tag{10}$$

Equating equations (9) and (10) requires the following design procedure:

$$\frac{1}{R_2C_1} = \frac{1}{R_4C_2} = \frac{\omega_o}{3} \tag{11}$$

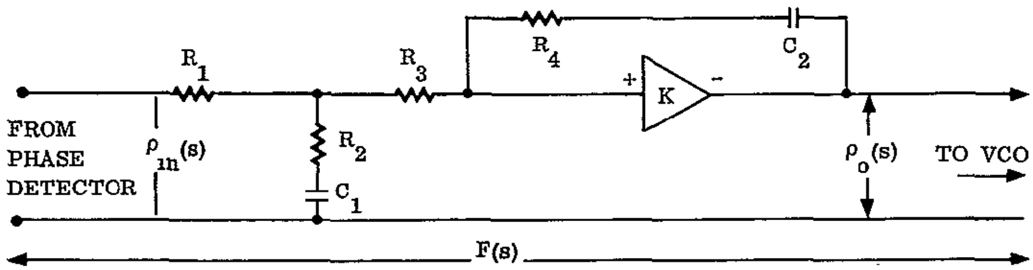

Figure 4-21. Subcarrier Loop Filter Implementation

and

$$\frac{9\,\omega_o}{4K_\phi K_v} = \left(\frac{R_2}{R_1 + R_2}\right)\left(\frac{R_4}{R_3}\right) \tag{12}$$

Resistors R_1, R_2, R_3, and R_4 are varied in discrete steps in accordance with the tracking bandwidth to satisfy equations (11) and (12) and also to satisfy the loading requirements assumed in equation (10). Capacitors C_1 and C_2 remain fixed for all tracking bandwidths to avoid transient problems when the loop bandwidth is changed.

The loop constant ω_o is calculated on the basis of the loop tracking bandwidth, from equation (8). Values of ω_o for the required loop tracking bandwidths are given in Table 4-11.

Table 4-11. ω_o for Loop Tracking Bandwidths

Tracking Bandwidth = B_n (Hz)	ω_o (rad/sec)
10	13.47
30	40.41
100	134.7
300	404.1
1000	1347
3000	4041

Comparison of equations (9) and (10) indicates that the actual transfer function differs from the ideal transfer function because of the imperfect integrators used. Instead of having a second-order pole at $s = 0$ we have a pole $s = \frac{1}{(R_1 + R_2)}\,C_1$ due to the imperfect passive inregrator and at $s = \frac{1}{KR_3C_2}$ due to the imperfect active integrator.

Because of the imperfect integrations the loop becomes first-order at very low frequencies. In order to determine the errors caused by approximating the double integration the poles of F(s), equation (10), are evaluated.

Let the phase detector gain constant, $K_\phi = 0.25$ volt/rad, and the VCO gain constant, $K_v = 0.47 \times 10^6$ rad/sec/volt. Also set $\frac{R_1 + R_2}{R_2} = 200$ and $K = 1 \times 10^6$.

From equation (12)

$$\frac{9\,\omega_o}{4K_\phi K_v} = 19.15 \times 10^{-6}\,\omega_o = \left(\frac{R_2}{R_1 + R_2}\right)\left(\frac{R_4}{R_3}\right)$$

$$\frac{R_4}{R_3} = 38.3 \times 10^{-4}\,\omega_o$$

From equation (11)

$$\frac{1}{R_2 C_1} = \frac{\omega_o}{3} \;;\; \frac{1}{R_4 C_2} = \frac{\omega_o}{3}$$

and

$$R_1 + R_2 = 200R_2 \;;\; R_4 = R_3\omega_o\,(38.3 \times 10^{-4})$$

Therefore the pole due to the passive integrator is

$$\frac{1}{(R_1 + R_2)\,C_1} = \frac{\omega_o}{600} = 6.74 \text{ rad/sec} \qquad \left\{\begin{array}{l} \omega_o = 4041 \text{ rad/sec} \\ B_n = 3000 \text{ Hz} \end{array}\right\}$$

and the pole due to the active integrator is:

$$\frac{1}{R_4 C_2} = \frac{1}{\omega_o\,(38.3 \times 10^{-4})\,R_3 C_2} = \frac{\omega_o}{3}$$

and

$$\frac{1}{KR_3C_2} = \frac{\omega_o^2 \,(38.3 \times 10^{-4})}{3\,(1 \times 10^6)} = \omega_o^2 \,(1.28 \times 10^{-9}) = 2.04 \times 10^{-2} \text{ rad/sec}$$

$$\omega_o = 4041 \text{ rad/sec}$$

$$B_n = 3000 \text{ Hz}$$

From the above relationship it can be seen that as the passive integrator is improved, that is increasing the ratio R_1/R_2, the pole at $\frac{1}{(R_1 + R_2)\,C_1}$ moves toward zero frequency, but the pole at $\frac{1}{KR_3C_2}$ moves away from zero frequency. The high amplifier gain, K, essentially removes the $\frac{1}{KR_3C_2}$ pole and closely approximates a perfect integrator. Practical amplifiers can be built with open loop gains in excess of 1×10^6.

The steady tracking error due to a frequency ramp is zero for the ideal third order loop with the open loop transfer function given in equation (5). However, because the integrations are not perfect, there is a steady state error. The error can be calculated by taking the pole at $\frac{1}{KR_3C_3}$ to be zero and letting the pole $\frac{1}{(R_1 + R_2)\,C_1} = \frac{\omega_o}{600}$. The open loop transfer function becomes:

$$G(s) = \frac{9\,\omega_o \left(s + \frac{\omega_o}{3}\right)^2}{4s^2 \left(s + \frac{\omega_o}{600}\right)} \tag{13}$$

and the error function is:

$$\frac{E(s)}{\theta_{in}(s)} = \frac{1}{1 + G(s)} = \frac{s^2 \left(s + \frac{\omega_o}{600}\right)}{s^2 \left(s + \frac{\omega_o}{600}\right) + \frac{9\,\omega_o}{4} \left(s + \frac{\omega_o}{3}\right)^2}$$

$$\frac{E(s)}{\theta_{in}(s)} = \frac{s^2\left(s + \frac{\omega_o}{600}\right)}{s^3 + \frac{1351\,\omega_o s^2}{600} + \frac{3}{2}\,\omega_o^2 s + \frac{\omega_o^3}{4}} \tag{14}$$

Let the frequency ramp (phase acceleration) input be $\theta_{in}(s) = \frac{\dot{\theta}}{s^3}$, the tracking error can be found by applying the final value theorem to equation (14), that is:

$$\begin{matrix} E(t) \\ \text{Steady} \\ \text{State} \end{matrix} = \lim_{t \to \infty} E(t) = \lim_{s \to 0} \left[s\,\theta_{in}(s) \left\{ \frac{E(s)}{\theta_{in}(s)} \right\} \right] \tag{15}$$

Multiplying equation (14) by $\left[s\,\frac{\ddot{\theta}}{s^3} \right]$ and taking the limit gives

$$\begin{matrix} E(t) \\ \text{Steady state} \end{matrix} = \frac{\left(\frac{\omega_o}{600}\right)\ddot{\theta}}{\frac{\omega_o^2}{4}} = \frac{\ddot{\theta}}{150\,\omega_o^2}.$$

since $B_n = 0.743\ \omega_o$

$$\begin{matrix} E(t) \\ \text{Steady state} \end{matrix} = \frac{\ddot{\theta}}{272\,(B_n)^2} \tag{16}$$

Where $\ddot{\theta}$ is the input frequency rate in radians/sec^2 and B_n is the one-sided loop noise bandwidth (tracking bandwidth) in Hz. The steady state tracking errors for the specified ramp inputs are shown in Table 4-12.

4.3.3.1 SUBCARRIER RECEIVER THRESHOLD ANALYSIS. When the RF signal-to-noise ratio deteriorates, the phase detector output noise as passed by the loop filter causes the VCO phase to fluctuate with respect to the received signal phase. Eventually, as the input signal drops, this random VCO phase error frequently exceeds $\pi/2$ radians and the system drops out of lock. This level is termed the system threshold. It is not a unique level, but rather a region where the probability of losing lock is sharply increased.

Table 4-12. Steady State Tracking Errors

Tracking Bandwidth (B_n) (Hz)	Frequency Rate Input (θ) (rad/sec^2)	Tracking Error (radians)
10	6.28×200	0.0462
30	$6.28 \times 2 \times 10^3$	0.0513
100	$6.28 \times 2 \times 10^4$	0.0462
300	$6.28 \times 2 \times 10^5$	0.0513
1000	$6.28 \times 2 \times 10^6$	0.0462
3000	$6.28 \times 2 \times 10^7$	0.0513

It has been demonstrated in other phase lock receivers using the third order phase locked loop analyzed here, that the carrier remains in lock down to signal-to-noise ratios of 3 db in the two-sided loop noise bandwidth ($2B_n$). Table 4-13 indicates the required sensitivity of the carrier receiver primary loop and the corresponding signal-to-noise ratio in $2B_n$, where B_n is the primary loop bandwidth. If the subcarrier receiver is to have the same sensitivity as the multifunction receiver it must hold lock at these same signal-to-noise ratios.

Table 4-13. Sensitivity of Carrier Receiver Primary Loop

Tracking Bandwidth B_n (Hz)	Threshold Level at Input to Receiver* (dbm)	S/N Ratio in $2B_n$** (db)
10	-157	5
30	-153	4
100	-148	4
300	-143	4
1000	-138	4
3000	-133	4

*Based on -172 dbm/Hz noise density at input to the receiver.
**3 db improvement due to maximal ratio squared combining.

Assuming 3 db signal-to-noise ratio in $2B_n$ to be absolute threshold, it can be seen from Table 4-13 that the specification can be met or exceeded. These thresholds are based on a receiver with a 2 db noise figure.

A noise analysis of the subcarrier receiver from the input to the ranging demodulator through the range tone output is carried out in Figure 4-22. Figure 4-23 illustrates the threshold

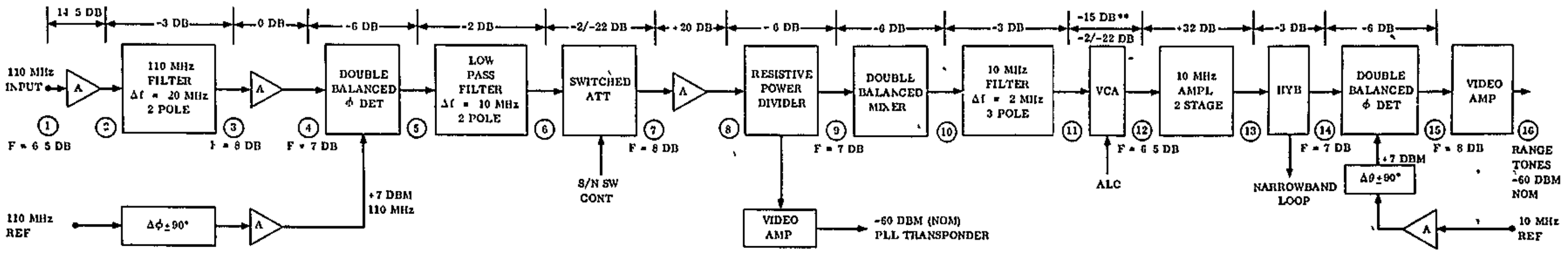

	1	2	3	4	5	6	7	8	9	10	11	12	13	14	15	16
NOISE BW	32 MHz	32 MHz	20 MHz	20 MHz	10 MHz	10 MHz	10 MHz	10 MHz	10 MHz	10 MHz	2 MHz	2 MHz	2 MHz	2 MHz	1 MHz	
SIGNAL INPUT	1	2	3	4	5	6	7	8	9	10	11	12	13	14	15	16
-159 DBM BOTH CH	S_i = -83 5	S_i = -69	S_i = -72	S_i = -72	S_i = -75	S_i = - 77	S_i = - 79	S_i = -59	S_i = -65	S_i = -71	S_i = -74	S_i = -89	S_i = -57	S_i = -60	S_i = -63	S_i = -60
	N_i = -24 5	N_i = -10	N_i = -15	N_i = -15	N_i = -21	N_i = - 23	N_i = - 25	N_i = - 6	N_i = -11	N_i = -17	N_i = -27	N_i = -42	N_i = -10	N_i = -13	N_i = -19	N_i = -22
	N_s = -92 5	N_s = -96	N_s = -93	N_s = -94	N_s = -99	N_s = -102	N_s = - 96	N_s = -98	N_s = -97	N_s = -101	N_s = -96	N_s = -104 5	N_s = -111	N_s = -104	N_s = -103	
±	N_t = -24 5	N_t = -10	N_t = -15	N_t = -15	N_t = -21	N_t = - 23	N_t = - 25	N_t = - 5	N_t = -11	N_t = -17	N_t = -27	N_t = -42	N_t = -10	N_t = -13	N_t = -19	
S/N/Mz	16 DB	16 DB	16 DB	16 DB	16 DB	16 DB	16 DB	16 DB	16 DB	16 DB	16 DB	16 DB	16 DB	16 DB	16 DB	
-50 DBM BOTH CH	S_i = -83 5	S_i = -69	S_i = -72	S_i = -72	S_i = -75	S_i = - 77	S_i = - 79	S_i = -59	S_i = -65	S_i = -71	S_i = -74	S_i = -89	S_i = -57	S_i = -60	S_i = -63	
	N_i = -97 6	N_i = -76 8	N_i = -81 7	N_i = -81 1	N_i = -87 2	N_i = - 88 9	N_i = - 90 7	N_i = -69 6	N_i = -75 6	N_i = -81 6	N_i = -91 6	N_i = -105 2	N_i = -70	N_i = -73	N_i = -79	
	N_s = -92 5	N_s = -96	N_s = -93	N_s = -94	N_s = -99	N_s = -102	N_s = - 96	N_s = -98	N_s = -97	N_s = -101	N_s = -96	N_s = -104 5	N_s = -111	N_s = -104		
	N_t = -91 3	N_t = -70 7	N_t = -81 4	N_t = -81 2	N_t = -86 9	N_t = - 88 7	N_t = - 89 6	N_t = -69 6	N_t = -75 6	N_t = -81 6	N_t = -90 2	N_t = -102	N_t = -70	N_t = -73		
S/N	82 8 DB	82 7 DB	82 4 DB	82 2 DB	81 9 DB	81 7 DB	80 6 DB	80 6 DB	80 6 DB	80 6 DB	79 2 DB	76 DB	76 DB	76 DB	76 DB	
-50 DBM BOTH CH 20 DB S/N RATIO SWITCH	S_i = -63 5	S_i = -49	S_i = -52	S_i = -52	S_i = -55	S_i = -57	S_i = -79	S_i = -59	S_i = -65	S_i = -71	S_i = -74	S_i = -89	S_i = -57	S_i = -60	S_i = -63	
	N_i = -99 2	N_i = -77 2	N_i = -82 1	N_i = -81 8	N_i = -87 6	N_i = -89 3	N_i = -103 3	N_i = -75 3	N_i = -81 3	N_i = -87 2	N_i = -97	N_i = -108 5	N_i = -71	N_i = -74	N_i = -80	
	N_s = -92 5	N_s = -96	N_s = -93	N_s = -94	N_s = -99	N_s = -82 0	N_s = -96	N_s = -98	N_s = -97	N_s = -101	N_s = -96	N_s = -104 5	N_s = -111	N_s = -104		
	N_t = -91 7	N_t = -77 1	N_t = -81 1	N_t = -81 6	N_t = -87 3	N_t = -81 3	N_t = -95 3	N_t = -75 3	N_t = -81 2	N_t = -87 0	N_t = -93 5	N_t = -103	N_t = -71	N_t = -74		
S/N	103 2 DB	103 1 DB	102 8 DB	102 6 DB	102 3 DB	94 3 DB	86 3 DB	86 3 DB	86 2 DB	86 DB	82 5 DB	77 DB	77 DB	77 DB	77 DB	

(1) ALL SIGNAL LEVELS IN DBM
(2) S = SIGNAL LEVEL
N_i = NOISE INPUT LEVEL
N_s = INT, GEN NOISE REF TO INPUT OF STAGE
N_t = N_i + N_s
(3) ASSUMING EQUAL CARRIER AND SIDEBAND POWER
(4) **VCA SET TO -15 DB FOR EQUAL POWER IN CARRIER AND SUBCARRIER

Figure 4-22. Subcarrier Receiver and Range Demodulator Gain Distribution and Noise Analysis

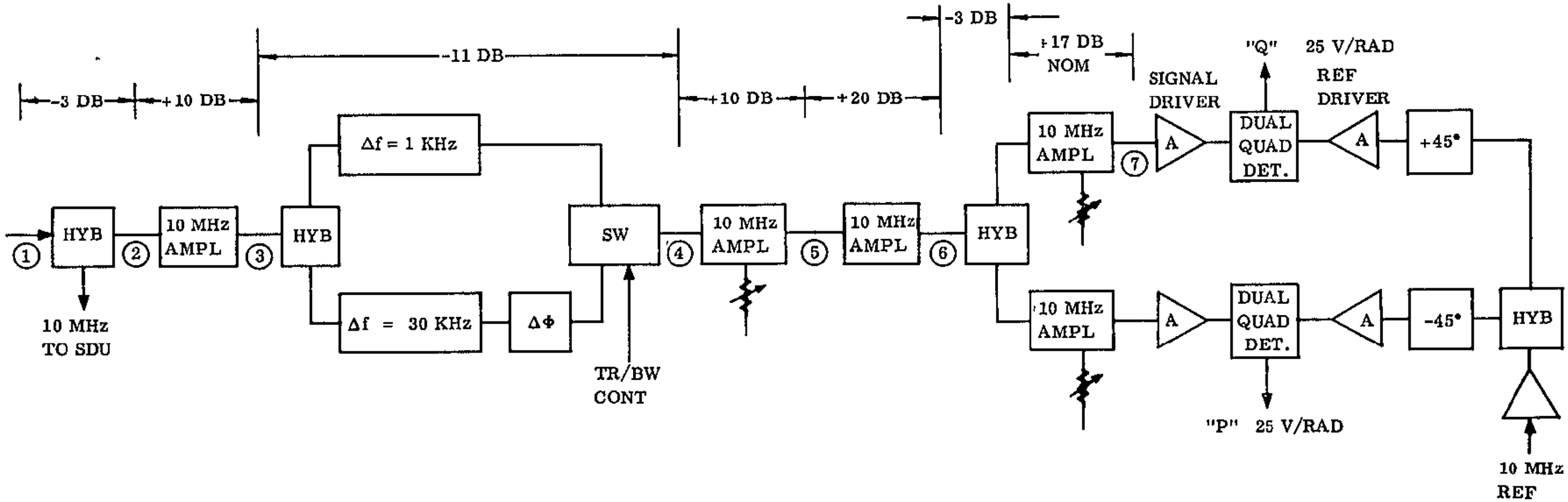

①	②	③	④	⑤	⑥	⑦	TR/BW	INPUT SIGNAL	S/N DENSITY	
			Δf = 1 KHz *							
S_i = -60	S = -63	S = -53	S = -64	S = -54	S = -34	S = -25	10 Hz	-159 DBM BOTH CH.	+16 DB/Hz	+3 DB in 10 Hz
N_i = -13	N = -16	N = -6	N = -48	N = -38	N = -18	N = -9				
			Δ_f = 30 KHz**							
S_i = -60	S = -63	S = -53	S = -64	S = -54	S = -34	S = -25	300 Hz	-145 DBM BOTH CH	+30 DB/Hz	+2 DB in 30 Hz
N_i = -27	N_i = -30	N_i = -20	N = -47	N = -37	N = -17	N = -8				

*NOISE BANDWIDTH = 1 57 KHz
**NOISE BANDWIDTH = 47 KHz

Figure 4-23. Threshold Noise Analysis, Narrowband Phase Lock Loop noise analysis for the narrowband phase lock loop. These numbers are based on a receiver noise figure of 2 db and an unmodulated subcarrier of equal power to the carrier.

Figure 4-24 illustrates the variation of the subcarrier signal power for different modulating conditions. From the figure it is seen that the subcarrier power equals the carrier power for a modulation index of 1.12 radians. An explanation of the numbers in Figure 4-14 may help to clarify their meaning and justification. The modulation indices for the subcarrier and for the range tones were obtained from Reference 3.

The unmodulated subcarrier results will be explained first. In column (1) a number of possible modulation indices are given ($\Delta\phi$) in peak radians. Column (2) the ratio of the power in the modulated carrier to the power in the unmodulated carrier or total power is calculated. For $\Delta\phi = 1.12$ radians this is:

$$\frac{P(\text{carrier})}{P(\text{total})} = 20 \log J_o(1.12)$$

From tables of Bessel function: $J_o(1.12) = 0.707$ then $\frac{P(\text{carrier})}{P(\text{total})} = -3$ db.

In column (3) the ratio of power in the subcarrier to power in the carrier is obtained as follows (assuming all the power is in the J_o and J_1 terms of the Bessel function):

$$\frac{P(\text{subcarrier})}{P(\text{carrier})} = 10 \log \left[\frac{2J_1^2(1.12)}{J_o^2(1.12)} \right]$$

where

$$J_1(1.12) = 0.5$$

$$J_o(1.12) = 0.707$$

$$\frac{P(\text{subcarrier})}{P(\text{carrier})} = 0 \text{ db}$$

Columns (4) and (5) are the carrier and noise levels into the phase detector at threshold. These levels are maintained by the AGC of the multifunction receiver. In other words, as the primary carrier is modulated the total power into the receiver must be increased to maintain carrier threshold or -72 dbm at the phase detector input. The total power increase necessary is just the inverse of the numbers in column (1). Therefore, the total power available at the input of the phase detector (6) is -72 dbm + 3 db = -69 dbm.

	Subcarrier Mod Index $\Delta\phi$ (rad)	P (Carrier)* / P (total) (db)	P (Subcarrier) / P (car) (db)	P (Carrier) to ϕ Det (dbm)	N_i into ϕ Det (dbm)	P (total) into ϕ Det ** (dbm)	P (Subcarrier) out of ϕ Det (dbm)	N out of ϕ Det (dbm)	S/N (10 MHz BW) (db)	S/N Hz (db)	Threshold of Unmodulated Subcarrier referred to (Carrier Threshold) +
	0	0	-	-72	-15	-72	-	-21	-	-	- db
VHF	0 5	- 54	-8.74	-72	-15	-71.46	-84.46	-21	-63.46	+ 6.57	+9 46
VHF	0.7	-1.08	-5 56	-72	-15	-70 92	-81.00	-21	-60.00	+10.00	+6.00
VHF	1.1	-2.88	-0.64	-72	-15	-69 12	-75.28	-21	-54.28	+15 72	+ 28
Equal Power →	1 12	-3	0	-72	-15	-69	-75	-21	-54	+16.00	0
S-Band	1.5	-5.8	+3 76	-72	-15	-66.2	-69.66	-21	-48.66	+21.34	-5.34
2 CH	0.75	-2.80	-4.6	-72	-15	-69 20	-78.70	-21	-67 70	+12.3	+3 7

*Total power increase to maintain Carrier Threshold

**ϕ Det = -6 dbm/1 12 rad for 0 dbm Signal Sensitivity

+ALC = 14 8 db Range for Unmodulated SC

SC $\Delta\phi$	Major Tone $\Delta\phi$	Minor Tone $\Delta\phi$	P (SCM) Δ P SC db	P (Major) P SC db	P (Minor) P SC db	Threshold of Modulated Subcarrier referred to (Carrier Threshold)
0.5	-	-	-	-	-	9.46 db
0.7	0.7	0.7	-2 3	-5.56	-5 56	+8.3
1 1	1.06	0.7	-3.7	-1	-5.56	+3 98
1 5	1.06	0 7	-3 7	-1	-5 56	-1.64
0.75	1.06	0.7	-3.7	-1	-5 56	+7.4

Δ 1 4 db Variation ALC

total ALC Range = 1 4 + 14 8 = 16.2 db ± index changes in transponder

Figure 4-24. Subcarrier Modulation Indices and Threshold Analysis

Column (7) depends on the modulation index and the particular phase detector used. Actual measurements on the phase detector to be used indicate a sensitivity of 0.143 volts/radian into 50 ohms for an input signal of 0 dbm and a reference input of +7 dbm. This amounts to -6 dbm for a 0 dbm signal modulated 1.12 radians. The loss to noise is taken to be 6 db.

Columns (8), (9), and (10) are self-explanatory. Column (11) gives the relative levels at which the carrier and subcarrier will reach threshold. From Figures 4-22 and 4-23 the worst case signal-to-noise ratio density is +16 dbm per Hz or a signal-to-noise ratio of 3 db in a two-sided noise bandwidth of 20 Hz. However, these numbers are based on an input signal of -159 dbm and the actual signal input at threshold is -157 dbm for a receiver with a 2 db noise figure. Therefore, the noise is decreased by 2 db and the signal-to-noise ratio at threshold in the 10 Hz tracking bandwidth is +5 db. This is the criteria used for phase-lock threshold from Table 4.3.4. Therefore, for a modulation index of 1.12 radians and an unmodulated subcarrier the subcarrier and carrier receivers lose lock at the same level.

From Figure 4-24 it can be seen that for modulation indices greater than 1.12 the multi-function receiver will drop lock before the subcarrier loses lock (-5.34 db for $\Delta\phi = 1.5$) and the subcarrier loses lock before the main receiver for modulation indices below 1.12 radians (+9.46 db for $\Delta\phi = 0.5$). The threshold of the subcarrier receiver is further degraded when range tones are applied. As indicated by Table II of Figure 4-24 the subcarrier is reduced by 2.2 to 3.7 db when range tones are applied. Therefore, the threshold for the subcarrier receiver varies from greater than 9.46 db above carrier threshold to 1.64 db below carrier threshold.

4.3.3.2 SUBCARRIER VCO PHASE NOISE ANALYSIS. At high signal levels, a residual phase noise error remains in the loop. This is caused by short-term instability in the VCO which is not completely corrected for because of the finite loop response time. The spectral density of the VCO phase noise function in general has a $\left(\frac{1}{\omega^2}\right)$ characteristic. A block diagram showing the representation of the oscillator phase noise injection is shown in Figure 4-25. The loop error is evaluated from equation (3) for a constant noiseless input.

$$E(s) = \frac{\theta_N(s)}{1 + G(s)}$$

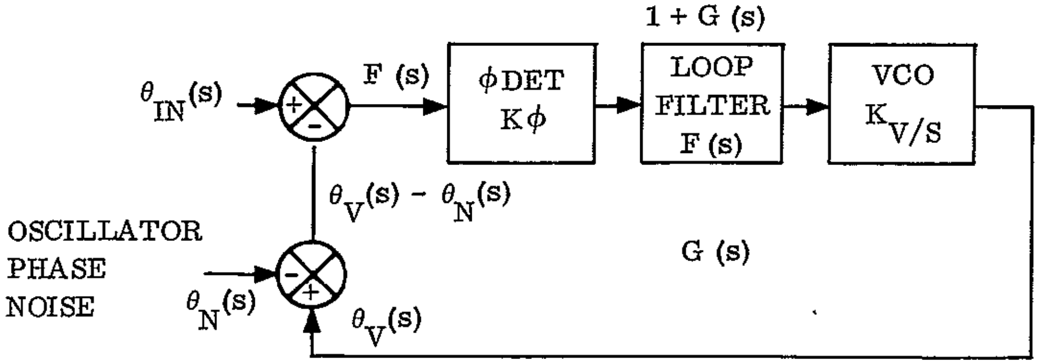

Figure 4-25. VCO Noise Injection Block Diagram

If we assume $\left|\theta_n(s)\right|^2 = \frac{2}{T_c s^2}$ from Reference 8, the mean square phase noise error $\overline{E(t)^2}$ can be evaluated in terms of T_c, the oscillator coherence time, and the loop noise bandwidth, $2B_n$, by means of the integral:

$$\overline{E(t)^2} = \frac{1}{2\pi} \int_{-\infty}^{\infty} \left|\theta_n(j\omega)\right|^2 \left|\frac{1}{1 + G(j\omega)}\right|^2 d(j\omega)$$

where

$$G(s) = \frac{9\,\omega_o \left(s + \frac{\omega_o}{3}\right)^2}{4s} \qquad \text{from equation (5)}$$

$$\overline{E(t)^2} = \frac{1}{2\pi} \int_{-\infty}^{\infty} \frac{2}{T_c (j\omega)^2} \left| \frac{(j\omega)^3}{\left(j\omega + \frac{\omega_o}{4}\right)\left(j\omega + \omega_o\right)^2} \right|^2 d(j\omega)$$

The evaluates from tables in Reference 9:

$$\overline{E(t)^2} = \frac{0.48}{T_c \omega_o} \qquad \text{(two-sided bandwidth)}$$

This becomes

$$\overline{E(t)^2} = \frac{0.24}{T_c \omega_o} = \frac{0.18}{B_n T_c} \text{ rad}^2 \qquad \text{(one-sided bandwidth)} \tag{17}$$

The noise which perturbs the VCO is not only the thermal noise within the oscillator, but also the noise introduced into the loop filter circuitry. The coherence time deteriorates as the oscillator deviation requirement is increased.

Recent experimental data obtained on wide deviation VCXO designs has suggested the following empirical relationship for determining coherence time.

$$T_c = 24 \left[\frac{2 \times 10^5}{\Delta F} \right]^2 \qquad (18)$$

where ΔF is the peak-to-peak VCO pulling range in Hz; for this case $\Delta F = 6 \times 10^5$ Hz.

From equation (18), the coherence time T_c is 2.66 seconds. Substituting this into equation (17) and setting $B_n = 10$ Hz gives

$$\overline{E(T)^2} = \frac{0.18}{10(2.66)} = 0.675 \times 10^{-2} \text{ rad}^2$$

The RMS phase error is

$$\sqrt{\overline{E(t)^2}} = (8.2 \times 10^{-2}) \text{ rad} \times 57.3 \text{ degrees/radian}$$

$$\sqrt{\overline{E(t)^2}} = 4.7 \text{ degrees}$$

Figure 4-26 illustrates two methods of achieving a wide pulling range low frequency VCO. In the first method (4-26A) the VCO is sidestepped to a low frequency and multiplied to the required tuning range. A second method of obtaining a large pulling range at low center frequency is illustrated in 4-26B.

In the second method two VCOs with opposite frequency control voltage slopes are mixed to obtain the difference frequency. If the difference, F, is chosen small the result is a low

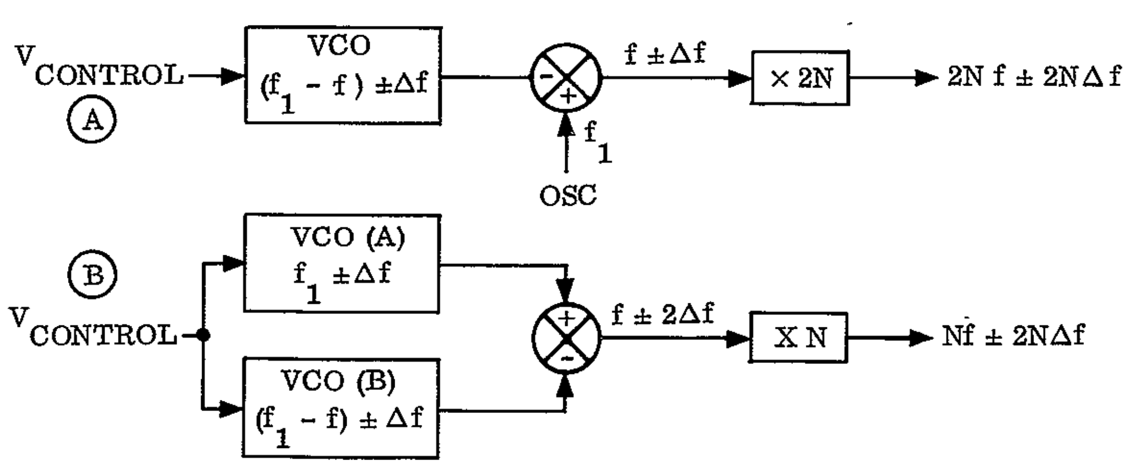

Figure 4-26. VCO Multiplier

frequency VCO with twice the tuning range of either VCO. In this case only one-half the multiplication is necessary to produce the required tuning range. The main advantage of this technique is that the resultant VCO has lower short-term phase jitter than one VCO of the same range. This is due to the rms addition of noise in the difference mixer compared to the multiplied noise from a single VCO.

The phase jitter improvement can be easily calculated. Assume a small difference frequency and equal pulling ranges for each VCO. Also assume a single VCO identical to either of these VCOs. Since the VCOs in question are essentially the same, also assume equal phase noise from each VCO, E(t). Let the required tuning range be $2N\Delta F$. The improvement is:

$$\frac{2NE(t)}{N\sqrt{\left(E_A(t)\right)^2 + \left(E_B(t)\right)^2}} = \frac{2NE(t)}{\sqrt{2}NE(t)} = \sqrt{2}$$

The subcarrier receiver will use the two VCO techniques to generate a wide-deviation VCO. The conditions assumed above can be very closely approximated to obtain maximum short-term stability improvement.

The rms phase noise then becomes

$$\frac{4.7°}{\sqrt{2}} = 3.3 \text{ degrees rms}$$

4.3.3.3 SUBCARRIER RECEIVER GROUP DELAY STABILITY. Receiver delay stability exerts a direct influence on the instrumental accuracy of the range and range rate measurements. The range error is directly related to an uncalibrated time delay, $\Delta\tau$, in the receiver. The absolute time delay can be initially calibrated out as part of the zero-set process, but it is desirable to keep this delay as low as possible since it is functionally related to total delay.

Table 4-14 tabulates the expected delay in the subcarrier receiver. The tabulation receives circuits from the range demodulator input (110 MHz) to the demodulated subcarrier range tone outputs. Maximally flat Butterworth filters are assumed. The gain map of Figure 4-22 shows the signal path for the table.

A possible source of delay variation is the ±300 KHz doppler shift on the subcarrier prior to mixing with the VCO. The major causes of delay here are the two-pole predetection and post-detection filters. An estimate of the order of magnitude of this variation can be gained from the following.

Table 4-14. Estimated Subcarrier Receiver Delay

Stage	3-db Bandwidth (MHz)	Total Delay (nanosec)
Two 110 MHz Amplifiers	150	3.5
2-Pole 110 MHz Filter	20	22.5
ϕ Detector	500	negligible
2-Pole 10 MHz Filter	10	45
10 MHz Amplifier	10	12.5
Balanced Mixer	500	negligible
3-Pole Filter	2	318
VCA	> 200	≈ 2
Two-stage 10 MHz IF Amplifier	80	7
Total Estimated Delay		410.5

The normalized time delay for a double-tuned circuit (critically coupled) is given by:

$$\text{normalized delay} = \frac{d\phi}{dx} = \frac{(x^2 + 1)}{x^4 + 1}$$

$$\text{where } x = \frac{\Delta f}{\Delta f_{3db}}; \quad \text{let} \left\{ \begin{aligned} \Delta f &= 300 \text{ KHz} \\ \Delta f_{3db} &= 20 \text{ MHz} \end{aligned} \right\} \quad \text{(predetection 110 MHz filter)}$$

The delay 300 KHz from center frequency is 1.000225 times the delay at center frequency. Thus, from table 4.3.5, the delay off center would be 22.505 nanosec for the 110 MHz filter and 1.001 × 45 = 45.045 nanosec for the 10 MHz filters. Thus, the total variation due to doppler shift is a negligible 0.05 nanosec.

Since the doppler is removed from the 10 MHz IF signal there is no delay variation due to doppler in the IF path. A cause of variation is the VCA which has a 20 db range. Actual measurements of the VCA show this to be 0.27 nanosec from 0 db to 20 db attenuation. Thus, the total delay variation due to doppler and control range in the subcarrier receiver is less than one nanosec.

4.3.4 AFC Analysis

The specification states that zero correction should be applied to the VCO under conditions where the signal level is below the threshold of the AFC discriminator. With conventional AFC systems, the output of the discriminator is amplified, filtered and applied to the VCO. The dc amplification must be sufficiently high so that the static error is held to a reasonably small percentage of the IF bandwidth. Therefore, when the signal is below the threshold level, small noise unbalances will be amplified and drive the VCO towards the end of its range. The Contractor has solved this problem in other equipment by the use of a small "dead zone" located in the center of the band in the AFC amplifier. Small error voltages which fit inside this "dead zone," such as noise unbalance, are not amplified and therefore do not pull the VCO.

To analyze the AFC loop, first consider the loop without the "dead zone" circuit. Figure 4-27 is a linear model of the AFC loop in Laplace notation.

K_1 = Discriminator constant, volts/rad/sec

K_2 = VCO constant, rad/sec/volt

$Y(s)$ = Laplace transform of loop filter

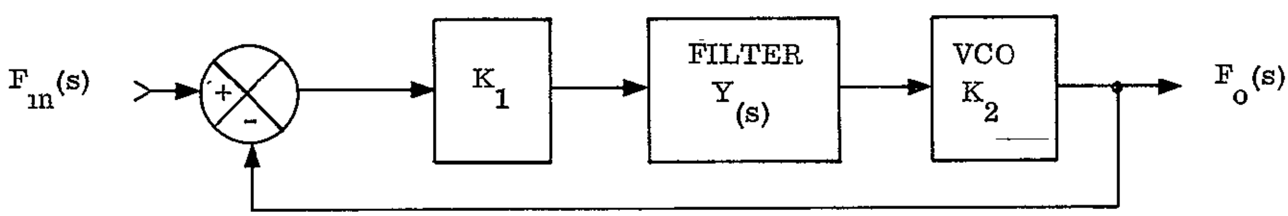

Figure 4-27. Linear Model of AFC Loop

The open loop gain is

$$G(s) = \frac{F_o(s)}{F_{in}(s) - F_o(s)} = K_1K_2Y(s)$$

The closed loop gain is

$$C(s) = \frac{G(s)}{1 + G(s)} = \frac{K_1K_2}{1 + K_1K_2Y(s)}$$

The error function is

$$E(s) = \frac{F_{in}(s)}{1 + K_1 K_2 Y(s)}$$

The loop filter, Y(s), is shown in Figure 4-28.

$$Y(s) = \frac{R_2}{R_1}\left(\frac{1}{R_2 C_1 s + 1}\right)$$

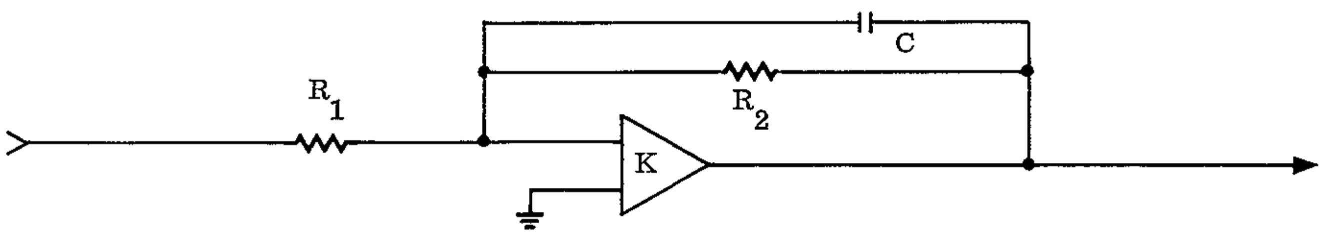

Figure 4-28. Loop Filter/Amplifier, Y(s)

Therefore, the érror function can be written

$$E(s) = \frac{F_{in}(s)}{1 + K_1 K_2\left[R_2/R_1\left(\frac{1}{R_2 Cs + 1}\right)\right]}$$

For a step frequency input, $F_{in}(s) = \frac{\Delta f}{s}$

$$\lim_{s \to 0} E_{(s)} \cdot s = \frac{\Delta f \cdot s}{s\left[1 + K_1 K_2 R_2/R_1\left(\frac{1}{R_2 Cs + 1}\right)\right]} = \frac{\Delta f\,(R_2 Cs + 1)}{\left[(R_2 Cs + 1) + K_1 K_2 R_2/R_1\right]}$$

$$\lim_{s \to 0} E_{(s)} \cdot s = \frac{\Delta f \cdot s}{1 + K_1 K_2 R_2/R_1} = \frac{\Delta f}{K_o}$$

where $K_o = 1 + K_1 K_2 R_2/R_1$

Therefore, the static error is inversely proportional to the open loop gain of the AFC loop. It is desirable to minimize the static error, but the gain must not be so large that errors due to noise offsets and operational amplifier drift are significant. A reasonable figure for static error is 5 percent of the IF bandwidth, or ±500 Hz for the 10 KHz IF/BW. The pulling range of the VCO is ±300 KHz. Therefore

$$\Delta f = K_o \cdot E$$

$$300(10^3) = K_o \cdot 500$$

$$K_o = 600$$

The noise unbalance from the discriminator may however, be of this same magnitude. In the absence of signal this noise unbalance would cause the VCO to be driven to its extreme range.

A solution to this problem is the use of an amplifier with a "dead zone." The familiar 'S' curve output from the discriminator is amplified and filtered and then passed through a pair of oppositely polarized diodes.

The results are indicated in Figure 4-29. The extent of the flat portion near the crossover is adjusted so that no output occurs for small outputs from the discriminator. Noise unbalance voltages from the discriminator will not cause a VCO frequency change. Using this technique it is possible to have the system automatically acquire a signal and to reacquire it in the case of a signal fade.

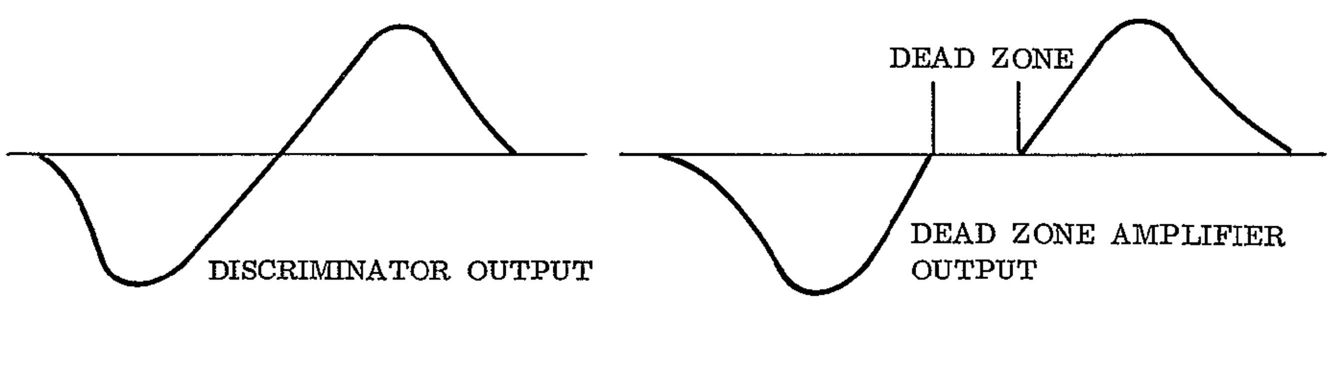

Figure 4-29. Dead Zone Amplifier Function

4.3.5 Maximal Ratio Diversity Combiner

The relationship for the output signal to noise power ratio, $(S_O/N_O)^2$, of a two channel maximal ratio diversity combiner is

$$\left(\frac{S_O}{N_O}\right)^2 = \left(\frac{S_A}{N_A}\right)^2 + \left(\frac{S_B}{N_B}\right)^2 \tag{1}$$

or

$$\frac{S_O}{N_O} = \sqrt{\left(\frac{S_A}{N_A}\right)^2 + \left(\frac{S_B}{N_B}\right)^2}$$

where S_A, S_B, N_A, and N_B are the signal and noise voltages at the input of the receiving system. If K_A = gain of Channel A and K_B = gain of Channel B, then

$$K_A = \frac{1}{S_A}, \quad K_B = \frac{1}{S_B}$$

Therefore, the noise input voltages at the combiner input are

$$N'_A = N_A K_A \text{ and } N'_B = N_B K_B$$

and the signal levels are

$$S'_A = S_A K_A, \; S'_B = S_B K_B \text{ and } S_A K_A = S_B K_B$$

That is, the receiver AGC system holds the input levels at the combiner to a constant normalized level. Figure 4-30 is a functional block diagram of the AGC and diversity combiner system.

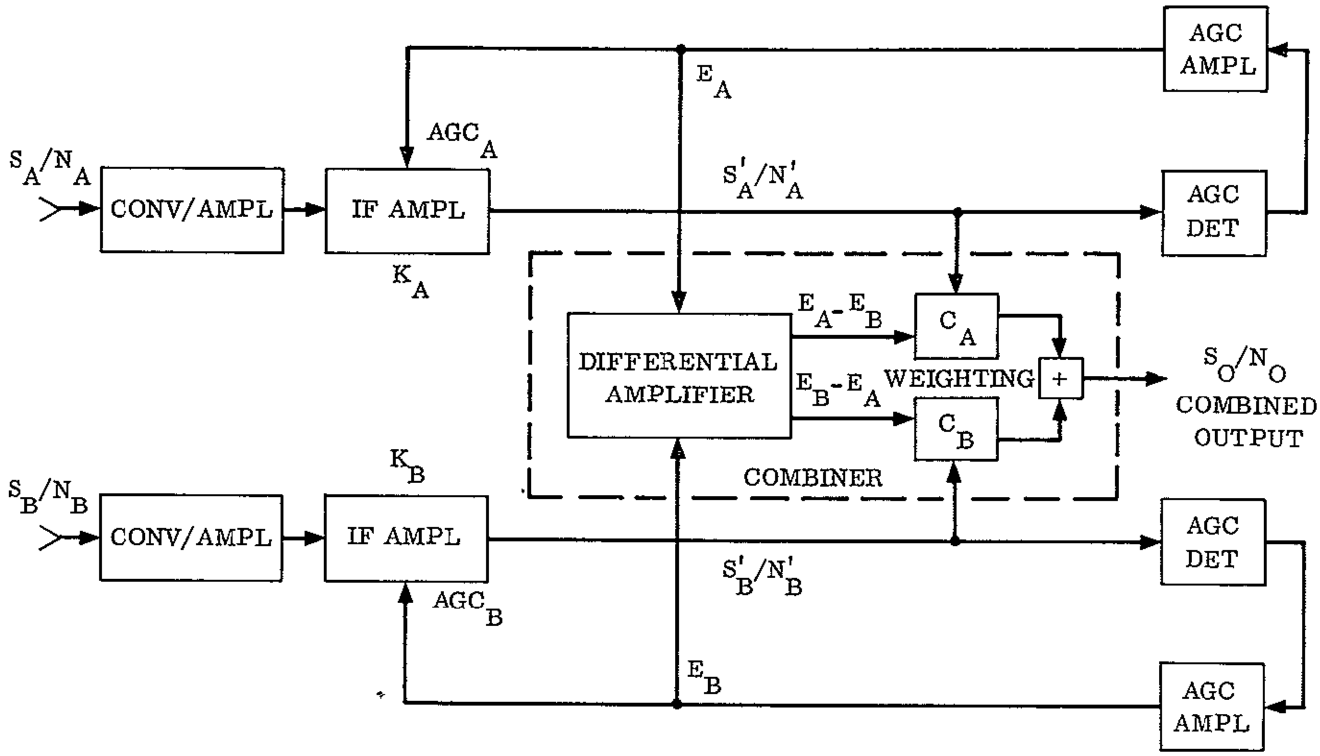

Figure 4-30. AGC System and Diversity Combiner Block Diagram

The combiner control weights each of the inputs according to the signal powers and maintains the output level from the combiner at a constant level. Therefore, the proper weighting functions, C_A and C_B, are defined by

$$\frac{C_A}{C_B} = \left(\frac{S_A}{S_B}\right)^2 \quad \text{and} \quad C_A + C_B = 1$$

The signals add coherently and the noise adds in an rms function so that the combined output signal, S_O, and noise, N_O, are

$$S_O = C_A S'_A + C_B S'_B$$

$$N_O = \left[(C_A N'_A)^2 + (C_B N'_B)^2\right]^{1/2}$$

Therefore, the combined output signal-to-noise ratio is:

$$\frac{S_O}{N_O} = \frac{C_A K_A S_A + C_B K_B S_B}{\left[(N_A K_A C_A)^2 + (N_B K_B C_B)^2\right]^{1/2}} \tag{2}$$

Defining the input signal voltage ratio $S_A/S_B = A = K_B/K_A$ and rewriting equation (2)

$$\frac{S_O}{N_O} = \frac{C_A S_A + AC_B S_B}{\left[(N_A C_A)^2 + (AN_B C_B)^2\right]^{1/2}} \tag{3}$$

$$\frac{S_O}{N_O} = \frac{S_A + \frac{S_B}{A}}{\left[(N_A)^2 + \left(\frac{N_B}{A}\right)^2\right]^{1/2}} \tag{4}$$

Since $N_A = N_B$, that is, the noise figures of the two channels are equal, then

$$\frac{S_O}{N_O} = \frac{S_A + \frac{S_B}{A}}{N\left(1 + \frac{1}{A^2}\right)^{1/2}} \tag{5}$$

Equation (5) determines the weighting function which the combiner control circuits must apply to the input voltages in order to yield a maximal ratio combined output.

The control signal for the combiner is derived from the AGC voltage, which changes as a linear function of the signal strength in db or

$$E_A = D \log S_A$$

where D is a gain factor determined by the AGC amplifier.

Therefore the differential AGC voltages are:

$$E_A - E_B = D \log S_A - D \log S_B = D \log \frac{S_A}{S_B} = D \log A$$
$$E_B - E_A = D \log S_B - D \log S_A = D \log \frac{S_B}{S_A} = D \log \frac{1}{A} \qquad (6)$$

The input signals to the combiner are held constant by the receiver AGCs. It is required, then, that the combiner control circuits weight the input signals in accordance with equation (5), making use of the differential AGC information, D log A and D log 1/A while maintaining the combiner output at a constant level. We can, therefore, calculate the required combining curve for each channel. Assume that the slope of the AGC voltage is 15 db/volt, which corresponds to a D factor of 0.667. With this selection, the variation of E_A and E_B is 7.4 volts over the receiver dynamic range of 111 db. If we have an AGC differential of $E_A - E_B = 0.4$ volts, this means that the signal difference is 6 db, with S_A the stronger signal.

For this example, the contributions out of the combiner must be 1:0.25. By choosing different 'A' ratios a plot of the required combiner response as a function of AGC differential is made. The data is tabulated in Table 4-15 and shown in Figure 4-31.

Table 4-15. Ideal Maximal Ratio Control Characteristics

S_A/S_B	20 log S_A/S_B (db)	$E_A - E_B$	C_A	C_B
1	0	0	0.5	0.5
1.414	3	0.2	0.667	0.333
2	6	0.4	0.8	0.2
2.828	9	0.6	0.889	0.111
4	12	0.8	0.941	0.059
5.66	15	1.0	0.97	0.03
8	18	1.2	0.985	0.015
16	24	1.4	0.996	0.004

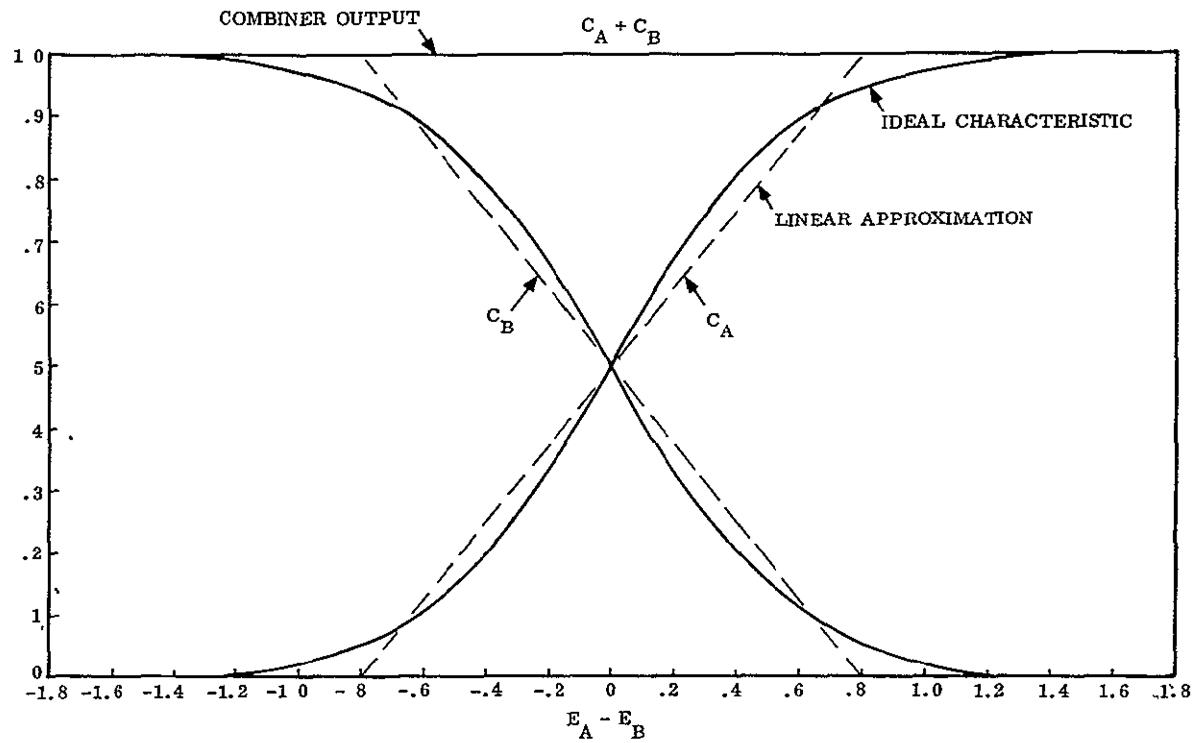

Figure 4-31. Diversity Combiner Characteristic

In the MFR diversity combiners, a linear approximation will be used since a linear characteristic is more easily implemented. The linear approximation chosen is shown in Figure 4-31. The approximation shown in the figure was chosen to minimize the deviation from the maximal ratio combiner characteristic. The error introduced by the approximation can be shown to be negligible by finding the ratio of the optimum S/N ratio to the actual S/N ratio for different points on the characteristic. For example, for an input signal difference of 6 db, the ratio of the optimum signal-to-noise ratio to the actual signal-to-noise radio is

$$\frac{S/N\ (OPT)}{S/N\ (ACT)} = 1.0078 \text{ or } 0.06 \text{ db}$$

Table 4-16 lists the errors for other signal level differences.

4.3.6 Group Delay Stability

The delay stability in the MFR must be maintained in order that range measurement accuracy is not degraded by receiver variations. In a diversity ranging system, the delay in each sum channel must be carefully controlled, and the delay of both sum channels must be closely matched. Otherwise indicated range variations would occur as the diversity combiner varies

Table 4-16. Errors Introduced by Linear Approximation

20 log S_A/S_B (db)	$\frac{S/N(OPT)}{S/N(ACT)}$ (db)
0	0
3	0.03
6	0.06
9	0.05
12	0.26
15	0.14
18	0.10
24	0.015

the contribution of each sum channel to the combined output. One potential source of group delay variation is the gain-controlled 110 MHz IF amplifier. The dynamic range of this unit is 111 db. The delay variation specification of 3.5 nanosec or less (Specification Paragraph 4.5.4.5.4.1) must be met over this range. Since the gain control is achieved by the use of VCAs (voltage controlled attenuators), the delay characteristics of these devices will determine the IF amplifier delay variation. The transistor amplifiers are a fixed-gain, broadband design which will not contribute to delay variations as a function of AGC.

The Contractor has recently developed a VCA which will be used in the MFR for gain controlling the IF amplifier. In the section describing the gain distribution for the receiver, it is seen that six VCAs, each of which contributes 18.5 db gain variation, are used to obtain the required 111 db total variation. Group delay measurements have been made on this device.

Over the gain range required in the MFR, each VCA will contribute 0.27 nanosec, for a total of 1.62 nanosec variation.

The delay variation in the diversity combiner will be appreciably less than the delay in the IF amplifier since only one VCA is used in each channel of the combiner.

The group delay variation between sum channels will be largely a function of the input and output filters at the second converter. The inputs filters are 50 MHz wide at the 0.5 db points or approximately 65 MHz at the 3 db points. The mid-frequency delay through a 5-pole Butterworth filter with these characteristics is 16 nanosec. The output filter is a two pole Butterworth design with a 3 db bandwidth of 32 MHz. The mid-band delay in this filter is 14 nanosec. The total delay 30 nanosec in these filters will be held to within 3 percent in order that this contribution to delay differential will be less than 1 nanosec.

4.4 SYSTEM SIGNAL SOURCE ANALYSIS

4.4.1 Carrier Frequency Generation Spurious Signal Analysis

Spurious outputs on the S-Band and VHF carrier frequency inputs to the transmitter are a minimum of 55 db below the carrier level for non-harmonically related spurious outputs and at least 45 db below for the harmonically related. The sources of the spurious signals present in the output are discussed below.

4.4.1.1 S-BAND. Non-harmonically related spurious signals from the HP5105A Synthesizer are at a minimum of 70 db below the selected output. In generating the S-Band carrier frequency, the synthesizer frequency is effectively multiplied by 4. This will degrade the spectral purity by 12 db resulting in a spurious level no greater than 58 db below the output.

A second contribution to spurious signals results from mixing the multiplied synthesizer input with the phase-modulated 200 MHz. No spurious below the ninth order are encountered, however, a ninth order crossover is present ($6f_{low} - 3f_{high}$). By using a double balanced mixer such as the AR/ANZAC SMX-10 in conjunction with correctly chosen mixer input signal levels, the output spurious content will be more than 55 db down.

In generating the fixed 25 MHz reference for the phase modulator, the 1 MHz reference from the synthesizer driver is used. Non-harmonically related spurious elements are in the order of 120 db down on the 1 MHz output. Multiplying first by 25, then by 8 (to 200 MHz), and then by 2 degrades the initial spectral purity by 52 db for a net contribution to carrier spurious in the order of 68 db below the output.

The process of multiplying the phase-modulated 25 MHz signal introduces further spurious content. In the design of the 25 MHz to 200 MHz multiplier, balanced doublers in conjunction with under-coupled two-pole interstage filters are employed to yield sufficient spur suppression without introducing objectionable phase distortion. The principal spurs occur at 200 MHz (±25 MHz) and are a minimum of 61 db below the 200 MHz signal and are consequently, a minimum of 55 db below the output carrier. The second harmonic of the carrier is greater than 45 db below the output.

4.4.1.2 VHF BAND. Spurious signals in the output carrier due to the HP5105A Synthesizer are a minimum of 70 db down. A ninth order crossover ($6f_{low} - 3f_{high}$) is present in the subtractive mixing of the synthesizer output with the phase-modulated 200 MHz signal but the resultant spur is more than 55 db below the carrier. The previous discussion concerning the 200 MHz spurious applies indicating spurious contributed by this source are more than 55 db down. An output filter limits harmonics of the carrier frequency to a level greater than 45 db below the output.

4.4.2 Transmitter Carrier Signal-to-Noise Ratio Analysis

For the HP5105A Synthesizer, the signal-to-noise ratio per Hz at 1 Hz is 60 db. Since the synthesizer output is multiplied by 4 to generate the S-Band output, the signal-to-noise ratio per Hz at 4 Hz from the carrier will be 12 db greater or 48 db. Since the phase noise spectral density varies inversely with frequency offset from the carrier, the signal-to-phase noise ratio will be 55 db at 20 Hz from the carrier. Therefore, in a 3 Hz bandwidth at 20 Hz from the carrier, the signal-to-phase noise ratio will be 50 db indicating a phase noise of approximately 3 milliradians. It is assumed in the foregoing that the additional phase noise introduced by frequency translation of the multiplied synthesizer output is negligible since, relatively speaking, the output from the HP5110B is spectrally pure.

The total phase jitter as measured with the phase coherent receiver specified in paragraph 4.2.3.1 of the specification may be estimated in the following manner. The signal-to-phase noise ratio per Hz after multiplication by 4 is 48 db. The phase noise power spectral density varies inversely as the square of the frequency offset from the carrier, that is,

$$\overline{\theta_n^2} = \frac{K}{s^2} \tag{1}$$

where K is a constant to be determined. Thus,

$$K = (2\pi \cdot 1)^2 \times 0.159 \times 10^{-4} \cong 6.3 \times 10^{-4}/\text{sec}^2 \tag{2}$$

The total phase jitter is measured at the output of the phase detector of the phase coherent receiver. The transfer function from input to output of the phase detector is 1 − H(S) which for the specified receiver is

$$1 - H(s) = \frac{\frac{9}{32B_L^2} s^2}{1 + \frac{3}{4B_L} s + \frac{9}{32B_L} 2\, s^2} \tag{3}$$

The total mean square phase jitter is

$$\overline{\theta_T^2} = \frac{1}{2\pi j} \int_{-j\infty}^{+j\infty} \frac{K}{s^2} \left| 1 - H(S) \right|^2 ds \tag{4}$$

which on being evaluated yields

$$\overline{\theta_T^2} = \frac{3K}{16B_L} \tag{5}$$

For a noise bandwidth of 10 Hz, the rms phase jitter is approximately 3.4 milliradians or about 0.2 degrees. The foregoing again neglects the relatively small additional phase jitter introduced by the translation process.

4.4.3 Phase Modulator and Group Delay

A highly-linear relationship between modulating voltage and phase deviation is required to attain the low degree of distortion required. The phase shifting characteristic of the network used (Figure 4-32) can be shown to be

$$\theta = \text{arc tan} - \frac{X(X + 2R)}{2R(R + X)} \tag{1}$$

$X = j(R - KV^a)$ where $-jKV^a$ is the capacitance of the voltage-variable capacitance (VVC) as a function of the reverse bias voltage V. For this design, R = 200 ohms and for the VVC, K = 104 and $V^a = V^{0.45}$.

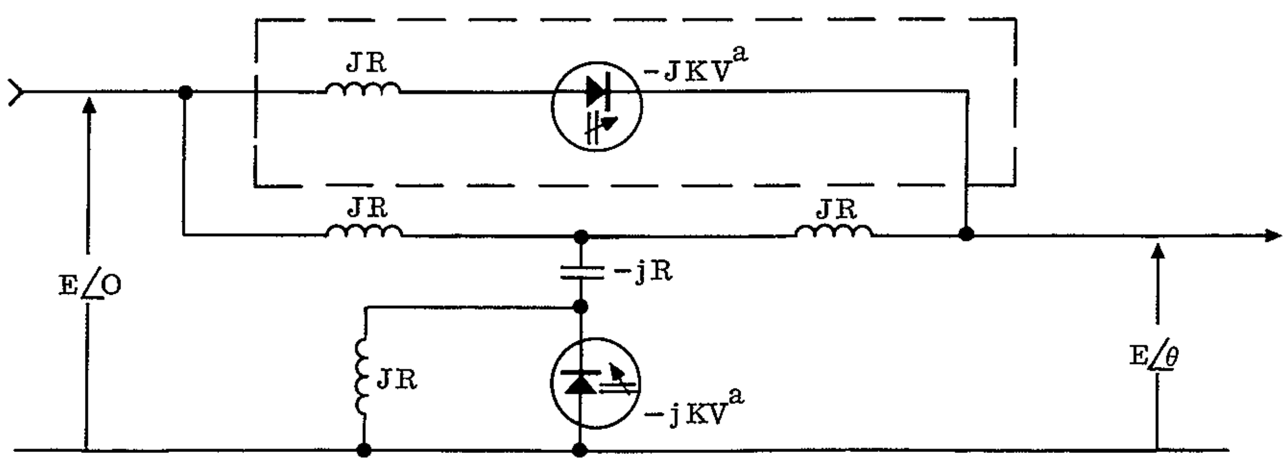

Figure 4-32. Phase Shifting Network

On substituting:

$$\theta = \text{arc tan } 1/2 \left\{ \frac{(K' V^{0.45} - 1)\,(K' V^{0.45} - 3)}{(K' V^{0.45} - 2)} \right\} \tag{2}$$

where $K' = 0.521$.

This result indicates an approximate linear relationship between θ and the instantaneous bias V for $\Delta\theta \leq 6/8$ radians and V between 0 and 20 volts with a sensitivity of approximately 6 degrees per volt. In practice the circuit has reduced sensitivity (~4-1/2 degrees) but comparable linearity. Distortion is in the order of 1 percent with a ±3/8 radian index. Fifth harmonic distortion is in the order of 0.1 percent.

Range measurement accuracy is directly related to the delay stability of the circuits following the phase modulator. The absolute time delay can be initially calibrated out as part of the zero-set process, but it is desirable to keep this delay as low as possible since it is fractionally related to total delay.

Table 4-17 tabulates the center frequency delay. The filters following the balanced doublers are under-coupled double-tuned circuits with coupling coefficients of approximately 0.6. This degree of coupling was chosen to minimize differential group delay in the filter passband.

Table 4-17. Center Frequency Delay

Filter	No. of Sections	3 db Filter BW	Center Freq Delay (nanosec)
Phase Modulator	-	-	90
High Pass Filter	4	20 MHz	18
Doubler (50 MHz)	2	5 MHz	86
Doubler (100 MHz)	2	10 MHz	43
Doubler (200 MHz)	2	20 MHz	22
Amplifier	1	20 MHz	16
Filter (900 MHz)	5	56 MHz	18
Filter (1800 MHz)	3	100 MHz	6
			Total: 299

In addition four transistor amplifier stages contribute 2 nanosec each and the three doublers each contribute 2 nanosec making the total 313 nanosec. After equipment warmup, the delay stability is less than 0.3 percent or about 0.9 nanosec per hour.

4.4.4 Receiver Signal Source - VCO Stability

The primary VCO must have sufficient short-term stability while locked in the 10 Hz tracking bandwidth to meet the 3-degrees rms phase noise requirement of the specification. By the development detailed in the discussion of the subcarrier VCO phase noise analysis (Paragraph 3.6.4), this stability requirement can be related to the oscillator coherence time (T_c).

Using the empirical relation for a single, wide deviation VCXO,

$$T_c = 24\left[\frac{2 \times 10^5}{\Delta f}\right]^2 \qquad (1)$$

The T_c for the ±300 KHz range would be 2.66 seconds.

The specification requires that:

$$T_c = \frac{0.18}{B_n E(t)^2} = \left[\frac{0.18}{(10\text{ Hz})}\right]\left[\frac{57.3°/\text{rad}}{3°}\right]^2 \qquad (2)$$

$$T_c = 6.56 \text{ sec}$$

which indicates the stability of a single VCXO is not adequate to meet this requirement.

The phase jitter can be improved to some extent by the technique of using two VCXO's as discussed in the subcarrier VCO analysis. The best improvement that could be hoped for would be to increase T_c by a factor of 2 indicating

$$E(t)\ (\text{rms phase noise}) = \sqrt{\frac{0.18}{10(2.65)(2)}}\ (57.3°/\text{rad}) = 3.34° \qquad (3)$$

The two VCO's used are not sufficiently identical to justify the assumptions made in demonstrating this degree of improvement can be attained. Specifically, the VCO's have different center frequencies and different pulling ranges; consequently they will not have equal uncorrelated phase noise contributions.

During the circuit development, techniques to improve the realizable phase stability of the VCO will be investigated.

4.5 ANTENNA ANALYSIS

4.5.1 Rosman, Tananarive, and Carnarvon Sites

4.5.1.1 TRANSMIT HORN. A theoretical analysis of expected horn patterns was made from the known dimensions of the feed. Phase deviation or error at the aperture is given for pyramidal horns in Reference 12 and is equal to:

$$\frac{b^2}{8\lambda l_e} \qquad \text{E-Plane}$$

$$\frac{a^2}{8\lambda l_h} \qquad \text{H-Plane}$$

where

a = H-plane aperture

b = E-plane aperture

λ = wavelength

l_e = horn length in E-plane

l_h = horn length in H-plane

Since a and b are equal, the phase deviation is the same for both planes and is equal to 0.296 wavelengths. From information in Reference 12, pattern characteristics may be computed. The results of this pattern development agree closely with patterns obtained from an ASI test report.

The pattern data obtained from the ASI test report and the patterns obtained by computation both indicate good performance in the H-plane. However, the patterns in the E-plane indicate that the shoulders of the first sidelobe are present on the sub-reflector. A comprehensive analysis of this is difficult since the sub-reflector is only 55 inches from the feed horn which has a far field of 154 inches.

The calculated efficiency of the present antenna system with the current feed horn, sub-reflector, and spar design has been pessimistically determined to be as low as 47 percent rather than the 77 percent which was indicated in the ASI test report. Since no unusual feed pattern or power distribution is indicated in the present design, the 47 percent efficiency could very well be realistic. The 54 percent efficienty was derived after subtracting the following losses:

Sub-reflector blockage	0.88 db
Spar blockage	0.48 db
Feed spillover efficiency	1.60 db
Illumination taper efficiency	0.35 db
Total Losses	3.31 db

Techniques for these computations were obtained from Reference 12 and Reference 13. This points up the fact that the performance to the transmit gain specification of 35.5 db may be more marginal than originally anticipated.

4.5.1.2 SYSTEM INSERTION LOSS. Total transmission line loss from the klystron output to the feed horn input is required to be 1.5 db or less. At Rosman there will be approximately 100 feet of WR430 waveguide between the new equipment building and the base of the antenna structure. This 100 feet of waveguide has a loss of 0.588 db at 1700 MHz, and at least 0.5 db loss at 1800 MHz.

Additionally there is 30 feet of guide up the antenna structure, and approximately 7 feet minimum to the transmitter location in the building. Waveguide losses, therefore, will account for at least 0.8 db loss at 1800 MHz. This leaves a budget of 0.7 db loss to be spread between two rotary joints, a transmit filter, miscellaneous flanges, bends, and flexguide, and a polarizer unit. Practical values of insertion loss for these elements are as follows:

Flanges, bends, and flexguide	0.25 db
Rotary joints 0.08 db each, total	0.16 db
Filter	0.18 db
Polarizer	0.10 db
Total	0.69 db

It is therefore indicated that the total insertion loss will be less than 1.5 db.

4.5.1.3 RECEIVE FEED PATTERNS. The E-plane and H-plane patterns of the receive feed aperture were calculated using the Universal radiation patterns of horns, the Huygen's source factor, and the two-element array factor. These patterns are plotted in Figures 4-33 and 4-34. These patterns indicate an edge illumination of approximately 11 db in the sum mode and a 2.5 db taper in the difference mode. Graphical integration of these patterns indicate a sub-reflector capture efficiency of approximately 53 percent. This is due to the double-cosine illumination function in the H-plane of the feed aperture. The direct result of this factor is a calculated 8 db sidelobe in the H-plane at 35 degrees of the axis of the feed.

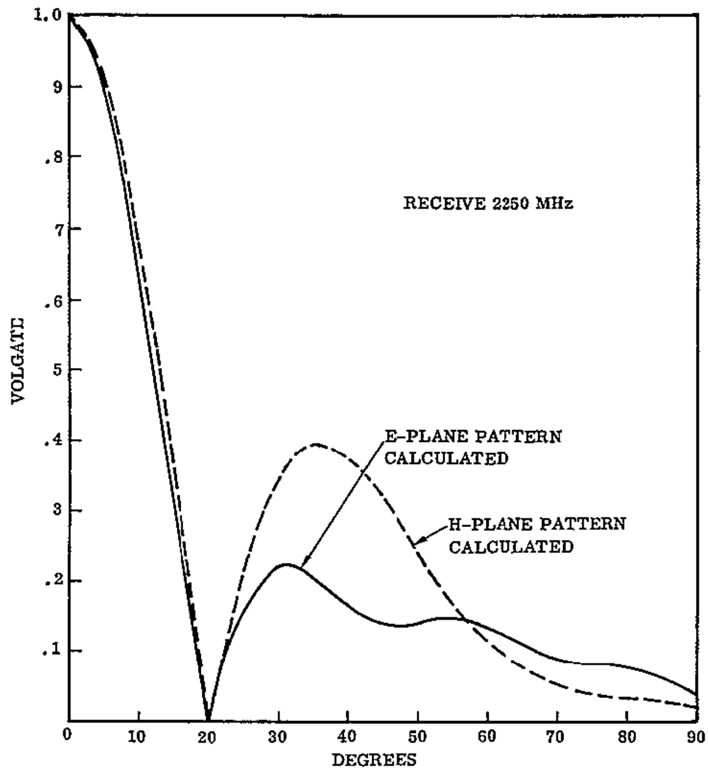

Figure 4-33. Receive Feed Patterns

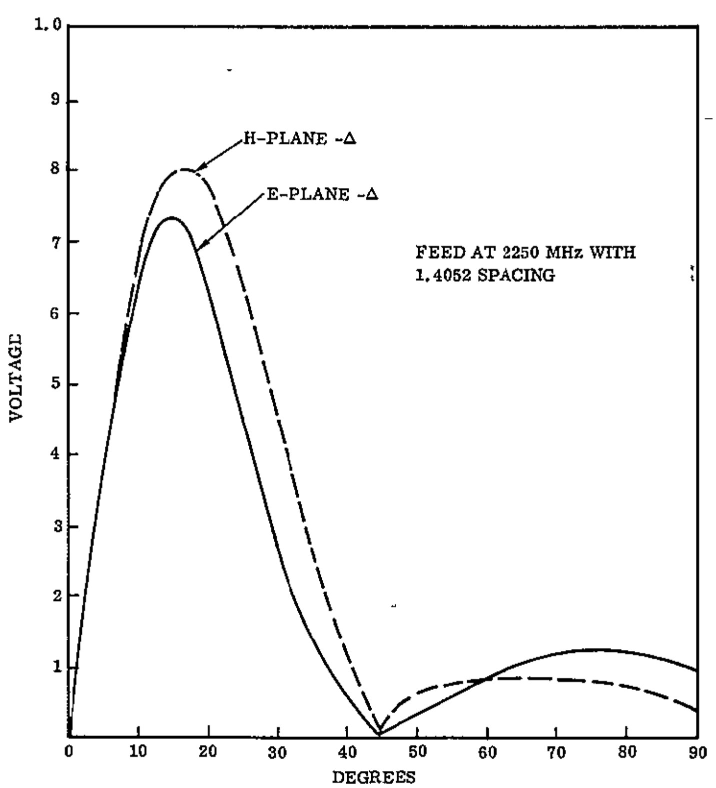

Figure 4-34. Difference Patterns

4.5.1.3.1 Gain. The subreflector capture efficiency of 53 percent combined with the aperture efficiency of the 14-foot parabola, including the blockage loss which is much higher than anticipated, yields a calculated overall efficiency of as low as 33 percent compared to the ASI test report indicated value of 36 percent. Scaling the existing designs to the new frequencies would yield a gain of 35.16 db if the calculated value of efficiency is limiting. A 46.5 percent efficiency would have to be realized to achieve the specified gain which is highly improbable in light of the calculated blockage losses. The blockage loss was calculated for a 3-foot diameter subreflector and two sets of 3-inch spars blocking the aperture of the 14-foot dish.

4.5.1.3.2 Sidelobes. Based on an illumination taper of 11 db, the first unperturbed sidelobe level for a circular aperture will be 25 db. The effect of the 8.25 percent aperture blockage is to raise the 25 db level to 15 db. Standard variations about this point due to reflection will result in marginal performance to the 15 db first sidelobe.

The previously-mentioned 8 db sidelobe of the feed in the H-plane at 35 degrees will result in the spillover energy at 35 degrees off axis of the 14-foot parabola being down only 25 db for the sum channel pattern. Reflections due to the site boresight inadequacies and aperture blockage effects will add to this.

It is doubtful, then that the existing antenna will provide a 25 db sidelobe. The performance could be pessimistically degraded by as much as 5 db from the specified value. The analysis of the difference patterns indicate a similar problem with high sidelobe levels. The first unperturbed sidelobe in the difference place for a 2.5 db taper would be 19 db. However, this value will vary due to the amplitude monopulse arrangement of the feed and the aperture blockage.

With reference to the subreflector capture angle of 17 degrees 2 minutes, and the calculated difference patterns of Figure 4-34, it is probable that the 25 db sidelobe level specification cannot be met either on the existing or the modified antenna. The spillover sidelobes in the area of 20 degrees are approximately 20 db below the sum channel gain and exceed the specified level by 5 db.

4.5.1.4 RECEIVE CHANNEL INSERTION LOSS. The receive channel insertion loss is estimated at 1.0 db or less and will be budgeted as follows:

Waveguide filter	0.24 db
6 feet of Spiroline	0.24 db
Monopulse comparator	0.32 db
Connectors and adaptors	0.20 db
Total	1.00 db

4.5.1.5 TRANSMIT FILTER HEAT ANALYSIS. The present high power klystron and related power supply is limited to a maximum power capability of 10 KW CW. The filter

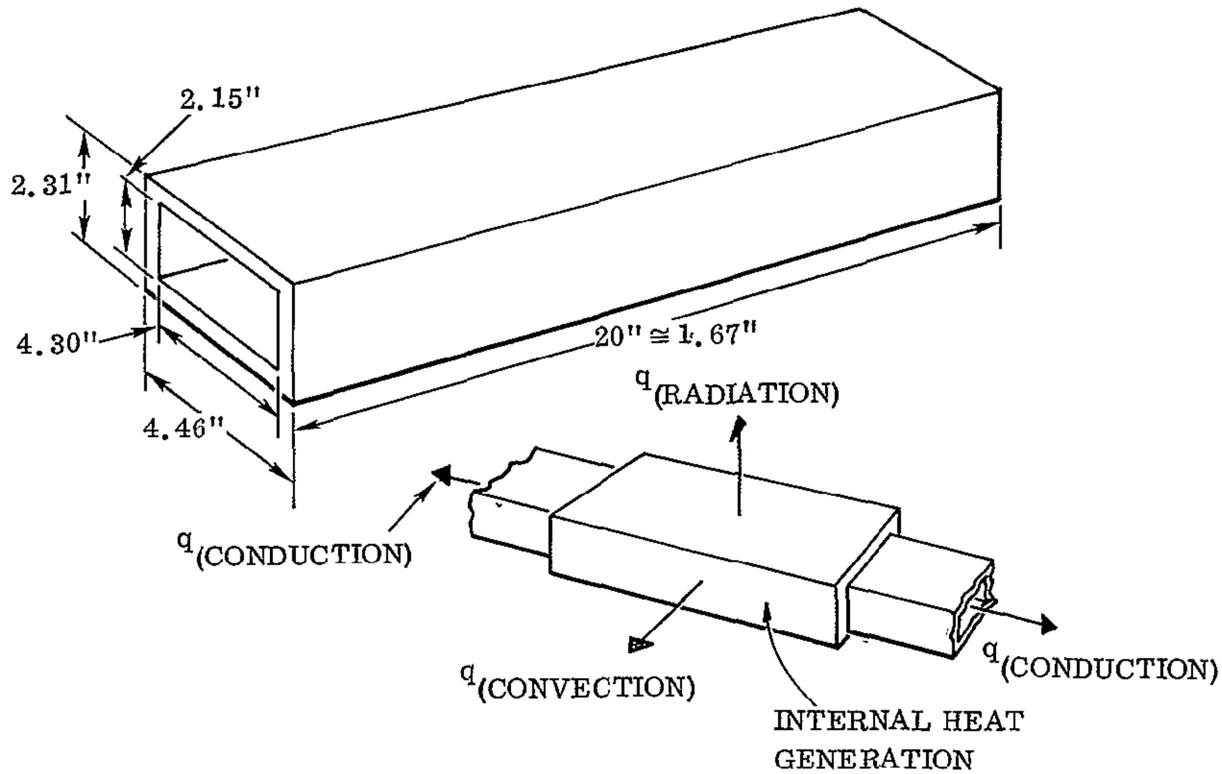

Figure 4-35. Transmit Filter Dimensions and Heat Balance

will be located at the base of the tower approximately 100 feet from the klystron output. The loss in waveguide WR430 at 1800 MHz is 0.57 db per 100 feet. Therefore, the actual power applied to the filter will be 8.8 KW. Presently available filters have an insertion loss in the pass band of between 0.03 db and 0.18 db. The maximum dissipated power in the filter is therefore 361 watts maximum and 88 watts minimum under full operating power conditions.

The following heat analysis was based on 8.8 KW applied power and 0.18 db insertion loss in the filter. The dissipated power for the purpose of the calculations is 361 watts. The size of the filter in the analysis is based on a filter proposed to General Dynamics by a qualified vendor. The dimensions are 2.3 × 4.5 × 20 inches. Refer to Figure 4-35.

Considering radiation cooling only:

$$\text{Surface area} = (2)(20)(2.31) + (2)(20)(4.46) = 270.85 \text{ in}^2$$

The heat flow in TBU/hr, q, can be expressed (per reference 14) as:

$$q = \sigma F_A F_\epsilon S (t_s^4 - t_R^4)$$

where

σ = Stefan-Boltzmann constant = 1.732×10^{-7}

t_R = temperature of the environment = 130° F = 589° R

t_s = surface temperature of the filter in degrees Rankine

The represented configuration is a completely enclosed small body, large comared to the enclosing body, in which case

S = Surface area of the filter

F_A = 1

F_ϵ = emissivity of the surface of the filter ≅ 0.89 for white epoxy paint

Now q = 1235 BTU/hr for 361 watts dissipation.

Substituting to obtain the worse case conditions:

$$1235 = (0.1732 \times 10^{-8})\ (1)\ (0.89)\ (1.88) \left[t_s^{\ 4}\ 1\ (589)^4\right]$$

Solving for t_s,

$$t_s = 860° R = 401° F$$

Therefore radiation alone is not sufficient to cool the filter.

Considering natural convection cooling, the heat transfer coefficients for heated horizontal plates are calculated (per reference 15) as follows:

a. Facing upward:

$$h_m = 0.27 \left[\frac{(\Delta t)_s}{L}\right]^{1/4}$$

b. Facing downward:

$$h_m = 0.12 \left[\frac{(\Delta t)_s}{L}\right]^{1/4}$$

where

L = length in ft.

$(\Delta t)_s$ = temperature difference between surface and air.

Averaging the two conditions:

$$h_m = 0.195 \left[\frac{(\Delta t)_s}{L}\right]^{1/4} \quad \text{BTU/ft}^2\text{/hr/°F}$$

The stabilized waveguide temperature, t_ω, can be obtained assuming a conduction of 10 watts/foot (34.2 BTU/hr) and a surface area of 1.18 ft^2.

Thus,

$$(t_\omega)^4 = \frac{34.2 \times 10^8}{(0.1732)\ (1)\ (0.89)\ (1.18)} + (589)^4$$

or,

$$t_\omega = 616°\text{R} = 157°\text{F}$$

Thus, the waveguides connectıng the filter will, in the worse case, be stabilized at 157° F.

The conduction heat loss, q, can then be expressed as:

$$q = \frac{KA}{L_{(ave)}} (\Delta t) = \frac{(100)\ (0.0073)}{0.4175} \left[t_s - t\omega\right]$$

where

$$K = 100 \text{ BTU/ft}^2/{}^\circ\text{F/ft for Aluminum alloy}$$

$$A = \text{cross-sectional area} = 0.0073 \text{ ft}^2.$$

$$L_{(ave)} = 0.4175 \text{ ft}$$

Since t_ω is a function of t_s, the waveguide temperature rise due to the filter is constrained in the analysis to 50° F or $t_\omega = 207°\text{F} = 666°\text{R}$.

Simplifying:

$$q = 3.5\, t_s - 2330$$

The total heat balance equation including the combined effects of radiation, convection, and conduction cooling is then

$$q = 1235 = h_m S(t_s - t_R) + \sigma F_A F_\epsilon S(T_s^4 - t_R^4) + \frac{KA}{L_{(ave)}}(t_s - t_\omega)$$

Substituting determined values and solving for t_s yields

$$t_s = 770°\text{R} = 311°\text{F}$$

It is obvious, then, that the combined effects of radiation, convection, and conduction cooling are still insufficient under the maximum conditions, and that it is necessary to evaluate the next step which is the use of radiating fins to increase the surface area of the filter.

The maximum ambient temperature by specification is 130° F. Under practical conditions, an ambient temperature of 100° F will be exceeded only a very small fraction of the time. Taking 160° F as the maximum surface temperature which can be tolerated to touch for long periods of time without injury would yield a temperature rise constraint of 60° F. Even under maximum ambient conditions, the surface temperature would then be 190° F, which can be touched without injury for short periods of time, and which represents an impractical case.

Using the 60° heat rise limitation, t_s would be 649° R. Solving for the heat loss components of radiation, convection, and conduction yields the following:

$$\begin{aligned} \text{Radiation } q &= 165 \text{ BTU/hr} \\ \text{Convection } q &= 53.8 \text{ BTU/hr} \\ \text{Conduction } \underline{q} &= \underline{105 \text{ BTU/hr}} \\ \text{Total } \quad q &= 324 \text{ BTU/hr} \end{aligned}$$

The filter will have to dissipate an additional 1235 - 324 = 911 BTU/hr to stabilize the temperature at 60° F differential.

The heat dissipated per foot for a waveguide fin may be approximated by the following expression taken from reference 16:

$$q/ft = 2\,\delta\,KN\,(t_o - t_g)\,\tanh\left(NW - \sqrt{N_\mu}\right)$$

where,

δ = 1/2 the fin thickness (ft)

K = conductivity (BTU/hr/ft/° F)

$N = \left(\frac{h}{K\delta}\right)^{1/2}$

t_o = surface temperature of filter (° F)

t_g = temperature of environment (130° F)

W = height of fin (ft)

N = Nusselt's number $= \frac{h\delta}{K}$

With $K = 100$, $h = 0.456$, $t_o = 90°$ F, and $\delta = 1/4''$, then q/ft = 23.05 BTU/hr.

To dissipate the additional 991 BTU/hr, there must be 42 linear feet of fin added to the filter surface. This requires that 25 fins be added. This requirement is within the feasibility limits of the filter physical size which would allow up to 28 fins of the stated size. A triangular shaped fin approach could possibly yield even better results.

The coefficient of thermal expansion for aluminum is 0.094×10^{-4} inches per inch per temperature differential in °F. The overall 20-inch length of the filter will therefore change to 20.011 inches; well within the machining tolerances of the filter. Therefore, no electrical or mechanical problems are anticipated with this filter design.

The conclusion of the analysis is that it is feasible to design a transmit filter having an insertion loss of 0.18 db and a capability for handling the required power without the use of external cooling, while exhibiting temperature rises which are neither hazardous to personnel nor productive of thermal expansion problems.

Since the filter will be a purchased item, General Dynamics does not intend to stipulate detail design techniques to its vendors, however, General Dynamics will assure that the selected vendor will conform to the temperature rise requirements.

4.5.1.6 CONCLUSIONS. The more comprehensive analysis of the existing 14-foot antennas has indicated that several potential problem areas may presently exist in performance which, if present in the existing antennas, could preclude the possibility of meeting some of the performance specifications. The full nature of these potential problems will not be assessed until the time of site turnover during which time parametric measurements must be made to determine the true performance of the existing antennas. The performance of the modified antennas will be as good or better than the existing antennas as determined at site turnover, but because of basic design limitations which have become apparent, it is not probable that a great degree of improvement can be realized.

4.5.2 Fairbanks Site

4.5.2.1 RECEIVE CHANNEL INSERTION LOSS. The feed assembly presently installed at the Fairbanks site has a specified insertion loss of 0.5 db from the feedhorn aperture to the receive filter outputs (not the preamplifier input). Low loss 0.5-inch Spiroline cables (Prodelin Part No. 51-500) with right-angle connectors (Prodelin Part No. 100-500) are used to connect the receive filters to the parametric amplifier assembly. The maximum length of cable used is 4 feet 3.5 inches which has an insertion loss of 0.17 db. (The Prodelin specification for this cable is 4 db per 100 ft.)

The connectors have an insertion loss of 0.02 db each. Therefore the total maximum loss for the communication path for the present Fairbanks site is calculated to be 0.71 db.

The present Fairbanks site has a three-channel parametric amplifier. The new parametric amplifier will be a six-channel unit. The maximum length of cable can then be expected to be approximately 6 feet with an attendent loss of 0.24 db. Using the same cable connectors would provide an additional loss of 0.04 db. Therefore th loss in the receive path will be 0.78 db under the most optimisitc prediction, and will be less than 1.0 db in the most pessimistic case.

4.6 RANGE TONE TRACKING

The 500 KHz, 100 KHz, and 20 KHz range tone tracking loops will be designed as second order loops. Two designs will be used: in the 1-Hz noise bandwidth mode, the loop filter will be active but with controlled dc gain, in the 0.1-Hz noise bandwidth mode, the loop filter will be active with effectively infinite dc gain. This is done such that reasonable values of resistors and capacitors can be used to obtain the required loop filter time constants and to minimize acquisition time. A block diagram for the phase lock loop is shown in Figure 4-36.

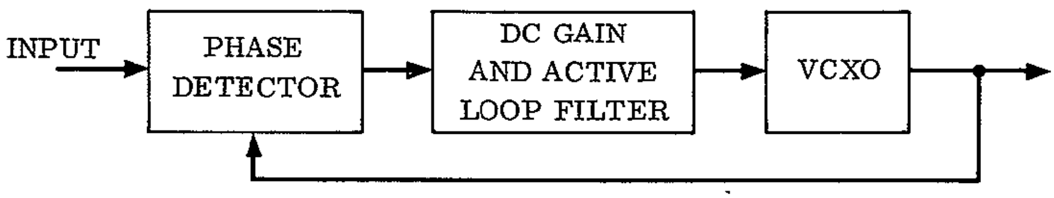

Figure 4-36. Block Diagram of a Range Tone Phase Lock Loop

4.6.1 Loop Design Parameters

The equations cited in the following discussion are taken from Reference 4. The loop transfer function for a loop with finite dc gain is

$$H_1(s) = \frac{\dfrac{K_V K_A K_D}{\tau_1 + \tau_2}(s\tau_2 + 1)}{s^2 + s\left(\dfrac{1 + K_A K_V K_D \tau_2}{\tau_1 + \tau_2}\right) + \dfrac{K_A K_V K_D}{\tau_1 + \tau_2}} \qquad (1)$$

where

K_D = sensitivity of ϕ_d in volts/radian $\left(\text{will be} \approx 1 \frac{\text{v}}{\text{rad}}\right)$

K_V = sensitivity of VCXO in $\frac{\text{radian}}{\text{volts}}$ $\left(\text{will be} \approx \pi \frac{\text{rad}}{\text{volt}}\right)$

$\tau_2 = R_2 C$

$\tau_1 = R_1 C$

$K_A = \frac{R_1}{R}$ (dc gain)

The loop filter configuration for this case is shown in Figure 4-37.

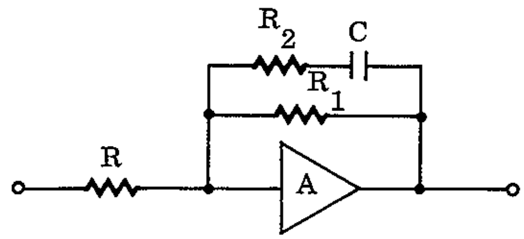

Figure 4-37. Finite DC Gain Loop

The loop transfer function for a loop with effectively infinite dc gain in the active loop filter is

$$H_2(s) = \frac{\frac{K_V K_D}{\tau_1}(s\tau_2 + 1)}{s^2 + s\frac{K_V K_D \tau_2}{\tau_1} + \frac{K_V K_D}{\tau_1}} \tag{2}$$

where

$$\tau_2 = R_2 C$$

$$\tau_1 = R_1 C$$

The loop filter configuration for this case is shown in Figure 4-38.

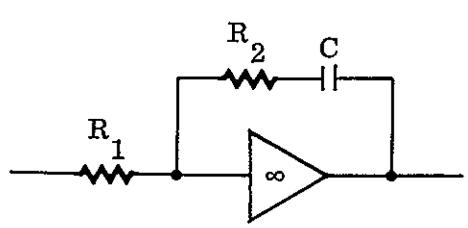

Figure 4-38. Infinite DC Gain Loop

These transfer functions may be rewritten in a more useful and familiar form, that of ξ (damping factor) and ω_n (natural angular frequency in $\frac{\text{rad}}{\text{sec}}$). These transfer functions become

$$H_1(s) = \frac{s\omega_n\left(2\xi - \frac{\omega_n}{K_V K_o K_d}\right) + \omega_n^2}{s^2 + 2\xi\,\omega_n\, s + \omega_n^2}\ , \tag{3}$$

$$H_2(s) = \frac{2\xi\,\omega_n\, s + \omega_n^2}{s^2 + 2\xi\,\omega_n\, s + \omega_n^2} \tag{4}$$

Equating like terms the loop parameters relationship can be found for ω_n and ξ. They are as follows:

For controlled dc gain in an active loop filter

$$\omega_n = \sqrt{\frac{K_A K_V K_D}{\tau_1 + \tau_2}}, \quad \xi = \frac{1}{2}\sqrt{\frac{K_A K_V K_D}{\tau_1 + \tau_2}}\left(\tau_2 + \frac{1}{K_A K_V K_D}\right) \tag{5}$$

For infinite dc gain in an active loop filter

$$\omega_n = \sqrt{\frac{K_V K_D}{\tau_1}}\ , \quad \xi = \frac{\tau_2}{2}\sqrt{\frac{K_V K_D}{\tau_1}} \tag{6}$$

The noise bandwidth is a key parameter and is

$$2B_n = \frac{1}{2\pi}\int_{-\infty}^{\infty} |H(j\omega)|^2\, d\omega \ \ \text{rad/sec} \tag{7}$$

where B_n is the one-sided noise bandwidth.

From both transfer functions, the noise bandwidth is

$$2B_n = \omega_n \left(\xi + \frac{1}{4\xi}\right) \text{ Hz} \tag{8}$$

where ω_n is given in rad/sec.

A damping factor of 0.707 will be used, therefore $2B_n = 1.06\ \omega_n$.

The determination of the loop gain for the 1 Hz two-sided noise bandwidth mode is a function of desired acquisition time and desired phase error. In general, a low gain is required for fastest acquisition, while high gain is required for minimum phase error.

When the frequency difference (as measured at the phase detector output) is within the lock-in frequency range of the loop, the maximum acqusition time may be approximated as

$$T_A \approx \frac{1}{\omega_n} \text{ seconds.} \tag{9}$$

Under this condition, the maximum acquisition time for the 1 Hz two-sided noise bandwidth is approximately 1 second. The approximate relationship for lock-in frequency range and thus maximum frequency difference to maintain this condition is

$$\begin{aligned} \Delta\omega_L &\approx 2\,\xi\omega_n \text{ rad/sec} \\ \Delta\omega_L &\approx 1.33 \\ \Delta f &\approx 0.212 \text{ Hz} \end{aligned} \tag{10}$$

Also

$$\Delta f = (\Delta E_D + \Delta E_A)\, K_A K_{VCO} + \Delta f_{VCXO} + \Delta f_{DOPPLER} \tag{11}$$

where

ΔE_D = dc drift of phase detector due to noise imbalance and temperature/ time drift (7 mv)

ΔE_A = operational amplifier dc offset drift (3 mv)

ΔF_{VCXO} = drift of VCXO (0.0413 Hz for 30-day period)

$\Delta f_{DOPPLER}$ = uncancelled doppler shift (0.0107 Hz or 500 KHz range tone)

Therefore

$$K_A = \frac{(0.212 - 0.053)}{(10 \text{ mv})(0.5 \text{ Hz/v})} \text{ Hz} = \frac{160 \times 10^{-3}}{5 \times 10^{-3}} = 32 \qquad (12)$$

Therefore to acquire within 1 sec, the dc gain of the operational amplifier cannot be greater than 32. Table 4-18 lists the loop parameters for the various operating conditions.

Table 4-18. Loop Parameters

Range Tone Frequency	DC Loop Gain in $\frac{1}{\text{Sec}}$	$2B_n$ in Hz	τ_1 in Sec	τ_2 in Sec
500 KHz	∞	0.1	350	15
	100	1	110.5	1.49
100 KHz	∞	0.1	350	15
	60	1	65.7	1.485
20 KHz	∞	0.1	350	15
	10	1	9.8	1.40

4.6.2 Systematic Phase Errors

The phase error of the loop is a function of the loop gain, doppler, doppler rate, the natural angular frequency of the loop, and parameter drifts. The following error equations will be accompanied by a numerical example using data for the 500 KHz range tone using the S-Band system.

The equation for the phase error for the loop with controlled active filter dc gain is

$$\theta_T = 360° \left(\frac{\Delta f}{K} + \frac{\Delta \dot{f}_D t}{K} + \frac{\Delta \dot{f}_D}{\omega_n^2}\right) + \left(\frac{\Delta E'}{K_D}\right) 57° \tag{13}$$

where

Δf = maximum uncancelled doppler plus 8-hour VCXO frequency drift = 0.0192 Hz for 500 KHz S-Band

$\Delta \dot{f}_D$ = maximum uncancelled doppler rate [assume that $\Delta \dot{f}_D T = \Delta f_D$] where Δf_D = 0.0107 Hz, $\Delta \dot{f}_D$ = 0.0043 Hz/sec

$K = K_A K_V K_D$ = (32)(3.14 rad/volt-sec)(1 volt/rad) = 100 sec^{-1}

ω_n = natural angular frequency = 0.943 rad/sec ($2B_n$ = 1 Hz)

$\Delta E'$ = dc drift of phase detector and operational dc amplifier in 8-hour period = 100 μv

Note that the maximum doppler and maximum doppler rate does not occur at the same time but they will be considered to occur at the same time as a worst case. Note also that the rate aiding reduces the phase dynamics to 0.03 percent for S-Band and to 0.3 percent for VHF.

$$\theta_T = 360° \left(\frac{0.0192}{100} + \frac{0.0107}{100} + \frac{0.0043}{(0.943)^2}\right) + 57.3° \left(\frac{0.1 \times 10^{-3}}{1}\right) \tag{14}$$

$$= 360° \left(1.92 \times 10^{-4} + 1.07 \times 10^{-4} + 4.9 \times 10^{-4}\right) + 0.0057°$$

$$= 0.2843° + 0.0057° = 0.29°$$

The equation for the phase error for the loop with infinite active filter dc gain ($2B_n$ = 0.1 Hz) is

$$\theta_T = \frac{360° \ \Delta \dot{f}_D}{\omega_n^2} + 57° \frac{\Delta E_D}{K_D} = 17.8° + 0.0057° \tag{13}$$

$$= 17.8°$$

4.6.3 Random Phase Errors

The error analysis above (except for phase detector offset) assumes noiseless conditions. The effects of input thermal noise and VCXO phase noise must also be considered.

The mean square phase error due to thermal noise is

$$\overline{\theta_n^2} \approx \frac{1}{2(\mathrm{SNR})_L} \mathrm{rad}^2 \text{ if } (\mathrm{SNR})_L > 10 \tag{14}$$

This error, being a function of signal level, is computed in the range error analysis.

The VCXO phase noise will be kept below 0.1 degree rms for the 500 KHz mode. The phase lock loop will improve on this value somewhat, but the bandwidths are small so that considering the error contribution of the VCXO as 0.1 degree rms is not a poor assumption.

4.6.4 Summary

Table 4-19 lists the maximum expected phase errors for various operating conditions in the absence of additive input thermal noise. It should be noted that the dynamic lag errors associated with the various bandwidths do not represent a practical case since the narrow bandwidth would not be used with high signal dynamics. In the practical case, the narrow bandwidth would be used only when dynamics were negligible but signal-to-noise ratio was low.

Table 4-19. RMS Phase Error at Strong Signal

Range Tone Frequency	$2B_n$ in Hz	S-Band Phase Error (Degrees)		VHF Phase Error (Degrees)	
		θ_{VCO}	θ_T	θ_{VCO}	θ_T
500 KHz	0.1	0.1°	17.8°		
	1.0	0.1°	0.29°		
100 KHz	0.1	0.02°	3.6°	0.02°	36°
	1.0	0.02°	0.078°	0.02°	0.726°
20 KHz	0.1	0.004°	0.72°	0.004°	7.35°
	1.0	0.004°	0.05°	0.004°	0.55°

4.7 RANGE ERROR ANALYSIS

The following error analysis for the ranging measurement groups errors in a manner consistent with the following definitions:

a. Resolution: includes all random and systematic errors due to the ground-equipment hardware operating with one polarization input in the presence of an infinitely high input signal-to-noise ratio. Resolution does not include the effects of additive input thermal noise, errors due to polarization diversity tracking, external effects such as propagation, or the effect of the transponder (or transponder simulator).

b. Instrumental Accuracy: includes all effects contributing to resolution plus additive input thermal noise.

c. Diversity Resolution: includes all effects contributing to resolution plus errors due to polarization diversity tracking.

d. Diversity Instrumental Accuracy: includes all effects contributing to diversity resolution plus additive input thermal noise.

The following paragraphs analyze error contributions from various sources under several conditions, including S-Band and VHF operation. The error analysis for VHF operation is based upon a multifunctional receiver operating with a VHF preamplifier converter. Although this configuration is not presently being implemented, it is understood that this is planned for the future. Since the modifications provided under this contract do not include the VHF receiver, General Dynamics cannot accurately or responsibly predict or control the performance of the existing VHF receiver. It is expected, however, that the results of the error analysis given herein for VHF operation will closely approximate the results of an error analysis for VHF operation with the existing VHF receiver since most of the error contributions stem from sources common to both.

The error analysis provided herein is applicable only for the Rosman, Tananarive, and Carnarvon sites.

4.7.1 Range Resolution

Range resolution is limited primarily by random and systematic time measurement errors. These appear as random and systematic variations on the measurement of the round-trip travel time for ranging signals.

4.7.1.1 RANDOM ERRORS. Random errors which contribute significantly to range resolution error take the form of quantizing error, jitter of the start and stop pulses and short-term instability of the time base (100 MHz clock signal). Contributions to start or stop pulse jitter come from such sources as the axis-crossing detectors, tracking loop oscillators, rate-aid circuit signals and reference signal generation and zero-set circuits.

For round-trip range measurement, the rms jitter of measured time delay, σ_T, is related to the range dispersion, σ_R, by:

$$\sigma_R = \frac{C}{2} \sigma_T$$

where C is the velocity of propagation.

The following paragraphs discuss the sources of random error contributions, and give representative calculations or state allowable design limits for the various errors. The errors are then summarized and predicted root-sum-square random errors are tabulated for operation with 500 KHz, 100 KHz, or 20 KHz as the highest range tone.

4.7.1.1.1 Reference Range Tone Jitter. The 500 KHz, 100 KHz, and 20 KHz reference range tones are produced from clocked pulses and are assigned a maximum time jitter of 3 nanosec. No correlation between the error on the returned tones and the reference tone at the time of return is assumed. Therefore the rms error contribution for the start pulse and for the stop pulse is:

$$\sigma_R = \frac{C}{2} \sigma_T = 0.45 \text{ meter}$$

4.7.1.1.2 Axis-Crossing Detectors. Axis-crossing detectors are used to generate a start pulse from the highest frequency reference range tone used in a specific mission and to generate a stop pulse from the returned tone after it has been filtered. Due to the method of implementation, the axis-crossing detection for the returned tone always occurs at 500 KHz regardless of the highest tone actually employed.

Jitter added to the signals by the axis-crossing detectors is a function of frequency. The allowable jitter value for each axis-crossing detector is:

Frequency	Jitter
500 KHz	3.5 nanosec
100 KHz	3.5 nanosec
20 KHz	20 nanosec

No correlation of jitter of the error contributions of the axis-crossing detectors is assumed. The rms value of range error contribution for each axis-crossing detection is:

σ_R = 0.525 meters for 500 KHz and 100 KHz

σ_R = 3.0 meters for 20 KHz

4.7.1.1.3 Rate-Aid Signal Jitter. Jitter on the rate-aid signal which is outside the pass band of the tracking loop in the range tone processor will appear in the output signal of the processor.

a. S-Band. Time jitter of the output signal for rate aid on the 500 KHz range tone is contributed primarily by spurious signal outputs of the 500 KHz to 5 MHz data converter and the two axis-crossing detectors operating on the data and reference 5 MHz signals.

Setting the maximum level of the spurious signal at -30 db yields a peak phase variation of 1.8 degrees at 5 MHz, or an rms phase jitter of 0.71 nanosec. Assuming an rms jitter of 1 nanosec for each axis-crossing detector yields an rms total contribution on the 1.5 MHz output for 500 KHz rate-aid of:

$$\sigma_T = \left[0.71^2 + 1^2 + 1^2\right]^{1/2} = 1.58 \text{ nanosec}$$

and an rms range error contribution of

$$\sigma_R = \frac{C}{2}\sigma_T = 0.24 \text{ meter}$$

for the 500 KHz range tone.

An additional axis-crossing detector operates on the output 1.5 MHz signal for scaling to generate rate-aid outputs for the 100 KHz and 20 KHz range tones. Assuming an rms jitter of 1.5 nanosec for this axis-crossing detector gives:

$$\sigma_T = \left[1.58^2 + 1.5^2\right]^{1/2} = 2.18 \text{ nanosec}$$

and

$$\sigma_R = \frac{C}{2}\sigma_T = 0.33 \text{ meter}$$

for the 100 KHz and 20 KHz range tones for S-Band operation.

b. VHF. The mixer conversion for VHF band operation is from 100 KHz to 420 KHz. Setting the maximum level of the spurious signal at -35 db yields a peak phase variation of 1.02 degrees at 420 KHz or an rms time jitter of 6.67 nanosec. An rms jitter of 3.5 nanosec is assumed for each of the two axis-crossing detectors used to produce the 1.5 MHz output signal. The rms jitter of the additional axis-crossing detector used to generate the aid signals is the same as for S-Band operation.

The resulting rms time jitter contribution for 100 KHz and 20 KHz range tones for VHF operation is·

$$\sigma_T = \left[6.67^2 + 3.5^2 + 3.5^2 + 1.5^2\right]^{1/2}$$

$$= 8.4 \text{ nanosec}$$

and an rms range error contribution of

$$\sigma_R = \frac{C}{2} \sigma_T = 1.27 \text{ meters}$$

4.7.1.1.4 Range Tone Tracking Filter VCXO. The short-term stability of the 1 MHz VCXO in the active range tone filter contributes a phase jitter to the 500 KHz input to the Digital Range Tone Extractor. The assigned maximum value of phase jitter for the VCXO in the narrow band condition is 0.1 degree at the 500 KHz output. This corresponds to·

$$\sigma_T = \frac{(0.1)}{(360)} \, 2 \, \mu\text{sec} = 0.55 \text{ nanosec}$$

$$\sigma_R = \frac{C}{2} \sigma_T = 0.08 \text{ meter}$$

This contribution applies for all modes and resolutions.

4.7.1.1.5 Quantizing. A 100 MHz clock is used to measure the time interval between a start pulse and a stop pulse. Either pulse can occur at any time relative to the clock pulse train. The maximum error of measurement of time between start and stop pulses is ±1 increment.

The effective rms error of measurement of the time interval (due to quantizing) is:

$$\left(\sigma_T\right)_q = \sqrt{2}\left(\frac{T_R}{\sqrt{12}}\right) = \frac{1}{\sqrt{6}\, f_R}$$

where:

f_R = counting rate (100 MHz)

T_R = time interval between clock pulses ±10 nanosec

Thus

$$\left(\sigma_T\right)_q = 4.1 \text{ nanosec}$$

and

$$\left(\sigma_R\right)_q = 0.61 \text{ meter}$$

The quantizing error is independent of the mode of operation or sampling rate.

4.7.1.1.6 Time Base Reference Jitter. The time base reference (100 MHz clock frequency) jitter results from short-term instability of the reference oscillator, which furnishes the 1 MHz reference, and jitter added by the 100 MHz synthesis circuitry (×100 multiplier). The error contribution by reference oscillator jitter is negligible. A 3 nanosec rms jitter of the synthesized 100 MHz signal is assumed. The maximum separation of the first and the last clock pulses of a range measurement interval can be large compared to the inverse of the clock filter bandwidth. Therefore no correlation is assumed between clock errors at start and end of the interval and the assumed error contribution is:

$$\sigma_R \quad \sqrt{2}\left(\frac{C}{2}\sigma_T\right) = 0.63 \text{ meter}$$

4.7.1.1.7 Time Interval Unit Gating. The time interval unit gate is turned on by a start pulse and turned off by a stop pulse. A random error of 1 nanosec is assumed for each operation. This gives an rms error of the interval of $\sqrt{2}$ nanosec and a range error:

$$\sigma_R = \frac{C}{2}\sigma_T = 0.21 \text{ meter}$$

4.7.1.1.8 Random Error Summary. A summary of the random error contributions and their root-sum-square value is shown in Table 4-20 for each of the three range tones.

Table 4-20. Range Random Error Summary

Source	σ_R (meters) for		
	500 KHz	100 KHz	20 KHz
Start Pulse			
Reference Range Tone	0.45	0.45	0.45
Axis-Crossing Detector	0.53	0.53	3.00
Stop Pulse			
Reference Tone	0.45	0.45	0.45
Axis-Crossing Detector	0.53	0.53	0.53
Rate Aid Circuit			
S-Band	0.24	0.33	0.33
VHF	--	1.27	1.27
Range Tone Tracking Filter			
VCXO	0.08	0.08	0.08
Quantizing	0.61	0.61	0.61
Time Base Reference	0.63	0.63	0.63
Time Interval Gates	0.21	0.21	0.21
RSS Random Error			
S-Band	1.36	1.38	3.26
VHF	--	1.84	3.48

4.7.1.2 SYSTEMATIC ERRORS. Systematic errors which contribute to the range resolution error take the form of cyclic group-delay variations within the equipment as a result of temperature change, doppler shift, signal level variation, power supply variation, and aging effects. The effect of the total group delay present in the system may be removed by a proper zero-set calibration. Group delay variations after zero-set produce an error in the range measurement. However, those variations which take place between the time of zero-set and the making of the measurements may be treated as a bias error and can be reduced significantly by data-processing techniques.

Equipment group delay variations which contribute significantly to the systematic error may result from differential drift of the start and stop pulses due to axis-crossing detector drift, drifts in the zero-set phase shifter and sidetone combiner circuitry, drifts in the modulator and the carrier/subcarrier receiver, dynamic lag errors in the range tone tracking filters, and drift of the time base reference frequency.

4.7.1.2.1 Axis-Crossing Detector Drift. The specified limits of drift and the resulting range errors for the start pulse and the stop pulse caused by the axis-crossing detectors are listed in Table 4-21.

Table 4-21. Start and Stop Pulse ACD Limits

Range Tone (KHz)	Time Drift (nanosec)	Range Error (meters)
500	1	0.15
100	5	0.75
20	25	3.75

Drifts for the start and stop pulse must be considered uncorrelated since they may be caused by independent influences on the circuitry.

4.7.1.2.2 PLL Input Filter Stability. The temperature stability and bandwidths of the range tone filters which precede the range tone tracking filter will be specified to give a long-term phase error and a corresponding range error for each tone not in excess of the value listed in Table 4-22.

Table 4-22. Range Tone Filter Stability

Tone (KHz)	Phase Shift (meters)	Range Error (meters)
500	1	0.833
100	1/5	0.833
20	1/5	4.16

4.7.1.2.3 Tracking Loop Dynamic Lag. Tracking loop performance is discussed in Section 4.6. Lag errors due to worst-case signal dynamics and incomplete rate aid to the range tone tracking filter are discussed in Section 4.6. The phase error and the equivalent range error for each range tone tracked with a two-sided noise bandwidth, B_n, of 1 Hz are given in Table 4-23.

Table 4-23. Range Tone Tracking Filter Dynamic Lag Errors With $2B_n$ = 1 Hz

Range Tone (KHz)	S-Band Lag Degrees	S-Band Lag Meters	VHF Lag Degrees	VHF Lag Meters
500	0.29	0.24		
100	0.078	0.33	0.726	3.0
20	0.05	1.04	0.55	11.5

4.7.1.2.4 Summary of Systematic Errors. The additional systematic errors are shown in Table 4-24 together with those which have been discussed in more detail.

Table 4-24. Systematic Range Error Summary

Source	σ_R (Meters) 500 KHz	100 KHz	20 KHz
Start Pulse			
Axis-Crossing Detector	0.15	0.75	3.75
Stop Pulse			
Zero-set Phase Shifter and Sidetone Combiner	0.15	0.75	3.75
Axis-Crossing Detector	0.15	0.75	3.75
Carrier/Subcarrier Receiver	0.75	0.75	0.75
PLL Input Filter Stability	0.833	0.833	4.16
Tracking Loop Dynamic Lag ($2B_n$ = 1 Hz)			
VHF	-	3.0	11.5
S-Band	0.24	0.33	1.04
RSS Systematic Error With Dynamics ($2B_n$ = 1 Hz)			
VHF	-	3.46	13.9
S-Band	1.18	1.75	7.82
RSS Systematic Error Without Dynamics			
VHF	-	1.72	7.75
S-Band	1.16	1.72	7.75

4.7.1.3 RANGE RESOLUTION SUMMARY. The range resolution is summarized in Table 4-25. The values in this table result from the random errors listed in Table 4-20. and the systematic errors listed in Table 4-24.

Table 4-25. Range Resolution Summary

Source	σ_R (Meters)				
	S-Band			VHF	
	500 KHz	100 KHz	20 KHz	100 KHz	20 KHz
Random Errors	1.36	1.38	3.26	1.84	3.48
Systematic Errors					
With Dynamics	1.18	1.75	7.82	3.46	13.9
Without Dynamics	1.16	1.72	7.75	1.72	7.75
Resolution					
With Dynamics	1.80	2.23	8.47	3.92	14.33
Without Dynamics	1.79	2.21	8.41	2.52	8.50

4.7.2 Range Instrumental Accuracy

Range instrumental accuracy includes all errors attributable to range resolution plus errors due to additive input thermal noise.

The random error in range due to thermal noise is a function of the signal-to-noise power density ratio at the input to the range tone tracking filter and the noise bandwidth of the tracking filter. The rms phase tracking error for a phase-locked loop is given by

$$\sigma_\phi = \left[N/2S\right]^{1/2} \text{ radian}$$

where

$N = 2 B_n \Phi$

B_n = one-sided noise bandwidth of the loop

Φ = noise power density about the tracked signal

Therefore,

$$\sigma_\phi = \left[B_n \left(\Phi/S\right)_R\right]^{1/2} \quad \text{radian}$$

where $(S/\Phi)_R$ is the signal-to-noise power density ratio for the demodulated highest frequency range tone.

The equivalent rms range error is

$$\sigma_R = \frac{C}{4\pi f_R}\,\sigma_\phi$$

$$= \left[\lambda_R/4\pi\right]\left[B_n(\Phi/S)_R\right]^{1/2}$$

where

C = velocity of propagation

f_R = frequency of highest range tone in use

λ_R = wavelength of that range tone

Now

$$(\Phi/S)_R = (\Phi/S)_T\left[(\Phi/S)_R\big/(\Phi/S)_T\right]$$

where

$(S/\Phi)_T$ = signal to noise power density ratio for total received signal

$(S/\Phi)_R/(S/\Phi)_T$ = ratio of signal to noise power density for demodulated highest frequency range tone to that for the total signal power received

Thus

$$\sigma_R = \left[\frac{\lambda_R}{4\pi}\right]\left[B_n\frac{(\Phi/S)_R}{(\Phi/S)_T}\right]^{1/2}\left[\left(\frac{\Phi}{S}\right)_T\right]^{1/2}$$

The values of $\lambda_R/4\pi$ for the three highest frequency range tones are listed in Table 4-26.

Table 4-26. Range Tone Error Ratio

Tone (f_R) (KHz)	$\lambda_R/4\pi$ (meters)
500	47.7
100	239
20	1183

The relationship between $(S/\phi)_R$ and $(S/\phi)_T$ depends upon the modulation conditions, and may be found in Tables 4-8 and 4-9. The relationship is shown graphically for three selected cases in Figure 4-39.

The relationship between $(S/\phi)_T$ and range is given in Figure 4.8 for S-Band and Figure 4.7 for VHF. (Attention is invited to the assumed transponder and loss conditions.) Combining the information from Figures 4-7, 4-8, and 4-39 gives $(S/\phi)_R$ as a function of of range. This is shown graphically in Figure 4-40 for the three tracking conditions.

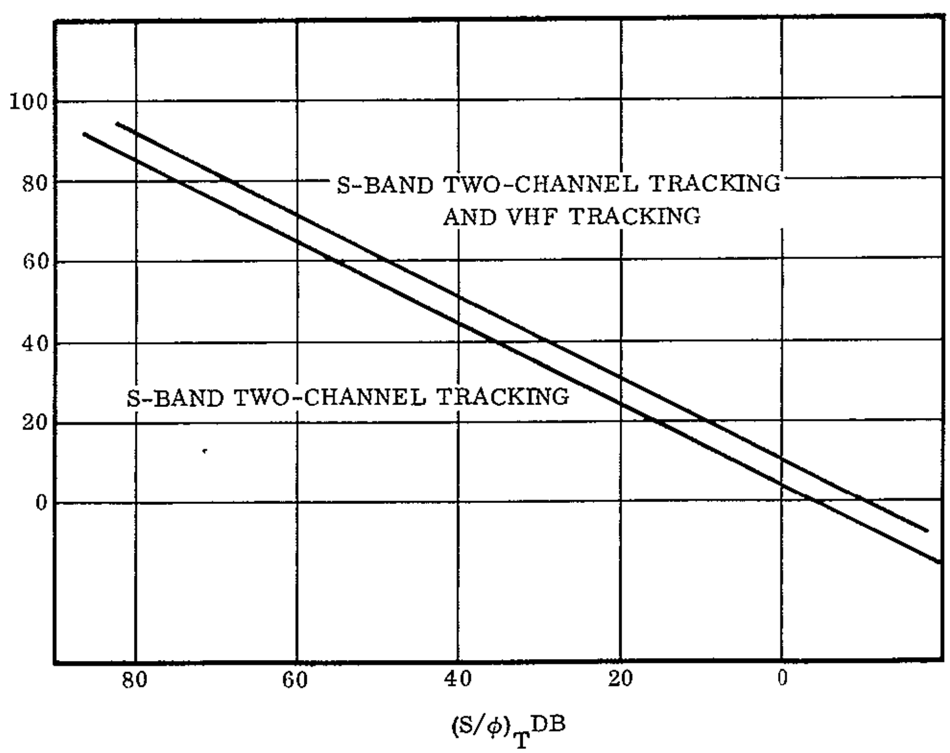

Figure 4-39. Power Density Relationships

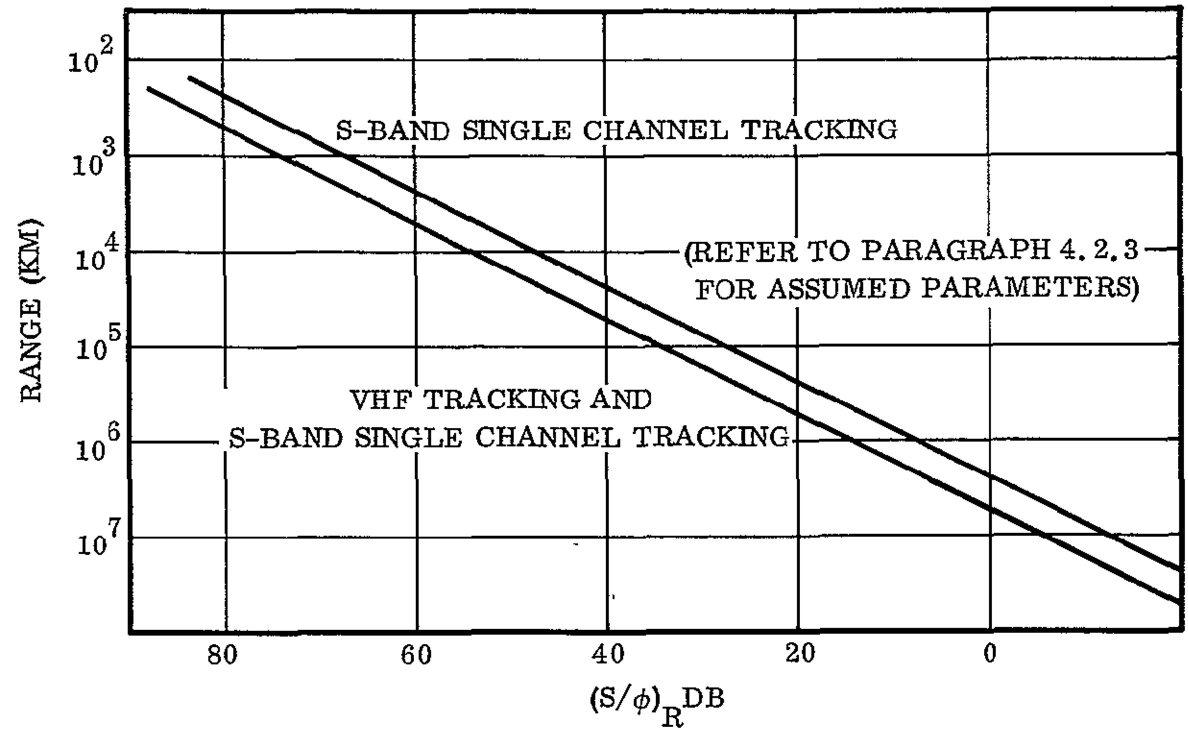

Figure 4-40. Signal-to-Noise Power Density vs. Range

The range instrumental accuracies obtained by combining range resolution and thermal noise errors are shown graphically in Figure 4-41 through 4-44 for various conditions. Figures 4-41 and 4-42 are for S-Band operation. Figure 4-41 is for the range tone tracking filter bandwidth ($2B_N$) of 1 Hz and includes maximum dynamic lag errors. Figure 4-42 is for the range tone tracking filter bandwidth ($2B_N$) of 0.1 Hz and includes no lag errors.

Figures 4-43 and 4-44 are for VHF operation. Figure 4-43 is for the 1 Hz bandwidth and maximum dynamics while Figure 4-44 is for the 0.1 Hz bandwidth and no dynamics.

4.7.3 Diversity Range Resolution and Instrumental Accuracy

The effects of polarization diversity tracking upon resolution and instrumental accuracy are not well known at this time. The effect will depend upon the relative phase and frequency differences which occur between the two polarizations as well as the relative signal strengths. At present, there is little data available which will allow realistic characterization of these differences at S-Band frequencies. Even after an appropriate model for input signal parameters is determined, the effect upon the data is difficult to assess.

Investigations in this area have begun and are continuing to be conducted by both General Dynamics and, under separate contract, by ADCOM, Inc. Through a cooperative effort,

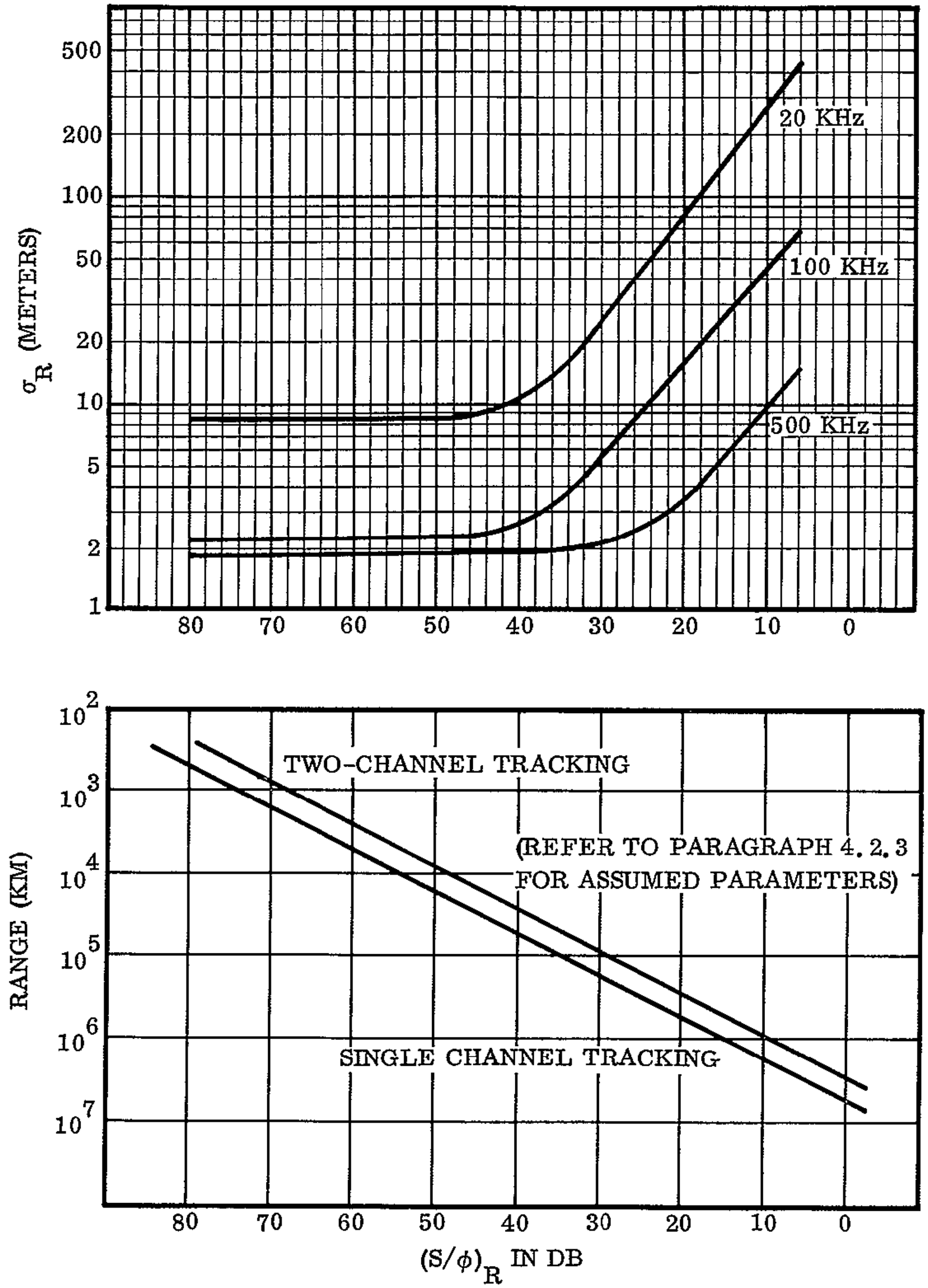

Figure 4-41. S-Band Range Instrumental Accuracy (1 Hz Range Tone Tracking Bandwidth With Maximum Doppler)

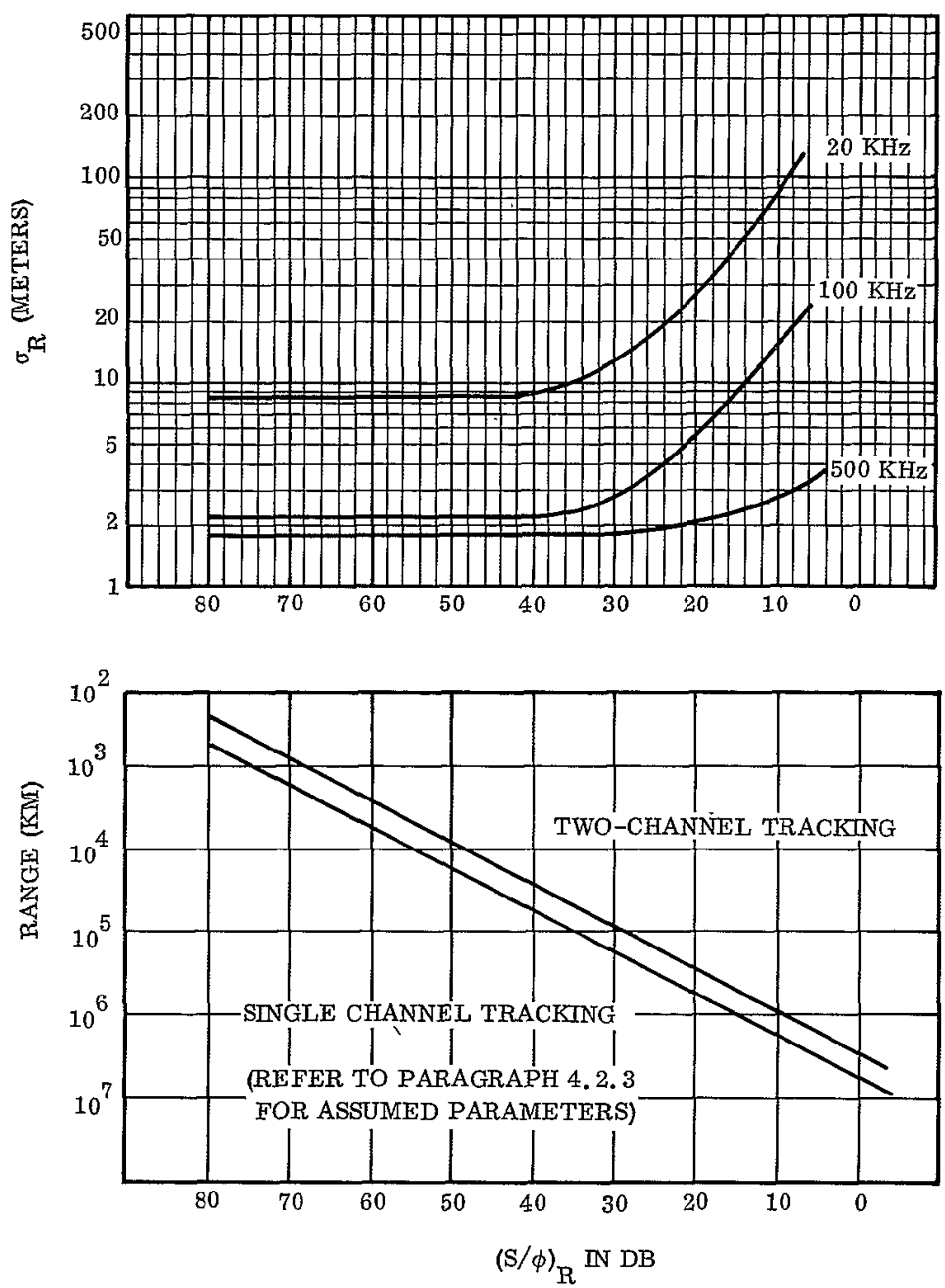

Figure 4-42. S-Band Range Instrumental Accuracy (0.1 Hz Range Tone Tracking Bandwidth With No Doppler)

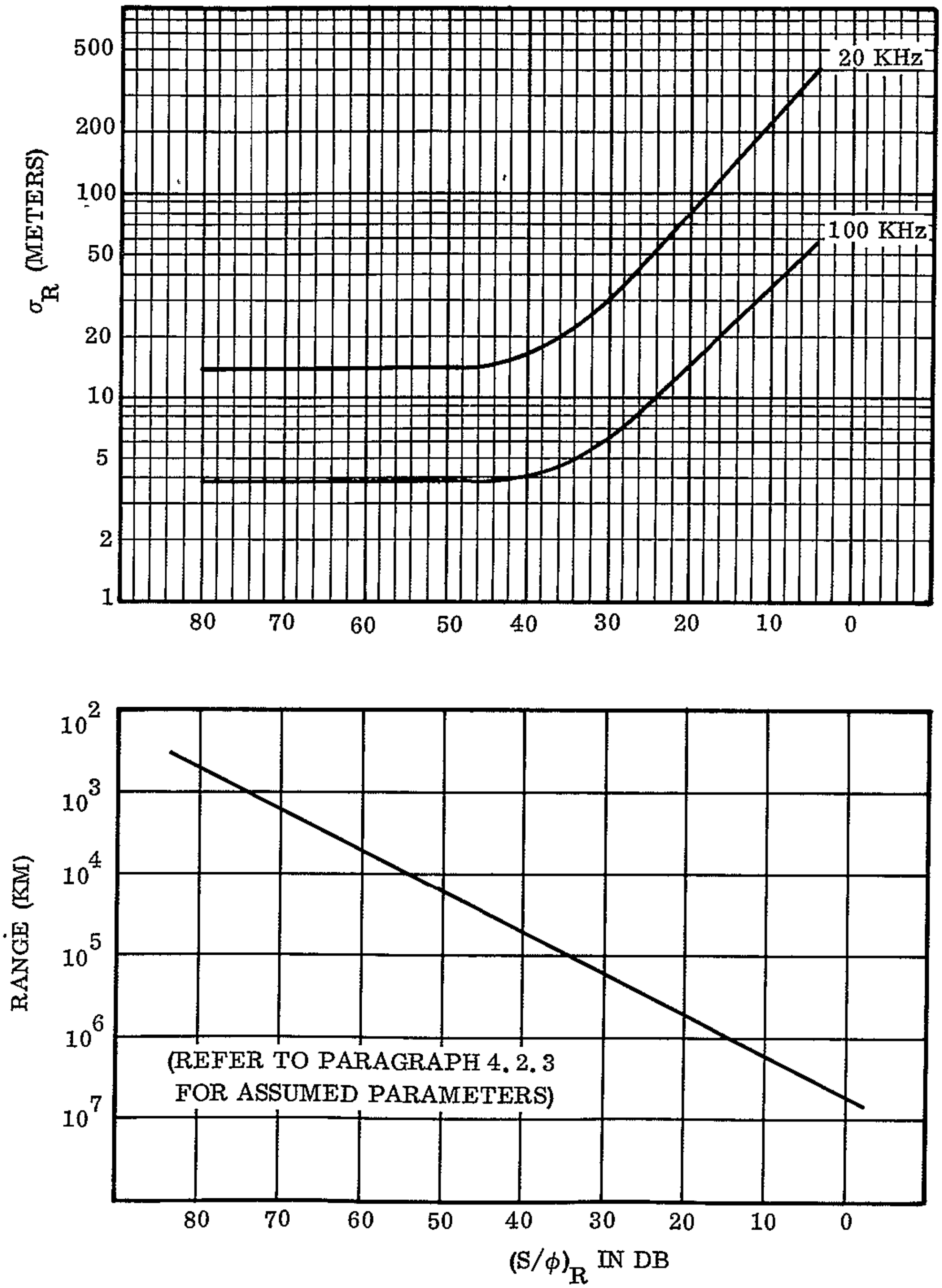

Figure 4-43. VHF Range Instrumental Accuracy (1 Hz Range Tone Tracking Bandwidth With Maximum Doppler)

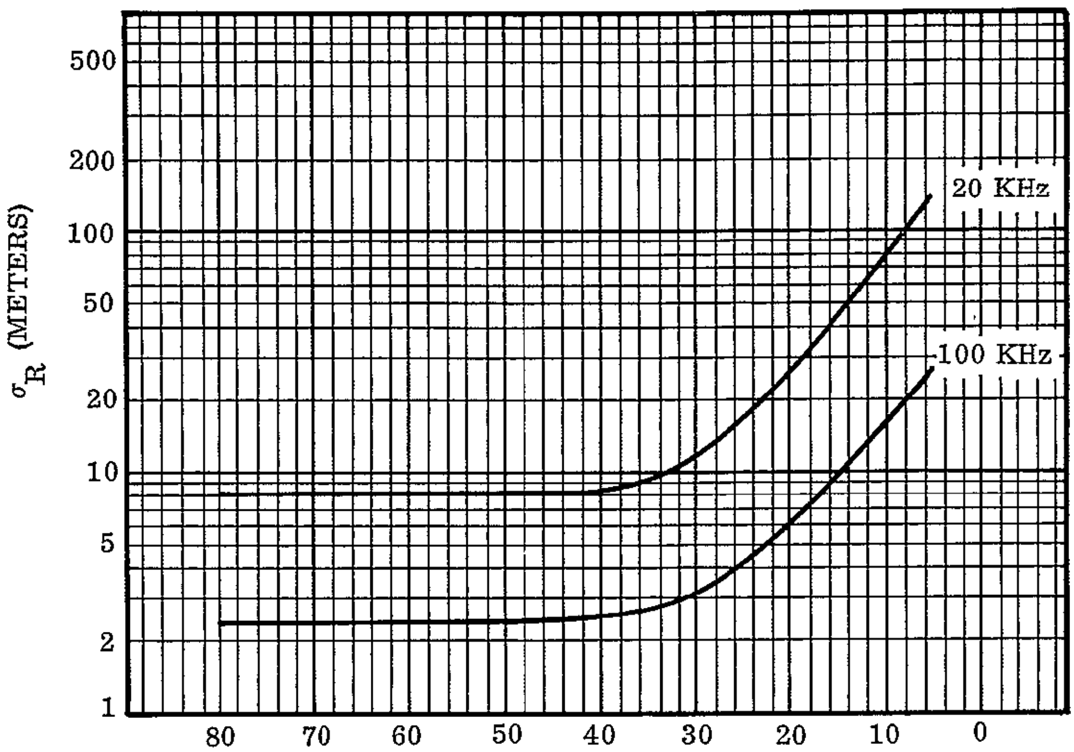

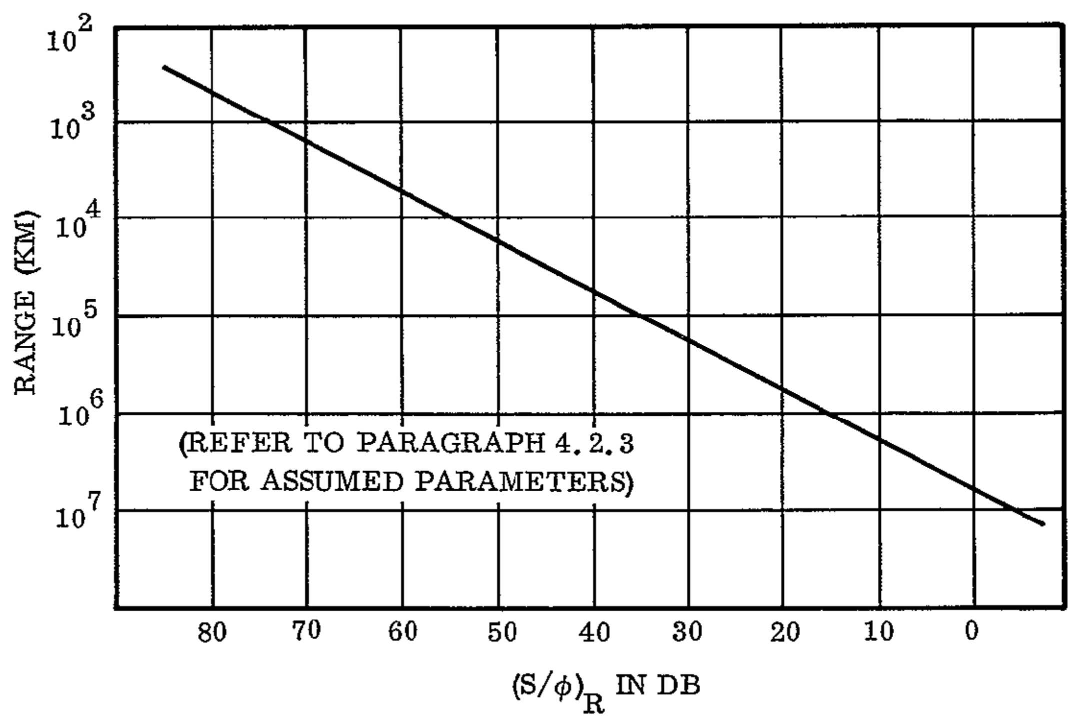

Figure 4-44. VHF Range Instrumental Accuracy (0.1 Hz Range Tone Tracking Bandwidth With No Doppler)

models for the input signals will be used in conjunction with a computer to determine the effects upon the data. The results of the investigation will be published in a separate document.

Although no specific data requirements have been established for diversity tracking, tests will be performed to the extent practicable to determine the effects of diversity and to compare the measured and predicted effects.

4.8 RANGE RATE ERROR ANALYSIS

The following error analysis for the range rate measurement discusses and groups errors in the same manner as the range error analysis. The definitions for resolution, instrumental accuracy, diversity resolution, and diversity instrumental accuracy given in Section 4.7 are applicable. As discussed in Section 4.7, the VHF error analysis is based upon a multifunctional receiver operating with a VHF preamplifier/converter. The analysis is applicable only for the Rosman, Tananarive, and Carnarvon sites.

4.8.1 Range Rate Resolution

Range rate resolution is limited by random and systematic errors of measurement of the time interval during which a specified number of cycles of a signal are observed. Error of measurement occurs as a result of both errors of measurement of the time interval and error of the time interval itself. In either case, the errors can be treated as errors of time measurement.

4.8.1.1 RANDOM ERRORS. Random errors which contribute significantly to range rate resolution take the form of quantizing error, jitter of the time interval counter start and stop times, and short term instability of the time base (≈10 MHz clock signal). Contributions to start or stop time jitter come from such sources as axis-crossing detectors, tracking loop and reference oscillators, and the high-speed gating circuitry of the time interval counter.

The doppler shift of the signal synthesized from the received carrier and subcarrier is determined by measuring the time interval corresponding to N cycles of a bias-plus-doppler signal. Thus:

$$N = (f_b + f_d)\,T$$

where

f_b = bias frequency

f_d = doppler frequency

N = total number of doppler-plus-bias cycles which are counted

T = the counting (or smoothing) time for N cycles of doppler plus bias

The doppler shift is determined by solving:

$$f_d = \frac{N}{T} - f_b$$

The dispersion of doppler shift resulting from a given dispersion of time measurement is determined by differentiating with respect to time to obtain:

$$\frac{\partial f_d}{\partial T} = -\frac{(f_b + f_d)^2}{N}$$

Thus the dispersion, σ_{fd}, of doppler measurement for given dispersion, σ_T, of time measurement is:

$$\sigma_{fd} = \frac{(f_b + f_d)^2}{N} \sigma_T$$

The resulting dispersion error in the determination of range rate is:

$$\sigma_{\dot{R}} = K \sigma_{fd} = K \frac{(f_b + f_d)^2}{N} \sigma_T$$

where K is a function of the carrier frequencies and coherence relationships of the transponder used in the measurement.

When operating with an S-Band or a VHF crystal transponder, the doppler shift observed corresponds to that which would be obtained if the transponder were to return the same frequency it received. In this case:

$$K_{XTAL} = C/2f_t = \lambda_t/2$$

where

C = velocity of propagation

f_t = carrier frequency transmitted from ground to the crystal transponder

λ_t = wavelength of transmitted carrier

K_{XTAL} = meters per sec per cycle per sec of doppler for XTAL transponder mode of operation

When operating with the S-Band PLL transponder, the observed doppler shift corresponds to round-trip transmission at a frequency 60 f_t/48. In this case:

$$K_{PLL} = C/2\left(\frac{60\, f_t}{48}\right) = \lambda_t'/2$$

where

f_t = carrier frequency transmitted from ground to PLL transponder

λ_t = 48 λ_t/60

λ_t' = wavelength of transmitted carrier

K_{PLL} = meters per sec per cycle per sec of doppler for PLL transponder mode of operation

The values of $(f_b + f_d)^2/N$ for the various modes and sampling rates are given in Table 4-27. The N values are from Table 2 of Specification Exhibit A. Values of $(f_b + f_d)$ maximum are 700 KHz for S-Band and 50 KHz for VHF.

Phase errors which appear at the bias-plus-doppler frequency $f_b + f_d$ are converted to time errors by

$$\sigma_T = \left(\frac{1}{f_b + f_d}\right)\sigma_\phi$$

Since

$$\sigma_{\dot{R}} = K\left(\frac{f_b + f_d}{N}\right)^2 \sigma_T$$

Table 4-27. Sampling Rates and Modes

Sampling Rate (Sec^{-1})	S-Band	VHF
	$(f_b + f_d)^2/N$	
4	7.48×10^6	6.11×10^5
2	3.74×10^6	3.05×10^5
1	2.14×10^6	1.74×10^5
0.1	1.56×10^5	1.37×10^4

then

$$\sigma_{\dot{R}} = K \left(\frac{f_b + f_d}{N} \right) \sigma \phi$$

4.8.1.1.1 Transmitted Carrier. The transmitted carrier is generated by using a synthesizer output at about 350 MHz which is multiplied by 4. The synthesizer output phase noise density in radians^2/Hz is approximately -63 db at 1 Hz and varies at $1/\omega^2$. It has a value, therefore, of approximately -47 db at one radian per second.

The rms phase errors is given by

$$\sigma_\phi = \left[\frac{1}{2\pi} \int_{-\infty}^{\infty} S_\phi(\omega) \, |H(\omega)|^2 \, d\omega \right]^{1/2}$$

and the rms error of angular frequency

$$\sigma = \sigma_{\dot{\phi}} = \left[\frac{1}{2\pi} \int_{-\infty}^{\infty} S_{\dot{\phi}}(\omega) \, |H(\omega)|^2 \, d\omega \right]^{1/2}$$

where $S_{\dot{\phi}}(\omega) = \omega^2 S_{\dot{\phi}}(\omega) = -47$ db

The transfer function in the worst case (largest noise bandwidth) is given by the product of the servo transfer function and a sin $(\omega T/2)/(\omega T/2)$ transfer function of the sampling filter used to compute range rate (doppler frequency).

Assuming the servo response is unity to 3000 Hz and that the sampling filter response is unity to 1/T Hz and falls off as $1/\omega$ beyond 1/T Hz, gives an equivalent rms angular frequency error of 0.018 rad/sec at the output of the synthesizer and 0.072 rad/sec at the S-Band transmitter output. The equivalent time jitter in the $(f_b + f_d)$ signal in the time interval gate is 4.1 nanosec.

The same synthesizer signal is used without multiplication for the VHF transmitter. The equivalent time jitter for the time interval gate is 14.3 nanosec for VHF.

4.8.1.1.2 First Local Oscillator. The spurious signal level specified for the 5 MHz system reference signal is -80 db. The signal is multiplied by 360 giving an increase in level of 51 db and a resulting spurious level of +29 db. This gives a possible phase modulation amplitude of $57.3(28.3\ \sqrt{2})=1.43$ degrees rms. The multiplier is specified to add not over 1 degree rms to this, giving a total of 1.75 degrees rms at S-Band. The spurious level for the VHF reference is -80 db and a multiplication of 63 is used. This raises the possible spurious level to $-80.0 + 36.0 = -44$ db. The resulting phase modulation rms value is $57.3\ (1.58\ \sqrt{2} \times 10^{2}) = 0.26$ degrees.

Assuming a 0.2 degree rms addition by the multiplier gives an error contribution of 0.328 degree rms for VHF. The resulting rms time errors from beginning to end of the time interval at the time interval counter are:

$$\sigma_T = \frac{\sqrt{2}\,\sigma_\phi}{360}\left(\frac{1}{f_b + f_d}\right) = 9.8 \text{ nanosec for S-Band}$$

$$= 31.7 \text{ nanosec for VHF}$$

4.8.1.1.3 Carrier/Subcarrier PLL VCXO Instability. The short-term instabilities of the VCXO's in the carrier PLL and the subcarrier PLL contribute a phase jitter to the start and the stop pulses of the time interval counter. The specified error for each VCXO operating closed loop with strong signal-to-noise ratio is 3 degrees rms. The rms error of the start pulse and of the stop pulse, due to VCXO noise, is therefore a $3\sqrt{2}$ degrees and the time interval error is $3\sqrt{2}\sqrt{2}\ =\ 6$ degrees.

Since the time jitter corresponding to σ_ϕ degrees rms of phase jitter is

$$\sigma_T = \frac{\sigma_\phi}{360}\left(\frac{1}{f_b + f_d}\right)$$

then, the rms time error contributed by the two VCXO's is

$$\sigma_T = \frac{6}{360}\left(\frac{1}{7 \times 10^5}\right) = 23.8 \text{ nanosec for S-Band}$$

$$= \left(\frac{6}{360}\right)\left(\frac{1}{5 \times 10^4}\right) = 333 \text{ nanosec for VHF}$$

4.8.1.1.4 Doppler Extractor Reference Signal. A spurious signal is present on the reference signal source at a level of -51 db. The signal is multiplied by 48 for S-Band operation and by 6 for VHF operation. This gives a possible increase of 34 db to a level of -21 db for S-Band and an increase of +15.6 db to -39.4 db for VHF.

The corresponding possible amplitude of phase modulation is 57.3/11.2 = 5.1 degrees for S-Band and 57.3/91.2 = 0.57 degrees for VHF.

Assuming a random relationship between the perturbation of the start pulse and the stop pulse, the rms phase errors are the same as the amplitudes given above and the resulting rms time interval errors are

$$\sigma_T = \frac{\sigma_\phi}{360}\left(\frac{1}{f_b + f_d}\right)$$

$$= \frac{5.1}{360}\left(\frac{1}{7 \times 10^5}\right) = 20.2 \text{ nanosec for S-Band}$$

$$= \frac{0.57}{360}\left(\frac{1}{5 \times 10^4}\right) = 31.7 \text{ nanosec for VHF}$$

4.8.1.1.5 Axis-Crossing Detector. An axis-crossing detector is used to generate the start pulse and the stop pulse from the doppler-plus-bias output signal of the doppler extractor. Time jitter added to the signal is a function of the signal frequency. The signal frequency in the S-Band mode is 500 KHz (±200 KHz). A rms jitter of 3.5 nanosec is assumed in this mode.

The signal frequency in the VHF mode is 30 KHz (±20 KHz). An rms jitter of 20 nanosec is assumed in this mode.

Assuming no correlation, the axis-crossing detector error contribution is

$$\sigma_T = 3.5\sqrt{2} = 4.95 \text{ nanosec S-Band}$$

$$= 28.28 \text{ nanosec VHF}$$

4.8.1.1.6 Quantizing. A clock frequency of approximately 10 MHz is used to measure the time interval between a start pulse and a stop pulse. Either pulse can occur at any time relative to the clock pulse train. Thus the rms error of measurement of the time interval (due to quantizing) is (as discussed in Section 4.7.1.1.5):

$$\left(\sigma_T\right)_q = 1/\sqrt{6}\, f_R = 41 \text{ nanosec}$$

4.8.1.1.7 Time Base Reference Jitter. The time base reference (10 MHz clock frequency) jitter results from short-term instability of the reference oscillator, which furnishes a 1 MHz reference, and jitter added by the 10 MHz synthesis circuitry (×10 multiplier). The error contribution by reference oscillator instability is negligible. A 3 nanosec jitter on the synthesized 10 MHz signal is assumed. Assuming no correlation of jitter error of the start and stop pulses, the resulting time base jitter is·

$$\sigma_T = 3\sqrt{2} = 4.24 \text{ nanosec}$$

4.8.1.1.8 Time Interval Unit Gating. The time interval unit gate is turned on by a start pulse and turned off by a stop pulse. A random error of 1 nanosec is assumed for each operation. This gives an rms error of the interval of $\sqrt{2}$ nanosec.

4.8.1.2 SYSTEMATIC ERRORS. Due to the short sampling interval, there are no significant systematic error contributions to the measurement of range rate.

4.8.1.3 RANGE RATE RESOLUTION SUMMARY. A summary of the time errors for range rate and the root-sum-square is shown in Table 4-28 for the S-Band and VHF crystal transponder cases. The corresponding range rate resolution for each sample rate is given in Table 4-29 using the values from Table 4-27 to convert time error to range rate error.

Table 4-28. Range Rate Time Error Summary

Source	σ_T (nanosec)	
	S-Band	VHF
Transmitted Carrier	4.1	14.3
1st Local Oscillator	9.8	31.7
Carrier/Subcarrier PLL VCXO Instability (3° each)	23.8	333
Doppler Extractor Reference Signal	20.2	31.7
Axis-Crossing Detector	4.95	28.3
Quantization	41	41
Time Base Reference	4.24	4.24
Time Interval Unit Gate	1.4	1.4
RSS	53	340.0

Table 4-29. Range Rate Resolution

Sample Rate	$\sigma_{\dot{R}}$ (meters/sec)	
	S-Band	VHF
4	0.034	0.21
2	0.017	0.105
1	0.00975	0.06
0.1	0.00071	0.0047

4.8.2 Range Rate Instrumental Accuracy

Range rate instrumental accuracy is obtained by combining the range rate resolution with errors due to additive input thermal noise.

The random error in range rate due to thermal noise is a function of the signal-to-noise power density ratio for the received carrier and subcarrier and the noise bandwidth of the PLL (phase-lock loop) for the carrier and the subcarrier PLL's. The rms phase tracking error for PLL is given by

$$\sigma_{\phi} = [N/2S]^{1/2} \text{ radian}$$

where

$N = 2B_n \Phi$

B_n = one-sided noise bandwidth of the PLL

Φ = noise power density about the tracked signal

Therefore

$$\sigma_{\phi} = [B_n \Phi/S]^{1/2} \text{ radian}$$

where S/Φ = the signal-to-noise power density ratio for the received carrier or subcarrier.

The equivalent rms time error is:

$$\sigma_T = \left[\frac{1}{2\pi(f_b + f_d)}\right]\sigma_{\phi}$$

and the resulting rms range rate error is:

$$\sigma_{\dot{R}} = K\left[\frac{f_b + f_d}{2\pi N}\right]\left[\frac{B_n \Phi}{S}\right]^{1/2}$$

The values of $(f_b + f_d)/2\pi N$ for the various modes and sampling rates are given in Table 4-30. The N values are from Table 2 of Specification Exhibit A. Values of $(f_b + f_d)$ max are 700 KHz for S-Band and 50 KHz for VHF.

Table 4-30. Values of $(f_b + f_d)/2\pi N$

Sampling Rate (sec^{-1})	S-Band	VHF
4	1.700	1.944
2	0.850	0.972
1	0.486	0.555
0.1	0.0356	0.0437

K is (as stated in Paragraph 4.8.1.1):

$$K_{PLL} = 48\,\lambda_t/60 \quad \text{for S-Band PLL transponder}$$

$$K_{XTAL} = \lambda_t/2 \quad \text{for VHF or S-Band XTAL transponder}$$

where λ_t = wavelength of transmitted carrier

In the XTAL transponder mode of operation, the RSS (root sum square) of the error contributions of the carrier PLL and the subcarrier PLL is:

$$\sigma_{\dot{R}} = \left[(\sigma_{\dot{R}})^2_c + (\sigma_{\dot{R}})^2_{sc}\right]^{1/2}$$

$$= \left[\frac{\lambda_t}{2}\right]\left[\frac{f_b + f_d}{2\pi N}\right]\left[\left(\frac{B_n\Phi}{S}\right)_c + \left(\frac{B_n\Phi}{S}\right)_{sc}\right]^{1/2}$$

Normally, equal values of B_n are used in the carrier and subcarrier loops and this is the assumed case

Therefore

$$\left[\left(\frac{B_n \Phi}{S}\right)_c + \left(\frac{B_n \Phi}{S}\right)_{sc}\right]^{1/2} = \left(\frac{B_n \Phi}{S}\right)_c^{1/2} \left[1 + \left(\frac{\Phi}{S}\right)_{sc} \bigg/ \left(\frac{\Phi}{S}\right)_c\right]^{1/2}$$

Also

$$\left(\frac{B_n \Phi}{S}\right)_c = \left(\frac{B_n \Phi}{S}\right)_T \left[\left(\frac{\Phi}{S}\right)_c \bigg/ \left(\frac{\Phi}{S}\right)_T\right]$$

Let

$$\left[\left(\frac{\Phi}{S}\right)_c \bigg/ \left(\frac{\Phi}{S}\right)_T\right] = a$$

and

$$\left[\left(\frac{\Phi}{S}\right)_{sc} \bigg/ \left(\frac{\Phi}{S}\right)_c\right] = b$$

Then

$$\sigma_{\dot{R}} = K_{\dot{R}} \left[\left(\frac{\Phi}{S}\right)_T\right]^{1/2}$$

where $K_{\dot{R}} = \left(\frac{\tau_t}{2}\right)\left[\frac{f_b + f_d}{2\pi N}\right] \left[B_n\, a\, (1 + b)\right]^{1/2}$

The values of $(S/\Phi)_c/S/\Phi)_T$ and $(S/\Phi)_{sc}/\ (S/\Phi)_c$ were tabulated in Section 4.2 for each mode of operation. The values of $(S/\Phi)_T$ versus range are plotted in Figure 4-7 for the VHF downlink and in Figure 4-8 for the S-Band downlink.

Three operating conditions have been selected for analysis. These are: (1) VHF Tracking (VHF case 3 from Table 4-8), (2) S-Band Single Channel Tracking (S-Band Single Channel case 2 from Table 4-9), and (3) S-Band Two-Channel Tracking (S-Band Two Channel case 3 from Table 4-9). All cases analyzed are for crystal transponders. The values of $\underline{a}$ and $\underline{b}$ in db and the resulting numerical value of $[a\ (1 + b)]^{1/2}$ are listed for each case in Table 4-31.

Table 4-31. Values for Selected Conditions

Condition	a (db)	b (db)	$[a\ (1 + b)]^{1/2}$ Numerical
VHF Tracking	+1.1	+6.9	2.75
S-Band Single Channel Tracking	+5.8	-1.1	2.60
S-Band Two-Channel Tracking	+2.5	+7.5	3.43

Two values of B_n are used for these calculations. They are B_n = 10 Hz and B_n = 1 KHz. The resulting values of $[B_n\ a\ (1 + b)]^{1/2}$ are listed in Table 4-32.

Table 4-32. Selected Modes and B_n Values

Condition	Value for B_n = 10 Hz	Value for B_n = 1 KHz
VHF Tracking	8.72	87.2
S-Band Single Channel Tracking	8.22	82.2
S-Band Two-Channel Tracking	10.85	108.5

Values of $\lambda_t/2$ for operation on the low side of the band are:

$\lambda_t/2$ = 1.021 meter for VHF (148 MHz)

$\lambda_t/2$ = 0.0856 meter for S-Band (1750 MHz)

Values of K_R resulting from operating in each of the three conditions, at each available data sampling rate, and with of B_n values of 10 Hz or 1,000 Hz are listed in Table 4-33.

Table 4-33. Sampling Rate Values of $K_{\dot{R}}$

Condition	Sampling Rate (sec^{-1})	$K_{\dot{R}}$	
		B_n = 10 Hz	B_n = 1000 Hz
VHF Tracking	4	17.3	173
	2	8.65	86.5
	1	4.94	49.4
	0.1	0.389	3.89
S-Band Single Channel Tracking	4	1.20	12.0
	2	0.598	5.98
	1	0.342	3.42
	0.1	0.025	0.25
S-Band Two-Channel Tracking	1	1.58	15.8
	2	0.79	7.9
	1	0.45	4.5
	0.1	0.033	0.33

The range rate instrumental accuracy is shown graphically for various conditions in Figures 4-45 and 4-46.

4.8.3 Diversity Range Rate Resolution and Instrumental Accuracy

Refer to Paragraph 4.7.3.

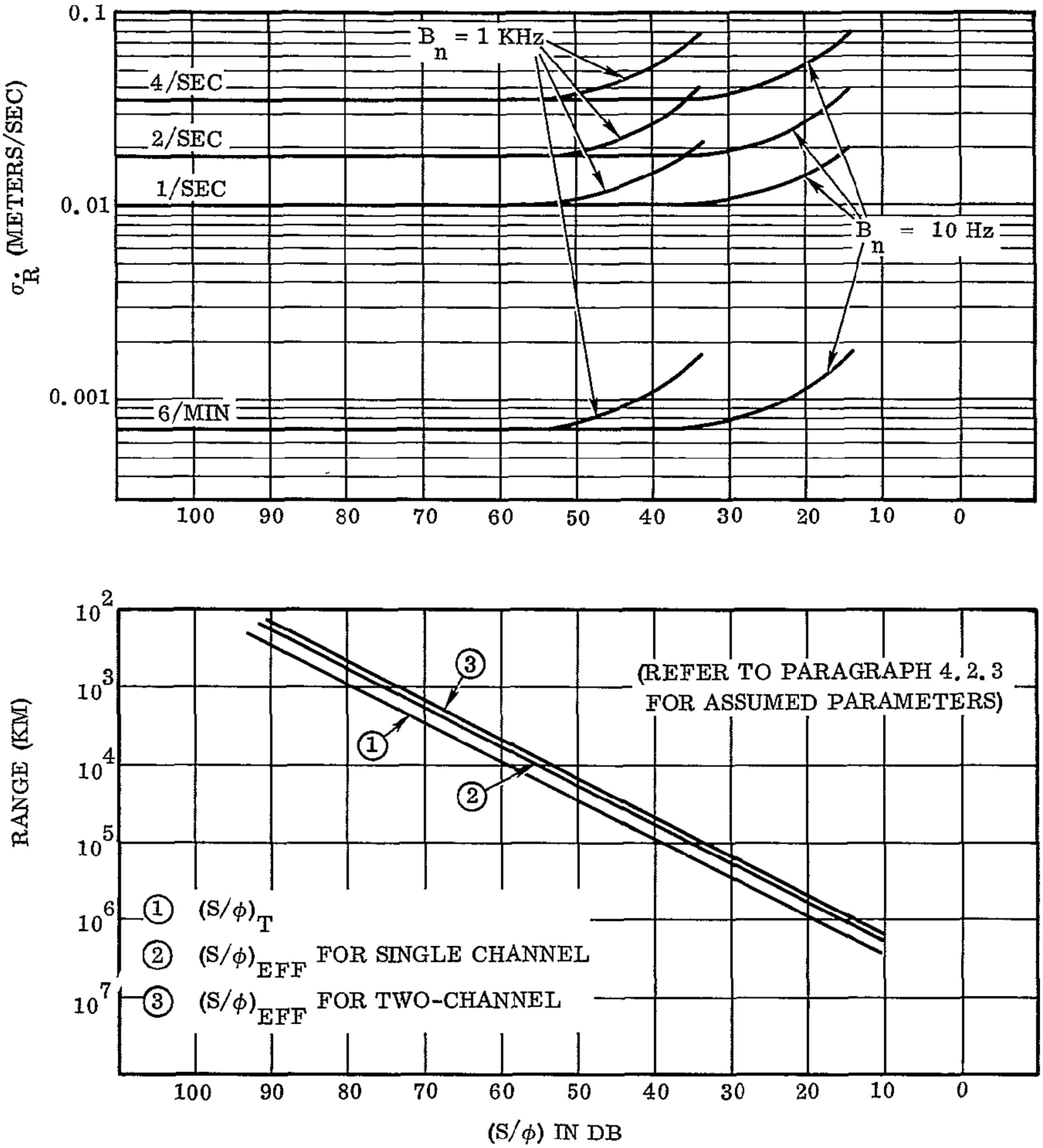

Figure 4-45. Range Rate Instrumental Accuracy S-Band Operation

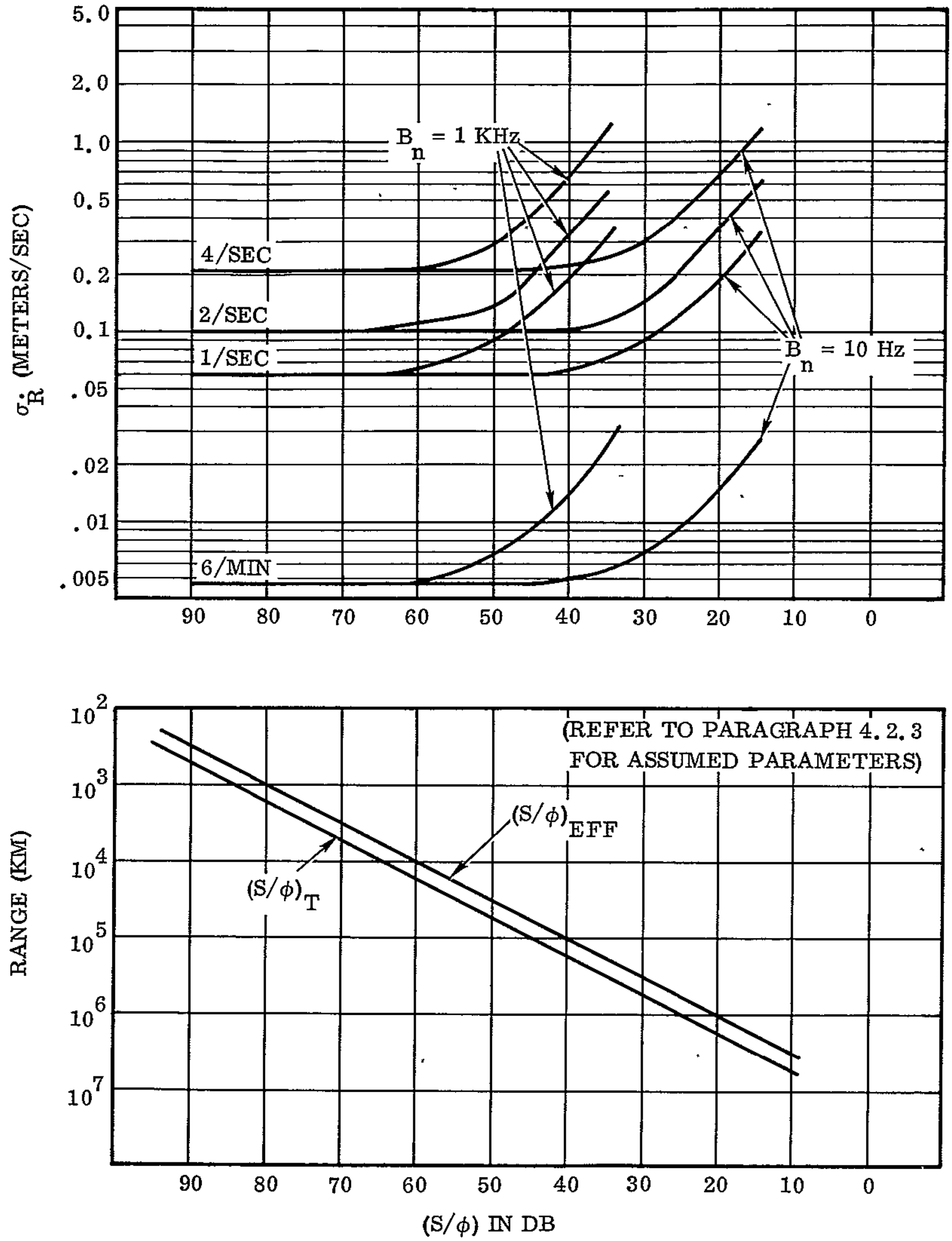

Figure 4-46. Range Rate Instrumental Accuracy VHF Operation

4.9 ANGLE DATA ERROR ANALYSIS

In general, modifications to the existing equipment will not affect the antenna pointing or angle tracking functions. The VHF antenna pointing and tracking system will not be affected whatsoever. For the S-Band system, no modifications are made for the purpose of affecting the antenna tracking system. Certain modifications made for other purposes, however, will inherently enter into the antenna tracking function. These include replacing the S-Band feed assembly and the S-Band receiver which supplies the autotrack error signals. Where these modifications do affect the antenna tracking function, the performance of the new equipment will be equal to or better than the existing equipment performance. In general, however, any change in performance of the angle tracking system will be negligible.

Angle tracking error analyses for the existing equipment may be found in the following documents:

a. Rosman, Carnarvon, and Tananarive Sites

   Motorola Report No. W2719-2-1 Goddard Range and Range Rate System Design Evaluation Report. November 1962. Contract No. NAS 5-1926.

b. Fairbanks Site

   General Electric — Goddard Range and Range Rate System (GRR-2) Design Evaluation Report — November 1964. Contract No. NAS 5-9731 and addendum thereto.

4.10 SYSTEM ACQUISITION

This subsection provides (1) an analysis to determine the required ambiguity resolving code (ARC) correlation time, and (2) acquisition time calculations for the entire system under various conditions.

4.10.1 Ambiguity Resolving Code Acquisition Analysis

Paragraph 3.7.1.6 described the Ambiguity Number Extraction Unit. This unit functions to determine a number from 0 to 63 which represents the number of 1/8-second ambiguities which must be added to the time interval measured by the sidetone ranging equipment to produce a time interval number representing the full unambiguous range. An analysis of the time required to determine the correlation between the received pseudo-random code and the local regenerated code follows. This time is principally a function of the code length and the received signal-to-noise ratio. Figure 4-47 is a simplified diagram of the correlation section of the Ambiguity Number Extraction Unit. Expressions for the associated signals follow.

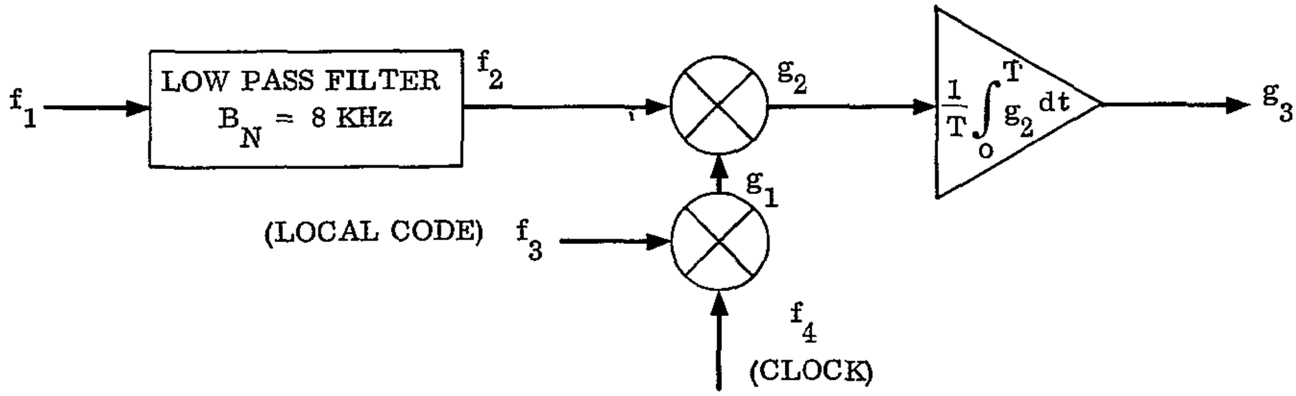

Figure 4-47. Correlation Section Block Diagram

If

$$f_3 = a(t + m\Delta t) \tag{1}$$

where

$a(t) = \pm 1$ (two-valued)

m = constant

Δt = bit period of clock

$$f_4 = +1 \qquad \Delta t = 0, 2, 4, \text{even}$$

$$f_4 = -1 \qquad \Delta t = 1, 3, 5, \text{odd}$$

then

$$g_1 = f_3 f_4 = a(t + m\Delta t)\Big|_{t=\text{even}} - a(t + m\Delta t)\Big|_{t=\text{odd}} \tag{2}$$

also

$$f_2 = A\, a(t) \sin \omega t + n'(t) \tag{3}$$

where

A = amplitude of signal

$a(t)$ = time-valued function describing the transmitted code

$\sin \omega t$ = sinusoid at frequency equaling the bit period

$n'(t)$ = band limited noise

then

$$g_2 = f_2 g_1 = (A\, a(t) \sin \omega t) \left[a(t + m\Delta t) \Big|_{t=\text{even}} - a(t + m\Delta t) \Big|_{t=\text{odd}} \right] \tag{4}$$

$$+ n'(t) \quad a(t) \left[a(t + m\Delta t) \Big|_{t=\text{even}} - a(t + m\Delta t) \Big|_{t=\text{odd}} \right]$$

Since $a(t)$ and $\sin \omega t$ have the same period for all t

$$g_2 = A\, a(t)\, a(t + m\Delta t)\, |\sin \omega t| + n(t) \tag{5}$$

Since $a(t + m\Delta t)$ is pseudo-random, it has approximately equal plus and minus values. Therefore $n'(t)$ is not affected except that its variance is reduced by one-half by the demodulation process.

After integration it becomes, if self-noise is neglected

$$g_3 = \frac{A}{T} \int_0^T a(t)\, a(t + m\Delta t)\, |\sin \omega t|\, dt \tag{6}$$

$$+ \frac{1}{T} \int_0^T n(t)\, dt$$

for

$$m \neq 0, \quad g_3 = 0$$

for

$$m = 0, \quad g_3 = \frac{A}{T}\int_0^T |\sin \omega t|\, dt = \frac{2A}{\pi}$$

The noise integral may be evaluated as follows.

Assuming band-limited noise, the integral can be approximated by

$$\frac{1}{T}\int_0^T n(t)\, dt \cong \frac{1}{N}\sum_{i=0}^{N} n_i \text{ with } N = B_n T \tag{7}$$

Now $1/B_n$ in this particular situation is related to Δt, the bit time of the code; in fact

$$1/B_n = 1/8 \text{ Hz} = \frac{\Delta t}{2} \tag{8}$$

Now the approximation is seen to be the sample mean. The expected value will be zero while the variance of the sample mean will be (from Reference 5):

$$\sigma_I^2 = \frac{\sigma_n^2}{N} = \frac{\sigma_n^2}{B_n T} = \left[\frac{\Delta t}{2T}\right]\sigma_n^2 = \left[\frac{\Delta t}{2T}\right]\left[\frac{\sigma_n'^2}{2}\right] \tag{9}$$

Now suppose that any decision will be based on the 3σ value of the noise term so that the probability of making an erroneous decision is 0.0027. Figure 4-48 shown below illustrates at what level a decision will be made.

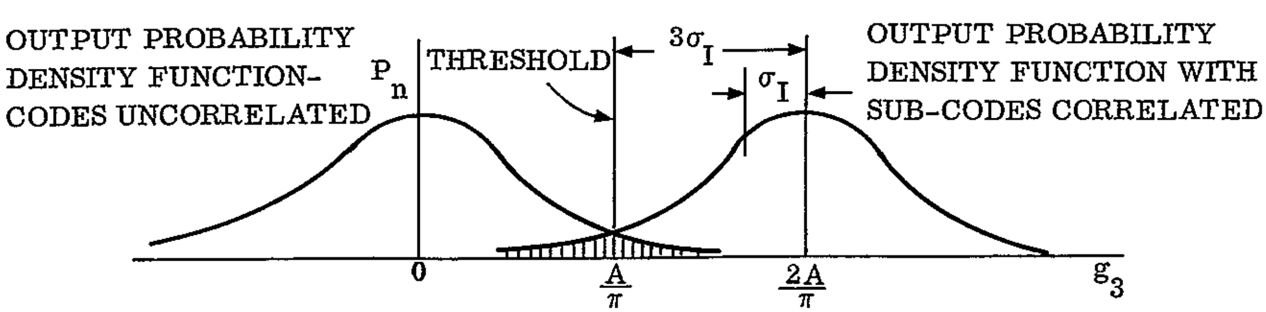

Figure 4-48. Correlator Output Probability Density Function

The two shaded areas represent the probability that an error will be made if one half the level of the signal output is chosen as threshold. This allows an equation to be written which will determine T, the integration time for each sub-code shift position. If g_3 is normalized with respect to A

$$\frac{g_3}{A} \leq \frac{2}{\pi} - \frac{3\sigma_1}{A} = \frac{2}{\pi} - \frac{3}{A}\left[\frac{\Delta t}{4T}\right]^{1/2} \sigma_n' \qquad m = 0 \tag{10}$$

$$\frac{g_3}{A} \geq \frac{3\sigma_I}{A} = \frac{3}{A}\left[\frac{\Delta t}{4T}\right]^{1/2} \sigma_n', \qquad m \neq 0 \tag{11}$$

Now since there can be only one threshold, the two equations can be equated and solved for T

$$T = \frac{9\pi^2 \Delta t}{4(A^2/\sigma_{n'}^2)} = \frac{9\pi^2 \Delta t}{8(S/N)_{input}} \tag{12}$$

where (S/N) is the power signal-to-noise ratio at the input to the g_2 multiplier.

The minimum signal-to-noise ratio into the g_2 multiplier is approximately -33 db. Substituting this S/N into the equation yields an integration of time of approximately 5.6 seconds.

4.10.1.1 SELF NOISE CONSIDERATIONS. In order to completely eliminate the effects of self noise, the integration time must be some multiple of the ambiguity code cycle time. However, the effect can be reduced to a point where it is negligible by integrating over 5 to 10 percent of the code cycle time (Reference 6). The code being used is 32,385 bits long with each bit corresponding to 1/4000-second so the minimum allowable integration time is

$$T_{MIN} = \frac{32,385}{4000}\ (0.05) \approx 0.4 \text{ second} \tag{13}$$

4.10.1.2 INTEGRATION TIMES. Using the information discussed above and considering what integration times are most easily implemented the following integration times have been chosen:

$$T_1 = 1.0 \text{ sec}$$

$$T_2 = 10.0 \text{ sec}$$

Note that a safety factor has been included in the maximum integration to allow for unexpected drops in signal power. A two-position switch mounted on the cabinet control panel allows either of the two integration times to be selected.

4.10.2 System Acquisition

Because of the wide variety of input signal conditions, system modes of operation, available bandwidths, etc., all possible cases of acquisition methods and resulting times cannot be practicably analyzed at this time. Two extreme cases and one practicable representative case are discussed below with the following conditions assumed:

a. The mode of operation requires acquiring:

(1) S-Band carrier
(2) Subcarrier
(3) Major range tone
(4) 7 minor range tones
(5) Ambiguity resolving code

b. With the selected bandwidths and integration times signal-to-noise ratios exist which allow correlation or lack of correlation to be properly recognized (no decision errors).

c. The ambiguity resolving code designate number has been preset so that one and only one integration period is required to acquire the code.

d. Automatic acquisition is used for each signal.

e. Antenna pointing is correct (angle acquisition is not required).

f. The various signals are acquired in the following manner:

<u>Carrier</u>: Phase-locked loop VCO is swept for specified period depending on selected bandwidth.

<u>Subcarrier</u>: Same as carrier

<u>Major Range Tone</u>: Phase-locked loop acquisition bandwidth encompasses signal. Bandwidth may be automatically reduced.

<u>Minor Range Tones</u>: Phase information is integrated for selected period and phase adjusted in 1/5 cycle increments. A minimum of two and a maximum of three integrations are required.

<u>ARC</u>: Correlation is checked by integrating for selected period.

4.10.2.1 STRONG SIGNAL CASE. In this case, it is assumed that sufficient signal exists to allow use of the widest bandwidths and shortest integration times. Table 4-34 lists the maximum and average acquisition times for each signal.

Table 4-34. Strong Signal Acquisition Times

Signal	Maximum Acquisition Time (Sec)	Average Acquisition Time (Sec)
Carrier	2.0	1.0
Subcarrier	2.0	1.0
Major Range Tone	2.5	2.0
7 Minor Range Tones	2.625	2.2
ARC	1.0	1.0
Total	10.125	7.2

4.10.2.2 WEAK SIGNAL CASE. In this case, it is assumed that the narrowest bandwidths and longest integration times must be used. It is still assumed, however, that with these conditions, correlation or lack of correlation will be properly recognized for each signal (no decision errors). Table 4-35 lists acquisition times for this case.

Table 4-35. Weak Signal Acquisition Times

Signal	Maximum Acquisition Time (Sec)	Average Acquisition Time (Sec)
Carrier	20.0	10.0
Subcarrier	20.0	10.0
Major Range Tone	2.5	2.0
7 Minor Range Tones	210.0	140.0
ARC	10.0	10.0
Total	262.5	172.0

4.10.2.3 MEDIUM SIGNAL CASE. In this case, it is assumed that carrier and subcarrier bandwidths of 100 Hz are selected, and that minor range tone and ARC integration times of 1 sec are selected. Again, it is assumed that correlation or lack of correlation will be properly recognized for each signal (no decision errors). Table 4-36 lists acquisition times for this case.

Table 4-36. Medium Signal Acquisition Times

Signal	Maximum Acquisition Time (Sec)	Average Acquisition Time (Sec)
Carrier	6.0	3.0
Subcarrier	6.0	3.0
Major Range Tone	2.5	2.0
7 Minor Range Tones	21.0	17.5
ARC	1.0	1.0
Total	36.5	26.5

4.10.2.4 SUMMARY. From Tables 4-34 and 4-35 it may be seen that the average acquisition time for the entire system will range from 7.2 seconds to 172 seconds depending upon the system selections necessarily made to be compatible with input signal level conditions. As may also be noted from the table, total acquisition time is most affected by the selected minor range tone integration period.

For most real missions (earth orbits), a 1-sec integration period is sufficient. Thus, for these missions, the average system acquisition time will be in the region of 20 to 30 sec.

4.11 TRANSPONDER TEST SET ANALYSIS

In the following discussion, two areas will be covered: (1) the effect of the subcarrier phase noise on the transmitter phase noise measurement, and (2) the delay time of the transponder simulator.

4.11.1 Transmitter Phase Noise Measurement

The specification on transmitter short-term stability requires that the oscillators be designed such that the total system phase jitter is less than 6 degrees rms at the subcarrier phase detector output. The transponder simulator reference oscillator, the carrier receiver oscillators, and the receiver subcarrier oscillator, as well as the transmitter oscillators (VCXO), contribute to system phase jitter.

The reference oscillator contributes negligible jitter since it is a stable crystal-controlled oscillator. The carrier receiver oscillators (VXCO and reference oscillator) contribute phase jitter only if there is imbalance between the amplitudes of the subcarrier sidebands (Reference 7). The formula predicting the amount of phase jitter due to sideband imbalance is

$$\theta_{SCC} = \left(\frac{\delta-1}{\delta+1}\right) \theta_c \tag{1}$$

where

θ_{SCC} = phase jitter on subcarrier due to phase jitter of carrier oscillators

θ_c = phase jitter of carrier oscillators

δ = imbalance factor (1.1 is 10 percent imbalance)

If 10 percent imbalance is assumed, then the phase jitter is $0.05\ \theta_c$. The phase jitter of the carrier receiver oscillators is almost the same as the phase jitter of the transmitter VCXO; therefore the phase jitter on the subcarrier due to the carrier is negligible in comparison with the transmitter VCXO jitter. The phase jitter as read at the output of the subcarrier phase detector is thus due only to the transmitter VCXO and the subcarrier VCO. If it is assumed that the mean square error (Reference 8) is as shown by

$$\left|\theta_N(s)\right|^2 = \frac{1}{T_c s^2}, \tag{2}$$

where T_c = coherence time of oscillator,

then the rms error for the second-order loop can be evaluated in terms of the T_c and the loop noise bandwidth, B_n, by means of the integral

$$\overline{E(t)^2} = \frac{1}{2\pi j} \int_{-\infty}^{\infty} - \frac{1}{T_c s^2} \left| \frac{s^2}{s^2 + 2\,\delta\,\omega_n s + \omega_n^2} \right| ds \tag{3}$$

The subcarrier loop has a damping factor (δ) of 0.707 and has 50 Hz as its narrowest noise bandwidth. For this type of loop, $\omega_n = 0.943B_n$ and the above integral becomes

$$\overline{E(t)^2} = \frac{0.353}{B_n T_c} \tag{4}$$

The expected value of T_c for the required transmitter VCXO is 4.5 sec, which will result in an rms phase jitter of 2.4 degrees. This error, when root-mean-squared with the phase jitter due to the subcarrier oscillator must produce an error of less than 6 degrees as measured at the subcarrier phase detector output. To find the maximum error that the subcarrier VCO can contribute, the following is used

$$\theta_{SCSC} = \sqrt{(6°)^2 - (2.4°)^2} \tag{5}$$

$$\theta_{SCSC} = 5.5° \text{ rms}$$

where θ_{SCSC} is the error in the subcarrier loop due to the subcarrier VCO.

4.11.2 Transponder Simulator Delay Time

The delay through the simulator is primarily a function of the RF path length and the delay of the wideband amplifier.

Referring to the block diagram given as Figure 3-132, the delay time of the RF path is the delay through the signal cables, the balanced mixer, the balanced modulator, the directional coupler, and the diplexer circulator. The total path will be about 3 feet, and the delay time can now be calculated using

$$\text{Delay Time} = \frac{\text{RF path length}}{K \times C} \tag{6}$$

where

C = speed of light in a vacuum, 3×10^8 meter/sec

K = velocity factor of the cable, 0.7

The delay time due to the RF path is therefor 4 nanosec.

The delay time for an RC-coupled amplifier can be found by differentiating the phase with respect to the frequency and can be shown to be

$$T.D. = \frac{0.318}{BW_{3\ DB}} \text{ sec} \tag{7}$$

For a transistor amplifier the constant (0.318) is not large enough since the gain is falling off somewhat faster than would be predicted for a one-pole amplifier. A better approximation would be

$$T.D. = \frac{0.450}{BW_{3\ DB}} \text{ sec} \tag{8}$$

To find the delay introduced by the wideband amplifier in the transponder simulator, it is necessary to know the number of stages to be used. Referring to Figure 3.11.8, note that the balanced modulator will require a drive level from the ×15 multiplier of +3 dbm; with 30 db of carrier suppression, this gives a carrier power of -27 dbm at the output of the balanced modulator.

To construct a suppressed carrier signal at this point, the sidebands must be at least 6 db above the carrier, or the sideband power must be -18 dbm. Assuming that the modulator has -7 db of conversion gain, then the modulator input power from the wideband amplifier must be -11 dbm. Assuming a conversion gain for the balanced mixer of -7 db and an input of -40 dbm, then the input power to the wideband amplifier is -47 dbm. The required gain, therefore, is 36 db. This gain will take a 3-stage amplifier offering 12 db gain per stage.

An obtainable bandwidth at this gain is about 100 MHz per stage; therefore the time delay is

$$T.D. = 3 \times \left[\frac{0.45}{10^8}\right] \tag{9}$$

$$T.D. = 13.5 \text{ nanosec}$$

To decrease the time delay more input power is required to reduce gain requirements and thus reduce the number of amplifier stages.

SECTION 5. RANGE AND RANGE RATE PERFORMANCE REQUIREMENTS

Range and range rate performance requirements to be used for acceptance testing were obtained by combining acceptable demonstration tolerances with the predicted performance given in Figures 4-41, 4-42, and 4-45. Only non-diversity S-Band operation is included.

The predicted and required range and range rate performance is shown in Figures 5-1, 5-2, and 5-3.

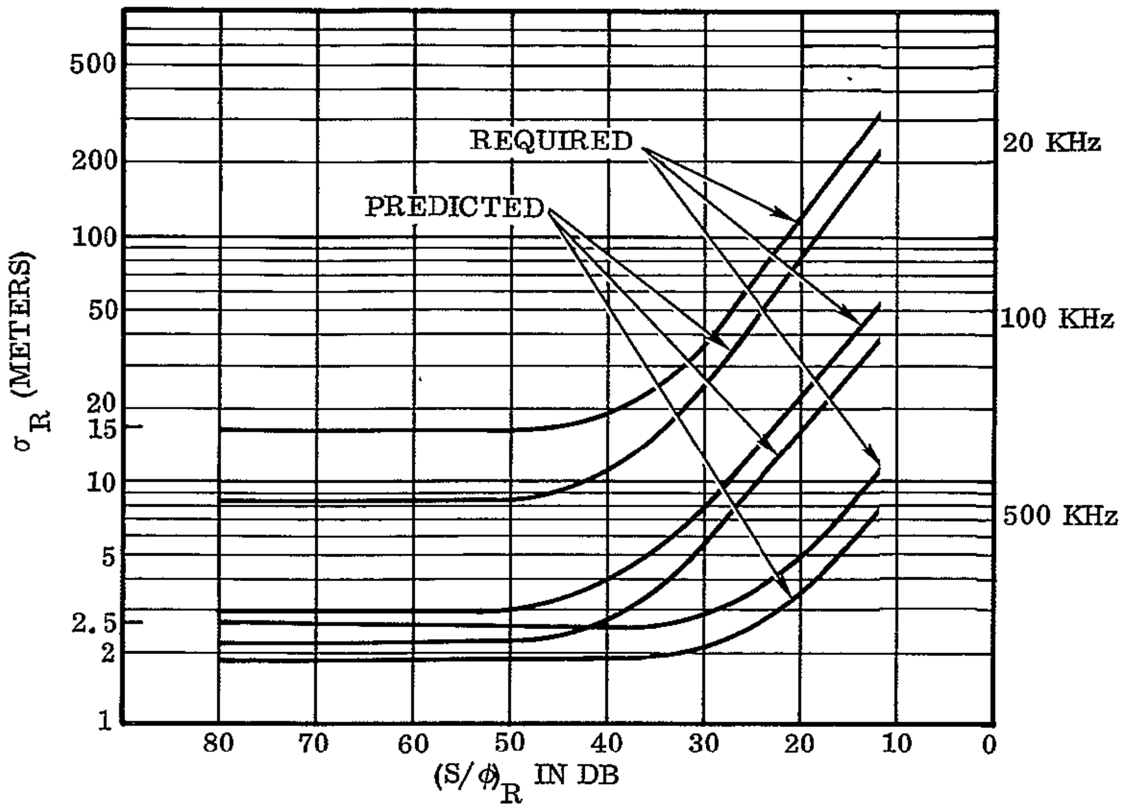

Figure 5-1. S-Band Range Instrumental Accuracy (1 Hz BW, Maximum Doppler)

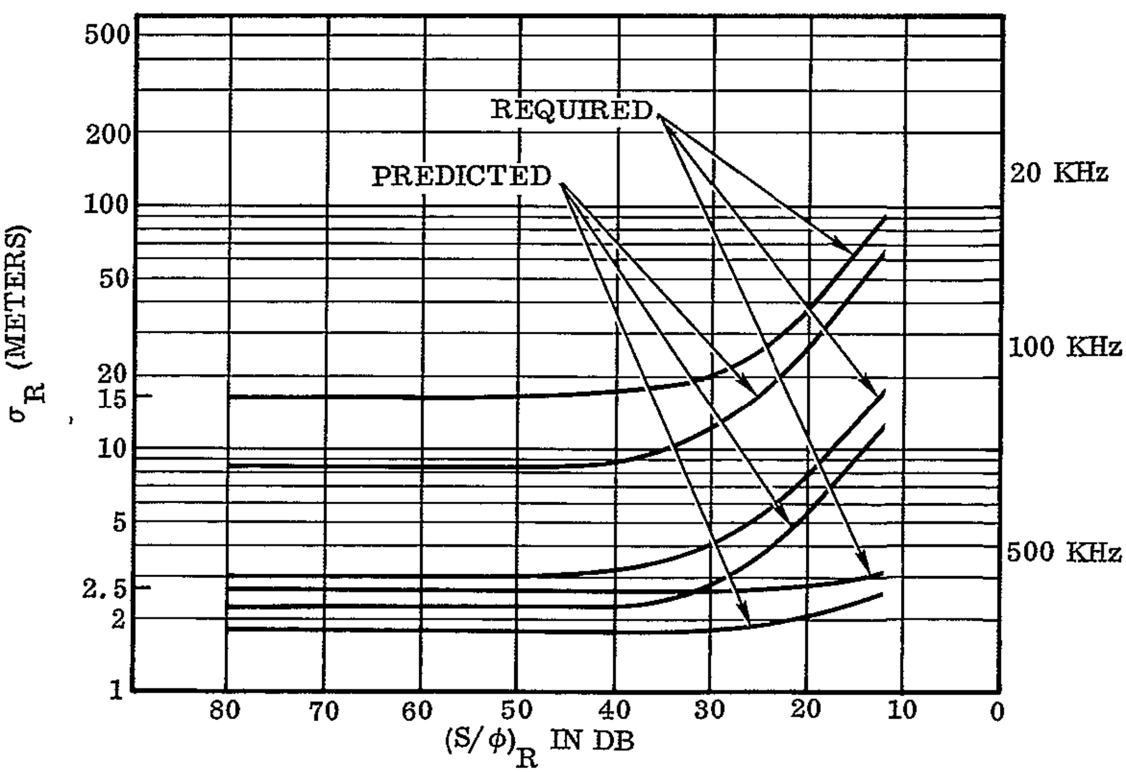

Figure 5-2. S-Band Range Instrumental Accuracy (0.1 Hz BW, No Doppler)

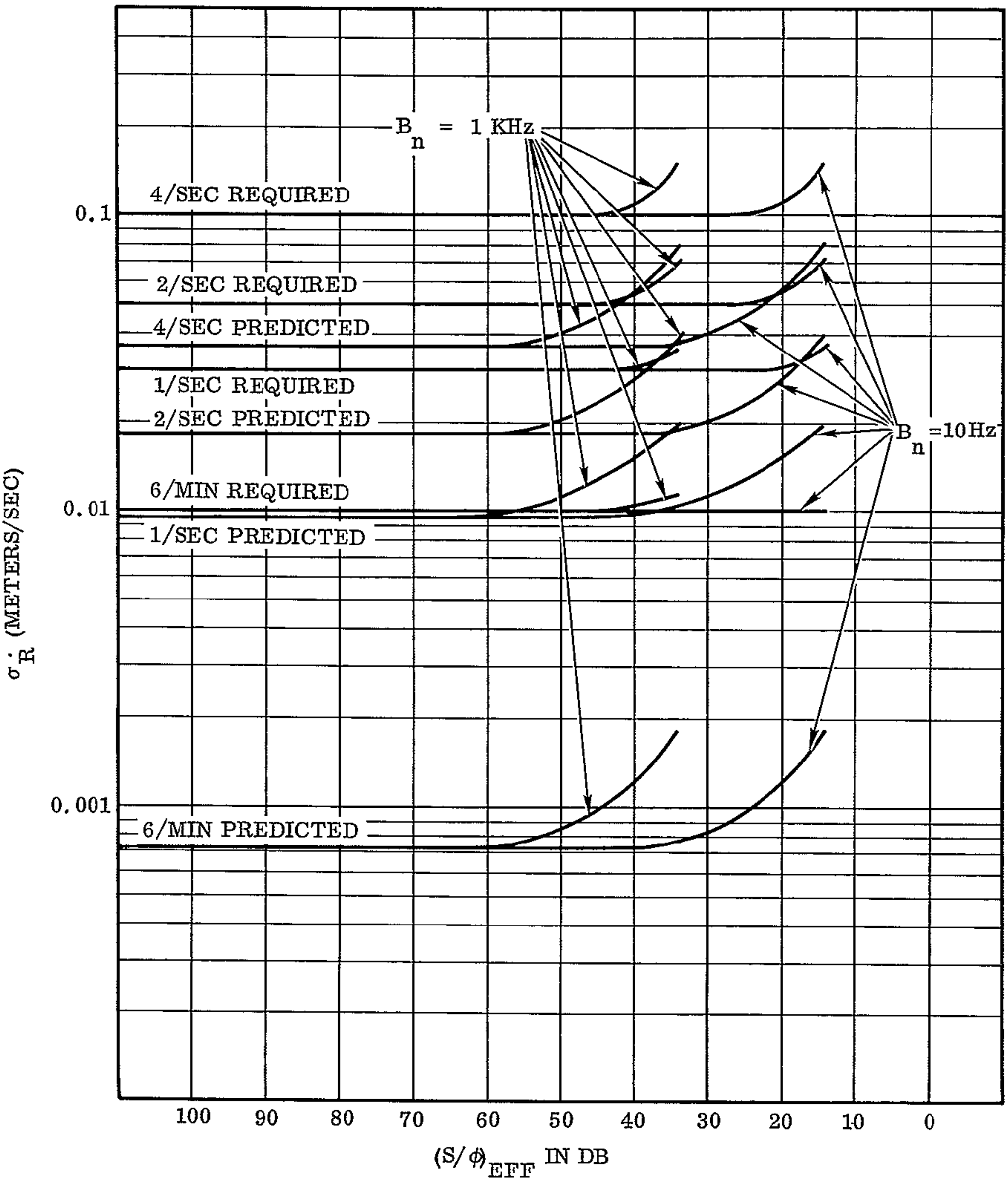

Figure 5-3. Range Rate Instrumental Accuracy, S-Band Operation

BIBLIOGRAPHY

1. Motorola Report No. W2719-2-1, Goddard Range and Range Rate System, Design Evaluation Report, November 1962.

2. Merrill I. Skolnik, Introduction to Radar Systems, McGraw-Hill, 1962.

3. GRARR Power Spectrum, Threshold Analysis, and Spectrum Diagrams, Goddard Space Flight Center, X-530-67-160, April 1967.

4. Gardner, Phaselock Techniques, Wiley, Inc., 1966.

5. Davenport and Root, Random Signals and Noise, p. 79, McGraw-Hill, 1958.

6. Jet Propulsion Laboratory Research Summary, No. 36-2, pp. 28-31.

7. Applications Technological Satellite Range and Range Rate Design Evaluation Report, Contract NAS 5-9808.

8. J. A. Develet, Jr., Fundamental Sensitivity Limitations for Second-Order Phase-Lock Loops, paper presented at URSI Meeting, Georgetown University, Washington, D. C., 4 May 1961.

9. James, Nichols and Phillips, Theory of Servomechanisms, p. 369, Rad. Lab. Series, Vol. 25, McGraw-Hill Book Company, 1947.

10. Frazier and Page, Phase Lock Loop Frequency Acquisition Study, IRE Transactions on Space Electronics and Telemetry, September 1962.

11. A. J. Mallinckrodt, Passive Ranging Doppler System, Phase A Completion Report, No. 961-R1, 2 November 1953, Ballistic Research Laboratory.

12. Henry Jasik, Antenna Engineering Handbook, Chapter 10, McGraw-Hill, 1961.

13. C. Larry Gray, Estimating the Effect of Feed Support Member Blocking an Antenna Gain and Sidelobe Level, Microwave Journal, March 1964.

14. Heat Flow and Extended Surfaces for Heat Transfer, Electro-Technology Magazine, C-M Technical Publications Corporation, 1961.

15. Theodore Baumeister, Mark's Mechanical Engineers Handbook, 6th Edition, McGraw-Hill, 1958.

16. P. J. Schneider, Conduction Heat Transfer, Addison-Wesley Publishing Co., 1955.